THE IMMUNOLOGY OF THE MALE GENITAL TRACT

EDITED BY: Yong-Gang Duan, Daishu Han and Kenneth Tung
PUBLISHED IN: Frontiers in Immunology

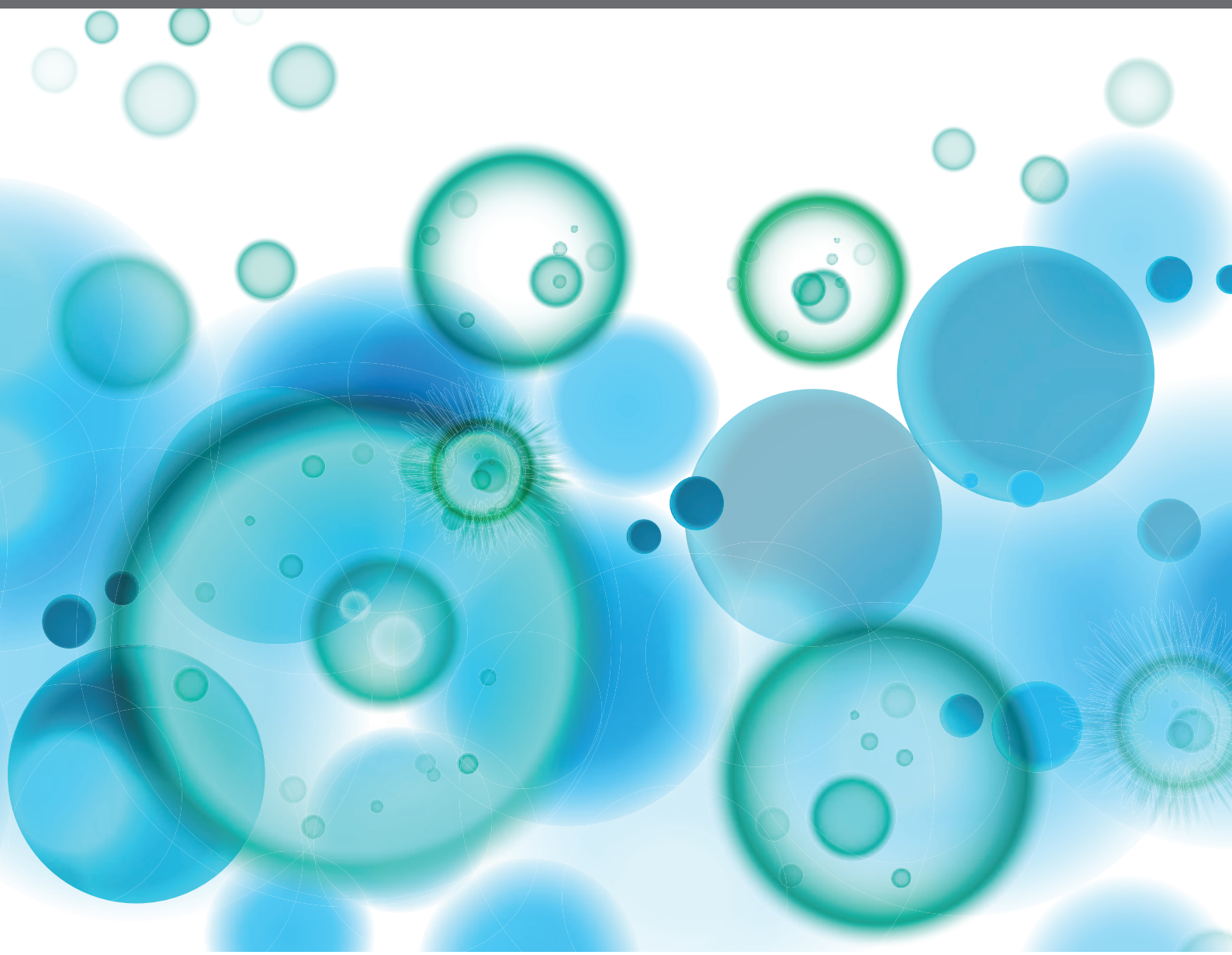

frontiers Research Topics

frontiers

ISSN 1664-8714
ISBN 978-2-83250-649-3
DOI 10.3389/978-2-83250-649-3

About Frontiers

Frontiers is more than just an open-access publisher of scholarly articles: it is a pioneering approach to the world of academia, radically improving the way scholarly research is managed. The grand vision of Frontiers is a world where all people have an equal opportunity to seek, share and generate knowledge. Frontiers provides immediate and permanent online open access to all its publications, but this alone is not enough to realize our grand goals.

Frontiers Journal Series

The Frontiers Journal Series is a multi-tier and interdisciplinary set of open-access, online journals, promising a paradigm shift from the current review, selection and dissemination processes in academic publishing. All Frontiers journals are driven by researchers for researchers; therefore, they constitute a service to the scholarly community. At the same time, the Frontiers Journal Series operates on a revolutionary invention, the tiered publishing system, initially addressing specific communities of scholars, and gradually climbing up to broader public understanding, thus serving the interests of the lay society, too.

Dedication to Quality

Each Frontiers article is a landmark of the highest quality, thanks to genuinely collaborative interactions between authors and review editors, who include some of the world's best academicians. Research must be certified by peers before entering a stream of knowledge that may eventually reach the public - and shape society; therefore, Frontiers only applies the most rigorous and unbiased reviews.
Frontiers revolutionizes research publishing by freely delivering the most outstanding research, evaluated with no bias from both the academic and social point of view. By applying the most advanced information technologies, Frontiers is catapulting scholarly publishing into a new generation.

What are Frontiers Research Topics?

Frontiers Research Topics are very popular trademarks of the Frontiers Journals Series: they are collections of at least ten articles, all centered on a particular subject. With their unique mix of varied contributions from Original Research to Review Articles, Frontiers Research Topics unify the most influential researchers, the latest key findings and historical advances in a hot research area! Find out more on how to host your own Frontiers Research Topic or contribute to one as an author by contacting the Frontiers Editorial Office: frontiersin.org/about/contact

THE IMMUNOLOGY OF THE MALE GENITAL TRACT

Topic Editors:
Yong-Gang Duan, Shenzhen Hospital, The University of Hong Kong, China
Daishu Han, Institute of Basic Medical Sciences, Chinese Academy of Medical Sciences and Peking Union Medical College, China
Kenneth Tung, University of Virginia, United States

The authors declare that the research was conducted in the absence of any commercial or financial relationships that could be construed as a potential conflict of interest.

Citation: Duan, Y.-G., Han, D., Tung, K., eds. (2022). The Immunology of the Male Genital Tract. Lausanne: Frontiers Media SA. doi: 10.3389/978-2-83250-649-3

Table of Contents

frontiers | Frontiers in Immunology

TYPE Editorial
PUBLISHED 17 October 2022
DOI 10.3389/fimmu.2022.1042468

OPEN ACCESS

EDITED AND REVIEWED BY
Nils Yngve Lycke,
University of Gothenburg, Sweden

*CORRESPONDENCE
Kenneth S. K. Tung
ksktung@googlemail.com

SPECIALTY SECTION
This article was submitted to Mucosal Immunity, a section of the journal Frontiers in Immunology

RECEIVED 12 September 2022
ACCEPTED 22 September 2022
PUBLISHED 17 October 2022

CITATION
Tung KSK, Han D and Duan Y-G (2022) Editorial: The immunology of the male genital tract. *Front. Immunol.* 13:1042468. doi: 10.3389/fimmu.2022.1042468

Editorial: The immunology of the male genital tract

Kenneth S. K. Tung[1]*, Daishu Han[2] and Yong-Gang Duan[3]

[1]Department of Pathology, Beirne B. Carter Center of Immunology, University of Virginia, Charlottesville, VA, United States, [2]School of Basic Medicine, Peking Union Medical College, Beijing, China, [3]Shenzhen Key Laboratory of Fertility Regulation, Center of Assisted Reproduction and Embryology, University of Hong Kong – Shenzhen Hospital, Shenzhen, China

KEYWORDS

editorial, male reproductive immunology, chronic epididymitis, experimental autoimmune orchitis (EAO), autoimmunity

Editorial on the Research Topic
The immunology of the male genital tract

Research on organ-specific autoimmune disease generally covers both systemic and local regulations. In contrast, studies on the testis are focused mainly on local mechanisms. This is because of the general belief that haploid germ cell-specific antigens (Ag) are sequestered within the seminiferous tubule (SFT) by the blood–testis barrier (BTB) and do not communicate with the immune system and that the late ontogeny of haploid germ cell Ag precludes neonatal tolerance induction. However, these arguments are not evidence-based, and recent findings indicate they are not valid.

As observed by Harakal et al., Ag sequestration applies only to some sperm Ag. Other haploid sperm Ag continuously egress the normal SFT. The physiological sperm Ag lactate dehydrogenase 3 (LDH3) enters the residual body (RB), egresses into the testis interstitial space, and forms immune complexes with circulating antibodies (Ab). LDH3 first egresses at postnatal week 5 when RB formation begins. Ag-specific systemic tolerance to LDH3 is documented in male wild-type (WT) mice, but not in male LDH3 -/- mice or Treg-depleted male WT mice. When Tregs are depleted from adult mice expressing the transgenic Foxp3-diphtheria toxin receptor, they spontaneously develop LDH3 Ab and severe autoimmune orchitis (AO), and both are preventable with Treg from WT male donors. Therefore, the egress of the sperm Ag from the SFT beyond the neonatal period is protected by Treg-dependent systemic tolerance. A similar mechanism applies to autoantigens in mouse stomachs, ovaries, prostates, and lacrimal glands (1–4). Although egress is documented herein only for LDH3, other investigators detected numerous rodent and human sperm proteins in the testis interstitial fluid and circulation *via* mass spectroscopy (5).

Normally sequestered sperm Ag are exemplified by the acrosomal zonadhesin (ZAN). Although systemic tolerance for ZAN is undetected in normal mice, when ZAN is exposed by unilateral vasectomy, it induces Ag-specific Treg-dependent tolerance in 7 days. Thus, when unilaterally vasectomized mice are immunized with the brain Ag or testis Ag, they develop an autoimmune disease in the brain but not in the testis. When

unilaterally vasectomized mice are 60% Treg-depleted, they develop ZAN Ab and severe bilateral AO.

The rapid Treg response to the exposed sequestered sperm Ag resembles the response against microbial Ag, which may reduce collateral tissue damage and enhance infection chronicity (6). The newly appreciated sequel of murine vasectomy suggests that should receive further investigation, and that vasectomy should be avoided in rodent infection models. The fact that the sequestered sperm Ag are protected by Treg-dependent tolerance also raises new questions regarding the high immunogenicity of the "foreign" cancer/testis Ag (7) and whether vasectomy can lead to a predisposition to neoplasia.

Lustig et al. reviewed the overall functional anatomy of the testis and described the cells located in the testis interstitial space. They also describe in detail local mechanisms that operate in rat experimental AO (EAO). First, indoleamine 2,3-dioxygenase (IDO) produced by Sertoli cells and other cell types. The essential amino acid trytophan is deprived by IDO, and it leads to the production of kynurenine. Second, the cytokines IL6 and TNFα disrupt the BTB integrity and expose sperm Ag. Third, the dendritic cells (DC) present testis Ag to T cells and include Treg in draining the lymph node (LN). (8). Fourth, Treg spreads in the testis and regional LN during EAO, but they do not suppress T-cell response. Fifth, the activins promote fibrosis. Sixth, the testis macrophages increase.

The study from Bhushan et al. details the macrophages in two unique locations. Those in close contact with Leydig cells are yolk sac-derived and they self-renew. They are essential for Leydig cell function, including steroidogenesis that maintains BTB integrity, the hypothalamic–pituitary–gonadal axis, and spermatogenesis. Moreover, the macrophages co-localized with the spermatogonia are BM-derived and renewed from blood, and they support pre-meiotic germ cell development. The peri-tubular macrophages may also process and present endogenous and exogenous Ag to Ag-specific T cells locally and in the regional LN. The M2 macrophages in a normal testis express high levels of CD163 and IL10 and minimal levels of nitric acid and TNFα. They stimulate a Treg response and maintain local and systemic tolerance for testis Ag. However, when the testis is inflamed from AO, infections, or LPS exposure, the macrophages switch from M2 to M1. M1 macrophages are major histocompatibility complex class II+ (MHC Class II+), and they produce proinflammatory cytokines (TNFα and IL6) and chemokines. A new *in vitro* study by Fan et al. on the small Ca^{2+} binding protein S100A9 documented its effect on the immunosuppressive property of M2 macrophages. The process requires the activation of the P13kt pathway; and S100A9 and/or P13K inhibitors prevent the activation of M2 macrophages *in vitro*.

The immunology of the epididymis is quite different from the immunology of the testis, as described by Pleuger et al. and Zhao et al. Importantly, the proximal caput epididymis is structurally and functionally distinct from the distal cauda epididymis. The caput has a complex epithelial lining with intraepithelial lymphocytes surrounded by a network of dendritic cells and F4/80+ and CD11c+ macrophages. The latter projects cytoplasmic processes into the lumen to contact intraluminal cell contents (9). Interestingly, the caput lumen is the location where most cytoplasmic droplets (CD) are discarded by the epididymal sperm. Because CD shares a common origin with the RB, the caput is potentially a location of sperm Ag exposure. Two regulatory pathways are documented in the caput. The first is TGFβ (10). Mice deficient in dendritic cell-specific TGFβ receptor 2 spontaneously develop epididymitis and sperm Ab and accumulate Treg in the epididymis and testis. The second is IDO, activated by activin A, and is expressed in the caput (11). Mice deficient in IDO express pro-inflammatory cytokines and show epididymitis and abnormal sperm contents. In contrast, the cauda epididymis is lined by a simple epithelium, and it is more responsive to mechanical injury (vasectomy) and bacterial infections. The caudal interstitial macrophages express NFκB and toll-like receptors, mount innate responses against infectious agents, and are prone to granulomata and fibrosis.

The findings in this review suggest future directions for exploration that may better clarify the nature of human gonadal diseases. Said findings include how an autoimmune disease develops as well as what and how testis autoantigens are selected based on different mechanisms of autoimmunity, including those driven by infection. Future studies will benefit from active collaboration between research on local and systemic mechanisms.

Author contributions

KT drafted the editorial, and DH and Y-GD contributed to the final submitted version. All authors contributed to the article and approved the submitted version.

Conflict of interest

The authors declare that the research was conducted in the absence of any commercial or financial relationships that could be construed as a potential conflict of interest.

Publisher's note

References

1. Taguchi O, Nishizuka Y. Self tolerance and localized autoimmunity: Mouse models of autoimmune disease that suggest tissue-specific suppressor T cells are involved in self tolerance. *J Exp Med* (1987) 165:146–56. doi: 10.1084/jem.165.1.146

2. Samy ET, Setiady YY, Ohno K, Pramoonjago P, Sharp C, Tung KSK. The role of physiological self-antigen in the acquisition and maintenance of regulatory T-cell function. *Immunol Rev* (2006) 212:170–84. doi: 10.1111/j.0105-2896.2006.00404.x

3. Setiady YY, Ohno K, Samy ET, Bagavant H, Qiao H, Sharp C, et al. Physiologic self antigens rapidly capacitate autoimmune disease-specific polyclonal CD4+ CD25+ regulatory T cells. *Blood* (2006) 107:1056–62. doi: 10.1182/blood-2005-08-3088

4. Savage PA, Klawon DEJ, Miller CH. Regulatory T cell development. *Annu Rev Immunol* (2020) 38:421–53. doi: 10.1146/annurev-immunol-100219-020937

5. O'Donnell L, Rebourcet D, Dagley LF, Sgaier R, Infusini G, O'Shaughnessy PJ, et al. Sperm proteins and cancer-testis antigens are released by the seminiferous tubules in mice and men. *FASEB J* (2021) 35:e21397. doi: 10.1096/fj.202002484R

6. Estrada Brull A, Rost F, Oderbolz J, Kirchner FR, Leibundgut-Landmann S, Oxenius A, et al. CD85k contributes to regulatory T cell function in chronic viral infections. *Int J Mol Sci* (2020) 22(1):31. doi: 10.3390/ijms22010031

7. Gjerstorff MF, Andersen MH, Ditzel HJ. Oncogenic cancer/testis antigens: Prime candidates for immunotherapy. *Oncotarget* (2015) 6(18):15772–87. doi: 10.18632/oncotarget.4694

8. Guazzone VA. Exploring the role of antigen presenting cells in male genital tract. *Andrologia* (2018) 50(11): e13120. doi: 10.3389/fimmu.2020.02115

9. Da Silva N, Cortez-Retamozo V, Reinecker HC, Wildgruber M, Hill E, Brown D, et al. A dense network of dendritic cells populates the murine epididymis. *Reproduction* (2011) 141:653–63. doi: 10.1530/REP-10-0493

10. Pierucci-Alves F, Midura-Kiela MT, Fleming SD, Schultz BD, Kiela PR. Transforming growth factor beta signaling in dendritic cells is required for immunotolerance to sperm in the epididymis. *Front Immunol* (2018) 9:1882. doi: 10.3389/fimmu.2018.01882

11. Gualdoni GS, Jacobo PV, Sobarzo CM, Pérez CV, Matzkin ME, Höcht C, et al. Role of indoleamine 2,3-dioxygenase in testicular immune-privilege. *Sci Rep* (2019) 9:15919. doi: 10.1038/s41598-019-52192-8

frontiers in Immunology

ORIGINAL RESEARCH
published: 09 September 2020
doi: 10.3389/fimmu.2020.574212

Influence of Experimental Autoimmune Prostatitis on Sexual Function and the Anti-inflammatory Efficacy of Celecoxib in a Rat Model

Yadong Zhang[1†], Xiangping Li[1†], Kuikui Zhou[2†], Mingkuan Zhou[1], Kai Xia[1], Yunlong Xu[2], Xiangzhou Sun[1], Yingjie Zhu[2], Chunyan Cui[3] and Chunhua Deng[1]**

[1] Department of Urology and Andrology, The First Affiliated Hospital, Sun Yat-sen University, Guangzhou, China, [2] Shenzhen Key Lab of Drug Addiction, The Brain Cognition and Brain Disease Institute (BCBDI), Shenzhen Institutes of Advanced Technology, Chinese Academy of Sciences, Shenzhen-HongKong Institute of Brain Science-Shenzhen Fundamental Research Institutions, Shenzhen, China, [3] Imaging and Minimally Invasive Intervention Center, Sun Yat-sen University Cancer Center (SYSUCC), Guangzhou, China

OPEN ACCESS

Edited by:
Yong-Gang Duan,
The University of Hong Kong, China

Reviewed by:
Emmanuele A. Jannini,
University of Rome Tor Vergata, Italy
Guiting Lin,
University of California,
San Francisco, United States

***Correspondence:**
Chunyan Cui
cuichy@sysucc.org.cn
Chunhua Deng
dengchh@mail.sysu.edu.cn

[†]These authors have contributed equally to this work

Specialty section:
This article was submitted to Mucosal Immunity, a section of the journal Frontiers in Immunology

Received: 19 June 2020
Accepted: 17 August 2020
Published: 09 September 2020

Citation:
Zhang Y, Li X, Zhou K, Zhou M, Xia K, Xu Y, Sun X, Zhu Y, Cui C and Deng C (2020) Influence of Experimental Autoimmune Prostatitis on Sexual Function and the Anti-inflammatory Efficacy of Celecoxib in a Rat Model. Front. Immunol. 11:574212. doi: 10.3389/fimmu.2020.574212

Experimental autoimmune prostatitis (EAP) is a well-established model induced by an autoimmune response to prostate antigen. The symptomatic, pathological, and immunological characteristics of EAP animals are highly consistent with human chronic prostatitis/chronic pelvic pain syndrome (CP/CPPS), which makes EAP an ideal model for this disease. Here, we investigate the influence of EAP on male rat sexual function and the efficacy of anti-inflammatory therapy with celecoxib. EAP rat models were established using male Wistar rats. Rats were randomly assigned to a normal control group, an EAP model group, or an EAP model with celecoxib treatment group (celecoxib group). Behavioral changes, sexual behavioral changes, and erectile function were estimated using an open-field test, a sucrose consumption test, mating experiments, and by intracavernous pressure/mean arterial pressure ratio (ICP/MAP). Histological changes in the prostate were observed by HE staining, and the serum inflammatory factors IL-1β and TNF-α levels were measured by enzyme-linked immunosorbent assay. In addition, serotonin (5-hydroxytryptamine, 5-HT), 5-HT_{1A} receptor, 5-HT_{2C} receptor, and serotonin transporter (SERT) expression levels in the hippocampus and spinal cord (T13–L1, L5–S2) were examined by immunohistochemistry and western blot analysis. Results showed that EAP rats exhibited characteristics of depression, decreased sexual drive, premature ejaculation, and increased threshold of penile erection. Moreover, all these changes were effectively alleviated by celecoxib. Significant increases in prostatic interstitial infiltration by inflammatory cells and in serum IL-1β and TNF-α levels were observed in EAP rats, and these were partially reduced by celecoxib. Additionally, the expression pattern of serotonin system regulators in the hippocampus and spinal cord were altered in EAP model rats, including a decrease in 5-HT levels and an increase in 5-HT_{1A} receptor levels. In conclusion, autoimmune prostatitis impaired rat sexual function, and this was effectively prevented by anti-inflammatory therapy with celecoxib. Moreover, a serotonin system disorder in the central nervous system was likely mediated via inflammation in EAP rats.

Keywords: experimental autoimmune prostatitis, chronic prostatitis/chronic pelvic pain (CP/CPP) syndrome, sexual dysfunction, depression, celecoxib, serotonin

INTRODUCTION

Chronic prostatitis/chronic pelvic pain syndrome (CP/CPPS) is an inflammatory disease affecting around 8.2% of the male population throughout the world (1). Common complications of CP/CPPS patients include sexual dysfunction and anxiety-related disorders (2, 3), as confirmed in our previous study (4). In our single-center study, the incidences of premature ejaculation (PE) and erectile dysfunction (ED) in CP/CPPS patients were about 45.3 and 47.4%, respectively (4), while the prevalence of PE was reported up to 64.1 and 36.9% in prostatitis-like symptom and chronic prostatitis group from another epidemiological investigation (5). According to a previous study (6), the incidence of anxiety-related disorders was reported to be 37–60%, including but not limited to depression, anxiety, and trauma-related disorders. Moreover, anxiety-related disorders comprised the highest risk factors for sexual dysfunction in CP/CPPS based on our data (4). However, the relationship among CP/CPPS, anxiety-related disorders, and sexual dysfunction was difficult to clarify because of the various confounding factors.

The cellular and molecular mechanisms underlying CP/CPPS remain largely unknown. Bacterial infection, urine reflux, autoimmune response, neuroendocrine disorder, and anxiety-related factors have been reported to associate with CP/CPPS (7). Based on the theory that immunopathogenic mechanisms (8) are involved, an experimental autoimmune prostatitis (EAP) animal model was established in rodents by generating an autoimmune response to various antigens, including an homogenate of male accessory glands (MAG) (9) or prostate (10), human prostate acid phosphatase (PAP) (11), prostate steroid binding protein (PSPB) (12), and peptide T2 (13). EAP rat is characterized by a prostate-specific cellular and humoral immune response with active inflammatory monocyte infiltration (14). In addition, the rodent model is associated with signs of chronic pelvic pain (15). Since the symptomatic, pathological, and immunological characteristics of the EAP model are highly consistent with human CP/CPPS, EAP rat is an ideal model to investigate effects related to prostate inflammation.

Celecoxib is a non-steroidal anti-inflammatory drug (NSAID) that reduces the production of prostaglandin by specifically inhibiting cyclooxygenase-2 (COX-2), thus producing anti-inflammatory and analgesic effects (16). Several clinical studies have reported that anti-inflammatory therapy with celecoxib alleviated the symptoms of CP/CPPS (17, 18). Also it's noteworthy that celecoxib was reported to benefit the treatment of depression (19, 20). As an important central neurotransmitter, serotonin (5-HT) is closely related to premature ejaculation and depression (21), which are both manifested in CP/CPPS patients. In clinical practice, selective serotonin reuptake inhibitors (SSRIs) are widely used to treat PE through the inhibition of reabsorption of serotonin in the synaptic gap (22). Thus, the association between inflammation and the serotonin system may be a factor of interest in these investigations.

In the present study, we report that autoimmune prostatitis caused depression-like behavior and impairment of sexual function in the EAP rat model. In addition, the expression patterns of serotonin system regulators in the central nervous system and serum inflammatory factors were altered in EAP rat, and these changes could be prevented by anti-inflammatory therapy with celecoxib.

MATERIALS AND METHODS

Experimental Animals

Specific pathogen-free (SPF) Wistar rats were procured from the experimental animal center of Sun Yat-sen University (Guangzhou, China). Rats were housed in an SPF environment in a standard housing room under controlled temperature (15–25°C), relative humidity (50–70%), and artificial light (12 h light/dark cycle), and were provided free access to food and water. All animal protocols were approved by the ethics committee of The First Affiliated Hospital of Sun Yat-sen University (Guangzhou, China).

Animal Model and Study Design

Adult male Wistar rats (3 months old, weighing 250–300 g) were randomly divided into EAP model group (n = 16), normal control group (n = 10), and EAP model with celecoxib treatment group (celecoxib group) (n = 10). In addition, prostate protein was extracted from another 18 adult male rats. The EAP rat model was established in the EAP model group and celecoxib group following a modified classical modeling method of two-step immunization (9). Briefly, prostates excised from Wistar rats were homogenized in 0.5% Triton X-100 (Sigma, Aldrich, United States) with an electric homogenizer (HZYBDJ, Hangzhou, China). Prostate protein extract was obtained by centrifugation (12,000 g, 30 min) of prostate homogenate and used as antigen. The protein concentration of the supernatant was determined using a BCA Protein Assay Kit (Cwbiotech, Beijing, China), and the supernatant was then diluted to 40 mg/mL. To generate the EAP model, a 1 mL suspension of prostate protein extract (20 mg) and complete Freund's adjuvant (0.5 mL, Sigma, Aldrich, United States) was injected subcutaneously on day 0, and a 1 mL suspension of prostate protein extract (20 mg) and incomplete Freund's adjuvant (0.5 mL, Sigma, Aldrich, United States) was injected on day 21 again. In the normal control group, 1 mL of 0.15 M saline was injected subcutaneously. On the day of model establishment, celecoxib (Pfizer Inc., New York, NY, United States) was administered in the celecoxib treatment group by gavage (18 mg/kg/day). In the model group and the normal control group, 0.15 M saline was administered by gavage (0.1 mL/kg/day).

Open-Field Test

Rats were tested in a self-made square box (80 cm by 80 cm; by 40 cm in height) painted black on the inside. The box bottom was divided into 25 small squares. At the start, the rat was positioned in the central square, and all movements within the next 5 min were recorded by camera. The number of squares that all four limbs of the rat had entered during exploration was taken as a

score of horizontal movement. The number of times the rats' forelegs lifted off the bottom or climbed the wall of the box was taken as a score of vertical movement. The tests were repeated twice by two researchers who were blinded to the grouping of rats, and an average value was taken as the final score. Each rat was tested before model establishment and 8 weeks after.

Sucrose Consumption Experiment

The Sucrose consumption experiment was performed according to previously published protocols (23). Prior to the start of the experiment, the rats were behaviorally adapted to drinking 1% sucrose water for 2 days. For the first 24 h, two bottles containing 1% sucrose water were placed in each cage. For the second 24 h, one bottle was filled with 1% sucrose water, and the other bottle with pure water. After 24 h water deprivation, each rat was given one bottle filled with 1% sucrose water and one bottle filled with pure water. The total liquid consumption and sucrose water consumption of each rat was determined 1 h later. The sucrose water preference was calculated as follows: Sucrose water preference = [(sucrose water consumption/total liquid consumption) × 100%]. Each rat was tested before model establishment and 8 weeks after.

Mating Experiment

For mating experiments, 36 adult female Wistar rats (3 months old, weighing 220–240 g) were castrated by bilateral ovariectomy following anesthesia by intraperitoneal injection of pentobarbital sodium (35 mg/kg). Two weeks after the procedure, estrus was induced in castrated female rats at 48 and 4 h prior to mating. Estrus was induced by subcutaneous injection of 20 μg estradiol benzoate (Kingyork, Tianjin, China) and 500 μg progesterone (Kingyork, Tianjin, China) dissolved in 0.1 mL olive oil. The mating experiment was conducted between 19:00 and 21:00. Each male rat was carefully placed into the observation cage for 10 min of adaptation. An estrous female rat was then carefully transferred into the cage. The mating behaviors over 30 min were observed and recorded by camera. The following parameters were evaluated: (i) Mount latency (ML), the time interval between the beginning of the test and the first time that the male rat mounts the female rat, with or without intromission; (ii) Intromission latency (IL), the time interval between the beginning of the test and the first time that the male rat intromits; (iii) Ejaculation latency (EL), the time interval between the first intromission and ejaculation; (iv) Mount Frequency (MF), a count of mount behaviors in 30 min; (v) Intromission frequency (IF), a counts of intromission behaviors in 30 min; (vi) Ejaculation Frequency (EF), a count of ejaculation in 30 min; (vii) Postejaculatory interval (PEI), the time interval between two successive ejaculations.

Intracavernous Pressure (ICP) and Mean Arterial Pressure (MAP) Measurement

Anesthesia was performed by intraperitoneal injection of pentobarbital sodium (35 mg/kg). The left common carotid artery was exposed by a median cervical incision and a PE-50 catheter connected to a pressure transducer was inserted for continuous MAP measurement. Crus penis and cavernous nerve (CN) were exposed by a lower abdominal incision. A bipolar electrode engaged the right CN with electrical stimulation (20 Hz, 5 V, 0.2 ms pulse duration) for 1 min. A 23G needle connected to a pressure transducer was inserted into either corpus cavernosum through the crus penis for ICP measurement. After 5 min, the electrical stimulation and measurement were repeated. To eliminate the interference of blood pressure, ICP/MAP was adopted to assess erectile function.

HE Staining of Prostate

After measuring ICP and MAP, the rat's prostate was harvested, washed with 0.15 M saline, fixed in 4% paraformaldehyde, and embedded in paraffin at 4°C overnight. Serial 4 μm thick sections were stained with hematoxylin and eosin (HE). After HE staining, pathological changes of the prostatic tissue in each group were observed under light microscopy (Olympus, Japan).

Serum TNF-α and IL-1β Enzyme-Linked Immunosorbent Assay (ELISA)

Blood samples were collected before rat sacrifice and centrifuged (3,000 *g*, 15 min, 4°C) to obtain serum. Serum was stored at −70°C until assayed. TNF-α and IL-1β were analyzed by ELISA kits (R&D Systems, Minneapolis, MN, United States) according to manufacturer's protocols. Serum TNF-α and IL-1β levels were determined following measurement of absorbance at 450 nm using a Bio-Rad microplate reader (Bio-Rad, Hercules, CA, United States).

Immunohistochemistry (IHC)

The expression levels of 5-HT, 5-HT_{1A} receptor, 5-HT_{2C} receptor, and SERT in the central nervous system were analyzed by IHC as follows. Brain and spinal cord (T13–L1 and L5–S2) tissues were harvested and fixed with 4% paraformaldehyde, dehydrated with ethanol and graded concentrations of xylene, and finally embedded in paraffin. The paraffinized tissues were then stored in liquid nitrogen until further processing. Sections of 4 μm thickness were blocked by BSA (Santa Cruz, CA, United States) for 1 h at room temperature, and then incubated overnight with primary antibodies against 5-HT (ab10385, Abcam, Cambridge, United Kingdom, 1:200), 5-HT_{1A} receptor (sc-10801, Santa Cruz, CA, United States, 1:200), 5-HT_{2C} receptor (sc-10802, Santa Cruz, CA, United States, 1:200), and SERT (sc-13997, Santa Cruz, CA, United States, 1:200) at 4°C. The sections were then washed and incubated with secondary antibodies and visualized using a DAB kit (K5007, DAKO, Glostrup, Denmark) according to manufacturer's protocols. Images were obtained using an LSM800 or LSM 710 confocal microscope (Zeiss, Heidenheim, Germany). For quantitative analysis, the results were presented as integrated optical density (IOD) using Image-Pro Plus 6.0 (Media Cybernetics, United States).

Western Blot

The expression levels of 5-HT, 5-HT_{1A} receptor, 5-HT_{2C} receptor, and SERT in the central nervous system were analyzed by western blot as follows. Brain and spinal cord (T13–L1 and L5–S2) tissues were lysed in 1 × RIPA buffer (Servicebio, Wuhan, China) to extract total protein. Total

protein concentrations were determined using the BCA Protein Assay Kit (Cwbiotech, Beijing, China). A standardized western blotting protocol was adopted. Briefly, 10–20 μg of protein per channel was separated through 10% SDS-PAGE and then transferred to polyvinylidene difluoride (PVDF) membranes (Millipore, Billerica, MA, United States). After blocking with BSA (Roche, Basel, Switzerland) for 1 h, membranes were incubated with primary antibodies against 5-HT (ab10385, Abcam, Cambridge, United Kingdom, 1:1000), 5-HT_{1A} receptor (sc-10801, Santa Cruz, CA, United States, 1:1000), 5-HT_{2C} receptor (sc-10802, Santa Cruz, CA, United States, 1:1000), and SERT (sc-13997, Santa Cruz, CA, United States, 1:1000) at 4°C overnight. The membranes were washed, incubated with secondary antibody, and visualized using the DAB Kit (Servicebio, Wuhan, China) according to the manufacturer's protocols. Specific bands were detected using a Gel Imaging System (Nikon, Japan). Gray values were quantified using Image-Pro Plus 6.0 (Media Cybernetics, United States) using β-actin as a control.

Statistical Analyses

SPSS 19.0 statistical software (SPSS Inc., Chicago, IL, United States) was used for statistical analyses. The data are presented as mean ± SD and comparisons between groups were performed using one-way ANOVA. A result with $P < 0.05$ was considered statistically significant.

RESULTS

Depression-Like Behaviors in EAP Rats

Behavioral changes were evaluated using the open-field test and the sucrose consumption test. EAP model rats exhibit typical depressive behaviors; thus, exploratory activity and sucrose water preference were reduced (**Figure 1**). These behaviors could be rescued by celecoxib treatment. Before model establishment, all rats exhibited normal active behaviors, and no significant difference in horizontal movement score, vertical movement score, or sucrose water preference was observed between the three groups ($P > 0.05$). However, 8 weeks after establishment of the EAP rat model, horizontal movement score (**Figure 1A**), vertical movement score (**Figure 1B**), and sucrose water preference (**Figure 1C**) were significantly reduced compared with the same rats before modeling ($P < 0.001$) or with the rats in the normal control and celecoxib groups ($P < 0.001$). No significant behavioral change was observed in the celecoxib or normal control groups during the study period ($P > 0.05$), and no difference was observed between the celecoxib group and the normal control group.

Sexual Behavior Changes and Erectile Function of EAP Rats

The sexual behavior and erectile function of rats in all three groups were analyzed. While sexual behavior changes

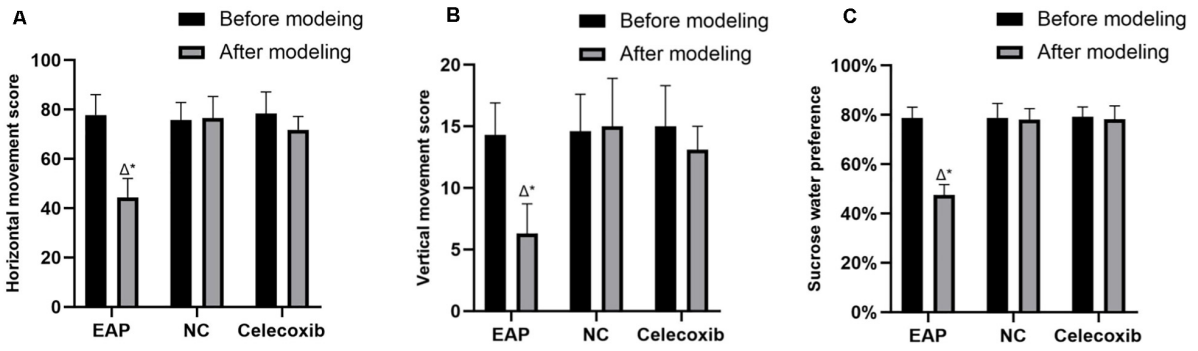

FIGURE 1 | Results of the open-field test and sucrose consumption test for all three rat groups. Horizontal movement score **(A)**, vertical movement score **(B)**, and sucrose water preference **(C)** of EAP rats were reduced compared with the same rats before modeling or with the rats in the normal control and celecoxib groups. $\Delta P < 0.001$ compared with the normal control group; $^*P < 0.001$ compared with rats from the same group before establishment of the model; NC, Normal Control Group.

TABLE 1 | Sexual behavior parameters of rats in different groups.

Parameters	EAP (n = 12)	NC (n = 10)	Celecoxib (n = 10)	F-value	P-value
Mount latency (ML) (s)	169.3 ± 52.9	117.0 ± 23.0**	124.2 ± 22.9**	6.489	0.005
Intromission latency (IL) (s)	180.8 ± 51.8	127.2 ± 21.7**	134.1 ± 22.0**	7.272	0.003
ejaculation latency (EL) (s)	192.5 ± 64.5	323.0 ± 80.0***	294.2 ± 85.5**	9.016	0.001
Postejaculatory interval (PEI) (s)	648.3 ± 140.5	391.0 ± 71.8***	388.0 ± 73.8***	23.308	0
Mount frequency (MF)	22.2 ± 3.7	30.4 ± 5.8**	31.5 ± 5.9***	11.002	0
Intromission frequency (IF)	15.9 ± 3.8	22.8 ± 4.9**	22.6 ± 4.0**	9.649	0.001
Ejaculation frequency (EF)	1.6 ± 0.5	2.2 ± 0.4*	2.2 ± 0.6*	5.095	0.013

*$P < 0.05$, **$P < 0.01$, ***$P < 0.001$ compared with EAP group.*

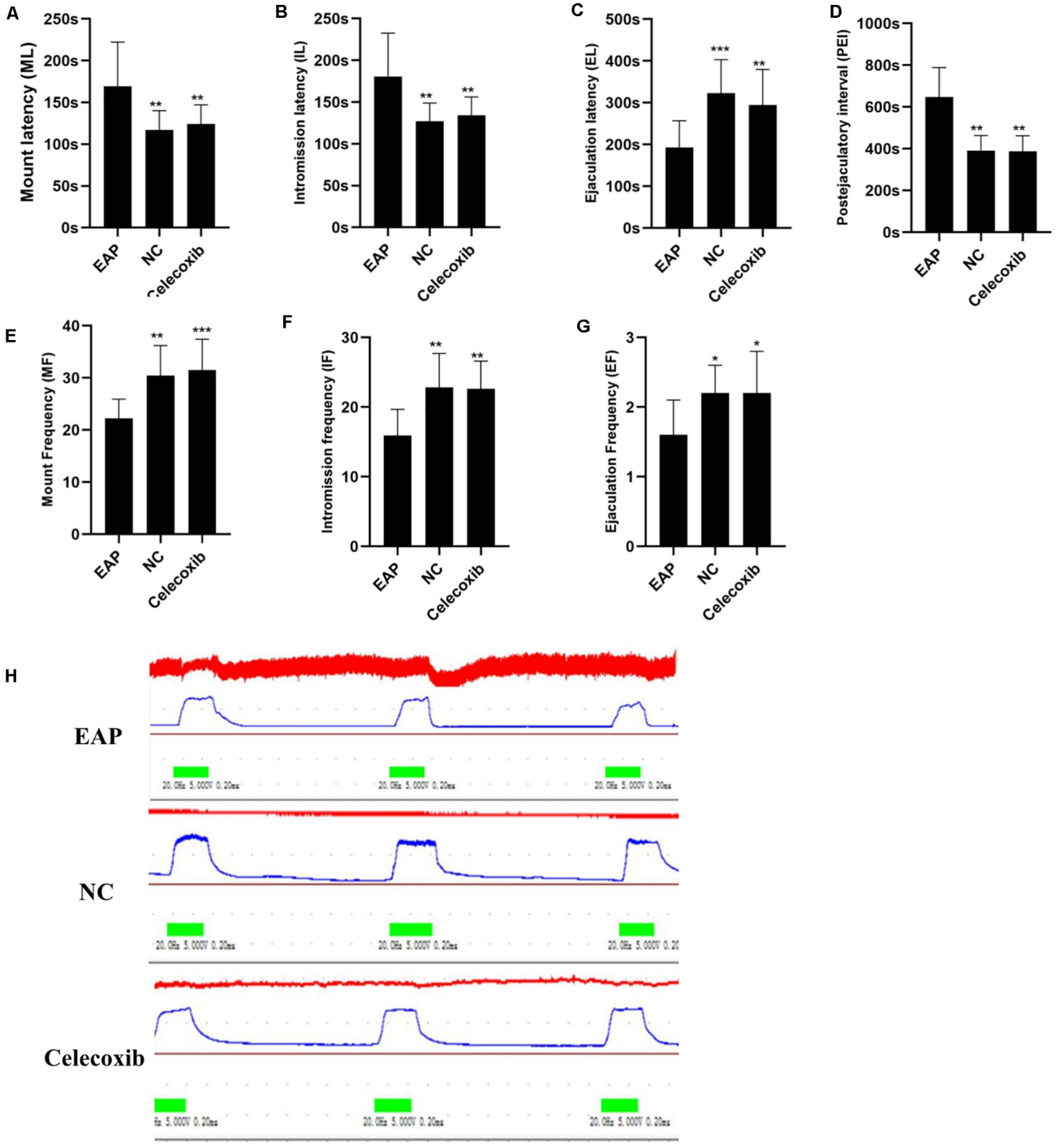

FIGURE 2 | Autoimmune prostatitis impaired rat sexual function. Mount latency (ML) was increased in EAP rats compared with celecoxib group and normal control group rats **(A)**. In addition, intromission latency (IL) was elongated **(B)**, and Ejaculation latency (EL) and postejaculatory interval (PEI) were shortened **(C,D)** in EAP rats. Mount frequency (MF), intromission frequency (IF), and ejaculation frequency (EF) were all reduced **(E–G)**. No significant differences between the celecoxib group and the normal control group were observed. The representative ICP/MAP of the rats in all three groups were all above 0.70 **(H)**. $^{*}P < 0.05$, $^{**}P < 0.01$, $^{***}P < 0.001$ compared with EAP group.

were observed in EAP rats when compared with the normal control group, no such changes were observed in the celecoxib group (**Table 1** and **Figures 2A–G**). Mount frequency (MF), intromission frequency (IF), and ejaculation frequency (EF) were all significantly reduced in EAP rats compared with the celecoxib and normal control groups ($P < 0.05$) (**Figures 2E–G**), and

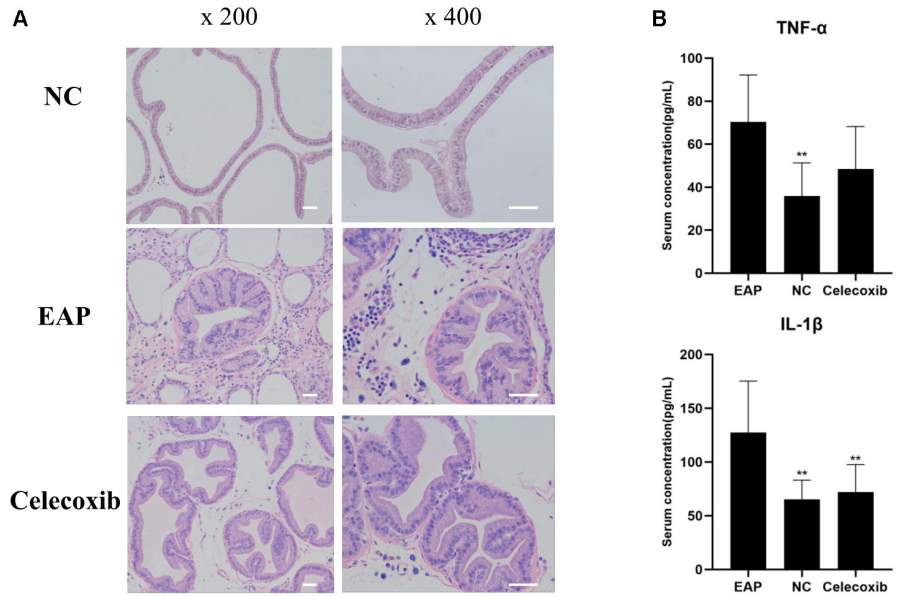

FIGURE 3 | Inflammatory changes of prostate and increased serum IL-1β in EAP rats. Representative inflammatory changes in the prostate gland (HE staining) in EAP rats are shown **(A)**; TNF-α and IL-1β levels were increased in EAP group rats compared with the normal control (NC) group **(B)**. $^{**}P < 0.01$ compared with EAP group. Scale bar = 25 μm.

mount latency (ML) was increased ($P < 0.05$) (**Figure 2A**). Moreover, intromission latency (IL) and postejaculatory interval (PEI) were increased in EAP rats (**Figures 2B,D**), while ejaculation latency (EL) was reduced (**Figure 2C**). No significant difference in any of the variables was observed between the celecoxib group and the normal control group ($P > 0.05$). The ICP/MAP were normal (above 0.70) in all three groups (**Figure 2H**), and no significant difference was observed between any two groups ($P > 0.05$).

Inflammatory Changes of Prostate and Increased Serum IL-1β in EAP Rats

To evaluate prostate and systemic inflammatory effects, histological examinations of rat prostate glands were performed and serum IL-1β and TNF-α concentrations were investigated. Characteristic inflammatory changes in the prostate gland were observed in 12 (out of 16) EAP group rats (**Figure 3A**). The lumens of these prostate glands were irregular in shape, secretions in the glandular cavity were scattered unevenly, the glandular epithelium showed segmental necrosis, and a large number of inflammatory cells had infiltrated into the interstitium. In the other 4 EAP group rats, HE staining showed normal morphology; this was adjudged to be due to the failure of modeling, and the data from these four rats were removed in all subsequent statistical analyses. In addition, serum IL-1β and TNF-α were both significantly increased compared with normal control group levels ($P < 0.01$) (**Figure 3B**). A comparison of celecoxib group and EAP group rats revealed that celecoxib treatment reduced infiltration of inflammatory cells and lowered serum IL-1β and TNF-α levels (**Figure 3B**); however, the observed reduction in TNF-α was not statistically significant. No significant differences were observed between celecoxib group and normal control group rats ($P > 0.05$) (**Figure 3B**).

Expression of 5-HT System Regulators Was Altered in Hippocampus of EAP Rats

To investigate changes in the 5-HT system in the hippocampus related to depression, the expression levels of 5-HT, 5-HT_{1A} receptor, 5-HT_{2C} receptor, and SERT in rat hippocampus were evaluated by immunohistochemistry and western blot analysis (**Figure 4**). In the EAP group, 5-HT expression in rat hippocampus was significantly decreased compared with the normal control group ($P < 0.05$) and celecoxib group ($P < 0.05$) rats (**Figures 4B,C**). In contrast, 5-HT_{1A}, 5-HT_{2C}, and SERT expression were all significantly increased ($P < 0.05$) (**Figures 4B,C**). No significant differences were observed between celecoxib group and normal control group rats. The western blot analyses were consistent with the results of quantitative analysis with IHC.

Expression of 5-HT System Regulators Was Altered in Spinal Cord (T13-L1, L5–S2) of EAP Rats

We also investigated changes in the 5-HT system in spinal segments controlling prostate sensation (**Figures 5**, **6**). Expression of 5-HT was significantly decreased in T13–L1 spinal cord segments in EAP rats and expression of 5-HT_{1A} receptor was increased compared with normal control group ($P < 0.05$) and celecoxib group ($P < 0.05$) rats (**Figures 5B,C**). Again, expression levels in celecoxib group rats were restored to

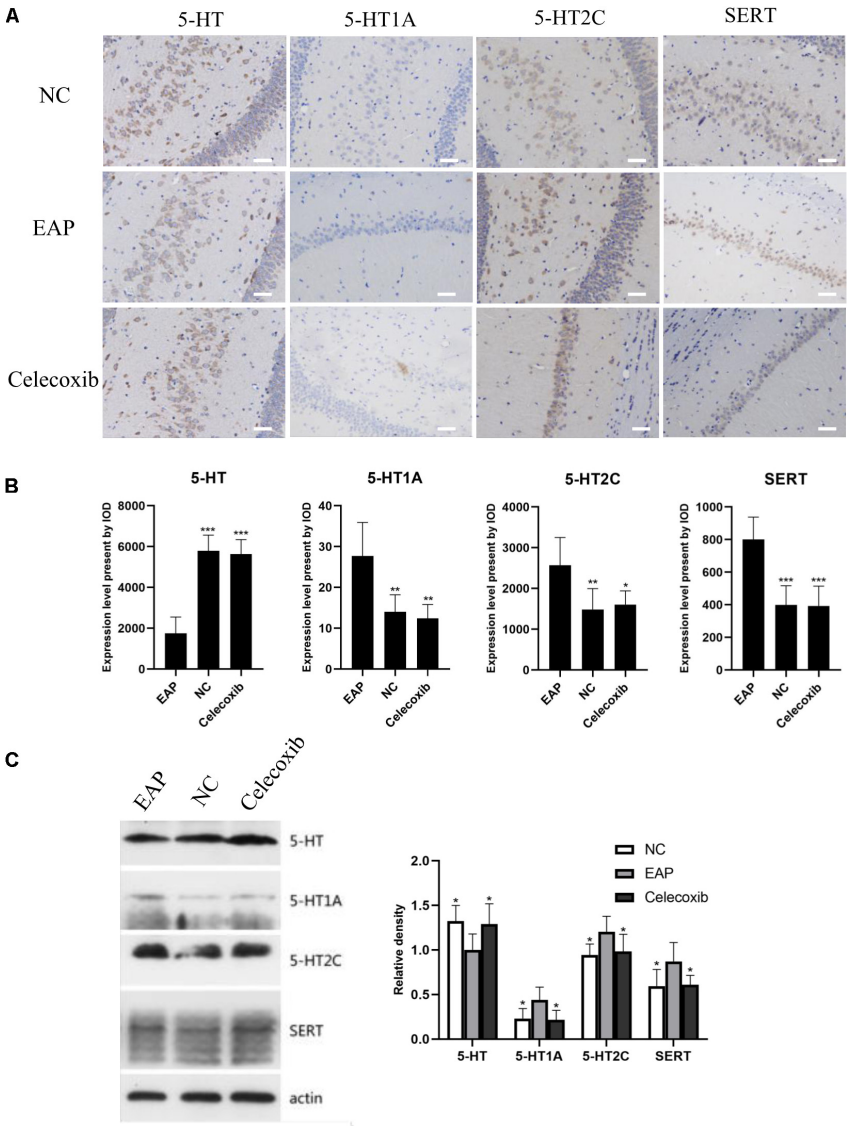

FIGURE 4 | Expression levels of 5-HT, 5-HT_{1A}, 5-HT_{2C} receptor, and SERT in rat hippocampus. In the EAP group (EAP), 5-HT was significantly decreased compared with the normal control group (NC) and celecoxib group (celecoxib), while 5-HT_{1A}, 5-HT_{2C}, and SERT were significantly increased **(B)**. Result were verified by IHC **(A)** and western blot **(C)**. $^{*}P < 0.05$, $^{**}P < 0.01$, $^{***}P < 0.001$ compared with EAP group. Scale bar = 25 μm.

similar levels as observed in normal control group rats. In L5–S2 segments of the spinal cord, 5-HT expression decreased, while 5-HT_{1A}, 5-HT_{2C}, and SERT expression levels increased in the EAP group, compared with the normal control group (**Figure 6**). In the celecoxib group, HT_{1A} and SERT expression levels were reduced compared with the EAP group (**Figures 6B,C**). However, no significant differences in 5-HT and 5-HT_{2C} expression levels were observed between the celecoxib group and the EAP group. Furthermore, no significant differences were observed between the celecoxib group and normal control group rats. Similar results were obtained from IHC and western blot. The expression levels of serotonin regulators in the central nervous system of EAP rat are compared with those of normal control group rats in **Table 2**.

DISCUSSION

Chronic prostatitis/chronic pelvic pain syndrome is a multifactorial disease. Therefore, it is difficult to recapitulate all the characteristics of CP/CPPS in a single animal model. Animal models of CP/CPPS commonly used include the EAP model (14), spontaneous prostatitis model (24), hormone and castration induced model (25), urine reflux model (26), and the chemically induced model (27). In each of these models, a specific trigger causes inflammation in the prostate via a non-bacterial route. This commonality confirms the central role of inflammation during the process of CP/CPPS initiation and development. Evidence supporting the association of CP/CPPS with autoimmunity is increasing, and includes the detection of

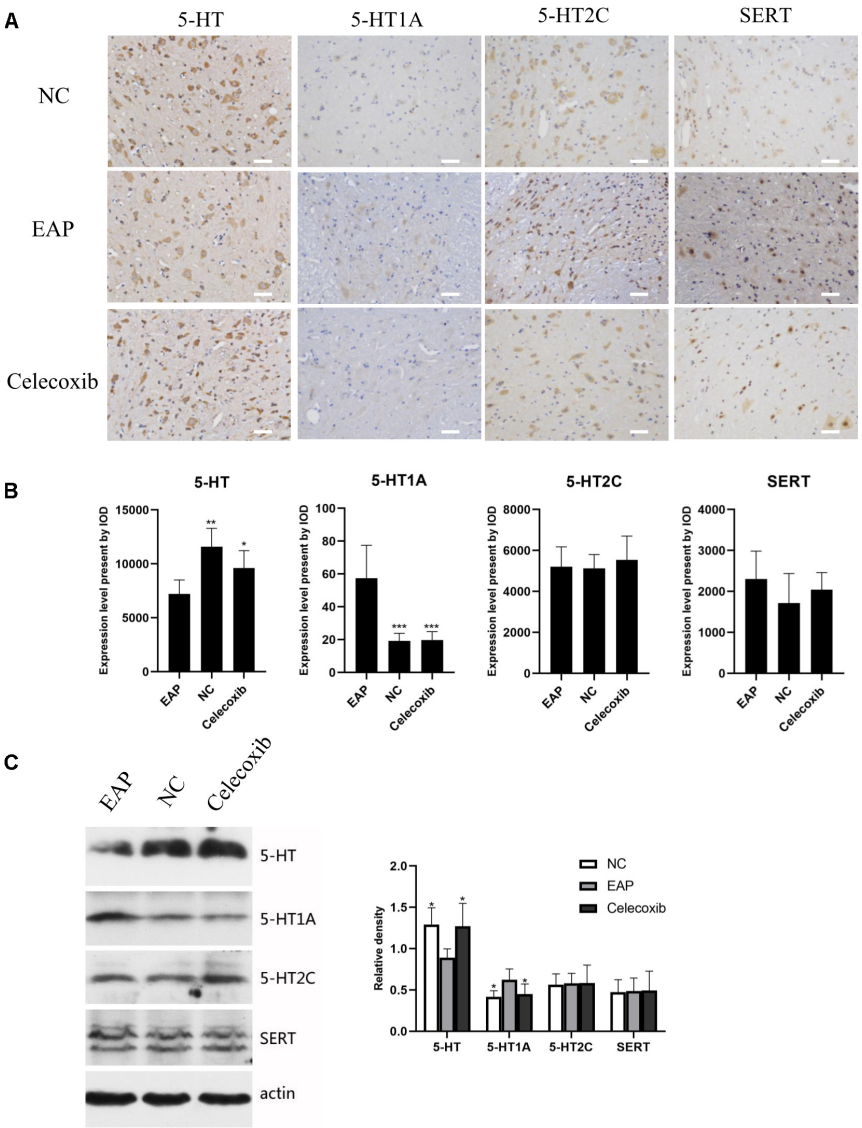

FIGURE 5 | Expression levels of 5-HT, 5-HT_{1A}, 5-HT_{2C} receptor, and SERT in rat T13–L1 segments of spinal cord. 5-HT levels were decreased and 5-HT_{1A} receptor levels were increased in the EAP group (EAP) compared with the normal control group (NC) and celecoxib group (celecoxib) **(B)**. Results were verified by IHC **(A)** and western blot **(C)**. $^{*}P < 0.05$, $^{**}P < 0.01$, $^{***}P < 0.001$ compared with EAP group. Scale bar = 25 μm.

prostate antigen specific T lymphocytes in CP/CPPS patients (28). No obvious signs of infection were found in most of the CP/CPPS patients with increased semen leukocytes (29).

It may be concluded that EAP provides an ideal animal model of CP/CPPS. The EAP model is characterized by prostate specific inflammation, good stability, and long-term maintenance (30). Nonetheless, the success rate of EAP model establishment varies according to method and rodent animal used. In the present study, we constructed EAP model rats with a success rate of 75% (12/16). Although the success rate in establishing EAP mouse models can reach 100%, by using the rat model, intromission and ejaculation can be clearly observed. Additionally, the average ejaculation latencies of rat and human are more similar (about 5 min), although there are, of course, large individual differences both in human and rats (21). The characteristic inflammatory changes in the prostate demonstrated in our model provide a basis for the study of behavioral changes, sexual behavioral changes, and erectile function in our animal model of CP/CPPS, and for investigating the anti-inflammatory therapy efficacy of celecoxib.

The high risk of depression associated with CP/CPPS was confirmed in a clinical study and in EAP mice (6, 31). The depressive state of animals is mainly manifested by a decrease in overall activity, reduced social communication activities, reduced exploratory activities, and defects in aggression and pleasure sensation (23, 32). In our present study, the depressive behavior pattern observed in EAP rat was relieved by celecoxib treatment.

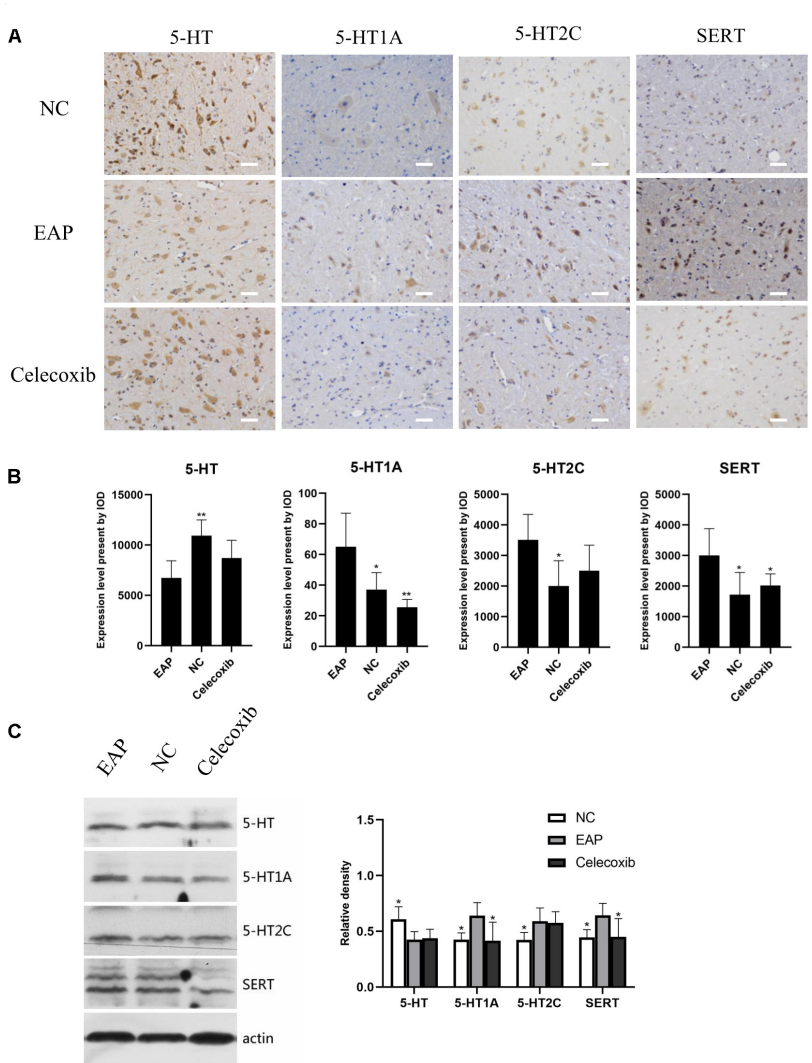

FIGURE 6 | Expression levels of 5-HT, 5-HT_{1A}, 5-HT_{2C} receptor, and SERT in rat L5–S2 segments of spinal cord. 5-HT levels were significantly decreased compared with normal control group (NC), while 5-HT_{1A}, 5-HT_{2C}, and SERT levels were significantly increased **(B)**. Result were verified by IHC **(A)** and western blot **(C)**. $^{*}P < 0.05$, $^{**}P < 0.01$, $^{***}P < 0.001$ compared with EAP group. Scale bar = 25 μm.

TABLE 2 | Serotonin regulators changes in EAP group compared to normal control group.

Regulators	Hippocampus	T13-L1	L5-S2
5-HT	L	L	L
5-HT1A	H	H	H
5-HT2C	H	N	N
SERT	H	N	H

L, lower than normal control group; H, higher than normal control group; N, No statistical significance.

Sexual dysfunction is common in CP/CPPS patients. However, sexual dysfunction in the EAP rat model has not been previously confirmed. In the current study, we report impaired sexual function in EAP rats, confirming that this is an ideal model to study CP/CPPS related sexual dysfunction. In mating experiments, reduced MF, IF, and EF, and elongated ML, all reflect a decline in sexual drive. Moreover, a shortened EL implied a reduced ejaculation threshold (or a condition with premature ejaculation), while elongated IL and shortened PEI indicated increased threshold of erection (33). Following anti-inflammatory treatment in the celecoxib group, all these parameters of sexual behavior were rescued to normal levels. This result provides further evidence that autoimmune inflammation is a critical factor in the pathological mechanisms underlying CP/CPPS. To our surprise, the ICP/MAP under electrical stimulation of CN showed no significant change, which may indicate that no apparent organic lesion was caused in EAP rats. However, under an electrical stimulation condition, we were not able to assess the erectile function of rats in the natural state. And it should be noted that male rats as well as many other mammals have a baculum

in the penis (34) which limit a rigorous assessment of erectile function.

Anti-inflammatory therapy using steroidal or non-steroidal anti-inflammatory drugs has been validated for the treatment of CP/CPPS. A meta-analysis has provided evidence that patients receiving anti-inflammatory treatment alone were 80% more likely to have favorable responses than patients receiving placebo. Moreover, α-blockers combined with anti-inflammatory treatment were associated with significantly better pain scores than placebo (18). In clinical practice, celecoxib has already been employed in the treatment of CP/CPPS, although the therapeutic effect faded 2 weeks after the end of treatment (17). The underlying mechanisms associated with prostate inflammation and anti-inflammation activity remain unclear. Several studies have shown that the proinflammatory factors TNF-α and IL-1β were increased in prostatic fluid, seminal plasma, or serum of CP/CPPS patients (35–37). Here, we detected significantly higher serum IL-1β and TNF-α levels in EAP rats compared with normal rats. In a comparison between the celecoxib and EAP groups, while IL-1β levels were significantly decreased in the celecoxib group, an observed decrease in TNF-α levels was not significant. These results demonstrate the anti-inflammatory efficacy of celecoxib and indicate that proinflammatory factors such as IL-1β are involved in CP/CPPS.

The serotonin system plays an important role in the occurrence of depression and male sexual dysfunction. However, studies researching the role of the serotonin system in sexual dysfunction are very limited. It has previously been suggested that low brain 5-HT levels (and 5-HT_{1A} receptor and 5-HT_{2C} receptor levels) were related to the pathogenesis of depression, though the conclusions are controversial (38). Increased serotonin levels in the central nervous system elevate the ejaculatory threshold (21, 22). However, 5-HT_{1A} receptors and 5-HT_{2C} receptors may play opposing biological roles in ejaculation. While 5-HT_{1A} receptors reduced ejaculation threshold, shortened ejaculation latency, and accelerated ejaculation, 5-HT_{2C} receptors delayed ejaculation (21). In addition, SERTs on the presynaptic membrane function by reabsorbing 5-HT, reducing the concentration of 5-HT in the synaptic gap, so as to increase ejaculation threshold and delay ejaculation (39). Based on these findings, we investigated the possible association between proinflammatory factors and the 5-HT system. Interestingly, the expression pattern of 5-HT system regulators was significantly altered in EAP rats. 5-HT expression levels were decreased and 5-HT_{1A} receptors expression levels were increased in the hippocampus and spinal cord (T13–L1 and L5–S2), and this may contribute to the depression-like behavior and PE. It is interesting to note that 5-HT_{1A} receptors are mainly distributed in the dorsal horn of the spinal cord and their expression can be upregulated by pain (40). Thus, pelvic pain in the EAP rat may attribute to the increased 5-HT_{1A} receptor expression in T13–L1 and L5–S2 segments, which are the segments of spinal cord controlling prostate sensation. Additionally, current evidence shows that depressive symptoms can be improved by administration of celecoxib in rats (19) as well as in humans (20), suggesting that celecoxib might relieve sexual dysfunction by psychological improvement exclusively, or combined with relief in prostate symptoms.

According to present understanding, proinflammatory cytokines can reduce 5-HT expression levels in the central nervous system in various ways (41): (i) an increase in proinflammatory cytokine levels leads to hyperactivity of the hypothalamic–pituitary–adrenal (HPA) axis, which stimulates the secretion of corticotropin releasing hormone (CRH) by paraventricular nuclei (PVN). CRH can reduce 5-HT release by acting on CRH receptors distributed in the limbic system (hippocampus, amygdala) and other parts of the brain; (ii) activation of indoleamine 2,3-dioxygenase (IDO) can be induced by NF-κB and p38 MAPK pathways. IDO can enhance the metabolism of tryptophan, a 5-HT precursor, and thus reduce the synthesis of 5-HT; (iii) the expression and activity of SERT can be up-regulated through the p38 MAPK pathway, which is activated by TNF-α and IL-1β. Uptake of 5-HT is promoted by SERT, and the level of 5-HT is lowered (42). Our findings support our preliminary hypotheses that inflammation can cause depression and sexual dysfunction via the serotonin system, and that this can be relieved by celecoxib via suppression of inflammatory factors. However, we acknowledge the limitations that the local levels of IL-1β and TNF-α in prostate were not assessed, and that other inflammatory factors related to CP/CPPS were not included in the present study. Moreover, the possible roles of the signal pathways mentioned above have not been elucidated. Therefore, more detailed studies are needed to understand the molecular mechanisms pertaining to inflammation and the 5-HT system.

In summary, our study provides a new insight into the mechanism of CP/CPPS in EAP rats. We demonstrate that autoimmune prostatitis can cause sexual function and depression in this rat model. And a serotonin system disorder in the central nervous system was likely mediated via inflammation in EAP rats. Moreover, we show that anti-inflammatory therapy with celecoxib was effective in relieving CP/CPPS characteristics in EAP rats.

DATA AVAILABILITY STATEMENT

The raw data supporting the conclusions of this article will be made available by the authors, without undue reservation.

ETHICS STATEMENT

The animal study was reviewed and approved by the Ethics Committee of The First Affiliated Hospital of Sun Yat-sen University (Guangzhou, China).

AUTHOR CONTRIBUTIONS

All authors contributed to the intellectual content of the manuscript and approved the manuscript version submitted for publication. YaZ, XL, and KZ have contributed equally to this work. YaZ, KZ, and MZ performed the experiments. YaZ, XL, KX, and YX analyzed the data and prepared the figures.

XL, KZ, YiZ, and YX interpreted the experimental results. YaZ and XL drafted the manuscript. CD and CC were responsible for the conception and design of the research and approved the final version of the manuscript. XS and CD edited and revised the manuscript.

FUNDING

This work was supported by the National Natural Science Foundation of China (Grant No. 81671449). KZ was supported by Guangzhou Regenerative Medicine and Health Guangdong Laboratory Grant (Grant No. 2018GZR110105006) and the National Natural Science Foundation of China (Grant No. 31900735).

ACKNOWLEDGMENTS

The authors would like to thank Dr. Tao Zheng and Prof. Xuenong Zou for excellent technical support and critically reviewing the manuscript.

REFERENCES

1. Magistro G, Wagenlehner FM, Grabe M, Weidner W, Stief CG, Nickel JC. Contemporary management of chronic prostatitis/chronic pelvic pain syndrome. *Eur Urol.* (2016) 69:286–97. doi: 10.1016/j.eururo.2015.08.061
2. Mehik A, Hellström P, Sarpola A, Lukkarinen O, Järvelin MR. Fears, sexual disturbances and personality features in men with prostatitis: a population-based cross-sectional study in Finland. *BJU Int.* (2001) 88:35–8. doi: 10.1046/j.1464-410x.2001.02259.x
3. Ku JH, Kim SW, Paick JS. Quality of life and psychological factors in chronic prostatitis/chronic pelvic pain syndrome. *Urology.* (2005) 66:693–701. doi: 10.1016/j.urology.2005.04.050
4. Zhang Y, Zheng T, Tu X, Chen X, Wang Z, Chen S, et al. Erectile dysfunction in chronic prostatitis/chronic pelvic pain syndrome: outcomes from a multi-center study and risk factor analysis in a single center. *PLoS One.* (2016) 11:e0153054. doi: 10.1371/journal.pone.0153054
5. Liang CZ, Hao ZY, Li HJ, Wang ZP, Xing JP, Hu WL, et al. Prevalence of premature ejaculation and its correlation with chronic prostatitis in Chinese men. *Urology.* (2010) 76:962–6. doi: 10.1016/j.urology.2010.01.061
6. Riegel B, Bruenahl CA, Ahyai S, Bingel U, Fisch M, Löwe B. Assessing psychological factors, social aspects and psychiatric co-morbidity associated with chronic prostatitis/chronic pelvic pain syndrome (CP/CPPS) in men–a systematic review. *J Psychosom Res.* (2014) 77:333–50. doi: 10.1016/j.jpsychores.2014.09.012
7. Nickel JC. Understanding chronic prostatitis/chronic pelvic pain syndrome (CP/CPPS). *World J Urol.* (2013) 31:709–10. doi: 10.1007/s00345-013-1121-4
8. Breser ML, Salazar FC, Rivero VE, Motrich RD. Immunological mechanisms underlying chronic pelvic pain and prostate inflammation in chronic pelvic pain syndrome. *Front Immunol.* (2017) 8:898. doi: 10.3389/fimmu.2017.00898
9. Depiante-Depaoli M, Pacheco-Rupil B. Experimental autoimmunity to rat male accessory glands (MAG). *Am J Reprod Immunol Microbiol.* (1985) 7:32–8. doi: 10.1111/j.1600-0897.1985.tb00260.x
10. Keetch DW, Humphrey P, Ratliff TL. Development of a mouse model for nonbacterial prostatitis. *J Urol.* (1994) 152:247–50. doi: 10.1016/s0022-5347(17)32871-9
11. Donadio AC, Depiante-Depaoli M. Inflammatory cells and MHC class II antigens expression in prostate during time-course experimental autoimmune prostatitis development. *Clin Immunol Immunopathol.* (1997) 85:158–65. doi: 10.1006/clin.1997.4427
12. Rivero V, Carnaud C, Riera CM. Prostatein or steroid binding protein (PSBP) induces experimental autoimmune prostatitis (EAP) in NOD mice. *Clin Immunol.* (2002) 105:176–84. doi: 10.1006/clim.2002.5281
13. Ihsan AU, Khan FU, Nawaz W, Khan MZ, Yang M, Zhou X. Establishment of a rat model of chronic Prostatitis/Chronic Pelvic Pain Syndrome (CP/CPPS) induced by immunization with a novel peptide T2. *Biomed Pharmacother.* (2017) 91:687–92. doi: 10.1016/j.biopha.2017.05.004
14. Motrich RD, Maccioni M, Riera CM, Rivero VE. Autoimmune prostatitis: state of the art. *Scand J Immunol.* (2007) 66:217–27. doi: 10.1111/j.1365-3083.2007.01971.x
15. Rudick CN, Schaeffer AJ, Thumbikat P. Experimental autoimmune prostatitis induces chronic pelvic pain. *Am J Physiol Regul Integr Comp Physiol.* (2008) 294:R1268–75. doi: 10.1152/ajpregu.00836.2007
16. Hoxha M, Buccellati C, Capra V, Garella D, Cena C, Rolando B, et al. In vitro pharmacological evaluation of multitarget agents for thromboxane prostanoid receptor antagonism and COX-2 inhibition. *Pharmacol Res.* (2016) 103:132–43. doi: 10.1016/j.phrs.2015.11.012
17. Zhao WP, Zhang ZG, Li XD, Yu D, Rui XF, Li GH, et al. Celecoxib reduces symptoms in men with difficult chronic pelvic pain syndrome (Category IIIA). *Braz J Med Biol Res.* (2009) 42:963–7. doi: 10.1590/s0100-879x2009005000021
18. Anothaisintawee T, Attia J, Nickel JC, Thammakraisorn S, Numthavaj P, McEvoy M, et al. Management of chronic prostatitis/chronic pelvic pain syndrome: a systematic review and network meta-analysis. *JAMA.* (2011) 305:78–86. doi: 10.1001/jama.2010.1913
19. Mesripour A, Shahnooshi S, Hajhashemi V. Celecoxib, ibuprofen, and indomethacin alleviate depression-like behavior induced by interferon-alfa in mice. *J Complement Integr Med.* (2019) 17:16. doi: 10.1515/jcim-2019-0016
20. Lehrer S, Rheinstein PH. Nonsteroidal anti-inflammatory drugs (NSAIDs) reduce suicidal ideation and depression. *Discov Med.* (2019) 28:205–12.
21. de Jong TR, Veening JG, Waldinger MD, Cools AR, Olivier B. Serotonin and the neurobiology of the ejaculatory threshold. *Neurosci Biobehav Rev.* (2006) 30:893–907. doi: 10.1016/j.neubiorev.2006.01.001
22. Mirone V, Arcaniolo D, Rivas D, Bull S, Aquilina JW, Verze P, et al. Results from a prospective observational study of men with premature ejaculation treated with dapoxetine or alternative care: the PAUSE study. *Eur Urol.* (2014) 65:733–9. doi: 10.1016/j.eururo.2013.08.018
23. Lewitus GM, Wilf-Yarkoni A, Ziv Y, Shabat-Simon M, Gersner R, Zangen A, et al. Vaccination as a novel approach for treating depressive behavior. *Biol Psychiatry.* (2009) 65:283–8. doi: 10.1016/j.biopsych.2008.07.014
24. Keith IM, Jin J, Neal D Jr., Teunissen BD, Moon TD. Cell relationship in a Wistar rat model of spontaneous prostatitis. *J Urol.* (2001) 166:323–8.
25. Wilson MJ, Woodson M, Wiehr C, Reddy A, Sinha AA. Matrix metalloproteinases in the pathogenesis of estradiol-induced nonbacterial prostatitis in the lateral prostate lobe of the Wistar rat. *Exp Mol Pathol.* (2004) 77:7–17. doi: 10.1016/j.yexmp.2004.02.004
26. Melman A, Tar M, Boczko J, Christ G, Leung AC, Zhao W, et al. Evaluation of two techniques of partial urethral obstruction in the male rat model of bladder outlet obstruction. *Urology.* (2005) 66:1127–33. doi: 10.1016/j.urology.2005.06.070
27. Chen CS, Chang PJ, Lin WY, Huang YC, Ho DR. Evidences of the inflammasome pathway in chronic prostatitis and chronic pelvic pain syndrome in an animal model. *Prostate.* (2013) 73:391–7. doi: 10.1002/pros.22580
28. Kouiavskaia DV, Southwood S, Berard CA, Klyushnenkova EN, Alexander RB. T-cell recognition of prostatic peptides in men with chronic prostatitis/chronic pelvic pain syndrome. *J Urol.* (2009) 182:2483–9. doi: 10.1016/j.juro.2009.07.067
29. Motrich RD, Cuffini C, Oberti JP, Maccioni M, Rivero VE. Chlamydia trachomatis occurrence and its impact on sperm quality in chronic prostatitis patients. *J Infect.* (2006) 53:175–83. doi: 10.1016/j.jinf.2005.11.007
30. Wang W, Naveed M, Baig M, Abbas M, Xiaohui Z. Experimental rodent models of chronic prostatitis and evaluation criteria. *Biomed Pharmacother.* (2018) 108:1894–901. doi: 10.1016/j.biopha.2018.10.010
31. Du HX, Chen XG, Zhang L, Liu Y, Zhan CS, Chen J, et al. Microglial activation and neurobiological alterations in experimental autoimmune

prostatitis-induced depressive-like behavior in mice. *Neuropsychiatr Dis Treat.* (2019) 15:2231–45. doi: 10.2147/NDT.S211288
32. Katz RJ, Roth KA, Carroll BJ. Acute and chronic stress effects on open field activity in the rat: implications for a model of depression. *Neurosci Biobehav Rev.* (1981) 5:247–51. doi: 10.1016/0149-7634(81)90005-1
33. Olivier B, Chan JS, Pattij T, de Jong TR, Oosting RS, Veening JG, et al. Psychopharmacology of male rat sexual behavior: modeling human sexual dysfunctions. *Int J Impot Res.* (2006) 18:S14–23. doi: 10.1038/sj.ijir.3901330
34. Cellerino A, Jannini EA. Male reproductive physiology as a sexually selected handicap? Erectile dysfunction is correlated with general health and health prognosis and may have evolved as a marker of poor phenotypic quality. *Med Hypotheses.* (2005) 65:179–84. doi: 10.1016/j.mehy.2004.10.020
35. Nadler RB, Koch AE, Calhoun EA, Campbell PL, Pruden DL, Bennett CL, et al. IL-1beta and TNF-alpha in prostatic secretions are indicators in the evaluation of men with chronic prostatitis. *J Urol.* (2000) 164:214–8.
36. Alexander RB, Ponniah S, Hasday J, Hebel JR. Elevated levels of proinflammatory cytokines in the semen of patients with chronic prostatitis/chronic pelvic pain syndrome. *Urology.* (1998) 52:744–9. doi: 10.1016/s0090-4295(98)00390-2
37. Lundh D, Hedelin H, Jonsson K, Gifford M, Larsson D. Assessing chronic pelvic pain syndrome patients: blood plasma factors and cortisol saliva. *Scand J Urol.* (2013) 47:521–8. doi: 10.3109/21681805.2013.769460
38. Benedetti F, Radaelli D, Poletti S, Locatelli C, Dallaspezia S, Lorenzi C, et al. Association of the C(-1019)G 5-HT1A promoter polymorphism with exposure to stressors preceding hospitalization for bipolar depression. *J Affect Disord.* (2011) 132:297–300. doi: 10.1016/j.jad.2011.02.024
39. Patel K, Hellstrom WJ. Central regulation of ejaculation and the therapeutic role of serotonergic agents in premature ejaculation. *Curr Opin Investig Drugs.* (2009) 10:681–90.
40. Zhang YQ, Gao X, Ji GC, Huang YL, Wu GC, Zhao ZQ. Expression of 5-HT1A receptor mRNA in rat lumbar spinal dorsal horn neurons after peripheral inflammation. *Pain.* (2002) 98:287–95. doi: 10.1016/s0304-3959(02)00026-x
41. Anisman H, Merali Z, Hayley S. Neurotransmitter, peptide and cytokine processes in relation to depressive disorder: comorbidity between depression and neurodegenerative disorders. *Prog Neurobiol.* (2008) 85:1–74. doi: 10.1016/j.pneurobio.2008.01.004
42. Zhu CB, Blakely RD, Hewlett WA. The proinflammatory cytokines interleukin-1beta and tumor necrosis factor-alpha activate serotonin transporters. *Neuropsychopharmacology.* (2006) 31:2121–31. doi: 10.1038/sj.npp.130102

Conflict of Interest: The authors declare that the research was conducted in the absence of any commercial or financial relationships that could be construed as a potential conflict of interest.

frontiers in Immunology

ORIGINAL RESEARCH
published: 25 September 2020
doi: 10.3389/fimmu.2020.583274

The Involvement of the Chemokine RANTES in Regulating Luminal Acidification in Rat Epididymis

Xiao Feng[1†], Bin-Fang Ma[1†], Bo Liu[1†], Peng Ding[1], Jin-Hua Wei[1], Pang Cheng[1], Sheng-Yu Li[1], Dong-Xu Chen[1], Zhi-Jian Sun[2] and Zhen Li[1]*

[1] Department of Human Anatomy, Histology and Embryology, Fourth Military Medical University, Xi'an, China, [2] The General Hospital of Northern Theater Command, Shenyang, China

Background: A complex interplay between different cell types in the epithelium leads to activation of the luminal acidifying capacity of the epididymis, a process that is crucial for sperm maturation and storage. Basal cells sense the luminal angiotensin II (ANG II) and stimulate proton secretion in clear cells through nitric oxide (NO). Our previous study has shown the chemokine regulated upon activation normal T-cell expressed and secreted (RANTES) was expressed in the F4/80 positive macrophages of human epididymis. The objective of this study was to explore the involvement of RANTES in regulating the luminal acidification in the rat epididymis.

Methods: The role of RANTES was investigated by *in vivo* perfusion with recombinant RANTES, Met-RANTES, and PBS of different pH values. Furthermore, rats vasectomy was performed to alter the epididymal luminal pH. RIA was used to measure the tissue homogenate ANG II concentration. Real time-PCR and western blot were employed to examine the expression levels of AGTR2, RANTES, CCR1, CCR5, and iNOS in epididymis.

Results: RANTES was restricted to the basal macrophages of epididymal ducts and co-localized with its receptors CCR1 and CCR5. Both V-ATPase and iNOS were up-regulated in the cauda epididymis after perfused with recombinant RANTES, while the antagonist Met-RANTES perfusion led to a complete abrogation of the increased expression of V-ATPase in the apical membrane of clear cells and iNOS in macrophages. Upon alkaline perfusion, RANTES expression was significantly increased and the apical accumulation of V-ATPase in the clear cells was induced in the cauda epididymis. The luminal pH in the cauda epididymis increased after vasectomy. The concentration of the ANG II and the expression levels of AGTR2, RANTES, CCR1, CCR5, and iNOS dropped in the cauda epididymis following vasectomy.

Conclusion: Upon the activation of basal cells, RANTES might induce the NO release from macrophages by interacting with its receptors, which increases proton secretion by adjacent clear cells. Thus, RANTES is possible to participate in the crosstalk among basal cells, macrophages and clear cells for the fine control of an optimum acidic luminal environment that is critical for male fertility.

Keywords: RANTES, epididymis, epididymal epithelium, luminal acidification, macrophages, iNOS

OPEN ACCESS

Edited by:
Yong-Gang Duan,
University of Hong Kong, China

Reviewed by:
Yao Bing,
Nanjing Medical University, China
Guo-Zhang Zhu,
Marshall University, United States

***Correspondence:**
Zhen Li
lizhenhe@fmmu.edu.cn

† These authors have contributed equally to this work

Specialty section:
This article was submitted to Mucosal Immunity, a section of the journal Frontiers in Immunology

Received: *14 July 2020*
Accepted: *07 September 2020*
Published: *25 September 2020*

Citation:
Feng X, Ma B-F, Liu B, Ding P, Wei J-H, Cheng P, Li S-Y, Chen D-X, Sun Z-J and Li Z (2020) The Involvement of the Chemokine RANTES in Regulating Luminal Acidification in Rat Epididymis. Front. Immunol. 11:583274. doi: 10.3389/fimmu.2020.583274

INTRODUCTION

The epididymis establishes a low luminal pH of 6.5–6.8 to maintain spermatozoa in a quiescent state during their maturation and storage in this organ (1). Acidification of the epididymal luminal fluid is critical for post-testicular maturation and acquirement of appropriate motility (2, 3), which is controlled by the intricate interaction of different types of cells in the highly specialized epididymal pseudostratified epithelium (4–6). Among the epithelial cells, angiotensin I (ANG I) is secreted by principal cells to the epididymal lumen (7), and is catalyzed by angiotensin-converting enzymes (ACE) to produce angiotensin II (ANG II) (8, 9). Then, ANG II binds with the receptor AGTR2, which is solely expressed on the surface of basal cells, stimulating the clear cells to increase the proton secretion via the activation of nitric oxide (NO)/cGMP pathway (4, 10). However, the intrinsic mechanism as to how AGTR2 activation regulates the NO production, still remains undiscovered.

Macrophages, as classical innate immune cells, play important roles in maintaining homeostasis such as phagocytizing foreign substances and secreting cytokines in the process of immunoreactivities (11, 12). In addition to their classical function in immune system, the non-classical function of macrophage in peripheral, non-lymphoid organs has been widely investigated (13). For example, in the small intestinal mucosal system (14, 15), macrophages can stretch out their long protuberances to the intestinal lumen to monitor the luminal composition changes so as to regulate the absorption of nutrients and secretion of goblet cells by interacting with intestinal epithelial cells (16, 17). Similar to the intestinal tract, macrophages in the initial segment of epididymis also extend long slender projections to the epididymal lumen to sample the fluid components in the lumen (18, 19). Besides, there still exists another type of macrophages whose morphology is distinct from those with long projections, presenting basal round-like distribution in the distal segments of the epididymis (4). The function of this subtype of macrophages still remain unknown.

The chemokine regulated upon activation normal T-cell expressed and secreted (RANTES) was initially recognized as a kind of chemo-attractant for immune cells (20–23). The receptors of RANTES include high affinity receptors CCR1 and CCR5, and low affinity receptor CCR3, all of which belong to seven transmembrane G protein coupled receptor family (22, 24). With the researches deepening, RANTES have been found to possess some new biological characteristics (25), such as facilitating breast tumor progression and metastasis (26, 27), and triggering drug-resistance in breast, ovarian, and prostate cancers (28–30). Our previous work has demonstrated that RANTES was mainly expressed in F4/80 positive macrophages in the basal region of human epididymal epithelium (31). RANTES has also been proved to promote the activity of macrophages by increasing their production of NO (32). Furthermore, it has been reported that the expression of RANTES can be promoted by ANG II in aorta (33) and glomerular endothelial cells (34).

Based on the aforementioned evidence, we hypothesized that RANTES expressed in the epididymal basal macrophages might be involved in the crosstalk between basal cells and clear cells when regulating the luminal acidification. To address this hypothesis, we examined the expression of RANTES and its receptors in rat epididymis and further investigated whether RANTES function in the acidification of the luminal fluid by *in vivo* perfusion and vasectomy model.

MATERIALS AND METHODS

Animals

Adult male Sprague Dawley (SD) rats were purchased from the Laboratory Animal Center of the Fourth Military Medical University. The animals were housed in individual cages and fed with food and water *ad libitum*. They were kept in a controlled environment on a 12 h/12 h light/dark cycle. The adult rats (12-week-old) were procured. Experimental procedures were approved by the local ethical committee.

Vasectomy

Adult male rats were distributed randomly into two groups: 8 weeks sham vasectomy (n = 7) and 8 weeks bilateral vasectomy (n = 7). Surgical procedures of animals vasectomy was accomplished as reported previously (35). The operative process was completed to minimize postoperative adhesion and inflammation. The surgery was performed under sodium pentobarbital anesthesia [60 mg/kg body weight, intraperitoneally (i.p.)].

In vivo Perfusion of the Distal Cauda Epididymis

Adult male Sprague-Dawley rats were anesthetized with sodium pentobarbital as described above. The vas deferens was cannulated through the lumen with a micro cannula (0.31 mm OD, 0.16 mm ID; Anilab Software & Instruments Co., PE-0402) connected to a 1-ml syringe. A small incision was made in the distal cauda epididymal region to allow the perfusate to exit the tubule. Perfusion was performed retrogradely at a rate of 20 μl/min using a syringe pump (78-0120S, Stoelting). The lumen was initially washed free of sperm with PBS (0.01M, pH 6.8) for usually 10 min. Then, vas deferens and cauda epididymis were perfused with recombinant RANTES (PeproTech, United States), Met-RANTES (R&D Systems, United States), and PBS of different pH values, respectively. The perfusion was performed retrogradely at a rate of 5 μl/min, and the luminal solution was sustained for 1 h. At the end of the experimental period, the cauda epididymis was harvested and extracted for the RNA and the protein. Or tissues were then washed in PBS, pH 7.4, and perfused with a solution containing 4% paraformaldehyde for 15 min for frozen sections.

Semi-Quantitative RT-PCR and Real-Time Quantitative RT-PCR

Total RNA was extracted from the caput, corpus, and cauda regions of the rat epididymis, using TRIzol Reagent (Takara, Shiga, Japan) according to the supplier instructions, and semi-quantitative RT-PCR for RANTES, CCR1, CCR3 and CCR5 were

performed as described previously (36). Real-time quantitative PCR analysis of V-ATPase, RANTES, CCR1 and CCR5, iNOS, AGTR2 expression in the different epididymal regions were performed with the MiniOpticon system (Bio-Rad, Hercules, CA, United States). Each reaction was performed in triplicate by using 10 ng of cDNA from each sample and SYBR Primix Ex Taq (TaKaRa, Shiga, Japan). The relative abundance of target transcript was quantified using the comparative Ct method. The β -actin or GAPDH from the same exacts were used as internal control. Data obtained from three independent experiments was calculated. Primers for PCR and qPCR were designed according to the rat sequences found in GenBank (**Supplementary Tables 1, 2**).

Western Blotting

The protocol for protein extracts from rat epididymis was designed, based on previously described procedures (36). Sample aliquots containing equal amounts of protein were separated via SDS-PAGE and transferred onto polyvinylidene difluoride membranes. The membranes were blocked in 5% non-fat milk for 1 h at room temperature, and incubated overnight at 4°C with rabbit anti-RANTES (Abcam, Cambridge, United Kingdom), rabbit anti-V-ATPase (GeneTex, Irvine, CA, United States), rabbit anti-iNOS (Abcam, Cambridge, United Kingdom), rabbit anti-AGTR2 (GeneTex, Irvine, CA, United States), rabbit anti-CCR1 (Abcam, Cambridge, United Kingdom), rabbit anti-CCR5 (GeneTex, Irvine, CA, United States), mouse anti-β-actin (Invitrogen, United States) and mouse anti-GAPDH (Invitrogen, United States). The membranes were then washed with TBST buffer and incubated with an appropriate secondary antibody (HRP-conjugated anti-rabbit IgG or HRP-conjugated anti-mouse IgG, Sigma, St. Louis, MO, United States) for 2 h at room temperature. After extensive washing, the densities of labeled protein bands on the blots were detected using an enhanced chemiluminescence reagent (Thermo, Rockford, IL, United States) and captured using a ChemiDoc MP System (Bio-Rad, Hercules, CA, United States).

Immunohistochemistry

The avidin-biotin technique was applied as previously described (31). After H_2O_2 treatment, paraffin-embedded sections were blocked for 30 min with 10% donkey serum at room temperature and incubated with the related anti-RANTES primary antibodies (5 mg/mL) overnight at 4°C, then followed by the 1:300-diluted biotinylated secondary antibody. The negative controls were performed in the absence of primary antibody. The same method was used in the experiment to detect the localization of CCR1 and CCR5 in rat epididymis, where the goat anti-CCR1 antibody and goat anti-CCR5 antibody (Santa Cruz Biotechnology) were used, with secondary antibodies, biotinylated anti-goat IgG (Sigma, St. Louis, MO, United States), applied for immunohistochemical staining.

Tissue Fixation and Immunofluorescence

Fixed tissues were dehydrated in 30% sucrose for 2 h at room temperature, embedded in Tissue-Tek OCT compound, and mounted and frozen on a cutting block. Tissues were cut in a Reichert Frigocut microtome at 10 μm thickness and sections were placed onto Superfrost Plus microscope slides. Sections were rehydrated in PBS for 10 min and pretreated with 1% (w/v) SDS. After three washes in PBS, slides were preincubated in 1% (w/v) BSA in PBS with 0.02% Na-azide for 30 min to block non-specific staining, after which they were incubated with different primary antibodies for 2 h at room temperature. The antibody included mouse anti-V-ATPase (Santa Cruz Biotechnology, Dallas, TX, United States) and rabbit anti-iNOS (Abcam, Cambridge, United Kingdom). Subsequently, the sections were incubated with an appropriate secondary antibody (FITC-conjugated goat anti-mouse, or Cy3-conjugated goat anti-rabbit, Beyotime, Shanghai, China) for 2 h at room temperature in the dark. Double Immunofluorescence Labeling with rabbit anti- RANTES antibody and rat anti-F4/80 antibody (Abcam, Cambridge, United Kingdom), the rabbit anti-RANTES antibody and goat anti-CCR1/CCR5 antibody, the goat anti-iNOS antibody and rat anti- F4/80 antibody, followed by the mixed secondary antibodies (Alexa 488-conjugated goat anti-rabbit, or Cy3-conjugated mouse anti-goat, Invitrogen, United States). The sections were then mounted in 50% glycerol and examined with the fluorescence microscope (Zeiss, Jena, Germany).

Statistical Analysis

All the results were expressed as mean ± SEM of independent experiments repeated for at least three times. Statistical analysis was performed with GraphPad Prism 5 software. Relative mRNA levels in different epididymal regions were compared by one-way ANOVA followed by Dunnett's multiple comparison test. Comparisons between two groups were carried out by Student's *t*-test. *P*-values < 0.05 were accepted as significant.

RESULTS

The Expression Profile of RANTES and Its Receptors in the Rat Epididymis

As a first step to determine the regional expression profile of RANTES in the rat epididymis, RT-PCR was performed in different segments and 430 bp positive products, the result of which indicated that RANTES was ubiquitously expressed in caput, corpus and cauda segments (**Figure 1A**). Moreover, the results of Western Blot analysis using the specific antibody against RANTES also confirmed the wide expression of RANTES in different segments of rat epididymis (**Figure 1B**). The immunohistochemical staining was carried out to elucidate the accurate localization of RANTES in the epithelium. Consistent with previous results (31), RANTES was found mainly distributed in the basal compartment of the caput, corpus and cauda segments while no detectable positive signals was found in the initial segment and in negative control (**Figure 1C**). Considering the specific morphology of these positive cells, which appear to be hemispherical, adhere to the basement membrane and locate underneath the columnar epithelial cells, we postulate that these cells could either be basal cells or basal macrophages. To further confirm the cell types that express RANTES, macrophage

markers, F4/80 antibody, was stained by immunofluorescence to distinguish the two cell types, showing the location of RANTES particularly in the macrophages (**Figure 1D**).

Several membrane receptors such as CCR1, CCR3, and CCR5 have been validated to be responsible for transducing the signal of RANTES in a context-dependent manner in different cellular processes (29). To identify the specific downstream receptors of RANTES in rat epididymis, we detected the expression profile of CCR1, CCR3 and CCR5 in the epididymis. We found the remarkable expression of CCR1 and CCR5 and the weak expression of the CCR3 in rat epididymis (**Figure 2A**). Similar to the distribution pattern of RANTES, the expression of CCR1 and CCR5 were mainly observed as positive brown granules in the basal compartment of the caput, corpus and cauda regions but disappeared in the initial segment and negative control (**Figure 2B**). The confocal imaging results also showed that both CCR1 and CCR5 proteins were co-localized with RANTES in the macrophages along the epididymis duct (**Figure 2C**). Thus, in rat epididymis, RANTES and its receptors CCR1 and CCR5 are predominantly expressed in the F4/80 positive macrophages which are located at the basal compartment of caput, corpus and cauda segments rather than the macrophages localized at the initial segment.

A significant difference was found in the morphology between the macrophages localized at the initial segment and those in other segments of the epididymal epithelium. The macrophages with long processes in the initial segment were mainly distributed in the adluminal compartment, while those in other segments of the epididymis exhibited basal round-like cells. No significant functional difference between these two subsets of macrophages was reported in previous studies. The unique localization of RANTES and its receptors in basal macrophages may indicate the difference of RANTES-mediated function between the two subtypes of macrophages which will be discussed later in the section "Discussion."

RANTES Induces the Epididymal Luminal Proton Secretion

In the epididymis, epithelial cells work in a concerted manner to establish a luminal acidic milieu which is essential for the post-testicular maturation and storage of spermatozoa. To examine whether RANTES is involved in the regulation of the unique acidic microenvironment in epididymal lumen, *in vivo* cauda microperfusion model was used to further determine the direct effects of RANTES on the luminal acid-base state. In the epididymal epithelium, V-ATPases in the clear cells are the final effectors which are responsible for the proton secretion and are sensitive indicators to evaluate the state of acid secretion. The effects of recombinant RANTES and Met-RANTES on V-ATPase were then examined in the *in vivo* perfusion model. After RANTES perfusion, the expression of V-ATPase was significantly up-regulated compared to the control group (pH of 6.8). Meanwhile, the immunofluorescent staining showed a notable accumulation of V-ATPases in the apical membrane of clear cells. Yet, the expression levels of V-ATPase were decreased with Met-RANTES replenishment compared with those in the RANTES perfusion group. Correspondingly, the immunofluorescent staining indicated that the accumulation of V-ATPases in the apical membrane of clear cell disappeared (**Figure 3A**).

Previous studies have elaborated that the expression of proton pumping V-ATPase in the apical membranes of epididymal clear cells is remarkably up-regulated via the activation of NO/cGMP pathway, leading to increased acid secretion. INOS is the enzyme which is responsible for NO production and used to assess the cellular ability to produce NO (37). We found that iNOS was also expressed in the F4/80 positive macrophages in the epididymal lumen (**Supplementary Figure 1**). So, it is possible that the intrinsic mechanism of RANTES regulates the expression of V-ATPases through the activation of NO/cGMP pathway. Real-time PCR and Western blot demonstrated that both mRNA and protein of iNOS were up-regulated by the addition of RANTES compared to the control group (pH of 6.8). Meanwhile, the immunofluorescent staining showed a stronger signal of iNOS in the macrophages. And the expression level of iNOS decreased with Met-RANTES replenishment compared with those in the RANTES perfusion group. The immunofluorescent staining, correspondingly, indicated weakened signal intensity of iNOS in macrophages (**Figure 3B**).

The Aberrant Alkaline Luminal Environment Induces the Expression of RANTES and Proton Secretion

While the pH values of the epididymal lumen in different segments are maintained at a relative stable state, the intrinsic mechanism still remains uncertain. To examine RANTES' role in maintaining the acidic environment, we used the alkaline perfusion model (PBS at pH 7.8) to simulate the luminal acid-base fluctuation. Compared with the control group (pH 6.8 PBS), the expression of RANTES in cauda epididymis were remarkably enhanced after perfusion with pH 7.8 PBS (**Figure 4A**). Besides, we also observed significantly upregulated mRNA of V-ATPase in cauda epididymis (**Figure 4B**), and intensive enrichment of V-ATPase in the apical membranes of clear cells under the alkaline condition, suggesting the induction of luminal acid secretion after alkaline microperfusion (**Figure 4C**). Therefore, we confirmed that abnormal alkaline environment could induce the production of RANTES, which could in turn promote acid secretion to restore the original acidic microenvironment.

RANTES Is Involved in the Abnormal Luminal Acid-Base State in the Vasectomy Model

Vasectomy is a classic surgical intervention for male contraception, which is also one of the frequently used animal models for the research into male reproductive function. Previous research has reported remarkable increase of lumen pH after vasectomy the yet no report regarding the underlying mechanism was found (35). Therefore, we constructed a rat vasectomy model to investigate whether RANTES is involved in the abnormal acid-base changes after vasectomy. Interestingly, after the vasectomy, we did find some prominent changes in the

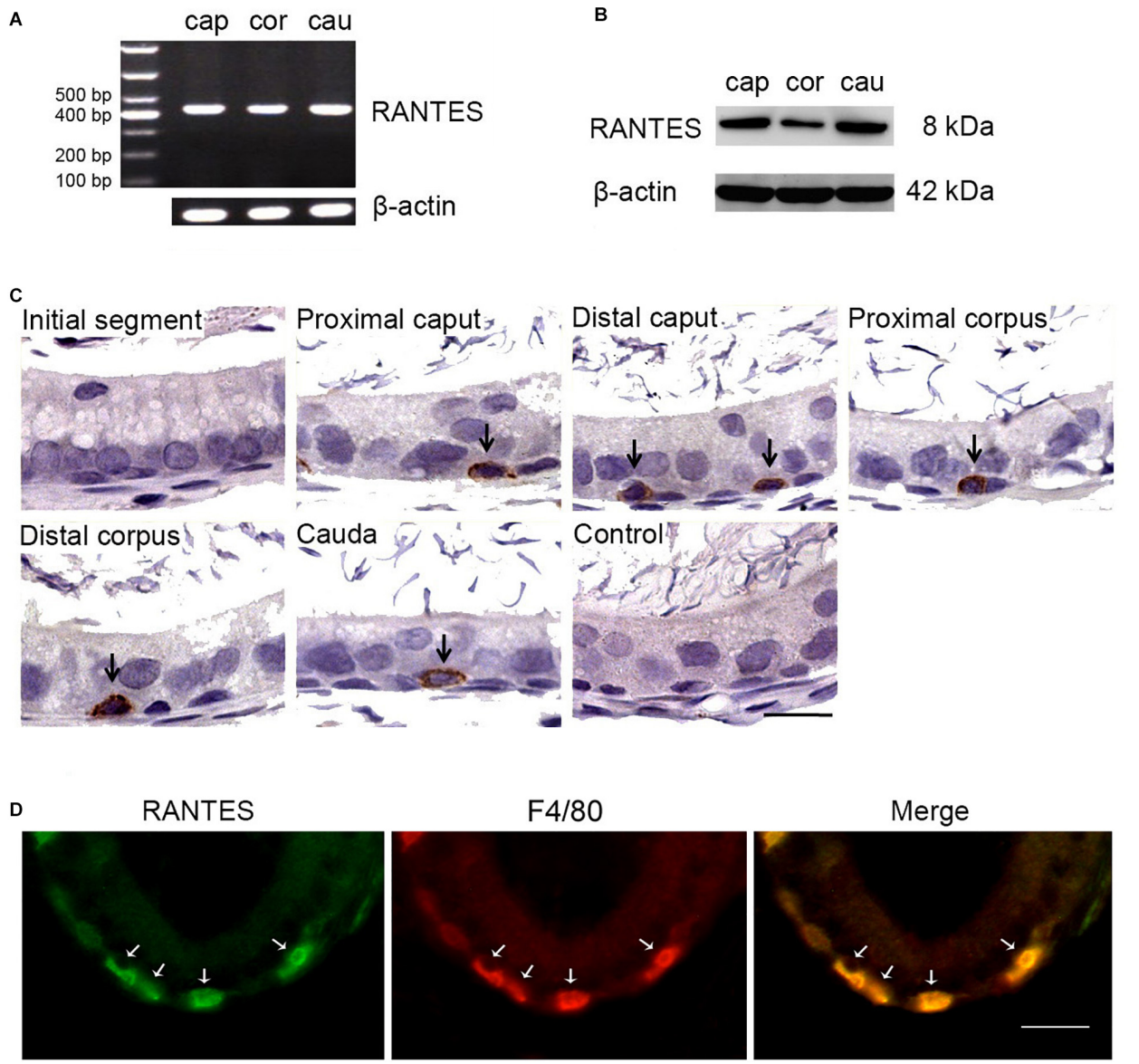

FIGURE 1 | Expression and cellular localization of RANTES in the adult rat epididymis. **(A)** RT-PCR analysis of RANTES in the caput (Cap), corpus (Cor) and cauda (Cau) regions of the epididymis. The PCR products were found in all three regions. **(B)** Protein extracted from different segments of the epididymis was analysis by WB. RANTES was detectable in the caput (Cap), corpus (Cor) and cauda (Cau). **(C)** Immunohistochemistry of RANTES in rat epididymis. Positive reactions were found restricted in partial basolateral cells (black arrows) of the epididymal ducts. **(D)** The cellular location of RANTES in cauda epididymis was detected by double IF. The green signal of RANTES (Alexa 488 labeled) coincide with the red signal of F4/80 (Cy3 labeled). White arrows: positive signals for RANTES or F4/80. Bar = 20 μm.

epididymal lumen. First, consistent with previous studies, the pH value of cauda in the experimental group was significantly higher than that in the sham-operated group (**Figure 5A**). Besides, the expression of V-ATPases in the apical membranes of clear cells was found decreased in the vasectomy group compared with the sham-operated group (**Figure 5B**), and iNOS was also found to decline in the cauda (**Figure 5C**). Finally, by real-time PCR and Western blot analysis were performed to detect the expression levels of RANTES and its receptors and we found both of them decreased significantly in the cauda segments (**Figure 5C**), suggesting the down-regulated expression of RANTES as a potential factor causing decreased acid secretion.

Though our research confirmed that aberrant RANTES expression could account for the abnormal outcome of alkaline luminal fluid after vasectomy, no investigation was done to reveal the upstream mechanism regulating RANTES expression. Recent reports showed that ANG II could stimulate V-ATPase-dependent proton extrusion and NO could be produced in the macrophages and function as one of the downstream effectors of AGTR2. These clues suggest that RANTES could be responsible

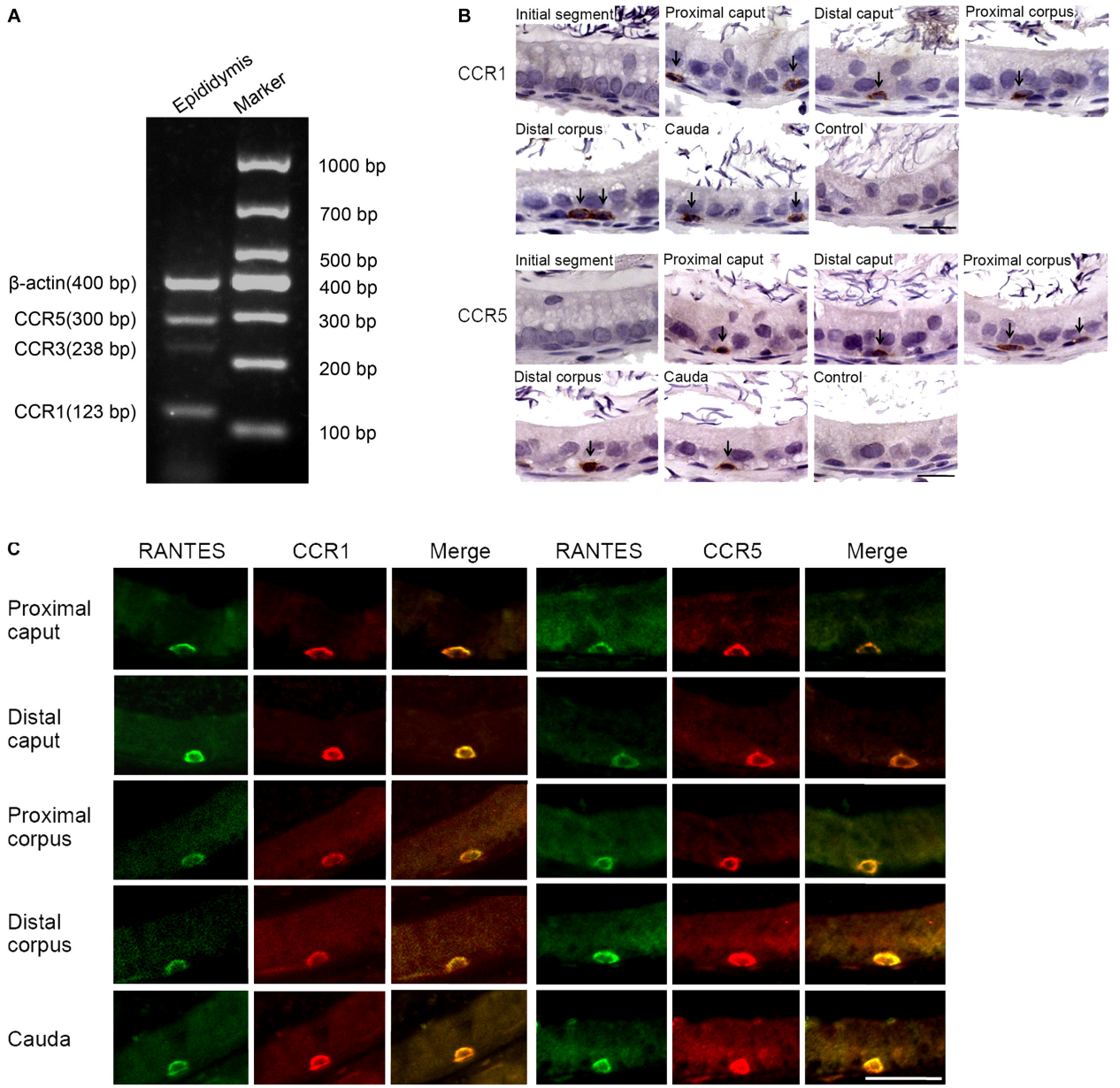

FIGURE 2 | Expression of RANTES receptors CCR1, CCR3 and CCR5 in the adult rat epididymis. **(A)** Expression of CCR1, CCR3 and CCR5 in rat epididymis were detected by RT -PCR. **(B)** Immunohistochemistry of CCR1 and CCR5 in rat epididymis. Black arrows: positive signals for CCR1 or CCR5. **(C)** Double IF staining was applied to detected the co-localization of RANTES with CCR1 and CCR5 in rat epididymis. The green signal of RANTES (Alexa 488 labeled) coincide with that of the red signal of CCR1 and CCR5 (Cy3 labeled). Bars = 20 μm.

for the transduction of ANG II/AGTR2 signal pathway in regulating NO synthesis. To further investigate the upstream pathway of RANTES, we measured the concentration of ANG II and the expression of AGTR2 in the vasectomy group and control group. As expected, the results showed a clear-cut demotion of ANG II in the vasectomy group (**Figure 5D**). Real-time PCR and Western blot were performed to detect the expression of AGTR2 and the data presented declined mRNA and protein of ANG II in the cauda of epididymis (**Figure 5D**). The results indicated that the decreased expression of RANTES may attribute to the abrogation of ANG II/AGTR2 signals but the direct regulatory relation between them needs to be validated in further experiments.

DISCUSSION

The results from the present study showed that RANTES and CCR1, CCR5 were constitutively expressed in the basal macrophages of rat epididymis, and played an essential role

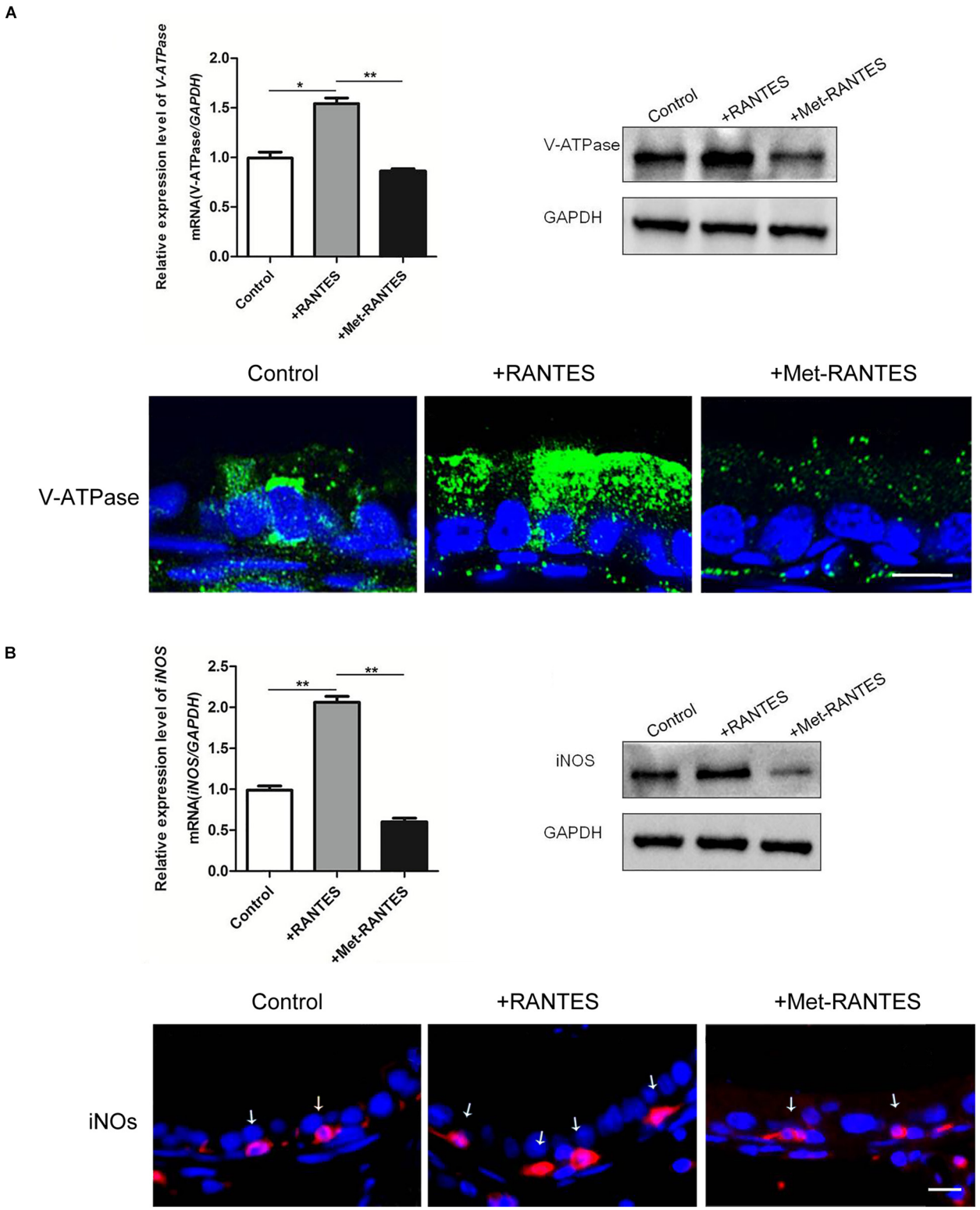

FIGURE 3 | Effects of RANTES and Met-RANTES on V-ATPase and iNOS in perfusion model. Rat cauda epididymis were perfused luminally *in vivo* with recombinant RANTES and Met-RANTES. Real-time PCR and WB analysis of the mRNA and protein levels of V-ATPase **(A)** and iNOS **(B)** were up-regulated by the addition of RANTES compared to the control group (pH of 6.8), but decreased with the antagonist Met-RANTES replenishment. Immunofluorescence staining showed a notable accumulation of V-ATPase in the apical membrane of clear cells **(A)** and a strong signal of iNOS (white arrows) in the epididymis **(B)** by the addition of RANTES, whereas it decreased with Met-RANTES replenishment. $^{**}P < 0.01$, $^{*}P < 0.05$, $N = 5–6$, Bar = 20 μm.

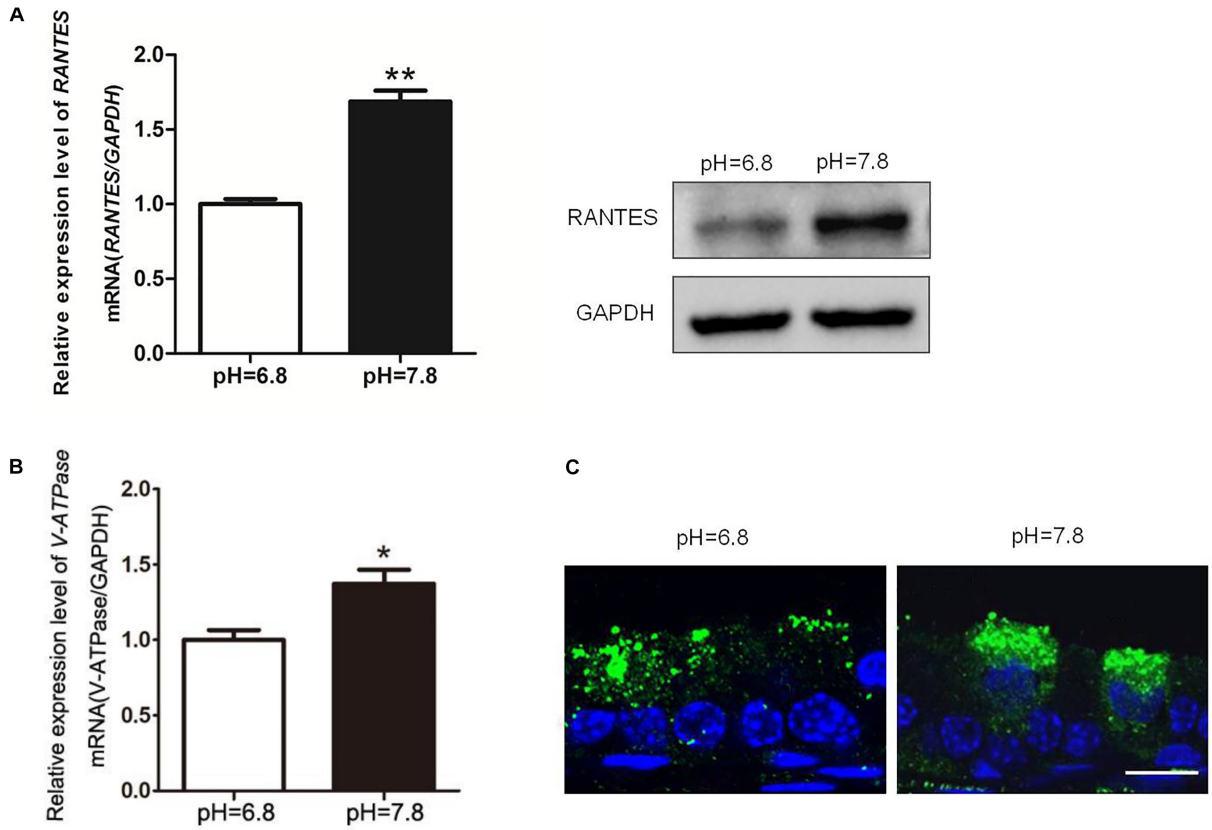

FIGURE 4 | Changes of RANTES and V-ATPase upon rat cauda epididymis alkaline perfusion. Rat cauda epididymal lumen was perfused *in vivo* with PBS (pH values 6.8 or 7.8). **(A)** Real-time PCR and WB revealed that upon alkaline treatment (pH of 7.8), the expression level of RANTES in cauda epididymis was significantly up-regulated compared with that in the control group (pH of 6.8). Meanwhile, **(B)** expression of V-ATPase mRNA was increased examined by real-time PCR, $N = 5–6$. **(C)** The Results of CLSM showed that the alkaline pH also induced the apical accumulation of V-ATPase in the clear cell. $^{**}P < 0.01$, $^{*}P < 0.05$, $N = 5–6$, Bar = 20 μm.

in the process of acidification in the luminal milieu. RANTES up-regulated the expression of iNOS in the macrophages and V-ATPase in the apical membrane of clear cells. Moreover, the expression of RANTES decreased and the pH value of the epididymal lumen increased following vasectomy.

In the epididymis, macrophages are widely distributed in different segments, exhibiting unique phenotypes and function to establish and maintain an appropriate environment for sperm maturation and storage (18, 38, 39). Epididymal macrophages can be divided into two subsets according to their distinguished appearances. Intraepithelial macrophages in the initial segment extend slender projections through the epithelial cells toward the lumen. This unique morphological characteristic was not observed in macrophages from the basal compartment of distal regions. Macrophages in the initial segment is mainly responsible for presenting antigen to the lymphocytes and eliminating defective epithelial cells and abnormal spermatozoa in epididymis, as well as the defense reaction in luminal infection (19, 40–42). Yet, the function of macrophages restricted to the basal region of the tubule is still unclear. Our study found that RANTES and its receptors CCR1 and CCR5 were specifically expressed in these basolateral macrophages, while they were absent in the initial segment. Thus, RANTES-positive macrophages might display some functions distinctive from those with long projections in the initial segment through its receptors CCR1 and CCR5.

In addition to the well-known chemotactic function, the non-canonical function of RANTES in sperm maturation seems more complicated than we previously thought (41). The present study showed the direct effects of RANTES on regulating the luminal acidification in the epididymis. RANTES perfusion induced the accumulation of V-ATPase in the apical membrane of clear cells and the expression of iNOS in the macrophages. A potent RANTES receptor antagonist Met-RANTES (43) was used to address the role of RANTES signaling through its receptors CCR1 and CCR5. Met-RANTES perfusion led to a complete abrogation of the increased expression of V-ATPase and iNOS in the epididymal epithelium. Since RANTES is a small protein of 8-kDa, we postulate that luminal perfused RANTES might directly bind to its specific 7-transmembrane G protein-coupled receptors, namely CCR1 and CCR5, on the surface of basal macrophages in the epithelium. Additional experiments such as using the methods of confocal microscopy and western blot should be done in the follow-up studies. It has been shown that

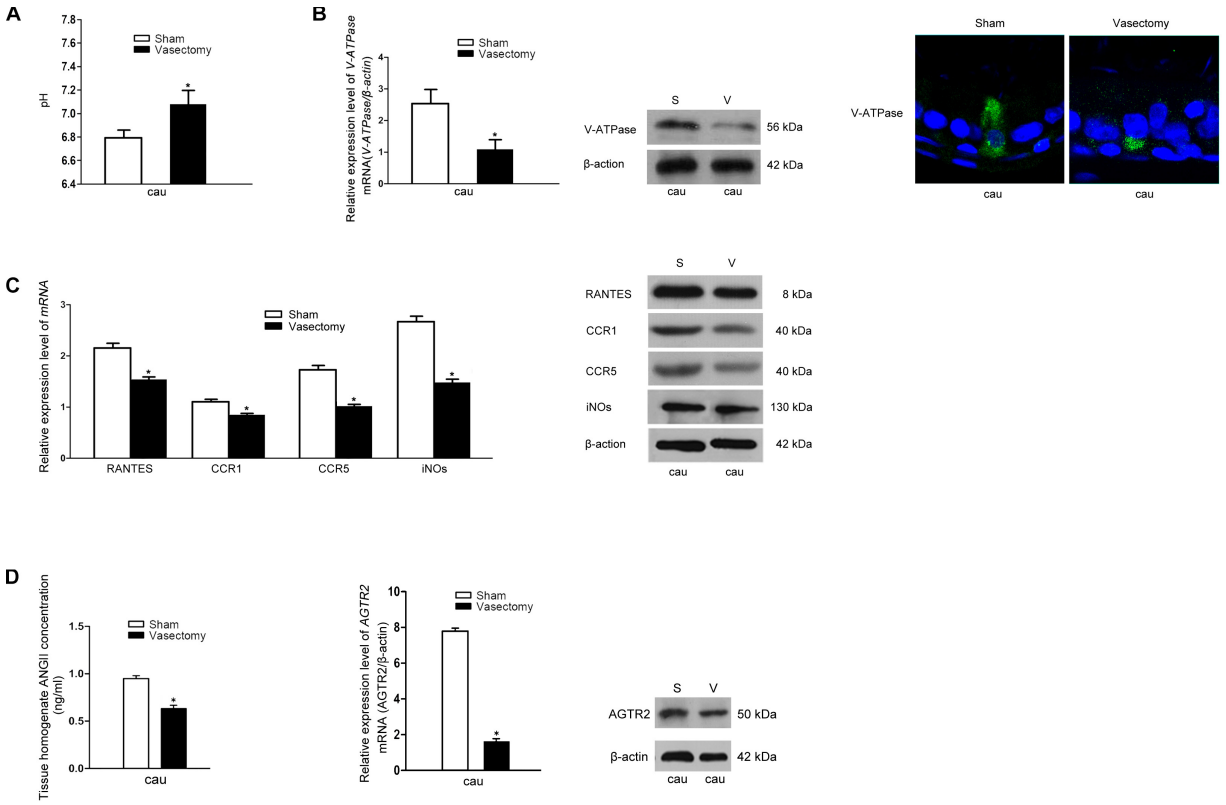

FIGURE 5 | Effects of rat vasectomy on the luminal pH and the expression of V-ATPase, RANTES, CCR1, CCR5, iNOS, and RAS. **(A)** 8 weeks after rat bilateral vasectomy, luminal fluid pH of cauda epididymis increased and remained alkaline. **(B)** The expression of V-ATPase in rat cauda epididymis was detected by Real time-PCR, WB and IF staining. **(C)** 8 weeks after rat bilateral vasectomy, the expression levels of RANTES, CCR1, CCR5, and iNOS mRNA and protein in cauda epididymis were decreased revealed by Real time-PCR and WB. **(D)** The tissue homogenate ANG II concentration were measured by RIA and the expression of AGTR2 was detected by Real time -PCR and WB. $^*P < 0.05$, $N = 5–6$, Bar = 20 μm.

proton was secreted by epididymal clear cells via activation of the NO/cGMP pathway (10). Therefore, RANTES might stimulate proton secretion by epididymal clear cells via activation of the NO released from macrophages. On the other hand, in the experiments detailed here, alkaline PBS induced the expression of RANTES within the epididymis and the accumulation of V-ATPase in the apical membrane of clear cells, indicating that the expression of RANTES could be increased responsively upon the exogenous luminal alkaline treatment in the epididymis.

We utilized the vasectomy model to further explore the function of RANTES in the epididymis. The luminal pH in the cauda epididymis increased as compared to control by 8 weeks post vasectomy, consistent with previous reports that luminal pH in the proximal cauda epididymis was significantly more alkaline (35). Accordingly, the accumulation of V-ATPase in the apical membrane of clear cells was decreased. Interestingly, the expression levels of RANTES, CCR1, CCR5, and iNOS were all significantly reduced in the cauda epididymis following vasectomy. This observation suggests that the decreased expression of RANTES and its receptors in the cauda epididymis may be one of the causes of the luminal alkaline pH in the vasectomy model. Previous study revealed that vasectomy altered the renin-angiotensin system (RAS) expression in the epididymis (7), which is coincided with our findings that both ANG II and AGTR2 decreased significantly in the cauda epididymis following vasectomy. It has been reported that ANG II promoted the expression of RANTES in glomerular endothelial cells through AGTR2 (34), and that AGTR2 was solely expressed in basal cells in the epididymal epithelium (10). All these studies strongly point to ANG II/AGTR2 as a factor regulating RANTES expression in the cauda epididymis to maintain the acidity of luminal fluid.

CONCLUSION

In conclusion, our findings indicate that macrophages at the basal part of epididymal duct facilitates the luminal acidification via RANTES. In another words, activation of AGTR2 in basal cells by luminal ANG II may stimulate RANTES in basal macrophages to induce the production of NO, which results in the accumulation of V-ATPase and increases proton secretion by adjacent clear cells (**Figure 6**). This study highlights a novel biological activity for RANTES, a chemokine best known for the ability to induce directional cellular recruitment. By participating in the crosstalk among basal cells, macrophages and clear cells,

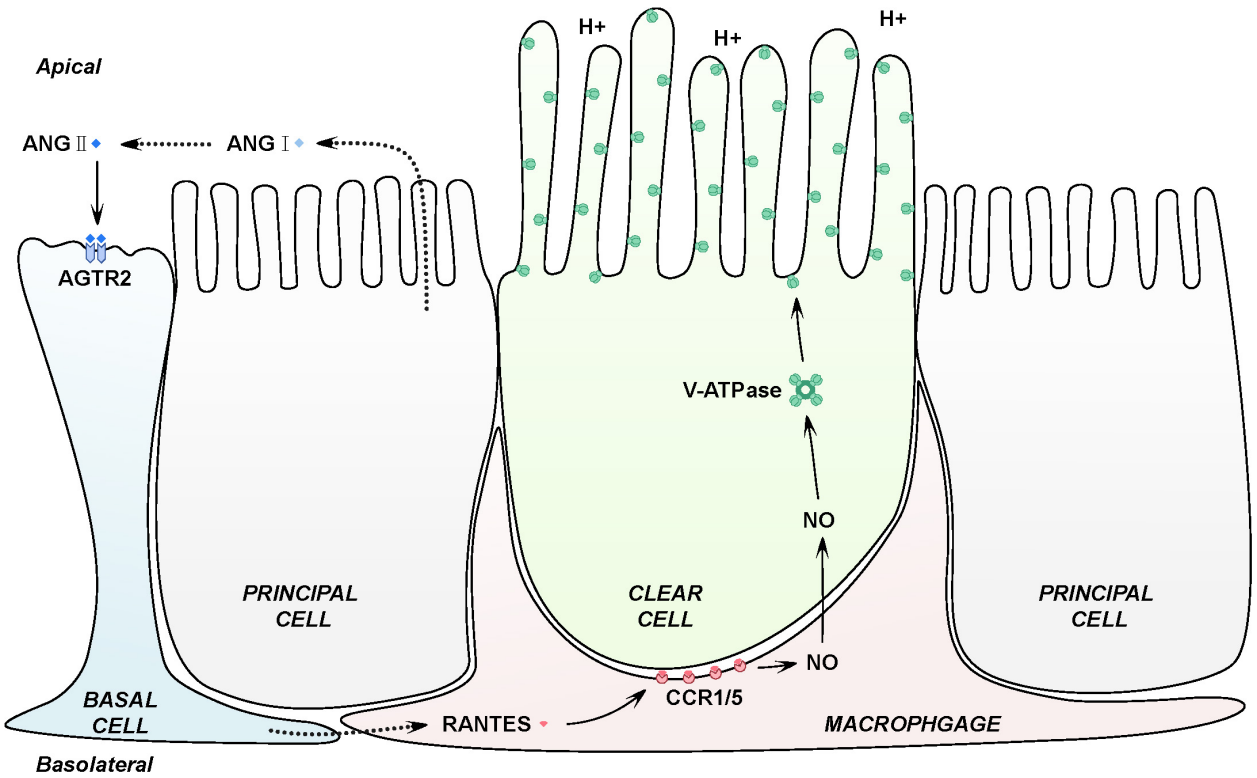

FIGURE 6 | Schematic representation of RANTES in the basal macrophages contributing to the intricate luminal acidic regulation in the epididymis. Firstly, epididymal luminal ANG II binds with its receptors AGTR2 expressed on the membrane of basal cells, inducing the expression of RANTES and its receptors, CCR1 and CCR5 in the basal macrophages. Secondly, RANTES could function with CCR1 and CCR5 to increase the expression of iNOs, which will lead to the up-regulation of NO. Finally, NO will diffuse to the adjacent clear cells to stimulate the expression of V-ATPase, causing the increased secretion of proton to the epididymal lumen to maintain the normal acidic microenvironment.

RANTES may regulate acidic luminal environment that is critical for male fertility.

DATA AVAILABILITY STATEMENT

All datasets presented in this study are included in the article/**Supplementary Material**.

ETHICS STATEMENT

The animal study was reviewed and approved by the Research Ethics Committee of the Fourth Military Medical University.

AUTHOR CONTRIBUTIONS

ZL, XF, and B-FM: conceived and designed the experiments. XF, B-FM, J-HW, PC, S-YL, and D-XC: performed the experiments. ZL, XF, B-FM, BL, and PD: analyzed the data. ZL and Z-JS: contributed to reagents, materials, and analysis tools. ZL, XF, and BL: wrote the manuscript. All authors contributed to the article and approved the submitted version.

FUNDING

This work was supported by the National Natural Science Foundation of China (Nos. 81170614 and 31871515) and the Natural Science Foundation of Liaoning Province, China (No. 20170540905).

ACKNOWLEDGMENTS

The content of this manuscript has been presented in poster presentations at the American-Sino Joint Meeting of Reproductive Immunology, the 38th Annual Meeting of the American Society for Reproductive Immunology, the 8th Annual Meeting of the Chinese Society for Reproductive Immunology. We are indebted to Miss. Qingyi Wang (Department of Foreign Language, Fourth Military Medical University, Xi'an, China) for her careful assistance during language editing of the manuscript.

SUPPLEMENTARY MATERIAL

The Supplementary Material for this article can be found online at: https://www.frontiersin.org/articles/10.3389/fimmu.2020.583274/full#supplementary-material

REFERENCES

1. Beaulieu V, Da SN, Pastor-Soler N, Brown CR, Smith PJ, Brown D, et al. Modulation of the actin cytoskeleton via gelsolin regulates vacuolar H+-ATPase recycling. *J Biol Chem.* (2005) 280:8452–63. doi: 10.1074/jbc.M412750200
2. Yeung CH, Breton S, Setiawan I, Xu Y, Lang F, Cooper TG. Increased luminal pH in the epididymis of infertile c-ros knockout mice and the expression of sodium-hydrogen exchangers and vacuolar proton pump H+-ATPase. *Mol Reprod Dev.* (2004) 68:159–68. doi: 10.1002/mrd.20067
3. Pastor-Soler N, Pietrement C, Breton S. Role of acid/base transporters in the male reproductive tract and potential consequences of their malfunction. *Physiology (Bethesda).* (2005) 20:417–28. doi: 10.1152/physiol.00036.2005
4. Breton S, Nair AV, Battistone MA. Epithelial dynamics in the epididymis: role in the maturation, protection, and storage of spermatozoa. *Andrology US.* (2019) 7:631–43. doi: 10.1111/andr.12632
5. Battistone MA, Merkulova M, Park YJ, Peralta MA, Gombar F, Brown D, et al. Unravelling purinergic regulation in the epididymis: activation of V-ATPase-dependent acidification by luminal ATP and adenosine. *J Physiol.* (2019) 597:1957–73. doi: 10.1113/JP277565
6. Pholpramool C, Borwornpinyo S, Dinudom A. Role of Na+ /H+ exchanger 3 in the acidification of the male reproductive tract and male fertility. *Clin Exp Pharmacol Physiol.* (2011) 38:403–9. doi: 10.1111/j.1440-1681.2011.05525.x
7. Saez F, Legare C, Laflamme J, Sullivan R. Vasectomy-dependent dysregulation of a local renin-angiotensin system in the epididymis of the cynomolgus monkey (*Macaca fascicularis*). *J Androl.* (2004) 25:784–96. doi: 10.1002/j.1939-4640.2004.tb02857.x
8. Kondoh G, Tojo H, Nakatani Y, Komazawa N, Murata C, Yamagata K, et al. Angiotensin-converting enzyme is a GPI-anchored protein releasing factor crucial for fertilization. *Nat Med.* (2005) 11:160–6. doi: 10.1038/nm1179
9. Gatti JL, Druart X, Guerin Y, Dacheux F, Dacheux JL. A 105- to 94-kilodalton protein in the epididymal fluids of domestic mammals is angiotensin I-converting enzyme (ACE); evidence that sperm are the source of this ACE. *Biol Reprod.* (1999) 60:937–45. doi: 10.1095/biolreprod60.4.937
10. Shum WW, Da SN, McKee M, Smith PJ, Brown D, Breton S. Transepithelial projections from basal cells are luminal sensors in pseudostratified epithelia. *Cell.* (2008) 135:1108–17. doi: 10.1016/j.cell.2008.10.020
11. Liu P, Peng J, Han GH, Ding X, Wei S, Gao G, et al. Role of macrophages in peripheral nerve injury and repair. *Neural Regen Res.* (2019) 14:1335–42. doi: 10.4103/1673-5374.253510
12. Lee HH, Ahn EK, Hong SS, Oh JS. Anti-inflammatory effect of tribulusamide D isolated from Tribulus terrestris in lipopolysaccharide-stimulated RAW264.7 macrophages. *Mol Med Rep.* (2017) 16:4421–8. doi: 10.3892/mmr.2017.7208
13. Zhao W, Beers DR, Thonhoff JR, Thome AD, Faridar A, Wang J, et al. Immunosuppressive functions of M2 macrophages derived from iPSCs of patients with ALS and healthy controls. *iScience.* (2020) 23:101192. doi: 10.1016/j.isci.2020.101192
14. Fink MY, Maloney J, Keselman A, Li E, Menegas S, Staniorski C, et al. Proliferation of resident macrophages is dispensable for protection during giardia duodenalis infections. *Immunohorizons.* (2019) 3:412–21. doi: 10.4049/immunohorizons.1900041
15. Erkelens MN, Goverse G, Konijn T, Molenaar R, Beijer MR, Van den Bossche J, et al. Intestinal macrophages balance inflammatory expression profiles via vitamin a and dectin-1-mediated signaling. *Front Immunol.* (2020) 11:551. doi: 10.3389/fimmu.2020.00551
16. McDole JR, Wheeler LW, McDonald KG, Wang B, Konjufca V, Knoop KA, et al. Goblet cells deliver luminal antigen to CD103+ dendritic cells in the small intestine. *Nature.* (2012) 483:345–9. doi: 10.1038/nature10863
17. Mazzini E, Massimiliano L, Penna G, Rescigno M. Oral tolerance can be established via gap junction transfer of fed antigens from CX3CR1(+) macrophages to CD103(+) dendritic cells. *Immunity.* (2014) 40:248–61. doi: 10.1016/j.immuni.2013.12.012
18. Battistone MA, Mendelsohn AC, Spallanzani RG, Brown D, Nair AV, Breton S. Region-specific transcriptomic and functional signatures of mononuclear phagocytes in the epididymis. *Mol Hum Reprod.* (2020) 26:14–29. doi: 10.1093/molehr/gaz059
19. Da SN, Cortez-Retamozo V, Reinecker HC, Wildgruber M, Hill E, Brown D, et al. A dense network of dendritic cells populates the murine epididymis. *Reproduction.* (2011) 141:653–63. doi: 10.1530/REP-10-0493
20. Aldinucci D, Casagrande N. Inhibition of the CCL5/CCR5 axis against the progression of gastric cancer. *Int J Mol Sci.* (2018) 19:1477. doi: 10.3390/ijms19051477
21. Homma T, Matsukura S, Hirose T, Ohnishi T, Kimura T, Kurokawa M, et al. Cooperative activation of CCL5 expression by TLR3 and tumor necrosis factor-alpha or interferon-gamma through nuclear factor-kappaB or STAT-1 in airway epithelial cells. *Int Arch Allergy Immunol.* (2010) 152(Suppl. 1):9–17. doi: 10.1159/000312120
22. Bruserud O, Ryningen A, Olsnes AM, Stordrange L, Oyan AM, Kalland KH, et al. Subclassification of patients with acute myelogenous leukemia based on chemokine responsiveness and constitutive chemokine release by their leukemic cells. *Haematologica.* (2007) 92:332–41. doi: 10.3324/haematol.10148
23. Reikvam H, Aasebo E, Brenner AK, Bartaula-Brevik S, Gronningsaeter IS, Forthun RB, et al. High constitutive cytokine release by primary human acute myeloid leukemia cells is associated with a specific intercellular communication phenotype. *J Clin Med.* (2019) 8:970. doi: 10.3390/jcm8070970
24. Ignatov A, Robert J, Gregory-Evans C, Schaller HC. RANTES stimulates Ca2+ mobilization and inositol trisphosphate (IP3) formation in cells transfected with G protein-coupled receptor 75. *Br J Pharmacol.* (2006) 149:490–7. doi: 10.1038/sj.bjp.0706909
25. Appay V, Rowland-Jones SL. RANTES: a versatile and controversial chemokine. *Trends Immunol.* (2001) 22:83–7. doi: 10.1016/s1471-4906(00)01812-3
26. Velasco-Velazquez M, Jiao X, De La Fuente M, Pestell TG, Ertel A, Lisanti MP, et al. CCR5 antagonist blocks metastasis of basal breast cancer cells. *Cancer Res.* (2012) 72:3839–50. doi: 10.1158/0008-5472.CAN-11-3917
27. Azenshtein E, Luboshits G, Shina S, Neumark E, Shahbazian D, Weil M, et al. The CC chemokine RANTES in breast carcinoma progression: regulation of expression and potential mechanisms of promalignant activity. *Cancer Res.* (2002) 62:1093–102.
28. Fang H, Jin J, Huang D, Yang F, Guan X. PAI-1 induces Src inhibitor resistance via CCL5 in HER2-positive breast cancer cells. *Cancer Sci.* (2018) 109:1949–57. doi: 10.1111/cas.13593
29. Kato T, Fujita Y, Nakane K, Mizutani K, Terazawa R, Ehara H, et al. CCR1/CCL5 interaction promotes invasion of taxane-resistant PC3 prostate cancer cells by increasing secretion of MMPs 2/9 and by activating ERK and Rac signaling. *Cytokine.* (2013) 64:251–7. doi: 10.1016/j.cyto.2013.06.313
30. Pasquier J, Gosset M, Geyl C, Hoarau-Vechot J, Chevrot A, Pocard M, et al. CCL2/CCL5 secreted by the stroma induce IL-6/PYK2 dependent chemoresistance in ovarian cancer. *Mol Cancer.* (2018) 17:47. doi: 10.1186/s12943-018-0787-z
31. Li Z, Sun Z, Liao C, Ma L, Ma B, Zhang Y. Regulated upon activation normal T-cell expressed and secreted originating from the epididymis differentially associates with viable and defective spermatozoa. *Fertil Steril.* (2010) 93:2661–7. doi: 10.1016/j.fertnstert.2010.01.053
32. Villalta F, Zhang Y, Bibb KE, Kappes JC, Lima MF. The cysteine-cysteine family of chemokines RANTES, MIP-1alpha, and MIP-1beta induce trypanocidal activity in human macrophages via nitric oxide. *Infect Immun.* (1998) 66:4690–5.
33. Guzik TJ, Hoch NE, Brown KA, McCann LA, Rahman A, Dikalov S, et al. Role of the T cell in the genesis of angiotensin II induced hypertension and vascular dysfunction. *J Exp Med.* (2007) 204:2449–60. doi: 10.1084/jem.20070657
34. Kashiwagi M, Masutani K, Shinozaki M, Hirakata H. MCP-1 and RANTES are expressed in renal cortex of rats chronically treated with nitric oxide synthase inhibitor. Involvement in macrophage and monocyte recruitment. *Nephron.* (2002) 92:165–73. doi: 10.1159/000064454
35. Caflisch CR, DuBose TJ. Effect of vasectomy on in situ pH in rat testis and epididymis. *Contraception.* (1990) 42:589–95. doi: 10.1016/0010-7824(90)90085-a
36. Cheng P, Zhao J, Qiao H, Ma H, Ma B, Wei J, et al. Colocalization of metastasis-associated proteins 1/2 and estrogen receptor alpha in rat epididymis. *Tissue Cell.* (2017) 49:582–8. doi: 10.1016/j.tice.2017.07.006
37. Wilmes V, Scheiper S, Roehr W, Niess C, Kippenberger S, Steinhorst K, et al. Increased inducible nitric oxide synthase (iNOS) expression in human

myocardial infarction. *Int J Legal Med.* (2020) 134:575–81. doi: 10.1007/s00414-019-02051-y
38. Wijayarathna R, Hedger MP. Activins, follistatin and immunoregulation in the epididymis. *Andrology US.* (2019) 7:703–11. doi: 10.1111/andr.12682
39. Shum WW, Smith TB, Cortez-Retamozo V, Grigoryeva LS, Roy JW, Hill E, et al. Epithelial basal cells are distinct from dendritic cells and macrophages in the mouse epididymis. *Biol Reprod.* (2014) 90:90. doi: 10.1095/biolreprod.113.116681
40. Smith TB, Cortez-Retamozo V, Grigoryeva LS, Hill E, Pittet MJ, Da SN. Mononuclear phagocytes rapidly clear apoptotic epithelial cells in the proximal epididymis. *Andrology US.* (2014) 2:755–62. doi: 10.1111/j.2047-2927.2014.00251.x
41. Guazzone VA. Exploring the role of antigen presenting cells in male genital tract. *Andrologia.* (2018) 50:e13120. doi: 10.1111/and.13120
42. Da SN, Barton CR. Macrophages and dendritic cells in the post-testicular environment. *Cell Tissue Res.* (2016) 363:97–104. doi: 10.1007/s00441-015-2270-0
43. Proudfoot AE, Power CA, Hoogewerf AJ, Montjovent MO, Borlat F, Offord RE, et al. Extension of recombinant human RANTES by the retention of the initiating methionine produces a potent antagonist. *J Biol Chem.* (1996) 271:2599–603. doi: 10.1074/jbc.271.5.2599

Conflict of Interest: The authors declare that the research was conducted in the absence of any commercial or financial relationships that could be construed as a potential conflict of interest.

frontiers in Immunology

MINI REVIEW
published: 25 September 2020
doi: 10.3389/fimmu.2020.583135

Pathomechanisms of Autoimmune Based Testicular Inflammation

Livia Lustig[1,2]*, *Vanesa A. Guazzone*[1,2], *María S. Theas*[1,2], *Christiane Pleuger*[3,4], *Patricia Jacobo*[1,2], *Cecilia V. Pérez*[2], *Andreas Meinhardt*[3,4] and *Monika Fijak*[3,4]*

[1] Departamento de Biología Celular e Histología/Unidad Académica II, Facultad de Medicina, Universidad de Buenos Aires (UBA), Buenos Aires, Argentina, [2] Instituto de Investigaciones Biomédicas (INBIOMED), Consejo Nacional de Investigaciones Científicas y Tècnicas (CONICET), Universidad de Buenos Aires (UBA), Buenos Aires, Argentina, [3] Department of Anatomy and Cell Biology, Justus-Liebig University Giessen, Giessen, Germany, [4] Hessian Centre of Reproductive Medicine, Justus-Liebig University Giessen, Giessen, Germany

Infection and inflammation of the male reproductive tract are relevant causes of infertility. Inflammatory damage occurs in the special immunosuppressive microenvironment of the testis, a hallmark termed testicular immune privilege, which allows tolerance to neo-antigens from developing germ cells appearing at puberty, long after the establishment of systemic immune tolerance. Experimental autoimmune orchitis (EAO) is a well-established rodent model of chronic testicular inflammation and organ specific autoimmunity that offers a valuable *in vivo* tool to investigate the pathological and molecular mechanisms leading to the breakdown of the testicular immune privilege. The disease is characterized by the infiltration of the interstitium by immune cells (mainly macrophages, dendritic cells, and T cells), formation of autoantibodies against testicular antigens, production of pro-inflammatory mediators such as NO, MCP1, TNFα, IL6, or activins and dysregulation of steroidogenesis with reduced levels of serum testosterone. EAO leads to sloughing of germ cells, atrophic seminiferous tubules and fibrotic remodeling, parameters all found similarly to changes in human biopsies from infertile patients with inflammatory infiltrates. Interestingly, testosterone supplementation during the course of EAO leads to expansion of the regulatory T cell population and inhibition of disease development. Knowledge of EAO pathogenesis aims to contribute to a better understanding of human testicular autoimmune disease as an essential prerequisite for improved diagnosis and treatment.

Keywords: testicular inflammation, autoimmunity, experimental autoimmune orchitis (EAO), infertility, testis immunoregulation

OPEN ACCESS

Edited by:
Daishu Han,
Chinese Academy of Medical Sciences and Peking Union Medical College, China

Reviewed by:
Jannette Marie Dufour,
Texas Tech University Health Sciences Center, United States
Megan K. L. MacLeod,
University of Glasgow, United Kingdom

***Correspondence:**
Livia Lustig
livialustig38@yahoo.com.ar
Monika Fijak
monika.fijak@anatomie.med.uni-giessen.de

Specialty section:
This article was submitted to Mucosal Immunity, a section of the journal Frontiers in Immunology

Received: *14 July 2020*
Accepted: *28 August 2020*
Published: *25 September 2020*

Citation:
Lustig L, Guazzone VA, Theas MS, Pleuger C, Jacobo P, Pérez CV, Meinhardt A and Fijak M (2020) Pathomechanisms of Autoimmune Based Testicular Inflammation. Front. Immunol. 11:583135. doi: 10.3389/fimmu.2020.583135

INTRODUCTION

Infection and inflammation of the male reproductive tract are relevant causes of infertility with a prevalence of 6–10% (1, 2). Bacterial infections eliciting epididymo-orchitis are either sexually transmitted or originate from urinary infections often resulting from ascending canalicular infections of the male excurrent ducts. Also, a number of systemically transmitted viruses (mumps virus, HIV and ZIKV virus, among others) are able to induce orchitis. Inflammation of the male reproductive tract is associated not only with infections but also with aging and diseases that damage germ cells (GC) including testis cancer, obesity, cryptorchidism and systemic autoimmune diseases, as well as trauma and toxic agents (3–7).

Autoimmune infertility has long been postulated as one of the causes of infertility, even though a well-defined entity has not yet been established. However, it is relevant that focal lymphocytic infiltrations have been detected in 25–30% of testicular biopsies from infertile patients (8, 9). Anti-sperm antibodies (ASA) have been mainly detected in patients with obstructive azoospermia (10). However, there is so far no close association between ASA and male genital tract inflammation (11, 12) except for some reports associating ASA with idiopathic granulomatous orchitis (13, 14) and a history of epididymitis/orchitis (15). Our own studies reported significantly elevated titers of autoantibodies against disulphide isomerase family A, member 3 (ER-60) in sera from infertile azoospermic patients with histologically confirmed low-grade testicular inflammation (16). Further, the major evidence for an autoimmune basis of human orchitis comes from patients with autoimmune polyendocrine syndrome APS-type 1 caused by AIRE gene mutation which induces testis impairment and antibodies to Leydig cell antigens (17).

Experimental autoimmune orchitis (EAO) is a well-established rodent model of organ specific autoimmunity that provides a very valuable *in vivo* tool to investigate pathological, immune and molecular mechanisms involved in chronic testicular inflammation.

EXPERIMENTAL MODELS OF AUTOIMMUNE ORCHITIS

Research on spontaneous autoimmune orchitis in mink (18, 19) and rodents after vasectomy (20), thymectomy (21, 22), or genetic manipulation (23) have constructed a body of evidence for better understanding of systemic and peripheral tolerance. Studies in classical rodent EAO models induced by antigen immunization have also clarified pathological mechanisms of autoimmune-based testicular inflammation [reviewed in (8, 24)].

The first report on a classical EAO model was published by Voisin et al. (25) who injected testicular tissue and adjuvants into guinea pigs. However, it was Freund et al. (26) who clarified the organ and species specificity of the model. In a murine model, EAO susceptibility depends of genetic background of each strain (27). Further progress on the pathogenesis of EAO has come from mouse and rat models, initiated by Tung and colleagues (28) and Doncel et al. (29), respectively. A description of the histopathology, mechanisms of disease initiation and testicular inflammation are discussed below.

Current rat and mouse EAO models utilizing testicular homogenate in complete Freund's adjuvant plus *pertussis* toxin (8), vasectomized mouse model (20), and mouse EAO model without adjuvants (30) have provided novel insights into orchitogenic antigens. Most of these antigens, identified by sera obtained from animals with EAO, are not testis-specific except zonadhesin or outer dense fiber major protein 2 (30–32).

IMMUNE PRIVILEGE OF THE TESTIS

Testicular homeostasis that protects GC from immune attack is known to be maintained by structural components such as the blood-testis barrier (BTB) and systemic and local tolerance mechanisms. In contrast with the previous testis antigen sequestration paradigm, some meiotic germ cell antigens, located in the adluminal compartment of the seminiferous tubules (ST) behind the BTB, are continuously released into the interstitial space despite an intact BTB. Systemic tolerance involving antigen-specific regulatory T cells (Tregs) is maintained in peripheral lymphoid organs by continuously egressing germ cell antigens via transcytosis in Sertoli cells (33). Originally, the testis was defined as an immune-privileged site since it was demonstrated that foreign-tissue grafts placed within the testis are tolerated and survive for several days longer than when these grafts are implanted in conventional body sites (34). Currently, testicular immune privilege is understood as the coordinated regulation of immunologic components to protect GC, including active processes associated with Sertoli cells, peritubular cells, Leydig cells, tolerogenic antigen-presenting cells, T cells and the production of immune-regulatory factors such as TGFβ, IL10, and activin [reviewed in (35–37)]. Several reviews suggest galectin-1 (*Lgals1*) as a putative candidate involved in the maintenance of testis immune privilege, mainly based on its expression by Sertoli cells (38–40). However, a significant reduction in the incidence and severity of EAO was observed in Lgals1$^{-/-}$ deficient vs. wild-type mice (41) adding a note of caution to this discussion. Indoleamine-2,3-dioxygenase (IDO) expression in porcine Sertoli cells and the ability of these cells to restore immune tolerance in NOD mice (42) point to a role of IDO in testis immune privilege. Current findings from functional *in vivo* experimental studies confirm that tryptophan metabolism modulates inflammatory immune response to spermatic antigens (43).

The BTB is formed by cell junctions of adjacent Sertoli cells at the base of the ST. It is constituted by multiple cell junction types including tight junctions, basal ectoplasmic specializations, gap junctions and desmosome-like junctions. Various integral tight junction proteins have been described between adjacent Sertoli cells with occludin and claudin 11 being the most important for barrier integrity (44). These proteins link to the actin cytoskeleton via cytoplasmic plaque proteins including zonula occludens-1,−2, and−3, and provide links to other junctional types (gap-, adherens-) in the BTB (45). Ectoplasmic specialization-mediated adhesion is largely constituted by the cadherin-catenin multifunctional complex (46). Gap junctions are cell-cell channels that allow diffusion of metabolites, second messengers, ions, and other molecules smaller than 1 kDa, being Cx43 the dominant gap junction protein within the ST (47). Testosterone, nitric oxide (NO), cytokines and growth factors regulate the stability or localization of proteins at the BTB (48–50). The BTB is a dynamic ultrastructure that transiently "opens" and "closes" during the movement of preleptotene/leptotene spermatocytes to the adluminal compartment without causing failure of BTB function. As leptotene spermatocytes transit toward the tubule lumen, junction disassembly ahead of spermatocytes is coordinated by junction assembly behind these GC so that the two spermatogenic events are synchronized (46). Moreover, the presence of specific transporters located along the basolateral membrane of Sertoli cells that allow the passage of

selective molecules while restricting the entry of others, makes the BTB a physiological barrier crucial for the development and maturation of GC.

HISTOPATHOLOGY AND MECHANISMS OF TESTICULAR INFLAMMATION IN RODENT EAO MODEL

Testis histopathology in EAO is characterized by an increase in the number of dendritic cells (DC), macrophages (Mϕ), mast cells and T lymphocytes (L) distributed in the interstitium close to ST, exhibiting different degrees of GC sloughing (mainly spermatids and spermatocytes). Germ cell apoptosis and multinucleated spermatids in the lumen of ST as well as vacuolization in the cytoplasm of Sertoli cell are frequently observed. Damage of ST is initially focal, followed by development of severe orchitis showing aspermatogenesis and fibrosis of the wall of most ST (**Figure 1**). L and Mϕ distributed in the interstitium might enter the ST in mice as well as in humans in contrast to rats. Large granulomae are frequently observed. Hyperplasia and hypertrophy of Leydig cells and an increased number of small blood vessels are also detected (**Figure 2**).

Blood Testis Barrier

During testicular inflammation BTB integrity is impaired—denoted by increased permeability to tracers (52, 53). Concomitantly, changes in expression of cell junction adhesion molecules were detected. A decrease in occludin and Cx43 expression and an increase in the expression of N-cadherin and α-catenin were observed in testis of rats with EAO (53, 54).

Increased levels of inflammatory cytokines in the EAO testis alter the normal function of the BTB. Local administration of IL17A into the rat testis increases BTB permeability by reducing occludin expression and delocalization of claudin-11 (55). IL6 impairs the Sertoli cell tight junction barrier in normal rats by perturbing the MAPK14 signaling pathway and inhibiting BTB-constituent protein degradation (54, 56). TNFα administered locally to adult rat testis inhibits the steady-state protein levels of occludin, ZO-1, and N-cadherin altering the BTB function (57).

Dendritic Cells

The maturation state of DC cells is regarded as a control point for the induction of peripheral tolerance or autoimmunity. Purified DC from EAO rat testes demonstrated significantly upregulated expression of the chemokine receptor CCR7, which is responsible for the migration of DC to the draining lymph nodes (58). Moreover, the expression of IL10 and IL12p35 transcripts were detectable only in DC from inflamed testes, pointing to a mature immunogenic state before imminent migration to the lymph nodes. DC in draining lymph nodes from rats with EAO are mature, present antigens to T cells, and stimulate an autoimmune response against testicular antigens, thereby causing immunological disturbances of the testis (59).

Macrophages

A large population of resident Mϕ subsets in the interstitium of normal testis is in close association with Leydig cells (60). Testicular Mϕ modulate spermatogenesis, steroidogenesis and also BTB permeability in the normal testis (61). Once testicular immune privilege is disrupted by immunization with spermatic antigens, the number of Mϕ progressively increases in the testicular interstitium. Chemokines, mainly MCP1, acting on endothelial cells, facilitate infiltration into the testis of $CD68^+$ $CD163^-$ monocytes from circulation, expressing the MCP1 receptor CCR2 (62, 63). Most of these infiltrating Mϕ express MHCII molecules and secrete pro-inflammatory mediators, mainly TNFα, IL6, and NO involved in BTB impairment, lymphocyte infiltration, and germ cell apoptosis (53, 64–66). Depletion of Mϕ by *in vivo* administration of liposomes containing clodronate significantly reduced the incidence and severity of EAO, thereby highlighting the requirement of these cells for disease induction (63).

T Cells

From the early focal EAO stage onwards, a large increase in the number of $CD4^+$ and $CD8^+$ T cells occurs in the interstitium in association with increasing damage of ST (67). Interestingly, in a mouse EAO testis, a population of double positive $CD4^+CD8^+$ T cells was detected (68). However, the function of these cells in the periphery is not very well-investigated. TNFα and IFNγ-producing Th1 cells and IL17-producing Th17 cells govern the early stage of EAO while $CD8^+$ T cells ($TNF\alpha^+$, $IFN\gamma^+$, and $IL17^+$) lead the disease to its chronic severe stage (69). Besides being the main source of Th1 and Th17 cytokines in the chronically inflamed testis, $CD8^+$ cells are the main subset expressing the CD25 activation marker (67). Together with the influx of auto-pathogenic T cells, $CD4^+$ and $CD8^+$ cells with regulatory phenotype (Tregs) also accumulate in EAO testis and in the lymph nodes draining the testis (TLN) (67, 70). These subsets show dynamic behavior during EAO progression; interstitial $CD4^+Foxp3^+$ Tregs reach a maximum number at the early stage of EAO and then decline at the chronic stage. However, the number of $CD8^+Foxp3^+$ subset that increases to a lesser extent than their $CD4^+$ $Foxp3^+$ counterparts during EAO onset remains stable throughout disease. The regulatory function of this subset was not evaluated. Most CD4+ Foxp3+ Tregs from TLN display an antigen-experienced phenotype and also express TGF-β. *In vitro* suppression studies showed that $CD4^+Foxp3^+$ Tregs derived from EAO TLN suppress T cell proliferation more efficiently than their counterparts derived from normal TLN, suggesting that EAO Tregs are over-activated by inflammation (70). However, Tregs present in the testicular inflammatory microenvironment fail to counteract deleterious autoimmune effects on GC; consequently, tissue damage progresses (71).

Germ Cells

In EAO testis, GC death occurs through apoptotic mechanisms involving FasL-Fas, TNFα-TNFR, IL6-IL6R, and NO-NOS systems, via autocrine or paracrine pathways. The number of apoptotic GC sloughed from the seminiferous epithelium expressing Fas, TNFR, or IL6R increases with progression of

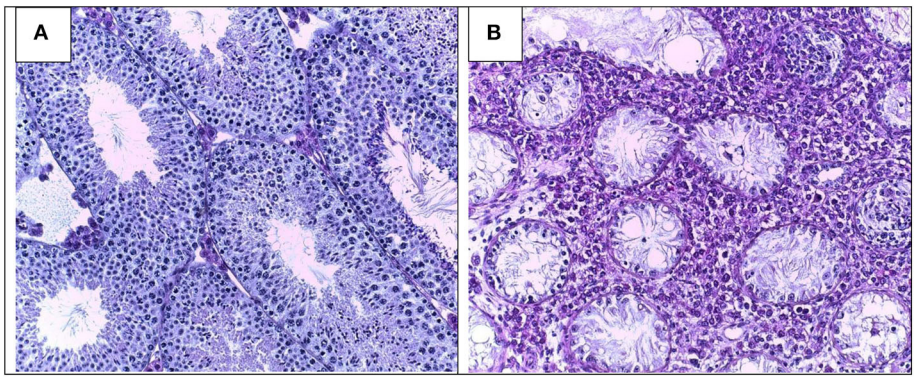

FIGURE 1 | Testicular histology in normal **(A)** and severe EAO **(B)** mouse testis. Typical histopathological changes include infiltration of the interstitium by immune cells, sloughing of germ cells leading to aspermatogenesis, vacuolization of Sertoli cells cytoplasm, thickening of lamina propria, extensive necrosis, and fibrosis of seminiferous tubules (magnification × 200).

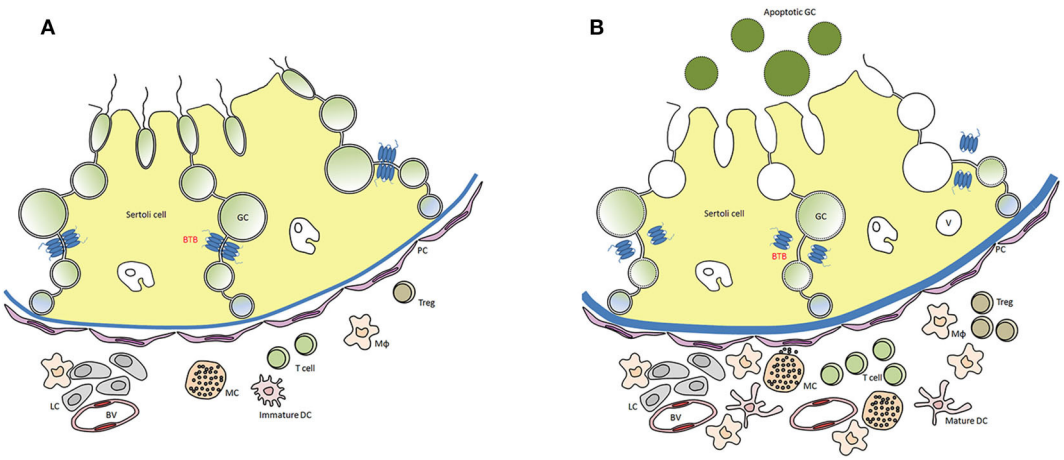

FIGURE 2 | Distribution of immune cells in a rodent testis section under normal **(A)** and inflammatory conditions (EAO) **(B)**. In EAO, dendritic cells (DC), macrophages (M*Φ*), T cells, regulatory T cells (Treg), and mast cells (MC) are increased in number and distributed in the interstitium, mainly in the peritubular area of damaged seminiferous tubules (ST). Some MC are located in a close proximity to peritubular cells (PC). Impairment of blood testis barrier (BTB) and disturbances of spermatogenesis (presence of apoptotic germ cells in the ST lumen) are illustrated; BV, blood vessel; v, vacuole in Sertoli cell cytoplasm [modified from (51)].

testicular damage (66, 72, 73). With the influx of T cells expressing FasL, the content of the soluble form of FasL increases in the interstitial fluid. This factor is capable of crossing the altered BTB in inflammation, and triggers Fas-sensitive germ cell apoptosis (74). TNFα produced in large quantities by resident Mϕ, infiltrating monocytes, and also by T cells induces apoptosis of spermatocytes and spermatids expressing TNFR1 (66, 72, 74). IL6 secreted by infiltrating Mϕ, Leydig, and peritubular cells activates executioner caspase-3, resulting in apoptosis of $IL6R^{+}$ GC (73).

An oxidative microenvironment is generated in EAO testis by high levels of NO, produced mainly by both resident and infiltrating Mϕ (65). NO reaches ST and induces basal germ cell apoptosis by activating the mitochondrial pathway. Spermatogonia are likely sensitive to oxidative stress generated by NO since DETA-NO, a compound that releases NO, induces cell cycle arrest and apoptosis in GC-1 cell line (75).

Apoptosis in EAO testis occurs via a cytokine-dependent amplification loop resulting from the activation of death receptors and oxidative damage of GC. This phenomenon is sustained by the ongoing influx of immune cells into the testicular interstitium.

FIBROTIC RESPONSE—INVOLVEMENT OF ACTIVIN A

In severe EAO fibrotic remodeling is a hallmark of the disease. Fibrotic changes are initiated around the ST and show excessive production and deposition of extracellular matrix proteins such as fibronectin and collagens and a thickening of the lamina propria. The fibrotic alterations are accompanied by changes in the morphological appearance and thickening of the α-smooth muscle actin layer in the peritubular cells, belonging to the

population of myofibroblasts in the testis (68, 76). Expression of fibronectin correlates positively with the disease damage score and fibrosis. Moreover, there is strong correlation between activin A concentrations and fibrotic damage in EAO testis (76). These changes show—also in human biopsies from patients with Sertoli cell only syndrom—a clear relationship between activin A expression—and lymphocytic infiltrates (76). Stimulation of peritubular cells by activin A increased levels of fibronectin and collagen I and IV implicating activin A as an important mediator of fibrotic remodeling during testicular inflammation (76). This underlines a function for activin A beside its classical endocrine function in inducing follicle stimulating hormone (FSH) secretion from the pituitary but increasingly as an important regulator of inflammation and fibrosis in many organs (77). Activin A is broadly expressed in testicular cells and stimulation of cultured Sertoli cells with TNFα leads to elevated expression of activin A (76). However, elevating circulating levels of follistatin, an endogenous antagonist of the activins prior to EAO induction was not sufficient to fully inhibit the disease development, although the severity of the disease and the extent of the fibrotic damage was reduced (52).

HORMONAL REGULATION DURING INFLAMMATORY PHASE OF THE DISEASE

The hormonal status of EAO animals shows disturbances of the hypothalamic-testicular axis at several levels. In EAO rats the levels of FSH are increased while the concentration of testosterone in serum is significantly downregulated (78–80). In contrast, the levels of intratesticular testosterone were either upregulated or unchanged, depending on the scientific report (78–80). Earlier *in vitro* experiments demonstrated that basal and human chorionic gonadotropin (hCG) stimulated testosterone production were significantly elevated in EAO testis (81). Moreover, Leydig cells from EAO testis *in vitro* showed an increased basal and hCG stimulated testosterone production compared to cells from control animals. Stimulation with TNFα inhibited this effect (72). Interestingly, testosterone substitution of EAO rats demonstrated a reduction of macrophage accumulation and CD4+ T cell influx at the testicular level, while the numbers of regulatory CD4+CD25+Foxp3+ T cells were increased. Testosterone treatment induced a strong increase in the number of regulatory T cells *in vivo* and *in vitro* (80, 82). Of note, androgens through androgen receptor modulate expression of Foxp3 (83) (**Table 1**).

INVOLVEMENT OF THE EPIDIDYMIS

In EAO mice, the epididymis underwent a region-specific immune response positively correlating to the severity of orchitis (28, 84). Similar to the observed differential immune responsiveness in a model of acute bacterial epididymitis (85, 86), the distally located cauda epididymidis and vas deferens show a severe immune reaction in EAO mice characterized by an upregulated expression of cytokines and immunomodulatory factors (*Tgfb1, Ccl2, Il1b, Il10, Tnf, Foxp3, Ido1*), immune cell infiltration, fibrosis and epithelial damage resulting in a loss of tissue integrity and subsequent aggregation of displaced spermatozoa within the interstitium (84). The proximal regions (initial segment and caput), in contrast, do not reveal histopathological alterations or an upregulated expression of cytokines, although these regions are more densely vascularized and harbor a high number of resident immune cells (87, 88). It needs to be noted though that data on epididymal reactions in EAO models are very scarce and thus the underlying molecular pathomechanisms remain unknown.

TABLE 1 | Pathological events leading to development of experimental autoimmune orchitis (EAO).

Structural and functional changes in Sertoli cells	Impairment of BTB structure and function by the action of pro-inflammatory cytokines mainly secreted by immune cells Vacuolization of Sertoli cell cytoplasm
Immunopathology	Testicular dendritic cells (DC) become mature, migrate to the testis-draining lymph nodes (TLN) and activate T cells
	Inflammatory macrophages (MΦ), DC, effector T lymphocytes (Th1, Th17, and $CD8^+$) and mast cells (MC), infiltrate the testis $CD4^+$ $Foxp3^+$ regulatory T lymphocytes (Tregs) actively accumulate within the testis and TLN Small vessels increase in number and chemokines enhance immune cell infiltration
	Tregs present in the testis fail to counterbalance immunoreactions that cause deleterious effects on germ cells (GC)
	Antigens released from damaged seminiferous tubules (ST) amplify the autoimmune response leading to continuous antigen presentation to T lymphocytes in TLN (chronification of orchitis)
Disturbances of spermatogenesis	GC apoptosis and sloughing in the tubular lumen mainly induced by the action of TNFα, IL6, NO, and Fas ligand
Hormonal changes	Impairment of androgen production
Chronic phase of disease	Aspermatogenesis, ST atrophy, fibrosis and thickening of ST wall Infertility

DISCUSSION

In summary, rodent models of EAO offer a valuable tool to discover the decisive mechanisms for the development of autoimmune-based epididymo-testicular inflammation. However, caution is necessary in extrapolating the data from rodent models to human due to several differences at the immunological and cellular level. Silent asymptomatic testicular inflammation in human is rather difficult to diagnose and treatment hampered due to missing non-invasive diagnostic tools. Possible therapeutical interventions and the development of new non-invasive diagnostic tools, such as serum assays may offer potential developments in the field gathered from the animal model. Several previous studies were already successfully dealing with the therapeutic inhibition of EAO by using e.g., depletion of Mϕ (63), blockade of pro-inflammatory

mediators (41, 52, 64, 89) or administration of testosterone (80). Supplementation of reduced testosterone levels in EAO rats led to inhibition of disease development and suggests testosterone as an immunoregulatory and immunosuppressive factor during testicular inflammation (80). Further studies are necessary to define the biomarkers and possible targets of autoimmune-based testicular inflammation.

MAIN OUTSTANDING QUESTIONS IN THE FIELD

To further our understanding of the immunopathology of autoimmune based impairment of fertility, the following aspects would warrant attention in future research: (a) the identification of molecular mechanism that trigger the autoimmune attack in the human testis without obvious presence of pathogens, (b) the evaluation of specific genetic predisposition in humans responsible for susceptibility to autoimmune diseases of the gonads, (c) elucidation of the common features of testis autoimmunity with autoimmune diseases of other organs, mainly in relation to Tregs behavior, and (d) the role of specific testicular somatic cells beside immune cells in the development of the disease.

AUTHOR CONTRIBUTIONS

LL, VG, MT, CP, PJ, CP, AM, and MF performed literature research and wrote the manuscript together. All authors reviewed and approved the final version of the manuscript.

FUNDING

International Research Training Group between Justus Liebig University of Giessen and Monash University, Melbourne (GRK 1871/1-2) on Molecular pathogenesis on male reproductive disorders funded by the Deutsche Forschungsgemeinschaft and Monash University. Universidad de Buenos Aires and Consejo Nacional de Investigaciones Científicas y Técnicas (CONICET).

REFERENCES

1. Rowe PJ, Comhaire F, Hargreave T, Mahmoud A. *WHO Manual for the Standarized Investigation, Diagnosis and Management of the Infertile Male.* Cambridge: Cambridge University Press (2000).
2. Weidner W, Pilatz A, Diemer T, Schuppe HC, Rusz A, Wagenlehner F. Male urogenital infections: impact of infection and inflammation on ejaculate parameters. *World J Urol.* (2013) 31:717–23. doi: 10.1007/s00345-013-1082-7
3. Frungieri MB, Calandra RS, Bartke A, Matzkin ME. Ageing and inflammation in the male reproductive tract. *Andrologia.* (2018) 50:1–9. doi: 10.1111/and.13034
4. Klein B, Haggeney T, Fietz D, Indumathy S, Loveland KL, Hedger M, et al. Specific immune cell and cytokine characteristics of human testicular germ cell neoplasia. *Hum Reprod.* (2016) 31:2192–202. doi: 10.1093/humrep/dew211
5. Leisegang K, Henkel R, Agarwal A. Obesity and metabolic syndrome associated with systemic inflammation and the impact on the male reproductive system. *Am J Reprod Immunol.* (2019) 82:e13178. doi: 10.1111/aji.13178
6. Jahnukainen K, Jorgensen N, Pollanen P, Giwercman A, Skakkebaek NE. Incidence of testicular mononuclear cell infiltrates in normal human males and in patients with germ cell neoplasia. *Int J Androl.* (1995) 18:313–20. doi: 10.1111/j.1365-2605.1995.tb00423.x
7. Nistal M, Riestra ML, Paniagua R. Focal orchitis in undescended testes: discussion of pathogenetic mechanisms of tubular atrophy. *Arch Pathol Lab Med.* (2002) 126:64–9. doi: 10.1043/0003-9985(2002)126<0064:FOIUT>2.0.CO;2
8. Fijak M, Pilatz A, Hedger MP, Nicolas N, Bhushan S, Michel V, et al. Infectious, inflammatory and "autoimmune" male factor infertility: how do rodent models inform clinical practice? *Hum Reprod Update.* (2018) 24:416–41. doi: 10.1093/humupd/dmy009
9. Schuppe H-C, Pilatz A, Hossain H, Diemer T, Wagenlehner F, Weidner W. urogenital infection as a risk factor for male infertility. *Dtsch Arztebl Int.* (2017) 114:339–46. doi: 10.3238/arztebl.2017.0339
10. Vickram A, Dhama K, Chakraborty S, Samad HA, Latheef SK, Sharun K, et al. Role of antisperm antibodies in infertility, pregnancy, and potential forcontraceptive and antifertility vaccine designs: research progress and pioneering vision. *Vaccines.* (2019) 7:116. doi: 10.3390/vaccines7030116
11. Marconi M, Pilatz A, Wagenlehner F, Diemer T, Weidner W. Are antisperm antibodies really associated with proven chronic inflammatory and infectious diseases of the male reproductive tract? *Eur Urol.* (2009) 56:708–15. doi: 10.1016/j.eururo.2008.08.001
12. Francavilla F, Barbonetti A. Male autoimmune infertility. In: Krause W, Naz R, editors. *Immune Infertility Impact of Immune Reactions on Human Fertility.* 2nd ed. Cham: Springer International Publishing (2017) p. 187–96.
13. Aitchison M, Mufti GR, Farrell J, Paterson PJ, Scott R. Granulomatous orchitis. review of 15 cases. *Br J Urol.* (1990) 66:312–4. doi: 10.1111/j.1464-410X.1990.tb14934.x
14. Roy S, Hooda S, Parwani A V. Idiopathic granulomatous orchitis. *Pathol Res Pract.* (2011) 207:275–8. doi: 10.1016/j.prp.2011.02.005
15. Tchiokadze S, Galdava G. Clinical and anamnestic characteristics of development of antisperm immunity in infertile men. *Georgian Med News.* (2015) 246:18–22.
16. Fijak M, Zeller T, Huys T, Klug J, Wahle E, Linder M, et al. Autoantibodies against protein disulfide isomerase ER-60 are a diagnostic marker for low-grade testicular inflammation. *Hum Reprod.* (2014) 29:2382–92. doi: 10.1093/humrep/deu226
17. Kisand K, Peterson P. Autoimmune polyendocrinopathy candidiasis ectodermal dystrophy: known and novel aspects of the syndrome. *Ann N Y Acad Sci.* (2011) 1246:77–91. doi: 10.1111/j.1749-6632.2011.06308.x
18. Pelletier RM. Cyclic formation and decay of the blood-testis barrier in the mink (Mustela vison), a seasonal breeder. *Am J Anat.* (1986) 175:91–117. doi: 10.1002/aja.1001750109
19. Pelletier R-M, Yoon SR, Akpovi CD, Silvas E, Vitale ML. Defects in the regulatory clearance mechanisms favor the breakdown of self-tolerance during spontaneous autoimmune orchitis. *Am J Physiol Regul Integr Comp Physiol.* (2009) 296:R743–62. doi: 10.1152/ajpregu.90751.2008
20. Wheeler K, Tardif S, Rival C, Luu B, Bui E, Del Rio R, et al. Regulatory T cells control tolerogenic versus autoimmune response to sperm in vasectomy. *Proc Natl Acad Sci USA.* (2011) 108:7511–6. doi: 10.1073/pnas.1017615108
21. Taguchi O, Nishizuka Y. Experimental autoimmune orchitis after neonatal thymectomy in the mouse. *Clin Exp Immunol.* (1981) 46:425–34.
22. Tung KS, Smith S, Matzner P, Kasai K, Oliver J, Feuchter F, et al. Murine autoimmune oophoritis, epididymoorchitis, and gastritis induced by day 3 thymectomy. *Am J Pathol.* (1987) 126:303–14.
23. Taurog JD, Rival C, van Duivenvoorde LM, Satumtira N, Dorris ML, Sun M, et al. Autoimmune epididymoorchitis is essential to the pathogenesis of male-specific spondylarthritis in HLA-B27-transgenic rats. *Arthritis Rheum.* (2012) 64:2518–28. doi: 10.1002/art.34480
24. Lustig L, Guazzone VA, Tung KSK. Autoimmune orchitis and autoimmune oophoritis. In: Rose N, Mackay I, editors. *The Autoimmune Diseases.* 6th ed. London: Elsevier Inc. (2019) p. 1235–51.

25. Voisin GA, Delauney A, Barber M. Sur les lesions testiculaires provoquee's chez les cobayes par iso- et autosensibilisation. *Ann Inst Pasteur.* (1951) 81:48–63.
26. Freund J, Lipton MM, Thompson GE. Aspermatogenesis in the guinea pig induced by testicular tissue and adjuvants. *J Exp Med.* (1953) 97:711–26. doi: 10.1084/jem.97.5.711
27. Teuscher C, Smith SM, Goldberg EH, Shearer GM, Tung KS. Experimental allergic orchitis in mice. I. genetic control of susceptibility and resistance to induction of autoimmune orchitis. *Immunogenetics.* (1985) 22:323–33. doi: 10.1007/BF00430916
28. Kohno S, Munoz JA, Williams TM, Teuscher C, Bernard CC, Tung KS. Immunopathology of murine experimental allergic orchitis. *J Immunol.* (1983) 130:2675–82.
29. Doncel GF, Di Paola JA, Lustig L. Sequential study of the histopathology and cellular and humoral immune response during the development of an autoimmune orchitis in Wistar rats. *Am J Reprod Immunol.* (1989) 20:44–51. doi: 10.1111/j.1600-0897.1989.tb00638.x
30. Terayama H, Hirai S, Naito M, Qu N, Katagiri C, Nagahori K, et al. Specific autoantigens identified by sera obtained from mice that are immunized with testicular germ cells alone. *Sci Rep.* (2016) 6:35599. doi: 10.1038/srep 35599
31. Fijak M, Iosub R, Schneider E, Linder M, Respondek K, Klug J, et al. Identification of immunodominant autoantigens in rat autoimmune orchitis. *J Pathol.* (2005) 207:127–38. doi: 10.1002/path.1828
32. Tardif S, Brady HA, Breazeale KR, Bi M, Thompson LD, Bruemmer JE, et al. Zonadhesin D3-polypeptides vary among species but are similar in *Equus* species capable of interbreeding. *Biol Reprod.* (2010) 82:413–21. doi: 10.1095/biolreprod.109.077891
33. Tung KSK, Harakal J, Qiao H, Rival C, Li JCH, Paul AGA, et al. Egress of sperm autoantigen from seminiferous tubules maintains systemic tolerance. *J Clin Invest.* (2017) 127:1046–60. doi: 10.1172/JCI89927
34. Head JR, Neaves WB, Billingham RE. Immune privilege in the testis. I. basic parameters of allograft survival. *Transplantation.* (1983) 36:423–31. doi: 10.1097/00007890-198310000-00014
35. Arck P, Solano ME, Walecki M, Meinhardt A. The immune privilege of testis and gravid uterus: same difference? *Mol Cell Endocrinol.* (2014) 382:509–20. doi: 10.1016/j.mce.2013.09.022
36. Fijak M, Meinhardt A. The testis in immune privilege. *Immunol Rev.* (2006) 213:66–81. doi: 10.1111/j.1600-065X.2006.00438.x
37. Schuppe HC, Meinhardt A. Immune privilege and inflammation of the testis. *Chem Immunol Allergy.* (2005) 88:1–14. doi: 10.1159/0000 87816
38. Chui K, Trivedi A, Cheng CY, Cherbavaz DB, Dazin PF, Huynh ALT, et al. Characterization and functionality of proliferative human Sertoli cells. *Cell Transplant.* (2011) 20:619–35. doi: 10.3727/096368910X536563
39. Dettin L, Rubinstein N, Aoki A, Rabinovich GA, Maldonado CA. Regulated expression and ultrastructural localization of galectin-1, a proapoptotic beta-galactoside-binding lectin, during spermatogenesis in rat testis. *Biol Reprod.* (2003) 68:51–9. doi: 10.1095/biolreprod.102.006361
40. Timmons PM, Rigby PWJ, Poirier F. The murine seminiferous epithelial cycle is pre-figured in the Sertoli cells of the embryonic testis. *Development.* (2002) 129:635–47.
41. Pérez C V, Gómez LG, Gualdoni GS, Lustig L, Rabinovich GA, Guazzone VA. Dual roles of endogenous and exogenous galectin-1 in the control of testicular immunopathology. *Sci Rep.* (2015) 5:12259. doi: 10.1038/srep12259
42. Fallarino F, Luca G, Calvitti M, Mancuso F, Nastruzzi C, Fioretti MC, et al. Therapy of experimental type 1 diabetes by isolated Sertoli cell xenografts alone. *J Exp Med.* (2009) 206:2511–26. doi: 10.1084/jem.20090134
43. Gualdoni GS, Jacobo P V, Sobarzo CM, Pérez C V, Matzkin ME, Höcht C, et al. Role of indoleamine 2,3-dioxygenase in testicular immune-privilege. *Sci Rep.* (2019) 9:15919. doi: 10.1038/s41598-019-52192-8
44. França LR, Hess RA, Dufour JM, Hofmann MC, Griswold MD. The Sertoli cell: one hundred fifty years of beauty and plasticity. *Andrology.* (2016) 4:189–212. doi: 10.1111/andr.12165
45. Stanton PG. Regulation of the blood-testis barrier. *Semin Cell Dev Biol.* (2016) 59:166–73. doi: 10.1016/j.semcdb.2016.06.018
46. Mruk DD, Cheng CY. The mammalian blood-testis barrier: its biology and regulation. *Endocr Rev.* (2015) 36:564–91. doi: 10.1210/er.2014-1101
47. Gerber J, Heinrich J, Brehm R. Blood-testis barrier and Sertoli cell function: lessons from SCCx43KO mice. *Reproduction.* (2016) 151:R15–27. doi: 10.1530/REP-15-0366
48. Lee NPY, Mruk DD, Wong C-H, Cheng CY. Regulation of Sertoli-germ cell adherens junction dynamics in the testis via the nitric oxide synthase (NOS)/cGMP/protein kinase G (PRKG)/beta-catenin (CATNB) signaling pathway: an *in vitro* and *in vivo* study. *Biol Reprod.* (2005) 73:458–71. doi: 10.1095/biolreprod.105.040766
49. Meng J, Holdcraft RW, Shima JE, Griswold MD, Braun RE. Androgens regulate the permeability of the blood-testis barrier. *Proc Natl Acad Sci USA.* (2005) 102:16696–700. doi: 10.1073/pnas.0506084102
50. Wang R-S, Yeh S, Chen L-M, Lin H-Y, Zhang C, Ni J, et al. Androgen receptor in sertoli cell is essential for germ cell nursery and junctional complex formation in mouse testes. *Endocrinology.* (2006) 147:5624–33. doi: 10.1210/en.2006-0138
51. Pérez C V, Theas MS, Jacobo P V, Jarazo-Dietrich S, Guazzone VA, Lustig L. Dual role of immune cells in the testis: protective or pathogenic for germ cells? *Spermatogenesis.* (2013) 3:e23870. doi: 10.4161/spmg.23870
52. Nicolas N, Muir JA, Hayward S, Chen JL, Stanton PG, Gregorevic P, et al. Induction of experimental autoimmune orchitis in mice: responses to elevated circulating levels of the activin-binding protein, follistatin. *Reproduction.* (2017) 154:293–305. doi: 10.1530/REP-17-0010
53. Pérez CV, Sobarzo CM, Jacobo PV, Pellizzari EH, Cigorraga SB, Denduchis B, et al. Loss of occludin expression and impairment of blood-testis barrier permeability in rats with autoimmune orchitis: effect of interleukin 6 on Sertoli cell tight junctions. *Biol Reprod.* (2012) 87:122. doi: 10.1095/biolreprod.112.101709
54. Pérez C, Sobarzo C, Jacobo P, Jarazo Dietrich S, Theas M, Denduchis B, et al. Impaired expression and distribution of adherens and gap junction proteins in the seminiferous tubules of rats undergoing autoimmune orchitis. *Int J Androl.* (2011) 34(Pt. 2):e566–77. doi: 10.1111/j.1365-2605.2011.01165.x
55. Pérez CV, Pellizzari EH, Cigorraga SB, Galardo MN, Naito M, Lustig L, et al. IL17A impairs blood-testis barrier integrity and induces testicular inflammation. *Cell Tissue Res.* (2014) 358:885–98. doi: 10.1007/s00441-014-1995-5
56. Zhang H, Yin Y, Wang G, Liu Z, Liu L, Sun F. Interleukin-6 disrupts blood-testis barrier through inhibiting protein degradation or activating phosphorylated ERK in Sertoli cells. *Sci Rep.* (2014) 4:4260. doi: 10.1038/srep04260
57. Li MWM, Xia W, Mruk DD, Wang CQF, Yan HHN, Siu MKY, et al. Tumor necrosis factor {alpha} reversibly disrupts the blood-testis barrier and impairs Sertoli-germ cell adhesion in the seminiferous epithelium of adult rat testes. *J Endocrinol.* (2006) 190:313–29. doi: 10.1677/joe.1.06781
58. Rival C, Guazzone VA, von Wulffen W, Hackstein H, Schneider E, Lustig L, et al. Expression of co-stimulatory molecules, chemokine receptors and proinflammatory cytokines in dendritic cells from normal and chronically inflamed rat testis. *Mol Hum Reprod.* (2007) 13:853–61. doi: 10.1093/molehr/gam067
59. Guazzone VA, Hollwegs S, Mardirosian M, Jacobo P, Hackstein H, Wygrecka M, et al. Characterization of dendritic cells in testicular draining lymph nodes in a rat model of experimental autoimmune orchitis. *Int J Androl.* (2011) 34:276–89. doi: 10.1111/j.1365-2605.2010.01082.x
60. Hutson JC. Physiologic interactions between macrophages and Leydig cells. *Exp Biol Med.* (2006) 231:1–7. doi: 10.1177/153537020623100101
61. Mossadegh-Keller N, Sieweke MH. Testicular macrophages: Guardians of fertility. *Cell Immunol.* (2018) 330:120–5. doi: 10.1016/j.cellimm.2018.03.009
62. Guazzone VA, Rival C, Denduchis B, Lustig L. Monocyte chemoattractant protein-1 (MCP-1/CCL2) in experimental autoimmune orchitis. *J Reprod Immunol.* (2003) 60:143–57. doi: 10.1016/j.jri.2003.08.001
63. Rival C, Theas MS, Suescun MO, Jacobo P, Guazzone V, van Rooijen N, et al. Functional and phenotypic characteristics of testicular macrophages in experimental autoimmune orchitis. *J Pathol.* (2008) 215:108–17. doi: 10.1002/path.2328
64. Jarazo Dietrich S, Fass MI, Jacobo PV, Sobarzo CMA, Lustig L, Theas MS. Inhibition of NOS-NO system prevents autoimmune orchitis development in rats: relevance of NO released by testicular macrophages in germ cell apoptosis and testosterone secretion. *PLoS ONE.* (2015) 10:e0128709. doi: 10.1371/journal.pone.0128709

65. Jarazo-Dietrich S, Jacobo P, Pérez C V, Guazzone VA, Lustig L, Theas MS. Up regulation of nitric oxide synthase-nitric oxide system in the testis of rats undergoing autoimmune orchitis. *Immunobiology.* (2012) 217:778–87. doi: 10.1016/j.imbio.2012.04.007
66. Theas MS, Rival C, Jarazo-Dietrich S, Jacobo P, Guazzone VA, Lustig L. Tumour necrosis factor-alpha released by testicular macrophages induces apoptosis of germ cells in autoimmune orchitis. *Hum Reprod.* (2008) 23:1865–72. doi: 10.1093/humrep/den240
67. Jacobo P, Guazzone VA, Jarazo-Dietrich S, Theas MS, Lustig L. Differential changes in CD4+ and CD8+ effector and regulatory T lymphocyte subsets in the testis of rats undergoing autoimmune orchitis. *J Reprod Immunol.* (2009) 81:44–54. doi: 10.1016/j.jri.2009.04.005
68. Nicolas N, Michel V, Bhushan S, Wahle E, Hayward S, Ludlow H, et al. Testicular activin and follistatin levels are elevated during the course of experimental autoimmune epididymo-orchitis in mice. *Sci Rep.* (2017) 7:42391. doi: 10.1038/srep42391
69. Jacobo P, Pérez CV, Theas MS, Guazzone VA, Lustig L. CD4+ and CD8+ T cells producing Th1 and Th17 cytokines are involved in the pathogenesis of autoimmune orchitis. *Reproduction.* (2011) 141:249–58. doi: 10.1530/REP-10-0362
70. Jacobo P, Guazzone VA, Pérez C V, Lustig L. CD4+ Foxp3+ regulatory T cells in autoimmune orchitis: phenotypic and functional characterization. *Am J Reprod Immunol.* (2015) 73:109–25. doi: 10.1111/aji.12312
71. Jacobo P. The role of regulatory T Cells in autoimmune orchitis. *Andrologia.* (2018) 50:e13092. doi: 10.1111/and.13092
72. Suescun MO, Rival C, Theas MS, Calandra RS, Lustig L. Involvement of tumor necrosis factor-alpha in the pathogenesis of autoimmune orchitis in rats. *Biol Reprod.* (2003) 68:2114–21. doi: 10.1095/biolreprod.102.011189
73. Rival C, Theas MS, Guazzone VA, Lustig L. Interleukin-6 and IL-6 receptor cell expression in testis of rats with autoimmune orchitis. *J Reprod Immunol.* (2006) 70:43–58. doi: 10.1016/j.jri.2005.10.006
74. Jacobo PV, Fass M, Pérez CV, Jarazo-Dietrich S, Lustig L, Theas MS. Involvement of soluble Fas Ligand in germ cell apoptosis in testis of rats undergoing autoimmune orchitis. *Cytokine.* (2012) 60:385–92. doi: 10.1016/j.cyto.2012.07.020
75. Ferreiro ME, Amarilla MS, Glienke L, Méndez CS, González C, Jacobo PV, et al. The inflammatory mediators TNFα and nitric oxide arrest spermatogonia GC-1 cell cycle. *Reprod Biol.* (2019) 19:329–39. doi: 10.1016/j.repbio.2019.11.001
76. Kauerhof AC, Nicolas N, Bhushan S, Wahle E, Loveland KA, Fietz D, et al. Investigation of activin A in inflammatory responses of the testis and its role in the development of testicular fibrosis. *Hum Reprod.* (2019) 34:1536–50. doi: 10.1093/humrep/dez109
77. Wijayarathna R, de Kretser DM. Activins in reproductive biology and beyond. *Hum Reprod Update.* (2016) 22:342–57. doi: 10.1093/humupd/dmv058
78. Suescun MO, Calandra RS, Lustig L. Alterations of testicular function after induced autoimmune orchitis in rats. *J Androl.* (1994) 15:442–8.
79. Suescun MO, Suescun MO, Lustig L, Calandra RS, Calandra RS, Groome NP, et al. Correlation between inhibin secretion and damage of seminiferous tubules in a model of experimental autoimmune orchitis. *J Endocrinol.* (2001) 170:113–20. doi: 10.1677/joe.0.1700113
80. Fijak M, Schneider E, Klug J, Bhushan S, Hackstein H, Schuler G, et al. Testosterone replacement effectively inhibits the development of experimental autoimmune orchitis in rats: evidence for a direct role of testosterone on regulatory T cell expansion. *J Immunol.* (2011) 186:5162–72. doi: 10.4049/jimmunol.1001958
81. Suescun MO, Calandra RS, Lustig L. Increased testosterone production *in vitro* by Leydig cells from rats with severe autoimmune orchitis. *Int J Androl.* (1997) 20:339–46. doi: 10.1046/j.1365-2605.1998.00076.x
82. Fijak M, Damm L-J, Wenzel J-P, Aslani F, Walecki M, Wahle E, et al. Influence of testosterone on inflammatory response in testicular cells and expression of transcription factor Foxp3 in T cells. *Am J Reprod Immunol.* (2015) 74:12–25. doi: 10.1111/aji.12363
83. Walecki M, Eisel F, Klug J, Baal N, Paradowska-Dogan A, Wahle E, et al. Androgen receptor modulates Foxp3 expression in CD4+CD25+Foxp3+ regulatory T-cells. *Mol Biol Cell.* (2015) 26:2845–57. doi: 10.1091/mbc.E14-08-1323
84. Wijayarathna R, Pasalic A, Nicolas N, Biniwale S, Ravinthiran R, Genovese R, et al. Region-specific immune responses to autoimmune epididymitis in the murine reproductive tract. *Cell Tissue Res.* (2020) 381:351–60. doi: 10.1007/s00441-020-03215-8
85. Michel V, Duan Y, Stoschek E, Bhushan S, Middendorff R, Young JM, et al. Uropathogenic *Escherichia coli* causes fibrotic remodelling of the epididymis. *J Pathol.* (2016) 240:15–24. doi: 10.1002/path.4748
86. Klein B, Bhushan S, Günther S, Middendorff R, Loveland KL, Hedger MP, et al. Differential tissue-specific damage caused by bacterial epididymo-orchitis in the mouse. *Mol Hum Reprod.* (2020) 26:215–27. doi: 10.1093/molehr/gaaa011
87. Da Silva N, Cortez-Retamozo V, Reinecker H-C, Wildgruber M, Hill E, Brown D, et al. A dense network of dendritic cells populates the murine epididymis. *Reproduction.* (2011) 141:653–63. doi: 10.1530/REP-10-0493
88. Battistone MA, Mendelsohn AC, Spallanzani RG, Brown D, Nair A V, Breton S. Region-specific transcriptomic and functional signatures of mononuclear phagocytes in the epididymis. *Mol Hum Reprod.* (2020) 26:14–29. doi: 10.1093/molehr/gaz059
89. Aslani F, Schuppe H-C, Guazzone VA, Bhushan S, Wahle E, Lochnit G, et al. Targeting high mobility group box protein 1 ameliorates testicular inflammation in experimental autoimmune orchitis. *Hum Reprod.* (2015) 30:417–31. doi: 10.1093/humrep/deu320

Conflict of Interest: The authors declare that the research was conducted in the absence of any commercial or financial relationships that could be construed as a potential conflict of interest.

frontiers in Immunology

MINI REVIEW
published: 30 September 2020
doi: 10.3389/fimmu.2020.583304

Immune Cell Subtypes and Their Function in the Testis

Sudhanshu Bhushan[1,2]*, *María S. Theas*[3,4], *Vanesa A. Guazzone*[3,4], *Patricia Jacobo*[3,4], *Ming Wang*[5], *Monika Fijak*[1,2], *Andreas Meinhardt*[1,2] *and Livia Lustig*[3,4]*

[1] Department of Anatomy and Cell Biology, Justus-Liebig University Giessen, Giessen, Germany, [2] Hessian Center of Reproductive Medicine, Justus-Leibig-University Giessen, Giessen, Germany, [3] Departamento de Biología Celular e Histología/Unidad Académica II, Facultad de Medicina, Universidad de Buenos Aires (UBA), Buenos Aires, Argentina, [4] Consejo Nacional de Investigaciones Científicas y Técnicas (CONICET), Facultad de Medicina, Instituto de Investigaciones Biomédicas (INBIOMED), Universidad de Buenos Aires (UBA), Buenos Aires, Argentina, [5] Medical Research Center, The First Affiliated Hospital of Zhengzhou University, Zhengzhou, China

OPEN ACCESS

Edited by:
Kenneth Tung,
University of Virginia, United States

Reviewed by:
Tony DeFalco,
Cincinnati Children's Hospital Medical Center, United States
Suresh Yenugu,
University of Hyderabad, India
Emily Bryan,
Queensland University of Technology, Australia

***Correspondence:**
Livia Lustig
livialustig38@yahoo.com.ar
Sudhanshu Bhushan
sudhanshu.bhushan@anatomie.med.uni-giessen.de

Specialty section:
This article was submitted to Mucosal Immunity, a section of the journal Frontiers in Immunology

Received: 14 July 2020
Accepted: 14 September 2020
Published: 30 September 2020

Citation:
Bhushan S, Theas MS, Guazzone VA, Jacobo P, Wang M, Fijak M, Meinhardt A and Lustig L (2020) Immune Cell Subtypes and Their Function in the Testis. Front. Immunol. 11:583304. doi: 10.3389/fimmu.2020.583304

Immunoregulation in the testis is characterized by a balance between immunosuppression (or immune privilege) and the ability to react to infections and inflammation. In this review, we analyze the phenotypes of the various immune cell subtypes present in the testis, and how their functions change between homeostatic and inflammatory conditions. Starting with testicular macrophages, we explore how this heterogeneous population is shaped by the testicular microenvironment to ensure immune privilege. We then describe how dendritic cells exhibit a tolerogenic status under normal conditions, but proliferate, mature and then stimulate effector T-cell expansion under inflammatory conditions. Finally, we outline the two T-cell populations in the testis: $CD4^+/CD8^+$ αβ T cells and $CD4^+/CD8^+$ $Foxp3^+$ regulatory T cells and describe the distribution and function of mast cells. All these cells help modulate innate immunity and regulate the immune response. By improving our understanding of immune cell behavior in the testis under normal and inflammatory conditions, we will be better placed to evaluate testis impairment due to immune mechanisms in affected patients.

Keywords: testis, immune privilege, macrophages, dendritic cells, T lymphocytes, mast cells

INTRODUCTION

The mammalian testis is divided into two main compartments: the convoluted seminiferous tubules, where spermatogenesis occurs, and the interstitial space where Leydig cells (LC) produce the male sex hormones (androgens). During spermatogenesis, germ cells divide and mature in close association with somatic Sertoli cells (SC) that extend from the basal membrane to the tubule lumen. Multiple highly specialized cell junctions namely tight, adherens and gap junctions extend between neighboring SC to form a blood-testis-barrier (BTB) that is permissive to the developing germ cells. Bordering the SC and spermatogonia, a basement membrane containing extracellular matrix proteins and a contractile peritubular cells (PTC, also known as myoid cells) sheet divides the seminiferous epithelium from the interstitium. Organization of the PTC sheet varies by species; in rodents, only one PTC layer is seen whereas in humans it typically consists of 5–7 layers (1). Immune cells in the testis are found exclusively in the interstitium, in close association with either PTC or LC, as well as with lymphatic and blood vessels (**Figure 1**). Some authors described that in rodents lymphatic vessels are restricted to the tunica

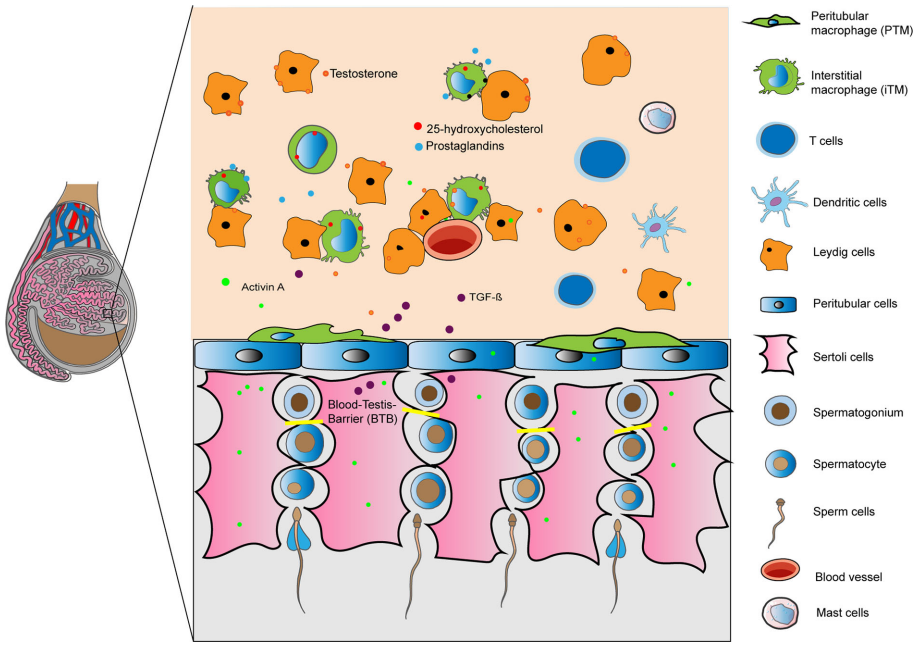

FIGURE 1 | Immunoregulation of the testis is mediated by a combination of structural (blood- testis barrier) and cellular derived factors. Illustration shows in a rodent testis, resident macrophages, tolerogenic dendritic cells, T cells and mast cells in the interstitium interacting with Leydig, Sertoli and peritubular cells releasing factors to create an optimal microenvironment for germ cells. Under inflammatory conditions immune cells are able to respond to invading pathogens.

albuginea (2–4), while others reported irregular channels incompletely bound by endothelial cells (5). In contrast, Kitadate et al. (6) described in mice testis parietal lymphatic endothelial cells (LE) that cover the surface of lymphatic space, mainly in the peritubular area close to the PTC layer contributing to the spermatogenic stem cell niche homeostasis through the supply of fibroblast growth factor ligands secreted by LE cells (6). Telocytes, a stromal cell type similarly localized as LE cells, have been recently identified in rodent and human testis (7, 8). It has been suggested a possible role of telocytes in the regulation of lymphatic capillary function (9). The immunomodulatory factor secreted by immune cells, and somatic cells (LC, SC, and PTC), in combination with BTB, forms a unique immunological environment that: (i) protects immunogenic germ-cell-specific neoantigens and transplants from immune attack, and (ii) responds to invading pathogens by eliciting a delicately balanced immune response to protect sensitive germ cells (10, 11).

The functions of the BTB, SC, LC, and PTC in preserving the immune privileged status of the testis has been described in details in previous reviews (11, 12). As such, we rather describe the different immune cells of the testis that maintain the immune privileged status and contribute to the immune response against inflammatory stressors.

MACROPHAGES

In the broadest sense, macrophages constitute an immune cell population with phagocytic characteristics, ingesting foreign particles and invading pathogens such as bacteria, and clearing cell debris. Given their essential role, macrophages are found in all mammalian organs where they perform immune and nonimmune functions (13). As is the case for other organs, macrophages are by far the most abundant and heterogeneous immune-cell population found in the testis (14, 15). The heterogeneity of these tissue-resident macrophages has been delineated based on cell surface marker expression, anatomical localization, gene expression profiles, ontogeny, and post-natal development. Under normal conditions, most testicular macrophages (TM) express the core macrophage markers F4/80, CD11b, AIF, and CX3CR1 (4, 16). The heterogeneity of the macrophages is evidenced by the differential expression of surface markers CD64 and major histocompatibility complex class II (MHC II), besides their localization relative to other cells within the testis (4, 16).

Under steady conditions, interstitial (iTM) and peritubular (pTM) macrophages predominate (16). iTM are characterized by $CD64^{hi}MHC^{lo}$ expression and are found adjacent to LC and blood vessels (**Figure 1**) (4, 16). By contrast, pTM are characterized by $CD64^{lo}MHC^{hi}$ expression and are found adjacent to the seminiferous tubules (**Figure 1**) (4, 16). Each TM subpopulation also expresses a unique transcriptional profile, which is indicative of functional specialization. For example, $CD64^{lo}MHC^{hi}$ pTM express high levels of antigen presentation genes, such as genes encoding the MHCII — H2Dmb, H2Eb1, and, H2K1. Conversely, $CD64^{hi}MHC^{lo}$pTM express high levels of immunosuppressive genes, namely, IL10 and Marco (16).

A recent study used single-cell mRNA sequencing (scRNA-seq) to identify two interstitial macrophage sub-populations of the lung, which were also found in the testis: Lyve1^{lo}MHCII^{hi} and Lyve1^{hi}MHCII^{lo}. These two subpopulations are distinct in localization, phenotype, and gene expression (17). Although TM seem to comprise only two main subsets, in-depth analyses using scRNA-seq and high powered confocal microscopy are needed to characterize the extent of heterogeneity in detail.

Resident macrophages in the brain, liver, and lung that arise embryonically either from the yolk sac or fetal liver; are maintained locally by self-renewal in adult life without notable contribution from blood monocytes (18). In other organs, such as the intestine, dermis, and pancreas, macrophage populations are maintained by replacement from blood monocytes (19–22). However, the exact contribution of embryonic progenitors and blood monocytes that give rise to tissue-resident macrophages in adult life is still controversial. Moreover, the mechanism by which adult tissue resident macrophages maintained in adult life is not yet completely understood.We have made great progress in recent years to unravel the ontogeny and functional heterogeneity of macrophage population in different organs, the origins of TM are still unclear. iTM are thought to originate from embryonic progenitors, whereas pTM seem to arise postnatally from bone marrow derived cells (16); however, the relative contributions of embryonic progenitors to the adult TM and the mechanisms of TM maintenance in adulthood are undefined.

Although all tissue-resident macrophages arise from distinct cellular origin, (23) upon organ entry, tissue-specific signals polarize macrophages to endow them with tissue- specific functions (24). For example, the intranasal transfer of progenitors from either the yolk sac, fetal liver, or bone marrow to the lungs of *Csf2rb*$^{-/-}$ mice lacking adult alveolar macrophages resulted in the polarization of macrophage progenitors with functional and transcriptional properties reminiscent of alveolar macrophages. These findings suggest that intrinsic factors rather than cellular origins, might imprint the resident macrophage phenotype (25). The testis microenvironment contains numerous immunomodulatory molecules — namely testosterone, prostaglandins, corticosterone, activin, and 25 hydroxy-cholesterol (25HC) — that might govern TM phenotype and function (**Figure 1**) (14, 26). Indeed, we found that testosterone, prostaglandins, and corticosterone present in the testicular interstitial fluid can polarize GM-CSF-derived macrophages to immunosuppressive macrophages by inducing CD163 and IL10 expression with concomitant low TNF-α production (14). Other molecules, such as 25-HC and activin, are also produced in large amounts in the testis (26, 27). Whether these molecules can influence TM phenotype and function has not been investigated, we speculate that they likely have a role.

Recent data primarily from *in vitro* studies suggest a role for TM in maintaining the immune privileged state of the testis (28, 29). Specifically, TM exhibit anergy to inflammatory stimuli, which serves to protect developing germ cells from the deleterious effects of pro-inflammatory cytokine. The mechanisms underlying this subdued inflammatory response of TM could be based on the low expression of toll like receptor (TLR) signaling genes and impaired ubiquitination and degradation of the NF-κB inhibitor IκBα that ultimately inactivates the inflammatory NF-κB signaling pathway (28).

TM are immunoregulatory, secreting high levels of IL10, and producing low levels of TNF-α and nitric oxide (NO) upon stimulation with the TLR4 ligand, lipopolysaccharide (LPS) (28, 29). In addition, TM suppress T-cell proliferation and activation, and induce naive T-cell differentiation into immunosuppressive regulatory T cells (Tregs) (14, 29). The TM immunoregulatory phenotype seems to be essential to preserve normal testis homeostasis: high TNF-α production impairs LC function and can breakdown the BTB, exposing the germs cell to cytotoxic inflammatory cytokines that ultimately impairs spermatogenesis (30). High NO production can also negatively affect LC function and consequently, steroidogenesis (31).

Besides acting as immune sentinel cells, TM are also equipped to perform testis-specific functions to maintain normal homeostasis, including: (1) supporting steroidogenesis by producing 25HC, (2) promoting spermatogenesis by expressing sp?A3B2 ? >ermatogonial proliferation- and differentiation-inducing factors such as colony stimulating factor 1 (CSF1) and enzymes involved in retinoic acid (RA) biosynthesis, and (3) guiding testis embryonic development by aiding blood vessel and spermatic cord formation (4, 26).

The number of TM increases during testis inflammation, as observed following acute LPS stimulation or in experimental models of murine chronic autoimmune epididymo-orchitis (EAO) induced by immunization with testis homogenate and adjuvants or pathogen-induced (*E. coli*) inflammation (epididymo-orchitis) (32–35). During LPS-induced inflammation, a transient influx of monocytes into the testis occurs that resolves after 72 h; whereas no changes in the number of TM was observed (32). Similarly, following *E. coli*-induced epididymo-orchitis, inflammation in the testis quickly resolves after the initial infiltration of immune cells and impairment of spermatogenesis. However, without therapeutic intervention, inflammation of the epididymis continues to remain (35). These observations suggest that the testis has a remarkable ability to resolve inflammation *via* mechanisms likely involving TM. Now, further studies are required to investigate how TM resolve inflammation and promote tissue repair.

We have gained mechanistic detail underlying the role of TM in resolving inflammation from the experimental autoimmune orchitis (EAO) model. Here, the number of TM subsets CD68^{+}CD163^{-} and (CD68^{+}CD163^{+}) increases progressively from the end of the immunization period to the severe orchitis stage, with minor changes in the number of resident CD163^{+} TM (33). At the same time, TM release large amounts of the pro-inflammatory mediators TNFα, IL6, IFNγ, and NO but not IL10 and GM-CSF (33, 36, 37). Infiltrating macrophages, but not resident CD163^{+} TM, express IL6, upregulate MHCII and reduce TNFα expression (33). Neither infiltrating (CD68^{+}CD163^{-}), intermediate (CD68^{+}CD163^{+}) nor resident (CD68^{-}CD163^{+}) TM up-regulate iNOS expression during EAO (37). The increase in NO production by TM during EAO mainly results from the large percentage of infiltrating and intermediate TM expressing iNOS; resident TM

contribute to NO production to a lesser extent. These events, as well as changes in other immune and nonimmune cell functions, ultimately disrupt testicular immune privilege and impair spermatogenesis and steroidogenesis (38).

The consequences of perturbed TM function are evident in infertile patients with hypospermatogenesis and Sertoli cell-only syndromes. Namely, patients present with an increased level of the TM-derived pro-inflammatory cytokines TNFα, IL1α, and IL1β (39, 40). Interstitial infiltration of activated macrophages and TNFα production is also a common feature in other models of testicular damage, such as testicular torsion (41), and in two models of transgenic male mice, one ectopically expressing humanP450 aromatase (AROM+), and the Tyro3, Axl and Mer (TAM) receptor tyrosine kinase triple knockout (42).

DENDRITIC CELLS

Dendritic cells (DC) are "professional" antigen-presenting cells and a cellular component of the adaptive immune system. DC constitute a heterogeneous population that includes classical DC, plasmacytoid DC, and monocyte-derived DC originating from hematopoietic stem cells in the bone marrow. DC are found in lymphoid and nonlymphoid tissues and have a role in T-cell activation and tolerance induction, both of which depend on many environmental signals (43). We found that normal rat testis and testicular draining lymph nodes (TLN) contain $CD103^+$ DC that express MHCII and B7 costimulatory molecules. However, functional data from *in vitro* assays revealed that these DC are unable to stimulate naïve T-cell proliferation (36, 44, 45). This finding suggests that DC support the immune privilege status of the testis as they adopt a tolerant status in the physiological testicular microenvironment.

DC isolated from normal testis also express the chemokine receptor CCR2, which is a marker of immature resident DC. Gao et al. showed that Sertoli cells may promote the differentiation of these immature DC into tolerogenic DC since mice prepuberal Sertoli cell-conditioned of mice DC down-regulate the expression levels of costimulatory molecules and decrease T-cell priming (46).

During EAO, $CD103^+$ $MHCII^+$ $CD80^+$ $CD86^+$ DC isolated from the testis and TLNs can activate T cells and produce IL12p70 (44, 45). Bioactive IL12p70 can bias activated T cells in favor of an inflammatory Th1 response (47). Moreover, DC isolated from EAO testes show an upregulation of chemokine receptor CCR7 expression, which directs DC migration to the TLN (45). In fact, mature $CD103^+$ DC accumulate in the lymph nodes (LN) that drain the EAO testis (44).

Based on our knowledge in the rat model thus far, we propose a putative model by which $CD103^+$ DC promote the induction and progression of orchitis. In the LN draining the immunization site, DC present orchitogenic antigens on their surface in the context of MHCII, then prime naïve T cells and polarize them toward effector functions. DC-sensitized T cells migrate to the testis, where they are attracted by local chemokines (CCL2 and CCL3) secreted by antigen presenting cells and somatic cells and contribute to testicular inflammation causing tissue damage (48, 49). Testicular DC take up spermatic antigens from the impaired seminiferous tubules to undergo immunogenic maturation, and subsequently travel to the TLN *via* the lymphatic system; alternatively, they might prime naïve T cells *in situ*. Consequently, this process would increase manifold in response to inflammatory signals leading to chronic orchitis.

LYMPHOCYTES

Depending on environmental signals, T cells commit to effector or regulatory lineages with opposing functions leading to inflammation or dominant immunologic tolerance (50). Flow cytometric analysis of the leukocytes present in the normal rat testis showed that nearly 25% of these cells are $CD3^+$ T cells, and that the percentage of $CD8^+$ T cells is 4-fold greater than that of $CD4^+$ T cells. Most $CD25^+$ T cells are found within the $CD8^+$ subset (51). Both subsets express proinflammatory mediators, such as TNFα, IFNγ, and FasL. A similar percentage of cells within the $CD4^+$ and $CD8^+$ T cell subsets express IFNγ; however, $CD8^+$ T cells are the main producers of FasL and TNFα. Testicular T cells expressing IL4 are occasionally observed under normal conditions (52, 53).

The presence of $Foxp3^+$ Tregs in the normal testis is well established (54–56). In the rat testis, ~2% of the cells within the $CD4^+$ and $CD8^+$ T-cell subsets express CD25 and Foxp3 (51). This percentage rises to 4% in the TLN (57). Most of these cells show a memory phenotype and produce TFG-β. Functional analysis of $CD4^+CD25^+Foxp3^+$ Tregs isolated from the TLN showed that these cells produce a potent proliferative response toward spermatic antigens and exert suppressive effects that prevent conventional T-cell proliferation (57). These results support that Tregs are activated *in vivo* by antigens from the seminiferous tubules. In fact, Tung et al. demonstrated that non sequestered germ cell antigens egressed from seminiferous tubules, enter the interstitium, and induce Tregs challenging the long-standing dogma that all germ cell neo-antigens are sequestered from the immune system (58). These phenomena elicit the expansion of Tregs in the TLN, where they may exert a basal and permanent suppression of auto-reactive T cells, thereby maintaining the tolerogenic environment (57, 58).

Under inflammatory conditions, pathogenic T cells can overwhelm the suppressive mechanisms of Tregs by altering the balance in favor of an autoimmune response (51). For example, during EAO, $CD4^+$, and $CD8^+$ T cells producing TNF-α, IFNγ, and FasL infiltrate the testis. Th1 and Th17 subsets serve as co-effector cells that govern the early stages of the disease whereas $CD8^+$ T cells producing Th1 and Th17 cytokines are relevant to establish chronic inflammation (51–53). Although Tregs accumulate in the testis and in the TLN, and despite that Tregs from the TLN are more effective at suppressing T-cell proliferation than their normal counterparts, these Tregs are unable to prevent germ cell attack. One proposal for this

paradigm is that cytokines in the inflammatory milieu might inhibit Tregs *in vivo*, compromising their function at inflammation sites (56, 57).

MAST CELLS

Mast cells (MC) are tissue resident immune cells with heterogeneous phenotypes localized within the subalbuginea area near blood vessels in rodents and/or in the interstitial compartment in humans (**Figure 1**). MC derive from $CD34^+$ hematopoietic progenitor cells, differentiating initially in the bone marrow and then locally in the specific organ that they have migrated to under the influence of estrogens (59). MC have diverse roles in innate immunity, tissue homeostasis and remodeling, and adaptive immunity. Pre-synthesized substances such as histamine, chymase, tryptase, carboxipeptidase A, and TNFα are stored in granules and are released immediately after MC activation (60). TNFα, IL6, and IL1β are synthesized *de novo* after MC activation (61). Direct interactions with autoreactive T cells may activate MC, inducing degranulation, and cytokine production.

During inflammation (such as in patients with defective spermatogenesis, varicocele, infertility, or EAO and testis torsion models) the number of MC increases. Here, the serine protease tryptase enhances fibroblast proliferation and collagen synthesis, inducing fibrosis of the seminiferous tubules (62). MC might also regulate fibrosis by activating matrix metalloproteinases (MMP) and tissue MMP inhibitors (63).

In the EAO model, MC mainly accumulate around the ST and especially the surrounding granulomas (64). Tryptase released by these MC activates proteinase-activated receptor-2 (PAR2) that is expressed by peritubular cells and TM to induce cell proliferation and cytokine production (64). Moreover, PAR2-derived peritubular cells drive an increase in the expression of inflammatory mediators MCP1, TGFβ2, and cyclooxygenase COX2.

Analyses of human testis biopsies from infertile patients found an increase in the number of MC within the walls of the seminiferous tubules; many of these cells were active and expressing tryptase (65). These MC were often localized near to spermatogonia and Sertoli cells, suggesting that MC might affect spermatogonia that express PAR2, possibly *via* their secreted products (65).

CONCLUSIONS AND FUTURE PERSPECTIVES

Immune cells have essential roles in maintaining testicular homeostasis by dampening the inflammatory response and supporting normal physiological functions. The attenuated inflammatory response of testicular immune cells, particularly TM, is essential as the testis is an immune privileged organ. Any inflammatory response can severely damage testicular function — namely steroidogenesis and spermatogenesis. Although substantial progress has been made in understanding testicular immune cell function, more detailed investigations are now required to delineate the interactions between these immune cells and neighboring nonimmune cells. The mechanisms underlying how immune cells help to resolve inflammation and promote tissue repair are to be studied in depth. Advances in this area will improve our understanding of male infertility problems and will pave the way for the development of innovative therapeutics.

AUTHOR CONTRIBUTIONS

All authors contributed to the article and approved the submitted version.

FUNDING

The support of the Deutsche Forschungsgemeinschaft (DFG) for the International Research Training Group (GRK 1871/2-1) on 'Molecular pathogenesis of male reproductive disorders' and the Faculty of Medicine of the Justus-Liebig-University of Giessen is gratefully acknowledged. SB is supported by DFG (BH93/1-4). The support from the University of Buenos Aires and CONICET is greatly acknowledged.

REFERENCES

1. Maekawa M, Kamimura K, Nagano T. Peritubular myoid cells in the testis: their structure and function. *Arch Histol Cytol* (1996) 59(1):1–13. doi: 10.1679/aohc.59.1
2. Hirai S, Naito M, Terayama H, Qu N, Kuerban M, Musha M, et al. The origin of lymphatic capillaries in murine testes. *J Androl* (2012) 33(4):745–51. doi: 10.2164/jandrol.111.015156
3. Svingen T, Francois M, Wilhelm D, Koopman P. Three-dimensional imaging of Prox1-EGFP transgenic mouse gonads reveals divergent modes of lymphangiogenesis in the testis and ovary. *PLoS One* (2012) 7(12):e52620. doi: 10.1371/journal.pone.0052620
4. DeFalco T, Potter SJ, Williams AV, Waller B, Kan MJ, Capel B. Macrophages Contribute to the Spermatogonial Niche in the Adult Testis. *Cell Rep* (2015) 12(7):1107–9. doi: 10.1016/j.celrep.2015.07.015
5. Hedger MP. "The Immunophysiology of Male Reproduction," in *Knobil and Neill's Physiology of Reproduction*. Amsterdam, Netherlands (2015). p. 805–92.
6. Kitadate Y, Jorg DJ, Tokue M, Maruyama A, Ichikawa R, Tsuchiya S, et al. Competition for Mitogens Regulates Spermatogenic Stem Cell Homeostasis in an Open Niche. *Cell Stem Cell* (2019) 24(1):79–92 e6. doi: 10.1016/j.stem.2018.11.013
7. Liu Y, Liang Y, Wang S, Tarique I, Vistro WA, Zhang H, et al. Identification and characterization of telocytes in rat testis. *Aging (Albany NY)* (2019) 11 (15):5757–68. doi: 10.18632/aging.102158
8. Marini M, Rosa I, Guasti D, Gacci M, Sgambati E, Ibba-Manneschi L, et al. Reappraising the microscopic anatomy of human testis: identification of telocyte networks in the peritubular and intertubular stromal space. *Sci Rep* (2018) 8(1):14780. doi: 10.1038/s41598-018-33126-2
9. Rosa I, Marini M, Sgambati E, Ibba-Manneschi L, Manetti M. Telocytes and lymphatic endothelial cells: Two immunophenotypically distinct and spatially

close cell entities. *Acta Histochem* (2020) 122(3):151530. doi: 10.1016/j.acthis.2020.151530
10. Fijak M, Pilatz A, Hedger MP, Nicolas N, Bhushan S, Michel V, et al. Infectious, inflammatory and 'autoimmune' male factor infertility: how do rodent models inform clinical practice? *Hum Reprod Update* (2018) 24 (4):416–41. doi: 10.1093/humupd/dmy009
11. Zhao S, Zhu W, Xue S, Han D. Testicular defense systems: immune privilege and innate immunity. *Cell Mol Immunol* (2014) 11(5):428–37. doi: 10.1038/cmi.2014.38
12. Arck P, Solano ME, Walecki M, Meinhardt A. The immune privilege of testis and gravid uterus: same difference? *Mol Cell Endocrinol* (2014) 382(1):509–20. doi: 10.1016/j.mce.2013.09.022
13. Bleriot C, Chakarov S, Ginhoux F. Determinants of Resident Tissue Macrophage Identity and Function. *Immunity* (2020) 52(6):957–70. doi: 10.1016/j.immuni.2020.05.014
14. Wang M, Fijak M, Hossain H, Markmann M, Nusing RM, Lochnit G, et al. Characterization of the Micro-Environment of the Testis that Shapes the Phenotype and Function of Testicular Macrophages. *J Immunol* (2017) 198 (11):4327–40. doi: 10.4049/jimmunol.1700162
15. Niemi M, Sharpe RM, Brown WR. Macrophages in the interstitial tissue of the rat testis. *Cell Tissue Res* (1986) 243(2):337–44. doi: 10.1007/BF00251049
16. Mossadegh-Keller N, Gentek R, Gimenez G, Bigot S, Mailfert S, Sieweke MH. Developmental origin and maintenance of distinct testicular macrophage populations. *J Exp Med* (2017) 214(10):2829–41. doi: 10.1084/jem.20170829
17. Chakarov S, Lim HY, Tan L, Lim SY, See P, Lum J, et al. Two distinct interstitial macrophage populations coexist across tissues in specific subtissular niches. *Science* (2019) 363(6432):1190–203. doi: 10.1126/science.aau0964
18. Hoeffel G, Chen J, Lavin Y, Low D, Almeida FF, See P, et al. C-Myb(+) erythro-myeloid progenitor-derived fetal monocytes give rise to adult tissue-resident macrophages. *Immunity* (2015) 42(4):665–78. doi: 10.1016/j.immuni.2015.03.011
19. Bain CC, Bravo-Blas A, Scott CL, Perdiguero EG, Geissmann F, Henri S, et al. Constant replenishment from circulating monocytes maintains the macrophage pool in the intestine of adult mice. *Nat Immunol* (2014) 15 (10):929–37. doi: 10.1038/ni.2967
20. Shaw TN, Houston SA, Wemyss K, Bridgeman HM, Barbera TA, Zangerle-Murray T, et al. Tissue-resident macrophages in the intestine are long lived and defined by Tim-4 and CD4 expression. *J Exp Med* (2018) 215(6):1507–18. doi: 10.1084/jem.20180019
21. Calderon B, Carrero JA, Ferris ST, Sojka DK, Moore L, Epelman S, et al. The pancreas anatomy conditions the origin and properties of resident macrophages. *J Exp Med* (2015) 212(10):1497–512. doi: 10.1084/jem.20150496
22. Tamoutounour S, Guilliams M, Montanana Sanchis F, Liu H, Terhorst D, Malosse C, et al. Origins and functional specialization of macrophages and of conventional and monocyte-derived dendritic cells in mouse skin. *Immunity* (2013) 39(5):925–38. doi: 10.1016/j.immuni.2013.10.004
23. Schulz C, Gomez Perdiguero E, Chorro L, Szabo-Rogers H, Cagnard N, Kierdorf K, et al. A lineage of myeloid cells independent of Myb and hematopoietic stem cells. *Science* (2012) 336(6077):86–90. doi: 10.1126/science.1219179
24. Lavin Y, Winter D, Blecher-Gonen R, David E, Keren-Shaul H, Merad M, et al. Tissue-resident macrophage enhancer landscapes are shaped by the local microenvironment. *Cell* (2014) 159(6):1312–26. doi: 10.1016/j.cell.2014.11.018
25. van de Laar L, Saelens W, De Prijck S, Martens L, Scott CL, Van Isterdael G, et al. Yolk Sac Macrophages, Fetal Liver, and Adult Monocytes Can Colonize an Empty Niche and Develop into Functional Tissue-Resident Macrophages. *Immunity* (2016) 44(4):755–68. doi: 10.1016/j.immuni.2016.02.017
26. Lukyanenko YO, Chen JJ, Hutson JC. Production of 25-hydroxycholesterol by testicular macrophages and its effects on Leydig cells. *Biol Reprod* (2001) 64 (3):790–6. doi: 10.1095/biolreprod64.3.790
27. Barakat B, O'Connor AE, Gold E, de Kretser DM, Loveland KL. Inhibin, activin, follistatin and FSH serum levels and testicular production are highly modulated during the first spermatogenic wave in mice. *Reproduction* (2008) 136(3):345–59. doi: 10.1530/REP-08-0140
28. Bhushan S, Tchatalbachev S, Lu Y, Frohlich S, Fijak M, Vijayan V, et al. Differential activation of inflammatory pathways in testicular macrophages provides a rationale for their subdued inflammatory capacity. *J Immunol* (2015) 194(11):5455–64. doi: 10.4049/jimmunol.1401132
29. Winnall WR, Muir JA, Hedger MP. Rat resident testicular macrophages have an alternatively activated phenotype and constitutively produce interleukin-10 in vitro. *J Leukoc Biol* (2011) 90(1):133–43. doi: 10.1189/jlb.1010557
30. Xia W, Wong EW, Mruk DD, Cheng CY. TGF-beta3 and TNFalpha perturb blood-testis barrier (BTB) dynamics by accelerating the clathrin-mediated endocytosis of integral membrane proteins: a new concept of BTB regulation during spermatogenesis. *Dev Biol* (2009) 327(1):48–61. doi: 10.1016/j.ydbio.2008.11.028
31. Weissman BA, Niu E, Ge R, Sottas CM, Holmes M, Hutson JC, et al. Paracrine modulation of androgen synthesis in rat leydig cells by nitric oxide. *J Androl* (2005) 26(3):369–78. doi: 10.2164/jandrol.04178
32. Gerdprasert O, O'Bryan MK, Nikolic-Paterson DJ, Sebire K, de Kretser DM, Hedger MP. Expression of monocyte chemoattractant protein-1 and macrophage colony-stimulating factor in normal and inflamed rat testis. *Mol Hum Reprod* (2002) 8(6):518–24. doi: 10.1093/molehr/8.6.518
33. Rival C, Theas MS, Suescun MO, Jacobo P, Guazzone V, van Rooijen N, et al. Functional and phenotypic characteristics of testicular macrophages in experimental autoimmune orchitis. *J Pathol* (2008) 215(2):108–17. doi: 10.1002/path.2328
34. Bhushan S, Hossain H, Lu Y, Geisler A, Tchatalbachev S, Mikulski Z, et al. Uropathogenic E. coli induce different immune response in testicular and peritoneal macrophages: implications for testicular immune privilege. *PLoS One* (2011) 6(12):e28452. doi: 10.1371/journal.pone.0028452
35. Klein B, Bhushan S, Gunther S, Middendorff R, Loveland KL, Hedger MP, et al. Differential tissue-specific damage caused by bacterial epididymo-orchitis in the mouse. *Mol Hum Reprod* (2020) 26(4):215–27. doi: 10.1093/molehr/gaaa011
36. Rival C, Lustig L, Iosub R, Guazzone VA, Schneider E, Meinhardt A, et al. Identification of a dendritic cell population in normal testis and in chronically inflamed testis of rats with autoimmune orchitis. *Cell Tissue Res* (2006) 324 (2):311–8. doi: 10.1007/s00441-005-0129-5
37. Jarazo-Dietrich S, Jacobo P, Perez CV, Guazzone VA, Lustig L, Theas MS. Up regulation of nitric oxide synthase-nitric oxide system in the testis of rats undergoing autoimmune orchitis. *Immunobiology* (2012) 217(8):778–87. doi: 10.1016/j.imbio.2012.04.007
38. Perez CV, Theas MS, Jacobo PV, Jarazo-Dietrich S, Guazzone VA, Lustig L. Dual role of immune cells in the testis: Protective or pathogenic for germ cells? *Spermatogenesis* (2013) 3(1):e23870. doi: 10.4161/spmg.23870
39. Frungieri MB, Weidinger S, Meineke V, Kohn FM, Mayerhofer A. Proliferative action of mast-cell tryptase is mediated by PAR2, COX2, prostaglandins, and PPARgamma : Possible relevance to human fibrotic disorders. *Proc Natl Acad Sci U S A* (2002) 99(23):15072–7. doi: 10.1073/pnas.232422999
40. Duan YG, Yu CF, Novak N, Bieber T, Zhu CH, Schuppe HC, et al. Immunodeviation towards a Th17 immune response associated with testicular damage in azoospermic men. *Int J Androl* (2011) 34(6 Pt 2):e536–45. doi: 10.1111/j.1365-2605.2010.01137.x
41. Rodriguez MG, Rival C, Theas MS, Lustig L. Immunohistopathology of the contralateral testis of rats undergoing experimental torsion of the spermatic cord. *Asian J Androl* (2006) 8(5):576–83. doi: 10.1111/j.1745-7262.2006.00146.x
42. Zhang Y, Li N, Chen Q, Yan K, Liu Z, Zhang X, et al. Breakdown of immune homeostasis in the testis of mice lacking Tyro3, Axl and Mer receptor tyrosine kinases. *Immunol Cell Biol* (2013) 91(6):416–26. doi: 10.1038/icb.2013.22
43. Tarbell KV, Rahman K. Dendritic cells in autoimmune disease. In: Rose N and Mackay I, editors. *The Autoimmune Diseases. 6th edition*. London: Elsevier Inc. (2019). p. 213–23.
44. Guazzone VA, Hollwegs S, Mardirosian M, Jacobo P, Hackstein H, Wygrecka M, et al. Characterization of dendritic cells in testicular draining lymph nodes in a rat model of experimental autoimmune orchitis. *Int J Androl* (2011) 34(3):276–89. doi: 10.1111/j.1365-2605.2010.01082.x
45. Rival C, Guazzone VA, von Wulffen W, Hackstein H, Schneider E, Lustig L, et al. Expression of co-stimulatory molecules, chemokine receptors and proinflammatory cytokines in dendritic cells from normal and chronically

inflamed rat testis. *Mol Hum Reprod* (2007) 13(12):853–61. doi: 10.1093/molehr/gam067
46. Gao J, Wang X, Wang Y, Han F, Cai W, Zhao B, et al. Murine Sertoli cells promote the development of tolerogenic dendritic cells: a pivotal role of galectin-1. *Immunology* (2016) 148(3):253–65. doi: 10.1111/imm.12598
47. Gately MK, Renzetti LM, Magram J, Stern AS, Adorini L, Gubler U, et al. The interleukin-12/interleukin-12-receptor system: role in normal and pathologic immune responses. *Annu Rev Immunol* (1998) 16:495–521. doi: 10.1146/annurev.immunol.16.1.495
48. Guazzone VA, Rival C, Denduchis B, Lustig L. Monocyte chemoattractant protein-1 (MCP-1/CCL2) in experimental autoimmune orchitis. *J Reprod Immunol* (2003) 60(2):143–57. doi: 10.1016/j.jri.2003.08.001
49. Guazzone VA, Jacobo P, Denduchis B, Lustig L. Expression of cell adhesion molecules, chemokines and chemokine receptors involved in leukocyte traffic in rats undergoing autoimmune orchitis. *Reproduction* (2012) 143(5):651–62. doi: 10.1530/REP-11-0079
50. Khan U, Ghazanfar H. T Lymphocytes and Autoimmunity. *Int Rev Cell Mol Biol* (2018) 341:125–68. doi: 10.1016/bs.ircmb.2018.05.008
51. Jacobo P, Guazzone VA, Jarazo-Dietrich S, Theas MS, Lustig L. Differential changes in CD4+ and CD8+ effector and regulatory T lymphocyte subsets in the testis of rats undergoing autoimmune orchitis. *J Reprod Immunol* (2009) 81(1):44–54. doi: 10.1016/j.jri.2009.04.005
52. Jacobo P, Perez CV, Theas MS, Guazzone VA, Lustig L. CD4+ and CD8+ T cells producing Th1 and Th17 cytokines are involved in the pathogenesis of autoimmune orchitis. *Reproduction* (2011) 141(2):249–58. doi: 10.1530/REP-10-0362
53. Jacobo PV, Fass M, Perez CV, Jarazo-Dietrich S, Lustig L, Theas MS. Involvement of soluble Fas Ligand in germ cell apoptosis in testis of rats undergoing autoimmune orchitis. *Cytokine* (2012) 60(2):385–92. doi: 10.1016/j.cyto.2012.07.020
54. Wheeler K, Tardif S, Rival C, Luu B, Bui E, Del Rio R, et al. Regulatory T cells control tolerogenic versus autoimmune response to sperm in vasectomy. *Proc Natl Acad Sci U S A* (2011) 108(18):7511–6. doi: 10.1073/pnas.1017615108
55. Nicolas N, Michel V, Bhushan S, Wahle E, Hayward S, Ludlow H, et al. Testicular activin and follistatin levels are elevated during the course of experimental autoimmune epididymo-orchitis in mice. *Sci Rep* (2017) 7:42391. doi: 10.1038/srep42391
56. Jacobo P. The role of regulatory T Cells in autoimmune orchitis. *Andrologia* (2018) 50(11):e13092. doi: 10.1111/and.13092
57. Jacobo P, Guazzone VA, Perez CV, Lustig L. CD4+ Foxp3+ regulatory T cells in autoimmune orchitis: phenotypic and functional characterization. *Am J Reprod Immunol* (2015) 73(2):109–25. doi: 10.1111/aji.12312
58. Tung KS, Harakal J, Qiao H, Rival C, Li JC, Paul AG, et al. Egress of sperm autoantigen from seminiferous tubules maintains systemic tolerance. *J Clin Invest* (2017) 127(3):1046–60. doi: 10.1172/JCI89927
59. Mechlin C, Kogan B. Mast cells, estrogens, and cryptorchidism: a histological based review. *Transl Androl Urol* (2012) 1(2):97–102. doi: 10.3978/j.issn.2223-4683.2012.06
60. Krystel-Whittemore M, Dileepan KN, Wood JG. Mast Cell: A Multi-Functional Master Cell. *Front Immunol* (2015) 6:620. doi: 10.3389/fimmu.2015.00620
61. Haidl G, Duan YG, Chen SJ, Kohn FM, Schuppe HC, Allam JP. The role of mast cells in male infertility. *Expert Rev Clin Immunol* (2011) 7(5):627–34. doi: 10.1586/eci.11.57
62. Moreno D, Sobarzo CM, Lustig L, Rodriguez Pena MG, Guazzone VA. Effect of ketotifen fumarate on experimental autoimmune orchitis and torsion of the spermatic cord. *Asian J Androl* (2020) 22(1):112–7. doi: 10.4103/aja.aja_30_19
63. Acikgoz A, Asci R, Aydin O, Cavus H, Donmez G, Buyukalpelli R. The role of ketotifen in the prevention of testicular damage in rats with experimental unilateral undescended testes. *Drug Des Devel Ther* (2014) 8:2089–97. doi: 10.2147/DDDT.S67941
64. Iosub R, Klug J, Fijak M, Schneider E, Frohlich S, Blumbach K, et al. Development of testicular inflammation in the rat involves activation of proteinase-activated receptor-2. *J Pathol* (2006) 208(5):686–98. doi: 10.1002/path.1938
65. Mayerhofer A, Walenta L, Mayer C, Eubler K, Welter H. Human testicular peritubular cells, mast cells and testicular inflammation. *Andrologia* (2018) 50(11):e13055. doi: 10.1111/and.13055

Conflict of Interest: The authors declare that the research was conducted in the absence of any commercial or financial relationships that could be construed as a potential conflict of interest.

frontiers in Immunology

REVIEW
published: 30 September 2020
doi: 10.3389/fimmu.2020.02115

The Immune Characteristics of the Epididymis and the Immune Pathway of the Epididymitis Caused by Different Pathogens

Hu Zhao[1†], *Caiqian Yu*[1†], *Chunyu He*[2], *Chunlei Mei*[2], *Aihua Liao*[2*] and *Donghui Huang*[2*]

[1] Department of Human Anatomy, Tongji Medical College, Huazhong University of Science and Technology, Wuhan, China, [2] Institute of Reproduction Health Research, Tongji Medical College, Huazhong University of Science and Technology, Wuhan, China

The epididymis is an important male accessory sex organ where sperm motility and fertilization ability develop. When spermatozoa carrying foreign antigens enter the epididymis, the epididymis shows "immune privilege" to tolerate them. It is well-known that a tolerogenic environment exists in the caput epididymis, while pro-inflammatory circumstances prefer the cauda epididymis. This meticulously regulated immune environment not only protects spermatozoa from autoimmunity but also defends spermatozoa against pathogenic damage. Epididymitis is one of the common causes of male infertility. Up to 40% of patients suffer from permanent oligospermia or azoospermia. This is related to the immune characteristics of the epididymis itself. Moreover, epididymitis induced by different pathogenic microbial infections has different characteristics. This article elaborates on the distribution and immune response characteristics of epididymis immune cells, the role of epididymis epithelial cells (EECs), and the epididymis defense against different pathogenic infections (such as uropathogenic *Escherichia coli*, *Chlamydia trachomatis*, and viruses to provide therapeutic approaches for epididymitis and its subsequent fertility problems.

Keywords: epididymis, epididymitis, epididymis epithelial cells, uropathogenic *Escherichia coli*, *Chlamydia trachomatis*, virus

OPEN ACCESS

Edited by:
Daishu Han,
Chinese Academy of Medical Sciences and Peking Union Medical College, China

Reviewed by:
Adrian Pilatz,
University Hospital Giessen, Germany
Baoxing Liu,
China-Japan Friendship Hospital, China

***Correspondence:**
Donghui Huang
jhsyyjs@126.com
Aihua Liao
aihua_liao@sina.com

[†]These authors have contributed equally to this work

Specialty section:
This article was submitted to Mucosal Immunity, a section of the journal Frontiers in Immunology

Received: *26 June 2020*
Accepted: *05 August 2020*
Published: *30 September 2020*

Citation:
Zhao H, Yu C, He C, Mei C, Liao A and Huang D (2020) The Immune Characteristics of the Epididymis and the Immune Pathway of the Epididymitis Caused by Different Pathogens. Front. Immunol. 11:2115. doi: 10.3389/fimmu.2020.02115

INTRODUCTION

Infertility is the third major issue affecting human health, experienced by ∼10–15% of couples when attempting to conceive a baby, among which 50% are related to male factor infertility (1). Infection and inflammation are involved in 13–15% of cases of male factor infertility. However, prevalence rates are up to 30% in regions with limited access to medical care (2, 3). Relevant diseases that can lead to infertility include epididymitis, combined epididymo-orchitis, and rarely, isolated orchitis (4, 5).

Acute epididymitis is one of the most common diseases related to male inflammation. Nicholson et al. have reported its incidence is ∼2.5–6.5/100 000 person-years (5, 6). Epididymitis can occur in men of any age. Pilatz et al. (7) investigated 237 patients with acute epididymitis aged 18–97 years and found the highest incidence rate was in the group aged between 48 and 57 years old. Redshaw et al. (8) showed that the annual incidence of acute epididymitis is ∼1.2/1,000 boys at the age of two to 13 years, while 43% of epididymitis cases occur among adult men aged 20–30 years.

It is well-known that men with epididymitis usually present with impaired semen quality as well as a high number of white blood cells (4, 9, 10). Pilatz et al. (11) found the sperm protein composition changed significantly in patients after epididymitis, which may be one of the factors contributing to subfertility/infertility in men after episodes of epididymitis.

Although conservative antimicrobial therapy is possible in the majority of patients and is usually sufficient to eradicate the pathogen, studies have shown that up to 40% of patients suffer from permanent oligospermia or azoospermia (12). Rusz et al. reported that persistent detrimental effects are not uncommon in patients with acute epididymitis even after a complete bacteriological cure (9). Recent data showed that this was related to pathogen damage, strong fibrotic transformation, and epithelial degeneration (13). However, the research of immunopathological mechanisms related to human epididymitis is hindered due to the limited access to tissue samples (14). Therefore, studies on the epididymis have been largely performed in rats and mice to assess the morphological changes and immune pathways (12). Evidence shows that models mimicking epididymitis have been instructive in a better understanding of the mechanisms of disease initiation and progression (5).

This study describes the immune characteristics of the epididymis and the immune pathways of the epididymitis triggered by various pathogenic infections (*E. coli*, *Chlamydia trachomatis*, viruses, etc.) in animal models to explore how the immune related-mechanisms of epididymitis can impair male fertility.

IMMUNE CHARACTERISTICS OF THE EPIDIDYMIS

Structure of the Epididymis

The epididymis is mainly composed of the epididymal tube. The inner layer of the epididymal duct is lined by a pseudostratified columnar ciliated epithelium, and the outer layer is surrounded by a peritubular layer of smooth muscle cells, in which there is interstitial tissue stroma containing the vasculature and lymphatics (15). Epididymis epithelial cells (EECs) are composed of many kinds of epithelial cells, including main cells, basal cells, lymphocyte or halo cells, clear cells, and monocyte phagocytes, among which the monocyte phagocytes include dendritic cells and macrophages (16), as shown in **Figure 1**.

The epididymis is divided into distinct segments according to its morphology and function (15). Usually, the epididymis is divided into three regions, including the caput, corpus, and cauda epididymis according to its anatomical structure (17, 18), but sometimes it is divided into four regions (the initial segment, caput, corpus, and cauda) (15, 19).

Blood-Epididymis Barrier

The epididymis has a certain barrier function, which is called the Blood-Epididymis Barrier (BEB). The fully functional BEB consists of anatomical, physiological, and immunological barriers (20). The anatomical barrier is made up of tight junctions, formed from the principal cells' basolateral and apical membranes, which restrict molecules and cells from coming into or out of the lumen. The physiological barrier comprised of transporters and channels, while the immunological barrier is comprised of different immune components inside and outside the tubule/duct (20).

The tight junctions and selective transport by the principal cells can create a high concentration of some molecules in the epididymis, such as carnitine and inositol, which is helpful for sperm storage and maturing (21, 22). In addition to creating a suitable environment for sperm maturation, the BEB also provides an immune-privileged environment for sperm with neoantigens (23).

The BEB, together with the blood-testis barrier, plays a key role in preventing autoimmune responses against antigenic post-pubertal germ cells (20). Compared with the blood-testis barrier, the tight junctions of the epididymis are much less effective (24). Itoh et al. (25) demonstrated that spermatic granulomas were formed after injection of spermatozoa or testicular germ cells into the mice epididymal interstitial space; in contrast, no infiltrate was detected, and spermatic granulomas were not formed in the interstitial space when similar studies were performed in the testis. Alterations in the BEB may also bring about the formation of inflammatory conditions such as sperm granulomas (22). Infection and inflammation also damage the BEB, resulting in loss of the barrier function. Maintaining the integrity of the BEB is essential for sperm maturation and immune privilege (26). Loss of the barrier function opens a pathway for the entry of physiological and immunological components, which can alter the luminal microenvironment and lead to autoimmunity against sperm antigens, finally resulting in male infertility (27).

EECs and TRLs

Toll-like receptors (TLRs) are innate immune pathogen pattern recognition receptors, which can recognize proteins, nucleic acids, and lipids of pathogenic microorganisms invading the body [such as viruses, bacteria, fungi, and protozoa (28)]. In rats, both EECs and immune cells express TLRs throughout the epididymis, which indicates that EECs also play an immune role (29). TLR1-TLR9 mRNA is abundantly expressed in the rat epididymis, while Tlr10 and Tlr11 are less abundantly expressed (30). However, the clear cells in the rat cauda epididymis do not express TLRs5–7 or TLR11 (29). TLRs1–4 are expressed by principal cells in all regions of the rat duct (30). The expression of TLR1-6 in the caput epididymis is similar to those in the testis, while the levels of TLR7, 9, and 11 in the mouse epididymis are higher (31).

IMMUNE CELLS IN THE EPIDIDYMIS

Dendritic Cells

Dendritic cells (DCs) are "professional" antigen-presenting cells that internalize and process allo- and autoantigens (32). The DC maturation state is a key point for balancing tissue tolerance and autoimmunity. Immature DCs have a strong ability to internalize antigens, but their ability to activate T cells is low, while mature DCs is a T cell stimulant (33).

The maturation process of DCs includes a decrease in endocytic capacity and an increase in the major

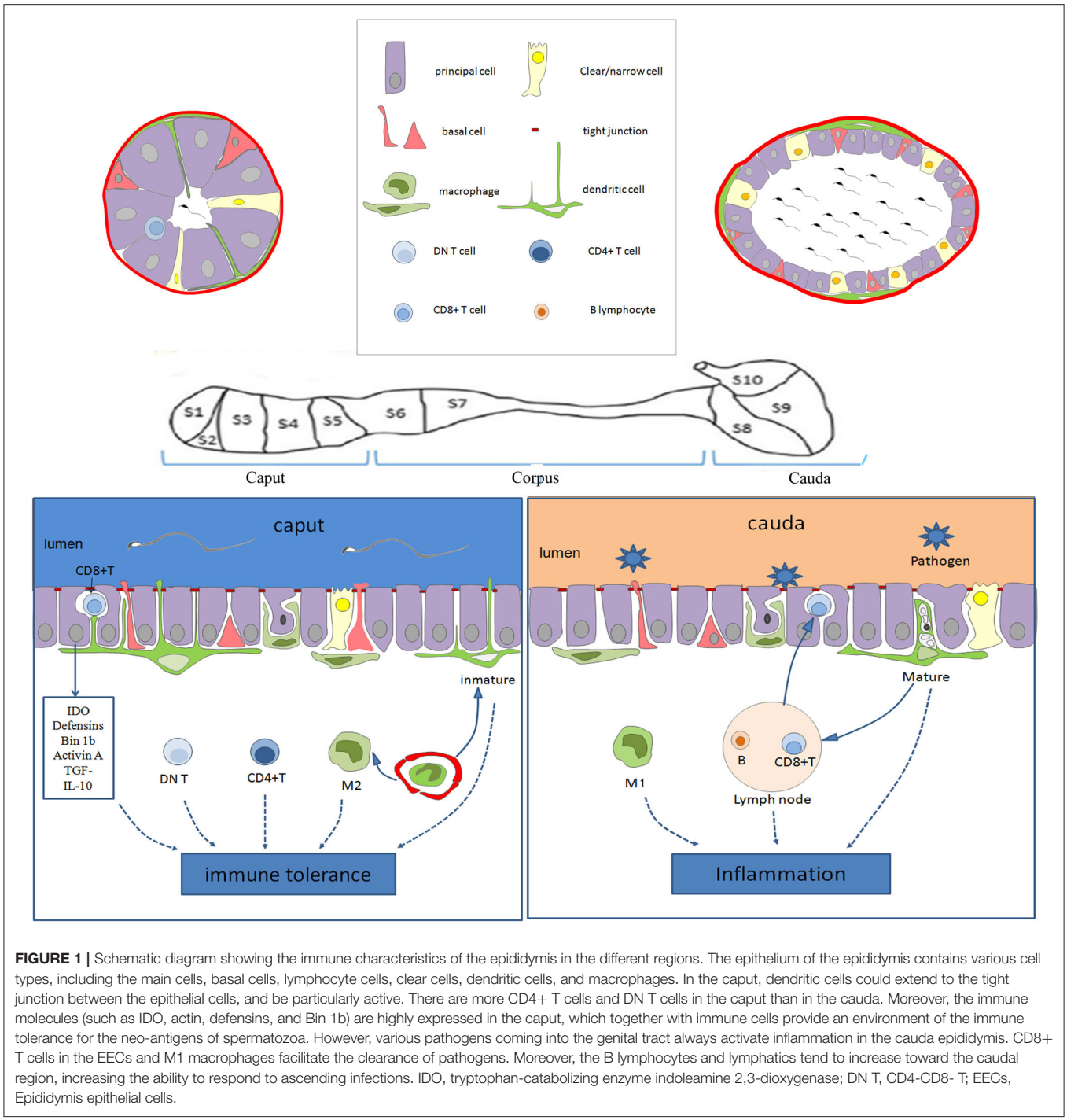

FIGURE 1 | Schematic diagram showing the immune characteristics of the epididymis in the different regions. The epithelium of the epididymis contains various cell types, including the main cells, basal cells, lymphocyte cells, clear cells, dendritic cells, and macrophages. In the caput, dendritic cells could extend to the tight junction between the epithelial cells, and be particularly active. There are more CD4+ T cells and DN T cells in the caput than in the cauda. Moreover, the immune molecules (such as IDO, actin, defensins, and Bin 1b) are highly expressed in the caput, which together with immune cells provide an environment of the immune tolerance for the neo-antigens of spermatozoa. However, various pathogens coming into the genital tract always activate inflammation in the cauda epididymis. CD8+ T cells in the EECs and M1 macrophages facilitate the clearance of pathogens. Moreover, the B lymphocytes and lymphatics tend to increase toward the caudal region, increasing the ability to respond to ascending infections. IDO, tryptophan-catabolizing enzyme indoleamine 2,3-dioxygenase; DN T, CD4-CD8- T; EECs, Epididymis epithelial cells.

histocompatibility complex and chemokine receptors (34). Upon receiving an activated signal associated with inflammation, an immature DC will turn into a mature DC and then produce many inflammatory cytokines, such as tumor necrosis factor-alpha (TNF-α), interleukin (IL)-20, IL-23, and TNF-related apoptosis-inducing ligand (35). In addition, mature DCs will induce T-cell proliferation and polarize T cells toward Th17 and Th1 (36). The physiological role of epididymal DC is to regulate the complex interactions between immune tolerance and activation, which is a balance point in determining male fertility (34, 37).

Da Silva et al. (38) found that DCs in the mouse epididymis form a dense dendritic network in the basal area of the epididymal epithelium and are highly active within the proximal caput, with its protuberance extending through the epithelium. They also reported a previously unrecognized dense network of

dendritic cells (CD11c+ CD103+ eDCs and CD11c+ CD103– eDCs) located at the base of the mouse epididymal epithelium, which displayed strong antigen-presenting and cross-presenting capabilities *in vitro*. DCs could collect antigens within the epididymal lumen and present them to the CD4+ T cells, thus regulating immunological reactions to spermatozoa and pathogens (39).

The conventional DCs in the murine epididymis are usually divided into cDC1 and cDC2 (40). The cDC1 type specifically deals with the cross-presentation of antigens (41), while cDC2 are mainly involved in T helper cell type responses (42). Voisin et al. (40) studied DC populations in the murine epididymis and found that cDCs1 account for 0.35 and 0.2% of the caput and cauda epididymis cells, respectively ($P < 0.05$) and that the cDC2 occupy 0.5% of the caput cells and 0.1% of the cauda cells ($P < 0.001$).

Wang et al. (37) showed that the number of CD11c+ DCs is relatively low in normal human epididymis unlike a dense network of CD11c+ DCs localized in the mouse epididymis. They concluded that the epididymis might have three phenotypically and functionally distinct subsets of DCs according to human and mouse data. They found that tolerogenic DC can: recognize normal sperm antigens; that immunogenic DCs detect and clear out abnormal sperm cells and exotic pathogens; and that inflammatory DCs: recruit Th17/Th1 cells (37).

Macrophages

Macrophages are the main phagocytes in tissue and can be specified for the detection, phagocytosis, and destruction of bacteria and other harmful organisms. They can also present antigens to T cells and initiate inflammation by releasing cytokines. Macrophages can be subcategorized as classical (M1) and alternative (M2) macrophages (43). M1 are characterized by a very high expression of pro-inflammatory cytokines (IL-6, TNF-α, and IL-12) and the production of reactive oxygen species and nitric oxide, which facilitates the clearance of microbial pathogens (44). In contrast, M2 are defined by high secretion of anti-inflammatory cytokines [IL-10, transforming growth factor-β (TGF-β)] and low expression of pro-inflammatory cytokines (IL-12, TNFα) (45). Therefore, M1/M2 polarization could affect the fate of inflamed or injured organs (46).

Macrophages are the most abundant immunocompetent cells in the murine epididymis (47). Macrophages are located chiefly in the interstitial and peritubular regions of the epididymis. Macrophages in the interstitial regions of the epididymis could express major histocompatibility complex class II antigens, which are necessary for antigen presentation to T cells (48). In contrast, most macrophages in the peritubular regions of the epididymis lack major histocompatibility complex class II expression, which is a common feature of mucosal epithelia (49). Da Silva et al. (38) reported that a network of mononuclear phagocytes (MPs) expressing macrophage and dendritic cell markers such as CD11c, F4/80, and CX3CR1, lines the base of the mouse epididymal tubule. Both macrophages and DCs are "professional" antigen-presenting cells, and play a complex dual role in the epididymis. On the one hand, they could inhibit responses to sperm antigens under normal conditions, but on the other hand, they might activate inflammatory responses to pathogens during infection (16, 34).

Lymphocyte

Lymphocytes present in the rat epididymal epithelium are often referred to as halo cells, which are named for the circular light-stained cytoplasm around the nucleus under light microscopy (50). Lymphocytes in the epididymis mainly consist of helper T lymphocytes (CD4+), cytotoxic T lymphocytes (CD8+), and B lymphocytes. CD4+ T cells are mainly located in the human epididymal stroma, while CD8+ T cells are the major lymphocytes within the epididymal epithelium (49). Voisin et al. used a single-cell isolation technique and observed that the numbers of CD4+ T cells were approximately equal in the murine caput and cauda epididymides (1.1 and 1%, respectively); the numbers of CD8+ T lymphocytes were similar as well between the caput and cauda (1.4 and 1.05%, respectively); however, the number of B lymphocytes in the cauda epididymis of was significantly higher than in the caput (0.7 and 0.35%, respectively) (40).

Surprisingly, natural killer and natural killer T cells were not detected in the murine epididymis (40). Given the very low incidence of epididymal tumors in humans (51), other populations or mechanisms may be involved in the anti-tumor effect in the epididymis (40). Voisin et al. (40) have described a new antigen-specific regulatory T cell population in the murine epididymis: double-negative (DN) T cells and found they were mainly located in the caput epididymis. This kind of cell has a strong cytotoxic effect on leukemia and lymphoma cell lines, but it does not affect normal cells. This supports the hypothesis that DN T cells could replace natural killer cells in the epididymis to prevent tumorigenesis (40).

Lymphocytes change in the epididymis at different ages (52). In young adult animals, the lymphocytes consist of helper T lymphocytes (CD4+) and cytotoxic T lymphocytes (CD8+), but there are no B lymphocytes, which indicate that immunoglobulin is not produced in the epididymis under normal conditions (52). A study of old brown Norwegian rats showed that B lymphocytes were rare in the epididymis epithelium of young rats, fewer than 1% of the total number of immune cells, but they were occasionally found in the epididymis epithelium of older rats, accounting for ∼5% of the total number of immune cells (53). The author postulated that the accumulation of damaged epithelial cells and antigens of germ cell origin, leaking through a dysfunctional blood-epididymis barrier, might contribute to the active recruitment of immune cells with age (53).

Basal Cell

Basal cells (BCs) are present in the epididymal epithelium of all mammalian species and are located in the basal region. Several manuscripts have reported BCs in the epididymis are similar to peritubular macrophages in their ultrastructural and antigenic aspects, and presumed that epididymal BCs from primates and rodents might originate from circulating progenitors and play some immunological role (54, 55). However, a recent article reported that mouse BCs have similar morphological

features compared to those of adjacent epithelial cells, and the authors proposed that BCs originate from the non-differentiated columnar epithelial cells instead of the MP system (56). Mammalian BCs not only have a hypothesized scavenger function but are also regarded as luminal sensors to regulate the activity of principal and clear cells (57).

Other Cells

The γδ T cells are typical mucosal cells and have recently been identified in the stroma and epididymal epithelium of the murine epididymis (40). The γδ T cells account for only a minor population of the T cells in the peripheral blood and lymphoid tissues in both mice and humans, but they are abundant in epithelial tissue (58). Epithelial γδ T cells exhibit tissue-specific restricted TCRs and show innate-like properties (59). Daley et al. (60) found that γδT cells could disable the immune system response against human pancreatic ductal adenocarcinoma. Considering the characteristics of the epididymis, γδT cells could also disable the immune system against sperm.

INNATE IMMUNE MOLECULES

Indoleamine 2,3-Dioxygenase

Indoleamine 2,3-dioxygenase (IDO) is an intracellular enzyme that catalyzes tryptophan to N-formalkynurenine, which is the first and key step in the kynurenine pathway (61). IDO is a ubiquitously expressed cytoplasmic protein typically activated by interferons (IFNs) (62). IDO has two main functions: one is to deplete tryptophan in an enclosed environment (such as in the epididymal duct lumen) to prevent bacterial or viral infection, and the other is to suppress T-cell-mediated immune responses against self-antigens, fetal antigens, or allogeneic antigens (63). IDO has been proven to suppress many kinds of immune responses, such as the regulation of tissue tolerance and the maintenance of immune privilege (64, 65).

Britan et al. (66) reported that IDO is highly expressed in the mouse caput epididymis and is mainly secreted by the principal and apical cells. The drosophila mothers against the decapentaplegic protein 2/3/4 signaling pathway activated by activin A, and could regulate the expression of IDO, suggesting that activin A may be an activator of IDO expression in the mouse proximal epididymis (67). Moreover, these immune regulators may induce a tolerogenic circumstance in DCs and T cells (67, 68). Jrad-Lamine et al. (69) have shown that pro-inflammatory cytokine expression is increased in the caput epididymitis of IDO-deficient mice. IDO-deficient mice possess significantly greater numbers of morphologically defective spermatozoa compared with wide-type controls. We propose that IDO activity, on the one hand, controlled the level of epididymal leukocytes and, on the other, regulated the involvement of the epididymal proteasome in clearing defective transiting spermatozoa (69).

Defensins

Defensins are not only important regulatory molecules in the biological immune system but are also important antimicrobial peptides with direct bactericidal functions (70). Multiple beta-defensins have been found in the epididymis of humans and mice with region-specific expression patterns, showing bacteria-killing activity and the promotion of sperm motility (71, 72).

Bin1b, exclusively expressed in the rat caput region of the epididymis, is a natural epididymis-specific antimicrobial peptide and can promote immature sperm to obtain motility (73). The specific expression of β-defensin 126 in the cattle epididymal tail can promote the acquisition of motility of epididymal sperm (74). Yenugu et al. (75) found that human and macaque sperm associated antigen 11 is involved in the mechanism of epididymal sperm maturation and host defense. Human β-defensin 114 can regulate lipopolysaccharide mediated inflammation and prevent the loss of sperm motility (76). Lack of human β-defensin 1 can lead to male infertility, which is manifested by poor sperm motility and reproductive tract infections (77).

Other Immune Molecules

The TGF-β superfamily comprises more than 30 members, including TGF-β isoforms, bone morphogenetic proteins, growth and differentiation factors, activins/inhibins, NODAL, and the anti-Müllerian hormone (78). Three isoforms of TGF-β have been identified in mammals: TGF-β1, TGF-β2, and TGF-β3. A recent study has revealed that TGF-β signaling in DCs is required for immunotolerance to sperm located in the epididymis, and that male mice lacking TGFβ signaling in DCs would develop severe epididymal inflammation (34). Voisin et al. (79) showed that EECs expressed the three TGF-β isoforms in all regions of the murine epididymis in pre-pubertal to adult mice, which indicated that the epididymal epithelium plays an active role in establishing a pro-tolerogenic environment necessary for the survival of immunogenic spermatozoa.

Activin A, a member of the TGF-β superfamily, is an important regulator of testicular and epididymal development and function, as well as inflammation and immunity (67). In the adult murine reproductive tract, activin A mRNA levels are highest in the caput epididymis and decrease progressively toward the distal vas deferens (80, 81). IL-10, a key effector regulatory cytokine, is located in the principal cells of the murine epididymal epithelium and may be involved in the protection of spermatozoa from autoimmune reactions (82). There are many other antimicrobial proteins (such as cathelicidins, mucins, lactoferrin, and chemokines) involved in the innate defense of EECs (83, 84).

CHARACTERISTICS OF EPIDIDYMIS IMMUNITY

In contrast to the immunologically privileged testis, the epididymis does not support prolonged allogeneic graft survival (85). Furthermore, epithelial tight junctions of the rodent epididymis may not be as effective as those of the blood-testis barrier, and direct interactions between intra-epithelial immune cells and either sperm antigens or ascending pathogens is possible (71). Therefore, the epididymis is more prone to inflammation and autoimmune responses than the testis.

It is worth noting that the type and number of immune cells and innate immune molecules are most abundant in the

murine epididymis head (40, 72). However, the distribution of epididymal lymphatics tends to increase toward the murine caudal region (86). It is widely accepted that immune tolerance exists in the caput epididymis, but pro-inflammatory circumstances prefer the cauda epididymis, as shown in **Figure 1**. Moreover, the closer the epididymis is to the testis, the lower the probability of inflammation, and the farther the testis is from the epididymis, the greater the odds of inflammation and its deleterious effect on reproduction (87). Epididymal immunity is based on a finely tuned equilibrium between efficient immune responses to pathogens and strong tolerance to spermatozoa (83).

IMMUNE PATHWAYS OF THE EPIDIDYMITIS CAUSED BY DIFFERENT PATHOGENS

Although epididymitis can occur in men of any age, the majority of epididymitis cases occur in men aged 20–39 and they are most often associated with sexually transmitted diseases (5). *Chlamydia trachomatis* and *Neisseria gonorrhea* account for ∼50% of cases of epididymitis associated with chlamydia and gonorrhea in men <39 years of age. After 39 years of age, the most common aetiologic agent responsible for epididymitis is *Escherichia coli* and other coliform bacteria found in the gastrointestinal tract (88). Weidner et al. (89) reported that enteric pathogens mainly occur in patients older than 35 years, sexually transmitted pathogens like Chlamydia trachomatis and Neisseria gonorrhoeae are often responsible in patients under 35 years. The different pathogens have different susceptible populations, and they have different inflammatory immune mechanisms. Therefore, it is helpful to understand the immune response of various pathogens for the treatment of epididymitis.

BACTERIAL INFECTION (UROPATHOGENIC *ESCHERICHIA COLI*)

Uropathogenic *Escherichia coli* (UPEC) is one of the most common causes of acute epididymitis, which is usually due to the retrograde progression of urethral pathogens and sexually transmitted bacterial infections (90). Silva et al. (91) reported that experimental epididymitis induced in rats by Gram-negative (LPS) and Gram-positive bacterial products resulted in differential patterns of acute inflammation in the cauda epididymis. LPS elicited a strong inflammatory reaction, as

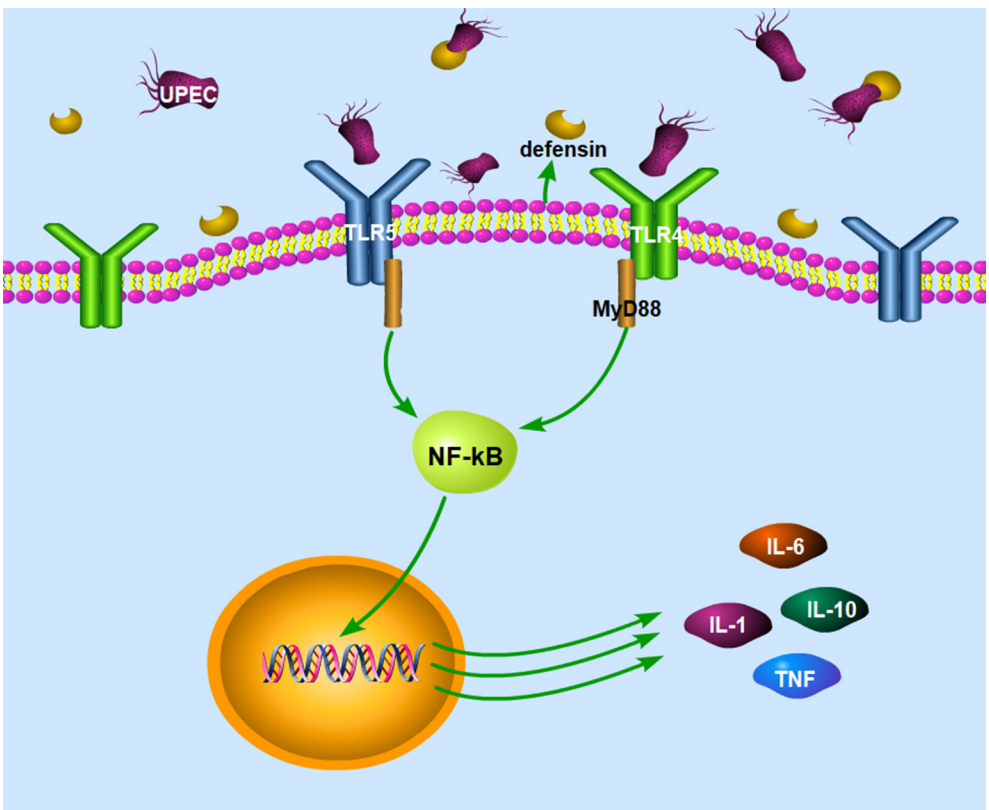

FIGURE 2 | The signaling pathways in the epididymitis induced by UEPC. The signaling pathway mainly includes two parts: (1) UPEC could activate TLR4 and TLR5 on epithelial cells and macrophages and induce the production of pro-inflammatory cytokines through the classical inflammatory NF-kB signaling pathway. (2) Epididymal cells can also limit pathogen infections by secreting defensins after infection with UPEC. UPEC, uropathogenic *Escherichia coli*; TLR4, toll like receptor 4; TLR5, toll like receptor 5; MyD 88, myeloid differentiation factor 88; NF-kB, nuclear factor kappa B; IL-1, interleukin-1; IL-6, interleukin-6; IL-10, interleukin-10; TNF, tumor necrosis factor.

reflected by the upregulation of the levels of mRNA for seven inflammatory mediators (IL-1b, TNF, IL-6, Interferon-gamma, IL-10, nitric oxide synthase 2, and nuclear factor-kappa-B inhibitor alpha), and the tissue concentrations of six cytokines/chemokines (IL-1a, IL-1b, IL-6, IL-10, CXCL2, and CCL2) within the first 24 h post-treatment (91).

Cheng et al. (92) found that the mouse epididymis infected by *E. coli* could activate TLR4 and TLR5 in the epididymis head epithelial cells and macrophages and induce the production of pro-inflammatory cytokines through the classical inflammatory NF-kappa B signaling pathway. Meanwhile, the natural immune response induced by UPEC in the epididymis of TLR4 and TLR5 knockout mice ($TLR4^{-/-}$, $TLR5^{-/-}$) was significantly lower than that induced in the wild-type mice (92), as shown in **Figure 2**. Although UPEC also activates TLR11, TLR11 cannot initiate innate immune responses in humans because there is no functional TLR11 (93). Moreover, UPEC induced the production of type 1 interferons by EECs through the activation of interferon regulatory factor 3 (92).

Epididymal cells can also limit pathogen infection by secreting defensins after infection with UPEC in the mouse model (34). Gene expression of defensin b2, defensin b21, and defensin 27 in the caput epididymis decreased in the LPS-induced rat epididymitis (94), while the gene expression of defensin b29, defensin b41, and defensin b42 remained unchanged after the treatment (95). Biswas et al. (96) demonstrated that the expression of defensins and sperm associated antigen 11 genes increased in the epididymis and testes in a UPEC induced rat epididymo-orchitis model. The recombinant defensin 21 significantly decreased the bacterial load in the epididymis and testis and proved to be more effective than gentamycin. Moreover, overexpression of Bin1b helps mice to resist *E. coli*-induced epididymitis (97).

Epididymitis also results in long-term problems in patients, such as the irreversible development of ductal obstructions and fibrotic tissue remodeling, even if full antibiotic treatment is provided (98). In the chronic UEPC murine epididymitis, the main pathological changes are dominated by lymphocytes, plasma cells, interstitial fibrosis (99), and even dead UEPC were able to disrupt testicular architecture after epididymal injection in the rat model (100). However, the mechanisms for this are unclear and need to be characterized in the future.

IMMUNE RESPONSE INDUCED BY *CHLAMYDIA TRACHOMATIS*

Chlamydia trachomatis (CT) is the most common sexually transmitted pathogen in high-income countries (101, 102) and is the most common etiology of STIs among sexually active males 14 to 35 years of age (88). Ito et al. (103) examined different microorganisms in men younger than 40 years of age with acute epididymitis and found that CT is a major pathogen (28%) while the prevalence of genital mycoplasmas (5%) and ureaplasmas were lower (5%). Screening for CT is advocated to control the transmission of chlamydia in sexually active young adults (104). However, there is an opposing option posited by another study, in which a population-based test for urogenital C trachomatis infection did not reduce the long-term risk of reproductive complications in women or epididymitis in men (105).

Approximately 50% of CT infections in men are asymptomatic (106, 107). The most important profile of a CT infection is a local immune response. First, the immune cells are recruited to the site of the infection and secrete pro-inflammatory cytokines such as interferon-γ (IFN-γ) (108, 109). IFN-γ has a dual function of inhibiting the growth of CT (110) in mice and inducing Th1 immune responses in CT-infected women (111). Studies have shown that IFN-γ activates host cells to restrict intracellular growth of CT by induction of IDO (112), as shown in **Figure 3**. The depletion of tryptophan by IDO has been proved to deprive CT of 5-hydroxytryptophan, which is essential for its differentiation into an infectious elementary body (112, 113). If IFN-γ is removed from the host cell, tryptophan synthesis will subsequently recover, and CT quickly forms into an infectious elementary body (114). In addition, CT infection of murine epithelial cells can induce the secretion of pro-inflammatory cytokines such as IL-1, Il-6, and TNF-α (115).

The most important features of CT infection are its chronic nature and the presence of a mild inflammation that remains subclinical in most individuals (116). Recognition of CT antigens is associated with TLR2, TLR4, and other CT antigens and pathogen recognition receptors (PRRs), which will induce a local secretion of cytokines/chemokines and consequently provoke chronic inflammation (116). This chronic inflammation can lead to cell proliferation, tissue remodeling, and scarring in the male genital tract (108).

INDUCTION OF ANTIVIRAL IMMUNE RESPONSES IN EPIDIDYMAL EPITHELIAL CELLS

Viruses can be divided into DNA viruses and RNA viruses. DNA viruses that can infect the male reproductive system include adeno-associated virus, cytomegalovirus, herpes simplex virus (HSV), hepatitis B virus, human papillomavirus, etc. (117). RNA viruses include mumps virus, enterovirus (enterovirus), human immunodeficiency virus (HIV), hepatitis C virus, etc. (118).

Mumps virus is the most common RNA virus that causes viral orchitis. The orchitis caused by Mumps virus is usually accompanied by viral epididymitis, and it severely impairs male fertility (119). Park et al. (120) investigated 18 patients with mumps orchitis and found 13 patients (72.2%) were accompanied with epididymitis. HSV-2 is the most common DNA virus that infects the male genitals, but most patients infected with HSV-2 have no obvious symptoms (121). The epididymis is a major target and reservoir of HIV (122). Pilatz et al. (11) investigated the etiology of acute epididymitis and found that viral epididymitis seems a rare condition.

Viral infections of the epididymis may sexually spread pathogens (123, 124). Different virus types that can infect the epididymis are associated with male infertility (123). Therefore, understanding the mechanisms underlying epididymal innate antiviral responses would aid in the development of preventive

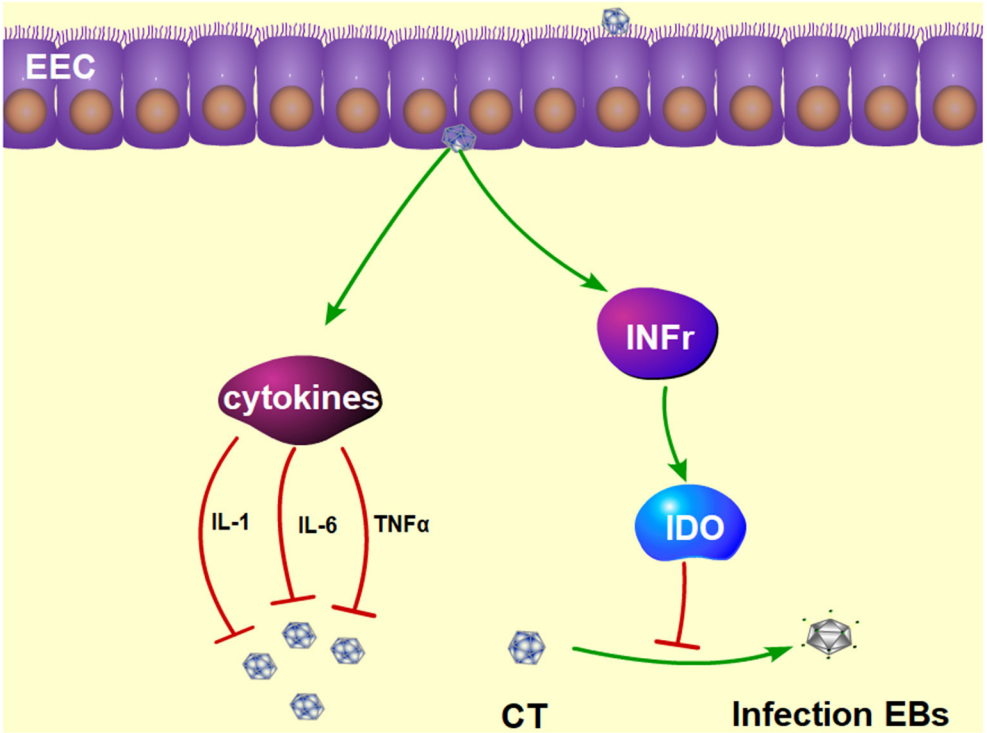

FIGURE 3 | The protective mechanism against CT infection in the epididymis. Interferon γ plays a functional role in inhibiting the growth of CT by induction of IDO, which prevents the CT from differentiating into infectious EBs. Furthermore, CT infection can induce the production of pro-inflammatory cytokines, such as IL-1, Il-6, and TNFα. IDO, tryptophan-catabolizing enzyme indoleamine 2,3-dioxygenase; EBs, elementary bodies; IL-1, interleukin-1; IL-6, interleukin-6; TNFα, tumor necrosis factor alpha.

and therapeutic strategies against viral infections of the epididymis (58).

The mouse EECs abundantly express viral sensors TLR3, the retinoic acid-inducible gene I (RIG-I), and DAI (31). TLR3 and retinoic acid-inducible gene I in EECs can be activated by synthetic double stranded RNA polyinosinic-polycytidylic acid, then significantly induce the expression of inflammatory cytokines (TNF-α and Monocyte chemokine-1, IFN-α and IFN-β) in EECs; the signaling pathway of DNA sensors can be initiated by HSV60 (31). HSV60 can significantly increase the expression of IFN-β, but not TNF-α and Monocyte chemokine-1 (31). Brown et al. (125) also showed that TLR3 and retinoic acid-inducible gene I-like receptors are enriched in human EECs from the corpus and cauda regions. Moreover, paired box 2, which was implicated in regulating antiviral response pathways, is required for basal expression of the DNA sensor, Z-DNA binding protein, and type I interferon, in caput but not in cauda cells (125).

CONCLUSION

Epididymitis is one of the common causes of male infertility. Persistent detrimental effects are common even after a complete bacteriological cure. This is related to the immune characteristics of the epididymis itself. Here, we elaborated on the distribution and role of the epididymis immune cells and the mechanisms of epididymis defenses against different pathogenic microbial infections. The purpose of this manuscript is to provide guidance for understanding the immune environment of the epididymis and to guide future therapeutic approaches to treating epididymitis. However, human data on different causes of acute epididymitis is spare, so more research is needed in the future.

AUTHOR CONTRIBUTIONS

HZ and CY wrote the article and performed literature searches and data compilation. CH and CM performed the necessary literature searches and data compilation. AL revised the article and gave valuable suggestions. DH designed the review and checked and approved the submitted manuscript. All authors have read and approved the final manuscript.

FUNDING

This work was supported by the National Natural Science Foundation of China (No. 81771575) and the Independent Innovation Foundation of Tongji Medical College of Huazhong University of Science and Technology (No. 5003510033).

REFERENCES

1. World Health Organization. *WHO Bulletin*. Geneva: World Health Organization (2010). p. 881–2.
2. Ahmed A, Bello A, Mbibu NH, Maitama HY, Kalayi GD. Epidemiological and aetiological factors of male infertility in northern nigeria. *Niger J Clin Pract*. (2010) 13:205–9. doi: 10.1007/s00063-010-1076-9
3. Eke AC, Okafor CI, Ezebialu IU. Male infertility management in a nigerian tertiary hospital. *Int J Gynaecol Obstet*. (2011) 114:85–6. doi: 10.1016/j.ijgo.2011.01.023
4. Schuppe HC, Pilatz A, Hossain H, Diemer T, Wagenlehner F, Weidner W. Urogenital infection as a risk factor for male infertility. *Dtsch Arztebl Int*. (2017) 114:39–346. doi: 10.3238/arztebl.2017.0339
5. Fijak M, Pilatz A, Hedger MP, Nicolas N, Bhushan S, Michel V, et al. Infectious, inflammatory and 'autoimmune' male factor infertility: how do rodent models inform clinical practice? *Hum Reprod Update*. (2018) 24:416–41. doi: 10.1093/humupd/dmy009
6. Nicholson A, Rait G, Murray-Thomas T, Hughes G, Mercer CH, Cassell J. Management of epididymo-orchitis in primary care: results from a large UK primary care database. *Br J Gen Pract*. (2010) 60:e407–22. doi: 10.3399/bjgp10X532413
7. Pilatz A, Hossain H, Kaiser R, Mankertz A, Schüttler CG, Domann E, et al. Acute epididymitis revisited: impact of molecular diagnostics on etiology and contemporary guideline recommendations. *Eur Urol*. (2015) 68:428–35. doi: 10.1016/j.eururo.2014.12.005
8. Redshaw JD, Tran TL, Wallis MC, deVries CR. Epididymitis: a 21-year retrospective review of presentations to an outpatient urology clinic. *J Urol*. (2014) 192:1203–7. doi: 10.1016/j.juro.2014.04.002
9. Rusz A, Pilatz A, Wagenlehner F, Linn T, Diemer T, Schuppe HC, et al. Influence of urogenital infections and inflammation on semen quality and male fertility. *World J Urol*. (2012) 30:23–30. doi: 10.1007/s00345-011-0726-8
10. Lang T, Dechant M, Sanchez V, Wistuba J, Boiani M, Pilatz A, et al. Structural and functional integrity of spermatozoa is compromised as a consequence of acute uropathogenic *E. coli*-associated epididymitis. *Biol Reprod*. (2013) 89:59. doi: 10.1095/biolreprod.113.110379
11. Pilatz A, Lochnit G, Karnati S, Paradowska-Dogan A, Lang T, Schultheiss D, et al. Acute epididymitis induces alterations in sperm protein composition. *Fertil Steril*. (2014) 101:1609–17.e1–5. doi: 10.1016/j.fertnstert.2014.03.011
12. Michel V, Pilatz A, Hedger MP, Meinhardt A. Epididymitis: revelations at the convergence of clinical and basic sciences. *Asian J Androl*. (2015) 17:756–63. doi: 10.4103/1008-682X.155770
13. Stammler A, Hau T, Bhushan S, Meinhardt A, Jonigk D, Lippmann T, et al. Epididymitis: ascending infection restricted by segmental boundaries. *Hum Reprod*. (2015) 30:1557–65. doi: 10.1093/humrep/dev112
14. Chakradhar S. Puzzling over privilege: how the immune system protects-and fails-the testes. *Nat Med*. (2018) 24:2–5. doi: 10.1038/nm0118-2
15. De Grava Kempinas W, Klinefelter GR. Interpreting histopathology in the epididymis. *Spermatogenesis*. (2015) 4:e979114. doi: 10.4161/21565562.2014.979114
16. Da Silva N, Smith TB. Exploring the role of mononuclear phagocytes in the epididymis. *Asian J Androl*. (2015) 17:591–6. doi: 10.4103/1008-682X.153540
17. Wang H, Kumar TR. Segment- and cell-specific expression of D-type cyclins in the postnatal mouse epididymis. *Gene Expr Patterns*. (2012) 12:136–44. doi: 10.1016/j.gep.2012.01.003
18. Légaré C, Sullivan R. Differential gene expression profiles of human efferent ducts and proximal epididymis. *Andrology*. (2020) 8:625–36. doi: 10.1111/andr.12745
19. Domeniconi RF, Souza AC, Xu B, Washington AM, Hinton BT. Is the epididymis a series of organs placed side by side? *Biol Reprod*. (2016) 95:10. doi: 10.1095/biolreprod.116.138768
20. Mital P, Hinton BT, Dufour JM. The blood-testis and blood-epididymis barriers are more than just their tight junctions. *Biol Reprod*. (2011) 84:851–8. doi: 10.1095/biolreprod.110.087452
21. Johnston DS, Turner TT, Finger JN, Owtscharuk TL, Kopf GS, Jelinsky SA. Identification of epididymis-specific transcripts in the mouse and rat by transcriptional profiling. *Asian J Androl*. (2007) 9:522–7. doi: 10.1111/j.1745-7262.2007.00317.x
22. Gregory M, Cyr DG. The blood-epididymis barrier and inflammation. *Spermatogenesis*. (2014) 4:e979619. doi: 10.4161/21565562.2014.979619
23. Cyr DG, Dufresne J, Gregory M. Cellular junctions in the epididymis, a critical parameter for understanding male reproductive toxicology. *Reprod Toxicol*. (2018) 81:207–19. doi: 10.1016/j.reprotox.2018.08.013
24. Hedger MP. Immunophysiology and pathology of inflammation in the testis and epididymis. *J Androl*. (2011) 32:625–40. doi: 10.2164/jandrol.111.012989
25. Itoh M, Xie Q, Miyamoto K, Takeuchi Y. Major differences between the testis and epididymis in the induction of granulomas in response to extravasated germ cells. I. A light microscopical study in mice. *Int J Androl*. (1999) 22:316–23. doi: 10.1046/j.1365-2605.1999.00186.x
26. Smith TB, Cortez-Retamozo V, Grigoryeva LS, Hill E, Pittet MJ, Da Silva N. Mononuclear phagocytes rapidly clear apoptotic epithelial cells in the proximal epididymis. *Andrology*. (2014) 2:755–62. doi: 10.1111/j.2047-2927.2014.00251.x
27. Dubé E, Cyr DG. The blood-epididymis barrier and human male fertility. *Adv Exp Med Biol*. (2012) 763:218–36. doi: 10.1007/978-1-4614-4711-5_11
28. Fitzgerald KA, Kagan JC. Toll-like receptors and the control of immunity. *Cell*. (2020) 180:1044–66. doi: 10.1016/j.cell.2020.02.041
29. Palladino MA, Savarese MA, Chapman JL, Dughi MK, Plaska D. Localization of Toll-like receptors on epididymal epithelial cells and spermatozoa. *Am J Reprod Immunol*. (2008) 60:541–55. doi: 10.1111/j.1600-0897.2008.00654.x
30. Palladino MA, Johnson TA, Gupta R, Chapman JL, Ojha P. Members of the toll-like receptor family of innate immunity pattern-recognition receptors are abundant in the male rat reproductive tract. *Biol Reprod*. (2007) 76:958–64. doi: 10.1095/biolreprod.106.059410
31. Zhu W, Zhao S, Liu Z, Cheng L, Wang Q, Yan K, et al. Pattern recognition receptor-initiated innate antiviral responses in mouse epididymal epithelial cell. *J Immunol*. (2015) 194:4825–35. doi: 10.4049/jimmunol.1402706
32. He Z, Zhu X, Shi Z, Wu T, Wu L. Metabolic regulation of dendritic cell differentiation. *Front Immunol*. (2019) 10:410. doi: 10.3389/fimmu.2019.00410
33. Rhodes JW, Tong O, Harman AN, Turville SG. Human dendritic cell subsets ontogeny, and impact on HIV infection. *Front Immunol*. (2019) 10:1088. doi: 10.3389/fimmu.2019.01088
34. Pierucci-Alves F, Midura-Kiela MT, Fleming SD, Schultz BD, Kiela PR. Transforming growth factor beta signaling in dendritic cells is required for immunotolerance to sperm in the epididymis. *Front Immunol*. (2018) 9:1882. doi: 10.3389/fimmu.2018.01882
35. Kemp TJ, Elzey BD, Griffith TS. Plasmacytoid dendritic cell-derived IFN-alpha induces TNF-related apoptosis-inducing ligand/Apo-2L-mediated antitumor activity by human monocytes following CpG oligodeoxynucleotide stimulation. *J Immunol*. (2003) 171:212–8. doi: 10.4049/jimmunol.171.1.212
36. Duan YG, Yu CF, Novak N, Bieber T, Zhu CH, Schuppe HC, et al. Immunodeviation towards a Th17 immune response associated with testicular damage in azoospermic men. *Int J Androl*. (2011) 34:e536–45. doi: 10.1111/j.1365-2605.2010.01137.x
37. Wang P, Duan YG. The role of dendritic cells in male reproductive tract. *Am J Reprod Immunol*. (2016) 76:186–92. doi: 10.1111/aji.12536
38. Da Silva N, Cortez-Retamozo V, Reinecker HC, Wildgruber M, Hill E, Brown D, et al. A dense network of dendritic cells populates the murine epididymis. *Reproduction*. (2011) 141:653–63. doi: 10.1530/REP-10-0493
39. Guazzone VA. Exploring the role of antigen presenting cells in male genital tract. *Andrologia*. (2018) 50:e13120. doi: 10.1111/and.13120
40. Voisin A, Whitfield M, Damon-Soubeyrand C, Goubely C, Henry-Berger J, Saez F, et al. Comprehensive overview of murine epididymal mononuclear phagocytes and lymphocytes: unexpected populations arise. *J Reprod Immunol*. (2018) 126:1–17. doi: 10.1016/j.jri.2018.01.003
41. den Haan JM, Lehar SM, Bevan MJ. $CD8^+$. but not $CD8^-$. dendritic cells cross-prime cytotoxic T cells *in vivo*. *J Exp Med*. (2000) 192:1685–96. doi: 10.1084/jem.192.12.1685

42. Schlitzer A, McGovern N, Ginhoux, F. Dendritic cells and monocyte-derived cells: two complementary and integrated functional systems. *Semin Cell Dev Biol*. (2015) 41:9–22. doi: 10.1016/j.semcdb.2015.03.011
43. Arora S, Dev K, Agarwal B, Das P, Syed MA. Macrophages: their role, activation and polarization in pulmonary diseases. *Immunobiology*. (2018) 223:383–96. doi: 10.1016/j.imbio.2017.11.001
44. Mosser DM, Edwards JP. Exploring the full spectrum of macrophage activation. *Nat Rev Immunol*. (2008) 8:958–69. doi: 10.1038/nri2448
45. Bhushan S, Meinhardt A. The macrophages in testis function. *J Reprod Immunol*. (2017) 119:107–12. doi: 10.1016/j.jri.2016.06.008
46. Kabat AM, Pearce EJ. Inflammation by way of macrophage metabolism. *Science*. (2017) 356:488–9. doi: 10.1126/science.aan2691
47. Nashan D, Malorny U, Sorg C, Cooper T, Nieschlag E. Immunocompetent cells in the murine epididymis. *Int J Androl*. (2015) 12:85–94. doi: 10.1111/j.1365-2605.1989.tb01289.x
48. Da Silva N, Barton CR. Macrophages and dendritic cells in the post-testicular environment. *Cell Tissue Res*. (2016) 363:97–104. doi: 10.1007/s00441-015-2270-0
49. Yakirevich E, Yanai O, Sova Y, Sabo E, Stein A, Hiss J, et al. Cytotoxic phenotype of intra-epithelial lymphocytes in normal and cryptorchid human testicular excurrent ducts. *Hum Reprod*. (2002) 17:275–83. doi: 10.1093/humrep/17.2.275
50. Flickinger CJ, Bush LA, Howards SS, Herr JC. Distribution of leukocytes in the epithelium and interstitium of four regions of the Lewis rat epididymis. *Anat Rec*. (1997) 248:380–90.
51. Yeung CH, Wang K, Cooper TG. Why are epididymal tumours so rare? *Asian J Androl*. (2012) 14:465–75. doi: 10.1038/aja.2012.20
52. Serre V, Robaire B. Segment-specific morphological changes in aging brown norway rat epididymis. *Biol Reprod*. (1998) 58:497–513. doi: 10.1095/biolreprod58.2.497
53. Serre V, Robaire B. Distribution of immune cells in the epididymis of the aging brown norway rat is segment-specific and related to the luminal content. *Biol Reprod*. (1999) 61:705–14. doi: 10.1095/biolreprod61.3.705
54. Yeung CH, Nashan D, Sorg C, Oberpenning F, Schulze H, Nieschlag E, et al. Basal cells of the human epididymis–antigenic and ultrastructural similarities to tissue-fixed macrophages. *Biol Reprod*. (1994) 50:917–26. doi: 10.1095/biolreprod50.4.917
55. Holschbach C, Cooper TG. A possible extratubular origin of epididymal basal cells in mice. *Reproduction*. (2002) 123:517–25. doi: 10.1530/reprod/123.4.517
56. Shum WW, Smith TB, Cortez-Retamozo V, Grigoryeva LS, Roy JW, Hill E, et al. Epithelial basal cells are distinct from dendritic cells and macrophages in the mouse epididymis. *Biol Reprod*. (2014) 90:90. doi: 10.1095/biolreprod.113.116681
57. Arrighi S. Are the basal cells of the ammalian epididymis still an enigma? *Reprod Fertil Dev*. (2014) 26:1061–71. doi: 10.1071/RD13301
58. Nielsen MM, Witherden DA, Havran WL. γδ T cells in homeostasis and host defence of epithelial barrier tissues. *Nat Rev Immunol*. (2017) 17:733–45. doi: 10.1038/nri.2017.101
59. Witherden DA, Johnson MD, Havran WL. Coreceptors and their ligands in epithelial γδ T cell biology. *Front Immunol*. (2018) 9:731. doi: 10.3389/fimmu.2018.00731
60. Daley D, Zambirinis CP, Seifert L, Akkad N, Mohan N, Werba G, et al. γδ T cells support pancreatic oncogenesis by restraining αβ T cell activation. *Cell*. (2016) 166:1485–99.e15. doi: 10.1016/j.cell.2016.07.046
61. Taylor MW, Feng GS. Relationship between interferon-gamma, indoleamine 2,3-dioxygenase, and tryptophan catabolism. *FASEB J*. (1991) 5:2516–22. doi: 10.1096/fasebj.5.11.1907934
62. Mellor AL, Munn DH. IDO expression by dendritic cells: tolerance and tryptophan catabolism. *Nat Rev Immunol*. (2004) 4:762–74. doi: 10.1038/nri1457
63. Dai X, Zhu BT. Indoleamine 2,3-dioxygenase tissue distribution and cellular localization in mice: implications for its biological functions. *J Histochem Cytochem*. (2010) 58:17–28. doi: 10.1369/jhc.2009.953604
64. Mellor AL, Munn DH. Creating immune privilege: active local suppression that benefits friends, but protects foes. *Nat Rev Immunol*. (2008) 8:74–80. doi: 10.1038/nri2233
65. Xu H, Zhang GX, Ciric B, Rostami A. IDO: a double-edged sword for T(H)1/T(H)2 regulation. *Immunol Lett*. (2008) 121:1–6. doi: 10.1016/j.imlet.2008.08.008
66. Britan A, Maffre V, Tone S, Drevet JR. Quantitative and spatial differences in the expression of tryptophan-metabolizing enzymes in mouse epididymis. *Cell Tissue Res*. (2006) 324:301–10. doi: 10.1007/s00441-005-0151-7
67. Wijayarathna R, Hedger MP. Activins, follistatin and immunoregulation in the epididymis. *Andrology*. (2019) 7:703–11. doi: 10.1111/andr.12682
68. Pallotta MT, Orabona C, Volpi C, Vacca C, Belladonna ML, Bianchi R, et al. Indoleamine 2,3-dioxygenase is a signaling protein in long-term tolerance by dendritic cells. *Nat Immunol*. (2011) 12:870–8. doi: 10.1038/ni.2077
69. Jrad-Lamine A, Henry-Berger J, Gourbeyre P, Damon-Soubeyrand C, Lenoir A, Combaret L, et al. Deficient tryptophan catabolism along the kynurenine pathway reveals that the epididymis is in a unique tolerogenic state. *J Biol Chem*. (2011) 286:8030–42. doi: 10.1074/jbc.M110.172114
70. Meade KG, O'Farrelly C. β-Defensins: farming the microbiome for homeostasis and health. *Front Immunol*. (2018) 9:3072. doi: 10.3389/fimmu.2018.03072
71. Guiton R, Voisin A, Henry-Berger J, Saez F, Drevet JR. Of vessels and cells: the spatial organization of the epididymal immune system. *Andrology*. (2019) 7:712–8. doi: 10.1111/andr.12637
72. Yamaguchi Y, Nagase T, Makita R, Fukuhara S, Tomita T, Tominaga T, et al. Identification of multiple novel epididymis-specific beta-defensin isoforms in humans and mice. *J Immunol*. (2002) 169:2516–23. doi: 10.4049/jimmunol.169.5.2516
73. Li P, Chan HC, He B, So SC, Chung YW, Shang Q, et al. An antimicrobial peptide gene found in the male reproductive system of rats. *Science*. (2001) 291:1783–5. doi: 10.1126/science.1056545
74. Fernandez-Fuertes B, Narciandi F, O'Farrelly C, Kelly AK, Fair S, Meade KG, et al. Cauda epididymis-specific beta-defensin 126 promotes sperm motility but not fertilizing ability in cattle. *Biol Reprod*. (2016) 95:122. doi: 10.1095/biolreprod.116.138792
75. Yenugu S, Hamil KG, French FS, Hall SH. Antimicrobial actions of human and macaque sperm associated antigen (SPAG). 11 isoforms: influence of the N-terminal peptide. *Mol Cell Biochem*. (2006) 284:25–37. doi: 10.1007/s11010-005-9009-2
76. Yu H, Dong J, Gu Y, Liu H, Xin A, Shi H, et al. The novel human β-defensin 114 regulates lipopolysaccharide (LPS)-mediated inflammation and protects sperm from motility loss. *J Biol Chem*. (2013) 88:12270–82. doi: 10.1074/jbc.M112.411884
77. Diao R, Fok KL, Chen H, Yu MK, Duan Y, Chung CM, et al. Deficient human β-defensin 1 underlies male infertility associated with poor sperm motility and genital tract infection. *Sci Transl Med*. (2014) 6:249ra108. doi: 10.1126/scitranslmed.3009071
78. Hinck AP, Mueller TD, Springer TA. Structural biology and evolution of the TGF-β family. *Cold Spring Harb Perspect Biol*. (2016) 8:a022103. doi: 10.1101/cshperspect.a022103
79. Voisin A, Damon-Soubeyrand C, Bravard S, Saez F, Drevet JR, Guiton R. Differential expression and localisation of TGF-β isoforms and receptors in the murine epididymis. *Sci Rep*. (2020) 10:995. doi: 10.1038/s41598-020-57839-5
80. Winnall WR, Wu H, Sarraj MA, Rogers PA, de Kretser DM, Girling JE, et al. Expression patterns of activin, inhibin and follistatin variants in the adult male mouse reproductive tract suggest important roles in the epididymis and vas deferens. *Reprod Fertil Dev*. (2013) 25:570–80. doi: 10.1071/RD11287
81. Wijayarathna R, Sarraj MA, Genovese R, Girling JE, Michel V, Ludlow H, et al. Activin and follistatin interactions in the male reproductive tract: activin expression and morphological abnormalities in mice lacking follistatin 288. *Andrology*. (2017) 5:578–88. doi: 10.1111/andr.12337
82. Veräjänkorva E, Pöllänen P, Hänninen A, Martikainen M, Sundström J, Antola H. Il-10 is highly expressed in the cryptorchid crypt epididymal epithelium: a probable mechanism preventing immune responses against autoantigenic spermatozoa in the epididymal

tubule. *Int J Androl*. (2002) 25:129–33. doi: 10.1046/j.1365-2605.2002.00336.x
83. Voisin A, Saez F, Drevet JR, Guiton R. The epididymal immune balance: a key to preserving male fertility. *Asian J Androl*. (2019) 21:531–9. doi: 10.4103/aja.aja_11_19
84. Collin M, Linge HM, Bjartell A, Giwercman A, Malm J, Egesten A. Constitutive expression of the antibacterial CXC chemokine GCP-2/CXCL6 by epithelial cells of the male reproductive tract. *J Reprod Immunol*. (2008) 79:37–43. doi: 10.1016/j.jri.2008.08.003
85. Guiton R, Henry-Berger J, Drevet JR. The immunobiology of the mammalian epididymis: the black box is now open! *Basic Clin Androl*. (2013) 23:8. doi: 10.1186/2051-4190-23-8
86. Hirai S, Naito M, Terayama H, Ning Q, Miura M, Shirakami G, et al. Difference in abundance of blood and lymphatic capillaries in the murine epididymis. *Med Mol Morphol*. (2010) 43:37–42. doi: 10.1007/s00795-009-0473-8
87. de Kretser DM, Huidobro C, Southwick GJ, Temple-Smith PD. The role of the epididymis in human infertility. *J Reprod Fertil Suppl*. (1998) 53:271–5.
88. Trojian TH, Lishnak TS, Heiman D. Epididymitis and orchitis: an overview. *Am Fam Phys*. (2009) 79:583–7. doi: 10.1186/1471-2296-10-23
89. Weidner W, Garbe C, Weissbach L, Harbrecht J, Kleinschmidt K, Schiefer HG, et al. Initial therapy of acute unilateral epididymitis using ofloxacin II. andrological findings. *Urologe A*. (1990) 29:277–80.
90. McConaghy JR, Panchal B. Epididymitis: an overview. *Am Fam Phys*. (2016) 94:723–6.
91. Silva EJR, Ribeiro CM, Mirim AFM, Silva AAS, Romano RM, Hallak J, et al. Lipopolysaccharide and lipotheicoic acid differentially modulate epididymal cytokine and chemokine profiles and sperm parameters in experimental acute epididymitis. *Sci Rep*. (2018) 8:103. doi: 10.1038/s41598-017-17944-4
92. Cheng L, Chen Q, Zhu W, Wu H, Wang Q, Shi L, et al. Toll-like receptors 4 and 5 cooperatively initiate the innate immune responses to uropathogenic *Escherichia coli* infection in mouse epididymal epithelial cells. *Biol Reprod*. (2016) 94:58. doi: 10.1095/biolreprod.115.136580
93. Zhang D, Zhang G, Hayden MS, Greenblatt MB, Bussey C, Flavell RA, et al. A toll-like receptor that prevents infection by uropathogenic bacteria. *Science*. (2004) 303:1522–6. doi: 10.1126/science.1094351
94. Biswas B, Yenugu S. Antimicrobial responses in the male reproductive tract of lipopolysaccharide challenged rats. *Am J Reprod Immunol*. (2011) 65:57–68. doi: 10.1111/j.1600-0897.2010.00937.x
95. Cao D, Li Y, Yang R, Wang Y, Zhou Y, Diao H, et al. Lipopolysaccharide-induced epididymitis disrupts epididymal beta-defensin expression and inhibits sperm motility in rats. *Biol Reprod*. (2010) 83:1064–70. doi: 10.1095/biolreprod.109.082180
96. Biswas B, Bhushan S, Rajesh A, Suraj SK, Lu Y, Meinhardt A, et al. Uropathogenic *Escherichia coli* (UPEC). induced antimicrobial gene expression in the male reproductive tract of rat: evaluation of the potential of defensin 21 to limit infection. *Andrology*. (2015) 3:368–75. doi: 10.1111/andr.12012
97. Fei Z, Hu S, Xiao L, Zhou J, Diao H, Yu H, et al. mBin1b transgenic mice show enhanced resistance to epididymal infection by bacteria challenge.Genes *Immun*. (2012) 13:45–51. doi: 10.1038/gene.2012.13
98. Michel V, Duan Y, Stoschek E, Bhushan S, Middendorff R, Young JM, et al. Uropathogenic *Escherichia coli* causes fibrotic remodelling of the epididymis. *J Pathol*. (2016) 240:15–24. doi: 10.1002/path.4748
99. Nashan D, Jantos C, Ahlers D, Bergmann M, Schiefer HG, Sorg C, et al. Immuno-competent cells in the murine epididymis following infection with *Escherichia coli*. *Int J Androl*. (1993) 16:47–52. doi: 10.1111/j.1365-2605.1993.tb01152.x
100. Lucchetta R, Clavert A, Meyer JM, Bollack C. Acute experimental *E. coli* epididymitis in the rat and its consequences on spermatogenesis. *Urol Res*. (1983) 11:17–20. doi: 10.1007/BF00257715
101. Frikh M, Mrimar N, Kasouati J, Hamzaoui A, Maleb A, Lemnouer A, et al. Prevalence and role of IgG anti-*Chlamydia trachomatis* in a population of infertile men in Morocco. *Prog Urol*. (2019) 29:612–8. doi: 10.1016/j.purol.2019.08.261
102. Hocking JS, Temple-Smith M, Guy R, Donovan B, Braat S, Law M, et al. Population effectiveness of opportunistic chlamydia testing in primary care in Australia: a cluster-randomised controlled trial. *Lancet*. (2018) 392:1413–22. doi: 10.1016/S0140-6736(18)31816-6
103. Ito S, Tsuchiya T, Yasuda M, Yokoi S, Nakano M, Deguchi T. Prevalence of genital mycoplasmas and ureaplasmas in men younger than 40 years-of-age with acute epididymitis. *Int J Urol*. (2012) 19:234–8. doi: 10.1111/j.1442-2042.2011.02917.x
104. Workowski KA, Bolan GA. Sexually transmitted diseases treatment guidelines 2015. *MMWR Recomm Rep*. (2015) 64:1–137. doi: 10.1016/j.annemergmed.2011.04.006
105. Andersen B, van Valkengoed I, Sokolowski I, Móller JK, Østergaard L, Olesen F. Impact of intensified testing for urogenital Chlamydia trachomatis infections: a randomised study with 9-year follow-up. *Sex Transm Infect*. (2011) 87:156–61.
106. Gonzales GF, Muñoz G, Sánchez R, Henkel R, Gallegos-Avila G, Díaz-Gutierrez O, et al. Update on the impact of *Chlamydia trachomatis* infection on male fertility. *Andrologia*. (2004) 36:1–23. doi: 10.1046/j.0303-4569.2003.00594.x
107. Moazenchi M, Totonchi M, Salman Yazdi R, Hratian K, Mohseni Meybodi MA, Ahmadi Panah M, et al. The impact of *Chlamydia trachomatis* infection on sperm parameters and male fertility: a comprehensive study. *Int J STD AIDS*. (2018) 29:466–73. doi: 10.1177/0956462417735245
108. Redgrove KA, McLaughlin EA. The role of the immune response in *Chlamydia trachomatis* infection of the male genital tract: a double-edged sword. *Front Immunol*. (2014) 5:534. doi: 10.3389/fimmu.2014.00534
109. Xu H, Su X, Zhao Y, Tang L, Chen J, Zhong G. Innate lymphoid cells are required for endometrial resistance to *Chlamydia trachomatis* infection. *Infect Immun*. (2020). 88:e00152-20. doi: 10.1128/IAI.00152-20
110. Coers J, Bernstein-Hanley I, Grotsky D, Parvanova I, Howard JC, Taylor GA, et al. *Chlamydia muridarum* evades growth restriction by the IFN-gamma-inducible host resistance factor Irgb10. *J Immunol*. (2008) 180:6237–45. doi: 10.4049/jimmunol.180.9.6237
111. Bakshi RK, Gupta K, Jordan SJ, Chi X, Lensing SY, Press CG, et al. An adaptive *Chlamydia trachomatis*-specific IFN-γ-producing $CD4^+$. T cell response is associated with protection against chlamydia reinfection in women. *Front Immunol*. (2018) 9:1981. doi: 10.33v89/fimmu.2018.01981
112. Somboonna N, Ziklo N, Ferrin TE, Hyuk Suh J, Dean D. Clinical persistence of *Chlamydia trachomatis* sexually transmitted strains involves novel mutations in the functional αββα tetramer of the tryptophan synthase operon. *mBio*. (2019) 10:e01464-19. doi: 10.1128/mBio.01464-19
113. Virok DP, Raffai T, Kókai D, Paróczai D, Bogdanov A, Veres G, et al. Indoleamine 2,3-dioxygenase activity in *Chlamydia muridarum* and *Chlamydia pneumoniae* infected mouse lung tissues. *Front Cell Infect Microbiol*. (2019) 9:192. doi: 10.3389/fcimb.2019.00192
114. Leonhardt RM, Lee SJ, Kavathas PB, Cresswell P. Severe tryptophan starvation blocks onset of conventional persistence and reduces reactivation of *Chlamydia trachomatis*. *Infect Immun*. (2007) 75:5105–17. doi: 10.1128/IAI.00668-07
115. Johnson RM. Murine oviduct epithelial cell cytokine responses to *Chlamydia muridarum* infection include interleukin-12-p70 secretion. *Infect Immun*. (2004) 72:3951–60. doi: 10.1128/IAI.72.7.3951-3960.2004
116. Mackern-Oberti JP, Motrich RD, Breser ML, Sánchez LR, Cuffini C, Rivero VE. *Chlamydia trachomatis* infection of the male genital tract: an update. *J Reprod Immunol*. (2013) 100:37–53. doi: 10.1016/j.jri.2013.05.002
117. Bezold G, Politch JA, Kiviat NB, Kuypers JM, Wolff H, Anderson DJ. Prevalence of sexually transmissible pathogens in semen from asymptomatic male infertility patients with and without leukocytospermia. *Fertil Steril*. (2007) 87:1087–97. doi: 10.1016/j.fertnstert.2006.08.109
118. Oliva A, Multigner L. Chronic epididymitis and grade III varicocele and their associations with semen characteristics in men consulting for couple infertility. *Asian J Androl*. (2018) 20:360–5. doi: 10.4103/aja.aja_78_17
119. Emerson C, Dinsmore WW, Quah SP. Are we missing mumps epididymo-orchitis? *Int J STD AIDS*. (2007) 18:341–2. doi: 10.1258/095646207780749754
120. Park SJ, Kim HC, Lim JW, Moon SK, Ahn SE. Distribution of epididymal involvement in mumps epididymo-orchitis. *J Ultrasound Med*. (2015) 34:1083–9. doi: 10.7863/ultra.34.6.1083

121. Ahmed HJ, Mbwana J, Gunnarsson E, Ahlman K, Guerino C, Svensson LA, et al. Etiology of genital ulcer disease and association with human immunodeficiency virus infection in two tanzanian cities. *Sex Transm Dis*. (2003) 30:14–9. doi: 10.1097/00007435-200302000-00004
122. Shehu-Xhilaga M, Kent S, Batten J, Ellis S, Van der Meulen J, O'Bryan M, et al. The testis and epididymis are productively infected by SIV and SHIV in juvenile macaques during the post-acute stage of infection. *Retrovirology*. (2007) 4:7. doi: 10.1186/1742-4690-4-7
123. Borges ED, Vireque AA, Berteli TS, Ferreira CR, Silva AS, Navarro PA. An update on the aspects of zika virus infection on male reproductive system. *J Assist Reprod Genet*. (2019) 36:1339–49. doi: 10.1007/s10815-019-01493-y
124. Spornraft-Ragaller P, Varwig-Janßen D. Sexually transmitted infections and male fertility. *Hautarzt*. (2018) 69:1006–13. doi: 10.1007/s00105-018-4300-9
125. Browne JA, Leir SH, Eggener SE, Harris A. Region-specific innate antiviral responses of the human epididymis. *Mol Cell Endocrinol*. (2018) 473:72–78. doi: 10.1016/j.mce.2018.01.004

Conflict of Interest: The authors declare that the research was conducted in the absence of any commercial or financial relationships that could be construed as a potential conflict of interest.

frontiers in Immunology

ORIGINAL RESEARCH
published: 23 October 2020
doi: 10.3389/fimmu.2020.570872

Prokineticin 2 *via* Calcium-Sensing Receptor Activated NLRP3 Inflammasome Pathway in the Testicular Macrophages of Uropathogenic *Escherichia coli*-Induced Orchitis

Yufang Su, Yuan Zhang, Zhiyong Hu, Liting He, Wei Wang, Jia Xu, Zunpan Fan, Chunyan Liu, Huiping Zhang and Kai Zhao**

Institute of Reproductive Health, Tongji Medical College, Huazhong University of Science and Technology, Wuhan, China

Reproductive tract infections contribute to the development of testicular inflammatory lesions, leading to male infertility. Previous research shows that the activation of the NLRP3 inflammasome in orchitis promotes the secretion and maturation of IL-1β and, thus, decreases male fertility. The calcium-sensing receptor (CaSR) is closely related to the secretion of proinflammatory cytokines. An increase in the CaSR level promotes the assembly and activation of the NLRP3 inflammasome. However, the role of CaSRs in orchitis is unknown. We first constructed a uropathogenic *Escherichia Coli* (UPEC) rat orchitis model and then detected the expression of CaSR and NLRP3 inflammatory pathway proteins in testicular macrophages (TM) through RT-PCR and WB, calcium levels in TM through flow cytometry, and proinflammatory factor IL-1β through ELISA. In addition, testosterone levels in the serum samples were detected using liquid chromatography–mass spectrometry (LC-MS). Here, we show that CaSR upregulation after infection in TM in a rat model of UPEC induces the activation of the NLRP3 inflammasome pathway and thereby enhances IL-1β secretion and reduces the testosterone level in the blood. Moreover, CaSR inhibitors can alleviate inflammatory impairment. After UPEC challenge *in vitro*, CaSR promoted NLRP3 expression and released IL-1β cleaved from TM into the supernatant. Overall, elevated CaSR levels in TM in testes with UPEC-induced orchitis may impair testosterone synthesis through the activation of the NLRP3 pathway and PK2 is an upstream regulatory protein of CaSR. Our research further shows the underlying mechanisms of inflammation-related male infertility and provides anti-inflammatory therapeutic targets for male infertility.

Keywords: calcium-sensing receptor, testicular macrophages, inflammasome, orchitis, prokineticin 2

OPEN ACCESS

Edited by:
Daishu Han,
Chinese Academy of Medical Sciences and Peking Union Medical College, China

Reviewed by:
Sudhanshu Bhushan,
Justus-Liebig-University Giessen, Germany
Yongning Lu,
Fudan University, China

****Correspondence:***
Huiping Zhang
zhpmed@126.com
Kai Zhao
kai_zhao@hust.edu.cn

Specialty section:
This article was submitted to Mucosal Immunity, a section of the journal Frontiers in Immunology

Received: *09 June 2020*
Accepted: *02 September 2020*
Published: *23 October 2020*

Citation:
Su Y, Zhang Y, Hu Z, He L, Wang W, Xu J, Fan Z, Liu C, Zhang H and Zhao K (2020) Prokineticin 2 via Calcium-Sensing Receptor Activated NLRP3 Inflammasome Pathway in the Testicular Macrophages of Uropathogenic Escherichia coli-Induced Orchitis. Front. Immunol. 11:570872. doi: 10.3389/fimmu.2020.570872

INTRODUCTION

Decline in male sperm quality and male infertility is a worldwide concern. Approximately 15% of male infertility cases are related to the inflammation of the reproductive system (1), and approximately 60% of such cases are caused by uropathogenic *Escherichia Coli* (UPEC) (2). Testicular impairment is usually caused by the immune system when it is killing pathogenic bacteria during an infection rather than by the direct toxicities of pathogens and their secretions to testicular cells (3). Therefore, studying the immune regulation of inflammation-related male infertility is of great significance to clinical diagnosis and treatment.

Testicular macrophages (TM) comprise the largest proportion of immune cells in the interstitial space of the testis (4). Rat TM account for approximately 20% of total immune cells, constituting the first line of defense against pathogens. Macrophages and NLRP3 inflammasomes are involved in the onset and development of orchitis (5). NLRP3 inflammasomes are composed of cytoplasmic sensor molecules, such as the PYD domain-containing protein 3 (NLRP3), adaptor proteins (e.g., caspase-recruiting domain [ASC] of apoptosis-associated speck-like proteins), and effector proteins (e.g., pre-caspase-1) (6–8). NLRP3 and ASC promote the cleavage of pro-caspase-1 and form an active complex, which triggers the cleavage of pro-IL-1β into mature IL-1β (9). In a murine model of UPEC orchitis, NLRP3, ASC, caspase-1, and IL-1β are clearly elevated in TM (10–12).

The calcium-sensing receptor (CaSR) can sense small changes in Ca^{2+} concentration, mediate signal transduction in the cytoplasm, promote the recruitment and assembly of NLRP3 inflammasomes, and cause an inflammatory response (13). Increasing evidence shows that the elevated circulating levels of proinflammatory cytokines are accompanied by changes in Ca^{2+} homeostasis (14). CaSR is expressed in BMDNs, promotes the assembly of NLRP3 inflammasomes by regulating Ca^{2+} concentration, and modulates the secretion and maturation of IL-1β (15). CaSR activates NLRP3 inflammasomes through the ERK1/2 signaling pathway in the preadipocyte line LS14 (16). However, the role of CaSR in UPEC-induced orchitis macrophages remains unclear.

Given the potential relationship between CaSR and NLRP3, we concluded that CaSR is closely related to UPEC-induced testicular inflammation. Based on our previous findings that PK2 promotes IL-1β secretion through the NLRP3 pathway (12), we speculated that PK2 and CaSR have a close relationship. In this study, we focused on the effect of CaSR on IL-1β secretion in TM during a UPEC infection to reveal the molecular mechanism that may ultimately damage male fertility.

MATERIALS AND METHODS

Animals

Adult male Wistar rats (8–10 weeks) were purchased from the Animal Center of Tongji Medical College. The rats were raised at 22°C in a 12 h light/12 h dark cycle and fed with standard food pellets and water. The study was conducted in strict accordance with the guidelines approved by the Animal Care and Use Committee of Tongji Medical College, Huazhong University of Science and Technology.

Bacterial Reproduction and Detection

The UPEC strain CFT073 (NCBI: AE014075, NC_004431) bacterial culture was shaken in an LB liquid medium and then grown to the exponential phase (OD600 = 0.6–0.8). The UPEC culture was centrifuged at 4000x*g* for 10 min at room temperature. The obtained pellets were washed with PBS and stored in DMEM 0F12:1. Then, a 9-cm LB solid medium plate was prepared, and the UPEC bacterial solution was diluted at different concentration gradients. Approximately 10 μL from each gradient solution was smeared evenly on the plate. Finally, the total number of CFU of UPEC was calculated.

Detection of bacteria in the testes of UPEC model rats: A small portion of each testis tissue sample was ground into a homogenate. After dilution with physiological saline, 10 μL of the homogenate was evenly spread on an LB solid medium, and the formation of UPEC CFU was observed on the next day.

UPEC-treated cells *in vitro*: Cells were infected with UPEC (Moi = 20) for 2 h.

UPEC Rat Model

After the rats were anesthetized, the testes and epididymides were fully exposed for the location of the vasa deferentia. Approximately 50 μL of 4×10^6 CFU UPEC CFT073 bacterial solution diluted with saline was injected into the vas deferens near the tail of the epididymis on both sides. The control group was injected with 50 μL of saline. After constructing the UPEC rat orchitis model, NPS2143 containing 0.5% DMSO was injected *in situ* into the testis of the rat the next day, and the concentration was 10 mg/kg according to the body weight of each rat.

Sample Collection

Collection of testis and epididymis tissues: Laboratory equipment was cleaned and disinfected at 125°C. After the rats were killed, the testes and epididymides were exposed immediately, and any damage to the seminiferous tubules was prevented by carefully removing the tissues.

For the collection of the testicular interstitial fluid, a 2-mm incision was made at the end of each testis, and then the white membrane was sutured at the top of the testis with four surgical threads. The testis was suspended in four refrigerators in a 15-mL centrifuge tube for 16 h and centrifuged at a speed of 200 RPM for 3 min. The resulting transparent tissue fluid was collected and stored in a refrigerator at −80°C.

Collection of the supernatant of the primary macrophages: Primary macrophages from each group adhered to the wall for 30–40 min. Each culture medium was changed for the stimulation of adherent macrophages and subsequent collection of supernatants.

Flow Cytometry

A stain buffer (100 μL) containing 1% BSA was used in the preparation of single-cell suspensions from primary TM. TM were broken, placed in an EP tube, and centrifuged at 300x*g* at 4°C for 10 min. The resulting pellets were collected, and impurities were

removed by resuspending the primary macrophages. Mouse anti-CD68-Alexa Fluor 488 (Bio-Rad, USA) and mouse anti-CD45-PE/Cy7 (BioLegend, USA) fluorescent antibody-labeled macrophages were prepared and incubated at 4°C in the dark for 50 min. The primary TM were washed again and centrifuged at 300x*g* for 10 min. The resulting pellets were collected, and the primary TM were resuspended after incubation for on-board testing.

Calcium ion detection: 350 μL of interstitial single-cell suspension (approximately 1×10^6 cells) and 2 μL of mouse anti-CD68-Alexa Fluor 488 (Bio-Rad, USA) and fluo4-am were used. After the exclusion of cell aggregation and bimodality according to the side scatter A (SSC-A) and SSC-H plots, flow cytometry analysis was performed using a flow cytometer (BD LSR II, USA), and data were analyzed using FlowJo version X.

Testicular Histopathology

Fresh testes from each group were removed and immediately placed in Bouins solution for 48 h. Testicular tissues were embedded in paraffin. The wax blocks were completely solidified and then cut into thin slices on a machine. The incised testicular tissues were dewaxed, stained with hematoxylin and eosin, and observed under a microscope.

Testes the same size as mung beans were collected form each group within 2 min and placed in a fixative solution. The testis microstructure was observed under an electron microscope.

Sperm Count and Sperm Forward-Movement Detection

The rats were anesthetized and sacrificed. Epididymal samples were collected, cut into small pieces, incubated in an F10 medium for 20 min, and counted under the microscope.

Cell Isolation

Isolation of adult Wistar rat TM. The testes were decapsulated and digested with 1 mg/mL collagenase I (Sigma, USA) at 34°C for 20 min. Then, mesenchymal cells and seminiferous tubules were separated through 200-mesh filtration. The cells were cultured in DMEM F12:1 (Life Technologies, USA). After 40 min, nonadherent cells were removed by culture medium washing. The remaining adherent interstitial cells were primarily TM.

Cell Viability Measurements

After the UPEC bacteria with MOI=20 stimulated the J774A.1 and Raw264.7 macrophage cell lines for 2 h, the cells were treated with the NPS2143 inhibitor for 4 h. According to the manufacturer's instructions, cell viability was assessed by Pierce LDH cytotoxicity assay (Beyotime, China) and neutral red toxicity assay (Beyotime, China) (17).

RT-PCR

Total RNA was isolated from TM using TRIzol reagent (Invitrogen, USA). Reverse transcription was performed using a PrimeScript™ RT kit. PCR was performed in 20 μL of a reaction mixture containing 2 μL of cDNA, 0.8 μL of forward primer, 0.8 μL of reverse primer (**Table 1**), and 10 μLSYBR Green PCR MasterMix. The amplification conditions were initial denaturation at 95°C for 30 s, 40 cycles of denaturation at 95°C for 5 s, annealing at 60°C for 30 s, and elongation at 72°C for 30 s. The $2^{-\Delta\Delta Ct}$ method was used in normalizing the relative expression level of the target gene to the relative expression level of the control.

Western Blot Analysis

Tissue and cell proteins were lysed on ice with radioimmunoprecipitation assay lysis buffer (Cwbio, Taizhou, China). Total proteins were collected after centrifugation. Then, 5 μL of 5× loading buffer was added to the proteins, which were denatured at 98°C and stored in a refrigerator at −20°C. Colloidal preparation, electrophoresis, membrane transfer, sealing, and other operations were carried out successively according to the kit's instructions. The following primary antibodies were used during incubation: goat anti-IL-1β polyclonal antibody (1:1000, R & D Systems, USA), rabbit anti-CaSR polyclonal antibody (6D4, 1:500, Santa Cruz Biotechnology, USA), rabbit anti-NLRP3 polyclonal antibody (1:500, Novus, USA), mouse anti-caspase-1 monoclonal antibody (1:500, Novus, USA), and mouse anti-β-actin polyclonal antibody (1:500, Boster, China). Protein bands were detected using ECL (Pierce, USA).

Enzyme-Linked Immunosorbent Assay

According to the manufacturer's instructions, the levels of IL-1β in the sera and supernatants were assessed using ELISA kits from R & D Systems (USA).

Immunofluorescence

Cells seeded in coverslips were washed with PBS and then fixed with prechilled 4% formaldehyde. Subsequently, the cells were blocked with 5% normal goat serum for 1 h at room temperature and then treated with rabbit anti-CaSR polyclonal antibody (1:200, Abcam, USA), PK2 polyclonal antibody (1:200, Abcam, USA), and rabbit anti-CaSR polyclonal antibody (1:500, Abcam, USA) and incubated overnight. The cells were washed twice with PBS and then treated with the following secondary antibodies: donkey antimouse IgG H & L (Alexa Fluoro® 647, 1:500, Abcam, USA) and goat antirabbit IgG H & L (FITC, 1:500, Abcam, USA) and left to stand at room temperature for 1 h. Nuclei were stained with DAPI.

Testosterone Test

For liquid chromatography–mass spectrometry (LC-MS), 200 μL of each sample was mixed with 800 μL of precooled methanol/acetonitrile (1:1) for the precipitation of the proteins. The mixtures were centrifuged at 15,000x*g* for 4 min at 4°C. Then, the supernatants were collected and dried under vacuum. A solution containing acetonitrile and water (1:1; 100 μL) was

TABLE 1 | Sequences of primer pairs used in the real-time quantitative PCR reactions.

Gene	Primer sequences (from 5' to 3')	Size (bp)
β-actin	F: GAGAGGGAAATCGTGCGT R: GGAGGAAGAGGATGCGG	93
CaSR	F: CTCCATTCCCTCCTCCTCCATCAG R: TTGCTGTTGCTTCTGCCTCTCTG	82
PK2	F: CAAGGACTCTCAGTGTGGA R: AAAATGGAACTTTCCGAGTC	128

added. The resulting solution was centrifuged at 14,000x*g* for 15 min at 4°C. The treated supernatants were analyzed using a liquid chromatograph LC-30A (SHIMADZU, Japan) and 4500 QQQ mass spectrometer (AB Sciex, USA).

pCMV-HA-PK2 Expression Plasmid

A pCMV-HA-PK2 expression plasmid was constructed (18). The recombinant plasmid was transiently transfected into J774A.1 and RAW264.7 macrophage cell lines and TM-3 cells with Lipofectamine 3000 (Invitrogen). Briefly, transfection complexes (including the optimized concentration of the plasmid and Lipofectamine 3000) were transferred to 80% fused TM-3 cells for 6 h, and then the cells were washed and further cultured in DMEM for 42 h.

Statistical Analysis

Statistical analysis was performed using the Social Science Statistics Package (SPSS) 18.0 and GraphPad Prism 5.0. Data were expressed as means and standard errors of the mean (SEM). Differences between two groups were analyzed through unpaired *t*-test. One-way analysis of variance and Tukey's HSD *post hoc* test were used in measuring differences between groups. $P < 0.05$ were considered significant.

RESULTS

Clear Decrease in Sperm Quality in UPEC Model Rats

We established a rat UPEC model according to previous methods. To verify the success of model construction, we compared the model using the control group. We found that the UPEC content in the seminal plasma of the injection group increased markedly (**Figure 1A**). Moreover, the testes were mashed and smeared on a bacterial plate. The generation of strains was visible to the naked eye (**Figure 1B**). Flow analysis showed that the purity of the primary macrophages extracted was as high as 92.2% (**Figure 1C**). To verify that UPEC bacteria can enter the testicular interstitium, we observed the complete form of UPEC bacteria under an electron microscope (**Figure 1D**). Semen parameter analysis showed that the total sperm count and forward motility of the sperm in the UPEC group decreased (**Figure 1E**). All these results indicate that the UPEC model was successfully constructed, and the sperm motility of the rats decreased visibly after infection.

CaSR Upregulates TM in Rat Testes With UPEC-Induced Orchitis

The role of CaSR in UPEC-induced orchitis was investigated. Seven days after UPEC infection, testicular volume decreased in the UPEC group (**Figure 2A**). The level of the *CaSR* gene was clearly elevated in the testicular group of the UPEC-infected rats (**Figure 2B**), and the expression level of the CaSR protein visibly increased (**Figure 2C**). Given that TM is the most abundant immune cell in the testicular interstitium, UPEC invasion and localization were detected. We focused on TM and isolated TM from UPEC-infected rats. The results show that CaSR gene and protein levels increased in the TM cells of the UPEC group (**Figures 2D, E**). Our previous results show that PK2 was upregulated in the TM of UPEC-induced rats. Our previous results indicate that PK2 is expressed in the rat TM nucleus, and UPEC infection induces the secretion of PK2 in the nucleus into

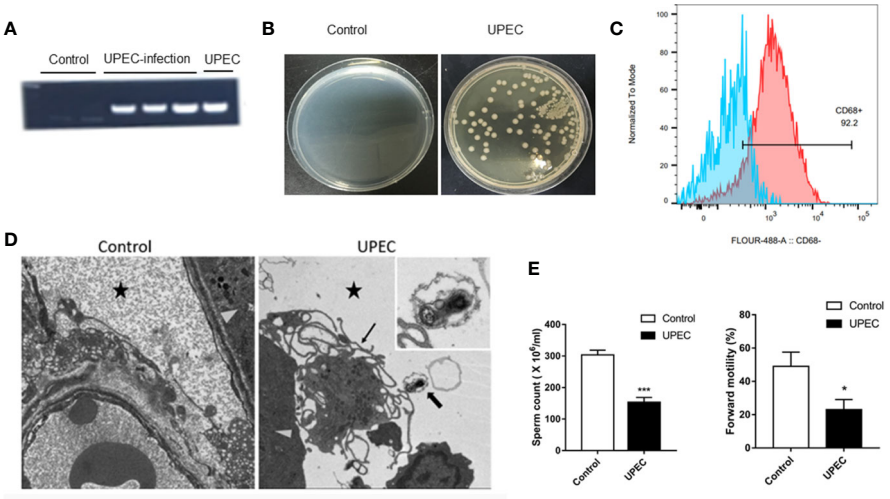

FIGURE 1 | The UPEC orchitis model was successfully constructed. **(A)** The expression of the PaPC gene in the control group, UPEC infection group, and the positive control group (*n*=5/group). **(B)** The growth of the colonies after homogenization and plating of testis tissues in the control and infection groups (*n*=5/group). **(C)** CD68 flow antibody was used in labeling primary TM (*n*=3/group). **(D)** The location of UPEC in the testes in the infected group. The triangular icon represents the seminiferous tubule area, the five-pointed star icon represents the interstitial area, the thick arrow indicates UPEC, and the thin arrow indicates the primary TM. The picture on the left is the infected group at ×1700 magnification, and the right is the infected group at ×5000 magnification (*n*=5/group). **(E)** Comparison of sperm count and forward sperm motility in normal saline control and UPEC infection groups (*n*=3/group). $^{*}P < 0.05$, $^{***}P < 0.001$ (*t*-test).

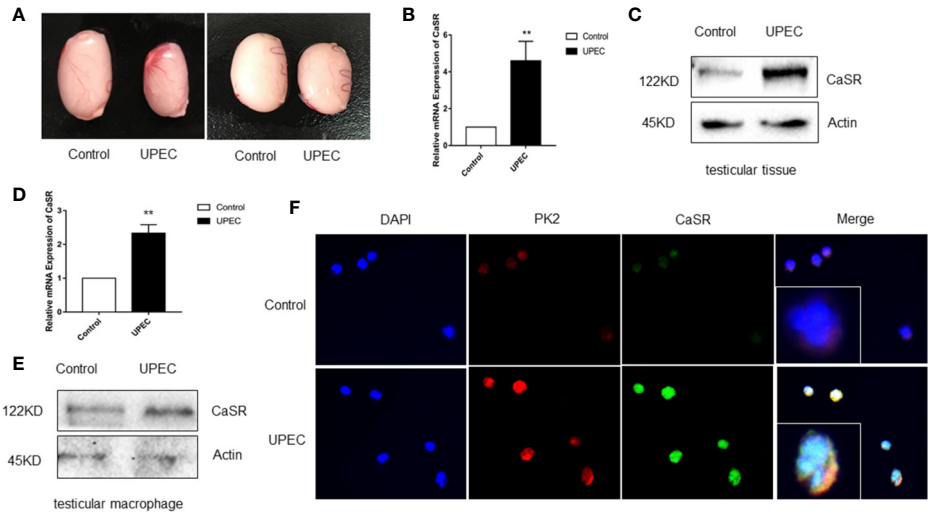

FIGURE 2 | CaSR expression was increased in UPEC-infected rat TM. **(A)** Comparison of testicle size between the saline control and UPEC infection groups (n=5/group). **(B)** CaSR mRNA expression in the testis tissues of the normal saline control and UPEC infected groups ($P < 0.01$) (n=5/group). **(C)** CaSR protein content in the testis tissues of the two groups of rats. **(D)** The expression of CaSR mRNA in the testes of two groups in primary macrophages ($P < 0.01$) (n=5/group). **(E)** CaSR protein expression in the primary testicular macrophages of the two groups of rats. **(F)** Localization of CaSR in primary testicular macrophages. $^{**}P < 0.01$ (t-test).

the cytoplasm to play a proinflammatory role. Therefore, we identified CaSR in TM by positioning PK2 in rat TM localization and immunofluorescence results show that CaSR was expressed in the TM nuclei of the control rats, and CaSR fluorescence increased after UPEC infection. However, UPEC infection induced CaSR expression in the cytoplasm. This result suggests that CaSR protein is involved in efficient production (**Figure 2F**). In conclusion, CaSR is highly expressed in the TM of rats infected with UPEC.

CaSR Inhibitor NPS2143 Relieves Orchitis Caused by UPEC

Given the proinflammatory effects of CaSR, its effects on inflammatory response and the male fertility process were studied. The CaSR inhibitor NPS2143 was injected into the testes of the UPEC-infected rats. CaSR activity was inhibited after injection. After UPEC infection, the renal tubules were inflamed, and testicular spermatogenic cells showed abnormal morphology. However, after treatment with NPS2143, inflammation was alleviated, and the severity of the damage to germ cells decreased. In the rats treated with NPS2143 alone, no significant changes in testicular morphology and parameters related to male reproduction were observed (**Figure 3A**). In addition, UPEC had a negative effect on sperm count and forward motility, and the UPEC + NPS2143 group showed the partial recovery of these factors (**Figures 3B, C**). The LC-MS results show that UPEC reduced the production of testosterone in the serum samples, and the UPEC + NPS2143 group displayed a partial recovery (**Figure 3D**). The UPEC strain was used to stimulate the macrophage cell lines J774A.1 and Raw264.7 to assess cell viability. The results show that, compared with the control group, the LDH released by the macrophage cell line increased in the UPEC group (**Figure 3E**), and the neutral red vitality test showed a significant decrease in cell metabolic activity (**Figure 3F**). However, NPS2143 inhibitors can be used to a certain extent to restore cell viability (**Figures 3E, F**). Our findings indicate that CaSR promoted testicular inflammation, thereby impairing male reproductive capacity, but the CaSR antagonist NPS2143 reduced inflammation and promoted sperm count recovery, forward motility, and testosterone production.

CaSR Regulates Ca^{2+} and Activates the NLRP3 Pathway

CaSR is a calcium-sensitive receptor. To explore the role of calcium ions in the activation of NLRP3 inflammasomes, we labeled intracellular calcium with Fluo4-AM. The results show that the calcium fluorescence signal in the macrophages of the control group was 6.4, whereas that in the UPEC group was 3.75 times of that value. The fluorescence signal in the UPEC + NPS2143 group was lower than that in the infected group (**Figures 4A, B**). Compared with the control group, the UPEC group had a higher calcium level ($P < 0.001$), and the UPEC + NPS2143 group had an obviously lower calcium level ($P < 0.05$) than the UPEC group (**Figure 4C**). The expression of the NLRP3 protein in the UPEC group was visibly higher than that in the control group, and the expression of the NLRP3 protein decreased in the UPEC + NPS2143 group (**Figure 4D**). In vitro and *in vivo*, the expression levels of CaSR and NLRP3 increased obviously after UPEC stimulation (**Figures 4D, E**). In the *in vivo* and *in vitro* experiments, the highest expression levels of CaSR and NLRP3 were observed after UPEC stimulation. Thus, UPEC clearly increased the level of intracellular Ca^{2+} in the primary macrophages, and CaSR mediated the assembly of functional NLRP3 inflammasomes though Ca^{2+}.

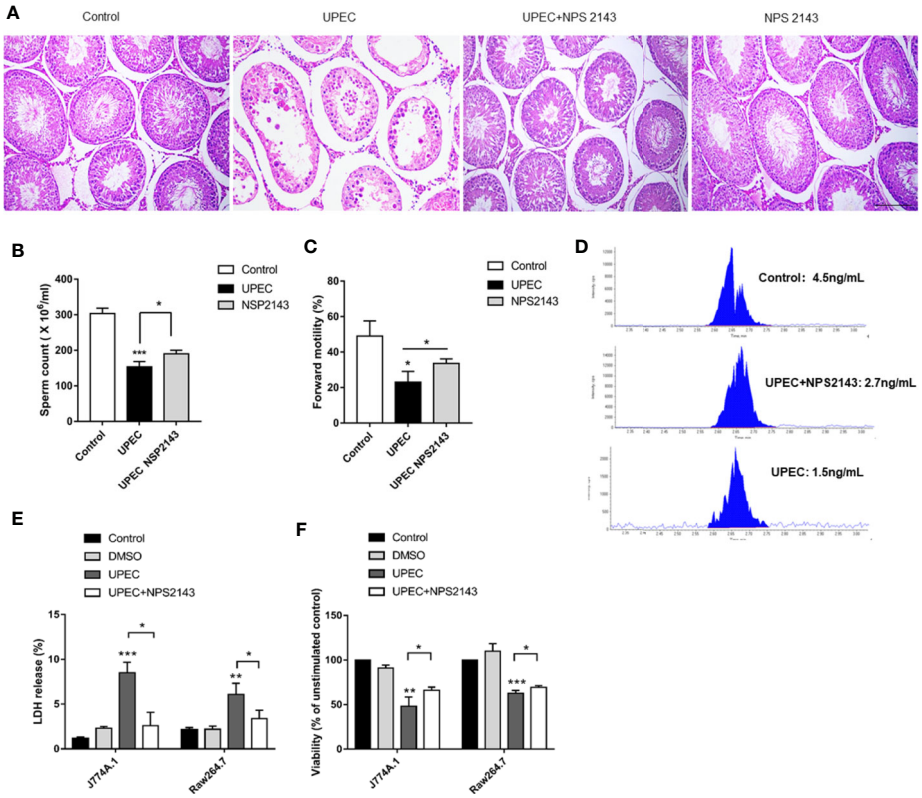

FIGURE 3 | CaSR inhibitor NPS-2143 can reduce UPEC-induced testicular inflammatory damage. **(A)** The morphology of the testicular tissues in the normal saline control group was intact; UPEC infection group showed obvious the irregular arrangement of spermatogenic epithelium, infiltration of inflammatory cells in the interstitium, and the destruction of many spermatogenic cell structures; UPEC+NPS-2143 inhibitor group. The inflammatory injury of the testis was relieved; the NPS-2143 negative control group showed no significant changes compared with the saline control group. Scale bar 100 um (n=5/group). **(B)** Comparison of the total number of sperm in normal saline control group, UPEC infection group, and NPS2143 rats (n=5/group). **(C)** The comparison of the forward movement speed of spermatozoa in the three groups (n=5/group). **(D)** The testosterone levels in the sera of rats were detected by LC-MS. **(E)** Assessment of LDH release from macrophage cell lines J774A.1 and Raw264.7 by UPEC strain. **(F)** Neutral red stains the macrophage cell lines J774A.1 and Raw264.7 in each group. $^{*}P < 0.05$, $^{**}P < 0.01$, $^{***}P < 0.001$ (t-test).

PK2 Activates the NLRP3 Pathway Through CaSR to Increase IL-1β Secretion

PK2 and its receptors follow the G protein-coupled receptor signaling pattern, activate PK2 transcription, release functional PK2 proteins from the cytoplasm to the extracellular environment, and further activate the NLRP3 pathway. Thus, we surmised that PK2 is associated with CaSR. The ELISA results of IL-1β show that IL-1β content was not detected in the supernatant of the control group, and the secretion level of IL-1β in the cell supernatant of the UPEC group increased obviously. However, the protein level of IL-1β decreased after treatment of TM with PKRA and NPS2143. It shows that PKRA and NPS2143 exerted inhibitory effects on IL-1β secretion (**Figure 5A**). To further confirm this effect, we divided the cells into ctrl, LPS, DMSO, LPS + UPEC + DMSO, LPS + UPEC + NPS2143, LPS + UPEC + MCC950, LPS + UPEC + VX-765, and LPS + UPEC + PK2 + DMSO, LPS + UPEC + PK2 + NPS2143, and LPS + UPEC + PK2 + MCC950, LPS + UPEC + PK2 + VX-765 groups. The results demonstrate that, under the action of three inhibitors, the level of PK2 and inflammatory PK2 increased. Meanwhile, NPS2143 inhibited the secretion of the inflammatory cytokine IL-1β, and the expression level of PK2 did not change after the addition of the NPS2143 inhibitor (**Figure 5B**). We transfected the PK2 plasmid into the macrophage cell lines and TM3 cell line, and the expression level of the PK2 gene was increased approximately 560-fold in TM3 cells (**Figure 5C**) and was increased approximately 3.4-fold in TM3 cells (**Figure 5D**). Total protein extracted from the transfected cells showed that, when PK2 was overexpressed, CaSR protein expression dramatically increased (**Figures 5E–G**). In summary, PK2 is an upstream regulator of the CaSR protein, and PK2 activates the NLRP3 pathway through CaSR, thereby increasing IL-1β secretion.

DISCUSSION

Our results indicate that UPEC infection can induce testicular inflammation by activating the NLRP3 inflammasome in TM. Interestingly, increase in CaSR level in TM enhances this process,

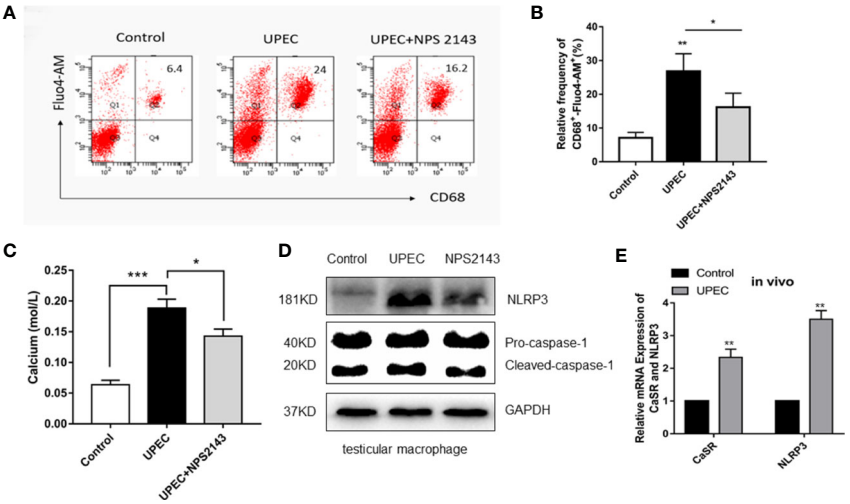

FIGURE 4 | CaSR promotes the recruitment and assembly of NLRP3 inflammasomes through Ca^{2+}. **(A)** The level of calcium ion in primary TM of each group was detected by flow cytometry (*n*=3/group). **(B)** Statistical analysis was performed on the results of the convection detection of calcium ion levels in the primary TM of each group. **(C)** The calcium level of each group labeled with the fluorescent indicator Fluo-am was detected using a microplate reader (*n*=3/group). **(D)** TM were isolated from the testes of rats in the control group and 7 days after UPEC treatment. After the collection of the macrophages, the protein levels of NLRP3 and caspase-1 in the macrophages were analyzed by Western blotting. **(E)** The expression of CaSR and NLRP3 genes in the two groups was detected (*n*=5/group). $^{*}P < 0.05$, $^{**}P < 0.01$, $^{***}P < 0.001$ (*t*-test).

and calcium content in the cytoplasm of a TM infected with UPEC increases obviously. CaSR can induce the production of various proinflammatory factors. In human preadipocytes, CaSR induces TNFα, thus leading to inflammation and abnormal fat functions (19). CaSR activation can promote the secretion of the proinflammatory factor IL-6 by rat peripheral blood polymorphonuclear neutrophils (20). After CaSR activation, T lymphocyte apoptosis can be increased through the TRPC3/6-IP3 signaling pathway (21). However, CaSR can be expressed in macrophages and has corresponding functions (22). The activation of CaSR can activate the NLRP3 inflammasome in macrophages and promote the secretion of proinflammatory factors, thereby causing inflammation (23). Knocking out CaSR can reduce the activation of the NLRP3 activator by inflammatory cells (15). We detected the upregulation of CaSR mRNA and protein in the testicular tissues of the UPEC-infected rats. In addition, TM isolated from the inflammation model demonstrated increased CaSR levels. Overall, we concluded that the direct stimulation of UPEC in the testicular matrix can elevate CaSR level.

Intracellular pathways triggered by CaSR stimulation depend on cell type, and ligands and physiological conditions have been widely accepted. Previous reports on the use of $CaCl_2$ to activate CaSR-dependent NLRP3 in human monocytes indicate that exposure to extracellular Ca^{2+} for 16 h triggers the proteolytic cleavage of pro-IL-1β protein (22). Data from a CaSR bias signal study indicate that Ca^{2+} alone triggers a p-ERK/ERK response, and the CaSR agonist cinacalcet can cause a higher p-ER/ERK response (24). Owing to the mobilization of Ca^{2+}, CaSR activation leads to an increase in intracellular Ca^{2+} concentration. In the BMDNs of bone marrow cells, CaSR can activate NLRP3 inflammasomes by increasing the concentration of Ca^{2+} and decreasing cAMP levels and thereby regulates the secretion and maturation of IL-1β. In summary, we investigated calcium ions in the cytoplasm of rat TM induced by UPEC, and our results indicate that the calcium content in rat TM infected with UPEC obviously increased. Given the upregulation of CaSR protein in TM, we speculate that CaSR promotes the maturation and secretion of IL-1β by regulating calcium ions in the cytoplasm.

To further study their relationship, we used the CaSR inhibitor NPS2143. NPS 2143 is a novel CaSR selective antagonist with anti-inflammatory activity (25, 26). NPS 2143, on the one hand, inhibits inflammation by reducing the expression of nitric oxide synthase, cyclooxygenase 2, and NF-κB. On the other hand, NPS 2143 relieves inflammation by activating the protein kinase AMPK (27, 28). In the UPEC infection model, the testis morphology recovered, and sperm motility increased after NPS2143 treatment. In the mass spectrometry, testosterone levels were elevated in NPS2143-treated rats compared to the UPEC-infected group. In addition, the CaSR inhibitor NPS2143 decreased the intracellular calcium content. For the first time, we systematically increased the expression of CaSR mRNA and protein in the TM of UPEC-infected rats.

The innate immune response of pathogens is associated with the assembly of inflammasomes (29, 30). When NS5 binds to NLRP3, Zika-induced IL-1β release occurs in human PBMC and mouse dendritic cells (31). The bacterium Acinetobacter baumannii induces IL-1β secretion *via* the NLRP3-ASC-caspase-1 pathway, thereby causing lung injury (32). UPEC promotes the cleavage of pro-IL-1β by promoting PK2 secretion and activating

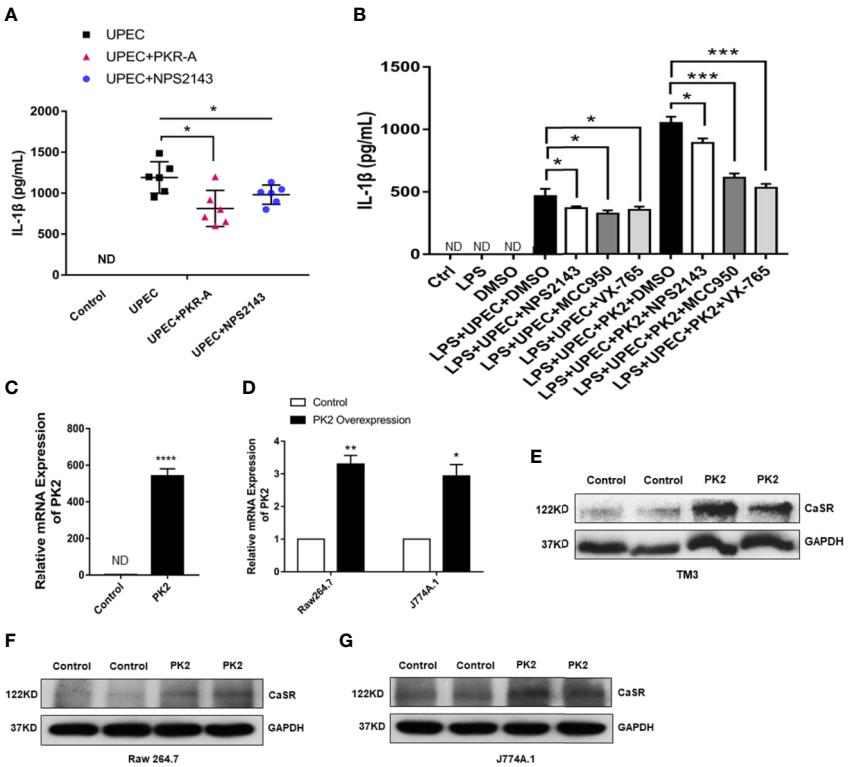

FIGURE 5 | NPS2143 blocks the PK2/CaSR pathway and promotes IL-1β secretion. **(A)** Testicular interstitial fluid was collected from each group, and IL-1β level in the primary TM interstitial fluid was analyzed by ELISA (*n*= 6/group). **(B)** LPS, 5% DMSO, 20 mg/kg NPS-2143, MCC950, VX-765, LPS + UPEC + PK2 + DMSO, LPS + UPEC + PK2 + NPS2143, LPS + UPEC + PK2 + MCC950, and LPS + UPEC + PK2 + VX-765 were used to stimulate macrophages for 120 min, and cell supernatants were collected. IL-1β levels in the supernatants of the primary TM were analyzed by ELISA (*n*=5/group). MCC950 was an inhibitor of NLRP3 protein, and VX-765 was an inhibitor of Caspase-1. **(C)** Transfection efficiency of PK2 in TM3 cell line (*n*=3/group). **(D)** Transfection efficiency of PK2 in RAW 264.7 and J774A.1 (n=3/group). **(E–G)** The protein level of CaSR was detected by Western blotting. $^{*}P < 0.05$, $^{**}P < 0.01$, $^{***}P < 0.001$, $^{****}P < 0.0001$ (*t*-test).

the NLRP3 inflammasome (12). Despite that NLRP3 and inflammation-related IL-1β are upregulated in UPEC-infected TM, whether CaSR induces NLRP3 inflammasome activity in the pathogenesis of orchitis is unclear. The relationship between CaSR and NLRP3 inflammasomes has received considerable attention. CaSR-induced ERK1/2 signaling mediates NLRP3 activation in LS14 preadipocytes (16). In the BMDNs of bone marrow cells, CaSR activates NLRP3 inflammasomes by increasing Ca^{2+} concentration and decreasing cAMP (15). The expression of NLRP3 was identified as a key marker of NLRP3 activation (33). Thus, we speculated that CaSR can activate NLRP3 inflammatory bodies in orchitis. Consistent with our results, NLRP3 protein expression was clearly upregulated in the TM of UPEC-infected rats. NLRP3 protein levels decreased after the use of the CaSR inhibitor NPS2143. Therefore, the increase in CaSR level in the TM of the UPEC-infected rats promoted the upregulation of NLRP3 mRNA and protein, and CaSR stimulation was involved in the activation of the NLRP3 inflammasome.

PK2 activates the maturation and secretion of IL-1β through NLRP3, and PK2 along with its receptors, follow the signaling pattern of a G protein-coupled receptor. Thus, CaSR is associated with PK2. LPS and bacterial DNA directly stimulate the upregulation of PK2 in Raw 264.7 cells (34). After UPEC infection, PK2 induces the activation of the NLRP3 inflammasome through the MAPK pathway, thereby promoting the maturation of IL-1β (12). This finding is consistent with our findings. The *in vivo* and *in vitro* experiments showed that PK2 promoted the secretion and maturation of IL-1β in the immune TM. To verify the role of CaSR and PK2, we overexpressed PK2 in the TM3 cell line through the PK2 plasmid transfection method. The results demonstrate that the CaSR protein was obviously upregulated in PK2-overexpressing TM3 cells. Therefore, PK2 may activate the NLRP3 inflammasome pathway through CaSR and thereby promote IL-1β secretion. We further improved the mechanism by which testicular inflammation impairs testicular function.

We find that CaSR promotes the secretion of proinflammatory factor IL-1β in the NLRP3 inflammatory corpuscle pathway in orchitis and that CaSR inhibitors reduce inflammatory damage to spermatogenic epithelial cells. After NPS2143 treatment, inflammation-induced testosterone reduction was inhibited, and thus, total sperm count and forward motility increased. In the rat serum samples, the inhibitor NPS2143 increased serum testosterone levels. Overall, CaSR plays an important role in the proinflammatory process of

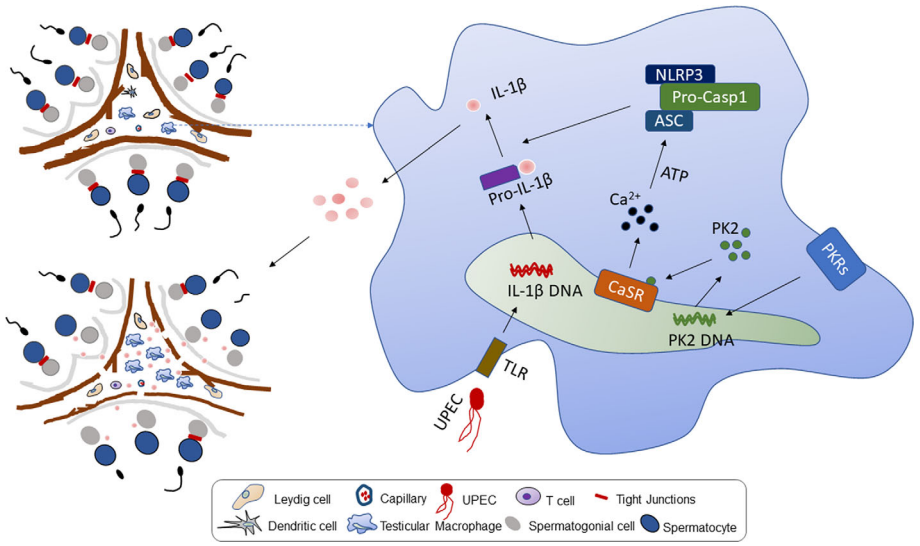

FIGURE 6 | Working model of UPEC-induced Prokineticin 2 *via* CaSR activated NLRP3 inflammasome in TM. Upper left: The model diagram of rat testis structure, including two parts of spermatogenic tubule and testicular interstitium. Right: After UPEC infection, NLRP3 inflammatory bodies in rat TM are activated to secrete a large amount of proinflammatory factor IL-1β. In the process, UPEC infection induces large amounts of PK2 secreted into the cytoplasm to stimulate the activation of CaSR, and activates the NLRP3 inflammasome by increasing the level of calcium ions in the cytoplasm of macrophages. Bottom left: The large amount of proinflammatory factor IL-1β secretion leads to a decrease in testosterone levels, and the normal physiological structure of testicular tissue is destroyed.

UPEC-induced orchitis by promoting the secretion of IL-1β in TM. This study introduces the mechanism for further alleviating orchitis. After UPEC infection, PK2 induced the activation of NLRP3 inflammasomes through a CaSR mechanism and promoted IL-1β maturation. IL-1β was released from TM to the testicular stroma, affecting adjacent Leydig cells, inhibiting testosterone synthesis and leading to impaired spermatogenesis and ultimately male infertility (**Figure 6**). Our research enriches knowledge of the role of CaSR in inflammatory diseases and provides new insights into the underlying mechanisms of inflammation-related male infertility.

DATA AVAILABILITY STATEMENT

The datasets presented in this study can be found in online repositories. The names of the repository/repositories and accession number(s) can be found in the article/**Supplementary Material**.

ETHICS STATEMENT

The animal study was reviewed and approved by the Institutional Animal Care and Use Committee of Tongji Medical College, Huazhong University of Science and Technology.

AUTHOR CONTRIBUTIONS

YS and KZ designed research studies, conducted experiments, analyzed data, and drafted the manuscript. YZ and ZH conducted rat model establishment, western blot, and propagation of bacteria. LH and ZF performed zebrafish assistance in immunofluorescence. WW and JX conducted sample collection and storage. CL and HZ provided intellectual input into planning of experiments and contributed to the writing of the manuscript. All authors contributed to the article and approved the submitted version.

FUNDING

This work was funded by National Key R&D Program of China (2018YFC1004300, 2018YFC1004304), National Natural Foundation of China (Grant numbers: 81871148, 81701539).

ACKNOWLEDGMENTS

We are grateful for the experimental platform provided by the Institute of Reproductive Health of Huazhong University of Science and Technology.

SUPPLEMENTARY MATERIAL

The Supplementary Material for this article can be found online at: https://www.frontiersin.org/articles/10.3389/fimmu.2020.570872/full#supplementary-material

REFERENCES

1. Schuppe HC, Meinhardt A, Allam JP, Bergmann M, Weidner W, Haidl G. Chronic orchitis: a neglected cause of male infertility? *Andrologia* (2008) 40 (2):84–91. doi: 10.1111/j.1439-0272.2008.00837.x
2. Wiles TJ, Kulesus RR, Mulvey MA. Origins and virulence mechanisms of uropathogenic Escherichia coli. *Exp Mol Pathol* (2008) 85(1):11–9. doi: 10.1016/j.yexmp.2008.03.007
3. Vazquez-Levin MH, Marín-Briggiler CI, Veaute C. Antisperm antibodies: invaluable tools toward the identification of sperm proteins involved in fertilization. *Am J Reprod Immunol* (2014) 72(2):206–18. doi: 10.1111/aji.12272
4. Wang M, Fijak M, Hossain H, Markmann M, Nüsing RM, Lochnit G, et al. Characterization of the Micro-Environment of the Testis that Shapes the Phenotype and Function of Testicular Macrophages. *J Immunol* (2017) 198 (11):4327–40. doi: 10.4049/jimmunol.1700162
5. Guazzone VA, Jacobo P, Theas MS, Lustig L. Cytokines and chemokines in testicular inflammation: A brief review. *Microsc Res Tech* (2009) 72(8):620–8. doi: 10.1002/jemt.20704
6. Shao BZ, Xu ZQ, Han BZ, Su DF, Liu C. NLRP3 inflammasome and its inhibitors: a review. *Front Pharmacol* (2015) 6:262. doi: 10.3389/fphar.2015.00262
7. Iyer SS, He Q, Janczy JR, Elliott EI, Zhong Z, Olivier AK, et al. Mitochondrial cardiolipin is required for Nlrp3 inflammasome activation. *Immunity* (2013) 39(2):311–23. doi: 10.1016/j.immuni.2013.08.001
8. Inoue M, Williams KL, Oliver T, Vandenabeele P, Rajan JV, Miao EA, et al. Interferon-β therapy against EAE is effective only when development of the disease depends on the NLRP3 inflammasome. *Sci Signal* (2012) 5(225):ra38. doi: 10.1126/scisignal.2002767
9. He Y, Hara H, Núñez G. Mechanism and Regulation of NLRP3 Inflammasome Activation. *Trends Biochem Sci* (2016) 41(12):1012–21. doi: 10.1016/j.tibs.2016.09.002
10. Hayrabedyan S, Todorova K, Jabeen A, Metodieva G, Toshkov S, Metodiev MV, et al. Sertoli cells have a functional NALP3 inflammasome that can modulate autophagy and cytokine production. *Sci Rep* (2016) 6:18896. doi: 10.1038/srep18896
11. Walenta L, Schmid N, Schwarzer JU, Köhn FM, Urbanski HF, Behr R, et al. NLRP3 in somatic non-immune cells of rodent and primate testes. *Reproduction* (2018) 156(3):231–8. doi: 10.1530/REP-18-0111
12. Li Y, Su Y, Zhou T, Hu Z, Wei J, Wang W, et al. Activation of the NLRP3 Inflammasome Pathway by Prokineticin 2 in Testicular Macrophages of Uropathogenic Escherichia coli- Induced Orchitis. *Front Immunol* (2019) 10:1872. doi: 10.3389/fimmu.2019.01872
13. Hendy GN, Canaff L. Calcium-sensing receptor, proinflammatory cytokines and calcium homeostasis. *Semin Cell Dev Biol* (2016) 49:37–43. doi: 10.1016/j.semcdb.2015.11.006
14. Lind L, Carlstedt F, Rastad J, Stiernström H, Stridsberg M, Ljunggren O, et al. Hypocalcemia and parathyroid hormone secretion in critically ill patients. *Crit Care Med* (2000) 28(1):93–9. doi: 10.1097/00003246-200001000-00015
15. Lee GS, Subramanian N, Kim AI, Aksentijevich I, Goldbach-Mansky R, et al. The calcium-sensing receptor regulates the NLRP3 inflammasome through Ca2+ and cAMP. *Nature* (2012) 492(7427):123–7. doi: 10.1038/nature11588
16. D'Espessailles A, Mora YA, Fuentes C, Cifuentes M. Calcium-sensing receptor activates the NLRP3 inflammasome in LS14 preadipocytes mediated by ERK1/2 signaling. *J Cell Physiol* (2018) 233(8):6232–40. doi: 10.1002/jcp.26490
17. Demirel I, Persson A, Brauner A, Särndahl E, Kruse R, Persson K. Activation of the NLRP3 Inflammasome Pathway by Uropathogenic Escherichia coli Is Virulence Factor-Dependent and Influences Colonization of Bladder Epithelial Cells. *Front Cell Infect Microbiol* (2018) 8:81. doi: 10.3389/fcimb.2018.00081
18. Li Y, Zhou T, Su YF, Hu ZY, Wei JJ, Wang W, et al. Prokineticin 2 overexpression induces spermatocyte apoptosis in varicocele in rats. *Asian J Androl* (2019) 22(5):500–6. doi: 10.4103/aja.aja_109_19
19. Mattar P, Bravo-Sagua R, Tobar N, Fuentes C, Troncoso R, Breitwieser G, et al. Autophagy mediates calcium-sensing receptor-induced TNFα production in human preadipocytes. *Biochim Biophys Acta Mol Basis Dis* (2018) 1864(11):3585–94. doi: 10.1016/j.bbadis.2018.08.020
20. Zhai TY, Cui BH, Zou L, Zeng JY, Gao S, Zhao Q, et al. Expression and Role of the Calcium-Sensing Receptor in Rat Peripheral Blood Polymorphonuclear Neutrophils. *Oxid Med Cell Longev* (2017) 2017:3869561. doi: 10.1155/2017/3869561
21. Wu QY, Sun MR, Wu CL, Li Y, Du JJ, Zeng JY, et al. Activation of calcium-sensing receptor increases TRPC3/6 expression in T lymphocyte in sepsis. *Mol Immunol* (2015) 64(1):18–25. doi: 10.1016/j.molimm.2014.10.018
22. Liu W, Zhang X, Zhao M, Zhang X, Chi J, Liu Y, et al. Activation in M1 but not M2 Macrophages Contributes to Cardiac Remodeling after Myocardial Infarction in Rats: a Critical Role of the Calcium Sensing Receptor/NRLP3 Inflammasome. *Cell Physiol Biochem* (2015) 35(6):2483–500. doi: 10.1159/000374048
23. D'Espessailles A, Santillana N, Sanhueza S, Fuentes C, Cifuentes M. Calcium sensing receptor activation in THP-1 macrophages triggers NLRP3 inflammasome and human preadipose cell inflammation. *Mol Cell Endocrinol* (2020) 501:110654. doi: 10.1016/j.mce.2019.110654
24. Rossol M, Pierer M, Raulien N, Quandt D, Meusch U, Rothe K, et al. Extracellular Ca2+ is a danger signal activating the NLRP3 inflammasome through G protein-coupled calcium sensing receptors. *Nat Commun* (2012) 3:1329. doi: 10.1038/ncomms2339
25. Yarova PL, Stewart AL, Sathish V, Britt RD Jr., Thompson MA, P Lowe AP, et al. Calcium-sensing receptor antagonists abrogate airway hyperresponsiveness and inflammation in allergic asthma. *Sci Transl Med* (2015) 7(284):284ra60. doi: 10.1126/scitranslmed.aaa0282
26. Mine Y, Zhang H. Calcium-sensing receptor (CaSR)-mediated anti-inflammatory effects of L-amino acids in intestinal epithelial cells. *J Agric Food Chem* (2015) 63(45):9987–95. doi: 10.1021/acs.jafc.5b03749
27. Lee JW, Park HA, Kwon OK, Park JW, Lee G, Lee HJ, et al. NPS 2143, a selective calcium-sensing receptor antagonist inhibits lipopolysaccharide-induced pulmonary inflammation. *Mol Immunol* (2017) 90:150–7. doi: 10.1016/j.molimm.2017.07.012
28. Li W, Qiu X, Jiang H, Zhi Y, Fu J, Liu J. Ulinastatin inhibits the inflammation of LPS-induced acute lung injury in mice via regulation of AMPK/NF-κB pathway. *Int Immunopharmacol* (2015) 29(2):560–7. doi: 10.1016/j.intimp.2015.09.028
29. Fullard N, O'Reilly S. Role of innate immune system in systemic sclerosis. *Semin Immunopathol* (2015) 37(5):511–7. doi: 10.1007/s00281-015-0503-7
30. Schroder K, Tschopp J. The inflammasomes. *Cell* (2010) 140(6):821–32. doi: 10.1016/j.cell.2010.01.040
31. Wang W, Li G, Wu D, Luo Z, Pan P, Tian M, et al. Zika virus infection induces host inflammatory responses by facilitating NLRP3 inflammasome assembly and interleukin-1β secretion. *Nat Commun* (2018) 9(1):106. doi: 10.1038/s41467-017-02645-3
32. Dikshit N, Kale SD, Khameneh HJ, Balamuralidhar V, Tang CY, Kumar P, et al. NLRP3 inflammasome pathway has a critical role in the host immunity against clinically relevant Acinetobacter baumannii pulmonary infection. *Mucosal Immunol* (2018) 11(1):257–72. doi: 10.1038/mi.2017.50
33. Bauernfeind FG, Horvath G, Stutz A, lnemri ES, MacDonald K, Speert D, et al. Cutting edge: NF-kappaB activating pattern recognition and cytokine receptors license NLRP3 inflammasome activation by regulating NLRP3 expression. *J Immunol* (2009) 183(2):787–91. doi: 10.4049/jimmunol.0901363
34. He X, Shen C, Lu Q, Li J, Wei Y, He L, et al. Prokineticin 2 Plays a Pivotal Role in Psoriasis. *EBioMedicine* (2016) 13:248–61. doi: 10.1016/j.ebiom.2016.10.022

Conflict of Interest: The authors declare that the research was conducted in the absence of any commercial or financial relationships that could be construed as a potential conflict of interest.

frontiers in Immunology

MINI REVIEW
published: 27 November 2020
doi: 10.3389/fimmu.2020.599594

Differential Immune Response to Infection and Acute Inflammation Along the Epididymis

Christiane Pleuger[1,2], Erick José Ramo Silva[3], Adrian Pilatz[2,4], Sudhanshu Bhushan[1,2] and Andreas Meinhardt[1,2]**

[1] Institute of Anatomy and Cell Biology, Justus-Liebig-University Giessen, Giessen, Germany, [2] Hessian Centre of Reproductive Medicine, Justus-Liebig-University Giessen, Giessen, Germany, [3] Department of Biophysics and Pharmacology, Institute of Biosciences of Botucatu, São Paulo State University (UNESP), Botucatu, Brazil, [4] Department of Urology, Pediatric Urology and Andrology, University Hospital, Justus-Liebig-University Giessen, Giessen, Germany

OPEN ACCESS

Edited by:
Daishu Han, Chinese Academy of Medical Sciences and Peking Union Medical College, China

Reviewed by:
Suresh Yenugu, University of Hyderabad, India
Rachel Guiton, Université Clermont Auvergne, France

***Correspondence:**
Andreas Meinhardt
Andreas.meinhardt@anatomie.med.uni-giessen.de
Christiane Pleuger
Christiane.pleuger@anatomie.med.uni-giessen.de

Specialty section:
This article was submitted to Mucosal Immunity, a section of the journal Frontiers in Immunology

Received: *27 August 2020*
Accepted: *03 November 2020*
Published: *27 November 2020*

Citation:
Pleuger C, Silva EJR, Pilatz A, Bhushan S and Meinhardt A (2020) Differential Immune Response to Infection and Acute Inflammation Along the Epididymis. Front. Immunol. 11:599594. doi: 10.3389/fimmu.2020.599594

The epididymis is a tubular structure connecting the vas deferens to the testis. This organ consists of three main regions—caput, corpus, and cauda—that face opposing immunological tasks. A means of combating invading pathogens is required in the distally located cauda, where there is a risk of ascending bacterial infections originating from the urethra. Meanwhile, immune tolerance is necessary at the caput, where spermatozoa with immunogenic neo-antigens originate from the testis. Consistently, when challenged with live bacteria or inflammatory stimuli, the cauda elicits a much stronger immune response and inflammatory-inflicted damage than the caput. At the cellular level, a role for diverse and strategically positioned mononuclear phagocytes is emerging. At the mechanistic level, differential expression of immunoprotective and immunomodulatory mediators has been detected between the three main regions of the epididymis. In this review, we summarize the current state of knowledge about region-specific immunological characteristics and unveil possible underlying mechanisms on cellular and molecular levels. Improved understanding of the different immunological microenvironments is the basis for an improved therapy and counseling of patients with epididymal infections.

Keywords: epididymis, epididymitis, mononuclear phagocytes, uropathogenic *E. coli*, infertility, bacterial infection

STRUCTURE AND FUNCTION OF THE EPIDIDYMIS

The epididymis is connected to the rete testis *via* efferent ducts that converge onto one single epididymal duct in the initial segment opposite the mediastinum testis. The epididymal duct meanders through three regions known as the caput (which contains the initial segment in rodents), corpus, and cauda epididymides (**Figure 1A**). Connective tissue septae segregate the epididymis further, producing 10 segments in mice (1) and 19 in rats (2). Septae in the human epididymis are present but poorly defined (3). The duct is lined by a two-layered pseudostratified epithelium, consisting of principal, basal, narrow/clear cells, and resident immune cells [mononuclear phagocytes (see *Immune-Cell Populations in the Rodent Epididymis*) and "halo cells" (4, 5)] and surrounded by a wall composed mostly of smooth muscle cells (**Figures 1B, C**). The interstitium is composed of blood vessels,

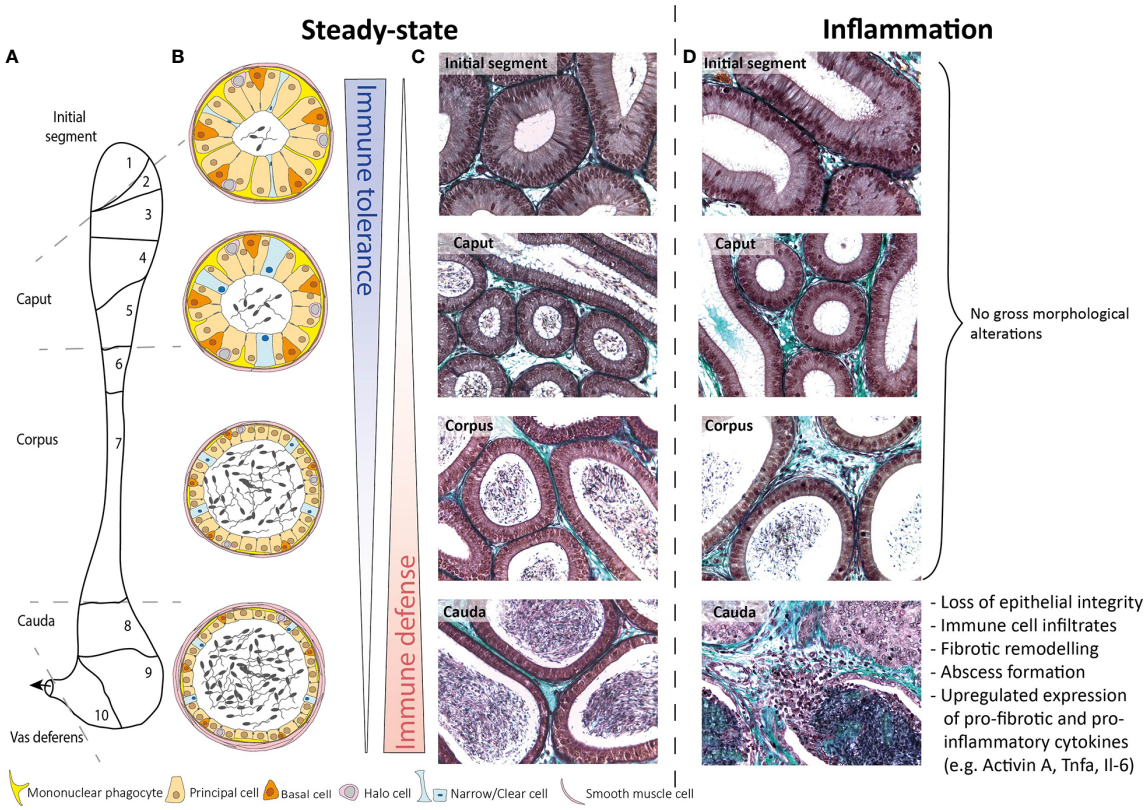

FIGURE 1 | Schematic overview of murine epididymal regions during steady-state and inflammatory conditions. **(A)** Based on structure and function, the murine epididymis is principally compartmentalized into four distinct anatomical regions, i.e. the initial segment (segment 1), caput (segments 2–5), corpus (segments 6–7), and cauda (segments 8–10). **(B)** The epididymal epithelium consists of diverse cell types, namely principal cells, basal cells, halo cells, and clear/narrow cells, whereby the epithelial composition and lumen diameter changes along the length of the single duct. To fulfill the main immunological functions—immune tolerance in the proximal regions and immune defense in the distal regions—mononuclear phagocytes are strategically positioned between adjacent epithelial cells and exhibit long protrusions within the initial segment, which are gradually shrinking towards the distal regions. **(C, D)** Under inflammatory conditions (10 days after infection with uropathogenic *E. coli*), the epididymis shows striking different immunological responses. While the initial segment, caput, and corpus remain mostly unaffected, the cauda epididymidis undergoes dramatic morphological alterations. Masson-Goldner-Trichrome staining, primary magnification 40×.

lymphatic vessels, leukocytes, and loose connective tissue, which increases in density in the septae. The luminal fluid provides a milieu necessary for the step-wise maturation of spermatozoa required to achieve full fertilizing capacity (6, 7). The blood-epididymal-barrier (BEB)—extending apically between adjacent principal cells—maintains the unique composition of the luminal fluid. However, its role in protecting spermatozoa from immune attack is likely not as robust as the blood-testis-barrier (8).

Emerging evidence on cellular and molecular levels has resulted in the hypothesis that the epididymis is "a series of organs side-by-side" (9). This hypothesis is evidenced by particular region-specific characteristics in regards to (a) the composition of the epithelium (4, 5), (b) the distribution and phenotype of resident immune cells subpopulations (10–13), and (c) differential gene expression profiles (1, 2, 14, 15). In line with that, septae segregate different segments and have been demonstrated to function as diffusion barriers, possibly creating distinct interstitial microenvironments (16, 17).

From the immunological perspective of the hypothesis that the epididymis is a "series of organs side-by-side," this duct faces two different immunological challenges at its opposing ends (**Figure 1B**). At the proximal end, mechanisms of strong local tolerance are required to avoid autoimmune reactions against post-testicular spermatozoa expressing sperm-specific neo-antigens (18). Conversely, at the distal end, mechanisms are required to react against bacterial pathogens ascending from the urethra (19). As pointed out below, there is accumulating evidence that different subsets of resident immune cell populations exist throughout the length of the epididymis that may play a role in the balance of immune tolerance and immune defense at the opposing ends of this organ.

LEUKOCYTES IN THE NORMAL EPIDIDYMIS

Immune-Cell Populations in the Rodent Epididymis

Different immune-cell populations, including heterogenous subsets of the mononuclear phagocyte (MP) system, T and B

lymphocytes reside within the rodent epididymis (4, 10, 11, 13, 18, 20–23). Two different T-cell populations [$CD4^-CD8^-$ (DN) and γδ T cells] have been identified recently: DN T cells are more abundant within the caput while γδ T cells are evenly distributed throughout the entire epithelium and interstitium (11). A region-specific role for these subpopulations remains elusive.

Generally, tissue-resident MPs are considered "guardians of the immune system," often found located at the interface with the external environment. MPs comprise heterogeneous subsets of monocytes, macrophages, and dendritic cells (DCs), which have a broad spectrum of common characteristics (i.e. migratory capabilities towards gradients of microbial signals or chemokines, engulfment and processing of microbial fragments or dying cells and antigen-presentation to the adaptive immune system, secretion of signaling molecules). Most notably, MP subsets are highly plastic, allowing them to regulate tissue homeostasis and immune responses in an organ-specific manner.

Within the epididymis, MPs constitute the majority of resident immune cells and comprise multiple closely related subpopulations that are strategically positioned throughout the different regions. As the composition and phenotype of epididymal MPs under normal circumstances has been comprehensively summarized elsewhere (24, 25), only a brief reflection will be provided here serving as a prerequisite to understand alterations seen in infection and inflammation. In brief, distinct MP populations at the periphery of the epithelium and within the interstitium are arranged as dense network with the highest abundance in the initial segment (IS). They are characterized by the expression of the chemokine (C-X3-C motif) receptor 1 (CX_3CR_1) as well as a region-specific morphology and transcriptomic signature (10, 13, 24). While peritubular $CX_3CR_1^+$ cells within the IS exhibit long arborizations between adjacent epithelial cells towards the tight junctions of the BEB, these gradually decline towards the distal segments until the cells finally appear flat in the cauda [**Figure 1B** (13)]. Interstitial MP do not exhibit a stellate morphology. Rather, they can be differentiated by their expression of the macrophage mannose receptor CD206 and lack of CD11c, pointing to a macrophage phenotype (13).

Epididymal MPs are currently classified into different subtypes based on the expression of surface markers traditionally used to distinguish macrophages from DCs (10, 13), i.e. the high-affinity IgG receptor FcγR CD64 *vs.* integrin alpha X CD11c expression, respectively (26, 27). However, several subsets have been described to express a complex combination of these markers in association with other markers (CX_3CR_1, CD11b, F4/80) (10). Thus, the original classification for epididymal MPs requires further consideration, with the benefit of techniques such as single cell RNA-sequencing and lineage tracing, to ultimately clarify the full extent of MP heterogeneity. Indeed, a recently published transcriptomic analysis revealed distinct gene expression profiles of $CX_3CR_1^+$ MPs isolated from different epididymal regions (10) suggesting a considerable level of MP heterogeneity and microenvironment-specific functions beside archetypical functions in all regions (i.e. phagocytosis and antigen-presentation). As an example, $CX_3CR_1^+$ MPs within the IS are differentially enriched with transcripts required for leukocyte transendothelial migration and cell adhesion (see below). Meanwhile, $CX_3CR_1^+$ MPs within the cauda are characterized by transcripts associated with NF-kappa B signaling, indicative of their protective role against invading luminal pathogens (10). Intriguingly, while both tubule-associated and interstitial MPs within the highly vascularized proximal regions (in particular the IS) can capture and process circulatory antigens, only interstitial MPs exhibit these properties in the more scarcely vascularized cauda (10). These spatial differences prompt the hypothesis that in the caput intraepithelial MPs could be involved in the continued capture of sperm autoantigens to maintain tolerance, while both the interstitially located MPs in the caput and cauda shall restrict microbial dissemination into the organ.

Immune-Cell Populations in the Human Epididymis

In contrast to experimental animals, human data on the epididymal leukocyte population are scarce and are almost exclusively derived using immune-based morphological methods (28). Human intraepithelial lymphocytes and macrophages are similar in terms of location to those found in rodents (29). Macrophages are the predominant immune cell population—except for intraepithelial leukocytes where T lymphocytes exceed—and express major histocompatibility complex class II (MHC-II) proteins in the interstitium. B cells are barely detectable, while DC consist of immature DC in the normal epididymis [$CD1a^+$ DC, $CD11c^+$ myeloid DC (mDC), and $CD209^+$ DC] (30, 31). Plasmacytoid DC and $CD83^+$ mature DC are only found in chronic epididymitis, similar to $CD4^+Th17^+$ T lymphocytes (30). Although not entirely clear, MHCII-restricted $CD4^+$ T lymphocytes seem to represent the predominant phenotype of T cells in the interstitium. As in other organs, $CD8^+$ T cells are the predominant phenotype in the epithelium and increase distally in the epididymis (31–33).

THE EPIDIDYMAL RESPONSE TO INFECTION AND INFLAMMATION

Various *in vivo* and *in vitro* models have clearly pointed to striking region-specific differences in the epididymal immune response. The clearest observation is that the cauda epididymidis is much more sensitive to inflammatory-inflicted damage than the caput epididymidis [**Figure 1D** (14, 34, 35)]. These observations are complemented by data from patients with acute bacterial epididymitis where in most cases the cauda is predominantly impacted, particularly in severe cases when an abscess is diagnosed (36).

Region-Specific Responses in Human Epididymitis

Acute epididymitis affects ~250 to 650 per 100,000 men each year (37). Three different forms can be distinguished: i) bacterial ascension through the male accessory glands (the most common

form), ii) concomitant epididymitis in the context of viral orchitis, and iii) a primarily viral epididymitis.

Molecular microbiological diagnostics can identify a causal bacterial pathogen in 87% of antibiotic-naïve cases (36). Both typical urinary tract pathogens [*Escherichia coli* (*E. coli*)] and sexually transmitted bacteria (*Chlamydia trachomatis, Neisseria gonorrhoeae*) are most relevant, regardless of age [**Figure 2** (36)]. As a result of bacterial ascension, 44% of patients experience isolated pain in the cauda epididymidis, 41% experience pain in the entire epididymis, and only 15% report isolated pain in the caput epididymidis (36). Abscess formation characterizes clinically severe forms of the disease. Interestingly, abscesses are typically located in the cauda, and very rarely in the caput epididymidis (36). Early studies that collected diagnostic epididymal biopsies identified polymorphonuclear cells in ~54% of cases and somewhat less frequently lymphocytic infiltrates (38). Of note, no differentiation of the inflammatory response in dependence of the etiology of the most relevant pathogens (e.g. *E. coli* vs. *Chlamydia trachomatis*) was ever conducted in human specimens. Research of this kind is limited by the low availability of specimens as histological evaluation is only performed in cases with a fulminant course, where secondary testicular infarction with the necessity of semi-castration occurs (36). Finally, persistent epididymal enlargement (usually of the cauda) >3 months post infection affects ~16% of patients (36).

Concomitant epididymitis in primary viral orchitis is possible both synchronously and metachronically, but the frequency is unclear. Data only exist for mumps orchitis from the era before mumps vaccination, and when scrotal ultrasound was unavailable (39). Currently, only one study has used ultrasound to describe the involvement of the epididymis in 23 cases of mumps orchitis. Interestingly, in 45% of the cases, no epididymal changes were visible (isolated orchitis), while in 30% only the caput was affected (diameter 11.1 mm instead of 6.5 mm) and in another 26% the entire epididymis was affected (40). These findings are in stark contrast to those of bacterial epididymitis, where the cauda is always primarily affected.

Only few studies carried out virological examinations in epididymitis patients. In a study investigating 28 epididymal biopsies, arbor and rhinoviruses were detected in only three cases (38); unfortunately corresponding histological reports were lacking. With epididymal biopsies now obsolete due to the risk of obstruction, another study isolated enteroviruses directly from the semen of patients with acute epididymitis and considered this as the etiologic pathogen (36). Moving forward, PCR-based urine diagnostics (STIs and 16s rDNA) are now recommended in the case of antibiotic pre-treatment with negative urine culture, while PCR diagnostics should be performed directly from the ejaculate if viral genesis is suspected (36).

Region-Specific Immune Responses in Rodent Models of Acute Bacterial Epididymitis

A frequently used rodent model to mimic ascending acute bacterial epididymitis uses uni- or bilateral intravasal inoculation of uropathogenic *E. coli* [UPEC, (19)]. After infection, fundamentally disparate immune responses and associated immunopathologies were observed in different epididymal regions (**Figures 1C, D**). The caput epididymidis remains mostly unaffected throughout the course of infection

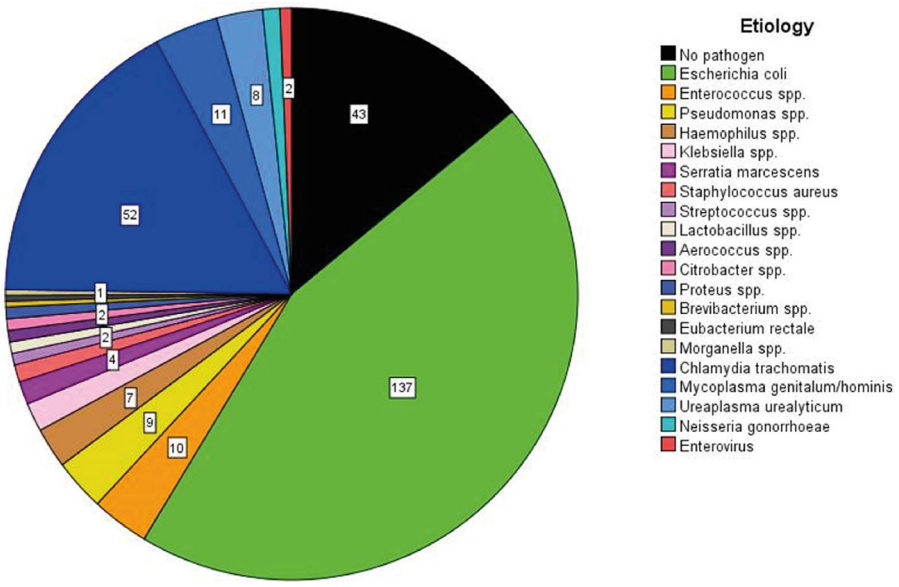

FIGURE 2 | The etiology of acute epididymitis in 284 patients without antimicrobial pre-treatment. A total of 307 pathogens are visualized due to two specimens being simultaneously detected in 23 patients. The pathogen detection rate is 85% with *E. coli* as the most common pathogen, followed by *Chlamydia trachomatis* as second most common. Data are obtained from a prospective study running since 2007 [modified according to (36)].

despite the presence of bacteria and the expression of signaling molecules required to sense bacteria and mount inflammatory responses against them [see *Region-Specific Immune Responses to LPS-Induced Epididymitis* (14, 34)]. Similar region-specific immune reactions have also been observed in a mouse model of experimental autoimmune epididymo-orchitis (35).

Immunotolerance in the Caput Epididymidis

A possible explanation for different immune responsiveness could lie in the unique requirements of the immune environment of the caput. Here, neoantigen-expressing spermatozoa originate from the immune-privileged testicular environment. As a result, multiple complementary mechanisms of peripheral immune tolerance are established to prevent autoimmune reactions against spermatozoa. At the cellular level, intraepithelial MPs sample sperm neoantigens *via* their characteristic thin protrusions (see *Immune-Cell Populations in the Rodent Epididymis*) that reach the epididymal lumen and—after migration to draining lymph nodes—induce regulatory T cells to suppress effector T cells (41). Although this mechanism was observed in men after vasectomy and may not reflect the steady-state situation, support for a more general mechanism in epididymal function has been obtained in the gut, an organ that faces similar challenges in inducing peripheral tolerance. In the gut, $CX_3CR_1^+$ macrophages (located within the lamina propria) capture luminal antigens and transfer them to $CD103^+$ DC in a connexin43-dependent manner (42). $CD103^+$ DC, in turn, migrate through lymphatics to the draining lymph node to induce the differentiation of antigen-specific regulatory T cells (42, 43).

In addition, MPs residing in the IS are in close contact with neighboring epithelial cells and possess a strong capacity to resolve arising inflammation—as shown by the rapid clearance of damaged epithelia (44). These and other means to preserve epithelial integrity are important mechanisms to maintain peripheral tolerance as a loss of epithelial integrity in the IS promotes autoimmune-associated responses against sperm antigens as seen in mice lacking the adhesive protein milk fat globule-EGF factor 8 protein MFGE8 (also known as SED1 or lactadherin) (45). Moreover, an important role for regulatory T cells was postulated in epididymal immune tolerance as depletion of these cells allowed induction of experimental auto immune-orchitis, at least under certain conditions (vasectomized B6AF1 mice) (46).

Molecular data point to the necessity to preserve immunotolerance not only in the IS and caput, where sperm first enter the epididymis, but throughout the organ. Here, it seems that transforming growth factor-beta (TGFβ) family members have a prominent role. TGFβ isoforms (TGF-β1, TGF-β2, TGF-β3) are expressed in all epididymal regions, but the active forms are preferentially found in the corpus (47). All isoforms activate the same receptor complex (TGFβ receptor 1 and 2) (48). Mice with DC-specific TGFβ receptor 2 deficiency develop severe leukocytosis in all regions, including the IS, which is triggered by an immune response specifically targeting sperm antigens (18).

Other immunomodulatory molecules, such as indolamine 2,3-dioxygenase [IDO (49)] or activin (50) are mostly enriched in the proximal region. Further protective mechanism in the proximal region of the epididymis could be based on the high expression of a large number of various anti-microbial peptides (51, 52). These include beta-defensins (*Defb* 3, 12, 15, 18, 20, 30, 42), lipocalin 2 (*Lcn2*), cathelicidin (*Camp*), pentraxin 3 (*Ptx3*), and *Lypd8* (Ly6/Plaur domain -containing protein 8). All of them were found in the top 50 significantly differential expressed genes with high baseline expression in the normal caput epididymis using whole transcriptome analysis (14). While beta-defensins are mostly expressed by epithelial cells, including proton-secreting clear cells with protrusions reaching into the lumen (53) for other anti-microbial peptides their cellular origin in the epididymis is not established, e.g. those controlling infection with gram-negative bacteria (*Lcn2*, *Lypd8*). It needs to be noted though that other defensins such as *Defb* 1, 2, and 9 are expressed at much higher levels in the cauda. This indicates a complex multitude of mechanisms that contribute to the maintenance of peripheral tolerance, whilst simultaneously providing sufficient resistance to bacteria-induced damage [reviewed in (54)], it is not clear to what extend their differential distribution contributes to immune tolerance and a dampened immune response towards microbes preferentially in the proximal epididymis.

Immune Defense in the Cauda Epididymidis

Conversely, the cauda is highly susceptible to damage as a result of inflammatory responses. UPEC-infected mice are characterized by interstitial and intraluminal immune cell infiltrates, epithelial detachment, and fibrosis that all contribute to irreversible epididymal duct obstruction [**Figure 1D** (14, 34)]. The immunopathological damage gradually decreases towards the corpus epididymidis. Besides the transcriptional differences underlying the immune responsiveness of epididymal MPs (10), segmental barriers serve to restrict the ascent of pathogens and spread of inflammatory modulators, at least for some time (16).

Intriguingly, the observed damage is mostly elicited by the magnitude of the host's immune response and only to a lesser extend due to bacterial virulence factors as evidenced by mice lacking the Myeloid Differentiation Primary Response Protein MYD88, which are characterized by a less pronounced immune reaction towards UPEC infection (34).

Although antibiotic interventions can eliminate epididymitis-associated pathogens, histopathological alterations and concomitant long-term fertility impairments are not preventable by antibiotics alone (55–59). However, a combined antibiotic (i.e. levofloxacin) and immunosuppressant (dexamethasone) regimen can successfully dampen adaptive (rather than innate) immune responses and the associated tissue damage in UPEC-induced mouse epididymitis (59). This treatment might thus constitute a promising strategy for fertility preservation in affected men (59).

Region-Specific Immune Responses to LPS-Induced Epididymitis

Considering the frequency of *E. coli*-induced epididymitis in men (see *Region-Specific Responses in Human Epididymitis*), lipopolysaccharide (LPS), a structural component of the outer membrane of Gram-negative bacteria such as *E. coli*, can be explored as agonist of the toll-like receptor 4 (TLR4) to investigate the role of TLR4 signaling in epididymitis

pathogenesis. To study region-specific immune responses, LPS can be applied systemically to circumvent the temporally different exposures of the epididymal regions to the inflammatory challenge, as seen in models of ascending bacterial infection (14, 34). In rodents, TLR4 is expressed in epididymal epithelial cells, smooth muscle cells and interstitial macrophages (60–63). TLR4 and associated signaling molecules [i.e. MYD88, cluster differentiation 14 (CD14), TIR-domain-containing adapter molecule-1 (TICAM1), and LPS-binding protein (LBP)] show a spatial expression pattern in the epididymis, adding further credence to region-specific inflammatory responses in the epididymis (14, 15, 61, 63, 64).

The first demonstration that TLR4 activation by LPS was sufficient to elicit epididymitis came from a rat model of experimentally induced systemic endotoxemia (61). Intravenous LPS (0.1–1.0 mg/kg) injection triggered rapid inflammatory responses in the epididymis that were mediated by TLR4-dependent NF-kappa B activation and an upregulation of inflammatory mediators [i.e. *Il1b*, *Tnf*, *Nos2*, *Bdkrb1* (61, 65)]. Intraperitoneal LPS (3.0 mg/kg) injection in mice results in a similar upregulation of pro-inflammatory cytokines and induces morphological alterations (immune cell infiltrates, fibrosis) that are mostly restricted to the cauda epididymis (66). This response is absent from $Tnf^{-/-}$ mice and wild-type mice treated with the TNFα inhibitor pomalidomide, indicating that the induced inflammatory response is the primary source of tissue damage (66).

Similar to the effects seen in the UPEC mouse model, retrograde intravasal LPS injection in rodents resulted in a severe inflammatory reaction within the cauda (66, 67). These responses were more robust than those generated by systemic LPS administration (66). Intriguingly, when LPS was directly injected into the mesenchyme of the caput epididymidis, this region was locally responsive as indicated by an upregulation of several members of interleukin, NF-kappa B, TNF families, and downregulation of β-defensins (68, 69).

The data from these studies point to the involvement of TLR4 signaling in mediating the immunopathological changes seen in acute bacterial epididymitis. However, the exact mechanism governing these events—such as the contributions of damage-associated molecular patterns (e.g. S100A) as enhancers (70), different TLR4-dependent signaling pathways (MYD88, TICAM), and downstream inflammatory mediators of epididymitis progression and severity—have only just begun to emerge.

CONCLUSIONS

The spatial differences in the structure and cellular composition of the epididymal epithelium and the region-specific gene expression patterns associated with sperm maturation are well known. Now, evidence is also accumulating to support a differential immune response throughout the epididymis. Most models point to a stronger inflammatory response to the same infectious or inflammatory challenges in the cauda compared to the caput epididymidis. The elevated immune response in the cauda prompts immunopathological alterations that can impair fertility. Although the caput is principally immunoreactive and the constituting cells can respond to inflammatory stimuli, the magnitude is at a much lesser extent. The data thus far have illustrated that strategically positioned MP subpopulations as well as region-specific expression of diverse immunomodulatory factors enable a precisely tuned balance between tolerance and defense at the opposing ends of the very same duct. Finally, the BEB seems to confer protection throughout the length of the epididymal duct, particularly from autoimmunity to sperm neoantigens. Going forward, research is necessary to better understand how this organ is able to maintain tolerance to autoimmunogenic spermatozoa at one end of the duct and ensure protection from ascending microbes at the other end. Then, work is warranted to delineate the functions of leukocytes in the steady-state epididymis, which currently remain an enigma.

AUTHOR CONTRIBUTIONS

CP, ES, AP, SB, and AM performed literature research and wrote the manuscript. All authors contributed to the article and approved the submitted version.

FUNDING

This work was supported by a GRK 1871/2 International Research Training Group Giessen-Monash grant on "Molecular pathogenesis of male reproductive disorders" (AM, CP, AP, and SB) and a project grant BH 93/1-4 (awarded to SB) from the Deutsche Forschungsgemeinschaft.

REFERENCES

1. Johnston DS, Jelinsky SA, Bang HJ, DiCandeloro P, Wilson E, Kopf GS, et al. The mouse epididymal transcriptome: transcriptional profiling of segmental gene expression in the epididymis. *Biol Reprod* (2005) 73:404–13. doi: 10.1095/biolreprod.105.039719
2. Jelinsky SA, Turner TT, Bang HJ, Finger JN, Solarz MK, Wilson E, et al. The rat epididymal transcriptome: comparison of segmental gene expression in the rat and mouse epididymides. *Biol Reprod* (2007) 76:561–70. doi: 10.1095/biolreprod.106.057323
3. Sullivan R, Mieusset R. The human epididymis: its function in sperm maturation. *Hum Reprod Update* (2016) 22:574–87. doi: 10.1093/humupd/dmw015
4. Shum WW, Smith TB, Cortez-Retamozo V, Grigoryeva LS, Roy JW, Hill E, et al. Epithelial basal cells are distinct from dendritic cells and macrophages in the mouse epididymis. *Biol Reprod* (2014) 90:90. doi: 10.1095/biolreprod.113.116681
5. Robaire B, Hinton B, Orgebincrist M. The Epididymis. In: *Knobil and Neill"s Physiology of Reproduction*. (Amsterdam, Boston: Elsevier Academic Press) (2006). p. 1071–148.
6. Skerget S, Rosenow MA, Petritis K, Karr TL. Sperm Proteome Maturation in the Mouse Epididymis. *PloS One* (2015) 10:e0140650. doi: 10.1371/journal.pone.0140650
7. Shum WW, Ruan YC, Da Silva N, Breton S. Establishment of cell-cell cross talk in the epididymis: control of luminal acidification. *J Androl* (2011) 32:576–86. doi: 10.2164/jandrol.111.012971

8. Gregory M, Cyr DG. The blood-epididymis barrier and inflammation. *Spermatogenesis* (2014) 4:e979619. doi: 10.4161/21565562.2014.979619
9. Domeniconi RF, Souza AC, Xu B, Washington AM, Hinton BT. Is the Epididymis a Series of Organs Placed Side By Side? *Biol Reprod* (2016) 95:10. doi: 10.1095/biolreprod.116.138768
10. Battistone MA, Mendelsohn AC, Spallanzani RG, Brown D, Nair AV, Breton S. Region-specific transcriptomic and functional signatures of mononuclear phagocytes in the epididymis. *Mol Hum Reprod* (2020) 26:14–29. doi: 10.1093/molehr/gaz059
11. Voisin A, Whitfield M, Damon-Soubeyrand C, Goubely C, Henry-Berger J, Saez F, et al. Comprehensive overview of murine epididymal mononuclear phagocytes and lymphocytes: Unexpected populations arise. *J Reprod Immunol* (2018) 126:11–7. doi: 10.1016/j.jri.2018.01.003
12. Guiton R, Voisin A, Henry-Berger J, Saez F, Drevet JR. Of vessels and cells: the spatial organization of the epididymal immune system. *Andrology* (2019) 7:712–8. doi: 10.1111/andr.12637
13. Da Silva N, Cortez-Retamozo V, Reinecker H-C, Wildgruber M, Hill E, Brown D, et al. A dense network of dend1ritic cells populates the murine epididymis. *Reproduction* (2011) 141:653–63. doi: 10.1530/REP-10-0493
14. Klein B, Bhushan S, Günther S, Middendorff R, Loveland KL, Hedger MP, et al. Differential tissue-specific damage caused by bacterial epididymo-orchitis in the mouse. *Mol Hum Reprod* (2020) 26:215–27. doi: 10.1093/molehr/gaaa011
15. Rinaldi VD, Donnard E, Gellatly KJ, Rasmussen M, Kucukural A, Yukselen O, et al. An atlas of cell types in the mouse epididymis and vas deferens. *Elife* (2020) e:55474. doi: 10.7554/eLife.55474
16. Stammler A, Hau T, Bhushan S, Meinhardt A, Jonigk D, Lippmann T, et al. Epididymitis: ascending infection restricted by segmental boundaries. *Hum Reprod* (2015) 30:1557–65. doi: 10.1093/humrep/dev112
17. Turner TT, Bomgardner D, Jacobs JP, Nguyen QA. Association of segmentation of the epididymal interstitium with segmented tubule function in rats and mice. *Reproduction* (2003) 125:871–8. doi: 10.1530/rep.0.1250871
18. Pierucci-Alves F, Midura-Kiela MT, Fleming SD, Schultz BD, Kiela PR. Transforming Growth Factor Beta Signaling in Dendritic Cells Is Required for Immunotolerance to Sperm in the Epididymis. *Front Immunol* (2018) 9:1882:1882. doi: 10.3389/fimmu.2018.01882
19. Fijak M, Pilatz A, Hedger MP, Nicolas N, Bhushan S, Michel V, et al. Infectious, inflammatory and 'autoimmune' male factor infertility: how do rodent models inform clinical practice? *Hum Reprod Update* (2018) 24:416–41. doi: 10.1093/humupd/dmy009
20. Flickinger CJ, Bush LA, Howards SS, Herr JC. Distribution of leukocytes in the epithelium and interstitium of four regions of the Lewis rat epididymis. *Anat Rec* (1997) 248:380–90. doi: 10.1002/(SICI)1097-0185(199707)248:3<380:AID-AR11>3.0.CO;2-L
21. Serre V, Robaire B. Distribution of immune cells in the epididymis of the aging Brown Norway rat is segment-specific and related to the luminal content. *Biol Reprod* (1999) 61:705–14. doi: 10.1095/biolreprod61.3.705
22. Nashan D, Malorny U, Sorg C, Cooper T, Nieschlag E. Immuno-competent cells in the murine epididymis. *Int J Androl* (1989) 12:85–94. doi: 10.1111/j.1365-2605.1989.tb01289.x
23. Seiler P, Wenzel I, Wagenfeld A, Yeung CH, Nieschlag E, Cooper TG. The appearance of basal cells in the developing murine epididymis and their temporal expression of macrophage antigens. *Int J Androl* (1998) 21:217–26. doi: 10.1046/j.1365-2605.1998.00116.x
24. Da Silva N, Smith TB. Exploring the role of mononuclear phagocytes in the epididymis. *Asian J Androl* (2015) 17:591–6. doi: 10.4103/1008-682X.153540
25. Da Silva N, Barton CR. Macrophages and dendritic cells in the post-testicular environment. *Cell Tissue Res* (2016) 363:97–104. doi: 10.1007/s00441-015-2270-0
26. Tamoutounour S, Henri S, Lelouard H, de Bovis B, de Haar C, van der Woude CJ, et al. CD64 distinguishes macrophages from dendritic cells in the gut and reveals the Th1-inducing role of mesenteric lymph node macrophages during colitis. *Eur J Immunol* (2012) 42:3150–66. doi: 10.1002/eji.201242847
27. McGovern N, Schlitzer A, Janela B, Ginhoux F. Protocols for the Identification and Isolation of Antigen-Presenting Cells in Human and Mouse Tissues. *Methods Mol Biol* (2016) 1423:169–80. doi: 10.1007/978-1-4939-3606-9_12
28. Hedger MP. Immunophysiology and pathology of inflammation in the testis and epididymis. *J Androl* (2011) 32:625–40. doi: 10.2164/jandrol.111.012989
29. Wang YF, Holstein AF. Intraepithelial lymphocytes and macrophages in the human epididymis. *Cell Tissue Res* (1983) 233:517–21. doi: 10.1007/BF00212221
30. Duan Y-G, Wang P, Zheng W, Zhang Q, Huang W, Jin F, et al. Characterisation of dendritic cell subsets in chronically inflamed human epididymis. *Andrologia* (2016) 48:431–40. doi: 10.1111/and.12463
31. Ritchie AW, Hargreave TB, James K, Chisholm GD. Intra-epithelial lymphocytes in the normal epididymis. A mechanism for tolerance to sperm auto-antigens? *Br J Urol* (1984) 56:79–83. doi: 10.1111/j.1464-410x.1984.tb07169.x
32. el-Demiry MI, Hargreave TB, Busuttil A, James K, Ritchie AW, Chisholm GD. Lymphocyte sub-populations in the male genital tract. *Br J Urol* (1985) 57:769–74. doi: 10.1111/j.1464-410x.1985.tb07051.x
33. Yakirevich E, Yanai O, Sova Y, Sabo E, Stein A, Hiss J, et al. Cytotoxic phenotype of intra-epithelial lymphocytes in normal and cryptorchid human testicular excurrent ducts. *Hum Reprod* (2002) 17:275–83. doi: 10.1093/humrep/17.2.275
34. Michel V, Duan Y, Stoschek E, Bhushan S, Middendorff R, Young JM, et al. Uropathogenic Escherichia coli causes fibrotic remodelling of the epididymis. *J Pathol* (2016) 240:15–24. doi: 10.1002/path.4748
35. Wijayarathna R, Pasalic A, Nicolas N, Biniwale S, Ravinthiran R, Genovese R, et al. Region-specific immune responses to autoimmune epididymitis in the murine reproductive tract. *Cell Tissue Res* (2020) 381(2):351–60. doi: 10.1007/s00441-020-03215-8
36. Pilatz A, Hossain H, Kaiser R, Mankertz A, Schüttler CG, Domann E, et al. Acute epididymitis revisited: impact of molecular diagnostics on etiology and contemporary guideline recommendations. *Eur Urol* (2015) 68:428–35. doi: 10.1016/j.eururo.2014.12.005
37. Çek M, Sturdza L, Pilatz A. Acute and Chronic Epididymitis. *Eur Urol Suppl* (2017) 16:124–31. doi: 10.1016/j.eursup.2017.01.003
38. Wolin LH. On the Etiology of Epididymitis. *J Urol* (1971) 105:531–3. doi: 10.1016/S0022-5347(17)61567-2
39. Wesselhoeft C. Orchitis in Mumps. *Boston Med Surg J* (1920) 183:458–61. doi: 10.1056/NEJM192010141831602
40. Park SJ, Kim HC, Lim JW, Moon SK, Ahn SE. Distribution of Epididymal Involvement in Mumps Epididymo-orchitis. *J Ultrasound Med* (2015) 34:1083–9. doi: 10.7863/ultra.34.6.1083
41. Rival C, Wheeler K, Jeffrey S, Qiao H, Luu B, Tewalt EF, et al. Regulatory T cells and vasectomy. *J Reprod Immunol* (2013) 100:66–75. doi: 10.1016/j.jri.2013.08.004
42. Mazzini E, Massimiliano L, Penna G, Rescigno M. Oral tolerance can be established via gap junction transfer of fed antigens from $CX3CR1_+$ macrophages to $CD103^+$ dendritic cells. *Immunity* (2014) 40:248–61. doi: 10.1016/j.immuni.2013.12.012
43. Worbs T, Bode U, Yan S, Hoffmann MW, Hintzen G, Bernhardt G, et al. Oral tolerance originates in the intestinal immune system and relies on antigen carriage by dendritic cells. *J Exp Med* (2006) 203:519–27. doi: 10.1084/jem.20052016
44. Smith TB, Cortez-Retamozo V, Grigoryeva LS, Hill E, Pittet MJ, Da Silva N. Mononuclear phagocytes rapidly clear apoptotic epithelial cells in the proximal epididymis. *Andrology* (2014) 2:755–62. doi: 10.1111/j.2047-2927.2014.00251.x
45. Raymond AS, Shur BD. A novel role for SED1 (MFG-E8) in maintaining the integrity of the epididymal epithelium. *J Cell Sci* (2009) 122:849–58. doi: 10.1242/jcs.041731
46. Wheeler K, Tardif S, Rival C, Luu B, Bui E, Del Rio R, et al. Regulatory T cells control tolerogenic versus autoimmune response to sperm in vasectomy. *Proc Natl Acad Sci U.S.A.* (2011) 108:7511–6. doi: 10.1073/pnas.1017615108
47. Voisin A, Damon-Soubeyrand C, Bravard S, Saez F, Drevet JR, Guiton R. Differential expression and localisation of TGF-β isoforms and receptors in the murine epididymis. *Sci Rep* (2020) 10:995. doi: 10.1038/s41598-020-57839-5
48. Shi Y, Massagué J. Mechanisms of TGF-β Signaling from Cell Membrane to the Nucleus. *Cell* (2003) 113:685–700. doi: 10.1016/S0092-8674(03)00432-X
49. Jrad-Lamine A, Henry-Berger J, Gourbeyre P, Damon-Soubeyrand C, Lenoir A, Combaret L, et al. Deficient tryptophan catabolism along the kynurenine pathway reveals that the epididymis is in a unique tolerogenic state. *J Biol Chem* (2011) 286:8030–42. doi: 10.1074/jbc.M110.172114

50. Wijayarathna R, Kretser DM, Sreenivasan R, Ludlow H, Middendorff R, Meinhardt A, et al. Comparative analysis of activins A and B in the adult mouse epididymis and vas deferens. *Reproduction* (2018) 155:15–23. doi: 10.1530/REP-17-0485
51. Hall SH, Yenugu S, Radhakrishnan Y, Avellar MC, Petrusz P, French FS. Characterization and functions of beta defensins in the epididymis. *Asian J Androl* (2007) 9:453–62. doi: 10.1111/j.1745-7262.2007.00298.x
52. Ribeiro CM, Silva EJ, Hinton BT, Avellar MC. β-defensins and the epididymis: contrasting influences of prenatal, postnatal, and adult scenarios. *Asian J Androl* (2016) 18:323–8. doi: 10.4103/1008-682X.168791
53. Battistone MA, Spallanzani RG, Mendelsohn AC, Capen D, Nair AV, Brown D, et al. Novel role of proton-secreting epithelial cells in sperm maturation and mucosal immunity. *J Cell Sci* (2019) 133(5):jcs233239. doi: 10.1242/jcs.233239
54. Wijayarathna R, Hedger MP. Activins, follistatin and immunoregulation in the epididymis. *Andrology* (2019) 7:703–11. doi: 10.1111/andr.12682
55. Greskovich F, Mathur S, Nyberg LM, Collins BS. Effect of early antibiotic treatment on the formation of sperm antibodies in experimentally induced epididymitis. *Arch Androl* (1993) 30:183–91. doi: 10.3109/01485019308987755
56. Vieler E, Jantos C, Schmidts HL, Weidner W, Schiefer HG. Comparative efficacies of ofloxacin, cefotaxime, and doxycycline for treatment of experimental epididymitis due to Escherichia coli in rats. *Antimicrob Agents Chemother* (1993) 37:846–50. doi: 10.1128/aac.37.4.846
57. Ludwig M, Johannes S, Bergmann M, Failing K, Schiefer HG, Weidner W. Experimental Escherichia coli epididymitis in rats: a model to assess the outcome of antibiotic treatment. *BJU Int* (2002) 90:933–8. doi: 10.1046/j.1464-410x.2002.03029.x
58. Ludwig M. Diagnosis and therapy of acute prostatitis, epididymitis and orchitis. *Andrologia* (2008) 40:76–80. doi: 10.1111/j.1439-0272.2007.00823.x
59. Klein B, Pant S, Bhushan S, Kautz J, Rudat C, Kispert A, et al. Dexamethasone improves therapeutic outcomes in a preclinical bacterial epididymitis mouse model. *Hum Reprod* (2019) 34:1195–205. doi: 10.1093/humrep/dez073
60. Palladino MA, Savarese MA, Chapman JL, Dughi M-K, Plaska D. Localization of Toll-like receptors on epididymal epithelial cells and spermatozoa. *Am J Reprod Immunol* (2008) 60:541–55. doi: 10.1111/j.1600-0897.2008.00654.x
61. Rodrigues A, Queiróz DB, Honda L, Silva EJ, Hall SH, Avellar MC. Activation of toll-like receptor 4 (TLR4) by in vivo and in vitro exposure of rat epididymis to lipopolysaccharide from Escherichia Coli. *Biol Reprod* (2008) 79:1135–47. doi: 10.1095/biolreprod.108.069930
62. Cheng L, Chen Q, Zhu W, Wu H, Wang Q, Shi L, et al. Toll-like Receptors 4 and 5 Cooperatively Initiate the Innate Immune Responses to Uropathogenic Escherichia coli Infection in Mouse Epididymal Epithelial Cells. *Biol Reprod* (2016) 94:58. doi: 10.1095/biolreprod.115.136580
63. Özbek M, Hitit M, Ergün E, Ergün L, Beyaz F, Erhan F, et al. Expression profile of Toll-like receptor 4 in rat testis and epididymis throughout postnatal development. *Andrologia* (2020) 52:e13518. doi: 10.1111/and.13518
64. Robertson MJ, Kent K, Tharp N, Nozawa K, Dean L, Mathew M, et al. Large-scale discovery of male reproductive tract-specific genes through analysis of RNA-seq datasets. *BMC Biol* (2020) 18:103. doi: 10.1186/s12915-020-00826-z
65. Silva EJ, Queiróz DB, Rodrigues A, Honda L, Avellar MC. Innate immunity and glucocorticoids: potential regulatory mechanisms in epididymal biology. *J Androl* (2011) 32:614–24. doi: 10.2164/jandrol.111.013565
66. Wang F, Liu W, Jiang Q, Gong M, Chen R, Wu H, et al. Lipopolysaccharide-induced testicular dysfunction and epididymitis in mice: a critical role of tumor necrosis factor alpha†. *Biol Reprod* (2019) 100:849–61. doi: 10.1093/biolre/ioy235
67. Silva EJ, Ribeiro CM, Mirim AF, Silva AA, Romano RM, Hallak J, et al. Lipopolysaccharide and lipotheicoic acid differentially modulate epididymal cytokine and chemokine profiles and sperm parameters in experimental acute epididymitis. *Sci Rep* (2018) 8:103. doi: 10.1038/s41598-017-17944-4
68. Song X, Lin N-H, Wang Y-L, Chen B, Wang H-X, Hu K. Comprehensive transcriptome analysis based on RNA sequencing identifies critical genes for lipopolysaccharide-induced epididymitis in a rat model. *Asian J Androl* (2019) 21:605–11. doi: 10.4103/aja.aja-21-19
69. Cao D, Li Y, Yang R, Wang Y, Zhou Y, Diao H, et al. Lipopolysaccharide-induced epididymitis disrupts epididymal beta-defensin expression and inhibits sperm motility in rats. *Biol Reprod* (2010) 83:1064–70. doi: 10.1095/biolreprod.109.082180
70. Wu Y, Li H, Qin Y. S100A4 Promotes the Progression of Lipopolysaccharide-induced Acute Epididymitis in Mice†. *Biol Reprod* (2020) 102(6):1213–24. doi: 10.1093/biolre/ioaa022

Conflict of Interest: The authors declare that the research was conducted in the absence of any commercial or financial relationships that could be construed as a potential conflict of interest.

frontiers in Immunology

ORIGINAL RESEARCH
published: 08 December 2020
doi: 10.3389/fimmu.2020.583276

Corticosterone Enhances the AMPK-Mediated Immunosuppressive Phenotype of Testicular Macrophages During Uropathogenic *Escherichia coli* Induced Orchitis

Zhengguo Zhang[1†], *Ziming Jiang*[1†], *Yiming Zhang*[1], *Yu Zhang*[1], *Yan Yan*[2], *Sudhanshu Bhushan*[3], *Andreas Meinhardt*[3], *Zhihai Qin*[2,4*] and *Ming Wang*[2*]

[1] Department of Urology, The First Affiliated Hospital of Zhengzhou University, Zhengzhou, China, [2] Medical Research Center, The First Affiliated Hospital of Zhengzhou University, Zhengzhou, China, [3] Department of Anatomy and Cell Biology, Justus-Liebig-University of Giessen, Giessen, Germany, [4] School of Basic Medical Sciences, The Academy of Medical Sciences of Zhengzhou University, Zhengzhou, China

Testicular macrophages (TM) play a central role in maintaining testicular immune privilege and protecting spermatogenesis. Recent studies showed that their immunosuppressive properties are maintained by corticosterone in the testicular interstitial fluid, but the underlying molecular mechanisms are unknown. In this study, we treated mouse bone marrow-derived macrophages (BMDM) with corticosterone (50 ng/ml) and uncovered AMP-activated protein kinase (AMPK) activation as a critical event in M2 polarization at the phenotypic, metabolic, and cytokine production level. Primary TM exhibited remarkably similar metabolic and phenotypic features to corticosterone-treated BMDM, which were partially reversed by AMPK-inhibition. In a murine model of uropathogenic *E. coli*-elicited orchitis, intraperitoneal injection with corticosterone (0.1mg/day) increased the percentage of M2 TM *in vivo*, in a partially AMPK-dependent manner. This study integrates the influence of corticosterone on M2 macrophage metabolic pathways, phenotype, and function, and highlights a promising new avenue for the development of innovative therapeutics for orchitis patients.

Keywords: Corticosterone, Testicular macrophage, AMPK, Fatty acid oxidation (FAO), Orchitis

OPEN ACCESS

Edited by:
Yong-Gang Duan,
University of Hong Kong, China

Reviewed by:
Daishu Han,
Chinese Academy of Medical Sciences and Peking Union Medical College, China
Sellappan Selvaraju,
National Institute of Animal Nutrition and Physiology (ICAR), India

****Correspondence:***
Ming Wang
wangmingheda@163.com
Zhihai Qin
zhihai@ibp.ac.cn

[†]These authors have contributed equally to this work

Specialty section:
This article was submitted to Mucosal Immunity, a section of the journal Frontiers in Immunology

Received: *14 July 2020*
Accepted: *10 November 2020*
Published: *08 December 2020*

Citation:
Zhang Z, Jiang Z, Zhang Y, Zhang Y, Yan Y, Bhushan S, Meinhardt A, Qin Z and Wang M (2020) Corticosterone Enhances the AMPK-Mediated Immunosuppressive Phenotype of Testicular Macrophages During Uropathogenic Escherichia coli Induced Orchitis. Front. Immunol. 11:583276. doi: 10.3389/fimmu.2020.583276

INTRODUCTION

Urogenital infection and immunological factors account for 13 to 15% of all cases of male infertility (1, 2). These are potentially curable or treatable conditions, but as yet sufficient knowledge of the underlying pathology or possible therapeutics is scarce. The testis is an immune-privileged organ that needs to tolerate autoantigens of germ cells and maintain immune homeostasis even under infectious or inflammatory conditions (3, 4). Testicular macrophages (TM), the main population of immune cells in the testis, play a key role in the maintenance of immune privilege (5–7), however, how they balance this function with defense against invading pathogens is largely unknown.

Much of our knowledge on TM has come from rat models, where these cells are largely anti-inflammatory, exhibiting reduced pro-inflammatory responses and an immunosuppressive phenotype, while retaining their phagocytic capacity (8, 9). Rat TM maintain their immunosuppressive function by secreting high amounts of the anti-inflammatory cytokine IL-10, and only low levels of pro-inflammatory cytokines such as TNF-α and IL-6 (10, 11). Most recently, corticosterone in the testicular interstitial fluid (TIF) was identified as an important mediator maintaining TM function and phenotype (12).

Clinically, corticosterone is a widely used immunosuppressive drug that belongs to the glucocorticoid family of steroid hormones, and elicits a wide range of biological effects including immunosuppressive and anti-inflammatory actions (13–15). *In vivo* corticosterone is mainly synthesized in the adrenal glands, and enters target organs *via* the bloodstream. However, corticosteroids can also be produced in extra-adrenal tissues such as the skin and intestine (16). In this regard, we found that corticosterone levels in TIF were significantly higher than in serum, even in rats following adrenalectomy (12). We uncovered significant intratesticular production of corticosterone by TM, suggesting an autocrine loop of corticosterone action in the testis. However, the underlying mechanisms of how corticosterone maintains the immunosuppressive function of TM and what the effects of corticosterone are on TM in infectious conditions are still not fully understood.

Two broad types of macrophages exist in tissues: classically activated pro-inflammatory M1 macrophages, and alternatively activated anti-inflammatory M2 macrophages. However, these phenotypes are not fixed, and most recently studies have revealed the importance of cellular metabolism in fate decision of macrophages. M1 and M2 macrophages rely on different metabolic pathways, namely glycolysis and oxidative phosphorylation, respectively, to maintain their specific phenotypes and functions (17, 18). Accordingly, a switch between these metabolic pathways can induce the alternation of macrophage phenotype: inhibiting oxidative phosphorylation not only suppresses the M2 macrophage state, but actively induces M1 macrophage polarization (19); while in contrast, activation of oxidative phosphorylation and PGC-1β reduces pro-inflammatory cytokine production in M1 macrophages (20). AMP-activated protein kinase (AMPK), a master-regulator of cellular and systemic energy homeostasis, has been identified as the key mediator of inflammatory signaling pathways in macrophages (21). AMPK activation facilitates macrophage differentiation to the anti-inflammatory M2 phenotype (22). Given the finding that corticosterone could impair the oxidative energy metabolism of the liver mitochondria (23), and based on these recent studies, we speculate that corticosterone could mediate the TM phenotype by altering their metabolic pathways.

Here we aimed to bring together recent findings on rat TM, corticosterone, and macrophage metabolism to ask about the pathways driving and maintaining the anti-inflammatory polarization of murine TM. Studying bone marrow derived monocytes (BMDM) and primary TM *in vitro* we found that corticosterone induced the activation of AMPK and fatty-acid oxidation pathways in BMDM, leading to M2 polarization, which phenocopied the anti-inflammatory features of TM. Similarly, *in vivo* in a uropathogenic *Escherichia coli* (UPEC)-elicited orchitis model, corticosterone treatment prevented UPEC-induced decreases in M2 TM in the mouse testis, which was partly AMPK-dependent.

MATERIALS AND METHODS

Animals

All mice were purchased from Charles River Laboratories (China). Animal experiments were conducted in accordance with the recommendations specified in the guide for the care and the protocols approved by the Ethics Committee of Zhengzhou University (Ethics Number: KY154). Mice (C57BL/6J, 8–10 weeks, male) were housed in groups of five in individually ventilated cages under a cycle of 12 h of light and 12 h of dark, in specific pathogen-free conditions with constant temperature (21°C) and 50–60% humidity. Mice were killed by isoflurane, and tissues were rapidly collected.

UPEC Orchitis Model

The bacteria-induced orchitis model was established as described previously (24). Briefly, after general anesthesia, a scrotal incision was made to expose the testes, epididymidis, and vasa deferentia. Ten μl of UPEC strain 536-saline (0.9% sodium chloride solution) suspension (about 5×10^5 bacteria) were injected bilaterally into the vas deferens proximal to the cauda epididymis using 30 G needles. Sham operated mice were injected with saline. The vasa deferentia were ligated close to the site of injection to prevent spreading of infection anterograde towards the urethra. From the second day after the operation, animals were intraperitoneally injected with corticosterone (0.1mg/day) and or Compound C (0.4 mg/kg, ABSIN, China, Shanghai). Mice were kept under standard housing conditions until being sacrificed at day 7 post operation. Both testes were removed aseptically for further analysis by flow cytometry or H&E staining.

Primary TM and PM Isolation

TM and PM were isolated from adult C57BL/6J mice as previously described (25, 26). Briefly, testes were decapsulated and collected into 10 ml of ice-cold endotoxin-free RPMI 1640 medium. The seminiferous tubules were gently separated as Hayes et al. described (27). The volume was adjusted to 50 ml and fragments were allowed to settle for 5 min, then the supernatant was recovered and centrifuged at 300 g for 10 min at 4°C. The interstitial cell pellet was resuspended in 5 ml RPMI 1640 culture medium and adjusted to a concentration of 5×10^6 cells/ml. After several washes with PBS, cells (2×10^6/well) were plated into six-well plates and incubated at 37°C in an atmosphere containing 5% CO_2 for 30 min. Contaminating cells were removed by extensive washing. Peritoneal exudate

cells were harvested by lavage with cold RPMI 1640 medium (10 ml per mouse). Cells were sedimented at 300 g for 10 min at room temperature. The cell pellet was resuspended in 10 ml medium, and 2×10^6 cells/well were seeded into six-well plates and incubated at 37°C in an atmosphere containing 5% CO_2 for 30 min to allow PM to adhere. Non-adherent cells were removed by washing thoroughly three times with RPMI 1640. Purity of TM and PM were analyzed by flow cytometry using antibodies against the macrophage markers F4/80 and CD11b, and found to be approximately 75–80% (TM) and 90% (PM), respectively (**Supplementary Figure 1**).

BMDM Isolation and Culture

Bone marrow-derived macrophages (BMDM) were generated from the femur and tibia of adult male mice. The bone marrow was rinsed into phosphate buffer saline (PBS) with a 1 ml syringe and centrifuged at 300 g for 5 min at RT. The cell pellet was resuspended in 5 ml red blood cells lysis buffer for 3 min to lyse the erythrocytes, then centrifuged at 300 g for 5 min at RT before being resuspended again in RPMI-1640 medium supplemented with 10% FBS and 1% penicillin/streptomycin. The cell concentration was adjusted to 5×10^6 cells/ml; 2×10^6 cells/well were seeded onto 12-well plates and incubated at 37°C in an atmosphere containing 5% CO_2 for 30 min. Contaminating cells were removed by extensive washing, taking advantage of the rapid adherence of macrophages. Finally, the isolated cells were cultured with RPMI 1640 medium containing 10% FBS, 1% penicillin/streptomycin, and 50 ng/ml granulocyte-macrophage colony-stimulating factor (GM-CSF, Biolegend, San Diego, USA).

ELISA

The ELISA Ready-SET-GO-Assays (TNFα, Cat#: 430901, Biolegend; IL-10, Cat#: 431411, Biolegend) were used to measure the concentrations of TNFα and IL-10 protein in BMDM and primary macrophage culture medium, according to the manufacturer's instructions.

RT-PCR

Total RNA was extracted from cells using Trizol Reagent. Complementary DNA was synthesized from 2 μg total RNA using for cDNA reverse transcription. Prime Script RT Master Mix (Applied TaKaRa, Otsu, Shiga, Japan) was used in accordance with the manufacturer's instructions. qRT-PCR was performed on an ABI PRISM 7300HT Sequence Detection System (Applied Biosystems, Foster City, CA, USA) using SYBR Green PCR Master Mix (TaKaRa). The primers used are listed in **Table 1**. The average threshold cycle number (CRtR) for each tested mRNA was used to quantify the relative expression according to the $2^{-\Delta\Delta Ct}$ method, and *Gapdh* was used as an internal control.

Western Blotting

Cell lysates were prepared in RIPA buffer (65 mM Tris-HCl, 150 mM NaCl, 1 mM EDTA, 1% NP-40, 0.5% sodium deoxycholate, 0.1% SDS, and protease inhibitor cocktail) and protein concentrations were measured by the Bio-Rad Protein Assay (Bio-Rad, Hercules, USA). Twenty μg of protein from each sample were subjected to SDS-PAGE and transferred onto nitrocellulose membranes. The membranes were incubated with 5% non-fat milk in TBST (0.5% Tween 20) for 1 h and washed three times with TBST washing buffer. After incubation with primary antibodies against p-AMPK (2535s, CST, Danvers, USA), AMPK (5831s, CST), p-ACC1 (3661s, CST), ACADM (118183, Abcam, Cambridge, UK), or ACADVL (118183, Abcam) at 4°C overnight, the membranes were washed and then incubated for 1h with HRP-conjugated anti-rabbit or anti-mouse secondary antibodies at room temperature. The blots were washed three times with TBST and developed with an ECL system (Bio-Rad). Actin (CST) was used as a loading control.

Flow Cytometry

To measure macrophage marker levels in primary TM and corticosterone-polarized BMDM flow cytometry was used. In brief, 1×10^6 cells were washed twice with washing buffer (1% BSA in PBS) and incubated with an anti-mouse CD16/32 antibody (553142, BD Biosciences, San Jose, USA) for 10 min. Then, anti-mouse CD45 (103128, Biolegend, APC-R700, 1:100), F4/80 (123118, Biolegend, APC-cy7, 1:100), CD11b (553310, BD, FITC, 1:100), and CD206 (141716, Biolegend, Percp 5.5, 1:100) antibodies were used to identify the macrophage populations. After incubating the cells with CD45, CD11b, F4/80 for 30 min on ice, cells were washed with PBS 1% w/v BSA, fixed, permeabilized, and labeled with anti-CD206 at 4°C for 30 minutes. Then cells were washed and re-suspended in washing buffer. Flow cytometric analysis was performed by using a FACS AriaII (BD) and data were analyzed with FlowJo software version X (Tree Star, Ashland, OR, USA).

TABLE 1 | The primers used in this paper.

Genes	Forward	Reverse
Tnfa	AAAGACCAGGTGGAGTGGAAGAAC	CTCAGTGCCGATGGAGTCCGAGTA
Il10	CCCATTCCTCGTCACGATCTC	TCAGACTGGTTTGGGATAGGTTT
Acc1	ACAGTGGAGCTAGAATTGGAC	ACTTCCCGACCAAGGACTTTG
Cpt1	CAGAGGATGGACACTGTAAAGG	CGGCACTTCTTGATCAAGCC
Acadm	TGGCATATGGGTGTACAGGG	CCAAATACTTCTTCTTCTGTTGATCA
Cd36	ATTGGTCAAGCCAGCT	TGTAGGCTCATCCACTAC
Fasn	AGCGGCCATTTCCATTGCCC	CCATGCCCAGAGGGTGGTTG
Acsl1	TCCTACAAAGAGGTGGCAGAACT	GGCTTGAACCCCTTCTGGAT
Gapdh	TCTCTGCTCCTCCCTGTTCC	TACGGCCAAATCCGTTCACA

FAO Enzyme Measurements

Analysis of fatty acid oxidation (FAO) was performed using a FAO flow cytometry kit (118183, Abcam). Levels of the FAO cycle enzymes ACADVL and ACADM were determined according to the manufacturer's instructions.

Seahorse XF96 Analysis

The Seahorse XF96 Extracellular Flux analyzer (Agilent, Santa Clara, USA) is a sensitive, high-throughput instrument that takes real-time measurements of respiration rates of cells with or without oxidative stress. Briefly, TM, PM, or corticosterone treated BMDM (10^4 cells/well) were seeded on Seahorse culture plates in assay medium (DMEM, 1% BSA, 25 mM glucose, and 2 mM glutamine, 1 mM pyruvate) and analyzed using a Seahorse XFe-96 system. For measuring extracellular acidification rate (ECAR), macrophages were stimulated accordingly with 10 mM glucose, 0.25 μM oligomycin (Calbiochem, Merck, Darmstadt, Germany), and 2-deoxyglucose (2-DG, 100 mM). To obtain the maximal respiratory and control values of cells, macrophages were stimulated with oligomycin (0.25 μM), Carbonyl cyanide 4-(trifluoromethoxy) phenylhydrazone (FCCP, 1 μM), and rotenone (1 μM)/antimycin A (1 μM) according to a standard protocol (28). The cell numbers were normalized to the cell protein concentrations. ECAR and OCR were measured with the XF96 Extracellular Flux Analyzer.

Histological Analysis

UPEC induced orchitis testes were collected and fixed in Bouin's fixative for 4 h and then embedded in paraffin. Tissue sections (6 μm) were stained with hematoxylin and eosin. After staining, images were acquired with a Vectra microscope (Akoya Biosciences, Menlo Park, USA).

Statistical Analyses

Statistical significance was calculated by Welch's t-test when comparing two groups or by one-way ANOVA. A p-value <0.05 was considered statistically significant.

RESULTS

Corticosterone Induces an Anti-Inflammatory Macrophage Phenotype *In Vitro*

Our previous study showed that corticosterone polarized GM-CSF-induced rat blood monocytes towards the anti-inflammatory M2 macrophage phenotype (12). To understand whether parallel effects occurred in murine macrophages, we first cultured mouse BMDM with 50 ng/ml of corticosterone for 7 days. As in rats, corticosterone treatment induced high levels of expression of the M2-marker CD206 on around half of macrophages (**Figures 1A, B**). Similarly, the relative mRNA level of *Cd206* was significantly higher in corticosterone-treated cultures, as was expression of the anti-inflammatory cytokine *Il10*; whereas expression of the pro-inflammatory cytokine *Tnfa* was significantly decreased by corticosterone treatment (**Figure 1C**). As macrophage polarization and pro-/anti-inflammatory cytokine production have recently been linked to changes in cellular metabolism, we next asked whether corticosterone was altering the metabolic pathways in murine BMDM. We cultured BMDM with or without corticosterone and assessed activity of the M1-linked glycolytic pathway and M2-linked oxidative phosphorylation (OXPHOS) by measuring the extracellular acidification rate (ECAR) and oxygen consumption rate (OCR), respectively (**Figure 1D**). Corticosterone significantly increased OCR and reduced ECAR in BMDM compared with the non-treated group (**Figure 1D**), which is consistent with the increased expression of M2 phenotypic markers and cytokines induced by corticosterone treatment seen above. Thus, corticosterone induces M2 polarization at the phenotypic, molecular, and metabolic level in murine BMDM *in vitro*.

We then asked how the effects of corticosterone on BMDM metabolism compared to the metabolic profiles of macrophages in the murine testis. We isolated an enriched population of primary TM (75–80% purity) and compared their ECAR/OCR profiles to those of primary PM (approximately 90% purity), which are known to have an M1 phenotype, and to the data from BMDM (**Figure 1D**). We found that the enriched TM population exhibited increased OCR and reduced ECAR relative to PM (**Figure 1E**), and that their metabolic profile closely resembled that of corticosterone-treated BMDM (**Figure 1D**). Taken together, an enriched primary TM population and corticosterone-treated BMDM both show comparably higher levels of OXPHOS and lower levels of glycolysis, consistent with an M2 anti-inflammatory phenotype.

Corticosterone Activates AMPK and Reprograms Fatty Acid Metabolism in BMDM

Having observed that corticosterone treatment induces an M2 polarization of BMDM that is metabolically similar to TM, we next aimed to identify the molecular mechanisms involved. The AMPK signaling pathway plays an important role in polarizing macrophages to an anti-inflammatory M2 phenotype (29); therefore we measured levels of phosphorylated AMPK (p-AMPK) in untreated BMDM and compared them with BMDM treated with corticosterone for 30–120 min. We found that both the abundance of p-AMPK and the ratio of p-AMPK to AMPK significantly increased in a time-dependent manner following corticosterone treatment (**Figure 2A**). When we compared these AMPK levels to those in a population enriched in primary TM, again we saw a striking resemblance between corticosterone-treated BMDM and TM, which exhibited high absolute levels of p-AMPK and a high ratio of p-AMPK to AMPK; while in contrast PM exhibited significantly less p-AMPK and lower ratios between p-AMPK and AMPK (**Figure 2B**). This suggested that TM express high levels of p-AMPK constitutively, while PM do not, and that BMDM require corticosterone to activate AMPK.

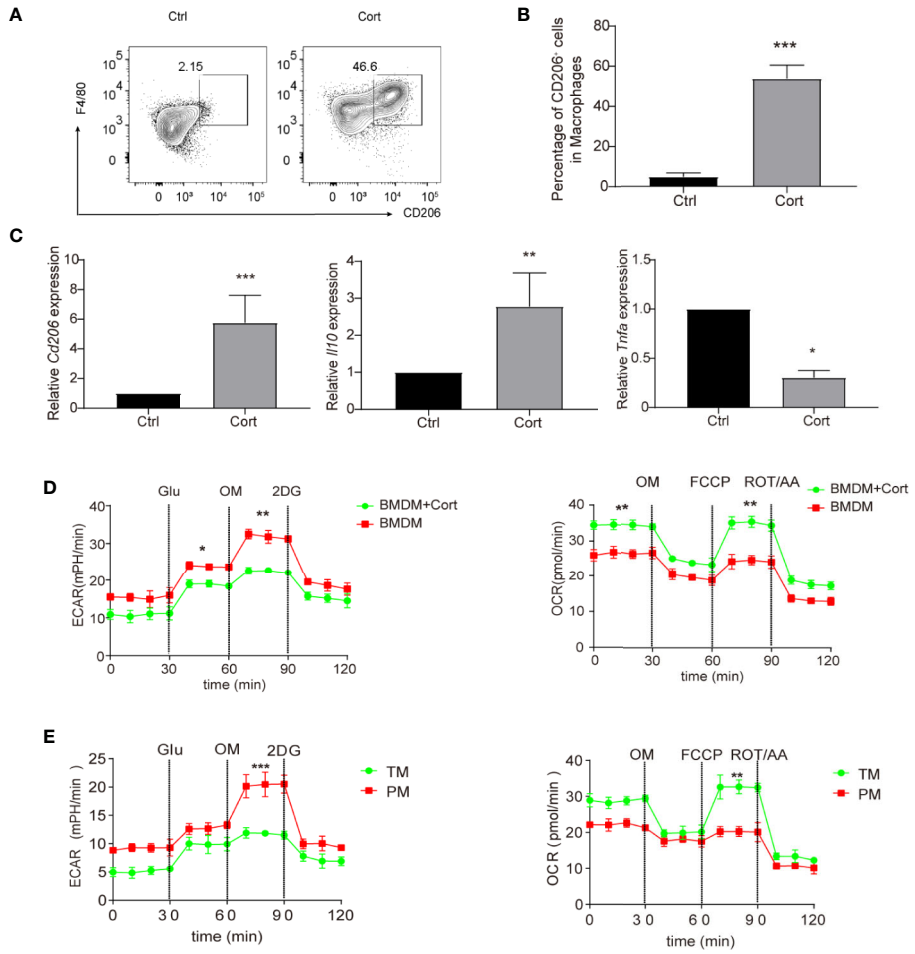

FIGURE 1 | Corticosterone induces M2 macrophage polarization in BMDM. **(A–D)** BMDM were derived by culture in RPMI 1640 medium supplemented with GM-CSF (50 ng/ml), before the addition of corticosterone (50 ng/ml) for 7 days. **(A, B)** The macrophage markers F4/80 and CD206 were identified by flow cytometry. Representative plots are shown **(A)**; alongside average percentage of macrophages expressing CD206 **(B)**. **(C)** The mRNA expression levels of *Cd206, Il10*, and *Tnfa* were quantified by qRT-PCR and normalized against *Actin*. **(D, E)** BMDM cultured with or without corticosterone **(D)**, and primary TM and PM **(E)** were seeded on XF96- Seahorse culture plates (10^4 per well). The ECAR and OCR were tested in XF-96 assay medium (see *Methods*) and normalized against protein concentration. After establishing a baseline, glucose (Glu, 10 mM), oligomycin (OM, 0.25 μM), 2-deoxyglucose (2-DG, 100 mM), or oligomycin (OM, 0.25 μM), FCCP (1 μM) and rotenone/antimycin A (ROT/AA, 1 μM) were sequentially added. Continuous ECAR and OCR values (pmoles/min/μg protein) are shown. Each repetition involved 4–5 mice per group and three replicates were performed (mean ± SD, Welch's t-test). *P < 0.05, **P < 0.01, ***P < 0.001.

Having shown that corticosterone treatment induces M2-like metabolic profiles in BMDM (**Figure 1D**) as well as inducing AMPK activation, we next asked how corticosterone impacted the AMPK-mediated fatty acid oxidation (FAO) pathway. As expected, corticosterone treatment of BMDM significantly increased the expression of key FAO enzymes including phosphorylated acetyl-CoA carboxylase (p-ACC), acyl-coenzyme A dehydrogenase (ACADM), and very long-chain specific acyl-CoA dehydrogenase (ACADVL) (**Figures 2C–E**). In addition, the mRNA levels of the FA transport gene transcript carnitine palmitoyltransferase 1 (*Cpt1*), the FA oxidation related gene transcripts acetyl-CoA carboxylase 1 (*Acc1*) and *Acadm*, and the FA synthesis gene transcript fatty acid synthase (*Fasn)* were also up-regulated after corticosterone stimulation (**Figure 2F**). Together, these data show that corticosterone treatment of BMDM induces AMPK activation and reprograms macrophages towards fatty acid metabolism, which is needed for M2 polarization. Moreover, similar relative levels of p-AMPK are present in corticosterone-treated BMDM and TM in the steady state.

AMPK Inhibition Reduces M2 Phenotypic and Metabolic M2 Polarization in BMDM and TM

To confirm the necessity of AMPK activation for the metabolic and phenotypic M2 polarization of corticosterone-treated BMDM, we conducted a series of experiments using the AMPK inhibitor Compound C. We first confirmed that Compound C treatment reversed corticosterone-mediated AMPK activation, while leaving overall AMPK levels

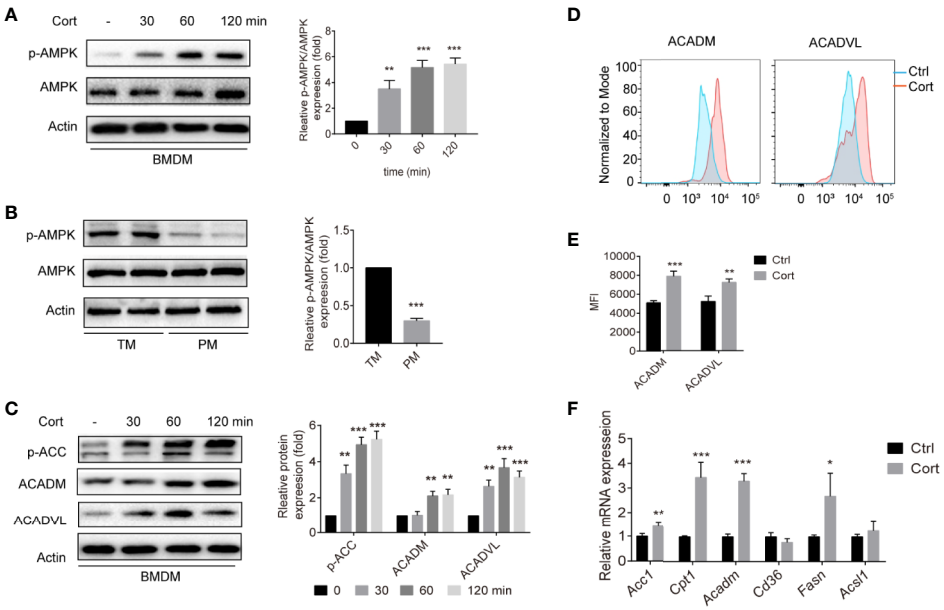

FIGURE 2 | Corticosterone increases p-AMPK levels and FA metabolism in BMDM. **(A, C)** BMDM were stimulated with corticosterone (50 ng/ml) from 30–120 min, the levels of AMPK/p-AMPK **(A)**, and p-ACC, ACADM, and ACADVL **(C)** were measured by Western blot. In each case, representative blots and average relative expression levels (determined by band intensity using Image J and normalized relative to BMDM control sample) are shown. **(B)** TM and PM were isolated and pooled from two mice (two mice for one sample, two samples were detected), p-AMPK/AMPK expression was measured by Western blot. Representative images of three independent experiments are shown. Relative amounts of p-AMPK detected on the blots were quantified as described in *Methods*. **(D, E)** BMDM were treated with corticosterone (50 ng/ml) for 7 days, cells were fixed and labeled for ACADM and ACADVL before analysis by flow cytometry. Representative MFI histogram **(D)** and the mean MFI **(E)** is shown (n = 4 per group). **(F)** The mRNA levels of FA metabolism genes were quantified by qRT-PCR and normalized against *Gapdh*. The data represent the means ± SD. Results are representative of four to five independent experiments. Welch's t-test, *p < 0.05, **p < 0.01, ***p < 0.001 as indicated.

unaffected, in BMDM (**Figure 3A**). We then asked what effect inhibiting AMPK activation would have on the observed metabolic polarization of BMDM. Compound C treatment significantly lowered OCR in corticosterone polarized BMDM (**Figure 3B**), and significantly inhibited the expression of the FAO-associated genes *Acc1*, *Cpt1*, and *Acadm* (**Figure 3C**). Moreover, Compound C treatment approximately halved the expression of the M2 macrophage marker CD206 at both the gene (**Figure 3D**) and population frequency (**Figure 3E**) level in corticosterone-treated BMDM. Collectively, these data showed that corticosterone-induced BMDM phenotypic and metabolic M2 polarization is AMPK dependent.

To understand whether AMPK activation was playing a parallel role in primary TM, we repeated the same analyses using these cells with PM for comparison. Again, we saw that Compound C treatment reduced p-AMPK levels in a dose-dependent fashion (**Figure 3F**). Similar to corticosterone-treated BMDM, we found that inhibition of AMPK activation led to significantly reduced OCR (**Figure 3G**), as well as significant reductions in *Cd206* expression (**Figure 3H**). Taken together, these results show that AMPK inhibition in BMDM and TM results in reduced FAO and decreased expression of the M2 marker *Cd206*. In BMDM this is accompanied by lowered expression of FAO-associated genes and a reduced frequency of cells showing M2 phenotypic polarization.

AMPK Is Required for Anti-Inflammatory Cytokine Production in Corticosterone-Polarized BMDM and in TM

Having shown that the phenotype and metabolic profile of corticosterone-polarized BMDM and TM relies on AMPK activation, we next investigated whether AMPK activation was needed for M2-associated cytokine production. Quantitative RT-PCR of cytokine gene expression showed that *Tnfa* transcript levels were elevated in corticosterone-treated BMDM in the presence or absence of the bacterial inflammatory stimulus LPS after 1 h, and were unaffected by Compound C treatment (**Figure 4A**). Expression levels equaled at 3 h post-LPS stimulation. In contrast, expression of the anti-inflammatory cytokine *Il10* gene was significantly increased following LPS treatment at 1 and 3 h, and inhibited by Compound C (**Figure 4A**). At the protein level, TNFα levels were high 3 h after LPS treatment of corticosterone-treated BMDM, and the addition of Compound C further enhanced this effect (**Figure 4B**). IL-10 protein levels confirmed the mRNA data, showing significant AMPK-activation-dependent induction following LPS exposure (**Figure 4B**). Thus, AMPK activation is crucial for the induction of immunosuppressive IL-10 in corticosterone-polarized BMDM in response to challenge with a common bacterial ligand.

We next asked whether there was evidence for comparable mechanisms in primary TM. Again, *Tnfa* expression was not

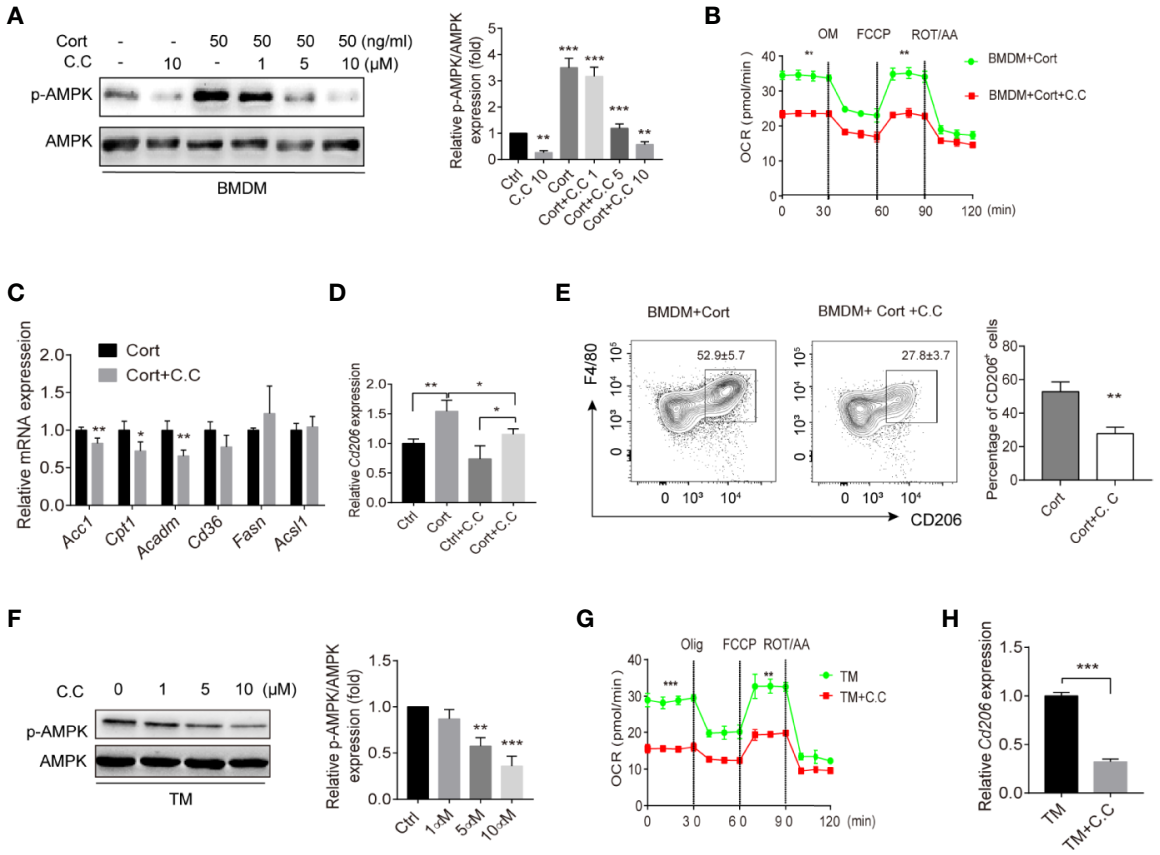

FIGURE 3 | AMPK inhibition suppresses M2 polarization of BMDM and TM. **(A)** Corticosterone (50 ng/ml, 7 days)-polarized BMDM were incubated with the AMPK inhibitor Compound C (1–10μM, 3h); p-AMPK protein expression was detected by Western blot. Bar blots represent the relative p-AMPK/AMPK protein level, which was determined from the band intensity using ImageJ software, and normalized relative to the BMDM control samples. **(B)** The OCR of corticosterone-polarized BMDM (same samples as in **Figure 1D**) were compared with BMDM+Compound C treatment. **(C, D)** The relative mRNA levels of fatty acid metabolism genes and *Cd206* in BMDM and corticosterone stimulated (50 ng/ml, 3 h) Expression of *Acc1*, *Cpt1*, *Acadm*, cluster of differentiation 36 (*Cd36*), *Fasn*, acyl-coA synthetase long chain family member 1 (*Acsl1*) in BMDM were quantified by qRT-PCR and normalized against *Gapdh* (means ± SD Welch's t-test for C, one way ANOVA for D.) **(E)** BMDM were stimulated with corticosterone for 7 days with/without daily Compound C (C. C; 10μM) administration. Levels of F4/80 and CD206 were identified by flow cytometry and the representative plot is shown. Bar blot shows the average of $CD206^+$ cell percentage (means ± SD, Welch's t-test). **(F)** TM were incubated with Compound C (1–10 μM, 3 h) and p-AMPK protein expression was detected by Western blot and quantified by using ImageJ **(G)**. The OCR of enriched populations of TM (same samples as in **Figure 1E**) and Compound C pre-treated TM (10 μM, 0.5 h) were measured in XF-96 assay medium and normalized against protein concentration **(H)**. The relative expression of *Cd206* in TM treated with or without Compound C was detected by qRT-PCR and normalized against *Gapdh*. In all graphs, the error bars represent SEM, whereas results designated with * were significant ($P < 0.05$), ** ($P < 0.005$) or (***$p < 0.001$). These experiments were repeated three times, Welch's t-test was used.

induced by LPS exposure of these cells, while instead abundant *Il-10* transcription was stimulated (**Figure 4C**). This is consistent with previous studies and confirms the immunosuppressive features of TM (10). Compound C pre-treatment significantly reduced both the *Il10* transcript and protein level in enriched populations of TM upon LPS stimulation (**Figures 4C, D**), suggesting that AMPK is important for expression of this key immunosuppressive cytokine by TM in response to a bacterial inflammatory stimulus.

Corticosterone Treatment Ameliorates UPEC-Elicited Orchitis *In Vivo*

The data so far have confirmed that corticosterone induces BMDM to develop an M2 phenotype, metabolic state, and immunosuppressive cytokine response, dependent on AMPK activation. We next wanted to ask about the possible roles of corticosterone *in vivo*. Therefore, the effects of corticosterone treatment on the inflammatory immune response and resulting testicular tissue impairment was assessed in a murine model of uropathogenic *Escherichia coli* (UPEC)-elicited orchitis, besides the role of AMPK (**Figure 5A**). Seven days after UPEC injection into the vas deferens, mice were sacrificed, immune cell suspensions were analyzed by flow cytometry, and testicular sections taken for histology. We found that UPEC induced a marked increase in frequency (**Figure 5B**) and absolute number (**Figure 5C**) of both $F4/80^{hi}$ resident TM and $CD11b^{hi}$ monocyte-derived macrophages in testis, consistent with the inflammation caused by UPEC infection. However, in mice

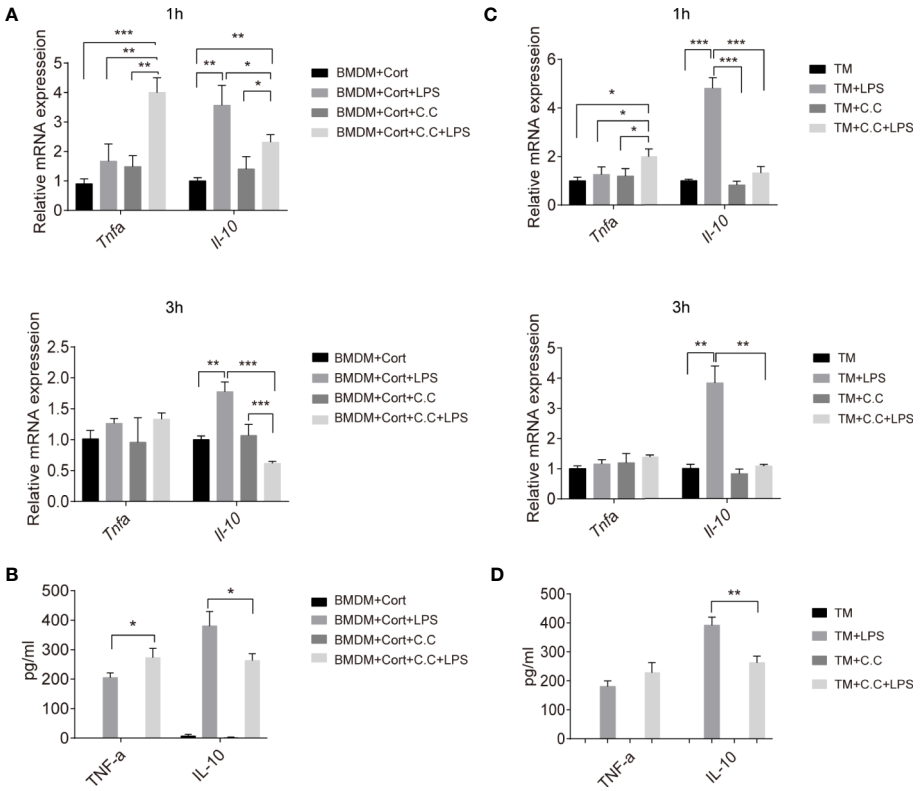

FIGURE 4 | Inhibition of inflammatory cytokine production in M2 phenotype BMDM and TM by Compound C. Enriched populations of TM **(C, D)** and corticosterone-induced BMDM **(A, B)** were pre-treated with Compound C (C. C, 0.5 μM, 30 min), then stimulated with LPS (1 ug/ml, 1 and 3 h, respectively). **(A, C)** The effects of AMPK inactivation on expression of *Il10* and *Tnfa* were examined by qRT-PCR. **(B, D)** After pretreatment with Compound C and LPS (3 h) cell supernatants were collected and the protein levels of TNF-α and IL-10 were measured by ELISA. Results are representative of three to four independent experiments. *p < 0.05; **p < 0.01; *p <0.001 as indicated. One-way ANOVA.

treated with corticosterone these increases were significantly less (**Figures 5B, C**), suggesting an anti-inflammatory function of corticosterone in the testis. By adding Compound C to the UPEC +corticosterone group, we uncovered a critical role for AMPK activation in mediating $CD11b^{hi}$ macrophage recruitment into the UPEC-inflamed testis (**Figures 5B, C**). We then looked at M2 marker expression in the $F4/80^{+}$ TM macrophages in each treatment group, and found that CD206 expression was significantly decreased by UPEC, but reinstated to control levels when corticosterone was applied (**Figures 5C, D**). AMPK activation was partially responsible for the change in frequency of CD206-expressing TM (**Figure 5D**). Moreover, compared to the UPEC treatment group, *Tnfa* expression was downregulated and *Acadm* expression was upregulated in enriched populations of TM isolated from the corticosterone treatment group—effects that were reversed by the addition of Compound C (**Figure 5E**). These data show that corticosterone reduced UPEC-induced inflammation in the murine testis by maintaining the immunosuppressive function of TM. When we examined control testis sections using H&E staining, we found a profound loss of germ cells in the seminiferous tubules (**Figure 5F**), consistent with the impaired spermatogenesis that often accompanies bacterial orchitis. In contrast, mice infected with UPEC and treated with corticosterone were less severely affected (**Figure 5F**). Again, the effects of corticosterone were partially reversed by Compound C treatment (**Figure 5F**), indicating an important role of AMPK signaling in corticosterone-mediated amelioration of UPEC-elicited orchitis. Taken together, corticosterone treatment protected testes from inflammation-associated tissue damage *via* a pathway involving AMPK activation and associated with maintaining TM M2 phenotype as well as reducing the abundance of infiltrating monocyte-derived macrophages.

DISCUSSION

The current study shows that corticosterone can help maintain the TM immunosuppressive phenotype under bacterial challenge, and that the AMPK pathway is responsible for part of the TM-mediated immunosuppression. In line with these findings, corticosterone treatment mediated profound changes to BMDM energy metabolism—inhibiting glycolysis and inducing FAO—to promote M2 polarization. Further experiments indicated that AMPK activation plays a major role in corticosterone-polarized M2 macrophage phenotype and

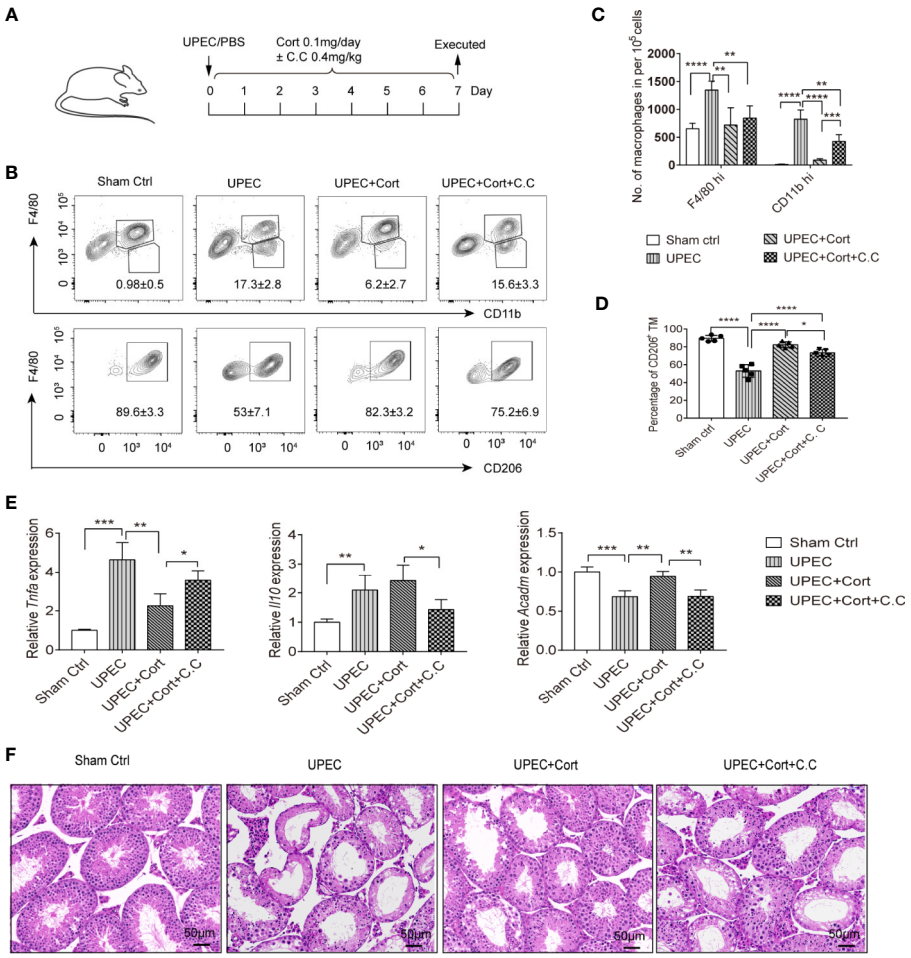

FIGURE 5 | Corticosterone treatment protects testis from UPEC-induced orchitis. **(A)** WT C57BL/6J mice were injected with saline or uropathogenic *Escherichia coli* into the vas deferens. Mice were then injected daily with corticosterone (0.1mg/day) ± Compound C (C.C, 0.4 mg/kg). Seven days post-infection mice were sacrificed and macrophage populations were measured in cells from testes by flow cytometry. Data are representative of two independent experiments. **(B)** Mean percentages of F4/80^{hi}CD11b^{lo} resident TM, F4/80^{lo}CD11b^{hi} monocyte-derived macrophages (upper panel) and the F4/80^{hi} CD206^{+} M2 TM (lower panel) in testes of the different treatment groups are presented. **(C)** The number of resident F4/80^{hi} macrophages and CD11b^{hi} monocyte-derived macrophages in testes of the different treatment groups is presented. **(D)** Percentage of CD206-expressing TM among F4/80^{hi}CD11b^{lo} resident macrophages in the different groups is shown; **(E)** TM were isolated and the relative expression of *Tnfa*, *Il10*, and *Acadm* were detected by RT-PCR. Mean ± SD; n = 5 for each group). The unpaired one-way ANOVA was employed for statistical analysis. *** $p < 0.001$, **$p < 0.01$, * $p < 0.01$. **(F)** Day 7 testicular tissue sections from each treatment group were stained with hematoxylin and eosin (magnification = 20× objective).

function. Moreover, corticosterone suppresses the pro-inflammatory response of BMDM, instead promoting IL-10 secretion in response to LPS. Similarly, *in vivo* in a UPEC elicited-orchitis mouse model, corticosterone treatment prevented UPEC-induced decreases in M2 TM and reduced tissue impairment in a partially AMPK-dependent manner. These findings highlight an important role for AMPK *in vivo* in TM, and demonstrate the therapeutic potential for corticosterone in maintaining the anti-inflammatory properties of TM and the immune privilege of the testis.

In previous studies in rats it was observed that TM play a crucial role in regulation of testicular inflammation by presenting an anti-inflammatory phenotype and secreting high amounts of IL-10 (10, 11). We further identified corticosterone as a main contributor to maintaining TM's immunosuppressive phenotype and function (10, 12). The anti-inflammatory function of corticosterone has been intensively investigated in many leucocytes, including macrophages, where it changes the phenotype and function of these cells (30). A recent study also showed that corticosterone attenuates LPS-induced inflammatory cytokine IL-1β secretion in BV2 mouse microglia-like cells (31), which occupy a similarly immune-privileged niche in the brain as TM do in the testis. However, until now the effects of corticosterone on murine TM and during testicular infection was unknown. It needs to be noted that isolated primary TM show a purity of approx. 80% and are

thus cautiously referred to as a TM enriched population with likely contaminants consisting of germ cells and Leydig cells that attach tightly to TM.

In this study, corticosterone treatment polarized BMDM towards a $F4/80^{+}CD206^{+}$ M2 anti-inflammatory phenotype with reduced TNF-α secretion and increased IL-10 production *in vitro*, similar to TM, suggesting a crucial role of corticosterone in mediating macrophage M2 polarization.

The underlying mechanism of corticosterone-mediated BMDM M2 polarization remained elusive. Recent advances in the immune-metabolism field have shown that the metabolic pathways and phenotypic polarization of macrophages are closely intertwined: macrophages can switch their phenotype and function by changing their metabolic pathways in response to the tissue microenvironment or upon encountering inflammatory cues (32, 33). Energy metabolism is not only a source of energy but also provides signals for macrophage polarization (17). Our study confirmed that, typically, M2 TM as well as corticosterone-polarized M2 BMDM showed increased FAO and decreased glycolysis, compared with M1 macrophage PM. Of note, we found that corticosterone upregulated expression of several FA metabolism-related genes in BMDM by activating AMPK, the master regulator of metabolism. The AMPK inhibitor Compound C reversed the anti-inflammatory property of corticosterone-polarized BMDM by inhibiting FAO. These results further confirmed that a switch of metabolic pathway can regulate macrophage phenotype and function and shed new light on the understanding of corticosterone-induced macrophage M2 polarization. However, how AMPK-mediates FA metabolism still needs further investigation.

Accumulating evidence has shown that AMPK activation exhibits anti-inflammatory features mainly by activating SIRT1 and PGC-1a, and by inhibiting several inflammatory pathways including NF-kB and AP-1 (34, 35). In rheumatoid arthritis, SIRT1/adenosine monophosphate enhances anti-inflammatory M2 macrophage polarization by activating AMPK signaling (36). Similarly, in this study we observed that corticosterone-mediated activation of AMPK polarized BMDM towards an immunosuppressive phenotype *in vitro* and supported maintenance of the M2 TM population *in vivo* under bacterial challenge. However, the mechanism of corticosterone-mediated AMPK activation is still not fully understood. In alignment with our findings, it has been recently reported that another glucocorticoid, dexamethasone, can improve therapeutic outcomes in a mouse model of UPEC-mediated epididymitis by inhibiting the immune response and tissue damage (37). Moreover, our *in vivo* data further demonstrated that corticosterone treatment ameliorates UPEC-elicited orchitis by increasing the percentage of M2 macrophages in the TM population; while Compound C treatment reduced the percentage of M2 macrophages, suggesting that the anti-inflammatory function of corticosterone depends at least partially on AMPK activation. In addition, corticosterone treatment significantly reduced the inflammatory $CD11b^{hi}$ monocytes population in the infected testis, and importantly, reduced inflammation-associated tissue damage.

Taken together, we have uncovered the underlying mechanisms of corticosterone-induced M2 BMDM polarization, in which AMPK activation-induced FAO plays a key role. We also evidence similar pathways in TM both *ex vivo* and *in vivo*, where corticosterone therapy ameliorated the tissue-damaging effects of UPEC-elicited orchitis by maintaining the population of M2 TM. Thus this work has uncovered key metabolic pathways and mediators underpinning the anti-inflammatory polarization of TM, and shed new light on the development of innovative therapeutics for orchitis patients.

DATA AVAILABILITY STATEMENT

The original contributions presented in the study are included in the article/**Supplementary Material**. Further inquiries can be directed to the corresponding authors.

ETHICS STATEMENT

The animal study was reviewed and approved by Ethics Committee of ZhengZhou University.

AUTHOR CONTRIBUTIONS

Conceptualization: SB, AM, and MW. Methodology: MW, ZZ, ZJ, YuZ, YiZ and YY. Formal analysis: MW, YY, and ZJ. Supervision and fund acquisition: MW, ZZ, and ZQ. Writing—review and editing: ZZ and MW. All authors contributed to the article and approved the submitted version.

ACKNOWLEDGMENTS

This work was financially supported by the National Natural Science Foundation of China (Grant No. 81901466 to MW, 81700609 to ZZ, and 81630068 to ZQ); Deutsche Forschungsgemeinschaft (DFG, Grant No. BH93/1-4 to SB) and Henan Science and Technology Foundation (Grant No. 2018020090). We acknowledge Lucy Robinson of Insight Editing London for assistance with manuscript editing.

SUPPLEMENTARY MATERIAL

The Supplementary Material for this article can be found online at: https://www.frontiersin.org/articles/10.3389/fimmu.2020.583276/full#supplementary-material

SUPPLEMENTARY FIGURE 1 | The purities of TM and PM were analyzed by flow cytometry. Isolated primary TM and PM were stained with anti-CD45, anti-F4/80, and anti-CD11b antibody, followed by FACS analysis. Representative plots are shown.

REFERENCES

1. Schuppe HC, Pilatz A, Hossain H, Diemer T, Wagenlehner F, Weidner W. Urogenital Infection as a Risk Factor for Male Infertility. *Dtsch Arztebl Int* (2017) 114(19):339–46. doi: 10.3238/arztebl.2017.0339
2. Isaiah IN, Nche BT, Nwagu IG, Nnanna II. Current studies on bacterospermia the leading cause of male infertility: a protégé and potential threat towards mans extinction. *N Am J Med Sci* (2011) 3(12):562–4. doi: 10.4297/najms.2011.3559
3. Head JR, Billingham RE. Immune privilege in the testis. II. Evaluation of potential local factors. *Transplantation* (1985) 40(3):269–75. doi: 10.1097/00007890-198509000-00010
4. Fijak M, Meinhardt A. The testis in immune privilege. *Immunol Rev* (2006) 213:66–81. doi: 10.1111/j.1600-065X.2006.00438.x
5. Schuppe HC, Meinhardt A. Immune privilege and inflammation of the testis. *Chem Immunol Allergy* (2005) 88:1–14. doi: 10.1159/000087816
6. Zhao S, Zhu W, Xue S, Han D. Testicular defense systems: immune privilege and innate immunity. *Cell Mol Immunol* (2014) 11(5):428–37. doi: 10.1038/cmi.2014.38
7. Li N, Wang T, Han D. Structural, cellular and molecular aspects of immune privilege in the testis. *Front Immunol* (2012) 3:152. doi: 10.3389/fimmu.2012.00152
8. Bhushan S, Meinhardt A. The macrophages in testis function. *J Reprod Immunol* (2017) 119:107–12. doi: 10.1016/j.jri.2016.06.008
9. Winnall WR, Hedger MP. Phenotypic and functional heterogeneity of the testicular macrophage population: a new regulatory model. *J Reprod Immunol* (2013) 97(2):147–58. doi: 10.1016/j.jri.2013.01.001
10. Bhushan S, Tchatalbachev S, Lu Y, Fröhlich S, Fijak M, Vijayan V, et al. Differential activation of inflammatory pathways in testicular macrophages provides a rationale for their subdued inflammatory capacity. *J Immunol* (2015) 194(11):5455–64. doi: 10.4049/jimmunol.1401132
11. Winnall WR, Muir JA, Hedger MP. Rat resident testicular macrophages have an alternatively activated phenotype and constitutively produce interleukin-10 in vitro. *J Leukoc Biol* (2011) 90(1):133–43. doi: 10.1189/jlb.1010557
12. Wang M, Fijak M, Hossain H, Markmann M, Nüsing RM, Lochnit G, et al. Characterization of the Micro-Environment of the Testis that Shapes the Phenotype and Function of Testicular Macrophages. *J Immunol* (2017) 198(11):4327–40. doi: 10.4049/jimmunol.1700162
13. Yang C, Nixon M, Kenyon CJ, Livingstone DE, Duffin R, Rossi AG, et al. 5α-reduced glucocorticoids exhibit dissociated anti-inflammatory and metabolic effects. *Br J Pharmacol* (2011) 164(6):1661–71. doi: 10.1111/j.1476-5381.2011.01465.x
14. Wei B, Zhu Z, Xiang M, Song L, Guo W, Lin H, et al. Corticosterone suppresses IL-1β-induced mPGE2 expression through regulation of the 11β-HSD1 bioactivity of synovial fibroblasts in vitro. *Exp Ther Med* (2017) 13(5):2161–8. doi: 10.3892/etm.2017.4238
15. Slominski RM, Tuckey RC, Manna PR, Jetten AM, Postlethwaite A, Raman C, et al. Extra-adrenal glucocorticoid biosynthesis: implications for autoimmune and inflammatory disorders. *Genes Immun* (2020) 21(3):150–68. doi: 10.1038/s41435-020-0096-6
16. Ahmed A, Schmidt C, Brunner T. Extra-Adrenal Glucocorticoid Synthesis in the Intestinal Mucosa: Between Immune Homeostasis and Immune Escape. *Front Immunol* (2019) 10:1438. doi: 10.3389/fimmu.2019.01438
17. Thapa B, Lee K. Metabolic influence on macrophage polarization and pathogenesis. *BMB Rep* (2019) 52(6):360–72. doi: 10.5483/BMBRep.2019.52.6.140
18. Galván-Peña S, O'Neill LA. Metabolic reprograming in macrophage polarization. *Front Immunol* (2014) 5:420. doi: 10.3389/fimmu.2014.00420
19. Orecchioni M, Ghosheh Y, Pramod AB, Ley K. Macrophage Polarization: Different Gene Signatures in M1(LPS+) vs. Classically and M2(LPS-) vs. Alternatively Activated Macrophages. *Front Immunol* (2019) 10:1084. doi: 10.3389/fimmu.2019.01084
20. Vats D, Mukundan L, Odegaard JI, Zhang L, Smith KL, Morel CR, et al. Oxidative metabolism and PGC-1beta attenuate macrophage-mediated inflammation. *Cell Metab* (2006) 4(1):13–24. doi: 10.1016/j.cmet.2006.05.011
21. Herzig S, Shaw RJ. AMPK: guardian of metabolism and mitochondrial homeostasis. *Nat Rev Mol Cell Biol* (2018) 19(2):121–35. doi: 10.1038/nrm.2017.95
22. Ma A, Wang J, Yang L, An Y, Zhu H. AMPK activation enhances the anti-atherogenic effects of high density lipoproteins in apoE(-/-) mice. *J Lipid Res* (2017) 58(8):1536–47. doi: 10.1194/jlr.M073270
23. Sun X, Luo W, Tan X, Li Q, Zhao Y, Zhong W, et al. Increased plasma corticosterone contributes to the development of alcoholic fatty liver in mice. *Am J Physiol Gastrointest Liver Physiol* (2013) 305(11):G849–61. doi: 10.1152/ajpgi.00139.2013
24. Klein B, Bhushan S, Günther S, Middendorff R, Loveland KL, Hedger MP, et al. Differential tissue-specific damage caused by bacterial epididymo-orchitis in the mouse. *Mol Hum Reprod* (2020) 26(4):215–27. doi: 10.1093/molehr/gaaa011
25. Mossadegh-Keller N, Sieweke MH. Characterization of Mouse Adult Testicular Macrophage Populations by Immunofluorescence Imaging and Flow Cytometry. *Bio Protoc* (2019) 9(5):e3178. doi: 10.21769/BioProtoc.3178
26. Zhang X, Goncalves R, Mosser DM. The isolation and characterization of murine macrophages. *Curr Protoc Immunol* (2008). Chapter 14(83):14.1.1–14. doi: 10.1002/0471142735.im1401s83
27. Hayes R, Chalmers SA, Nikolic-Paterson DJ, Atkins RC, Hedger MP. Secretion of bioactive interleukin 1 by rat testicular macrophages in vitro. *J Androl* (1996) 17(1):41–9. doi: 10.1002/j.1939-4640.1996.tb00585.x
28. Trotta AP, Gelles JD, Serasinghe MN, Loi P, Arbiser JL, Chipuk JE. Disruption of mitochondrial electron transport chain function potentiates the pro-apoptotic effects of MAPK inhibition. *J Biol Chem* (2017) 292(28):11727–39. doi: 10.1074/jbc.M117.786442
29. Sag D, Carling D, Stout RD, Suttles J. Adenosine 5'-monophosphate-activated protein kinase promotes macrophage polarization to an anti-inflammatory functional phenotype. *J Immunol* (2008) 181(12):8633–41. doi: 10.4049/jimmunol.181.12.8633
30. Meinhardt A, Wang M, Schulz C, Bhushan S. Microenvironmental signals govern the cellular identity of testicular macrophages. *J Leukoc Biol* (2018) 104(4):757–66. doi: 10.1002/JLB.3MR0318-086RR
31. Liu J, Mustafa S, Barratt DT, Hutchinson MR. Corticosterone Preexposure Increases NF-κB Translocation and Sensitizes IL-1β Responses in BV2 Microglia-Like Cells. *Front Immunol* (2018) 9:3. doi: 10.3389/fimmu.2018.00003
32. Hobson-Gutierrez SA, Carmona-Fontaine C. The metabolic axis of macrophage and immune cell polarization. *Dis Model Mech* (2018) 11(8):dmm034462. doi: 10.1242/dmm.034462
33. Koo SJ, Garg NJ. Metabolic programming of macrophage functions and pathogens control. *Redox Biol* (2019) 24:101198. doi: 10.1016/j.redox.2019.101198
34. Cantó C, Auwerx J. PGC-1alpha, SIRT1 and AMPK, an energy sensing network that controls energy expenditure. *Curr Opin Lipidol* (2009) 20(2):98–105. doi: 10.1097/MOL.0b013e328328d0a4
35. Salminen A, Hyttinen JM, Kaarniranta K. AMP-activated protein kinase inhibits NF-κB signaling and inflammation: impact on healthspan and lifespan. *J Mol Med (Berl)* (2011) 89(7):667–76. doi: 10.1007/s00109-011-0748-0
36. Park SY, Lee SW, Lee SY, Hong KW, Bae SS, Kim K, et al. SIRT1/Adenosine Monophosphate-Activated Protein Kinase α Signaling Enhances Macrophage Polarization to an Anti-inflammatory Phenotype in Rheumatoid Arthritis. *Front Immunol* (2017) 8:1135. doi: 10.3389/fimmu.2017.01135
37. Klein B, Pant S, Bhushan S, Kautz J, Rudat C, Kispert A, et al. Dexamethasone improves therapeutic outcomes in a preclinical bacterial epididymitis mouse model. *Hum Reprod* (2019) 34(7):1195–205. doi: 10.1093/humrep/dez073

Conflict of Interest: The authors declare that the research was conducted in the absence of any commercial or financial relationships that could be construed as a potential conflict of interest.

frontiers in Immunology

ORIGINAL RESEARCH
published: 19 February 2021
doi: 10.3389/fimmu.2021.582858

Uropathogenic *Escherichia coli* Infection Compromises the Blood-Testis Barrier by Disturbing mTORC1-mTORC2 Balance

Yongning Lu[1]*, *Miao Liu*[1], *Nicholas J. Tursi*[2], *Bin Yan*[1], *Xiang Cao*[1], *Qi Che*[1], *Nianqin Yang*[1]* and *Xi Dong*[1]

[1] Reproductive Medicine Centre, Zhongshan Hospital, Fudan University, Shanghai, China, [2] Department of Biology, University of Pennsylvania, Philadelphia, PA, United States

OPEN ACCESS

Edited by:
Daishu Han,
Chinese Academy of Medical Sciences and Peking Union Medical College, China

Reviewed by:
Wing-Yee Lui,
The University of Hong Kong, Hong Kong
Marco G. Alves,
Independent Researcher, Porto, Portugal

***Correspondence:**
Yongning Lu
yongninglu1981@126.com
Nianqin Yang
yang.nianqin@zs-hospital.sh.cn

Specialty section:
This article was submitted to Mucosal Immunity, a section of the journal Frontiers in Immunology

Received: 13 July 2020
Accepted: 19 January 2021
Published: 19 February 2021

Citation:
Lu Y, Liu M, Tursi NJ, Yan B, Cao X, Che Q, Yang N and Dong X (2021) Uropathogenic Escherichia coli Infection Compromises the Blood-Testis Barrier by Disturbing mTORC1-mTORC2 Balance. Front. Immunol. 12:582858. doi: 10.3389/fimmu.2021.582858

The structural and functional destruction of the blood-testis barrier (BTB) following uropathogenic *E. coli* (UPEC) infection may be a critical component of the pathologic progress of orchitis. Recent findings indicate that the mammalian target of the rapamycin (mTOR)-signaling pathway is implicated in the regulation of BTB assembly and restructuring. To explore the mechanisms underlying BTB damage induced by UPEC infection, we analyzed BTB integrity and the involvement of the mTOR-signaling pathway using *in vivo* and *in vitro* UPEC-infection models. We initially confirmed that soluble virulent factors secreted from UPEC trigger a stress response in Sertoli cells and disturb adjacent cell junctions *via* down-regulation of junctional proteins, including occludin, zonula occludens-1 (ZO-1), F-actin, connexin-43 (CX-43), β-catenin, and N-cadherin. The BTB was ultimately disrupted in UPEC-infected rat testes, and blood samples from UPEC-induced orchitis in these animals were positive for anti-sperm antibodies. Furthermore, we herein also demonstrated that mTOR complex 1 (mTORC1) over-activation and mTORC2 suppression contributed to the disturbance in the balance between BTB "opening" and "closing." More importantly, rapamycin (a specific mTORC1 inhibitor) significantly restored the expression of cell-junction proteins and exerted a protective effect on the BTB during UPEC infection. We further confirmed that short-term treatment with rapamycin did not aggravate spermatogenic degeneration in infected rats. Collectively, this study showed an association between abnormal activation of the mTOR-signaling pathway and BTB impairment during UPEC-induced orchitis, which may provide new insights into a potential treatment strategy for testicular infection.

Keywords: blood-testis barrier, uropathogenic *E. coli*, orchitis, mammalian target of rapamycin, male infertility

INTRODUCTION

Approximately 6% to 15% of male infertility is attributed to infections or inflammation of the urogenital tract (1). Compared with the impacts of urethritis and prostatitis, the sequelae of epididymitis or orchitis are more likely to result in reduced fertility—as spermatogenetic, sperm maturational, and storage microenvironments may be directly exposed to pathogens and inflammatory products. Uropathogenic *Escherichia coli* (UPEC) is one of the major pathogens involved in ascending, non-sexually transmitted epididymo-orchitis (2–4). The elimination of invading pathogens by antibiotic administration is currently the major standardized therapy prescribed in acute bacterial epididymo-orchitis (4–6). Unfortunately, in most cases antibiotic treatment alone cannot guarantee the full restoration of fertility due to permanent tissue damage or immunologic impairment within these organs (2, 6, 7). A better understanding of the mechanisms by which uropathogen-related orchitis disturbs testes functions may assist clinicians in developing better treatment strategies for fertility protection.

Investigations into the immunopathological mechanisms implicated in orchitis are particularly noteworthy considering the role of testicular immune privilege with respect to spermatogenic conservation. The blood-testis barrier (BTB) is one of the most well studied functional tissue barriers, and contributes to maintaining the special immune microenvironment in the testis (8, 9). This barrier is located at the interface of juxtaposed Sertoli cells, and is comprised of multiple junctional complexes—including tight junctions (TJs), gap junctions, adhesion junctions, and desmosomes (10, 11). The BTB sequesters meiotic spermatocytes and antigen-expressing, post-meiotic spermatids away from the immune system (10). Despite being one of the tightest blood-tissue barriers, the BTB undergoes restructuring during stage VIII-XI of the seminiferous epithelial cycle to support preleptotene spermatocytes that transit through this barrier (9, 12). In this process, a "new" BTB is assembled behind the transiting spermatocytes while the "old" BTB noted above is disassembled (10). The remodeling mechanisms of the BTB guarantee immunologic barrier integrity and prevent the development of autoimmune responses against germ cells.

Although the BTB restructuring mechanism has yet to be fully understood, accumulating evidence suggests that the mammalian target of rapamycin (mTOR) contributes to the regulation of this physiologic process during the epithelial cycle of spermatogenesis (13, 14). Two functionally and structurally distinct mTOR-signaling complexes (mTOR complex 1 [mTORC1] and 2 [mTORC2]) are formed depending upon whether their partner proteins Raptor (regulatory-associated protein of mTOR) or Rictor (rapamycin-insensitive companion of mTOR) combine with the core component (15). These two mTOR complexes exert their antagonistic effects to facilitate the transition of preleptotene spermatocytes across this immunologic barrier, as well as to maintain structural and functional integrity of the BTB. Recent evidence also indicates that mTORC1 promotes BTB disassembly by inducing redistribution and endocytosis of junctional proteins (16, 17). Conversely, mTORC2 contributes to the maintenance of BTB integrity and the assembly of a "new" barrier (18). A delicate mTORC1-mTORC2 balance is thus critical for the preservation of BTB function. In the context of pathologic situations, it was found that viral infection or inflammation caused BTB impairment by triggering the release of cytokines, such as TNF-α, and activating inflammatory-signaling pathways, including the p38 mitogen-activated protein (MAP) kinase pathway (19, 20). However, the role of the mTOR pathway remains arcane with respect to potential alterations of the BTB during bacterially-induced orchitis.

Using *in vivo* and *in vitro* infection models, our previous studies showed that the inflammatory response in the testis and damage to the Sertoli cells was caused by UPEC. In the present study, we further elucidated the dynamic alterations of the BTB in UPEC-induced orchitis and explored the possibility of preserving BTB structure and function by manipulating the balance between mTORC1 and mTORC2.

MATERIALS AND METHODS

Bacterial Propagation and Preparation of Culture Supernatant

The uropathogenic *Escherichia coli* (UPEC) strain CFT073 was purchased from American Type Culture Collection (ATCC, Gaithersburg, Maryland, USA) and propagated as previously described (21). UPEC was propagated overnight on agar plates. A single bacterial clone was then inoculated in lysogeny broth (LB) agar medium until grown to early exponential phase (OD600 = 0.4~0.8) at 37°C in a shaking incubator. The viable bacterial concentration was estimated using standard growth curves. Bacteria were centrifuged at 4500×g for 8 min at room temperature and the pellet was washed once with PBS and resuspended in DMEM/F12 medium or sterile saline. The concentrated bacterial suspension was then adjusted to 1×10^9 colony-forming units (CFU) per milliliter. For *in vivo* experiments, the bacterial suspension was diluted with sterile saline to achieve 1×10^6 CFU of bacteria in 100 µl. For Sertoli cell *in vitro* stimulation, the bacterial suspension was subsequently centrifuged at 4500×g for 10 minutes, and the collected supernatant was ultimately filtered with 0.1-µm filters before use.

Rat Orchitis Model

All experiments were approved by the Ethical Committee of Zhongshan Hospital and performed in accordance with the Guide for the Care and Use of Laboratory Animals. Nine-week-old male Sprague-Dawley (SD) rats were purchased from CAVENS (Changzhou, Jiangsu, China) and housed in 12 h light/12 h dark standard conditions, with water and food provided *ad libitum* for at least 1 week prior to experimentation. The orchitis model was modified on the basis of previous studies (21). Adult rats (270–300 g) were injected intramuscularly with Zoletil™ 20 (Virbac, Carros, France; 50 mg/kg of body weight) for anesthetization. Fifty microliters of UPEC bacterial suspension per side (0.5×10^6 CFU) was percutaneously injected into both testes of rats in the infected groups using 30-gauge needles. The

same volume of 0.9% saline was applied as a control. In the rapamycin-treated groups, different doses of rapamycin (2, 5, or 10 mg/kg/day) were administrated intraperitoneally on day 7 post infection for seven days based on a previous report (22). The remaining infected rats received the same amount of vehicle (5% ethanol +5% PEG 400 + 5% Tween 80 + 85% saline) as the vehicle-treated group. Euthanasia of animals was conducted at certain time-points. After recording body and testis weights, serum, and testes were collected for further experiments. In each group there were 12 (control group)–15 (infected and rapamycin-treated groups) rats used for all experiments. The bilateral testes from six animals in each group were fixed for transmission electron microscopy and paraffin-section assessments. The testes of the remaining animals were assigned for biotin assay, frozen sections, and western blotting analysis. For the biotin penetration assay, 100 µl of EZ-Link™ sulfo-NHS-LC-biotin was loaded into the testes and organs were harvested as described in the literature (23). Rats that were intraperitoneally (i.p.) injected with $CdCl_2$ (3 mg/kg body weight) served as positive controls, and testes were collected after three days.

Sertoli Cell Culture and Treatment With Bacterial Supernatants

The mouse Sertoli cell line TM4 was purchased from ATCC and cultured in complete growth medium according to ATCC instructions. Primary Sertoli cells were isolated from the testes of 4-week-old male Sprague-Dawley (SD) rats as previously described (24). The purity of the Sertoli cells was determined to be >95% by immunofluorescence evaluation using antibodies against vimentin (**Supplementary Figure 1**). Sertoli cells were cultured in serum-free DMEM/F12 (ThermoFisher Scientific, Asheville, NC, USA) supplemented with penicillin/streptomycin. In the infected groups, Sertoli cells were exposed to different amounts of filtered UPEC supernatant (40 or 60 µl per 200 µl of culture medium) with or without rapamycin (Selleckchem, Houston, TX, USA) and cultured for 24 or 40 hours. Rapamycin dissolved in DMSO (at a storage concentration of 10 mM) was used to treat cells at a final concentration of 0.1 nM or 0.1 µM based on a previous report (17, 25) and our pilot study. Culture medium was replaced every 10–12 hours.

Detection of Anti-Sperm Antibodies

Serum samples were collected from animals at 3 months post infection and sperm-bound total immunoglobulins were detected using an ELISA kit (BIOSH Biotechnology Limited Company, Shanghai, China), following the manufacturer's instructions. Fifty microliters of each serum sample—as well as positive/negative control solutions provided in the kit—was added to a 96-well assay plate coated with specific capture antigens for anti-sperm antibodies and incubated for 30 minutes. Horseradish peroxidase (HRP)-conjugated detection antibody was subsequently added and tetramethylbenzidine served as the substrate. We detected the optical density (OD) at a wavelength of 450 nm using a microplate reader (ThermoFisher Scientific, Asheville, NC, USA).

Electron Microscopy

To reveal changes in BTB ultrastructure after infection, 1 mm^3 of testicular tissues were fixed in 2.5% glutaraldehyde/0.1 M sodium phosphate (pH, 7.35) and ultra-thin sections (70 nm) were prepared for subsequent evaluation using transmission electron microscopy (HITACHI HT7800, TOKYO, Japan) at 80 kV. The connections between cultured TM4 cells were observed with scanning electron microscopy (SEM) using cells fixed on glass coverslips.

Histologic Assessment of the Testes

For assessment of testicular histopathology, sections (4 µm in thickness) of modified Davidson's fluid-fixed and paraffin-embedded testis were stained with hematoxylin and eosin as previously described (21). Three sections from different regions of each testis were then used for histopathologic evaluation. The percentage of abnormal seminiferous tubules in cross sections was calculated by assessing over 200 tubules in each testis.

Immunofluorescence Staining

Frozen-tissue sections of testes (8 µm in thickness) and Sertoli cells grown on glass coverslips were fixed with ice-cold methanol and permeabilized with 0.1% Triton-X 100. Immunofluorescence analyses were performed as described by Bhushan et al (24). Sections of testes were blocked with 5% BSA +5% goat serum for 1 hour at room temperature. Primary antibodies were incubated at 4°C overnight, followed by rinsing 3 times with Tris-buffered saline (TBS). Incubation with anti-rabbit or anti-mouse secondary antibody was performed in the dark for 1 hour, and CoraLite®594-conjugated phalloidin was applied to identify F-actin filaments. Slides were mounted with antifade mounting medium using Hoechst 33342 (P0133, Beyotime Biotechnology, Shanghai, China) for nuclear staining prior to assessment with an inverted laser scanning confocal microscope (TiE-A1 plus, Nikon-instruments, Tokyo Metropolis, Japan). The list of antibodies used is provided in the **Supplementary Materials**.

Western Immunoblotting Analysis

Different groups of Sertoli cells and testicular tissue homogenates were lysed with RIPA buffer (P0013B, Beyotime Institute of Biotechnology, Shanghai, China) supplemented with a proteinase-inhibitor cocktail (Roche, Basel, Switzerland). Thirty micrograms of protein from each sample was resolved using 4–12% or 8% SDS-PAGE and subsequently transferred onto 0.22-µm PVDF membranes (at 200 mA for 3.5 hours). The nonspecific binding sites were blocked by incubating the membranes in 5% BSA in TBS with 0.1% Tween (TBS-T) for 1 hour. The membranes were subsequently incubated with primary antibodies in blocking solution overnight at 4°C and then rinsed 3 times with TBS-T. Membranes were ultimately incubated for 1 hour with anti-mouse or anti-rabbit antibody conjugated with HRP and then rinsed 3 times with TBS-T. Protein expression was measured as previously reported (24). The antibodies used are listed in the **Supplementary Materials**. ImageJ (https://imagej.nih.gov) was used to quantify the intensity of bands after western blotting. Uncropped original

figures of all blots shown in this manuscript are presented in **Supplementary PowerPoint**.

Statistical Analysis

Measurement data are presented as mean ± standard deviation (SD), and statistical significance between/among groups was analyzed using Student's *t* test, one-way ANOVA, or Mann–Whitney U test (2-sided). Differences were considered to be statistically significant when $p<0.05$ (we used $^{*}p<0.05$, $^{**}p<0.01$, and $^{***}p<0.001$).

RESULTS

BTB Alterations and Anti-Sperm Antibody Detection in UPEC-Infected Rats

Our previous study indicated that the BTB appeared to remain functionally intact 7 days post-UPEC infection (21). However, the long-term effects of bacterial invasion on the BTB and the testicular immune microenvironment are still largely unknown. To further elucidate the possible changes of the BTB in orchitis-model rats over time, we first investigated alterations in BTB ultrastructure at different time-points within 1-month after infection (**Figure 1A**). In control rat testes (**Figure 1A-1**), tight junctions (TJ, indicated by white arrow), bundles of F-actin filaments (black arrowhead), and endoplasmic reticulum (ER, black arrow) in adjoining Sertoli cells were readily identified. There was no significant abnormality in TJs in the first few days after bacterial injection (**Figure 1A-2**), although actin filaments and ER became less distinct. As time passed, the structure of the TJs turned more obscure by Day 7 (**Figure 1A-3**) and even more indistinguishable at Days 14 and 30 (**Figures 1A-4, 5**). Moreover, the anti-sperm antibody showed positivity in infected animals three months after UPEC injection (**Figure 1B**). Collectively, our present findings provide a more complete observation on the dynamic alterations in BTB ultrastructure, suggesting that UPEC infection disturbed testicular immune privilege.

The Expression of Sertoli Cell Junctional Proteins Decreases in the Testes of Orchitis-Model Rats

The BTB is composed of a series of junctional complexes between adjacent Sertoli cells—including tight junctions, gap junctions, basal ectoplasmic specialization (ES, a testis-specific actin-rich adhesion junction), and desmosomes. To further investigate the impact of UPEC infection on the BTB, we evaluated the expression patterns of Sertoli cell junctional proteins at different time-points post infection using immunofluorescence staining (**Figure 2**). Occludin, one of the tight-junction proteins, was observed between neighboring Sertoli cells and germ cells in control testes. However, occludin expression was significantly decreased from day 3 after infection,

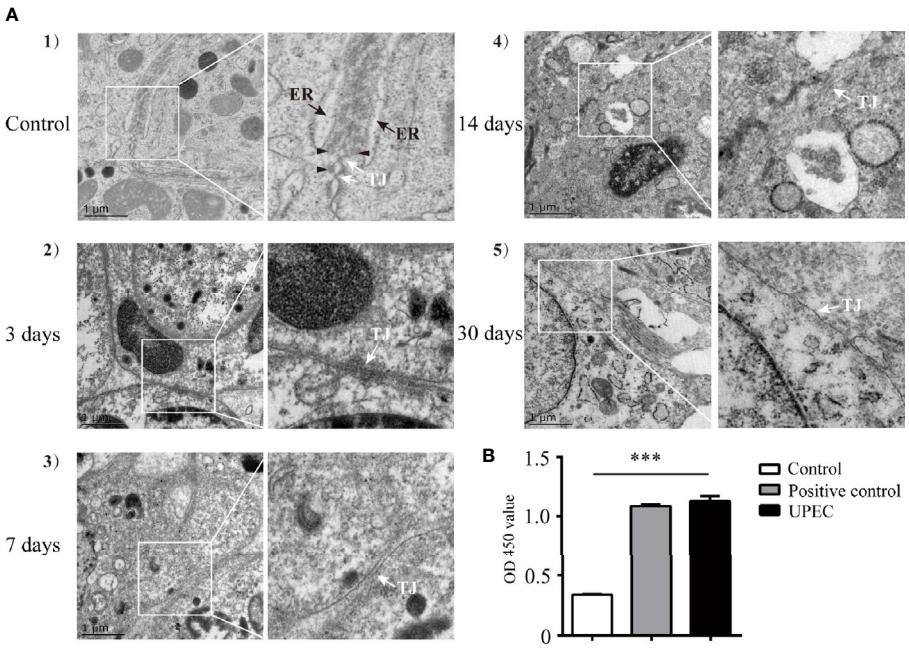

FIGURE 1 | UPEC infection disrupts BTB structure and results in an elevation of serum anti-sperm antibodies in an orchitis rat model. A bacterial suspension (0.5×10^6 CFU/50 μl) or 50 μl of saline was bilaterally injected into testes of 10–11-week-old SD rats. **(A)** Animals were sacrificed at the indicated time-points and BTB structure in the testis was observed using TEM. Scale bar, 1 μm. White arrow, TJ (tight junction); black arrow, ER (endoplasmic reticulum); black arrowhead, F-actin bundles. The photographs in the right column are the enlarged images of the white box regions. **(B)** Serum samples were collected from rats after three months, and anti-sperm antibodies in serum were detected with ELISA kits. Histograms show quantitative results, and *p* value was determined with ANOVA; $^{***}p<0.001$.

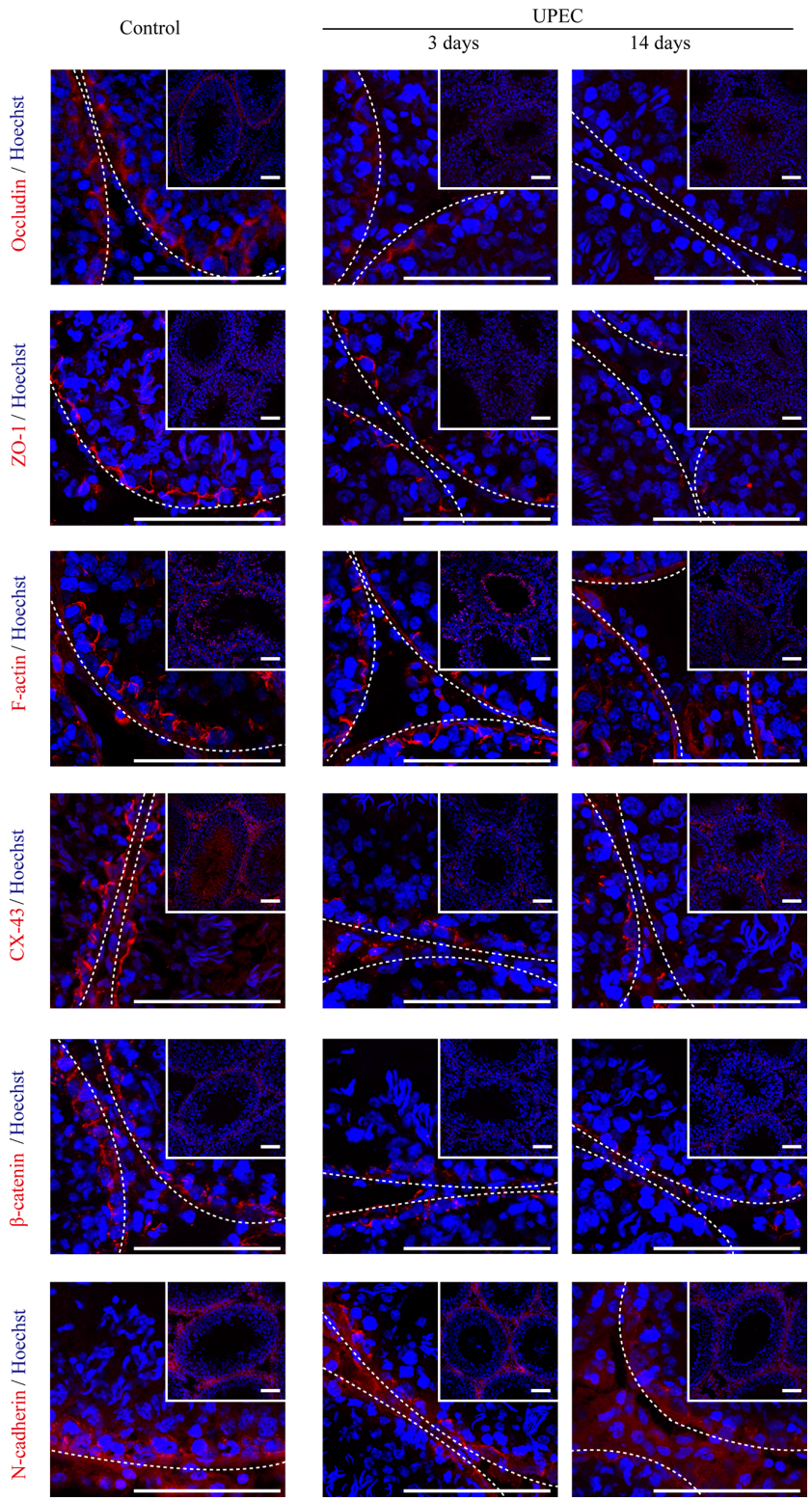

FIGURE 2 | UPEC infection down-regulates the expression of cell-junction proteins in the testes of orchitis-model rats. In the orchitis model, rats were sacrificed at the indicated times, and we evaluated the expression of cell-junction proteins in seminiferous epithelium using immunofluorescence staining under an inverted laser scanning confocal microscope. Red, cell-junction proteins; blue, Hoechst 33342 nuclear staining. The images in the insets are the same testes cross-sections at lower magnification (scale bar, 100 μm). The white broken lines indicate the relative location of the basement membrane adjacent to the BTB of the seminiferous tubules.

continually declined at later time-points, and was barely detectable in affected seminiferous tubules on day 14. A similar time-dependent pattern of decreasing expression was found for tight junction adaptor protein zonula occludens-1 (ZO-1), the cell-skeleton protein filamentous actin (F-actin), gap junction protein connexin-43 (CX-43), and adhesion junction proteins (β-catenin and N-cadherin). These results confirmed that UPEC infection induced extensive down-regulation of a variety of BTB constituent proteins in the testis of rats induced with orchitis.

UPEC Bacterial Supernatant Disrupts Connections Between Sertoli cells and Down-regulates the Expression of Cell Junctional Proteins

To verify the influence of UPEC infection on the connections between Sertoli cells, we treated primary Sertoli cells and the Sertoli cell line TM4 with UPEC culture supernatant (**Figure 3**). Although adjacent TM4 cells were observed to be closely attached to each other in the control group using SEM, cells became more and more dissociated after bacterial supernatant stimulation in a dose- and time-dependent manner (**Figure 3A**). In an *in vitro* culture system of primary Sertoli cells, we evaluated the expression of occludin, ZO-1, and F-actin. Similar to what we observed in orchitis-model rat testes, the expression of these 2 cell-junction proteins was markedly diminished in primary Sertoli cells treated with a low dose of UPEC supernatant for 40 hours (**Figures 3B, C**); the down-regulation of junctional proteins was even more significant when the dose was increased. The density of the F-actin network (which was stained with CoraLite®594-conjugated phalloidin) was found to be negligible and disorganized in infected primary Sertoli cells. Collectively, our findings using *in vivo* and *in vitro* models provided compelling evidence that indicated that UPEC infection decreased Sertoli cell junctional protein expression and eventually undermined the BTB.

mTORC1-mTORC2 Balance Is Disturbed in Infected Sertoli Cells

Recent studies suggest that the balance between mTORC1 and mTORC2 plays a pivotal role in the regulation of BTB dynamics (13, 26). We thus investigated the impact of UPEC infection on the mTOR-signaling pathway using an *in vitro* model. In primary Sertoli cells treated with UPEC bacterial culture supernatant, we observed increased phosphorylation of both

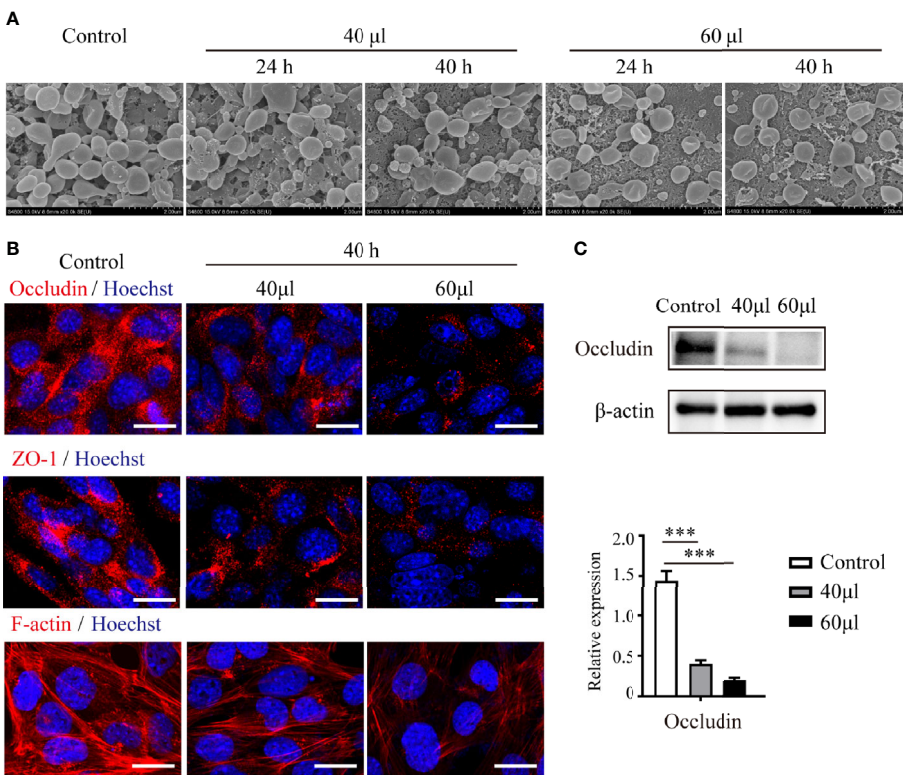

FIGURE 3 | UPEC-secreted virulence factors in cell culture supernatant disturb Sertoli cell connections and down-regulate the expression of cell-junction proteins. Sertoli cells treated with the indicated amounts of supernatant from UPEC bacterial cultures for 24 or 40 hours. **(A)** TM4 cellular connections were observed using SEM. Scale bar, 2 μm. **(B)** Expression of cell-junction proteins in primary Sertoli cells were evaluated using immunofluorescence and observed under confocal microscopy. Scale bar, 20 μm. **(C)** The expression levels of occludin in primary Sertoli cells were evaluated using immunoblotting analysis, and representative blots are depicted. Data are presented as mean ± SD from triplicate experiments. Histograms shows quantitative results and *p* values were determined by ANOVA; ***p < 0.001.

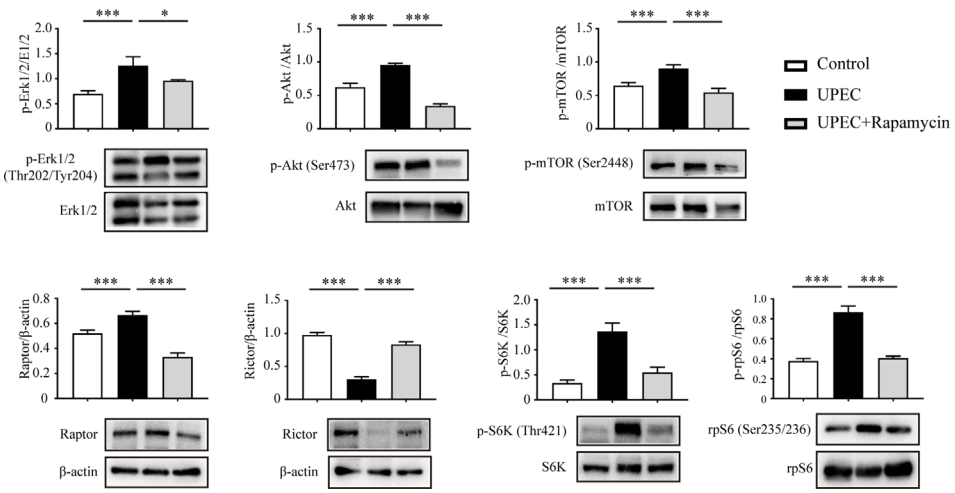

FIGURE 4 | UPEC-derived soluble virulence factors activate the mTORC1-signaling pathway and disturb mTORC1-mTORC2 balance. Primary Sertoli cells were treated with UPEC culture supernatant for 40 hours, with either vehicle solution (UPEC) or with 0.1 μM rapamycin as supplement (UPEC + rapamycin). We extracted proteins in RIPA buffer and determined expression levels using western blotting analysis. Representative blots are shown. Data are presented as mean ± SD from triplicate experiments. Histograms show quantitative results, and *p* value was determined by ANOVA; $^{*}p < 0.05$, $^{***}p < 0.001$.

Erk1/2 and Akt (**Figure 4**), which are the upstream enzymes regulating the mTORC1 pathway (27, 28). Consequently, we found mTORC1 activation as indicated by the phosphorylation of mTOR Ser2448, as well as the upregulation of Raptor, whereas the key component of mTORC2—Rictor—was accordingly downregulated by approximately 70% in Sertoli cells treated with bacterial culture supernatant. P70 ribosomal S6 kinase (S6K)—the downstream substrate of mTORC1—was subsequently activated and, consequently, the phosphorylation of the S6K substrate—S6 ribosomal protein (rpS6)—was also significantly increased. Significantly, each of the changes observed in the investigated signaling pathways was abolished by rapamycin treatment. These findings suggest that mTORC1 was over-activated while mTORC2 was suppressed in Sertoli cells during UPEC infection.

Rapamycin Partially Rescues the Down-regulation of Cell Junctional Proteins in Infected Sertoli Cells

Considering the role of mTOR signaling on BTB regulation, we next evaluated the possibility of restoring the mTORC1-mTORC2 balance and the expression of junctional proteins in Sertoli cells using the mTORC1-specific inhibitor rapamycin (**Figure 5**). Consistent with the above findings using immunoblotting, it was confirmed in infected Sertoli cells *via* immunofluorescence that Raptor and Rictor were upregulated and downregulated, respectively. Of note, these impacts were abolished by administering a rapamycin supplement (**Figure 5A**) that induced the suppression of mTORC1 and reactivation of mTORC2. Importantly, the administration of rapamycin partially restored the expression and distribution of cell-junction proteins that we observed in primary Sertoli cells (**Figures 5B, C**). These findings further suggested an mTORC1-mTORC2 imbalance may contribute to the disruption of Sertoli cell connections caused by UPEC infection.

The Expression of Sertoli Cell Junctional Proteins Is Restored by Rapamycin in Orchitis-Model Rats

To assess the *in vivo* effectiveness of rapamycin treatment on restoring Sertoli cell junctional proteins, we administrated rapamycin (5 mg/kg/day) daily from day 7 onward for one extra week in UPEC-infected rats. Animals were sacrificed on day 14 and sections of rat testes were collected (as described in Materials and Methods). We determined the expression of a series of cell-junction proteins on frozen sections of testes using immunofluorescence (**Figure 6A**) and, similar to the results observed through *in vitro* experiments, each of these proteins were down-regulated by approximately 30–50% in UPEC-infected rats. Notably, the expression of selected cell-junction proteins rebounded moderately after one week of rapamycin treatment. Similar results were further confirmed by immunoblotting analysis using total testicular tissue proteins (**Figure 6B**). These data confirmed that rapamycin partially restored the expression of BTB proteins after UPEC infection.

Rapamycin Treatment Partially Reinforces BTB Integrity in Infected Rats Without Additional Spermatogenic Disruption

To further investigate the potential value of rapamycin treatment in BTB maintenance in rats with orchitis, BTB integrity was evaluated using a biotin-infiltration assessment (**Figures 7A, B**). The testes of $CdCl_2$-treated rats served as positive controls since this chemical is known to cause irreversible disruption of the

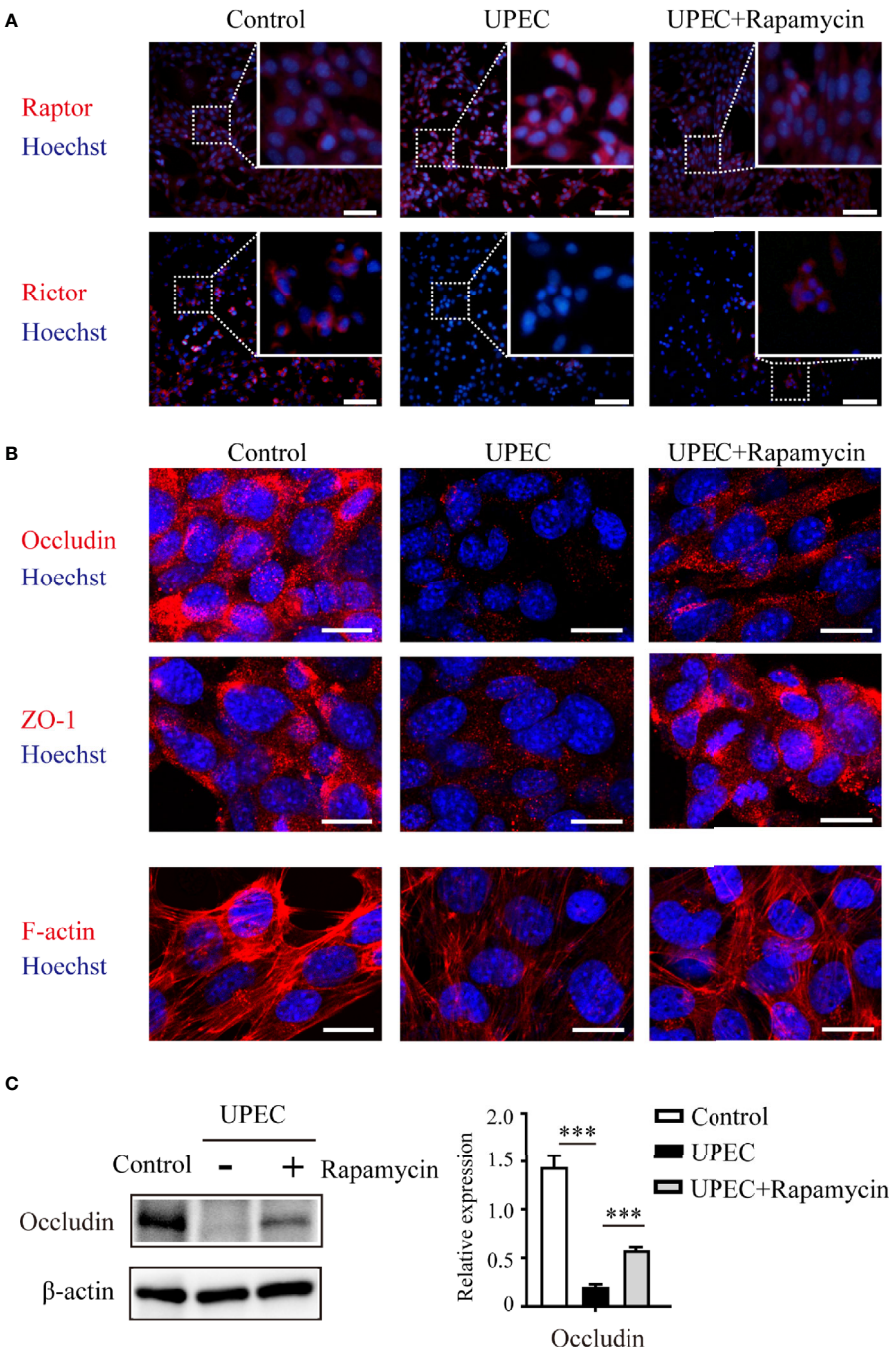

FIGURE 5 | Rapamycin restores mTORC1-mTORC2 balance and rescues UPEC-induced down-regulation of cell-junction proteins in Sertoli cells. Primary Sertoli cells were treated with UPEC culture supernatant for 40 hours with vehicle solution (UPEC) or with 0.1 μM rapamycin supplement (UPEC+Rapamycin). Expression of Raptor and Rictor **(A)**, as well as cell-junction proteins **(B)**, was evaluated using immunofluorescence staining. Scale bars: **(A)** 50 μm, **(B)** 20 μm. **(C)** The occludin expression levels in Sertoli cells were further confirmed using western blotting, and representative blots are shown. Data are presented as mean ± SD from triplicate experiments. Histograms show quantitative results, and *p* value was determined by ANOVA; ***$p < 0.001$.

BTB (29). In the saline-injected control group, the BTB remained intact as biotin migration was restricted to the basement membrane instead of penetrating into the abluminal compartment. In contrast, the BTB was completely compromised in the testes of $CdCl_2$-treated animals as indicated by the infiltration of biotin into the lumen of the seminiferous tubules. Similarly, BTB integrity was also greatly abolished in UPEC-infected rat testes, with biotin freely penetrating across the abluminal compartment in a

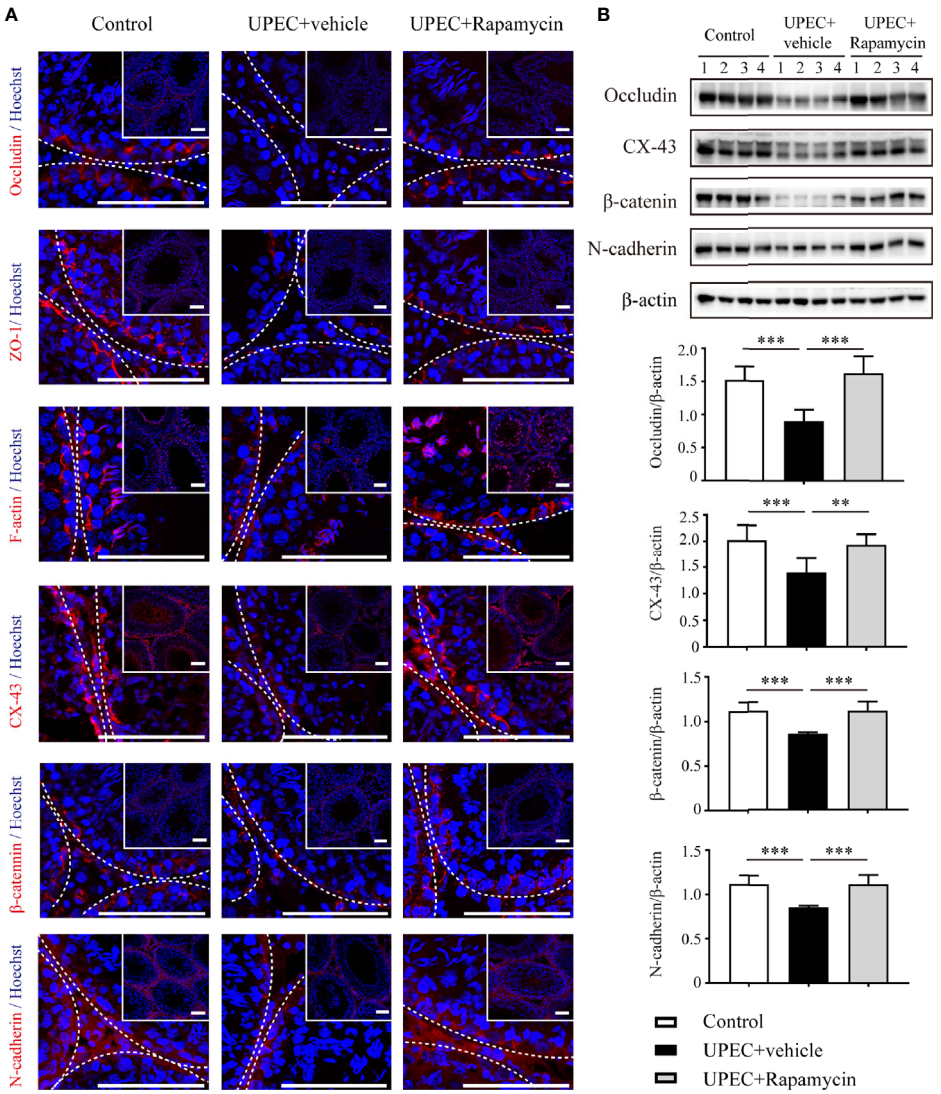

FIGURE 6 | Rapamycin (5 mg/kg/day) treatment for seven days partially rescues down-regulation of cell-junction proteins in UPEC-infected testes. **(A)** We evaluated cell-junction protein expression in all three groups using immunofluorescence staining and confocal microscopy. The images in the insets are the same testes cross-sections at lower magnification (scale bar, 100 μm). The white broken lines indicate the relative location of the basement membrane adjacent to the BTB of the seminiferous tubules. **(B)** Representative blots show the expression patterns of selected junctional proteins in the testes from all three groups animals (n=4 in each group). Histograms show quantitative results, and *p* value was determined by ANOVA; $^{**}p < 0.01$, $^{***}p < 0.001$.

majority of tubules. Intriguingly, the distance of biotin infiltration was significantly reduced in rapamycin-treated orchitis rats, supporting the assumption that rapamycin contributed to the maintenance of BTB integrity in orchitis.

It has been reported, however, that long-term administration of rapamycin leads to a reversable impairment of spermatogenesis by inhibiting mTOR signaling (30–32). Given the function of mTORC1, it is reasonable to question whether 7-day treatment with rapamycin further perturbs spermatogenesis in orchitis animals. Therefore, a histopathological assessment was performed on the cross-sections of testes (**Figures 7C, D**), and the ratios of testis to body weights in three (control, UPEC-infected and vehicle-treated, and UPEC-infected and rapamycin-treated) groups were calculated (**Figure 7E**). Consistent with our previous report (21), UPEC infection caused various degrees of spermatogenic impairment and immune cell infiltration (**Figures 7C** *b*, *h–j*). Importantly, the number of abnormal seminiferous tubules was slightly lower in the rapamycin-treated group (22.7 ± 8.6%) compared with vehicle-treated animals (30.8 ± 15%), although this difference was not statistically significant (**Figure 7D**). Furthermore, the ratios of testis to body weights were similar in control and rapamycin groups on day 14, whereas the ratios in UPEC-infected and vehicle-treated groups showed a tendency to be lower (although again not statistically significant)

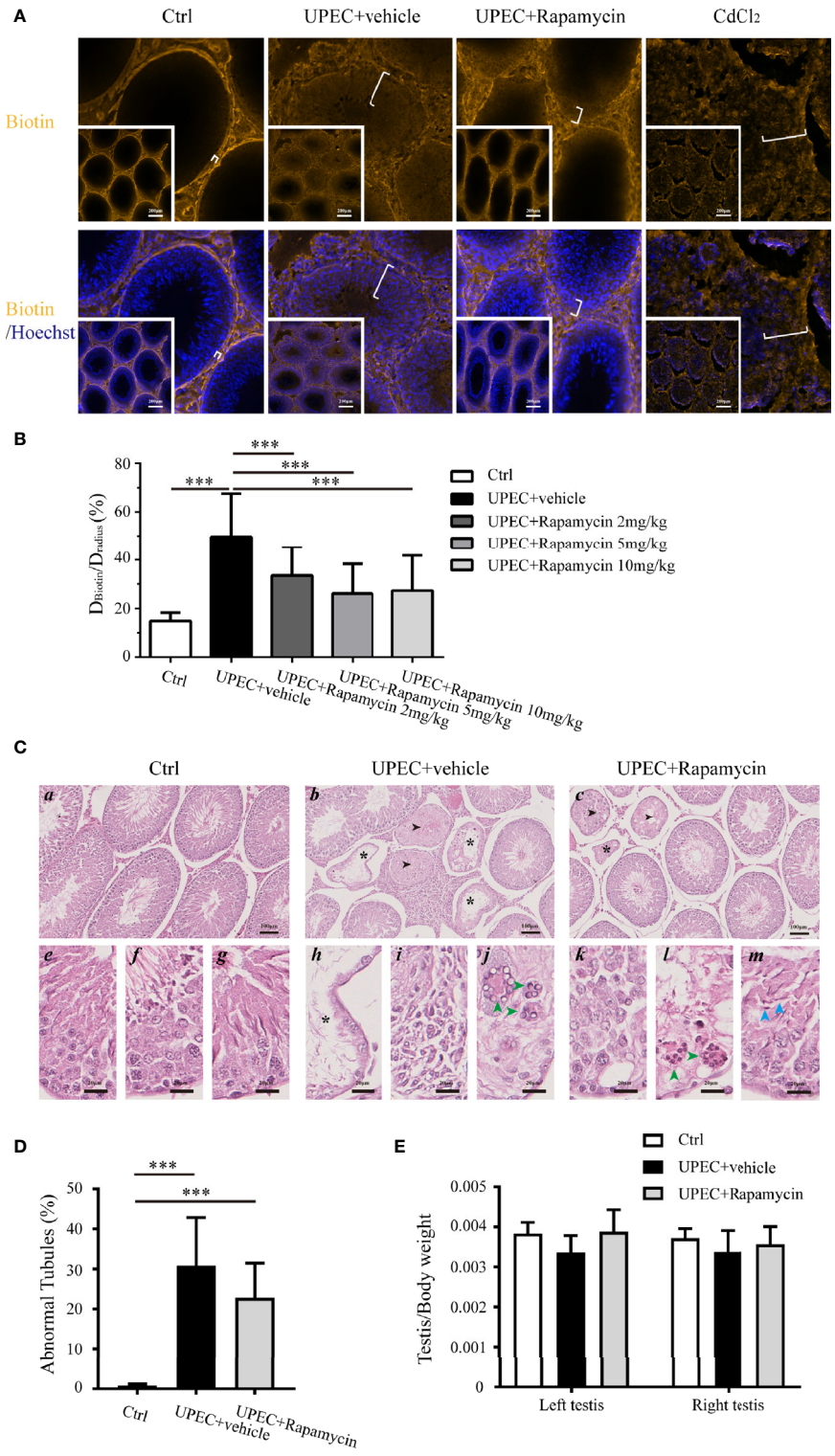

FIGURE 7 | Continued

FIGURE 7 | Rapamycin treatment reduces biotin infiltration through the BTB and does not perturb spermatogenesis in testes from UPEC-infected rats. **(A)** BTB integrity was functionally evaluated using a sulfo-NHS-LC-biotin diffusion assay, and the representative images of biotin diffusion in the testes of different groups are shown. The testes of $CdCl_2$-treated rats served as positive controls. The white brackets indicate the distance penetrated by biotin. The images in the insets are the same testes cross sections at lower magnification (scale bar, 200 μm). **(B)** Semi-quantified data from the sulfo-NHS-LC-biotin diffusion assay are demonstrated as a bar graph. For an oval-shaped tubule from an oblique cross-section, we calculated the radius using the mean of the longest and shortest radii. Approximately 50 tubules were randomly scored per testis. D_{Biotin}, distance penetrated by biotin in seminiferous tubule; D_{radius}, the radius of the corresponding seminiferous tubule. *p* value was determined with ANOVA, ***$p<0.001$. **(C)** Paraffin sections of testes (4 μm) were stained with hematoxylin and eosin. Histopathologic evaluation was performed on the testes of control (n=4), UPEC + vehicle-treated (n=6), and rapamycin-treated animals (n=6) using light microscopy. The images were captured using a NanoZoomer S210 system and representative figures are depicted (*a*-*c*: scale bar, 100 μm; *e*-*m*: scale bar, 20 μm). Seminiferous tubules marked with asterisks indicate Sertoli cell-only tubules (*b*, *c*, *h*); those marked with arrowheads indicate hypospermatogenic tubules (*b and c*). *e*–*g*: higher-magnification images showing seminiferous epithelium at stages II-III, VIII, and XIII in control rat testes, respectively; *h*–*j*: higher-magnification images demonstrating typical pathologic changes in UPEC-infected rats testes (*h*, extensive germ-cell loss, and only Sertoli cells remained in the seminiferous epithelium; *I*, infiltration of inflammatory cells in the interstitial compartment; *j*, the presence of multinucleated, round spermatids are indicated by green arrowheads); *k*–*m*, higher-magnification images show pathologic changes in testes from orchitis-model animals treated with rapamycin (*k*, disordered seminiferous epithelium with germ cell exfoliation; *l*, the presence of multinucleated round spermatids are indicated by green arrowheads; *m*, elongated spermatids with defects in polarity are indicated by blue arrowheads, in which the spermatid heads were misoriented by pointing 45°–90° away from the basement membrane). **(D)** The percentage of abnormal seminiferous tubules in each testicular cross-section was calculated by assessing over 200 tubules in every sample. The data are presented as mean ± SD and shown in the histogram. *p* value was determined by ANOVA; ***$p<0.001$. **(E)** The ratios of testis to body weight in the three groups are presented as mean ± SD and shown in the histogram. *p* value was determined using ANOVA.

(**Figure 7E**). Taken together, our findings suggest a role for short-term rapamycin treatment in BTB protection, without inducing further spermatogenic dysfunction during UPEC infection.

DISCUSSION

We previously demonstrated that the BTB appeared to remain functionally intact at one single time-point in the early stage of UPEC infection (21). In addition, we also observed that the bacteria migrated across the seminiferous epithelium and reached the interstitial compartment of the testis (21). We therefore speculated that UPEC either utilized epithelial transcytosis or caused a transient disruption of the BTB to reach the interstitium. Considering the role of the BTB in the maintenance of testicular immuno-privilege, the impacts of infection or inflammation on this barrier have attracted increasing attention. Wu et al. found that the mumps virus could disrupt the BTB through the induction of TNF-α in Sertoli cells (19), and other investigators reported that a lipopolysaccharide (LPS) challenge induced occludin down-regulation and compromised BTB integrity (33). In our previous study we demonstrated UPEC-derived α-hemolysin caused Sertoli cell necrosis by inducing calcium influx and mitochondrial dysfunction (34). Given that UPEC bacteria possess multiple virulence factors that include LPS and α-hemolysin, it is reasonable to assume that the presence of UPEC inside the testis would disrupt the BTB formed by neighboring Sertoli cells. Herein, we therefore investigated the continuous dynamic changes in the BTB during UPEC invasion, and partially deduced the potential mechanism underlying BTB impairment in orchitis.

Compared to the infection models we had used previously, we slightly modified the UPEC-infection model used in the present study. For the *in vivo* orchitis model, a lower number of bacteria were directly injected into the testis rather than through the vas deferens, as pathogens can migrate to the interstitium (21). In addition, the UPEC culture supernatant was applied to *in vitro* experimentation primarily based upon two rationales. First, our previous studies indicated that soluble virulence factors, such as α-hemolysin, are the dominant factors inducing Sertoli cell necrosis (34), and second, in our experience MOI (multiplicity of infection) is difficult to control precisely in cell-culture experiments over several days due to the constant proliferation of bacteria. With our modified infection models, we first demonstrated that UPEC invasion caused structural and functional impairment of the BTB in a time-dependent manner. Moreover, our results suggested that an mTORC1-mTORC2 imbalance plays a pivotal role in BTB disruption, which can be partially restored by the specific mTORC1 inhibitor rapamycin.

Rather than only examining samples on day 7 post-infection as in our previously published research, in the present study we observed ultrastructural disruption of the BTB at multiple time-points using TEM, which showed additional and significant morphologic changes over time. We also found anti-sperm antibody positivity in the sera of orchitis-model rats after three months of modeling. Using *in vivo* and *in vitro* models, our results showed that UPEC infection or bacterial culture supernatant decreased to varying degrees of the expression of Sertoli cell junctional proteins that comprise the BTB. These findings confirmed a progressive destruction of the BTB by bacterial invasion, and subsequent compromise of the testicular immune-privileged microenvironment.

A series of experiments have shown that BTB cell-junction proteins are not only essential for barrier integrity, but also indispensable for supporting spermatogenesis. For example, occludin-knockout mice were infertile by 36–60 weeks of age, with an absence of spermatocytes and spermatids in the seminiferous tubules (35, 36). It was also reported that spermatogonia failed to differentiate beyond type A in CX-43 Sertoli cell specific-knockout mice (37). Moreover, BTB assembly delay during postnatal development caused by diethylstilbestrol treatment resulted in meiotic failure of spermatocytes and a delay in spermiation (38). Indeed, we also noted spermatogenic dysfunction in our UPEC-induced orchitic animals that was accompanied by BTB destruction. Given our previously published findings, the down-regulation of BTB cell-junction

proteins in response to UPEC infection may be an important mechanism contributing to degeneration of the seminiferous epithelium in our orchitis model. In this context, safeguarding BTB integrity in orchitis is particularly important in preserving testicular function.

The underlying molecular mechanisms controlling BTB "opening" and "closing" are of particular interest in the context of orchitis. A number of recent studies indicated that the delicate balance between mTORC1 and mTORC2 occupies a key role in the regulation of BTB restructuring under normal physiologic conditions (13, 14). However, the role of mTORC1-mTORC2 in orchitis-related BTB disruption remains unclear. Herein, we noted that mTORC1, as well as the upstream kinases Erk1/2 and Akt, were all activated, whereas mTORC2 was suppressed in Sertoli cells facing a challenge from UPEC-soluble virulence factors. The hyperactivation of mTORC1 and attenuation in mTORC2 both promote an "open/leaky" state with respect to the BTB, and this imbalance likely contributes to the disruption of barrier integrity during UPEC infection. We also observed that rapamycin, an mTORC1- specific inhibitor, abolished mTORC1 hyperactivation and partially restored the expression of all our selected junctional proteins in infected Sertoli cells. Consistent with our *in vitro* data, we also confirmed the rescue effects of rapamycin in an orchitis rat model following UPEC infection. This further suggested that disequilibrated mTORC1-mTORC2 contributed to UPEC-induced BTB damage, which could then provide a potential therapeutic target in orchitis.

Previous studies have shown that mTOR signaling is directly involved in the nutritional support of spermatogenesis (39). In addition, mTOR is required for the proliferation and differentiation of spermatogonial stem cells as opposed to survival and maintenance (40). Serra et al. established that raptor-knockout led to incomplete meiosis by spermatogonia and no production of mature spermatozoa (41). Busada et al. demonstrated that mTORC1 inhibition with rapamycin resulted in a blockade of spermatogonial differentiation (42). Infertility is consistently one of the most common side effects experienced by men undergoing organ transplantation and long-term rapamycin treatment to prevent organ rejection (31, 43, 44). This immunosuppressant potentially causes a reversible diminution in a series of sperm parameters such as sperm count, motility, and vitality (32, 45). Given the critical role of mTORC1 in germ cell differentiation and rapamycin's side effects on fertility, it is of critical importance to ascertain whether short-term rapamycin treatment is detrimental to spermatogenesis. Congruent with our earlier study, UPEC infection induced considerable disruption of spermatogenesis and induced the infiltration of immune cells. It is noteworthy that we uncovered herein a tendency to decrease in the number of abnormal tubules in infected rats treated with rapamycin compared to the vehicle-treated controls (although this was not statistically significant). This suggests that at least seven days of rapamycin treatment (up to 10 mg/kg) at the acute phase of infection may actually exert a protective effect instead of aggravating the degeneration of seminiferous epithelium in infected testes. Thus, this may constitute a promising finding that sheds new light on the treatment of orchitis, providing an alternative to the sole use of antibiotics.

However, there are still some limitations to the present study. For example, it will be necessary in the future to fully evaluate the safety of our remedy strategy using rapamycin alone in control animals, and to investigate the impact on spermatozoa. Further study is also required to explore the long-term effects on spermatogenesis and fertility. It was recently reported that a rapamycin analog with 40 times more selectivity for mTORC1 reduced off-target inhibition of mTORC2, substantially decreasing metabolic and immunologic side effects (46). However, further investigation is required to determine the optimal dosage and treatment duration with an appropriate mTORC1 inhibitor. Moreover, it is essential to identify the principal virulence factor(s) that induces BTB dysfunction to better understand the underlying mechanism(s) of orchitis-related infertility.

In summary, the present study illustrated that an imbalance in mTORC1-mTORC2 contributed to disruptive alterations of the BTB following UPEC infection. Restoring these two complexes to their normal antagonistic function may provide a complementary strategy for treating bacterial orchitis. Our results thus revealed the possibility of further protecting testicular structure and function from infection/inflammation-induced tissue damage.

DATA AVAILABILITY STATEMENT

The raw data supporting the conclusions of this article will be made available by the authors, without undue reservation.

ETHICS STATEMENT

The animal study was reviewed and approved by the Ethical Committee of the Zhongshan Hospital.

AUTHOR CONTRIBUTIONS

NY and YL designed the experiments, YL wrote the manuscript, and NT provided manuscript revision. YL, ML, QC, and BY performed the cell culture and molecular biology experiments. YL and ML performed the animal experiments and analyzed the data, and XC and XD provided intellectual input and coordination. All authors contributed to the article and approved the submitted version.

FUNDING

This work was funded by project grants from the National Natural Science Foundation of China (nos. 81300473, 82071643, and 81971345).

ACKNOWLEDGMENTS

The authors acknowledge the assistance of Huijuan Shi and Yihua Gu (Shanghai Institute of Planned Parenthood Research) for providing experimental facilities. The authors also appreciate the technical support and suggestions from Andreas Meinhardt, Sudhanshu Bhushan and Monika Fijak (Justus-Liebig-University, Giessen, Germany), and Ke Zhu and Xuehai Zhou (Fudan University). We thank LetPub for its linguistic assistance during the preparation of this manuscript.

SUPPLEMENTARY MATERIAL

The Supplementary Material for this article can be found online at: https://www.frontiersin.org/articles/10.3389/fimmu.2021.582858/full#supplementary-material

Supplementary Table 1 | List of antibodies.

Supplementary Figure 1 | Immunofluorescence staining of vimentin in primary Sertoli cells Supplementary PowerPoint Original western blots.

Supplementary PowerPoint | Original western blots.

REFERENCES

1. Fijak M, Pilatz A, Hedger MP, Nicolas N, Bhushan S, Michel V, et al. Infectious, inflammatory and 'autoimmune' male factor infertility: how do rodent models inform clinical practice? *Hum Reprod Update* (2018) 24 (4):416–41. doi: 10.1093/humupd/dmy009
2. Schuppe HC, Meinhardt A, Allam JP, Bergmann M, Weidner W, Haidl G. Chronic orchitis: a neglected cause of male infertility? *Andrologia* (2008) 40 (2):84–91. doi: 10.1111/j.1439-0272.2008.00837.x
3. Wiles TJ, Kulesus RR, Mulvey MA. Origins and virulence mechanisms of uropathogenic Escherichia coli. *Exp Mol Pathol* (2008) 85(1):11–9. doi: 10.1016/j.yexmp.2008.03.007
4. Pilatz A, Hossain H, Kaiser R, Mankertz A, Schuttler CG, Domann E, et al. Acute epididymitis revisited: impact of molecular diagnostics on etiology and contemporary guideline recommendations. *Eur Urol* (2015) 68(3):428–35. doi: 10.1016/j.eururo.2014.12.005
5. Ryan L, Daly P, Cullen I, Doyle M. Epididymo-orchitis caused by enteric organisms in men > 35 years old: beyond fluoroquinolones. *Eur J Clin Microbiol Infect Dis* (2018) 37(6):1001–8. doi: 10.1007/s10096-018-3212-z
6. Comhaire FH, Mahmoud AM, Depuydt CE, Zalata AA, Christophe AB. Mechanisms and effects of male genital tract infection on sperm quality and fertilizing potential: the andrologist's viewpoint. *Hum Reprod Update* (1999) 5 (5):393–8. doi: 10.1093/humupd/5.5.393
7. Salonia A, Bettochi C, Carvalho J, Corona G, Jones TH, Kadioğlu A, et al. EAU Guidelines on Sexual and Reproductive Health 2020. In: *European Association of Urology Guidelines 2020 Edition. presented at the EAU Annual Congress Amsterdam 2020. Arnhem*. The Netherlands: European Association of Urology Guidelines Office (2020).
8. Zhao S, Zhu W, Xue S, Han D. Testicular defense systems: immune privilege and innate immunity. *Cell Mol Immunol* (2014) 11(5):428–37. doi: 10.1038/cmi.2014.38
9. Mruk DD, Cheng CY. The Mammalian Blood-Testis Barrier: Its Biology and Regulation. *Endocr Rev* (2015) 36(5):564–91. doi: 10.1210/er.2014-1101
10. Stanton PG. Regulation of the blood-testis barrier. *Semin Cell Dev Biol* (2016) 59:166–73. doi: 10.1016/j.semcdb.2016.06.018
11. Wen Q, Tang EI, Li N, Mruk DD, Lee WM, Silvestrini B, et al. Regulation of Blood-Testis Barrier (BTB) Dynamics, Role of Actin-, and Microtubule-Based Cytoskeletons. *Methods Mol Biol* (2018) 1748:229–43. doi: 10.1007/978-1-4939-7698-0_16
12. Cheng CY, Mruk DD. The blood-testis barrier and its implications for male contraception. *Pharmacol Rev* (2012) 64(1):16–64. doi: 10.1124/pr.110.002790
13. Mok KW, Mruk DD, Cheng CY. Regulation of blood-testis barrier (BTB) dynamics during spermatogenesis via the "Yin" and "Yang" effects of mammalian target of rapamycin complex 1 (mTORC1) and mTORC2. *Int Rev Cell Mol Biol* (2013) 301:291–358. doi: 10.1016/B978-0-12-407704-1.00006-3
14. Oliveira PF, Cheng CY, Alves MG. Emerging Role for Mammalian Target of Rapamycin in Male Fertility. *Trends Endocrinol Metab* (2017) 28(3):165–7. doi: 10.1016/j.tem.2016.12.004
15. Shimobayashi M, Hall MN. Making new contacts: the mTOR network in metabolism and signalling crosstalk. *Nat Rev Mol Cell Biol* (2014) 15(3):155–62. doi: 10.1038/nrm3757
16. Mok KW, Chen H, Lee WM, Cheng CY. rpS6 regulates blood-testis barrier dynamics through Arp3-mediated actin microfilament organization in rat sertoli cells. An in vitro study. *Endocrinology* (2015) 156(5):1900–13. doi: 10.1210/en.2014-1791
17. Mok KW, Mruk DD, Silvestrini B, Cheng CY. rpS6 Regulates blood-testis barrier dynamics by affecting F-actin organization and protein recruitment. *Endocrinology* (2012) 153(10):5036–48. doi: 10.1210/en.2012-1665
18. Mok KW, Mruk DD, Lee WM, Cheng CY. Rictor/mTORC2 regulates blood-testis barrier dynamics via its effects on gap junction communications and actin filament network. *FASEB J* (2013) 27(3):1137–52. doi: 10.1096/fj.12-212977
19. Wu H, Jiang X, Gao Y, Liu W, Wang F, Gong M, et al. Mumps virus infection disrupts blood-testis barrier through the induction of TNF-alpha in Sertoli cells. *FASEB J* (2019) 33(11):12528–40. doi: 10.1096/fj.201901089R
20. Jia X, Xu Y, Wu W, Fan Y, Wang G, Zhang T, et al. Aroclor1254 disrupts the blood-testis barrier by promoting endocytosis and degradation of junction proteins via p38 MAPK pathway. *Cell Death Dis* (2017) 8(5):e2823. doi: 10.1038/cddis.2017.224
21. Lu Y, Bhushan S, Tchatalbachev S, Marconi M, Bergmann M, Weidner W, et al. Necrosis is the dominant cell death pathway in uropathogenic Escherichia coli elicited epididymo-orchitis and is responsible for damage of rat testis. *PloS One* (2013) 8(1):e52919. doi: 10.1371/journal.pone.0052919
22. Han W, Wang H, Su L, Long Y, Cui N, Liu D. Inhibition of the mTOR Pathway Exerts Cardioprotective Effects Partly through Autophagy in CLP Rats. *Mediators Inflammation* (2018) 2018:4798209. doi: 10.1155/2018/4798209
23. Chen H, Lui WY, Mruk DD, Xiao X, Ge R, Lian Q, et al. Monitoring the Integrity of the Blood-Testis Barrier (BTB): An In Vivo Assay. *Methods Mol Biol* (2018) 1748:245–52. doi: 10.1007/978-1-4939-7698-0_17
24. Bhushan S, Tchatalbachev S, Klug J, Fijak M, Pineau C, Chakraborty T, et al. Uropathogenic Escherichia coli block MyD88-dependent and activate MyD88-independent signaling pathways in rat testicular cells. *J Immunol* (2008) 180(8):5537–47. doi: 10.4049/jimmunol.180.8.5537
25. Edwards SR, Wandless TJ. The rapamycin-binding domain of the protein kinase mammalian target of rapamycin is a destabilizing domain. *J Biol Chem* (2007) 282(18):13395–401. doi: 10.1074/jbc.M700498200
26. Li N, Cheng CY. Mammalian target of rapamycin complex (mTOR) pathway modulates blood-testis barrier (BTB) function through F-actin organization and gap junction. *Histol Histopathol* (2016) 31(9):961–8. doi: 10.14670/HH-11-753
27. Wang L, Harris TE, Lawrence JCJr. Regulation of proline-rich Akt substrate of 40 kDa (PRAS40) function by mammalian target of rapamycin complex 1 (mTORC1)-mediated phosphorylation. *J Biol Chem* (2008) 283(23):15619–27. doi: 10.1074/jbc.M800723200
28. Ma L, Chen Z, Erdjument-Bromage H, Tempst P, Pandolfi PP. Phosphorylation and functional inactivation of TSC2 by Erk implications for tuberous sclerosis and cancer pathogenesis. *Cell* (2005) 121(2):179–93. doi: 10.1016/j.cell.2005.02.031
29. Li SYT, Yan M, Chen H, Jesus T, Lee WM, Xiao X, et al. mTORC1/rpS6 regulates blood-testis barrier dynamics and spermatogenetic function in the testis in vivo. *Am J Physiol Endocrinol Metab* (2018) 314(2):E174–E90. doi: 10.1152/ajpendo.00263.2017
30. Moreira BP, Oliveira PF, Alves MG. Molecular Mechanisms Controlled by mTOR in Male Reproductive System. *Int J Mol Sci* (2019) 20(7):1633. doi: 10.3390/ijms20071633

31. Huyghe E, Zairi A, Nohra J, Kamar N, Plante P, Rostaing L. Gonadal impact of target of rapamycin inhibitors (sirolimus and everolimus) in male patients: an overview. *Transpl Int* (2007) 20(4):305–11. doi: 10.1111/j.1432-2277.2006.00423.x
32. Rovira J, Diekmann F, Ramirez-Bajo MJ, Banon-Maneus E, Moya-Rull D, Campistol JM. Sirolimus-associated testicular toxicity: detrimental but reversible. *Transplantation* (2012) 93(9):874–9. doi: 10.1097/TP.0b013e31824bf1f0
33. Pan Y, Liu Y, Wang L, Xue F, Hu Y, Hu R, et al. MKP-1 attenuates LPS-induced blood-testis barrier dysfunction and inflammatory response through p38 and IkappaBalpha pathways. *Oncotarget* (2016) 7(51):84907–23. doi: 10.18632/oncotarget.12823
34. Lu Y, Rafiq A, Zhang Z, Aslani F, Fijak M, Lei T, et al. Uropathogenic Escherichia coli virulence factor hemolysin A causes programmed cell necrosis by altering mitochondrial dynamics. *FASEB J* (2018) 32(8):4107–20. doi: 10.1096/fj.201700768R
35. Saitou M, Furuse M, Sasaki H, Schulzke JD, Fromm M, Takano H, et al. Complex phenotype of mice lacking occludin, a component of tight junction strands. *Mol Biol Cell* (2000) 11(12):4131–42. doi: 10.1091/mbc.11.12.4131
36. Takehashi M, Kanatsu-Shinohara M, Miki H, Lee J, Kazuki Y, Inoue K, et al. Production of knockout mice by gene targeting in multipotent germline stem cells. *Dev Biol* (2007) 312(1):344–52. doi: 10.1016/j.ydbio.2007.09.029
37. Carette D, Weider K, Gilleron J, Giese S, Dompierre J, Bergmann M, et al. Major involvement of connexin 43 in seminiferous epithelial junction dynamics and male fertility. *Dev Biol* (2010) 346(1):54–67. doi: 10.1016/j.ydbio.2010.07.014
38. Toyama Y, Ohkawa M, Oku R, Maekawa M, Yuasa S. Neonatally administered diethylstilbestrol retards the development of the blood-testis barrier in the rat. *J Androl* (2001) 22(3):413–23.
39. Jesus TT, Oliveira PF, Silva J, Barros A, Ferreira R, Sousa M, et al. Mammalian target of rapamycin controls glucose consumption and redox balance in human Sertoli cells. *Fertil Steril* (2016) 105(3):825–33 e3. doi: 10.1016/j.fertnstert.2015.11.032
40. Serra ND, Velte EK, Niedenberger BA, Kirsanov O, Geyer CB. Cell-autonomous requirement for mammalian target of rapamycin (Mtor) in spermatogonial proliferation and differentiation in the mousedagger. *Biol Reprod* (2017) 96(4):816–28. doi: 10.1093/biolre/iox022
41. Serra N, Velte EK, Niedenberger BA, Kirsanov O, Geyer CB. The mTORC1 component RPTOR is required for maintenance of the foundational spermatogonial stem cell pool in micedagger. *Biol Reprod* (2019) 100(2):429–39. doi: 10.1093/biolre/ioy198
42. Busada JT, Niedenberger BA, Velte EK, Keiper BD, Geyer CB. Mammalian target of rapamycin complex 1 (mTORC1) Is required for mouse spermatogonial differentiation in vivo. *Dev Biol* (2015) 407(1):90–102. doi: 10.1016/j.ydbio.2015.08.004
43. Bererhi L, Flamant M, Martinez F, Karras A, Thervet E, Legendre C. Rapamycin-induced oligospermia. *Transplantation* (2003) 76(5):885–6. doi: 10.1097/01.TP.0000079830.03841.9E
44. Zuber J, Anglicheau D, Elie C, Bererhi L, Timsit MO, Mamzer-Bruneel MF, et al. Sirolimus may reduce fertility in male renal transplant recipients. *Am J Transplant* (2008) 8(7):1471–9. doi: 10.1111/j.1600-6143.2008.02267.x
45. Skrzypek J, Krause W. Azoospermia in a renal transplant recipient during sirolimus (rapamycin) treatment. *Andrologia* (2007) 39(5):198–9. doi: 10.1111/j.1439-0272.2007.00787.x
46. Schreiber KH, Arriola Apelo SI, Yu D, Brinkman JA, Velarde MC, Syed FA, et al. A novel rapamycin analog is highly selective for mTORC1 in vivo. *Nat Commun* (2019) 10(1):3194. doi: 10.1038/s41467-019-11174-0

Conflict of Interest: The authors declare that the research was conducted in the absence of any commercial or financial relationships that could be construed as a potential conflict of interest.

frontiers in Immunology

ORIGINAL RESEARCH
published: 19 February 2021
doi: 10.3389/fimmu.2021.580454

Characterization of an Antiviral Component in Human Seminal Plasma

Ran Chen[1†], Wenjing Zhang[1†], Maolei Gong[1†], Fei Wang[1], Han Wu[2], Weihua Liu[1], Yunxiao Gao[3], Baoxing Liu[3], Song Chen[4], Wei Lu[4], Xiaoqin Yu[1], Aijie Liu[1], Ruiqin Han[1], Yongmei Chen[1] and Daishu Han[1]*

[1] Institute of Basic Medical Sciences, School of Basic Medicine, Peking Union Medical College, Chinese Academy of Medical Sciences, Beijing, China, [2] Department of Immunology, Shenzhen University School of Medicine, Shenzhen, China, [3] Department of Andrology, China-Japan Friendship Hospital, Beijing, China, [4] Science and Technology Innovation Center, Guangzhou University of Chinese Medicine, Guangzhou, China

OPEN ACCESS

Edited by:
Jose Luis Subiza, Inmunotek SL, Spain

Reviewed by:
Jan Muench, University of Ulm, Germany
Nathalie Dejucq-Rainsford, Institut National de la Santé et de la Recherche Médicale (INSERM), France

***Correspondence:**
Daishu Han
dshan@ibms.pumc.edu.cn

[†]These authors have contributed equally to this work

Specialty section:
This article was submitted to Viral Immunology, a section of the journal Frontiers in Immunology

Received: 29 July 2020
Accepted: 04 January 2021
Published: 19 February 2021

Citation:
Chen R, Zhang W, Gong M, Wang F, Wu H, Liu W, Gao Y, Liu B, Chen S, Lu W, Yu X, Liu A, Han R, Chen Y and Han D (2021) Characterization of an Antiviral Component in Human Seminal Plasma. Front. Immunol. 12:580454. doi: 10.3389/fimmu.2021.580454

Numerous types of viruses have been found in human semen, which raises concerns about the sexual transmission of these viruses. The overall effect of semen on viral infection and transmission have yet to be fully investigated. In the present study, we aimed at the effect of seminal plasma (SP) on viral infection by focusing on the mumps viral (MuV) infection of HeLa cells. MuV efficiently infected HeLa cells *in vitro*. MuV infection was strongly inhibited by the pre-treatment of viruses with SP. SP inhibited MuV infection through the impairment of the virus's attachment to cells. The antiviral activity of SP was resistant to the treatment of SP with boiling water, Proteinase K, RNase A, and DNase I, suggesting that the antiviral factor would not be proteins and nucleic acids. PNGase or PLA2 treatments did not abrogate the antiviral effect of SP against MuV. Further, we showed that the prostatic fluid (PF) showed similar inhibition as SP, whereas the epididymal fluid and seminal vesicle extract did not inhibit MuV infection. Both SP and PF also inhibited MuV infection of other cell types, including another human cervical carcinoma cell line C33a, mouse primary epididymal epithelial cells, and Sertoli cell line 15P1. Moreover, this inhibitory effect was not specific to MuV, as the herpes simplex virus 1, dengue virus 2, and adenovirus 5 infections were also inhibited by SP and PF. Our findings suggest that SP contains a prostate-derived pan-antiviral factor that may limit the sexual transmission of various viruses.

Keywords: seminal plasma, prostate fluid, antiviral factor, mumps virus, sexual transmission

INTRODUCTION

Many types of viruses can be detected in human semen, which poses a risk for the sexual spread of pathogens (1, 2). While 17 of 32 viruses present in semen are sexually transmissible (3), the efficiency of sexual transmission is variable. The efficiency of viral transmission is generally associated with seminal viral load and tropism for the ano-genital tract, and the mucosal barrier plays an important role in restricting sexual transmission of viruses (4). Growing evidences indicate that human semen may impact viral infection (5), which has yet to be intensively investigated.

Studies on the role of SP in viral infection have thus far shown conflicting results. Early studies showed that human seminal plasma (SP) significantly inhibited HIV-1 infection (6), and that multiple cationic polypeptides in SP played an anti-HIV-1 role (7). Seminal exosomes inhibit HIV-1 infection by blocking the interaction between HIV-1 and target cells (8–11). Recent studies showed that SP also inhibited ZIKV and cytomegalovirus (HCMV) infections (12, 13). In contrast, human semen-derived amyloid fibrils enhance HIV-1 infection, herpes simplex virus (HSV), HCMV, and EBOV infections (14–17). Moreover, SP may differentially impact HIV-1infection in a cell-specific manner (18), and the inflammatory status of the male genital tract can alter SP inhibition of HIV-1infection (19). These previous observations suggest that different mechanisms underlie the effect of SP on viral infection and are worthy of clarification.

MuV is the causative pathogen of mumps, a contagious disease worldwide (20). MuV also has a high tropism for the testis and induces orchitis, an etiologic factor of male infertility (21). MuV can be detected in mumps orchitis (22). MuV can efficiently replicate in most types of testicular cells and thereby perturb testicular functions (23–27). Sialic acid and Axl/Mer receptor tyrosine kinases play roles in MuV infection of testicular cells (28). In fact, MuV can infect various cell types *via* its receptor α2,3-sialic acid (29, 30). While MuV infects various cells of the male genital tract, it is not sexually transmitted. In the present study, we hypothesized that SP inhibits viral infection, and we attempted to elucidate the antiviral effect of SP on different cell types against various viruses. We found that SP potently inhibited MuV infection of different cell types of the genital tract and the infection of HeLa cells by various virus types, including MuV, herpes simplex virus 1 (HSV-1), adenovirus 5 (AV-5), and dengue virus 2 (DeV-2).

MATERIALS AND METHODS

Cell Culture

Vero E6 (CRL-1586), HeLa (CCL-2), and 15P1 (CRL-2618) cell lines were purchased from ATCC (Manassas, VA, USA). C33A (HTB-31) cell line was obtained from the cell center of the Peking Union Medical College (PUMC, Beijing, China). The primary epididymal epithelial cells (EEC) were isolated from 3-week-old C57BL/6J mice based on previous described procedures (31). The cells were cultured in Dulbecco's modified Eagle's medium (DMEM) (Thermo Fisher Scientific, Waltham, MA, USA) and supplemented with 5% fetal calf serum (FCS) (Thermo Fisher Scientific), 1.2 mg/ml sodium bicarbonate, 100 U/ml penicillin, and 100 mg/ml streptomycin, under a humidified atmosphere of 5% CO_2 in compressed air at 37°C.

Sample Collection

All of the human samples were obtained from the Andrology Department of the China-Japan Friendship Hospital. We collected 20 semen samples from healthy individuals between 30 and 40 years of age. After liquefaction at 37°C for 1 h, SP was obtained by centrifugation of semen at 12,000 × g for 10 min and collection of the cell-free supernatant. The SP was then stored at −80°C as individual or pooled samples. Ten prostatic fluids (PF) were obtained from healthy individuals 30 to 40 years of age. The prostate was massaged by urologist using a finger inserted through the anus to collect PF in a 1.5-ml microcentrifuge tube. PF were centrifuged at 12,000 × g for 10 min, and supernatants were collected. After a 10-fold dilution in PBS, individual and pooled PF were stored at −80°C. We obtained three seminal vesicles and epididymides from prostatic carcinoma patients aged 48 and 50 years. Epididymal fluids (EF) were diluted 10-fold in PBS. The seminal vesicles were cut into small pieces (<1 mm^3) in PBS at a concentration of 1 g/ml to extract seminal vesicle fluids (SVF). After vortex for 2 min, the SVF were obtained by collecting supernatant after centrifugation at 12,000 × g for 10 min. The SVF were then pooled and stored at −80°C. All of the samples were used after informed consent had been given by donors and approved by the ethics committee of the PUMC.

Viral Preparations

MuV, HSV-1, AV-5, and DeV-2 were kindly provided by laboratories of the PUMC (Beijing, China), and all viruses were amplified and titrated in Vero cells. Briefly, Vero cells (5×10^6) were seeded in 100-mm culture dishes with 10 ml of DMEM supplemented with 10% FCS. After 24 h, the cells were infected with viruses at a multiplicity of infection (MOI) of 1.0. Seven days after infection, we collected the culture medium and lysed the cells by freezing in liquid nitrogen and thawing at 37°C three times. After centrifugation at 2,000 rpm for 10 min, the supernatants were collected. Viral preparations were maintained in PBS at a density of 1×10^9 plaque-forming units/ml and then stored at −80°C.

Treatments of Viruses, SP, and PF

For the pre-treatment of viruses with fluids from the male genital tracts, we incubated viruses with the defined concentration of the fluids in complete medium at 37°C for the specific durations. For heat treatment, SP and PF were heated in boiling water for 15 min. After a centrifugation at 12,000 × g for 10 min, supernatants were collected. To treat samples with enzymes, SP and PF were incubated with individual enzymes, including 300 μg/ml proteinase K (ProK) (P6565, Sigma-Aldrich, St. Louis, MO, USA), 200 U/ml DNase I (2270A, Takara Bio., Dalian, China), 200 μg/ml RNase A (GE101, TransGen Biotech, Beijing China), 200 U/ml PNGase F (G5166, Sigma), and 100 U/ml lipase (L8620, Solarbio Life Sciences Ltd. Co, Beijing, China), at 37°C for 5 h. SP and PF were then heated in boiling water for 5 min to inactivate enzymes.

Cell Infection

Target cells were cultured in 6-well plates at 5×10^5 cells/well. After 24 h, cell culture media were replaced with the pre-incubated mixtures of viruses and fluids, and the cells were incubated at 37°C for 1 h. The culture media were then replaced with virus- and fluid-free media. MuV binding to HeLa cells was determined after incubating the cells with 50 MOI MuV on ice

for 1 h. After three washes with PBS, cells were collected for virus detection. For MuV entry, cells were incubated with 50 MOI MuV for 1 h at 37°C and the surface-bound MuV was removed by treating cells with 0.25% trypsin (Thermo Fisher Scientific) for 5 min. The cells were then collected for MuV detection.

$TCID_{50}$

Vero cells were seeded in 96-well plates at a density of 5×10^3 cells/well in 100 µl of culture media. After 24 h in an incubator with 5% CO_2 at 37°C, a serial dilution of MuV was added into plate wells. Ten days later, we calculated 50% tissue-culture effective dose ($TCID_{50}$) values according to the Reed-Muench method.

Cellular Viability

Cellular viability was assessed using a Cell Counting Kit-8 (CCK-8) assay kit (Dalian Meilun Biotechnology Co., Ltd., Dalian, China) according to the manufacturer's instructions. Briefly, HeLa cells were seeded in 96-well plates at a density of 5×10^3 cells/well in 100 µl culture media. At specific durations after MuV infection, 10 µl of the CCK-8 solution was added to each well. Two hours later, NADH produced by viable cells transformed colorless WST®-8 to orange color WST®-8 formazan. We measured the absorbance at 450 nm; the ratio of the absorbance value to the control (set as "1") represented cellular viability.

Immunofluorescence Staining

HeLa cells were cultured in 35-mm culture dishes and fixed with refrigerated 4% methanol at −20°C for 3 min. After washing them twice with PBS, the cells were permeabilized with 0.2% Triton X-100 (Zhongshan Biotechnology Co.) in PBS for 10 min and blocked with 5% normal goat serum (Zhongshan Biotechnology Co.) for 1 h at room temperature. The cells were subsequently incubated with mouse anti-MuV-NP monoclonal antibody (sc-57922) (Santa Cruz Biotechnology, Dallas, TX, USA) at 4°C in a humidified chamber for 24 h. After washing them twice with PBS, the cells were incubated with tetramethyl rhodamine isothiocyanate (TRITC)-conjugated goat anti-mouse secondary antibodies (Zhongshan Biotechnology Co.) for 1 h. Nuclei were counterstained with 4′, 6′-diamidino-2-phenylindole (DAPI) (Zhongshan Biotechnology Co.) according to the manufacturer's instructions. The cells were then mounted with antifade mounting medium (Zhongshan Biotechnology Co.) and observed under a fluorescence microscope BX-51 (Olympus, Tokyo, Japan).

Real-Time Quantitative RT-PCR (qRT-PCR)

Total RNA was extracted using Trizol reagents (Thermo Fisher Scientific) according to the manufacturer's instructions. The total RNA (1 µg) was reverse-transcribed into cDNA in a 20-µl reaction mixture containing 2.5 µM of random hexamers, 2 µM of deoxynucleotide triphosphates, and 200 units of Moloney murine leukemia virus reverse transcriptase (Promega, Madison, WI, USA). We performed PCR in a 20-µl reaction mixture containing 0.2 µl of cDNA, 0.5 µM of forward and reverse primers, and 10 µl of Power SYBR Green PCR Master Mix (Applied Biosystems, Foster City, CA, USA) on an ABI PRISM 7300 real-time cycler (Applied Biosystems). Relative mRNA levels were determined using the $2^{-\Delta\Delta Ct}$ method, as described in the Applied Biosystems User Bulletin No. 2 (P/N 4303859). The primer sequences for PCR are listed in **Table 1**.

Western Blot Analysis

Cells were lysed in a lysis buffer containing a protease inhibitor cocktail (Sigma-Aldrich), and the protein concentrations were determined using a bicinchoninic acid protein assay kit (Pierce Biotechnology, Rockford, IL, USA). Proteins (20 µg/well) were separated using 10% SDS-PAGE and then electro-transferred onto polyvinylidene fluoride membranes (Millipore, Bedford, MA, USA). The membranes were blocked with Tris-buffered saline (pH 7.4) containing 5% non-fat milk for 1 h at room temperature and then incubated with mouse anti-MuV-NP (ab9880) (Abcam, Cambridge, UK) or anti-β-Actin (66009-1-lg) (Sigma-Aldric) mAbs for 24 h at 4°C. After washing them twice with Tris-buffered saline containing 0.1% Tween-20, the membranes were incubated with HRP-conjugated secondary antibodies for 1 h at room temperature. Protein bands were visualized with an Enhanced Chemiluminescence Detection Kit (Zhongshan Biotechnology Co.).

Ultrafiltration of SP and PF

SP and PF were separated to four fractions (<3 kDa, >3 kDa, <100 kDa, >100 kDa) by ultrafiltration using Amicon® Ultra-0.5 Centrifugal Filter Devices (Merck Millipore Co., Darmstadt, Germany) according to manufacturer's instructions. Briefly, 500 µl of sample was added to filter device and capped it. The device was spun at 12,000 × g for 30 min. The filtrate was collected. The retentate was washed twice with PBS by repeating centrifugation. The filter device was placed upside down in a 1.5 ml micro-centrifuge tube and spun at 1,000 × g for 2 min to obtain the retentate. The retentate was diluted to a final volume of 500 µl.

TABLE 1 | Primers used for real-time qRT-PCR.

Target genes	Forward (5' → 3')	Reverse (5' → 3')
MuV-NP	TCAGATCAATCGCATCGGGG	CTTGCGACTGTGCGTTTTGA
HSV-1-UL49	GGTGTTCGTCGTCTTCGGAT	CTTCAGGTATGGCGAGTCCC
AV-5-Hexon	GGTGGCCATTACCTTTGACTCTTC	CCACCTGTTGGTAGTCCTTGTATTTAGTATCATC
DeV-2-NS1	AATCCGCTCAGTAACAAG	GTTTCGGGACCATCAATA
ACTB	CATGTACGTTGCTATCCAGGC	CTCCTTAATGTCACGCACGAT
Actb	GAAATCGTGCGTGACATCAAAG	TGTAGTTTCATGGATGCCACAG

NP, nuclear protein; UL, unique long gene; NS, non-structural protein.

Statistical Analysis

Statistical difference between two groups was determined using Student's *t* test. A one-way ANOVA with Bonferroni's (selected pairs) *post-hoc* test was used for multiple comparisons. We performed calculations using SPSS version 13.0 (SPSS Inc., Chicago, IL, USA). Data were presented as the means ± SEM of at least three experiments. A *P*-value <0.05 was considered to be statistically significant.

RESULTS

MuV Infection of HeLa Cells

To evaluate MuV infection and replication *in vitro*, human cervical epithelium cancer-derived HeLa cells were used as host cells. Real-time qRT-PCR results showed that MuV efficiently infected HeLa cells and replicated within them in a time-dependent manner (**Figure 1A**). The RNA levels of MuV nuclear protein (MuV-NP) gene were dramatically increased within cells at 24 and 48 h after infection with MuV at a MOI of 1.0. Accordingly, the protein levels of MuV-NP were increased in HeLa cells in a time-dependent manner after infection (**Figure 1B**). MuV-NP was further confirmed using immunofluorescence staining, which showed much greater fluorescent densities in cells at 24 and 48 h after infection (**Figure 1C**, lower panels). $TCID_{50}$ assay results also showed that viral loads in the HeLa cell culture medium significantly increased in a time-dependent manner (**Figure 1D**). MuV infection did not significantly affect cellular viability (**Figure 1E**).

Inhibition of MuV Infection by SP

To analyze the effect of SP on MuV infection, MuV-NP level was examined in HeLa cells after inoculation with a pre-incubation mixture of SP and MuV. A 2-h pre-incubation of 1.0 MOI MuV with SP at 37°C significantly attenuated MuV-NP RNA levels in HeLa cells in a dose-dependent manner at 48 h after infection (**Figure 2A**). In addition, Western blot analysis showed that MuV-NP protein levels were reduced by the presence of SP (**Figure 2B**). A 2-h pre-incubation of MuV with 1.0% SP dramatically inhibited MuV infection. The inhibitory efficiency of 1.0% SP on MuV infection depended upon the duration of the pre-incubation of MuV with SP; that is, the 2-h pre-incubation of 1.0 MOI MuV with 1.0% SP markedly reduced MuV-NP RNA (**Figure 2C**) and protein (**Figure 2D**) levels. Accordingly, SP significantly reduced MuV loads in the culture medium in a pre-incubation time-dependent manner 48 h after infection (**Figure 2E**). The presence of 1.0% SP for up to 2 h did not impair HeLa cell viability (**Figure 2F**). These results suggested that SP contains an antiviral factor that potently inhibits MuV infection. However, the presence of 1.0% SP for long terms could significantly reduce cell viability (**Figure S1**). We therefore incubated HeLa cells with SP for 1 h to avoid the cytotoxic effect in the present study.

To confirm whether SP acted on viruses or target cells, we firstly treated HeLa cells with 1.0% SP for 1 h, and the cells were then infected with 1.0 MOI MuV. The pre-treatment of HeLa cells with SP did not affect MuV infection (**Figure S2**). Further, we compared MuV infection after the pre-incubation of MuV with SP at 37, 4, or 45°C for 2 h to determine the association between the antiviral effect

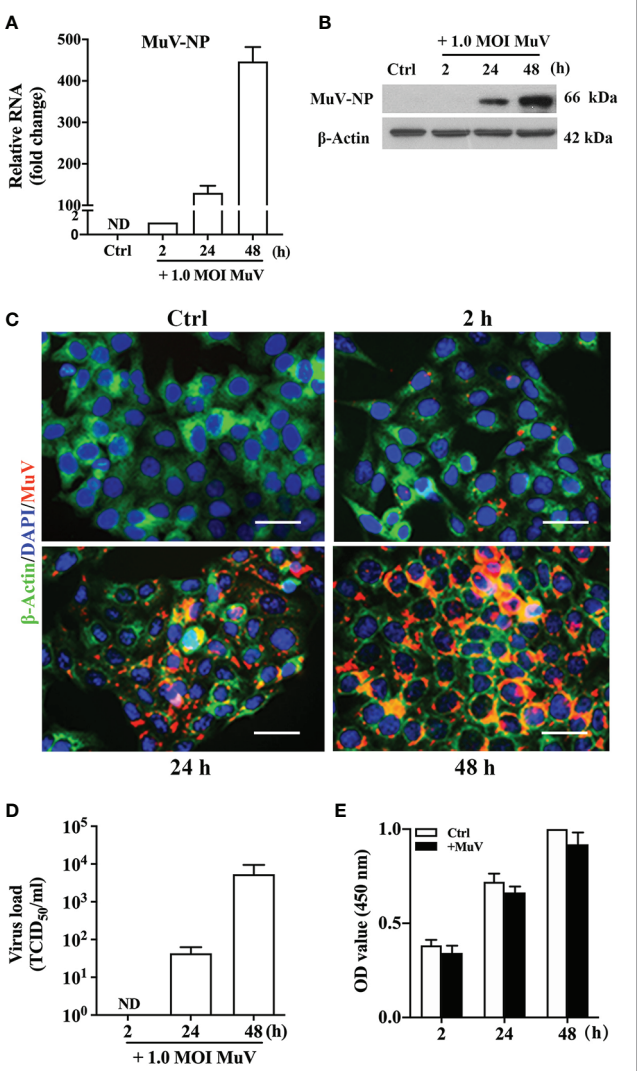

FIGURE 1 | MuV replication in HeLa cells. **(A)** Time-dependent MuV replication. HeLa cells were infected with MuV at a MOI of 1.0, and cells without MuV infection served as controls (Ctrl). Total RNA was extracted at specific times after infection, and the relative RNA levels of MuV-NP were analyzed using real-time qRT-PCR. **(B)** Protein levels of MuV-NP. HeLa cells were infected with MuV as described in **(A)**. At the indicated time-points after infection, MuV-NP protein levels in the cellular lysates were determined using Western blot analysis. **(C)** Intracellular MuV-NP. HeLa cells were infected with MuV as described in **(A)**. We determined intracellular distribution of MuV-NP (red) using immunofluorescence staining. The cytoplasm and nuclei were localized by immunofluorescence staining for β-Actin (green) and DAPI (blue). **(D)** Viral loads. HeLa cells were infected with 1.0 MOI MuV for the indicated periods of time. MuV loads in culture medium were determined using a $TCID_{50}$ assay. **(E)** Cell viability. After infection with MuV at a MOI of 1.0 for the indicated durations, the HeLa cell viability was determined using the CCK-8 assay. Images represent at least three independent experiments. Data are presented as means ± SEM of three separate experiments. Scale bar = 20 μm. ND, not detectable.

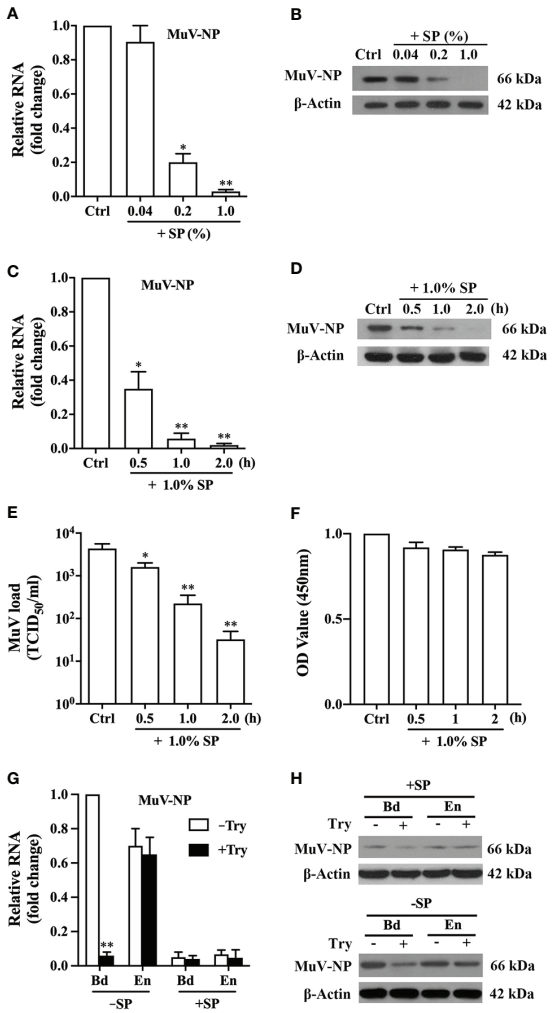

FIGURE 2 | Inhibition of MuV infection by SP. **(A)** Dose-dependent SP inhibition of MuV infection. MuV was pre-incubated with the indicated doses of SP for 2 h, and MuV without SP treatment served as controls (Ctrl). HeLa cells were infected with MuV. Total RNA was extracted at 48 h after MuV infection, and MuV-NP RNA levels were determined using real-time qRT-PCR. **(B)** HeLa cells were treated as described in **(A)**. The protein levels of MuV-NP were determined using Western blot analysis. **(C, D)** Time-dependent SP inhibition of MuV infection. MuV was pre-incubated with 1.0% SP for the specific durations. HeLa cells were infected with MuV for 48 h. MuV-NP RNA **(C)** and protein **(D)** levels were determined with real-time qRT-PCR and a Western blot analysis, respectively. **(E)** MuV loads in culture medium. MuV was treated, and HeLa cells were infected as described in **(C)**. Culture supernatants were collected at 48 h after MuV infection, and MuV loads in culture supernatants were determined using the $TCID_{50}$ assay. **(F)** Cell viability. HeLa cells were treated as described in **(C)**, and the cell viability was assessed using the CCK-8 assay. **(G, H)** MuV binding (Bd) and entry (En). MuV was pre-incubated in the absence (–SP) or the presence (+SP) of 1.0% SP for 2 h. HeLa cells were inoculated with 50 MOI of MuV on ice for 1 h to detect MuV binding to cells. HeLa cells were inoculated with 50 MOI of MuV at 37°C for 1 h to examine MuV entry into cells. MuV bound to cells was removed by treatment with 0.25% trypsin (+Try) for 5 min. MuV-NP RNA **(G)** and protein **(H)** levels were determined using real-time qRT-PCR and Western blot analysis, respectively. Images represent at least three independent experiments. Data are presented as means ± SEM of three experiments. $^*P < 0.05$, $^{**}P < 0.01$.

of SP and temperature. MuV infection was significantly inhibited by the pre-incubation at 4°C while the inhibition was evidently reduced in comparison with the pre-incubation at 37°C (**Figure S3**). However, MuV infection was completely abolished at 45°C in both the presence and absence of SP.

To determine which step of the viral infection cascade was inhibited by SP, we detected MuV binding and entry. MuV efficiently bound (Bd) with and entered (En) into HeLa cells in the absence of SP (**Figure 2G**). Treatment of cells with 0.25% trypsin for 5 min significantly removed bound MuV-NP RNA, but did not affect the entered MuV-NP RNA level. The 2-h pre-incubation of MuV with SP almost completely blocked MuV binding and entry to cells because Bd and En MuV-NP RNA levels were extremely low. Western blotting results confirmed that the pre-incubation of MuV with SP markedly reduced Bd and En MuV-NP protein levels (**Figure 2H**, upper panel). Trypsin evidently reduced Bd MuV-NP but did not affect En MuV-NP levels (**Figure 2H**, lower panel). The diminished MuV entry in the presence of SP was most likely due to the impairment of virus binding as it is essential for virus entry.

Characterization of Seminal Antiviral Factor

To characterize the properties of the antiviral factor, SP was treated with protein- and nucleic acid-degrading enzymes for 5 h at 37°C. Treatments of SP with either ProK, DNase I, or RNase A did not alter MuV-NP RNA (**Figure 3A**, left panel) or protein (right panel) levels in HeLa cells 48 h after infection. ProK, DNase I, and RNase A efficiently digested seminal proteins, isolated DNA and RNA from HeLa cells, respectively (**Figure S4**). Moreover, the treatment of SP with PNGase F and lipase retained the SP inhibition of MuV infection (**Figure S5**). In controls, the treatment of MuV with each enzyme alone without SP did not affect MuV infection (**Figure S6**). The results suggest that proteins, nucleic acids, glycosylated molecules, and lipids were not responsible for the antiviral effect of SP.

The molecular size of the antiviral factor was assessed by SP filtration through 100-kDa and 3-kDa filters. A 2-h pre-incubation of MuV with the retentate (Ret) of both filters dramatically reduced MuV-NP RNA (**Figure 3B**, left panel) and protein (right panel) levels. The SP filtrate (Fil) of 100-kDa filter also evidently reduced MuV-NP levels, whereas the filtrate of 3-kDa filter did not affect MuV infection. Moreover, the treatment of the retentate of two filters with boiling water did not markedly reduced the inhibitory effects on MuV infection (**Figure 3C**). Notably, SDS-PAGE results showed that the retentate of 100-kDa filter contained abundant <100 kDa molecules, whereas the filtrate of 100-kDa filter did not contain proteins of >100-kDa (**Figure S7**), which indicate that the ultrafiltration through 100-kDa filter did not efficiently separated >100-kDa molecules from smaller molecules. These results suggest that the antiviral component exists in >3kDa fraction, but not in <3 kDa fraction.

Inhibition of MuV Infection by Prostate Fluids

Given that SP is mostly produced by the prostate, seminal vesicle, and epididymis, we examined the antiviral effect of the prostatic

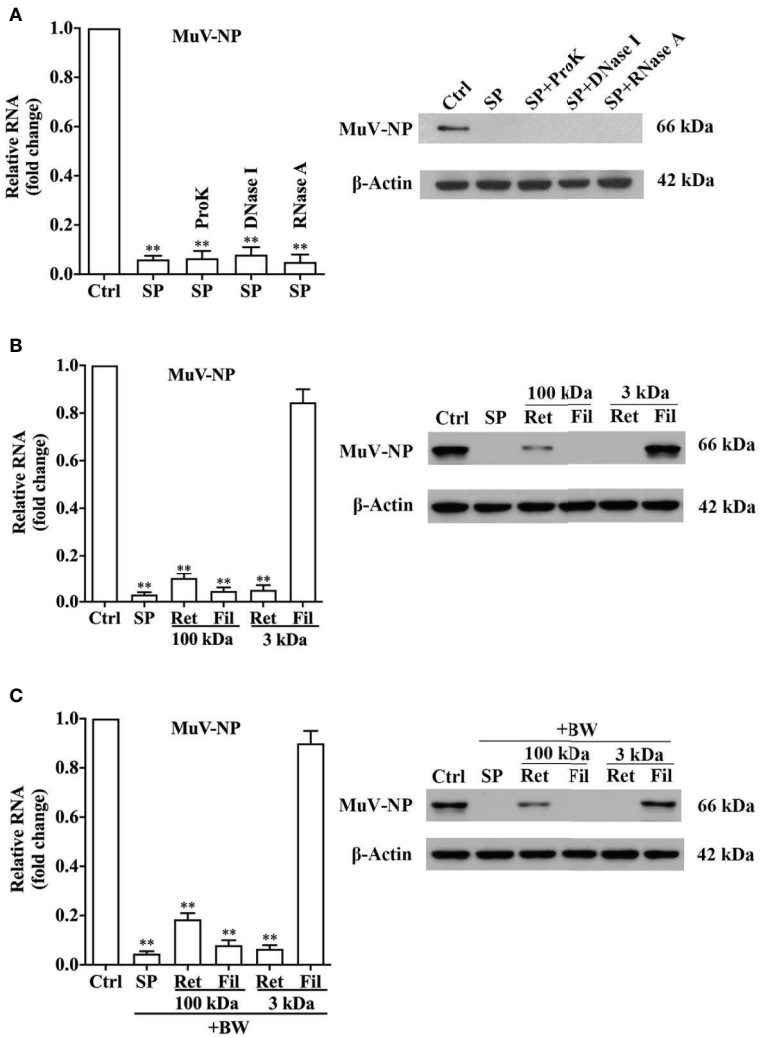

FIGURE 3 | Characterization of antiviral component. **(A)** Physical properties of the antiviral component. SP was treated with proteinase K (ProK), DNase I, or RNase A at 37°C for 5 h. MuV was incubated with SP for 2 h, and MuV without treatment served as the control (Ctrl). HeLa cells were infected with 1.0 MOI of MuV. At 48 h post-infection, MuV-NP RNA (left panel) and protein (right panel) levels were determined using real-time qRT-PCR and a Western blot, respectively. **(B)** Size analysis of the antiviral component. SP was filtered through 100 kDa and 3 kDa filters. Filtrate (Fil) and retentate (Ret) fractions were collected. MuV was incubated with fractions for 2 h, and HeLa cells were infected with MuV. MuV-NP RNA (left panel) and protein (right panel) levels were determined. **(C)** Heat resistance of the antiviral component. The Fil and Ret fractions of ultrafiltration were treated with boiling water (BW) for 10 min, and then incubated with MuV for 2 h. MuV-NP RNA (left) and protein (right) levels were determined. Images represent at least three independent experiments. Data are presented as means ± SEM of three experiments, $^{**}P < 0.01$.

fluids (PF), seminal vesicle fluids (SVF), and epididymal fluids (EF). The pre-incubation of MuV with PF at doses of 0.2 and 1% significantly reduced MuV-NP RNA levels in HeLa cells 48 h after infection, whereas SVF and EF did not affect MuV-NP RNA levels (**Figure 4A**, left panel). Accordingly, PF markedly reduced MuV-NP protein level at a dose of 1% (**Figure 4A**, right panel). The retentate of PF through a 3-kDa filter dramatically reduced MuV-NP RNA (**Figure 4B**, left panel) and protein (right panel) levels, although the filtrate did not affect MuV-NP levels. Both the retentate and filtrate through a 100-kDa filter significantly inhibited MuV infection. Treatment of PF with boiling water (BW), proteinase K (ProK), DNase I, or RNase A did not affect MuV-NP RNA (**Figure 4C**, left panel) and protein levels (right panel). The 2-h pre-incubation of MuV with PF dramatically diminished bound and entered MuV-NP RNA (**Figure 4D**, left panel) and protein (right panel) levels. These observations are similar to the those for SP, suggesting that the antiviral component in SP is most likely produced by the prostate gland.

Individual Variations in Antiviral Effect

To compare the antiviral activities of SP and PF from individual donors, we examined the antiviral effect of 20 SP and 10 PF samples.

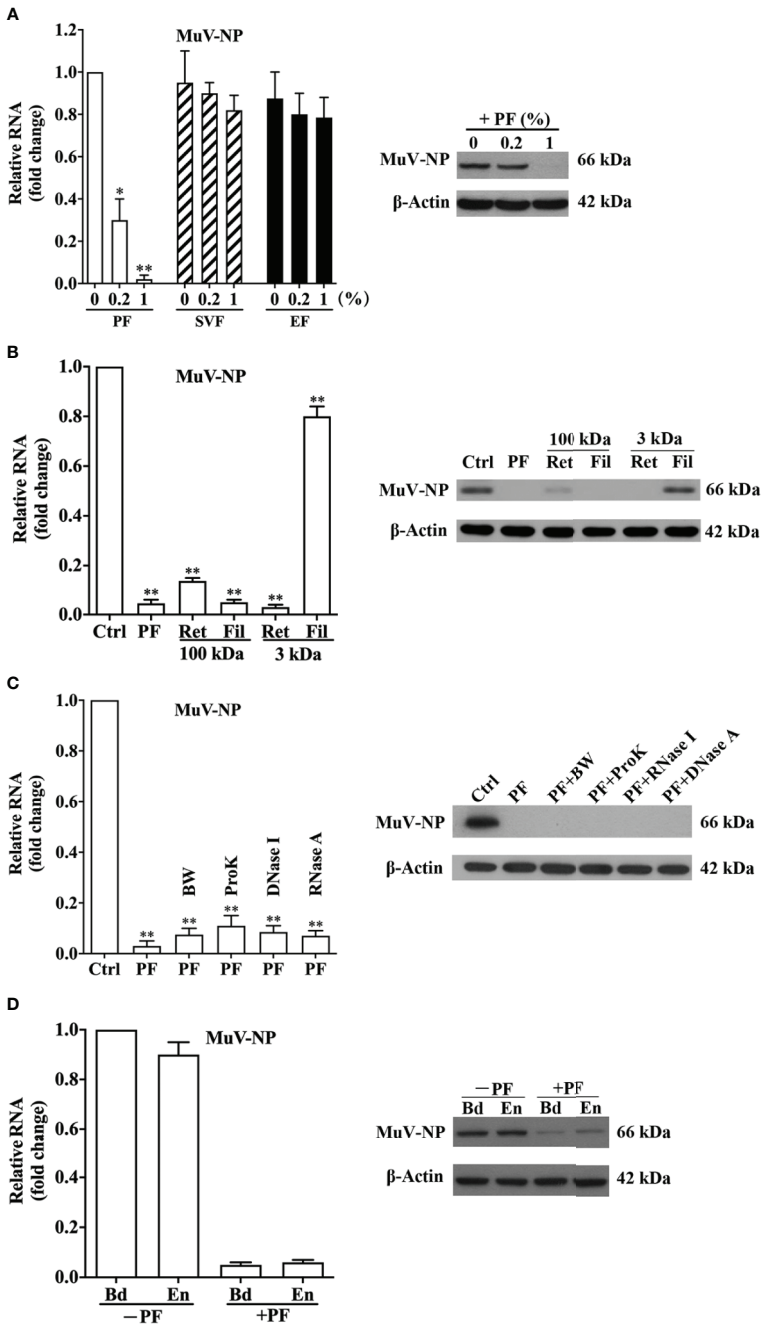

FIGURE 4 | Antiviral effect of male genital tract fluids. **(A)** Antiviral effect of prostatic fluids (PF), seminal vesicle fluids (SVF), and epididymal fluids (EF). MuV was incubated with the indicated doses of PF, SVF, or EF at 37°C for 2 h, and HeLa cells were infected with 1.0 MOI of MuV. At 48 h after infection, MuV-NP RNA levels (left panel) were determined using real-time qRT-PCR. The inhibition of PF on MuV-NP protein level (right panel) was analyzed by a Western blot. **(B)** Antiviral effect of PF fractions. PF were filtered through a 3-kDa filter, and MuV was incubated with either 1% filtrate (Fil) or 1% retentate (Ret) at 37°C for 2 h. MuV without treatment served as the control (Ctrl). HeLa cells were infected with 1.0 MOI of MuV. MuV-NP RNA (left panel) and protein (right panel) levels were determined 48 h after infection. **(C)** Properties of the antiviral factor in PF. PF were treated in boiling water (BW) for 5 min, or incubated with Proteinase K (ProK), DNase I, or RNase A at 37°C for 5 h, followed by heating inactivation in BW for 5 min. MuV was incubated with 1% PF for 2 h, and HeLa cells were infected with 1.0 MOI of MuV. MuV-NP RNA and protein levels were determined 48 h after infection. **(D)** MuV binding (Bd) and entry (En). MuV was pre-incubated with 1% PF (+PF) or without PF (-PF) at 37°C for 2 h. HeLa cells were inoculated for 1 h with 50 MOI MuV on ice for binding or at 37°C for entry. MuV-NP RNA (left panel) and protein (right panel) levels were determined. Images represent at least three independent experiments. Data are presented as means ± SEM of three experiments. *P < 0.05, **P < 0.01.

All 20 of the SP samples at a dose of 1% dramatically reduced the MuV-NP RNA level in HeLa cells 48 h after MuV infection (**Figure 5A**). In contrast, 0.2% SP exhibited great variation in inhibiting MuV infection. Although the 0.2% SP treatment of samples 7, 9, 12, and 18 greatly reduced MuV-NP RNA levels, other SP samples did not significantly inhibit MuV infection at a dose of 0.2%. Similarly, 1% of all PF samples substantially decreased MuV-NP RNA levels (**Figure 5B**). Although 8 of 10 PF samples significantly reduced MuV-NP RNA levels at the dose of 0.2%, samples 6 and 7 did not significantly reduce MuV-NP RNA at this dose (**Figure 5B**). These results indicated that the antiviral effect is a general property of human SP and PF with variation in individual donors.

Pan-Antiviral Effect of the Antiviral Factor

To determine whether the SP inhibition of MuV infection is a cell line-specific effect, we performed the experiments on three other cell types, including C33A, EEC, and 15P1. Similar to the observations in HeLa cells, the pre-incubation of MuV with 1.0% SP remarkably reduced MuV infection in all these cells (**Figure 6A**). To examine whether the antiviral factor specifically inhibits MuV infection or generally inhibits infection by other viruses, we analyzed the effect of SP and PF on the infection of HeLa cells by HSV-1, AV-5, and DeV-2. The pre-incubation of these viruses with 1.0% SP or PF dramatically reduced the RNA levels of HSV-1 (**Figure 6B**, left panel), AV-5 (middle panel), and

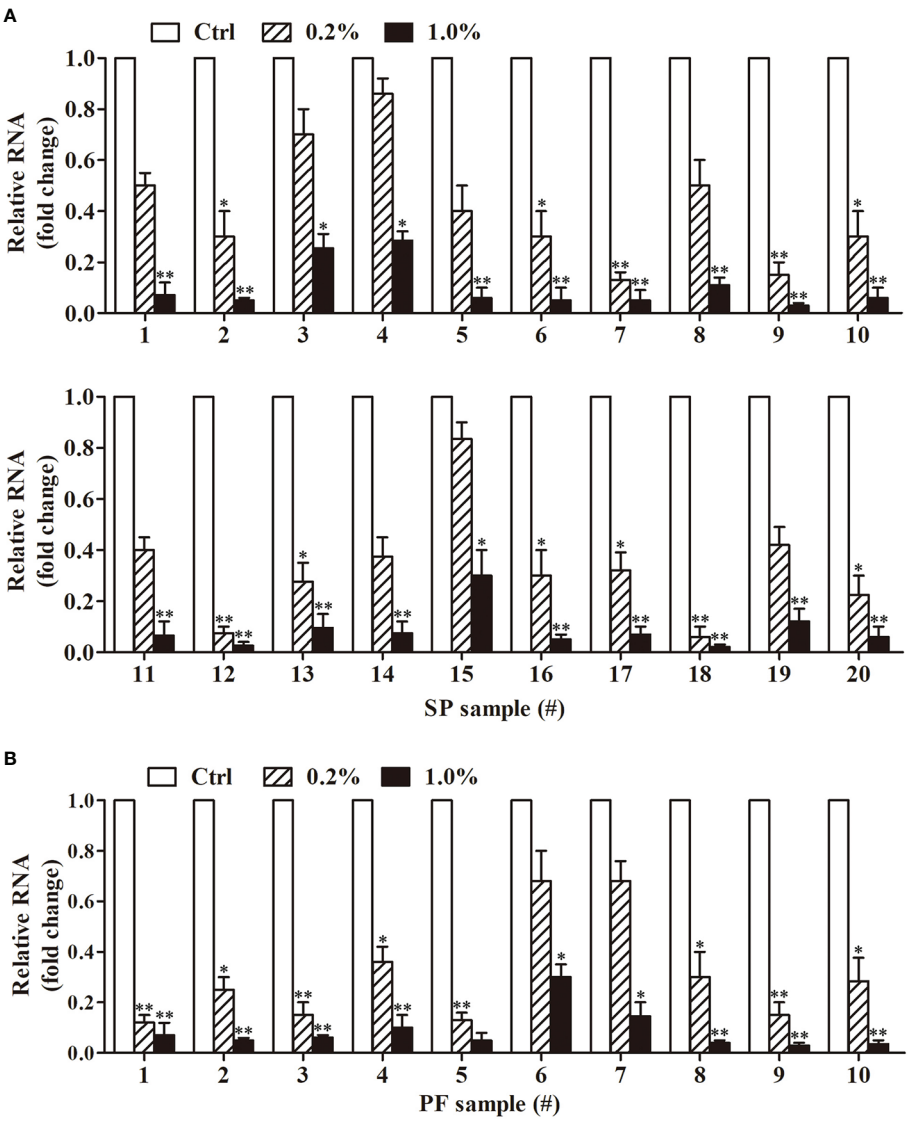

FIGURE 5 | Antiviral effect of SP and PF from individual donors. **(A)** Antiviral effect of SP. SP samples were collected from 20 individual donors. MuV was incubated with 0.2 or 1.0% individual SP samples for 2 h. MuV without treatment served as the control (Ctrl). HeLa cells were infected with 1.0 MOI of MuV. Total RNA was extracted from cells 48 h after MuV infection. MuV-NP RNA levels were determined using real-time qRT-PCR. **(B)** Antiviral effect of individual PF samples. Individual PF samples were collected from 10 donors. MuV was incubated with individual PF, and HeLa cells were infected as described in **(A)**. MuV-NP RNA levels were determined 48 h after infection. Data are presented as means ± SEM of three experiments. $^{*}P < 0.05$, $^{**}P < 0.01$.

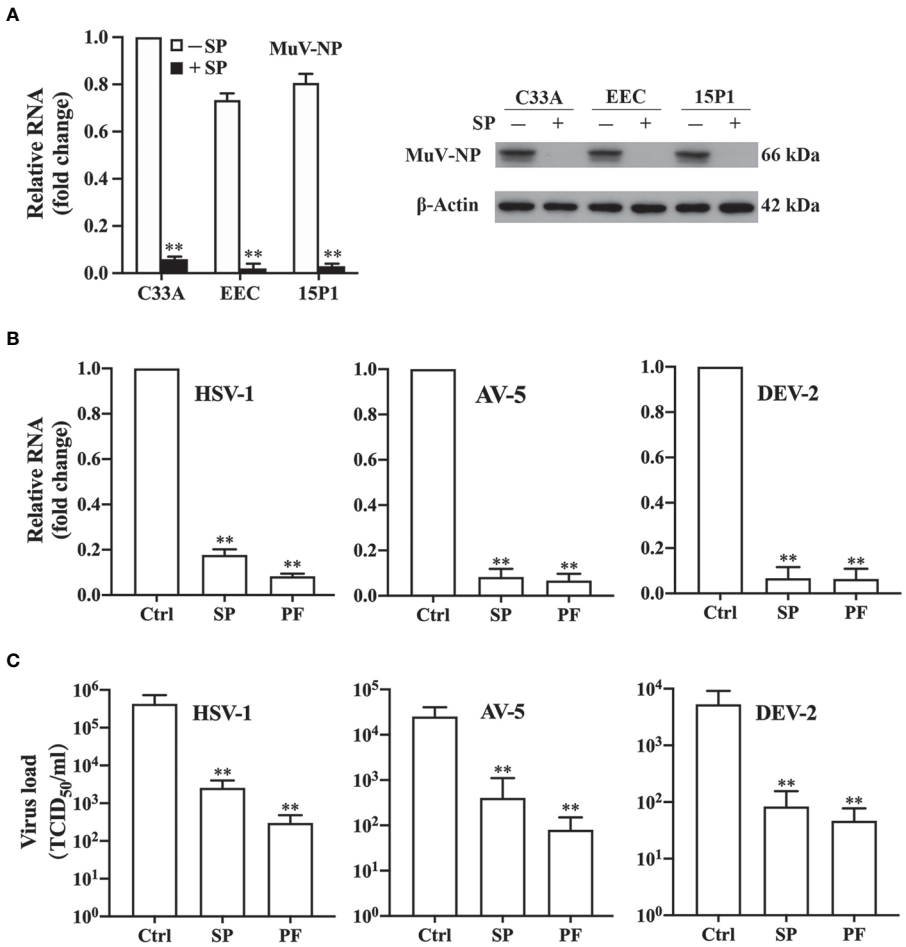

FIGURE 6 | Pan-antiviral effects of antiviral factor. **(A)** SP effect on MuV infection of different cell types. MuV was incubated with (+) 1% SP or without (–) SP at 37°C for 2 h. Human cervical squamous carcinoma cell line C33A, mouse primary epididymal epithelial cell (EEC), and mouse Sertoli cell line 15P1 were infected with 1.0 MOI MuV. MuV-NP RNA (left panel) and protein (right panel) levels were determined at 48 h after MuV infection. **(B, C)** Antiviral effect of SP against different viruses. **(B)** Viral RNA. Herpes simplex virus 1 (HSV-1), adenovirus 5 (AV-5), and dengue virus 2 (DeV-2) were incubated with 1% SP or PF for 2 h. Viruses without treatment served as the controls (Ctrl). HeLa cells were infected with each virus at a MOI of 1.0. RNA levels of HSV-1 (left panel), AV-5 (middle panel), and DeV-2 (right panel) were determined using real-time qRT-PCR 48 h after infection. **(C)** Viral loads in culture medium. Viruses were treated, and HeLa cells were infected with each virus, as described in **(B)**. Culture medium was collected 48 h after infection. Viral loads of HSV-1 (left panel), AV-5 (middle panel), and DeV-2 (right panel) in the medium were determined using $TCID_{50}$. Data are presented as means ± SEM of three experiments. $^{**}P < 0.01$.

DeV-2 (right panel) in HeLa cells 48 h after infection. Similarly, SP and PF significantly attenuated loads of HSV-1 (**Figure 6C**, left panel), AV-5 (middle panel), and DeV-2 (right panel) in the culture medium. These results indicated that the antiviral factor in SP and PF exerts a pan-antiviral activity.

DISCUSSION

The presence of viruses in semen is a risk for sexual spread of pathogens. Semen is not only a passive vector for viral spread, but also impacts viral transmission. The facilitative and inhibitory effects of semen on HIV-1 transmission have been documented (32). In the present study, we examined the antiviral effect of SP. We demonstrated that human SP decidedly inhibited MuV, HSV-1, AV-5, and DeV-2 infection, which suggest a pan-antiviral effect of SP.

The male reproductive system is a potential refuge for harboring viruses due to its immunosuppressive environment for protecting immunogenic germ cells from autoimmune responses (33). The mammalian testis, in particular, is a remarkably immunoprivileged organ wherein viruses can escape from immune surveillance and impair testicular function (34, 35). The antiviral effect of SP constitutes an important strategy for restricting the sexual transmission of viruses. MuV manifests a tropism for the testis and frequently induces orchitis (21). While natural MuV-induced diseases have been only observed in human beings, MuV can infect different species (29). Accordingly, the present study showed that several cell types from the human female genital tract and the mouse

male genital tract were efficiently infected *in vitro* by MuV, and that SP potently inhibited MuV infection of the target cells. These results suggest that the antiviral effect of SP is a general property independent target cells.

The effect of semen on HIV-1infection has been intensively studied because sexual transmission is a major route of viral spread. Semen may inhibit HIV-1 infection through distinct mechanisms. Early studies showed that SP abrogated HIV-1 infection through gp17 glycoprotein, cationic polypeptides, DC-SIGN (7, 36). Several other studies demonstrated that exosomes in human semen were involved in the inhibition of HIV-1 infection (8–10). Recent studies showed that seminal exosomes and salivary extracellular vesicles inhibited ZIKV infection through the impairment of viral attachment to target cells by acting on cells (12, 37). These mechanisms could not explain SP inhibition of MuV infection in the present study. We demonstrated that SP acted on MuV and did not target host cells. Moreover, the fraction of <100 kDa potently inhibited MuV infection, which did not support the involvement of exosomes. While the retentate of 100 kDa filter also significantly inhibited MuV infection, we could not conclude that it was indeed the effect of a >100 kDa component because this fraction contained abundant <100 kDa components. We also demonstrated that heating at boiling water did not affect the inhibitory effect of SP on MuV infection, and that neither proteins nor glycosylated molecules were involved in the SP inhibition of MuV infection, which corresponded the observations in the inhibition of semen on ZIKV infection (12). We further excluded the involvement of nucleic acids and lipids because the treatments of SP with respective enzymes did not restrain the inhibition of MuV infection. After the exclusion of these macromolecules, it is hard to image what the antiviral factor is. We may speculate that a small molecule that naturally binds to the macromolecules poses the virucidal effect of SP. Since the antiviral factor likely produced by the prostate, the analysis on the products of the prostatic cells *in vitro* would aid in the identification of the antiviral factor. The antiviral component in SP potently inhibited viral infection because 1% SP profoundly inhibited viral infection. The antiviral effect of SP is an interesting issue that is worthy of further investigation.

To understand the mechanisms by which SP inhibited MuV infection, we explored the targets acted upon by the antiviral factor. A time-dependent pre-incubation of MuV with SP was required for the antiviral effect. By contrast, the pre-treatment of HeLa cells with SP did not alter MuV infection. These results suggest that the antiviral factor acted on viruses and did not act on target cells. These results differ the observation that semen inhibited ZIKV infection by acting on target cells *via* extracellular vesicles (12), suggesting that semen possesses different antiviral components against viral infection through distinct mechanisms. Although SP is highly toxic to cell culture *in vitro*, we used a low dose of 1% SP and treated cells for a short time of 1 h to reduce the cytotoxicity. We provided evidence that the treatment of HeLa cells with 1% SP up to 2 h did not significantly impair cell viability and did not inhibit MuV infection, which excluded involvement of the cytotoxic effect in the SP inhibition of MuV infection.

SP is principally produced by accessory sex glands, including the seminal vesicle and prostate glands, which contribute to approximately 70 and 25% of SP, respectively (38, 39). The epididymis also produces ~5% of SP. An antiviral effect was only observed with PF, whereas SVF and EF did not inhibit MuV infection, suggesting that the antiviral component in SP was produced by the prostate. Numerous viruses have been found and persist long-term in the testis because of the testicular immunoprivileged status (3). Viruses may be shed from the testis into semen. In addition to the mucosal barrier and viral tropism, the production of an antiviral factor by the prostate gland should restrict the overall sexual transmission of viruses.

In contrast to the antiviral effects of semen, several previous studies focused on the role of semen in facilitating HIV-1 infection (32). These studies demonstrated that seminal amyloid fibrils enhanced HIV-1 infection by facilitating the attachment of HIV-1 to targets cells (14). This enhancement was also reported for HCMV infection (16). Notably, a recent study demonstrated that SP inhibited HCMV infection (13). Our present study provided substantial evidence that SP inhibited MuV infection of different cell types, including human cervical carcinoma cell lines, mouse primary epididymal epithelial cells, and a mouse Sertoli cell line. We showed that the antiviral component produced by the prostate and acted directly on the virus. Moreover, we found that SP also inhibited HSV-1, AD-5, and DeV-2 infection. The discrepancies in the results from these different studies have yet to be resolved. We realize that seminal amyloid fibrils always promote infection of different viruses, whereas the effect of whole SP on viral infection remain controversial. Considering that different virus strains and target cells were used in the previous studies, the effect of SP on viral infection should depend on the virus strains and host cells through different mechanisms. The virus- and host cell-specific antiviral effect of SP is an interesting issue for future study. Notably, the infected or inflammatory status of the male genital tract may impact HIV-1 infection (19). Since MuV has a tropism for the testis and epididymis and induces a severe inflammation in these organs, the potential modification of SP due to inflammation in the male genital tract may impact the antiviral effect of SP, which should be considered and worthy of clarification.

In summary, the immunoprivileged status of the male reproductive tract provides a sanctuary for viruses to escape immune surveillance. These viruses may shed into semen, thereby transmitting *via* sexual activity. It is important for the male reproductive system to adopt mechanisms that inhibit viral infection for restricting sexual transmission of the viruses. In the present study, we characterized a pan-antiviral property of SP and PF that potently inhibited infection of various types of cells by different viruses. Our results provided novel insights into the antiviral effect of SP and we believe that the isolation of specific antiviral factors from semen may benefit antiviral therapy.

DATA AVAILABILITY STATEMENT

The original contributions presented in the study are included in the article/**Supplementary Material**. Further inquiries can be directed to the corresponding author.

ETHICS STATEMENT

The studies involving human participants were reviewed and approved by the Institutional Review Board of Institute of Basic Medical Sciences, Chinese Academy of Medical Sciences. The patients/participants provided their written informed consent to participate in this study. Written informed consent was obtained from the individual(s) for the publication of any potentially identifiable images or data included in this article.

AUTHOR CONTRIBUTIONS

RC, WZ, MG, and DH designed the experiments. RC, WZ, MG, FW, HW, WLi, YG, BL, SC, WLu, XY, and AL performed the experiments. RC, WZ, MG, FW, RH, YC, and DH analyzed the data. DH, RC, WZ, and MG wrote the paper, with the other authors providing editorial comments. All authors contributed to the article and approved the submitted version.

FUNDING

This work was supported by grants from the National Key R&D program of China (Nos. 2018YFC1003900 and 2016YFA0101001), the National Natural Science Foundation of China (No. 82071633), CAMS Initiative for Innovative Medicine (Nos. 2017-I2M-B&R-06 and 2017-I2M-3-007).

SUPPLEMENTARY MATERIAL

The Supplementary Material for this article can be found online at: https://www.frontiersin.org/articles/10.3389/fimmu.2021.580454/full#supplementary-material

Supplementary Figure 1 | Long-term effect of SP on cell viability. HeLa cells were incubated with 1.0% SP for the specific durations. Culture media were replaced with fresh complete media without SP. The cell viability was assessed using the CCK-8 assay 48 h after the medium replacements. Data are presented as means ± SEM of three experiments. $^{*}P < 0.05$, $^{**}P < 0.01$.

Supplementary Figure 2 | SP effect on cells and MuV. HeLa cells were pre-incubated with 1% SP (C+SP) for 1 h and then transfected with 1.0 MOI MuV. MuV was pre-incubated with 1% SP (MuV+SP) and then transfected HeLa for 1 h. HeLa cells were transfected with MuV without SP served as the control (Ctrl). At 48 h after infection, MuV-NP RNA (left panel) and protein (right panel) levels were determined using real-time qRT-PCR and Western blot, respectively. Data are the means ± SEM of three experiments and images represent at least three independent experiments. $^{**}P < 0.01$.

Supplementary Figure 3 | Temperature-dependent antiviral effect of SP. MuV was incubated with 1% SP (+) or without SP (–) for 2 h at 4, 37, or 45°C. HeLa cells were infected with 1.0 MOI MuV. MuV-NP RNA and protein levels were determined using real-time qRT-PCR and Western blot. Data are the means ± SEM of three experiments. Images represent three independent experiments. $^{*}P < 0.05$, $^{**}P < 0.01$.

Supplementary Figure 4 | Efficiency of enzymes. **(A)** Proteinase K (ProK). Seminal plasma (SP) was incubated with 300 μg/ml (+) or without (–) ProK at 37°C for 5 h and then heated in boiling water for 5 min. Each sample (2 μl/well) was loaded for SDS-PAGE with 10% polyacrylamide gel. Proteins were visualized after staining with Coomassie blue and following by decoloration. Molecular sizes were referred by protein markers (M). **(B, C)** Nucleic acid enzymes. Genomic DNA and total RNA were isolated from HeLa cells. DNA **(B)** or RNA **(C)** were treated with 200 U/ml DNase I or 200 μg/ml RNase A at 37°C for 5 h. DNA and RNA were determined after electrophoresis in 1% agarose. Images are the representatives of at least three independent experiments.

Supplementary Figure 5 | PNGase F and lipase treatments. Seminal plasma (SP) was treated with 200 U/ml PNGase F or 100 U/ml lipase at 37°C for 5 h. MuV was incubated with SP for 2 h. MuV without SP served as the control (Ctrl). HeLa cells were infected with 1.0 MOI MuV. MuV-NP RNA (left panel) and protein (right panel) levels were determined at 48 h after infection using real-time qRT-PCR and Western blot, respectively. Images represent three experiments. Data are the means ± SEM of three experiments. $^{**}P < 0.01$.

Supplementary Figure 6 | Effect of enzymes on MuV infection. **(A)** Proteinase K (ProK), DNase I, and RNase A were heated in boiling water for 5 min. MuV was incubated with 300 μg/ml Pro K, 200 U/ml DNase I, and 200 μg/ml RNase A for 5 h. MuV without enzymes served as the control (Ctrl). HeLa cells were infected with 1.0 MOI MuV, and MuV-NP RNA (left panel) and protein (right panel) were determined at 48 h after MuV infection. **(B)** PNGase F and lipase were heated in boiling water for 5 min. MuV was incubated with 200 U/ml PNGase F or 100 U/ml lipase for 5 h. HeLa cells were infected and MuV-NP was determined as described in **(A)**. Data are the means ± SEM of three experiments, and images are the representatives of three experiments.

Supplementary Figure 7 | Fractions of seminal plasma (SP). SP was separated to four fractions by ultrafiltration using 100 kDa and 3 kDa filter devices. The retentates (Ret) and filtrates (Fil) of the two filters were subjected to SDS-PAGE with 10% polyacrylamide gel. The protein components were visualized after Coomassie blue staining and decoloration. Protein sizes were referred by molecular markers (M). Images represent three experiments.

REFERENCES

1. Salam AP, Horby PW. The breadth of viruses in human semen. *Emerg Infect Dis* (2017) 23(11):1922–4. doi: 10.3201/eid2311.171049
2. Feldmann H. Virus in Semen and the Risk of Sexual Transmission. *N Engl J Med* (2018) 378(15):1440–1. doi: 10.1056/NEJMe1803212
3. Le Tortorec A, Matusali G, Mahe D, Aubry F, Mazaud-Guittot S, Houzet L, et al. From ancient to emerging infections: the odyssey of viruses in the male genital tract. *Physiol Rev* (2020) 100(3):1349–414. doi: 10.1152/physrev.00021.2019
4. Frouard J, Le Tortorec A, Dejucq-Rainsford N. In vitro models for deciphering the mechanisms underlying the sexual transmission of viruses at the mucosal level. *Virology* (2018) 515:1–10. doi: 10.1016/j.virol.2017.11.023
5. Sabatte J, Remes Lenicov F, Cabrini M, Rodriguez Rodrigues C, Ostrowski M, Ceballos A, et al. The role of semen in sexual transmission of HIV: beyond a carrier for virus particles. *Microbes Infect* (2011) 13(12-13):977–82. doi: 10.1016/j.micinf.2011.06.005
6. O'Connor TJ, Kinchington D, Kangro HO, Jeffries DJ. The activity of candidate virucidal agents, low pH and genital secretions against HIV-1 in vitro. *Int J STD AIDS* (1995) 6(4):267–72. doi: 10.1177/095646249500600409

7. Martellini JA, Cole AL, Venkataraman N, Quinn GA, Svoboda P, Gangrade BK, et al. Cationic polypeptides contribute to the anti-HIV-1 activity of human seminal plasma. *FASEB J* (2009) 23(10):3609–18. doi: 10.1096/fj.09-131961
8. Madison MN, Jones PH, Okeoma CM. Exosomes in human semen restrict HIV-1 transmission by vaginal cells and block intravaginal replication of LP-BM5 murine AIDS virus complex. *Virology* (2015) 482:189–201. doi: 10.1016/j.virol.2015.03.040
9. Madison MN, Roller RJ, Okeoma CM. Human semen contains exosomes with potent anti-HIV-1 activity. *Retrovirology* (2014) 11:102. doi: 10.1186/s12977-014-0102-z
10. Welch JL, Kaddour H, Schlievert PM, Stapleton JT, Okeoma CM. Semen exosomes promote transcriptional silencing of HIV-1 by disrupting NF-kB/Sp1/Tat circuitry. *J Virol* (2018) 92(21):e00731–18. doi: 10.1128/JVI.00731-18
11. Ouattara LA, Anderson SM, Doncel GF. Seminal exosomes and HIV-1 transmission. *Andrologia* (2018) 50(11):e13220. doi: 10.1111/and.13220
12. Muller JA, Harms M, Kruger F, Gross R, Joas S, Hayn M, et al. Semen inhibits Zika virus infection of cells and tissues from the anogenital region. *Nat Commun* (2018) 9(1):2207. doi: 10.1038/s41467-018-04442-y
13. Lippold S, Braun B, Kruger F, Harms M, Muller JA, Gross R, et al. Natural Inhibitor of Human Cytomegalovirus in Human Seminal Plasma. *J Virol* (2019) 93(6):e01855–18. doi: 10.1128/jvi.01855-18
14. Munch J, Rucker E, Standker L, Adermann K, Goffinet C, Schindler M, et al. Semen-derived amyloid fibrils drastically enhance HIV infection. *Cell* (2007) 131(6):1059–71. doi: 10.1016/j.cell.2007.10.014
15. Torres L, Ortiz T, Tang Q. Enhancement of herpes simplex virus (HSV) infection by seminal plasma and semen amyloids implicates a new target for the prevention of HSV infection. *Viruses* (2015) 7(4):2057–73. doi: 10.3390/v7042057
16. Tang Q, Roan NR, Yamamura Y. Seminal plasma and semen amyloids enhance cytomegalovirus infection in cell culture. *J Virol* (2013) 87 (23):12583–91. doi: 10.1128/JVI.02083-13
17. Bart SM, Cohen C, Dye JM, Shorter J, Bates P. Enhancement of Ebola virus infection by seminal amyloid fibrils. *Proc Natl Acad Sci U S A* (2018) 115 (28):7410–5. doi: 10.1073/pnas.1721646115
18. Sabatte J, Faigle W, Ceballos A, Morelle W, Rodriguez Rodrigues C, Remes Lenicov F, et al. Semen clusterin is a novel DC-SIGN ligand. *J Immunol* (2011) 187(10):5299–309. doi: 10.4049/jimmunol.1101889
19. Camus C, Matusali G, Bourry O, Mahe D, Aubry F, Bujan L, et al. Comparison of the effect of semen from HIV-infected and uninfected men on CD4+ T-cell infection. *AIDS* (2016) 30(8):1197–208. doi: 10.1097/QAD.0000000000001048
20. Rubin S, Eckhaus M, Rennick LJ, Bamford CG, Duprex WP. Molecular biology, pathogenesis and pathology of mumps virus. *J Pathol* (2015) 235 (2):242–52. doi: 10.1002/path.4445
21. Masarani M, Wazait H, Dinneen M. Mumps orchitis. *J R Soc Med* (2006) 99 (11):573–5. doi: 10.1258/jrsm.99.11.573
22. Bjorvatn B. Mumps virus recovered from testicles by fine-needle aspiration biopsy in cases of mumps orchitis. *Scand J Infect Dis* (1973) 5(1):3–5. doi: 10.3109/inf.1973.5.issue-1.02
23. Wu H, Zhao X, Wang F, Jiang Q, Shi L, Gong M, et al. Mouse Testicular Cell Type-Specific Antiviral Response against Mumps Virus Replication. *Front Immunol* (2017) 8:117. doi: 10.3389/fimmu.2017.00117
24. Jiang Q, Wang F, Shi L, Zhao X, Gong M, Liu W, et al. C-X-C motif chemokine ligand 10 produced by mouse Sertoli cells in response to mumps virus infection induces male germ cell apoptosis. *Cell Death Dis* (2017) 8(10): e3146. doi: 10.1038/cddis.2017.560
25. Le Goffic R, Mouchel T, Ruffault A, Patard JJ, Jegou B, Samson M. Mumps virus decreases testosterone production and gamma interferon-induced protein 10 secretion by human leydig cells. *J Virol* (2003) 77(5):3297–300. doi: 10.1128/jvi.77.5.3297-3300.2003
26. Wu H, Jiang X, Gao Y, Liu W, Wang F, Gong M, et al. Mumps virus infection disrupts blood-testis barrier through the induction of TNF-alpha in Sertoli cells. *FASEB J* (2019) 33(11):12528–40. doi: 10.1096/fj.201901089R
27. Le Tortorec A, Denis H, Satie AP, Patard JJ, Ruffault A, Jegou B, et al. Antiviral responses of human Leydig cells to mumps virus infection or poly I:C stimulation. *Hum Reprod* (2008) 23(9):2095–103. doi: 10.1093/humrep/den207
28. Wang F, Chen R, Jiang Q, Wu H, Gong M, Liu W, et al. Roles of Sialic Acid, AXL, and MER Receptor Tyrosine Kinases in Mumps Virus Infection of Mouse Sertoli and Leydig Cells. *Front Microbiol* (2020) 11:1292:1292. doi: 10.3389/fmicb.2020.01292
29. Xu P, Huang Z, Gao X, Michel FJ, Hirsch G, Hogan RJ, et al. Infection of mice, ferrets, and rhesus macaques with a clinical mumps virus isolate. *J Virol* (2013) 87(14):8158–68. doi: 10.1128/jvi.01028-13
30. Kubota M, Takeuchi K, Watanabe S, Ohno S, Matsuoka R, Kohda D, et al. Trisaccharide containing alpha2,3-linked sialic acid is a receptor for mumps virus. *Proc Natl Acad Sci U S A* (2016) 113(41):11579–84. doi: 10.1073/pnas.1608383113
31. Zhu W, Zhao S, Liu Z, Cheng L, Wang Q, Yan K, et al. Pattern recognition receptor-initiated innate antiviral responses in mouse epididymal epithelial cells. *J Immunol* (2015) 194(10):4825–35. doi: 10.4049/jimmunol.1402706
32. Doncel GF, Joseph T, Thurman AR. Role of semen in HIV-1 transmission: inhibitor or facilitator? *Am J Reprod Immunol* (2011) 65(3):292–301. doi: 10.1111/j.1600-0897.2010.00931.x
33. Dejucq N, Jegou B. Viruses in the mammalian male genital tract and their effects on the reproductive system. *Microbiol Mol Biol Rev* (2001) 65(2):208–31. doi: 10.1128/mmbr.65.2.208-231.2001
34. Liu W, Han R, Wu H, Han D. Viral threat to male fertility. *Andrologia* (2018) 50(11):e13140. doi: 10.1111/and.13140
35. Li N, Wang T, Han D. Structural, cellular and molecular aspects of immune privilege in the testis. *Front Immunol* (2012) 3:152. doi: 10.3389/fimmu.2012.00152
36. Autiero M, Gaubin M, Mani JC, Castejon C, Martin M, el Marhomy S, et al. Surface plasmon resonance analysis of gp17, a natural CD4 ligand from human seminal plasma inhibiting human immunodeficiency virus type-1 gp120-mediated syncytium formation. *Eur J Biochem* (1997) 245(1):208–13. doi: 10.1111/j.1432-1033.1997.00208.x
37. Conzelmann C, Groß R, Zou M, Krüger F, Görgens A, Gustafsson MO, et al. Salivary extracellular vesicles inhibit Zika virus but not SARS-CoV-2 infection. *J Extracell Vesicles* (2020) 9(1):1808281. doi: 10.1080/20013078.2020.1808281
38. Gonzales GF. Function of seminal vesicles and their role on male fertility. *Asian J Androl* (2001) 3(4):251–8.
39. Verze P, Cai T, Lorenzetti S. The role of the prostate in male fertility, health and disease. *Nat Rev Urol* (2016) 13(7):379–86. doi: 10.1038/nrurol.2016.89

Conflict of Interest: The authors declare that the research was conducted in the absence of any commercial or financial relationships that could be construed as a potential conflict of interest.

frontiers in Immunology

MINI REVIEW
published: 18 March 2021
doi: 10.3389/fimmu.2021.582946

Mumps Orchitis: Clinical Aspects and Mechanisms

Han Wu[1,2], *Fei Wang*[2], *Dongdong Tang*[3] *and Daishu Han*[2]*

[1] Department of Immunology, Shenzhen University School of Medicine, Shenzhen, China, [2] Institute of Basic Medical Sciences, School of Basic Medicine, Peking Union Medical College, Chinese Academy of Medical Sciences, Beijing, China, [3] Reproductive Medicine Center, Department of Obstetrics and Gynecology, The First Affiliated Hospital of Anhui Medical University, Hefei, China

The causative agent of mumps is a single-stranded, non-segmented, negative sense RNA virus belonging to the *Paramyxoviridae* family. Besides the classic symptom of painfully swollen parotid salivary glands (parotitis) in mumps virus (MuV)-infected men, orchitis is the most common form of extra-salivary gland inflammation. Mumps orchitis frequently occurs in young adult men, and leads to pain and swelling of the testis. The administration of MuV vaccines in children has been proven highly effective in reducing the incidence of mumps. However, a recent global outbreak of mumps and the high rate of orchitis have recently been considered as threats to male fertility. The pathogenesis of mumps orchitis remains largely unclear due to lack of systematic clinical data analysis and animal models studies. The alarming increase in the incidence of mumps orchitis and the high risk of the male fertility have thus become a major health concern. Recent studies have revealed the mechanisms by which MuV-host cells interact and MuV infection induces inflammatory responses in testicular cells. In this mini-review, we highlight advances in our knowledge of the clinical aspects and possible mechanisms of mumps orchitis.

Keywords: mumps, MuV, orchitis, testis, infertility

OPEN ACCESS

Edited by:
Michael H. Lehmann, Ludwig Maximilian University of Munich, Germany

Reviewed by:
Nadine Krüger, Deutsches Primatenzentrum, Germany
Benhur Lee, Icahn School of Medicine at Mount Sinai, United States

***Correspondence:**
Daishu Han
dshan@ibms.pumc.edu.cn

Specialty section:
This article was submitted to Viral Immunology, a section of the journal Frontiers in Immunology

Received: *11 August 2020*
Accepted: *04 March 2021*
Published: *18 March 2021*

Citation:
Wu H, Wang F, Tang D and Han D (2021) Mumps Orchitis: Clinical Aspects and Mechanisms. Front. Immunol. 12:582946. doi: 10.3389/fimmu.2021.582946

INTRODUCTION

Mumps is a worldwide contagious disease caused by mumsp virus (MuV). MuV is mainly transmitted via the respiratory route. MuV infection results in painful inflammatory symptoms, such as parotitis, orchitis, oophoritis, aseptic meningitis, encephalitis and pancreatitis (1). Besides the typical painfully swollen parotitis in infected males, orchitis is the most common extra-salivary inflammation and an important etiological factor of male infertility (2).

Mumps orchitis generally manifests around a week after the onset of parotitis (1, 3). Approximately 30% of mumps orchitis in post pubertal males suffer from infertility or subfertility (3). Mumps orchitis may lead to the atrophy of germinal epithelium with spermatogenesis arrest and the disruption of steroidogenesis. MuV complications are not lethal, therefore lacking human samples to examine disease pathogenesis.

Current information on pathogenesis after MuV infection is largely based on investigation using animal models (4–8). We have recently examined mechanisms underlying MuV infection of testicular cells, MuV-induced immune responses and impairment of testicular functions in mouse

models, which provide novel insights into the pathology of mumps orchitis and related male infertility (9–11). In this mini review, we briefly summarize MuV biology and focus on mechanisms underlying pathogenesis of mumps orchitis.

MUV AND COMPLICATIONS

MuV belongs to the *Paramyxoviridae* family, which consists of enveloped particles that contain a non-segmented single negative-strand RNA genome (**Figure 1**). The MuV genome consists 15,384 nucleotides that encodes seven proteins: nucleoprotein (NP), polymerase (L), phosphoprotein (P), matrix protein (M), hemagglutinin/neuraminidase (HN), fusion protein (F), and small hydrophobic protein (SH) (12). MuV strains can be classified into 12 genotypes based on the nucleotide diversity of the SH gene (13, 14). Viral RNA encapsulated by NP is the template for replication. A complex of L and P acts as a replicase to transform the negative-strand RNA to a positive-strand RNA and as a transcriptase to generate mRNA. HN and F glycoproteins cooperatively mediate virus attachment and internalization to host cells via its receptor sialic acid that is present on the surface of most mammalian cell types.

MuV is initially transmitted via the respiratory route by the inhalation of contaminated droplets from an infected respiratory tract. Based on the array of symptoms, MuV would initially replicate within the lymphoid and reticuloendothelial tissue of the respiratory tract, which then lead to a transient viremia that may spread viruses into multiple organs (12). While it is assumed that MuV first infects the respiratory epithelium, the primary target cells for early infection and replication remain unclear. However, MuV has rarely been detected in blood, probably due to the coincident development of specific antibodies.

Besides asymptomatic and mild respiratory diseases in approximately 30% of infections, the typical characteristics of mumps include swollen parotitis, which is used to diagnose the disease. Parotid gland swelling is mostly bilateral, occurs 2–3 weeks after transmission, and lasts for 2–3 days. The symptom may persist for a week or more in minor cases. Following parotitis, MuV infection can lead to inflammation in the reproductive and central nerve systems, including orchitis, oophoritis, encephalitis, and meningitis (1). MuV may also result in myocarditis, pancreatitis and nephritis. While the complications are mostly self-limiting, long-term sequelae such as infertility, paralysis, hydrocephalus and deafness can occur. Mumps orchitis is the most concerned extra-parotid gland inflammation due to its detrimental effect on human reproduction.

CLINICAL ASPECTS OF MUMPS ORCHITIS

Vaccination and Incidences of Mumps Orchitis

In the pre-vaccine era, mumps was an infectious disease that was most commonly transmitted among children and was mainly

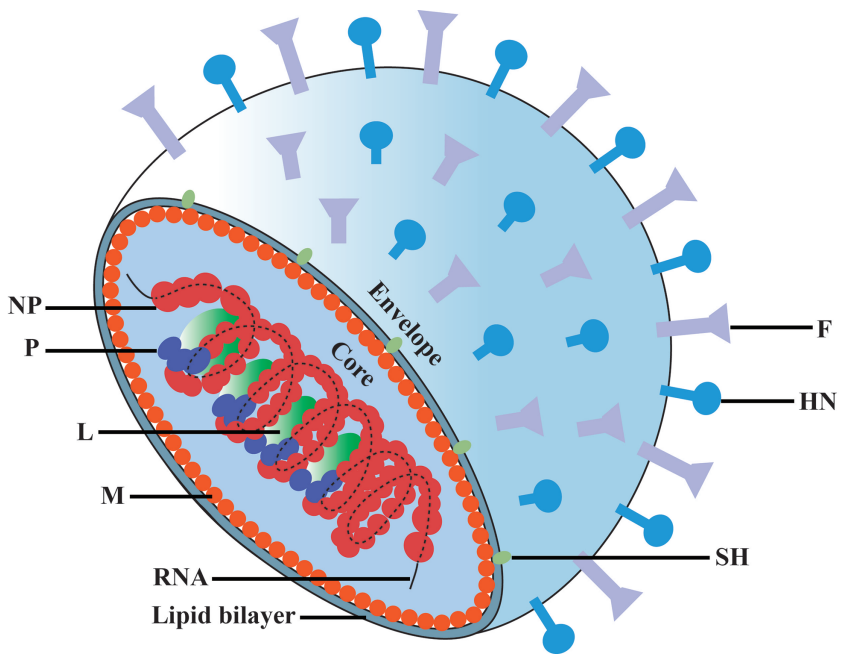

FIGURE 1 | Schematic diagram of mumps virus. The MuV core is enveloped by matrix protein (M) and lipid bilayer containing small hydrophobic protein (SH), spike fusion protein (F) and hemagglutinin-neuramindase (HN). The genomic RNA combines with nucleoprotein (NP), polymerase (L) and phosphoprotein (P) to form the core of the helical nucleocapsid.

complicated with parotitis (15, 16). With routine MuV vaccination, mumps incidence has dramatically declined. However, there have been large outbreaks of mumps worldwide in the past decades, including vaccinated populations (17–31). In China, the mumps vaccine was first introduced in the National Immunization Program in 2007 (32). From June 2020, the policy had changed to receive two doses of trivalent measles, mumps and rubella (MMR) vaccine. The annual occurrence of mumps cases from 2009 to 2019 is shown in **Figure 2**. After high vaccination coverage, mumps incidence dropped by half in 2016 from its peak in 2012. Notably, mumps incidences slightly increased from 2017 to 2019. This may be due to the fact that more than 10 years have passed since the first one dose vaccine was administered, and vaccine effectiveness has declined.

The recent resurgence of mumps mainly involved adolescents and young adults, with high rates of orchitis frequently reported (3, 33–35). Orchitis is the most common complication of mumps and occurs in as high as 40% of all mumps cases in young adult men (36). Mumps orchitis is mostly unilateral, but can occur bilaterally in 10–30% of cases (37). Unvaccinated postpubertal males are susceptible to virus outbreaks and are at high risk of developing mumps orchitis. In China, the vaccination rate of men born in the 1990s, who are now 30 years old, is low due to lacking MMR vaccination program in less developed areas. Thus, it is essential to be aware of this epidemiological shift and the resurgence of mumps orchitis in the clinic. Cases of orchitis following MMR vaccination are reported in post-pubertal adults, suggesting that the MMR vaccination may have an adverse effect on the testis in certain young adults (38–41). Therefore, whether unvaccinated male in this age group should be offered the MMR vaccine requires in-depth and carefully evaluation.

Clinical Manifestations

Mumps orchitis usually occurs at about one week after the onset of parotitis in young adult males with MuV infection. The onset of orchitis is associated with constitutional symptoms, such as headache and fever and later manifests as testicular swollen and pain. Examination of the scrotum generally indicates swelling testes, associated tenderness, and inflammation of the scrotum. Epididymitis also occurs in most of the mumps orchitis cases and results in mumps epididymo-orchitis (42, 43). A recent study demonstrates that the epididymal head is mostly involved in mumps epididymo-orchitis, which is in contrast to bacterial epididymitis that commonly occurs in the cauda epididymis (44, 45). During the acute phase, the endocrine function of the testes is altered, e.g., decreased testosterone levels. Some cases also show increased luteinizing hormone (LH) and follicle-stimulating hormone (FSH) levels (46). The acute symptoms can resolve within two weeks; however, testicular atrophy can occur in half of the orchitis patients and is characterized by an oblong shape, low echogenicity, and decreased vascularity based on ultrasonographic findings (3, 47). However, seminal abnormalities, including sperm count, motility and morphology, may sustain for years after recovery (37), suggesting the abnormal spermatogenesis can occur.

Diagnostic and Therapeutic Approaches

There is no standard criteria procedure for MuV diagnosis because it is not a common condition that is observed in hospital. Diagnosis of MuV is mainly based on clinical complication and laboratory testing. Orchitis characteristically presents with swollen and pain testes. Ultrasonography can provide image features, including low echogenicity, hypervascularity, and increased volume of the testes and epididymis (43, 48). Testicular inflammation and hydrocele could also be detected. The routine urine analysis is necessary for diagnosing the mumps orchitis to rule out bacterial infection (33).

The definitive diagnosis of mumps orchitis should be based on laboratory tests. The presence of MuV in saliva or seminal fluid can be determined by real time RT-PCR. The MuV-specific IgM and IgG antibodies in blood can be measured by ELISA for serological markers of MuV infection. A positive serum IgM or a four-fold increase in IgG level is considered serologically positive for MuV infection (49). While MuV can be isolated from the seminal fluid within two weeks after symptom onset (50), the test for viral infectivity is usually not performed in the clinical diagnosis due to the complicated procedure for this test.

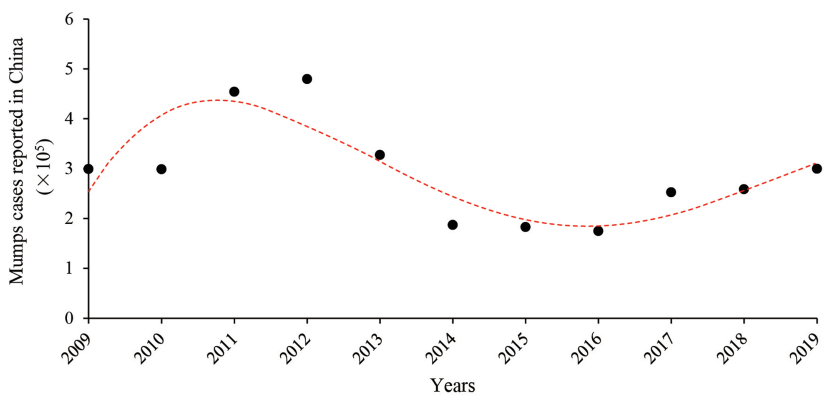

FIGURE 2 | Annual mumps cases reported in China from 2009 to 2019. Data come from reports of the National Health Commission of China.

MuV infection is mostly self-limiting, and there is currently no specific antiviral therapy available. The treatment for mumps orchitis generally includes supportive procedures, including bed rest, scrotal support, and analgesic and anti-inflammatory drugs against pain and fever. Symptoms can resolve with treatment in 4–10 days (51). Steroid drugs were used to diminish testicular pain and swelling, but it does not alter the clinical course and prevent subsequent atrophy. Interferon has been used in a series of cases to cure mumps orchitis; however, this is a controversial method because there is conflicting evidence on its therapeutic effect. Erpenbach et al. claimed to have prevented testicular damage and infertility in four patients who had bilateral mumps orchitis by using systematic interferon for seven days (52). However, Yeniyol et al. found that interferon is not effective in preventing testicular atrophy because 40% of patients presents evidence of total atrophy of seminiferous tubules on testicular biopsies performed during follow-up (53). A recent study that assessed a series of 56 cases of mumps orchitis treated with interferon also showed some kind of hormone or sperm impairment in most patients during the later follow up period, while only two patients (14%) were considered free of sequelae (3). Although some treatments can diminish the complications of acute mumps orchitis, the preventive and therapeutic approaches of the orchitis-caused testicular damage and subfertility/infertility require establishment.

MECHANISMS OF MUMPS ORCHITIS

It is difficult to study the pathogenesis of mumps orchitis in humans due to the lack of samples. Recent studies using mouse models provide insights to mechanisms by which MuV infects testicular cells and impairs testicular functions (**Figure 3**).

MuV Receptors and Testis Tropism

It is well-known that MuV has high tropism to the testis (57). Thus, understanding the mechanism of receptor recognition by MuV is very important. Sialic acid, which is expressed on the cell surface as a terminal component of sugar chains, plays a role in mediating infection of many viruses, including influenza viruses (58), the Middle East respiratory syndrome coronavirus (59), and Zika virus (ZIKV) (60). A previous study demonstrated that MuV used a trisaccharide containing α2,3-linked sialic acid on the cell surface as a receptor that interacts with MuV attachment protein HN (61). The MuV-HN-receptor interaction triggers the activation of the F protein, causing fusion of the viral envelope with the plasma membrane and allowing cell entry (62). A very recent study has confirmed the presence of sialic acid on the surface of Sertoli cells (SCs) and Leydig cells (LCs) (63). Depletion of sialic acid by sialidase decreases MuV internalization into SCs and LCs, but does not affect MuV binding to these cells (63). These results suggest that other co-receptors for MuV binding to testicular cells exist. Recently, two novel glycan motifs, sialyl Lewis^X (SLe^X) and the GM2 ganglioside (GM2-glycan), have been shown to serve as MuV receptors (64). Whether these receptors function for MuV tropism toward testicular cells requires further investigation.

Other types of cell receptors such as AXL and MER, which are members of a subfamily of receptor tyrosine kinases, have been suggested as potential candidates for MuV tropism. AXL and MER are abundantly expressed in SCs and LCs and play important roles in regulating testicular immune privilege (65). Both AXL and MER can interact with the ligands Gas6 and protein S that in turn bind to the surface of enveloped viruses (66). Several studies have demonstrated that AXL facilitates infection of multiple viruses, including Ebola virus (67), influenza virus (68), and ZIKV (69). AXL and MER have been suggested to function as binding or entry factors for MuV based on the observation that these are highly expressed in the testis during MuV infection (63, 70). Knockout of *Axl*, *Mer*, and both *Axl* and *Mer* did not affect MuV binding to SCs and LCs, and the levels of MuV internalized into SCs and LCs were comparable (63). Thus, AXL and MER were not required as binding or entry factors for MuV in these cells. However, a genetic study showed that double knockout of both *Axl* and *Mer* remarkably decreased MuV replication, whereas single knockout of either *Axl* or *Mer* barely affected MuV replication. Additionally, a study using an inhibitor of AXL and MER showed no change in MuV replication in type 1 interferon receptor knockout (*Ifnar1*$^{-/-}$) SCs and LCs, while it significantly decreased in wild-type cells, suggesting a redundant role of AXL and MER in facilitating MuV replication in SCs and LCs by inhibiting the antiviral IFN signaling (63). These findings on the mechanism underlying receptors-mediated MuV binding, internalization and replication (**Figure 3**) may be helpful discovering the targets for the prevention of MuV infection.

MuV-Induced Immune Response in Testicular Cells

Due to the lack of testicular biopsy from mumps orchitis patients, it is difficult to investigate MuV infection and pathogenesis in the testis. Although humans are believed to be the only natural reservoir, MuV was experimentally used to infect various animal models to evaluate protective immunity against MuV (8, 71). Unfortunately, studies on the pathogenesis of orchitis in the animal models are limited. A current study found that MuV can infect the majority of mouse testicular cells, including SCs, LCs, testicular macrophages (TMs), and male germ cells (GCs) (9). However, MuV differentially replicates in these testicular cells. MuV replicated at relatively high efficiency rate in SCs compared with LCs and TMs. In contrast, MuV does not replicate in male GCs. These findings suggest that testicular cells exhibit different innate antiviral responses against MuV replication.

To understand the mechanisms underlying MuV-induced orchitis, a recent study investigated the pattern recognition receptors-initiated innate immune responses of testicular cells to MuV infection (11). MuV induces innate immune responses in mouse SCs and LCs through the activation of Toll-like receptor 2 (TLR2) and retinoic acid-inducible gene I (RIG-I) signaling pathways. MuV-initiated TLR2 signaling mainly induces pro-inflammatory cytokines (TNF-α and IL-6) as well as chemokines (MCP-1 and CXCL10), whereas the RIG-I

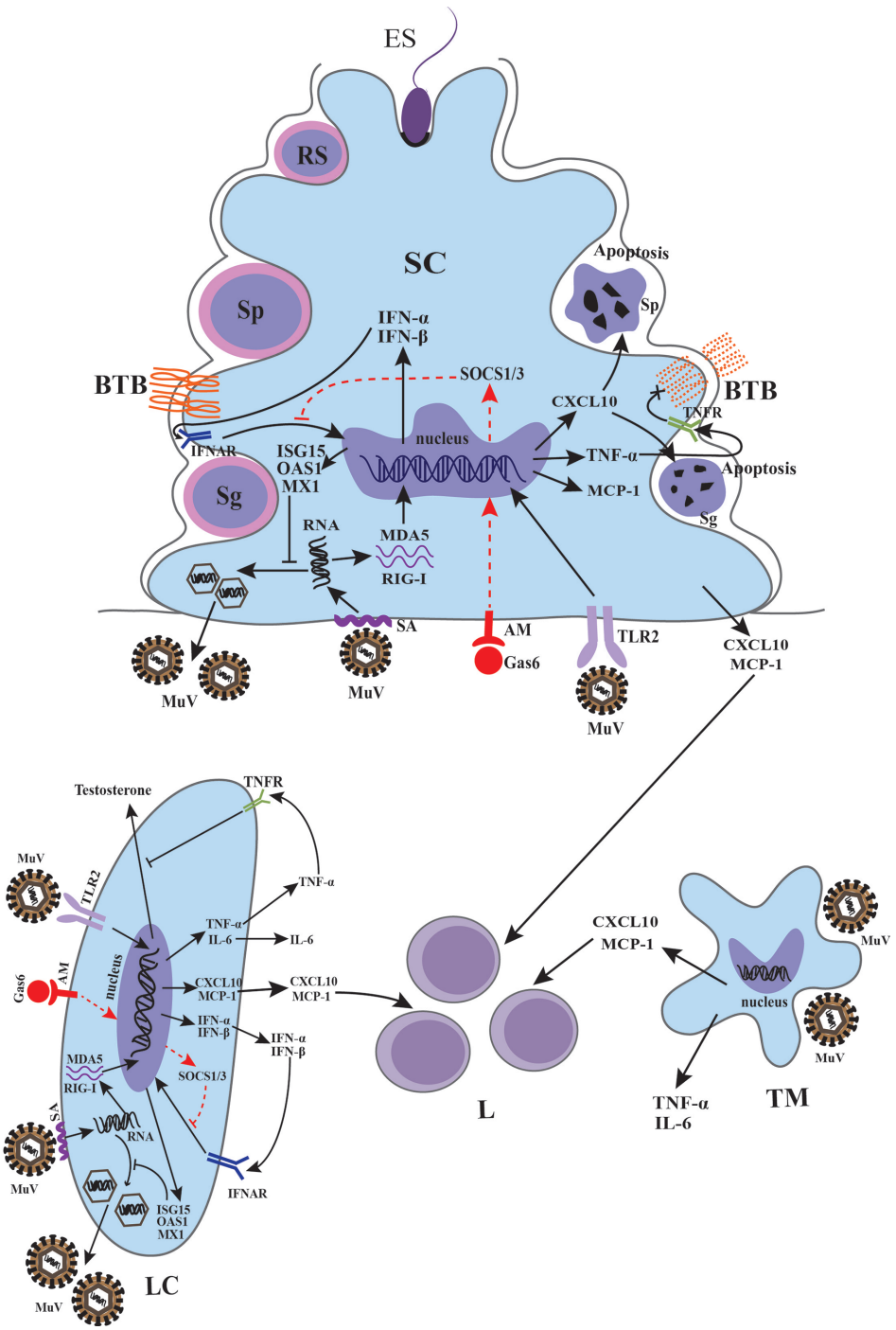

FIGURE 3 | Schematic of MuV infection of testicular somatic cells and downstream effects. Sialic acid (SA) on the surface of Sertoli cells (SCs) and Leydig cells (LCs) mediated MuV entry into cells. Gas6 and Axl/Mer (AM) receptor tyrosine kinase system facilitates MuV replication by inhibiting antiviral response. MuV triggers Toll-like receptor 2 (TLR2) and cytosolic RNA sensors MDA5/RIG-I signaling pathways, thereby inducing the expression of various immunoregulatory cytokines, including pro-inflammatory factors TNF-α and IL-6, chemokines CXCL10 and MCP-1, and type 1 interferons INF-α and IFN-β. IFN-α and IFN-β then induce the expression of various proteins, including ISG15, OAS1 and Mx1, that can inhibit MuV replication. MuV infection also induces the production of CXCL10, MCP-1, TNF-α and IL-6 by testicular macrophages (TM). CXCL10 produced by SC in response to MuV infection induces apoptosis of germ cells, whereas TNF-α disrupts blood-testis barrier (BTB) integrity and permeability. MuV infection of LC inhibits testosterone synthesis. MuV-induced TNF-α is presumably responsible for the MuV inhibition of testosterone synthesis. MCP-1 and CXCL10 produced by SC, LC and TM may recruit leukocytes (L), resulting in orchitis. Sg, spermatogonium; Sp, spermatocyte; RS, round spermatid; ES, elongated spermatid. SOCS, suppressor of cytokine signaling. →, promotion; ⊥, inhibition; ×, disruption of BTB. The red dashed line indicates a possible signaling pathway in SCs and LCs according to previous findings (54–56).

pathway principally participated in the induction of type 1 interferons (IFN-α and IFN-β). In response to MuV infection, SCs produced relatively high levels of pro-inflammatory cytokines and chemokines, but low levels of IFN-α and IFN-β compared to LCs. A previous study using a mouse model showed that mumps-associated gene geranylgeranyl diphosphate synthase 1 deficiency in SCs resulted in male infertility and abnormal activation of MAPK and NF-κB downstream of TLR2 signaling (72). These investigations suggest that TLR2 plays a crucial role in initiating the innate immune responses to MuV infection in testicular cells. However, the TLR2 ligand in MuV has yet to be identified. In contrast, TNF-α, IL-6, MCP-1, CXCL10, IFN-α and IFN-β were nearly undetectable in male GCs after MuV infection, suggesting a low level of innate immune response in GCs (11). MCP-1 and CXCL10 produced by TMs, SCs and LCs in response to MuV infection should facilitate the recruitment of leukocytes into the testis for MuV orchitis (**Figure 3**).

Usually, viral replication in infected cells is restricted by cellular innate antiviral responses. The production of IFNs is a universal mechanism of the host's defense against viral infection (73). IFN-β can inhibit MuV replication in SCs, LCs, and TMs by inducing the expression of antiviral proteins, including ISG15, OAS1, and MX1, but not in GCs. Remarkably, GCs and TMs are equipped with autophagy machineries, and autophagy restricts MuV replication in these cells. In contrast, autophagy is not involved in limiting MuV replication in LCs and SCs. These findings suggest a cell type-specific innate antiviral mechanisms against MuV replication in testicular cells.

Notably, viral infection in male GCs may be sexually transmitted to female partners and fetus, thus leading to virus parallel and vertical transmission (74). The antiviral defense of male GCs is particularly important not only for male fertility but also for limiting virus transmission. The innate antiviral responses in most type of cells after viral infection produce type 1 IFNs and various pro-inflammatory cytokines (75). The increased levels of certain pro-inflammatory cytokines can be harmful to spermatogenesis (76). However, autophagy directly uptakes and degrades viruses that invade GCs, without the induction of pro-inflammatory cytokines (77). Therefore, autophagy of male GCs should be suitable for the antiviral defense without harming spermatogenesis.

MuV Infection Damages Testis Function

The cytokines induced by viral infection can mediate organ dysfunction and tissue damage (78). We recently found that MuV infection induced the production of various pro-inflammatory cytokines and inhibited testosterone synthesis in LCs (11). The production of pro-inflammatory cytokines such as TNF-α by LCs after MuV infection may be responsible for the inhibition of testosterone synthesis by reducing the expression of enzymes for testosterone synthesis (79). However, one study showed that the testicular testosterone level was reduced in TNF-α knockout mice, which was probably caused by the augmentation of Mullerian inhibiting substance in the testis (80). TNF-α may play dual roles in the protection and disruption of the tissue functions dependent on its level under pathophysiological conditions. The high level of TNF-α in the testis due to infection and inflammation disrupts testicular functions (81, 82). Moreover, we demonstrated that the production of TNF-α and CXCL10 in SCs after MuV infection impaired blood-testis barrier (BTB) and induced GC apoptosis, respectively (10, 83). The BTB plays an important role in maintaining normal spermatogenesis. TNF-α produced by SCs in response to MuV infection impaired BTB formation by reducing the levels of occludin and zonula occludens 1 (ZO-1) (83). The finding is supported by a previous study that occludin is one of the target proteins of TNF-α in rat SCs (84). Moreover, a recent study showed that the exposure of SCs to inflammatory mediators derived from ZIKV-infected macrophages also led to the degradation of the ZO-1 protein, which correlated with increased BTB permeability (85). These findings suggest an adverse role of virus-induced production of inflammatory cytokines such as TNF-α. During spermatogenesis, a large number of novel antigens are produced by post-meiotic spermatids in seminiferous tubules after immune self-tolerance has been established (86). The production of autoantibodies against GC antigens is a common feature for orchitis patients. This may explain why mumps orchitis often causes male infertility in postpubertal and young adult men but rarely affects children when the spermatids have not yet been produced in the testes.

The deleterious effects of MuV infection on male GCs have also been examined in a recent study (10). The study showed that TNF-α produced by mouse SCs in response to MuV induced CXCL10 expression in autocrine manner. CXCL10 is a pleiotropic cytokine capable of exerting various functions, including the chemotaxis of leucocytes and induction of apoptosis (87). CXCR3, as the receptor of CXCL10, is expressed on the surface of male GCs. CXCL10 activates caspase-8/3 through CXCR3 that in turn induces GC apoptosis (10). Therefore, blocking CXCL10-CXCR3 signaling may alleviate GC degeneration caused by MuV infection.

Laboratory animal models are critical for the studies on the pathogenesis of MuV-induced diseases. Unfortunately, mice are not susceptible to MuV infection. Although MuV efficiently replicates in mouse testicular cells *in vitro*, this is not evident *in vivo* (11). The detrimental effects of ZIKV on the testis are only occurred in mice lacking interferon signaling but not in WT mice (88). A recent study showed that mice lacking type 1 interferon signaling were susceptible to MuV infection (71). Whether orchitis is generated in *Ifnar1*$^{-/-}$ mice after MuV inoculation remain unknown, and thus requires further investigation. Alternatively, a mouse cell-adapted MuV strain may be used to establish an orchitis model, but how far the observations in mouse models are relevant to human remains questionable.

CONCLUSIONS

The recent outbreaks occurring in highly vaccinated populations have sparked renewed interest in mumps and complications, particularly orchitis. There is a growing concern that a group of

mumps cases has shifted from children to young adults and is associated with a high rate of orchitis and severe reproductive problems. The mechanisms behind the development of mumps and orchitis are unknown. Several recent studies on MuV based on primary cells have improved our understanding of mumps virus pathogenesis with regard to MuV receptors-testicular cells interaction, innate immune responses to MuV infection, and detrimental effects on testicular function using mouse models. However, a number of knowledge gaps remain. MuV can effectively replicate in mouse testicular cells *in vitro*. The testis is an immunoprivileged organ for the protection of the spermatozoon from adverse immune response (89). Whether the testicular immune privilege status provides a refuge for MuV replication to escape immune surveillance requires clarification. Rare orchitis cases after the MMR vaccination were reported, suggesting a potential risk of the vaccination (38–41, 71). The pathogenesis of the vaccination-related orchitis remains uncertain and is worth investigating further. In-depth understanding of these questions would help in the development of preventative and therapeutic approaches for mumps orchitis and male infertility.

AUTHOR CONTRIBUTIONS

DH and HW designed the concept and wrote the manuscript. DT and FW collected materials and prepared figures. All authors contributed to the article and approved the submitted version.

FUNDING

This work was supported by grants from the National Key R&D program of China (Nos. 2018YFC1003900 and 2016YFA0101001), and the National Natural Science Foundation of China (Nos. 81701430 and 82071633).

REFERENCES

1. Hviid A, Rubin S, Mühlemann K. Mumps. *Lancet* (2008) 371:932–44. doi: 10.1016/s0140-6736(08)60419-5
2. Masarani M, Wazait H, Dinneen M. Mumps orchitis. *J R Soc Med* (2006) 99:573–5. doi: 10.1258/jrsm.99.11.573
3. Ternavasio-de la Vega HG, Boronat M, Ojeda A, Garcia-Delgado Y, Angel-Moreno A, Carranza-Rodriguez C, et al. Mumps orchitis in the post-vaccine era (1967-2009): a single-center series of 67 patients and review of clinical outcome and trends. *Med (Baltimore)* (2010) 89:96–116. doi: 10.1097/MD.0b013e3181d63191
4. Rozina EE, Hilgenfeldt M. Comparative study on the neurovirulence of different vaccine strains of parotitis virus in monkeys. *Acta Virol* (1985) 29:225–30.
5. McCarthy M, Jubelt B, Fay DB, Johnson RT. Comparative studies of five strains of mumps virus in vitro and in neonatal hamsters: evaluation of growth, cytopathogenicity, and neurovirulence. *J Med Virol* (1980) 5:1–15. doi: 10.1002/jmv.1890050102
6. Kilham L, Margolis G. Induction of congenital hydrocephalus in hamsters with attenuated and natural strains of mumps virus. *J Infect Dis* (1975) 132:462–6. doi: 10.1093/infdis/132.4.462
7. Parker L, Gilliland SM, Minor P, Schepelmann S. Assessment of the ferret as an in vivo model for mumps virus infection. *J Gen Virol* (2013) 94:1200–5. doi: 10.1099/vir.0.052449-0
8. Xu P, Huang Z, Gao X, Michel FJ, Hirsch G, Hogan RJ, et al. Infection of mice, ferrets, and rhesus macaques with a clinical mumps virus isolate. *J Virol* (2013) 87:8158–68. doi: 10.1128/JVI.01028-13
9. Wu H, Zhao X, Wang F, Jiang Q, Shi L, Gong M, et al. Mouse Testicular Cell Type-Specific Antiviral Response against Mumps Virus Replication. *Front Immunol* (2017) 8:117. doi: 10.3389/fimmu.2017.00117
10. Jiang Q, Wang F, Shi L, Zhao X, Gong M, Liu W, et al. C-X-C motif chemokine ligand 10 produced by mouse Sertoli cells in response to mumps virus infection induces male germ cell apoptosis. *Cell Death Dis* (2017) 8:e3146. doi: 10.1038/cddis.2017.560
11. Wu H, Shi L, Wang Q, Cheng L, Zhao X, Chen Q, et al. Mumps virus-induced innate immune responses in mouse Sertoli and Leydig cells. *Sci Rep* (2016) 6:19507. doi: 10.1038/srep19507
12. Rubin S, Eckhaus M, Rennick LJ, Bamford CG, Duprex WP. Molecular biology, pathogenesis and pathology of mumps virus. *J Pathol* (2015) 235:242–52. doi: 10.1002/path.4445
13. Jin L, Orvell C, Myers R, Rota PA, Nakayama T, Forcic D, et al. Genomic diversity of mumps virus and global distribution of the 12 genotypes. *Rev Med Virol* (2015) 25:85–101. doi: 10.1002/rmv.1819
14. Johansson B, Tecle T, Orvell C. Proposed criteria for classification of new genotypes of mumps virus. *Scand J Infect Dis* (2002) 34:355–7. doi: 10.1080/00365540110080043
15. Galazka AM, Robertson SE, Kraigher A. Mumps and mumps vaccine: a global review. *Bull World Health Organ* (1999) 77:3–14. doi: 10.1007/bf02727158
16. Edmunds WJ, Gay NJ, Kretzschmar M, Pebody RG, Wachmann H. Network EPES-e. The pre-vaccination epidemiology of measles, mumps and rubella in Europe: implications for modelling studies. *Epidemiol Infect* (2000) 125:635–50. doi: 10.1017/s0950268800004672
17. Vandermeulen C, Roelants M, Vermoere M, Roseeuw K, Goubau P, Hoppenbrouwers K. Outbreak of mumps in a vaccinated child population: a question of vaccine failure? *Vaccine* (2004) 22:2713–6. doi: 10.1016/j.vaccine.2004.02.001
18. Westphal DW, Eastwood A, Levy A, Davies J, Huppatz C, Gilles M, et al. A protracted mumps outbreak in Western Australia despite high vaccine coverage: a population-based surveillance study. *Lancet Infect Diseases* (2019) 19:177–84. doi: 10.1016/s1473-3099(18)30498-5
19. Qin W, Wang Y, Yang T, Xu XK, Meng XM, Zhao CJ, et al. Outbreak of mumps in a student population with high vaccination coverage in China: time for two-dose vaccination. *Hum Vaccin Immunother* (2019) 15:2106–11. doi: 10.1080/21645515.2019.1581526
20. Ma R, Lu L, Zhou T, Pan J, Chen M, Pang X. Mumps disease in Beijing in the era of two-dose vaccination policy, 2005-2016. *Vaccine* (2018) 36:2589–95. doi: 10.1016/j.vaccine.2018.03.074
21. Beleni AI, Borgmann S. Mumps in the Vaccination Age: Global Epidemiology and the Situation in Germany. *Int J Environ Res Public Health* (2018) 15:1618. doi: 10.3390/ijerph15081618
22. Willocks LJ, Guerendiain D, Austin HI, Morrison KE, Cameron RL, Templeton KE, et al. An outbreak of mumps with genetic strain variation in a highly vaccinated student population in Scotland. *Epidemiol Infect* (2017) 145:3219–25. doi: 10.1017/S0950268817002102
23. Patel LN, Arciuolo RJ, Fu J, Giancotti FR, Zucker JR, Rakeman JL, et al. Mumps Outbreak Among a Highly Vaccinated University Community-New York City, January-April 2014. *Clin Infect Dis* (2017) 64:408–12. doi: 10.1093/cid/ciw762
24. Havlickova M, Limberkova R, Smiskova D, Herrmannova K, Jirincova H, Novakova L, et al. Mumps in the Czech Republic in 2013: Clinical Characteristics, Mumps Virus Genotyping, and Epidemiological Links. *Cent Eur J Public Health* (2016) 24:22–8. doi: 10.21101/cejph.a4512
25. Nedeljkovic J, Kovacevic-Jovanovic V, Milosevic V, Seguljev Z, Petrovic V, Muller CP, et al. A Mumps Outbreak in Vojvodina, Serbia, in 2012 Underlines the Need for Additional Vaccination Opportunities for Young Adults. *PloS One* (2015) 10:e0139815. doi: 10.1371/journal.pone.0139815

26. Sane J, Gouma S, Koopmans M, de Melker H, Swaan C, van Binnendijk R, et al. Epidemic of mumps among vaccinated persons, The Netherlands, 2009-2012. *Emerg Infect Dis* (2014) 20:643–8. doi: 10.3201/eid2004.131681
27. Gilliland SM, Jenkins A, Parker L, Somdach N, Pattamadilok S, Incomserb P, et al. Vaccine-related mumps infections in Thailand and the identification of a novel mutation in the mumps fusion protein. *Biologicals* (2013) 41:84–7. doi: 10.1016/j.biologicals.2012.09.007
28. Barskey AE, Schulte C, Rosen JB, Handschur EF, Rausch-Phung E, Doll MK, et al. Mumps outbreak in Orthodox Jewish communities in the United States. *N Engl J Med* (2012) 367:1704–13. doi: 10.1056/NEJMoa1202865
29. Roberts C, Porter-Jones G, Crocker J, Hart J. Mumps outbreak on the island of Anglesey, North Wales, December 2008-January 2009. *Euro Surveill* (2009) 14:19109. doi: 10.2807/ese.14.05.19109-en
30. Cortese MM, Jordan HT, Curns AT, Quinlan PA, Ens KA, Denning PM, et al. Mumps vaccine performance among university students during a mumps outbreak. *Clin Infect Dis* (2008) 46:1172–80. doi: 10.1086/529141
31. Castilla J, Garcia Cenoz M, Barricarte A, Irisarri F, Nunez-Cordoba JM, Barricarte A. Mumps outbreak in Navarre region, Spain, 2006-2007. *Euro Surveill* (2007) 12:E070215.070211. doi: 10.2807/esw.12.07.03139-en
32. Zheng J, Zhou Y, Wang H, Liang X. The role of the China Experts Advisory Committee on Immunization Program. *Vaccine* (2010) 28 Suppl 1:A84–7. doi: 10.1016/j.vaccine.2010.02.039
33. Davis NF, McGuire BB, Mahon JA, Smyth AE, O'Malley KJ, Fitzpatrick JM. The increasing incidence of mumps orchitis: a comprehensive review. *BJU Int* (2010) 105:1060–5. doi: 10.1111/j.1464-410X.2009.09148.x
34. Centers for Disease Control and Prevention (CDC). Mumps epidemic–Iowa, 2006. *MMWR Morb Mortal Wkly Rep* (2006) 55:366–8.
35. Tae BS, Ham BK, Kim JH, Park JY, Bae JH. Clinical features of mumps orchitis in vaccinated postpubertal males: a single-center series of 62 patients. *Korean J Urol* (2012) 53:865–9. doi: 10.4111/kju.2012.53.12.865
36. A retrospective survey of the complications of mumps. *J R Coll Gen Pract* (1974) 24:552–6.
37. Bartak V. Sperm count, morphology and motility after unilateral mumps orchitis. *J Reprod Fertil* (1973) 32:491–4. doi: 10.1530/jrf.0.0320491
38. Clifford V, Wadsley J, Jenner B, Buttery JP. Mumps vaccine associated orchitis: Evidence supporting a potential immune-mediated mechanism. *Vaccine* (2010) 28:2671–3. doi: 10.1016/j.vaccine.2010.01.007
39. Kanda T, Mochida J, Takada S, Hori Y, Yamaguchi K, Takahashi S. Case of mumps orchitis after vaccination. *Int J Urol* (2014) 21:426–8. doi: 10.1111/iju.12305
40. Abdelbaky AM, Channappa DB, Islam S. Unilateral epididymo-orchitis: a rare complication of MMR vaccine. *Ann R Coll Surg Engl* (2008) 90:336–7. doi: 10.1308/003588408X285694
41. Suzuki M, Takizawa A, Furuta A, Yanada S, Iwamuro S, Tashiro K. A case of orchitis following vaccination with freeze-dried live attenuated mumps vaccine. *Nihon Hinyokika Gakkai Zasshi* (2002) 93:577–9. doi: 10.5980/jpnjurol1989.93.577
42. Wharton IP, Chaudhry AH, French ME. A case of mumps epididymitis. *Lancet* (2006) 367:702. doi: 10.1016/S0140-6736(06)68274-3
43. Tarantino L, Giorgio A, de Stefano G, Farella N. Echo color Doppler findings in postpubertal mumps epididymo-orchitis. *J Ultrasound Med* (2001) 20:1189–95. doi: 10.7863/jum.2001.20.11.1189
44. Park SJ, Kim HC, Lim JW, Moon SK, Ahn SE. Distribution of Epididymal Involvement in Mumps Epididymo-orchitis. *J Ultrasound Med* (2015) 34:1083–9. doi: 10.7863/ultra.34.6.1083
45. Yang DM, Kim SH, Kim HN, Kang JH, Seo TS, Hwang HY, et al. Differential diagnosis of focal epididymal lesions with gray scale sonographic, color Doppler sonographic, and clinical features. *J Ultrasound Med* (2003) 22:135–42; quiz 143-134. doi: 10.7863/jum.2003.22.2.135
46. Adamopoulos DA, Lawrence DM, Vassilopoulos P, Contoyiannis PA, Swyer GI. Pituitary-testicular interrelationships in mumps orchitis and other viral infections. *Br Med J* (1978) 1:1177–80. doi: 10.1136/bmj.1.6121.1177
47. Choi HI, Yang DM, Kim HC, Kim SW, Jeong HS, Moon SK, et al. Testicular atrophy after mumps orchitis: ultrasonographic findings. *Ultrasonography* (2020) 39:266–71. doi: 10.14366/usg.19097
48. Basekim CC, Kizilkaya E, Pekkafali Z, Baykal KV, Karsli AF. Mumps epididymo-orchitis: sonography and color Doppler sonographic findings. *Abdom Imaging* (2000) 25:322–5. doi: 10.1007/s002610000039
49. Krause CH, Molyneaux PJ, Ho-Yen DO, McIntyre P, Carman WF, Templeton KE. Comparison of mumps-IgM ELISAs in acute infection. *J Clin Virol* (2007) 38:153–6. doi: 10.1016/j.jcv.2006.10.010
50. Jalal H, Bahadur G, Knowles W, Jin L, Brink N. Mumps epididymo-orchitis with prolonged detection of virus in semen and the development of anti-sperm antibodies. *J Med Virol* (2004) 73:147–50. doi: 10.1002/jmv.10544
51. Casella R, Leibundgut B, Lehmann K, Gasser TC. Mumps orchitis: report of a mini-epidemic. *J Urol* (1997) 158:2158–61. doi: 10.1016/s0022-5347(01)68186-2
52. Erpenbach KH. Systemic treatment with interferon-alpha 2B: an effective method to prevent sterility after bilateral mumps orchitis. *J Urol* (1991) 146:54–6. doi: 10.1016/s0022-5347(17)37713-3
53. Yeniyol CO, Sorguc S, Minareci S, Ayder AR. Role of interferon-alpha-2B in prevention of testicular atrophy with unilateral mumps orchitis. *Urology* (2000) 55:931–3. doi: 10.1016/s0090-4295(00)00491-x
54. Rothlin CV, Ghosh S, Zuniga EI, Oldstone MB, Lemke G. TAM receptors are pleiotropic inhibitors of the innate immune response. *Cell* (2007) 131:1124–36. doi: 10.1016/j.cell.2007.10.034
55. Fenner JE, Starr R, Cornish AL, Zhang JG, Metcalf D, Schreiber RD, et al. Suppressor of cytokine signaling 1 regulates the immune response to infection by a unique inhibition of type I interferon activity. *Nat Immunol* (2006) 7:33–9. doi: 10.1038/ni1287
56. Piganis RA, De Weerd NA, Gould JA, Schindler CW, Mansell A, Nicholson SE, et al. Suppressor of cytokine signaling (SOCS) 1 inhibits type I interferon (IFN) signaling via the interferon alpha receptor (IFNAR1)-associated tyrosine kinase Tyk2. *J Biol Chem* (2011) 286:33811–8. doi: 10.1074/jbc.M111.270207
57. Bjorvatn B. Mumps virus recovered from testicles by fine-needle aspiration biopsy in cases of mumps orchitis. *Scand J Infect Dis* (1973) 5:3–5. doi: 10.3109/inf.1973.5.issue-1.02
58. Weis W, Brown JH, Cusack S, Paulson JC, Skehel JJ, Wiley DC. Structure of the influenza virus haemagglutinin complexed with its receptor, sialic acid. *Nature* (1988) 333:426–31. doi: 10.1038/333426a0
59. Li W, Hulswit RJG, Widjaja I, Raj VS, McBride R, Peng W, et al. Identification of sialic acid-binding function for the Middle East respiratory syndrome coronavirus spike glycoprotein. *Proc Natl Acad Sci U S A* (2017) 114:E8508–17. doi: 10.1073/pnas.1712592114
60. Tan CW, Huan Hor CH, Kwek SS, Tee HK, Sam IC, Goh ELK, et al. Cell surface alpha2,3-linked sialic acid facilitates Zika virus internalization. *Emerg Microbes Infect* (2019) 8:426–37. doi: 10.1080/22221751.2019.1590130
61. Kubota M, Takeuchi K, Watanabe S, Ohno S, Matsuoka R, Kohda D, et al. Trisaccharide containing alpha2,3-linked sialic acid is a receptor for mumps virus. *Proc Natl Acad Sci U S A* (2016) 113:11579–84. doi: 10.1073/pnas.1608383113
62. Kubota M, Okabe I, Nakakita SI, Ueo A, Shirogane Y, Yanagi Y, et al. Disruption of the Dimer-Dimer Interaction of the Mumps Virus Attachment Protein Head Domain, Aided by an Anion Located at the Interface, Compromises Membrane Fusion Triggering. *J Virol* (2020) 94:e01732–19. doi: 10.1128/JVI.01732-19
63. Wang F, Chen R, Jiang Q, Wu H, Gong M, Liu W, et al. Roles of Sialic Acid, AXL, and MER Receptor Tyrosine Kinases in Mumps Virus Infection of Mouse Sertoli and Leydig Cells. *Front Microbiol* (2020) 11:1292. doi: 10.3389/fmicb.2020.01292
64. Kubota M, Matsuoka R, Suzuki T, Yonekura K, Yanagi Y, Hashiguchi T. Molecular Mechanism of the Flexible Glycan Receptor Recognition by Mumps Virus. *J Virol* (2019) 93:e00344–19. doi: 10.1128/JVI.00344-19
65. Deng T, Chen Q, Han D. The roles of TAM receptor tyrosine kinases in the mammalian testis and immunoprivileged sites. *Front Biosci (Landmark Ed)* (2016) 21:316–27. doi: 10.2741/4390
66. Bhattacharyya S, Zagorska A, Lew ED, Shrestha B, Rothlin CV, Naughton J, et al. Enveloped viruses disable innate immune responses in dendritic cells by direct activation of TAM receptors. *Cell Host Microbe* (2013) 14:136–47. doi: 10.1016/j.chom.2013.07.005
67. Shimojima M, Takada A, Ebihara H, Neumann G, Fujioka K, Irimura T, et al. Tyro3 family-mediated cell entry of Ebola and Marburg viruses. *J Virol* (2006) 80:10109–16. doi: 10.1128/JVI.01157-06
68. Shibata T, Habiel DM, Coelho AL, Kunkel SL, Lukacs NW, Hogaboam CM. Axl receptor blockade ameliorates pulmonary pathology resulting from

primary viral infection and viral exacerbation of asthma. *J Immunol* (2014) 192:3569–81. doi: 10.4049/jimmunol.1302766
69. Richard AS, Shim BS, Kwon YC, Zhang R, Otsuka Y, Schmitt K, et al. AXL-dependent infection of human fetal endothelial cells distinguishes Zika virus from other pathogenic flaviviruses. *Proc Natl Acad Sci U S A* (2017) 114:2024–9. doi: 10.1073/pnas.1620558114
70. Wang H, Chen Y, Ge Y, Ma P, Ma Q, Ma J, et al. Immunoexpression of Tyro 3 family receptors–Tyro 3, Axl, and Mer–and their ligand Gas6 in postnatal developing mouse testis. *J Histochem Cytochem* (2005) 53:1355–64. doi: 10.1369/jhc.5A6637.2005
71. Pickar A, Xu P, Elson A, Zengel J, Sauder C, Rubin S, et al. Establishing a small animal model for evaluating protective immunity against mumps virus. *PloS One* (2017) 12:e0174444. doi: 10.1371/journal.pone.0174444
72. Wang XX, Ying P, Diao F, Wang Q, Ye D, Jiang C, et al. Altered protein prenylation in Sertoli cells is associated with adult infertility resulting from childhood mumps infection. *J Exp Med* (2013) 210:1559–74. doi: 10.1084/jem.20121806
73. Sadler AJ, Williams BR. Interferon-inducible antiviral effectors. *Nat Rev Immunol* (2008) 8:559–68. doi: 10.1038/nri2314
74. Apari P, de Sousa JD, Muller V. Why sexually transmitted infections tend to cause infertility: an evolutionary hypothesis. *PloS Pathog* (2014) 10:e1004111. doi: 10.1371/journal.ppat.1004111
75. Kumar H, Kawai T, Akira S. Pathogen recognition by the innate immune system. *Int Rev Immunol* (2011) 30:16–34. doi: 10.3109/08830185.2010.529976
76. Guazzone VA, Jacobo P, Theas MS, Lustig L. Cytokines and chemokines in testicular inflammation: A brief review. *Microsc Res Tech* (2009) 72:620–8. doi: 10.1002/jemt.20704
77. Wileman T. Autophagy as a defence against intracellular pathogens. *Essays Biochem* (2013) 55:153–63. doi: 10.1042/bse0550153
78. Spencer JV, Religa P, Lehmann MH. Editorial: Cytokine-Mediated Organ Dysfunction and Tissue Damage Induced by Viruses. *Front Immunol* (2020) 11:2. doi: 10.3389/fimmu.2020.00002
79. Diemer T, Hales DB, Weidner W. Immune-endocrine interactions and Leydig cell function: the role of cytokines. *Andrologia* (2003) 35:55–63. doi: 10.1046/j.1439-0272.2003.00537.x
80. Suh JH, Gong EY, Hong CY, Park E, Ahn RS, Park KS, et al. Reduced testicular steroidogenesis in tumor necrosis factor-alpha knockout mice. *J Steroid Biochem Mol Biol* (2008) 112:117–21. doi: 10.1016/j.jsbmb.2008.09.003
81. Wang F, Liu W, Jiang Q, Gong M, Chen R, Wu H, et al. Lipopolysaccharide-induced testicular dysfunction and epididymitis in mice: a critical role of tumor necrosis factor alphadagger. *Biol Reprod* (2019) 100:849–61. doi: 10.1093/biolre/ioy235
82. Theas MS, Rival C, Jarazo-Dietrich S, Jacobo P, Guazzone VA, Lustig L. Tumour necrosis factor-alpha released by testicular macrophages induces apoptosis of germ cells in autoimmune orchitis. *Hum Reprod* (2008) 23:1865–72. doi: 10.1093/humrep/den240
83. Hughes EG. The effectiveness of ovulation induction and intrauterine insemination in the treatment of persistent infertility: a meta-analysis. *Hum Reprod* (1997) 12:1865–72. doi: 10.1093/humrep/12.9.1865
84. Siu MK, Lee WM, Cheng CY. The interplay of collagen IV, tumor necrosis factor-alpha, gelatinase B (matrix metalloprotease-9), and tissue inhibitor of metalloproteases-1 in the basal lamina regulates Sertoli cell-tight junction dynamics in the rat testis. *Endocrinology* (2003) 144:371–87. doi: 10.1210/en.2002-220786
85. Siemann DN, Strange DP, Maharaj PN, Shi PY, Verma S. Zika Virus Infects Human Sertoli Cells and Modulates the Integrity of the In Vitro Blood-Testis Barrier Model. *J Virol* (2017) 91:e00623–17. doi: 10.1128/JVI.00623-17
86. Yule TD, Montoya GD, Russell LD, Williams TM, Tung KS. Autoantigenic germ cells exist outside the blood testis barrier. *J Immunol* (1988) 141:1161–7.
87. Liu M, Guo S, Hibbert JM, Jain V, Singh N, Wilson NO, et al. CXCL10/IP-10 in infectious diseases pathogenesis and potential therapeutic implications. *Cytokine Growth Factor Rev* (2011) 22:121–30. doi: 10.1016/j.cytogfr.2011.06.001
88. Krause KK, Azouz F, Shin OS, Kumar M. Understanding the Pathogenesis of Zika Virus Infection Using Animal Models. *Immune Netw* (2017) 17:287–97. doi: 10.4110/in.2017.17.5.287
89. Li N, Wang T, Han D. Structural, cellular and molecular aspects of immune privilege in the testis. *Front Immunol* (2012) 3:152. doi: 10.3389/fimmu.2012.00152

Conflict of Interest: The authors declare that the research was conducted in the absence of any commercial or financial relationships that could be construed as a potential conflict of interest.

frontiers in Immunology

ORIGINAL RESEARCH
published: 25 June 2021
doi: 10.3389/fimmu.2021.639239

Obesity Causes Abrupt Changes in the Testicular Microbiota and Sperm Motility of Zebrafish

Yufang Su[1,2], Liting He[1], Zhiyong Hu[1], Ying Li[3], Yuan Zhang[1], Zunpan Fan[1], Kai Zhao[1], Huiping Zhang[1] and Chunyan Liu[1]**

[1] Institute of Reproductive Health, Tongji Medical College, HuaZhong University of Science and Technology, Wuhan, China, [2] Department of Oncology, Jiangxi Maternal and Child Health Hospital, Nanchang, China, [3] Prenatal Diagnostic Center, People's Hospital of Guangxi Zhuang Autonomous Region, Nanning, China

OPEN ACCESS

Edited by:
Kenneth Tung,
University of Virginia,
United States

Reviewed by:
Allan Zhao,
Guangdong University of Technology,
China
Reet Mändar,
University of Tartu, Estonia

***Correspondence:**
Huiping Zhang
zhpmed@126.com
Chunyan Liu
lchy2019@hust.edu.cn

Specialty section:
This article was submitted to Mucosal Immunity, a section of the journal Frontiers in Immunology

Received: 08 December 2020
Accepted: 04 June 2021
Published: 25 June 2021

Citation:
Su Y, He L, Hu Z, Li Y, Zhang Y, Fan Z, Zhao K, Zhang H and Liu C (2021) Obesity Causes Abrupt Changes in the Testicular Microbiota and Sperm Motility of Zebrafish. Front. Immunol. 12:639239. doi: 10.3389/fimmu.2021.639239

Background: Obesity is a recognized risk factor for low fertility and is becoming increasingly prevalent in many countries around the world. Obesity changes intestinal microbiota composition, causes inflammation of various organs, and also reduces sperm quality. Several microorganisms are present in the testis. However, whether obesity affects the changes of testicular microbiota and whether these changes are related to reduced fertility in obese men remain to be elucidated.

Methods: In the present study, a zebrafish obesity model was established by feeding with egg yolk powder. Sperm motility was measured by the Computer Assisted Sperm Analysis system, testicular microbial communities was assessed *via* 16s RNA sequencing, the immune response in zebrafish testis was quantified by quantitative real-time polymerase chain reaction and enzyme-linked immunosorbent assay, and the testicular tissue structure was detected by electron microscopy and hematoxylin–eosin staining.

Results: Compared with the control group, zebrafish sperm motility was dramatically reduced, the expression of testicular proinflammatory cytokines in the testes was upregulated, and the blood–testis barrier structure was disrupted in the obese group. In addition, testicular microbiome composition was clearly altered in the obese group.

Conclusion: Obesity alters testicular microbiota composition, and the reason behind the decreased sperm motility in obese zebrafish may be related to changes in the testicular microbial communities.

Keywords: testicular microbiota, obesity, zebrafish, intestinal microbiota, sperm motility

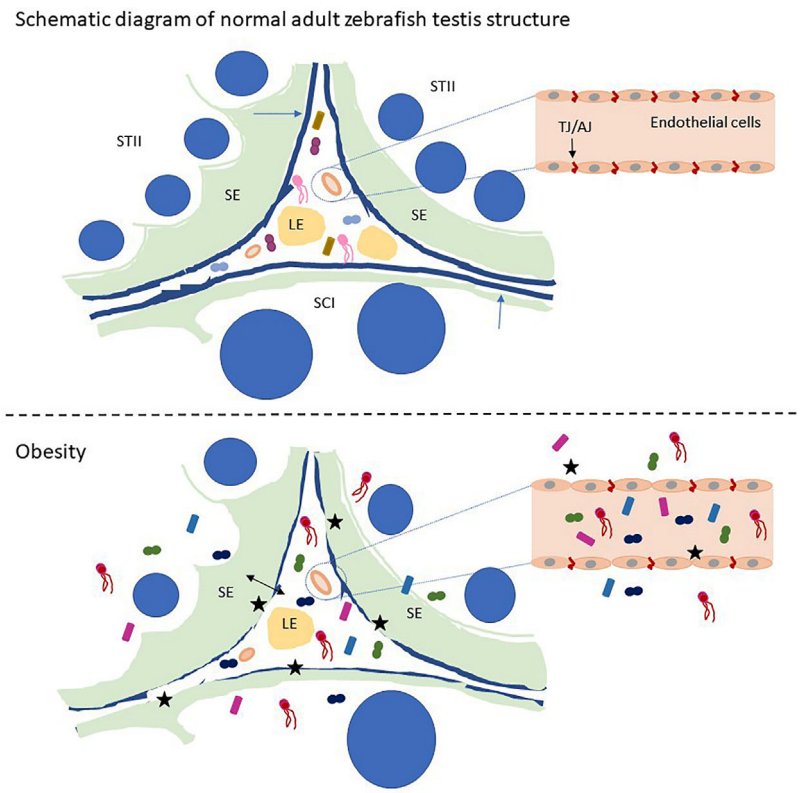

GRAPHICAL ABSTRACT | Schematic of zebrafish testis microbiological disturbance and BTB disruption caused by obesity. STII, spermatids at the second phase of spermiogenesis; SCI, primary spermatocytes; LE, Leydig cells in the interstitium; SE, Sertoli cells. The blue arrow indicates the basement membrane of the zebrafish testis, and the black stars indicate the breach of the zebrafish BTB and the vascular barrier. Small graphics in the picture represent microorganisms.

HIGHLIGHTS

Changes in the composition of testicular microbiota in obese zebrafish.

Decreased sperm motility in obese zebrafish.

Defective tight junction of blood–testis barrier in obese zebrafish.

Zebrafish testicular immune response is activated.

Altered testicular microbiota in obese zebrafish are related to changes in their gut microbes.

INTRODUCTION

In recent decades, the number of obese men of childbearing age has almost doubled (1, 2). In 2000, 65% of adult men had a body mass index (BMI) over 25 (overweight), and 30% had a BMI higher than 30 (obesity) (3). Cohort analysis demonstrated that the total sperm count and sperm motility were lower in obese than in healthy donors (4, 5). Endocrine disorders (disorders of testosterone levels) (6, 7), genetics, autophagy (8), and physical or chemical factors are all involved in low fertility caused by obesity in men.

There are approximately 10^{13}–10^{14} bacteria in the human intestine (9). The gut microbiota can regulate liver metabolism by reducing energy expenditure and promoting obesity (10). *Faecalibacterium prausnitzii*, an anti-inflammatory bacterium, was found to be significantly decreased in the intestine of morbidly obese diabetic patients (11, 12). In previous studies, obese mice fed on a high-fat diet (HFD) had increased intestinal permeability, and the abundance of *Bacteroides*, *Clostridium*, and *Bifidobacterium* in the intestine of mice decreased by 50% (13, 14). The richness of *Enterobacter cloacae strain B29* was significantly aggrandized in the intestinal microorganisms of obese individuals (15, 16). The above findings demonstrated that High-fat-diet reduces the abundance of predominant bacteria in the intestine and accelerates the richness of pathogenic bacteria, thereafter the metabolites of the changed microbiota may contribute to obesity, which destroys the intestinal vascular barrier. The human testis has tissue-associated symbiotic bacteria, with *Actinomycetes*, *Bacteroides*, *Pachybacteria*, and *Proteus* being the most abundant microorganisms in the men with testicular tumor (seminoma) with normozoospermic (17). A study showed that *Clostridium* spp. are related to the vitality and morphology of human sperm (18). Cohort studies have found that an increase in *Actinomycetes* and *Sclerotinia* changes the testicular microbiota

in male patients with non-obstructive azoospermia. Moreover, patients with complete germ cell aplasia did not have Clostridia in their testes (17). All of the above findings suggest that changes in testicular microorganisms may be associated with decreased male fertility.

An article found that adult males over 35 years of age may develop epididymitis caused by intestinal pathogens (19). Studies have shown that the permeability of the blood–testis barrier (BTB) is increased and testicular development is altered in obese mice when their intestinal microbiota composition was changed (20–22). However, whether obesity changes the testicular microorganism composition and whether defects in testicular function caused by obesity are related to changes in testicular microorganism composition remain to be elucidated. Thus, we constructed a zebrafish obesity model through HFD feeding. After 8 weeks, the sperm motility and integrity of the BTB were measured. Based on 16s RNA sequencing, the testicular and intestinal microbial community composition was analyzed to reveal the association between obese infertility and testicular microbiota.

MATERIALS AND METHODS

Chemicals and Materials

Egg yolk powder (59% fat, 32% proteins, 2% carbohydrates) with a purity >98% was obtained from Solarbio (Cat # E8200, China). Fragments and coverslip for zebrafish sperm motility testing were purchased from Hamilton Thorne - 203L-72 (Lot # 559599, USA). Oil Red O was purchased from Sigma (Lot # SLBT6544, USA).

Fish Maintenance and HFD Feeding

Zebrafish embryos were provided by the Institute of Reproductive Health, Tongji Medical College, Huazhong University of Science and Technology. Zebrafish were maintained in a flow-through system containing charcoal-filtered water on a 14 h light/10h dark photoperiod at 28 ± 0.5°C.

AB zebrafish strains were utilized because these strains have become the most commonly used zebrafish for studying obesity and obesity-related experiments (22–25). We randomly assigned 80 3-month-old adult zebrafish to two diet groups. One group (40 per group) was fed with red worms to maintain physiological energy requirements, whereas the other group was given 30 mg of egg yolk powder per fish per day while feeding an equivalent number of red worms. Zebrafish were maintained in 5 L tanks for every 10 fish and were fed twice daily. They were fasted overnight and sacrificed in the eighth week (26).

Measurement of Zebrafish Length, Weight, Blood Glucose, and Cholesterol

The body weight and length of zebrafish were recorded and calculated to obtain the BMI. We collected blood samples from the dorsal artery and pooled blood samples for every 8 fish for one exemplary feeding experiment. Fasting blood glucose was measured using a glucometer (Safe blood glucose meter, Sannuo), and cholesterol levels were determined using the Amplex® Red Cholesterol Assay Kit (Invitrogen) (26).

Histology

Cryosections from zebrafish liver were prepared by embedding freshly isolated liver tissue in 4% paraformaldehyde (Sigma-Aldrich, St. Louis, Missouri, USA). The slides were stained at room temperature with Oil Red O in the dark overnight, and images were captured under an Olympus microscope (Tokyo, Japan) (27). Anatomically comparable sections of subcutaneous fat were stained with hematoxylin–eosin (HE), and microscopic images were obtained at 40× magnification under an Olympus microscope (Tokyo, Japan). Put a fresh zebrafish testis sample of about 1-2 mm^3 into the electron microscope fixation solution within 2 minutes, fix it with osmium acid, dehydrate, infiltrate, and embed it, and cut it into a thickness of 80-100nm (Leica, EM UC7, Germany), double staining with uranium and lead, and dry at room temperature Overnight, observe the microstructure of the tissue under the electron microscope (FEI, Tecnai G2 20 TWIN, American).

Zebrafish Sperm Motility Test

Zebrafish semen was manually squeezed out and placed in a 100 μL Eppendorf tube with 10 μL of D-Hank's solution. The mixed droplets of sperm were placed on a 20 μm slide and then added with 5 μL of 0.1% bovine serum albumin solution (activated). The slide was immediately covered with a coverslip and pushed under the HT Computer Assisted Sperm Analysis (CASA) II Animal (Hamilton Thorne, USA). Each group randomly selected 6 fish for sperm motility test, and repeated the test for each fish 5 times, and the average was determined. Sperm motility test for each fish was completed within 1 h after fresh zebrafish semen was collected.

Enzyme-Linked Immunosorbent Assay

Serum IL-1β levels were determined by using the Fish IL-1β ELISA Kit (MyBioSource), and serum testosterone levels were quantified by using Testosterone ELISA Kit (Cayman) following the manufacturer's instructions.

Detection of Gene Expression

Prepare enough sterile dissecting instruments, anesthetize the zebrafish on ice, and extract fresh zebrafish testis samples in a sterile ultra-clean bench. Each zebrafish dissection instrument is not reused. DNA was extracted from the fresh testicular tissue according to the instructions of the EZNA® Soil DNA Kit (Omega Biotechnology Company, Norcross, Georgia, USA). We pooled the bilateral testes of 10 zebrafish in each group into an experimental group for DNA extraction. Total RNA was extracted from zebrafish testis by using TRIzol reagent (Takara Biochemicals, Japan) following the manufacturer's protocol. RNA reverse transcriptase reaction was conducted using a PrimeScript RT kit (Takara, Kusatsu, Japan). Real-time polymerase chain reaction (RT-PCR) was performed on a StepOnePlus Real-Time PCR instrument (Applied Biosystems). The gene expression levels of *β-actin*, *tnf-α*, *il-1β*, and *il-8* were detected *via* an SYBR Green system (DBI Bioscience) using oligonucleotide primers (**Table 1**) (28, 29). Each tested gene was repeated three times for qRT-PCR.

TABLE 1 | Sequences of primer pairs used in the real-time quantitative PCR reactions.

Gene	Primer sequences (from 5' to 3')	Size (bp)
β-actin	F: ATGGATGAGGAAATCGCTGCC R: CTCCCTGATGTCTGGGTCGTC	127
tnf-α	F: GGGCAATCAACAAGATGGAAG R: GCAGCTGATGTGCAAAGACAC	250
il-1β	F: TGGTGGATTCAGTGCCGTCT R: AGGCCAGGTACAGGTTACTTTTG	246
il-8	F: GTCGCTGCATTGAAACAGAA R: CTTAACCCATGGAGCAGAGG	158

16s RNA Sequencing and Bioinformatics Analysis

Taking into account that zebrafish are aquatic animals, feces are not easy to collect, our gut microbes and testis microbe specimens come from the entire zebrafish intestine or testis (30). Prepare enough sterile dissecting instruments, anesthetize the zebrafish on ice, and extract fresh zebrafish testis samples in a sterile ultra-clean bench. Each zebrafish dissection instrument is not reused. We pooled the bilateral testes of 10 zebrafish in each group into an experimental group for DNA extraction. DNA was extracted from the fresh testicular tissue according to the instructions of the EZNA® Soil DNA Kit (Omega Biotechnology Company, Norcross, Georgia, USA), and the quality of DNA was detected by 2% agarose gel electrophoresis. The DNA concentration and purity were determined by using NanoDrop2000. Then, the 16S rRNA V3-V4 gene (338F 5'-ACTCCTACGGGAGGCAGCAG-3' and 806R 5'-GGACTACHVGGGTWTCTAAT-3') was amplified by PCR, and the PCR product was recovered on a 2% agarose gel. The recovered product was purified by using the AxyPrep DNA Gel Extraction Kit (Axygen Biosciences, Union City, CA, USA) and detected by 2% agarose gel electrophoresis using a Quantus™ Fluorometer (Promega, USA). The NEXTFLEX Rapid DNA-Seq Kit was used to build the library. Sequencing was performed on the Miseq PE300 platform (Illumina).

Trimmomatic software was used for sequencing the original sequences for quality control. FLASH software was employed for splicing. UPARSE software (version 7.1) was applied to cluster the sequences into OTUs based on 97% similarity and remove the chimeras. RDP classifier (2.11) was applied to annotate species classification for each sequence. 16S rRNA sequencing data were analyzed using QIIME 1.9.1 (31). To minimize the effects of false sequences, we deleted OTUs that were less than 0.005% of the total number of sequences and performed data flattening. The sequences were compared using Mothur 1.30.2 for alpha diversity analyses. The genome of the gut microbiome was deduced from the 16S rRNA sequence by PICRUSt (32).

Data Analyses

Data were quantified as the difference relative to that of the control group and are shown as mean ± standard error of the mean. The data were verified for normality and homogeneity of variance using the Kolmogorov–Smirnov one-sample test and Levene's test. Intergroup differences were assessed by one-way ANOVA followed by Dunnett's *post hoc* test. All statistical analyses were conducted by SPSS 18.0. The level of statistical significance was set at $P < 0.05$, indicated by an asterisk.

RESULTS

Construction of a Zebrafish Obesity Model

After 8 weeks of HFD feeding, we compared parameters related to obesity, including body weight, BMI, and condition index. The presence of early obesity-related metabolic alterations was investigated by quantifying blood glucose levels and cholesterol levels to determine whether the modeling was successful. Compared with the control group, the abdomen of zebrafish in the obese group was enlarged, as shown by the black arrow in **Figure 1A**. The bodyweight increased by approximately 1.4 times, the body length increased by approximately 1.2 times, and the BMI increased from 27–28 to 32–34 ($P < 0.0001$) (**Figures 1B–D**). A significant enhancement in the number of subcutaneous adipocytes in zebrafish was observed. The space between subcutaneous muscle fibers was enlarged by adipocytes, and the volume of each adipocyte increased by approximately 2–3 times under a 10× microscope (**Figure 1E**). Consistent with the expected results, the number of zebrafish liver fat vacuoles was higher in the obese group than in the control group (**Figure 1F**). We detected the expression levels of cholesterol and glucose in the blood of zebrafish, compared with the control group, the blood cholesterol level in the obese group increased ($P < 0.01$) (**Figure 1G**), and the blood glucose levels increased ($P < 0.05$) (**Figure 1H**). The above data indicated the successful construction of the zebrafish obesity model.

Sperm Motility Decline in the Obese Zebrafish Model

We analyzed the effects of obesity on zebrafish sperm motility. **Figure 2A** shows a visual representation of zebrafish sperm motility within 120 s, where green indicates motile sperm, blue indicates progressive sperm, purple indicates slow sperm, and red indicates immobile sperm. In 80 s, the number of stationary sperm was higher than that of the control group. The zebrafish motile time and the motile average path velocity (VAP) in the obese group markedly decreased ($P < 0.01$) (**Figures 2B, C**). In addition, the percentage of zebrafish sperm forward motion and the progressive VAP of zebrafish sperm were distinctly reduced (**Figures 2D, E**). Electron microscopy revealed that the zebrafish sperm heads in the obese group had lesions, as shown by the red arrow in **Figure 2F**, and the count of head lesions of zebrafish sperm in the obese group was

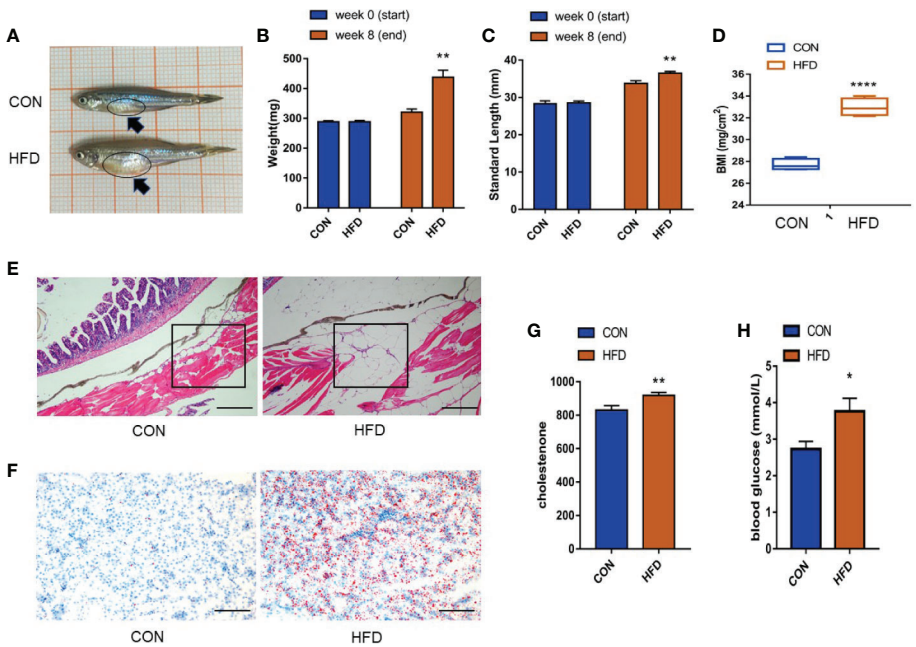

FIGURE 1 | Successful establishment of the obesity model. **(A)** Male zebrafish appearance in control and obese groups. A clearly larger abdomen can be seen in zebrafish in the obese group as shown by the dark blue arrow. **(B, C)** Measurement of body weight and length of zebrafish before and after exposure. **(D)** Significant differences in the BMI index. **(E)** Expression of subcutaneous fat in zebrafish (scale bar = 100 μm). **(F)** Expression of fat droplets in the liver (scale bar = 100 μm). **(G, H)** Determination of cholesterol in the blood and detection of blood glucose. Values are mean ± SME (n = 5). The asterisk represents a statistically significant difference when compared with the controls; *, ** and **** at $P < 0.05$, $P < 0.01$ and $P < 0.0001$, respectively.

obviously increased in the control group ($P < 0.001$) (**Figure 2G**). The above results indicate that diet-induced obesity reduces the sperm quality of adult zebrafish, which in turn has a negative impact on the fertility of male zebrafish.

Obesity Destroys Zebrafish BTB Structure and Accelerates Testicular Inflammation

To investigate whether the testicular tissue structure is affected by obesity, we compared the HE staining of zebrafish testes. Unlike mammalian seminiferous tubules, each of the seminiferous vesicles encased by the Sertoli cells in the zebrafish's seminary is the same type of seminiferous cells. In the **Figure 3A**, as shown by the yellow stars, each seminiferous vesicle contains equally developed spermatogenic cells, and the tissue structure of the seminiferous vesicles and the seminiferous epithelium is clear. The red arrow indicates the area between the two seminiferous epitheliums. However, the testes in the obese group had disordered seminiferous tubules and blurred contour boundaries (**Figure 3A**). We examined the BTB structure under an electron microscope. The control group had a normal BTB physiological structure, whereas the obese group had a significant disorder. Large number of vacuoles, irregular arrangement of tight junction in the gap link between the Sertoli cells and the spermatogenic cells was observed in the obese group (**Figure 3B**). Therefore, obesity increases the permeability of the BTB.

Obesity is related to direct damage to testicular function. Therefore, we investigated the changes in blood testosterone levels between the two groups and found that the plasma testosterone levels in the obese group were dramatically decreased ($P < 0.001$) (**Figure 3C**). Compared with the control group, the expression levels of *il-8*, *tnf-α*, and *il-1β* in zebrafish testes of the obese group were increased (**Figure 3D**). and the protein levels of IL-1β in the plasma of the obese group was increased ($P < 0.01$) (**Figure 3E**). Therefore, our results suggest that diet-induced obesity contributes to the inflammatory response in zebrafish testes.

High-Fat Diet-Induced Obesity Changes the Intestinal Microorganism Composition

Obesity induced by high-fat diet can change the composition of intestinal microbiota, so we tested the intestinal microbiota in the zebrafish obesity model. Consistent with our expectations, the analysis of the intestinal microbial composition revealed that the abundance of the dominant intestinal bacteria *Plesiomonas* (from 26.39% to 3.87%) and *Vibrio* (from 12.42% to 6.45%) remarkably decreased, and the pathogenic bacteria *Aeromonas* (from 5.35% to 29.49%) dramatically increased in the obese group compared with the control group (**Figure 4A**). At the genus level, the bacterial community compositions in the control and obese groups were also different in terms of abundance and diversity. Each group contained unique bacteria. Sixty-eight types of bacteria and seven species of different bacteria were observed in the two groups (**Figure 4B**). In addition, based on the phylum level abundance indicated that obesity induced by a high-fat diet

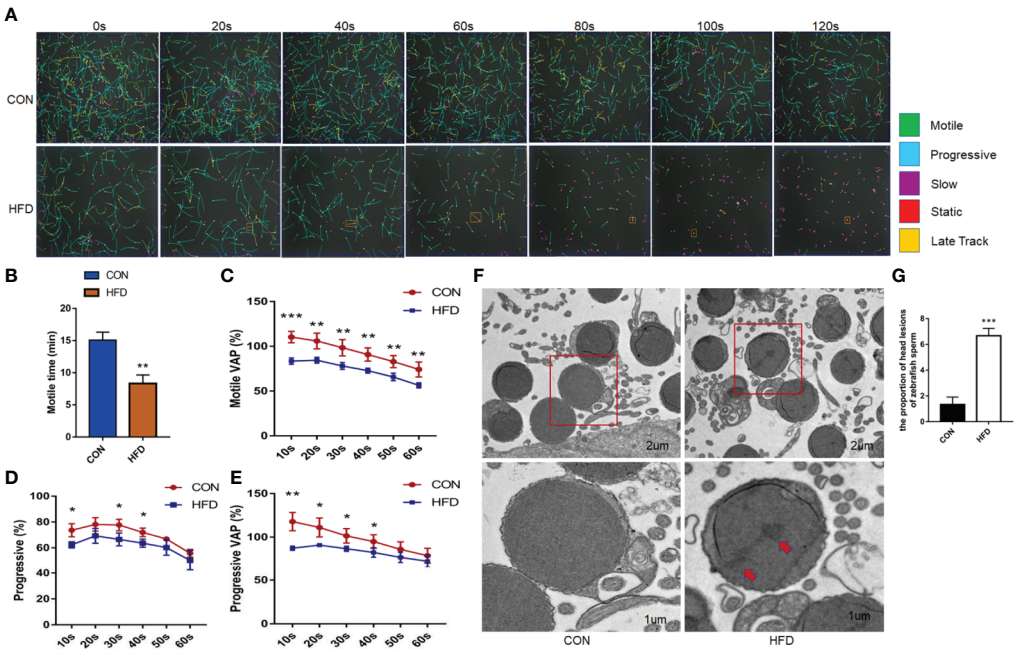

FIGURE 2 | Effects of obesity on the sperm motility of zebrafish. **(A)** Intuitive CASA image of zebrafish sperm movement under a microscope. **(B)** Sperm MOT between the two groups. **(C–E)** Percentage of motile VAP and progressive VAP (%) of adult zebrafish. **(F)** Comparison of sperm morphology between the two groups under the electron microscope. **(G)** The obese group had lesions on the head of the sperm as shown by the red arrow. Data represent mean ± SME (n = 6). *, ** and *** at $P < 0.05$, $P < 0.01$ and $P < 0.001$, respectively.

clearly changes the composition of gut microbes, compared with the control group, *Proteobacteria* (from 97.49% to 91.27%) increased in the obese group, while *Fusobacteria* (from 5.74% to 0.22%) and *Firmicutes* (from 2.38% to 0.97%) decreased (**Figure S1**). Based on LEfSe multi-level species discriminant analysis, we observed a conspicuous difference, in which 26 bacterial groups showed self-evident relative abundance in the obese and control groups (**Figure 4C**), indicating a palpable difference in intestinal microbiota after obesity.

High-Fat Diet-Induced Obesity Changes the Testicular Microorganism Composition

To understand the relationship between the obesity-related decrease in male fertility and testicular microbial communities, 16s RNA sequencing analysis of the microbial communities was performed. The testis microbe data from one sample of the obese group were excluded because they were deemed non-compliant. The statistical analysis demonstrated that *Pseudomonas*, *Lactobacillus*, and *Bifidobacterium* are the main genera in the testis. However, compared with the control group, the relative abundance of *Lactobacillus* in the obese group was increased, whereas the richness of *Bifidobacterium* decreased (**Figure 5A**). On the phylum level abundance indicated that obesity induced by a high-fat diet changes the testicular microbes, compared with the control group, *Proteobacteria* (from 57.93% to 58.56%) and *Firmicutes* (from 29.61% to 32.84%) increased in the obese group, while and *Actinobacteria* (from 12.39% to 8.36%) decreased (**Figure S2**). Alpha diversity analysis of the testicular microbes revealed that obesity was associated with a reduction in species diversity in the testis (Wilcoxon rank-sum test, $P = 0.03$; **Figure 5B**). Analysis of the differences in the testicular microbiota of the two groups screened out an additional 15.28% of *Escherichia-Shigella* in the obese group. However, *Plesiomonas* and *Vibrio* were not found in the pie chart of the obese group (**Figure 5C**). These data indicated that the diversity of bacteria in the obese group decreased.

In addition, we performed a sample-to-species analysis to display the distribution ratio of dominant species in each group of microbiotas and the distribution ratio of predominant species in different groups (**Figure S3**). At the genus level, each group contained unique bacteria. The bacterial community composition in the control and obese groups was also visibly different in terms of abundance and diversity (**Figure 5D**). Fifty-one common bacterial species were observed in the two groups. The heatmap and sample cluster tree analyses of 50 species of testicular microorganisms in different groups (**Figure S4**) showed significant differences in the predominant testicular microorganism composition after obesity.

To study the changes in the function and metabolism of the microbial community in the testis between the obese and control groups, we deduced the genome from 16S rRNA data and analyzed the functional potential of the intestinal microbiota using PICRUSt. Differences in 25 related genes were screened. In the obese group, the functions of signal transduction mechanism, amino acid transport and metabolism, lipid transport and

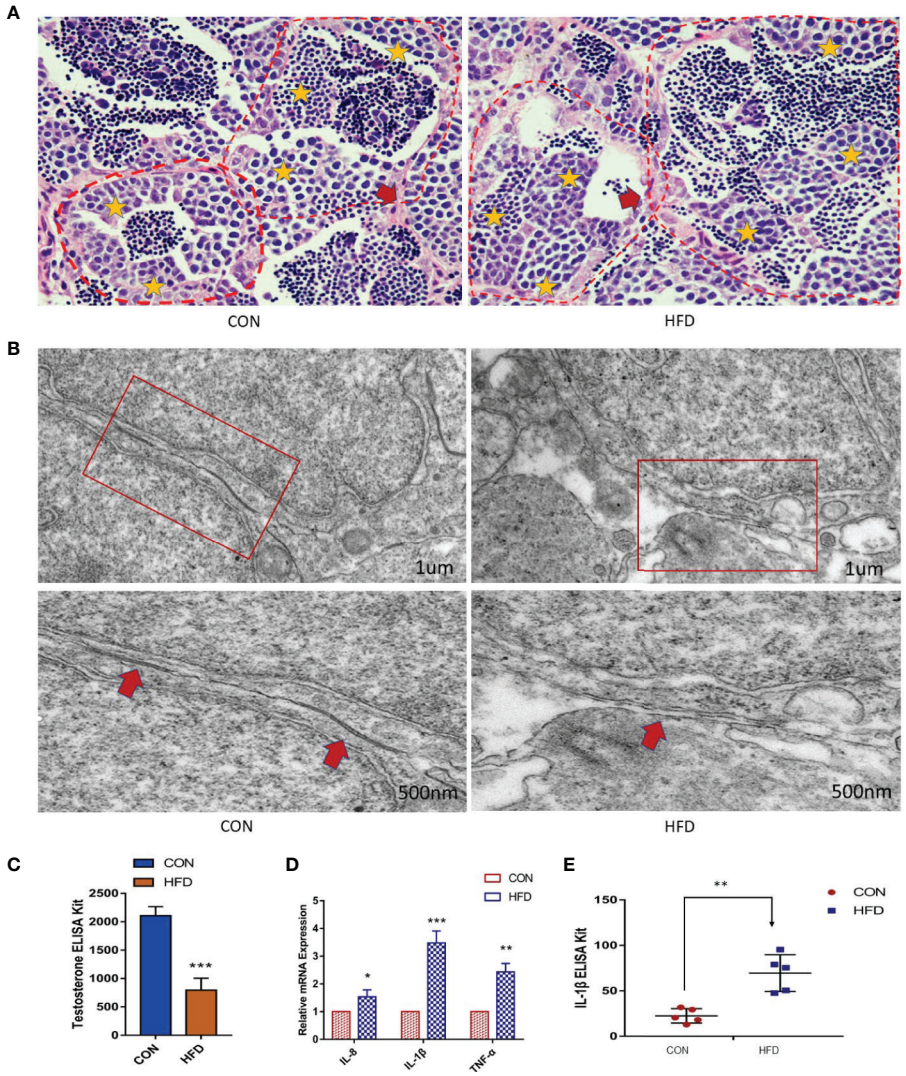

FIGURE 3 | Obesity causes the destruction of zebrafish BTB structure and testicular inflammation. **(A)** Testicular HE staining in the control and obese groups. Yellow stars indicate sperm vesicles of the same type of spermatogenic cells in the zebrafish testis, and the red arrow indicates the interstitial part. Obviously, the zebrafish spermatogenic cells were disorderly arranged, and the interstitium was thickened. **(B)** Ultrastructure of zebrafish BTB. Red boxes indicate connections between Sertoli cells and germ cells in zebrafish testis. In the enlarged image, the BTB structure of the obese group is damaged, as shown by the red arrow. **(C)** Detection of testosterone in the blood. The testosterone level of the obese group was markedly decreased ($P < 0.001$). **(D)** Effects of ODP exposure on the mRNA levels of *tnf-α*, *il-1β*, and *il-8* in zebrafish testis. **(E)** Detection of IL-1β expression in the blood by ELISA. Data represent mean ± SME (n = 5). The asterisk represents a statistically significant difference when compared with the corresponding controls; *, ** and *** at $P < 0.05$, $P < 0.01$ and $P < 0.001$, respectively.

metabolism, carbohydrate transport metabolism, and coenzyme transport and metabolism all decreased, especially signal transduction mechanism and amino acid transport and metabolism (**Figure 5E**). 16s RNA functional prediction analysis data indicate that the changes in metabolic indications may be related to the decline of sperm motility caused by obesity.

Comparison Between Testicular Microbiota and Intestinal Microbiota

Our results indicated that testicular and intestinal microbes have their predominant microbiota. For instance, *Plesiomonas* (26.39%), *Vibrio* (12.42%), and *Aeromonas* (5.35%) were highly expressed in the control intestinal microorganisms, whereas *Lactobacillus* and *Bifidobacterium* accounted for 19.94% and 12.19% in the testicular microorganisms, respectively. *Pseudomonas* had the highest composition in the gut and testicular microorganisms regardless of whether the zebrafish was obese or not (**Figure 6A** and **Figure S5**). Predominant bacteria such as *Vibrio*, *Plesiomonas*, *Aeromonas*, and *Pseudomonas* were all expressed in normal intestinal and testicular microbes. However, after obesity, the abundance of *Vibrio* and *Plesiomonas* was dramatically decreased in testicular and intestinal microbes (**Figure 6B**). The expression of

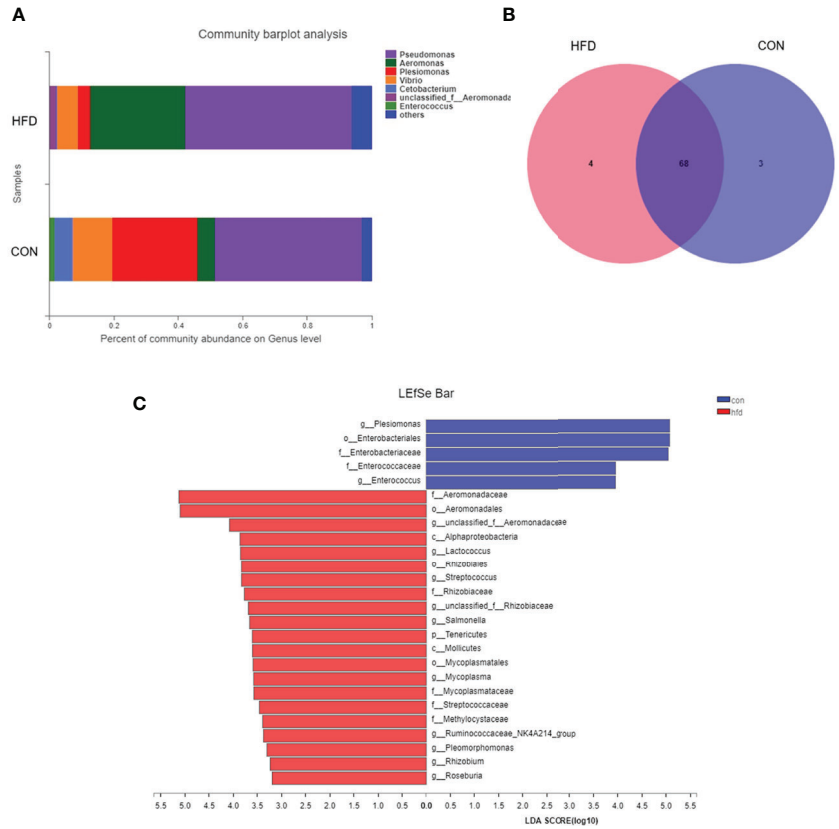

FIGURE 4 | Differences in intestinal microbial composition after High-fat diet-induced obesity. **(A)** Composition of intestinal microbial communities in the control and obese groups. **(B)** Venn plot population analysis results in gut microbes between the control and obese groups. **(C)** LEfSe multi-level species discriminant analysis using non-parametric factorial Kruskal–Wallis rank sum test and LDA to find groups that significantly differ in abundance. Data represent mean ± SME (n = 3).

Escherichia-Shigella in the intestinal and testicular microbes of the control group and intestinal microorganisms of the obese group was low (less than 0.15%) but accounted for 15.28% in the testicular microbes of the obese group (**Figures 6A, B**). The above data demonstrate that the composition of predominant intestinal and testicular microorganisms has changed, and there may be a connection between these changes and obesity.

DISCUSSION

To our knowledge, this study is the first to report on the relationship between obesity and testicular microorganisms. Our results demonstrated that the sperm motility index and blood testosterone levels of the obese group were reduced compared with the control group. Obesity can cause disorders in the BTB structure, and the expression of IL-1β protein remarkably increased in the blood. Based on the above research, we began to consider the role of testicular microbes in obesity and their relationship with intestinal microbes, the changes in testicular microbes, the cause of the changes, and whether these variables may be related to alterations in gut microbes.

Previous studies indicate that the permeability of the testicular BTB was increased in a diet-induced obese mouse model (33). This is consistent with our research results, obesity caused zebrafish disordered seminiferous tubules and blurred contour boundaries, and the structure of the tight junction protein involved in the gap link between the Sertoli cells and the spermatogenic cells was destroyed. BTB permeability may cause testicular inflammation, and cytokines can be employed as markers of inflammation (34, 35). Our results show, the expression levels of *il-8*, *tnf-α*, and *il-1β* in zebrafish testes of the obese group were increased, and the protein levels of IL-1β in the plasma of the obese group was increased in the obese group. Obesity can lead to hypogonadism (lower testosterone levels) in men through the effects of enterotoxin (36), and our results indicated that the zebrafish serum testosterone level decreased after obesity. The above-mentioned obesity leads to the destruction of the zebrafish testis structure, increases the expression of inflammatory factors, and decreases the level of testosterone.

A growing number of evident have shown that obesity is regulated by multiple organs. For instance, certain bacteria and their metabolites may directly target the brain through vagal nerve stimulation or immune nerves, and the endocrine

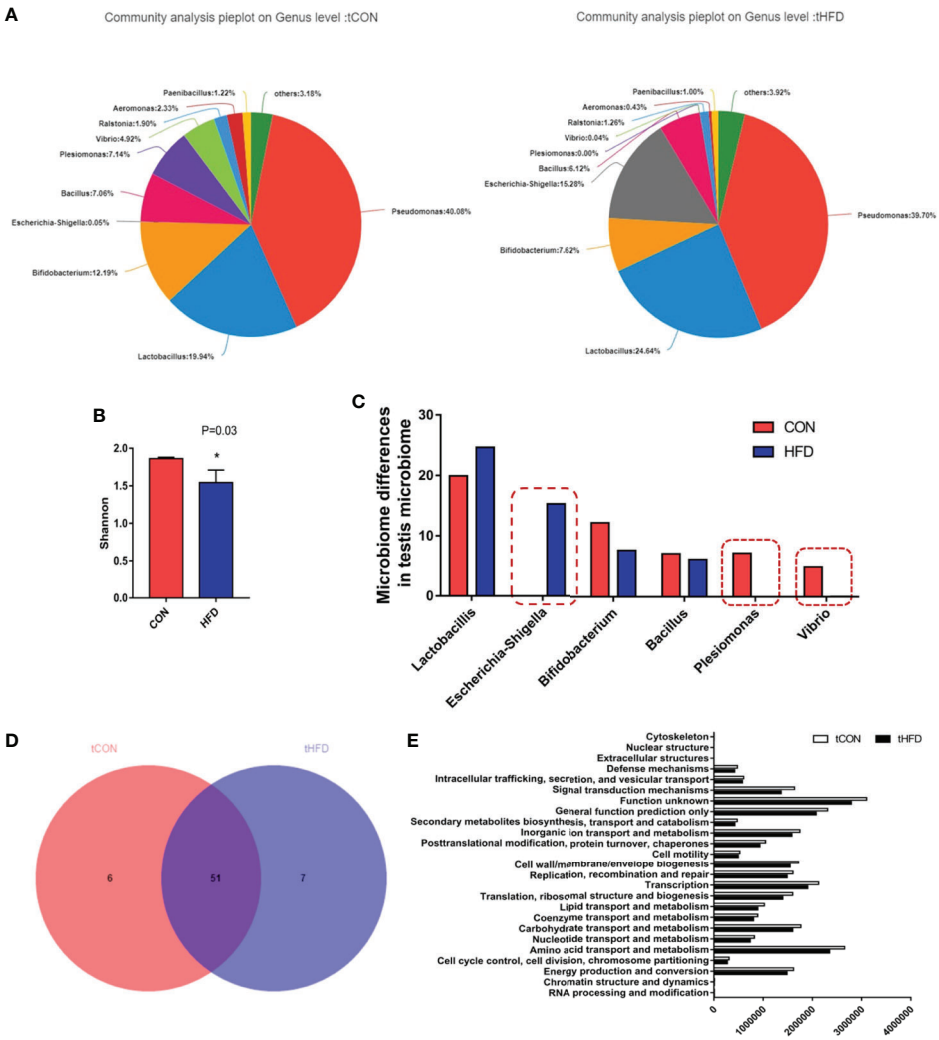

FIGURE 5 | Microbial community composition analysis in the testes of normal and obese male zebrafish showing marked microbial differences between the two groups. **(A)** The pie chart shows the community species composition information of testicular microbes at the gate level in the control and HFD groups. **(B)** Shannon diagram of alpha diversity analysis of testicular microorganisms ($P = 0.03$). **(C)** Analysis and selection of dominant strains of testicular microbial communities that were markedly differently expressed in the two groups. **(D)** Venn plot population analysis results between the two groups. **(E)** Predictive analysis of microbiota function. Data represent mean ± SME ($n = 3$). * at $P < 0.05$.

mechanism targets the brain indirectly (37, 38). Chronic kidney disease (39, 40) and non-alcoholic fatty liver disease (41) can cause significant changes in the composition and function of intestinal microbiota, which can cause systemic inflammation. First, our results demonstrated that *Plesiomonas* and *Vibrio* were the predominant testicular microorganisms in the obese group. Moreover, the relative abundance of *Lactobacillus* and *Bifidobacterium* was decreased in the testes of the obese group, indicating that obesity can cause reduced diversity of testicular microorganisms. Moreover, *no rank-c-Cyanobacteria* and *Bacteroides* are normally expressed in the intestinal microbes but not in the testicular microbes of the control group. However, they were observed in the testicular microbes of the obese group. Of note, the abundance of *Escherichia-Shigella* was increased by 15.28% in the obese group, whereas it was less than 0.15% in the control group and intestinal microorganisms. The above findings indicate that there may be a connection between intestinal and testicular microorganisms.

Under healthy conditions, there may be bacterial translocation between adjacent organs, and intestinal microbiota generally cannot enter other organs under healthy conditions. An article on HFD-fed mice may provide a mechanism for intestinal vascular barrier leakage and the passage of macromolecules and bacteria, due to the translocation of intestinal bacteria transferred to the liver and the destruction of intestinal vascular barrier by bacteria or virulent factors (42). However, with the help of the

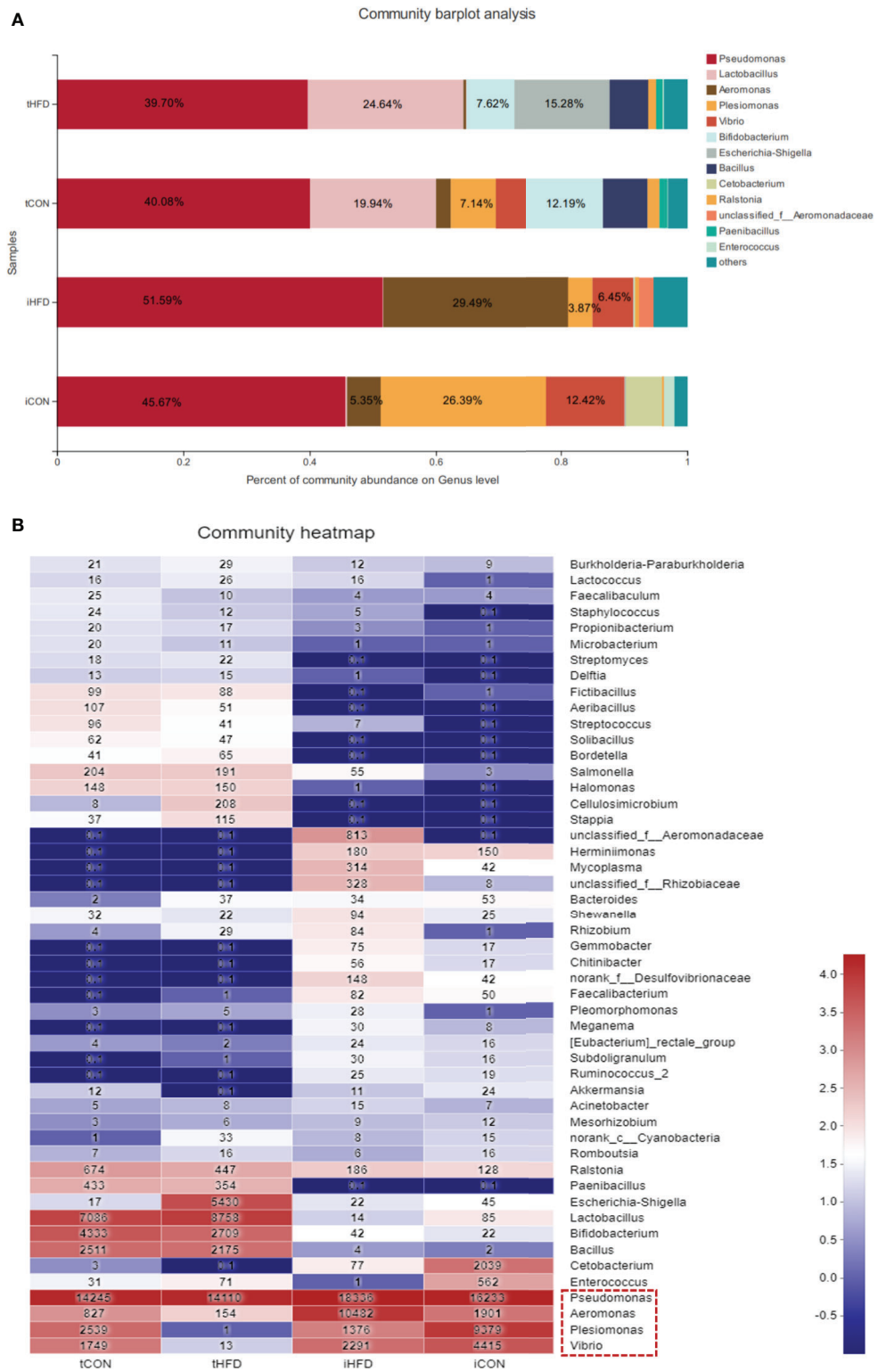

FIGURE 6 | Comparison between testicular and intestinal microorganisms. **(A)** Analysis of the microbial community composition of the testis and intestinal samples in the control and obese groups. The histogram results show that the dominant species are the same at the gate level for different samples, but the relative abundance is different. **(B)** The heatmap shows the species composition and sample cluster tree analysis of 50 species of bacterial communities in the testis and intestinal tracts of different groups at the genus level. Red indicates high bacterial abundance, whereas blue indicates low abundance. Data represent mean ± SME (n = 3).

pathogenicity island 2-encoded type III secretion system and reduced intestinal endothelial cell-dependent β-catenin signaling, certain pathogens can penetrate the intestinal vascular barrier to reach these organs and induce systemic immune response (43). The leakage of bacteria and their metabolites can also affect the function of the vascular wall barrier of the brain (44, 45), eyes (46), and testes (18). Our results indicate that obesity leads to reduced sperm motility, affects sperm quality, destroys the BTB, and causes a highly inflammatory state in zebrafish testis. Endotoxins can dramatically increase the permeability of the intestinal wall and damage the mucosa to form inflammation and ulcers (47, 48). Therefore, we speculate that the disturbances of intestinal microbes may affect testicular microbes through the leakage of pathogenic bacteria and their metabolites.

A study on intestinal microbes and sperm quality indicated that endotoxemia and epididymal inflammation are caused by an imbalance in intestinal microbiota in mice, which are the main factors attributed to sperm quality and motility. The authors transplanted intestinal microorganisms from HFD-fed mice to mice fed with a normal diet. After 15 weeks, the endotoxins in the blood nearly increased by threefold, and sperm motility was also affected (49). The results suggested that obesity alters intestinal microbiota composition and reduces sperm motility. This finding further validated the speculation that intestinal microorganisms may be transferred to the testis *via* the destruction of the intestinal vascular barrier and through the blood, thereby affecting testicular microbiota composition.

A study on the intestinal microbiota of individuals with polycystic ovary syndrome (PCOS) and clinical indicators associated with imbalanced microbiota found substantial differences in the types of intestinal microorganisms between PCOS and non-obese control groups. A positive correlation was observed between the abundance of *Shigella* and *Streptococcus* with testosterone and BMI (50). PCOS is a systemic disease of the female genital ovaries related to obesity (51). In male reproductive diseases associated with obesity, *Escherichia-Shigella* may be positively correlated with testosterone and BMI.

CONCLUSION

We speculate that the disturbance of intestinal microbes causes the imbalance of testicular microbiota through the production of endotoxemia, which increases the richness of *Escherichia-Shigella* and causes testicular inflammation. On the one hand, *Escherichia-Shigella* promotes the process of endotoxemia, and on the other hand, it further exacerbates testicular inflammation, leading to orchitis. Under the action of a large number of inflammatory factors and toxins, the BTB is damaged. While affecting the structure of the testis, the physiological functions of the testis were also adversely affected. Testosterone levels and sperm quality dramatically decreased. In short, the decline of sperm motility in obesity may be caused by an imbalance in testicular microbiota, leading to the destruction of the BTB structure and inflammatory response in the testis. Despite our findings, this study has some limitations. For example, our sample size is limited. And because of the small size of zebrafish (the mean testis weight of zebrafish was 4.7 ± 0.2 mg), the microbiological samples we collect are mixed samples.

DATA AVAILABILITY STATEMENT

The datasets presented in this study can be found in online repositories. The names of the repository/repositories and accession number(s) can be found below: NCBI AND PRJNA722878.

ETHICS STATEMENT

The study was conducted in strict accordance with the guidelines approved by the Animal Care and Use Committee of Tongji Medical College, Huazhong University of Science and Technology.

AUTHOR CONTRIBUTIONS

YS and CL designed research studies, conducted experiments, analyzed data, and drafted the manuscript. ZH assisted in 16sRNA mapping analysis. LH and YZ conducted Zebrafish model establishment. KZ and YL performed zebrafish execution and electron microscopy. ZF conducted sample collection and storage. CL and HZ provided intellectual input into planning of experiments and contributed to the writing of the manuscript. All authors contributed to the article and approved the submitted version.

FUNDING

This study was supported by National Key Research and Development Project (2018YFC1004300) and Wuhan Youth Science and technology plan (2017050304010291).

ACKNOWLEDGMENTS

We are grateful for the experimental platform given by the Institute of Reproductive Health of Huazhong University of Science and Technology.

SUPPLEMENTARY MATERIAL

The Supplementary Material for this article can be found online at: https://www.frontiersin.org/articles/10.3389/fimmu.2021.639239/full#supplementary-material

Supplementary Figure 1 | Analysis of the microbial community composition of the intestinal samples on the phylum level.

Supplementary Figure 2 | Analysis of the microbial community composition of the testis samples on the phylum level.

Supplementary Figure 3 | Analysis of the relationship between samples and species of two groups of testicular microorganisms was performed to show the distribution ratio of dominant species in each group of bacteria and the distribution ratio of each dominant species in different groups.

Supplementary Figure 4 | Species composition at different levels of the testicular bacterial community at the gate level and heatmap and sample cluster tree analyses.

Supplementary Figure 5 | Venn plot population analysis results of all samples, including gut and testicular microbes.

REFERENCES

1. Ramlau-Hansen CH, Thulstrup AM, Nohr EA, Bonde JP, Sørensen TI, Olsen J. Subfecundity in Overweight and Obese Couples. *Hum Reprod* (2007) 22(6):1634–7. doi: 10.1093/humrep/dem035
2. Palmer NO, Bakos HW, Fullston T, Lane M. Impact of Obesity on Male Fertility, Sperm Function and Molecular Composition. *Spermatogenesis* (2012) 2(4):253–63. doi: 10.4161/spmg.21362
3. Hedley AA, Ogden CL, Johnson CL, Carroll MD, Curtin LR, Flegal KM. Prevalence of Overweight and Obesity Among US Children, Adolescents, and Adults, 1999-2002. *JAMA* (2004) 291(23):2847–50. doi: 10.1007/s00018-015-2061-5
4. Wang EY, Huang Y, Du QY, Yao GD, Sun YP. Body Mass Index Effects Sperm Quality: A Retrospective Study in Northern China. *Asian J Androl* (2017) 19(2):234–7. doi: 10.4103/1008-682X.169996
5. Ma J, Wu L, Zhou Y, Zhang H, Xiong C, Peng Z, et al. Association Between BMI and Semen Quality: An Observational Study of 3966 Sperm Donors. *Hum Reprod* (2019) 34(1):155–62. doi: 10.1093/humrep/dey328
6. Chavarro JE, Toth TL, Wright DL, Meeker JD, Hauser R. Body Mass Index in Relation to Semen Quality, Sperm DNA Integrity, and Serum Reproductive Hormone Levels Among Men Attending an Infertility Clinic. *Fertil Steril* (2010) 93(7):2222–31. doi: 10.1016/j.fertnstert.2009.01.100
7. Liu Y, Zhao W, Gu G, Lu L, Feng J, Guo Q, et al. Palmitoyl-Protein Thioesterase 1 (PPT1): An Obesity-Induced Rat Testicular Marker of Reduced Fertility. *Mol Reprod Dev* (2014) 81(1):55–65. doi: 10.1002/mrd.22281
8. Mu Y, Yan WJ, Yin TL, Zhang Y, Li J, Yang J. Diet-Induced Obesity Impairs Spermatogenesis: A Potential Role for Autophagy. *Sci Rep* (2017) 7(1):43475. doi: 10.1038/srep43475
9. Eckburg PB, Bik EM, Bernstein CN, Purdom E, Dethlefsen L, Sargent M, et al. Diversity of the Human Intestinal Microbial Flora. *Science* (2005) 308 (5728):1635–8. doi: 10.1126/science.1110591
10. Braniste V, Al-Asmakh M, Kowal C, Anuar F, Abbaspour A, Tóth M, et al. The Gut Microbiota Influences Blood-Brain Barrier Permeability in Mice. *Sci Trans Med* (2014) 6(263):263ra158–263ra158. doi: 10.1126/scitranslmed.3009759
11. Sokol H, Pigneur B, Watterlot L, Lakhdari O, Bermúdez-Humarán LG, Gratadoux JJ, et al. Faecalibacterium Prausnitzii is an Anti-Inflammatory Commensal Bacterium Identified by Gut Microbiota Analysis of Crohn Disease Patients. *Proc Natl Acad Sci U S A* (2008) 105(43):16731–6. doi: 10.1073/pnas.0804812105
12. Furet JP, Kong LC, Tap J, Poitou C, Basdevant A, Bouillot JL, et al. Differential Adaptation of Human Gut Microbiota to Bariatric Surgery-Induced Weight Loss: Links With Metabolic and Low-Grade Inflammation Markers. *Diabetes* (2010) 59(12):3049–57. doi: 10.2337/db10-0253
13. Ley RE, Bäckhed F, Turnbaugh P, Lozupone CA, Knight RD, Gordon JI. Obesity Alters Gut Microbial Ecology. *Proc Natl Acad Sci U S A* (2005) 102 (31):11070–5. doi: 10.1073/pnas.0504978102
14. Cani PD, Bibiloni R, Knauf C, Waget A, Neyrinck AM, Delzenne NM, et al. Changes in Gut Microbiota Control Metabolic Endotoxemia-Induced Inflammation in High-Fat Diet-Induced Obesity and Diabetes in Mice. *Diabetes* (2008) 57(6):1470–81. doi: 10.2337/db07-1403
15. Gérard P. Gut Microbiota and Obesity. *Cell Mol Life Sci* (2016) 73(1):147–62. doi: 10.1007/s00018-015-2061-5
16. Fei N, Zhao L. An Opportunistic Pathogen Isolated From the Gut of an Obese Human Causes Obesity in Germfree Mice. *ISME J* (2013) 7(4):880–4. doi: 10.1038/ismej.2012.153
17. Alfano M, Ferrarese R, Locatelli I, Ventimiglia E, Ippolito S, Gallina P, et al. Testicular Microbiome in Azoospermic Men—First Evidence of the Impact of an Altered Microenvironment. *Hum Reprod* (2018) 33(7):1212–7. doi: 10.1093/humrep/dey116
18. Weng SL, Chiu CM, Lin FM, Huang WC, Liang C, Yang T, et al. Bacterial Communities in Semen From Men of Infertile Couples: Metagenomic Sequencing Reveals Relationships of Seminal Microbiota to Semen Quality. *PloS One* (2014) 9(10):e110152. doi: 10.1371/journal.pone.0110152
19. Ryan L, Daly P, Cullen I, Doyle M. Epididymo-Orchitis Caused by Enteric Organisms in Men > 35 Years Old: Beyond Fluoroquinolones. *Eur J Clin Microbiol Infect Dis* (2018) 37(6):1001–8. doi: 10.1007/s10096-018-3212-z
20. Al-Asmakh M, Stukenborg JB, Reda A, Anuar F, Strand ML, Hedin L, et al. The Gut Microbiota and Developmental Programming of the Testis in Mice. *PloS One* (2014) 9(8):e103809. doi: 10.1371/journal.pone.0103809
21. Tainaka T, Shimada Y, Kuroyanagi J, Zang L, Oka T, Nishimura Y, et al. Transcriptome Analysis of Anti-Fatty Liver Action by Campari Tomato Using a Zebrafish Diet-Induced Obesity Model. *Nutr Metab (Lond)* (2011) 8:88. doi: 10.1186/1743-7075-8-88
22. Hiramitsu M, Shimada Y, Kuroyanagi J, Inoue T, Katagiri T, Zang L, et al. Eriocitrin Ameliorates Diet-Induced Hepatic Steatosis With Activation of Mitochondrial Biogenesis. *Sci Rep* (2015) 4(1):3708. doi: 10.1038/srep03708
23. Shimada Y, Kuninaga S, Ariyoshi M, Zhang B, Shiina Y, Takahashi Y, et al. E2F8 Promotes Hepatic Steatosis Through FABP3 Expression in Diet-Induced Obesity in Zebrafish. *Nutr Metab* (2015) 12(1):17. doi: 10.1186/s12986-015-0012-7
24. Oka T, Nishimura Y, Zang L, Hirano M, Shimada Y, Wang Z, et al. Diet-Induced Obesity in Zebrafish Shares Common Pathophysiological Pathways With Mammalian Obesity. *BMC Physiol* (2010) 10(1):21. doi: 10.1186/1472-6793-10-21
25. Landgraf K, Schuster S, Meusel A, Garten A, Riemer T, Schleinitz D, et al. Short-Term Overfeeding of Zebrafish With Normal or High-Fat Diet as a Model for the Development of Metabolically Healthy Versus Unhealthy Obesity. *BMC Physiol* (2017) 17(1):4. doi: 10.1186/s12899-017-0031-x
26. Zhou T, Wei J, Su Y, Hu Z, Li Y, Yuan H, et al. Triclocarban at Environmentally Relevant Concentrations Induces the Endoplasmic Reticulum Stress in Zebrafish. *Environ Toxicol* (2019) 34(3):223–32. doi: 10.1002/tox.22675
27. Bernhard F, Landgraf K, Klöting N, Berthold A, Büttner P, Friebe D, et al. Functional Relevance of Genes Implicated by Obesity Genome-Wide Association Study Signals for Human Adipocyte Biology. *Diabetologia* (2013) 56(2):311–22. doi: 10.1007/s00125-012-2773-0
28. Wei J, Zhou T, Hu Z, Li Y, Yuan H, Zhao K, et al. Effects of Triclocarban on Oxidative Stress and Innate Immune Response in Zebrafish Embryos. *Chemosphere* (2018) 210:93–101. doi: 10.1016/j.chemosphere.2018.06.163
29. Kuczynski J, Stombaugh J, Walters WA, González A, Caporaso JG, Knight R. Using QIIME to Analyze 16S rRNA Gene Sequences From Microbial Communities. *Curr Protoc Bioinf* (2011) Chapter 10:Unit 10.7–10.7. doi: 10.1002/0471250953.bi1007s36
30. Chen L, Hu C, Lok-Shun Lai N, Zhang W, Hua J, Lam PKS, et al. Acute Exposure to PBDEs at an Environmentally Realistic Concentration Causes Abrupt Changes in the Gut Microbiota and Host Health of Zebrafish. *Environ Pollut* (2018) 240:17–26. doi: 10.1016/j.envpol.2018.04.062
31. Langille MGI, Zaneveld J, Caporaso JG, McDonald D, Knights D, Reyes JA, et al. Predictive Functional Profiling of Microbial Communities Using 16S rRNA Marker Gene Sequences. *Nat Biotechnol* (2013) 31(9):814–21. doi: 10.1038/nbt.2676
32. Fan Y, Liu Y, Xue K, Gu G, Fan W, Xu Y, et al. Diet-Induced Obesity in Male C57bl/6 Mice Decreases Fertility as a Consequence of Disrupted Blood-Testis Barrier. *PloS One* (2015) 10(4):e0120775. doi: 10.1371/journal.pone.0120775
33. Tremellen K. Gut Endotoxin Leading to a Decline in Gonadal Function (GELDING) - a Novel Theory for the Development of Late Onset Hypogonadism in Obese Men. *Basic Clin Androl* (2016) 26(1):7. doi: 10.1186/s12610-016-0034-7
34. Li Y, Su Y, Zhou T, Hu Z, Wei J, Wang W, et al. Activation of the NLRP3 Inflammasome Pathway by Prokineticin 2 in Testicular Macrophages of Uropathogenic Escherichia Coli- Induced Orchitis. *Front Immunol* (2019) 10:1872. doi: 10.3389/fimmu.2019.01872
35. Shin N, Whon TW, Bae J. Proteobacteria: Microbial Signature of Dysbiosis in Gut Microbiota. *Trends Biotechnol* (2015) 33(9):496–503. doi: 10.1016/j.tibtech.2015.06.011
36. Zanoni I, Tan Y, Di Gioia M, Broggi A, Ruan J, Shi J, et al. An Endogenous caspase-11 Ligand Elicits Interleukin-1 Release From Living Dendritic Cells. *Science* (2016) 352(6290):1232–6. doi: 10.1126/science.aaf3036

37. Dinan TG, Cryan JF. The Microbiome-Gut-Brain Axis in Health and Disease. *Gastroenterol Clin North Am* (2017) 46(1):77–89. doi: 10.1016/j.gtc.2016.09.007
38. Schachter J, Martel J, Lin CS, Chang CJ, Wu TR, Lu CC, et al. Effects of Obesity on Depression: A Role for Inflammation and the Gut Microbiota. *Brain Behav Immun* (2018) 69:1–8. doi: 10.1016/j.bbi.2017.08.026
39. Kanbay M, Onal EM, Afsar B, Dagel T, Yerlikaya A, Covic A, et al. The Crosstalk of Gut Microbiota and Chronic Kidney Disease: Role of Inflammation, Proteinuria, Hypertension, and Diabetes Mellitus. *Int Urol Nephrol* (2018) 50 (8):1453–66. doi: 10.1007/s11255-018-1873-2
40. Sabatino A, Regolisti G, Cosola C, Gesualdo L, Fiaccadori E. Intestinal Microbiota in Type 2 Diabetes and Chronic Kidney Disease. *Curr Diabetes Rep* (2017) 17 (3):16. doi: 10.1007/s11892-017-0841-z
41. Loomba R, Seguritan V, Li W, Long T, Klitgord N, Bhatt A, et al. Gut Microbiome-Based Metagenomic Signature for Non-invasive Detection of Advanced Fibrosis in Human Nonalcoholic Fatty Liver Disease. *Cell Metab* (2017) 25(5):1054–62.e5. doi: 10.1016/j.cmet.2017.04.001
42. Mouries J, Brescia P, Silvestri A, Spadoni I, Sorribas M, Wiest R, et al. Microbiota-Driven Gut Vascular Barrier Disruption is a Prerequisite for non-Alcoholic Steatohepatitis Development. *J Hepatol* (2019) 71(6):1216–28. doi: 10.1016/j.jhep.2019.08.005
43. Spadoni I, Zagato E, Bertocchi A, Paolinelli R, Hot E, Di Sabatino A, et al. A Gut-Vascular Barrier Controls the Systemic Dissemination of Bacteria. *Science* (2015) 350(6262):830–4. doi: 10.1126/science.aad0135
44. Fiorentino M, Sapone A, Senger S, Camhi SS, Kadzielski SM, Buie TM, et al. Blood–Brain Barrier and Intestinal Epithelial Barrier Alterations in Autism Spectrum Disorders. *Mol Autism* (2016) 7(1):49. doi: 10.1186/s13229-016-0110-z
45. Mokhtari Z, Gibson DL, Hekmatdoost A. Nonalcoholic Fatty Liver Disease, the Gut Microbiome, and Diet. *Adv Nutr* (2017) 8(2):240–52. doi: 10.3945/an.116.013151
46. Andriessen EM, Wilson AM, Mawambo G, Dejda A, Miloudi K, Sennlaub F, et al. Gut Microbiota Influences Pathological Angiogenesis in Obesity-Driven Choroidal Neovascularization. *EMBO Mol Med* (2016) 8(12):1366–79. doi: 10.15252/emmm.201606531
47. Schultz C. Isoenzyme Analysis of typhoid-Shigella and Escherichia-Shigella Hybrid Vaccines and Their Parental Strains. *J Clin Microbiol* (1989) 27 (12):2838–41. doi: 10.1128/jcm.27.12.2838-2841.1989
48. Bin P, Tang Z, Liu S, Chen S, Xia Y, Liu J, et al. Intestinal Microbiota Mediates Enterotoxigenic Escherichia Coli-Induced Diarrhea in Piglets. *BMC Veterinary Res* (2018) 14(1):385. doi: 10.1186/s12917-018-1704-9
49. Ding N, Zhang X, Zhang XD, Jing J, Liu SS, Mu YP, et al. Impairment of Spermatogenesis and Sperm Motility by the High-Fat Diet-Induced Dysbiosis of Gut Microbes. *Gut* (2020) 69(9):1608–19. doi: 10.1136/gutjnl-2019-319127
50. Liu R, Zhang C, Shi Y, Zhang F, Li L, Wang X, et al. Dysbiosis of Gut Microbiota Associated With Clinical Parameters in Polycystic Ovary Syndrome. *Front Microbiol* (2017) 8:324. doi: 10.3389/fmicb.2017.00324
51. Patel S. Polycystic Ovary Syndrome (PCOS), an Inflammatory, Systemic, Lifestyle Endocrinopathy. *J Steroid Biochem Mol Biol* (2018) 182:27–36. doi: 10.1016/j.jsbmb.2018.04.008

Conflict of Interest: The authors declare that the research was conducted in the absence of any commercial or financial relationships that could be construed as a potential conflict of interest.

frontiers in Immunology

REVIEW
published: 21 July 2021
doi: 10.3389/fimmu.2021.658432

Impacts of Immunometabolism on Male Reproduction

Lijun Ye[1†], Wensi Huang[1†], Su Liu[1], Songchen Cai[1], Ling Hong[1], Weiqiang Xiao[2], Kristin Thiele[3], Yong Zeng[1], Mingzhe Song[2] and Lianghui Diao[1*]*

[1] *Shenzhen Key Laboratory for Reproductive Immunology of Peri-implantation, Clinical Research Center for Reproductive Medicine, Shenzhen Zhongshan Urology Hospital, Shenzhen, China,* [2] *Shenzhen Zhongshan Institute for Reproduction and Genetics, Fertility Center, Shenzhen Zhongshan Urology Hospital, Shenzhen, China,* [3] *Division of Experimental Feto-Maternal Medicine, Department of Obstetrics and Fetal Medicine, University Medical Center Hamburg-Eppendorf, Hamburg, Germany*

The physiological process of male reproduction relies on the orchestration of neuroendocrine, immune, and energy metabolism. Spermatogenesis is controlled by the hypothalamic-pituitary-testicular (HPT) axis, which modulates the production of gonadal steroid hormones in the testes. The immune cells and cytokines in testes provide a protective microenvironment for the development and maturation of germ cells. The metabolic cellular responses and processes in testes provide energy production and biosynthetic precursors to regulate germ cell development and control testicular immunity and inflammation. The metabolism of immune cells is crucial for both inflammatory and anti-inflammatory responses, which supposes to affect the spermatogenesis in testes. In this review, the role of immunometabolism in male reproduction will be highlighted. Obesity, metabolic dysfunction, such as type 2 diabetes mellitus, are well documented to impact male fertility; thus, their impacts on the immune cells distributed in testes will also be discussed. Finally, the potential significance of the medicine targeting the specific metabolic intermediates or immune metabolism checkpoints to improve male reproduction will also be reassessed.

Keywords: immunometabolism, immune privilege, metabolic reprogramming, immune cells, male reproduction, hypothalamic-pituitary-testicular axis

OPEN ACCESS

Edited by:
Yong-Gang Duan,
University of Hong Kong, China

Reviewed by:
Yongning Lu,
Fudan University, China
Pallav Sengupta,
Mahsa University, Malaysia
Yao Bing,
Nanjing Medical University, China

****Correspondence:***
Lianghui Diao
diaolianghui@gmail.com
Mingzhe Song
smz798018@163.com

[†]These authors have contributed equally to this work

Specialty section:
This article was submitted to Mucosal Immunity, a section of the journal Frontiers in Immunology

Received: *25 January 2021*
Accepted: *29 June 2021*
Published: *21 July 2021*

Citation:
Ye L, Huang W, Liu S, Cai S, Hong L, Xiao W, Thiele K, Zeng Y, Song M and Diao L (2021) Impacts of Immunometabolism on Male Reproduction. Front. Immunol. 12:658432. doi: 10.3389/fimmu.2021.658432

INTRODUCTION

Male reproduction is a multi-step process starting from the production of germ cells in testes and transport of sperm to the sperm-egg binding site in the fallopian tube, which is orchestrated by the sophisticated regulation of the endocrine and immune system (1–3). Spermatogenesis is a complex and highly-coordinated cellular differentiation process controlled by the hypothalamic-pituitary-testicular (HPT) axis that modulates gonadal steroid hormones in testes (4, 5). Whereas, spermatogenesis presents a unique challenge to the immune system because meiosis and subsequent cellular differentiation events involved in spermatogenesis occur long after the systemic tolerance is established (6, 7). In order to protect the testicular germ cells from detrimental immune responses, the male reproductive system adopts an exclusive immune milieu, which is referred to as the blood-testis barrier (BTB) in testes. The BTB anatomically divides the seminiferous epithelium into the basal compartment containing meiotic (leptotene,

zygotene, and pachytene spermatocytes) germ cells and the adluminal compartments. All subsequent post-meiotic (round and elongating spermatids) germ cells, thus, allowing early-stage germ cells (spermatogonia) localized outside of BTB to become autoantigenic foreign bodies to the immune system (8, 9). Except for the above testicular physical barriers, the testicular immune privilege will be sustained by coordinating systemic immune tolerance, and antigen-specific regulatory immunoregulation (10). Infection or physical trauma of the testis can perturb testicular immune privilege, causing inappropriate immune responses or inflammation, which may result in altered tissue and cellular metabolic function, and eventually leading to impairment of spermatogenesis, autoimmune disorders, and male infertility (11–13).

Metabolism cooperation among testicular cells is crucial for normal spermatogenesis since increased energy requirements during reproduction and metabolic factors play a predominant role in controlling the functional activity of the reproduction endocrine and immunity in testes (14). The establishment of BTB physically and physiological compartmentalize the seminiferous epithelium into two different milieus forming a microenvironment to support spermatogenesis. Metabolic regulation is essential for developing germ cells into mature spermatids due to the specific metabolic demands of germ cells (15). The BTB is composed of specialized junctions between adjacent Sertoli cells, which is located near the basement membrane, is responsible for maintaining the different levels of substances between rete testis fluid and the lymph or plasma (16). Sertoli cells provide structural and functional support for the development of the germ cells due to their role in maintaining the suitable ionic and metabolic microenvironment in testes (17, 18). They use different metabolic substrates, including glucose and fatty acids, and growth factors to meet their metabolic demands and nurture germ cells (19–22). Because the testis is a naturally hypoxic organ, Sertoli cells preferentially use glucose and go through anaerobic glycolysis rather than the tricarboxylic acid cycle to meet the specific metabolic demands of germ cell development (18, 23). Besides, Sertoli cells regulate testicular immune tolerance by producing anti-inflammatory cytokines and prostanoid molecules, slowing leukocyte migration and inhibiting complement activation and membrane-associated cell lysis (24). In the interstitium, Leydig cells also contribute to the spermatogonial microenvironment by secreting growth factors and steroid hormones whose metabolism is notable in testes (25, 26). Androgens in Leydig cells are derived from cholesterol, which metabolizes to progesterone and, subsequently, testosterone (26). Testosterone regulates spermatogenesis and contributes to the maintenance of the BTB (27). In addition to Sertoli cells and Leydig cells, immune cells presenting in the interstitium, such as macrophages, mast cells, T cells, natural killer (NK) cells, are responsible for the regulation of sperm generation (28, 29). Metabolism, as well as the key signaling pathway mediating metabolic activity in various immune cells of human blood or rodent animals, have been elaborated in recently published reviews (30–33). However, even though all testicular cells, including germ cells, Sertoli cells, Leydig cells, testicular macrophages and lymphocytes, can regulate local immunity in the testis, the specific metabolic functions of testicular immune cells and the different metabolic pathways of testicular immune cells in physiological and pathological states have been neglected (29).

Immunometabolism is a recently emerging area of research that focuses on the crosstalk between the immune and metabolic systems, and studies in the field of reproduction have shown that immunometabolic disorders may be associated with infertility (34–36). Accumulating data from cellular and animal researches focusing on how metabolism regulated immune cell function have been reported, which provide new therapeutic opportunities for many diseases related to immune system dysregulation like autoimmune diseases and cancer (37–39). However, little literature on the immunometabolism or metabolism of immune cells in the male reproductive system, neither in animals nor in humans. In addition, metabolic factors play a dominant role in controlling the functional activity of the HPT axis in men due to the increased energy requirements during reproduction. Therefore, men who are overweight and suffer from metabolic syndrome may be at higher risk of infertility than their healthy counterparts (14). In this review, we will focus on the following topics (a) functional impacts of the neuroendocrine-immune systems on male reproduction; (b) the normal metabolic state of immune cells in testes and their alteration in metabolic diseases; (c) potential therapeutic strategies for male infertility based on key immunometabolic targets.

REGULATION OF HPT AXIS AND IMMUNE ON MALE REPRODUCTION

Regulation of HPT Axis on Male Reproduction

Both positive and negative feedback regulatory mechanisms homeostatically regulate the HPT axis. The gonadotropin-releasing hormone (GnRH) is the central regulator of the HPT axis and is secreted from the hypothalamus in a periodic pulsatile manner and regulates the synthesis and secretion of gonadotropins, which are luteinizing hormone (LH) and follicle-stimulating hormone (FSH), by the pituitary gland. Gonadotropins, in turn, acts on testes to stimulate the synthesis of sex gonadal steroid hormones and modulates the testicular-specific morphological changes and functions (40). Conversely, testosterone secreted by the testes provides continuous negative feedback to the hypothalamus and pituitary gland to maintain a steady GnRH, LH, and FSH secretion state. Thus, these gonadal steroids, together with pituitary gonadotropins, explicitly establish physiological homeostasis *via* feedback regulatory mechanisms to keep healthy male reproductive function (4, 41).

Inside testes, the Sertoli cells provide morphogenetic support through cell-cell interactions, nutrients, and biochemical components through lactate, hormones, and cytokines to facilitate spermatogenesis (22). Leydig cells are the major site

for the synthesis of the predominant male steroid hormone (testosterone), and cytokines, such as macrophage-migration-inhibitory factor (MIF), for the regulation and maintenance of spermatogenesis and extra-testicular androgenic and anabolic and anti-inflammatory functions (42, 43). All the above components of the HPT axis coordinate to produce sex steroid hormones, maintain spermatogenesis and sperm counts and quality (27, 44).

Regulation of metabolic process in testes is another crucial factor that has a direct influence on male reproduction. Germ cells have specific metabolic requirements for their development, preferentially utilizing lactate as a substrate for ATP production (21). Sertoli cells fulfill the energy requirement of the germ cells and themselves through glycolysis and fatty acid oxidation (18). FSH and sex steroid hormones from the HPT axis have been proven as the regulatory factors that modulate Sertoli cell metabolism (18, 45). FSH regulates glycolytic metabolism in mature Sertoli cells through increasing glucose uptake and both pyruvate and lactate production. Meanwhile, FSH has a regulatory effect on lipid metabolism by influencing lipid esterification in Sertoli cells (18, 46, 47). Androgens and estrogens also regulate Sertoli cell metabolism. 5α-Dihydrotestosterone and 17β-estradiol are reported to regulate glucose uptake and lactate production in Sertoli cells isolated from humans (48). A recent genome-wide study of androgen and estrogen receptor binding sites proved that sex hormones regulate lipid metabolism in adult Sertoli cells from rats by transcriptionally controlling the expression of the genes (49). Despite energy metabolism for germ cell development, Leydig cells are stimulated by LH and metabolize cholesterol to testosterone and other steroid hormones, which are required for spermatogenesis and other functions for male reproduction (26).

Impact of GnRH and Pituitary Gonadotropins on Immune Function

The immune system does not work in isolation as neuro-endocrine-immune and central nervous systems are integrated through a complex network (50) of signal molecules, including cytokines, hormones, and neurotransmitters (51, 52). Evidence suggests the hypothalamic-pituitary-gonadal (HPG) axis and related hormonal system may modulate immune function (53). Physiologically, GnRH acts as an autocrine or paracrine factor to regulate both neuroendocrine and immune functions. Immunoreactive and bioactive GnRH receptor (GnRH-R) has been identified in human peripheral lymphocytes, implicating that GnRH may function as an autocrine or paracrine factor to regulate immune functions (54–56). Blockade of central and peripheral GnRH-R during maturation of both the HPG axis and brain-thymus-lymphoid axis remarkably impairs the development of the immune system (57). The administration of GnRH antagonist into rodent and primate fetuses resulted in the suppression in the numbers of thymocytes and immune cell development, suggesting GnRH plays a crucial role in immune system modulation and development (56, 58). In mammals, GnRH induces the expression of cytokines such as interleukin-2 (IL-2) and interferon-γ (IFN-γ), promoting their proliferation and activation of immune cells (59). Taken together, these pieces of evidence indicate that GnRH may be directly involved in the cell-mediated and humoral immune response.

Nevertheless, a paucity of studies illustrating the immunomodulatory actions of FSH and LH experimental and clinical evidence suggested that these two gonadotropins induce the proliferation of immune cells and modify cytokine (e.g., IL-10, interferon-γ) production (60, 61). After treatment with gonadotropin, the immune cell populations were altered in male patients with idiopathic hypogonadotropic hypogonadism (IHH), suggesting that gonadotropin could modulate both cell-mediated and humoral immunity (62).

Collectively, Sertoli cell metabolism plays a decisive role in the male reproductive physiology process. And FSH and sex steroid hormones (androgens and estrogens) from the HPT axis have been shown to regulate Sertoli cell metabolism.

Impact of Sex Steroid Hormones on Immune Function

Besides sexual differentiation and reproduction, sex steroid hormones also influence immune function due to the presence of hormone receptors on immune cells (63, 64). Owing to lipophilic properties, sex steroid hormones can alter membrane properties of immune cells by integrating into their membrane, leading to changes in the immune cell functions (51). Androgens and estrogens represent the two major gonadal steroid hormones produced by the testes. Estrogens and androgens exert their effects through binding to their well-recognized estrogen receptors (ERs) and androgen receptors (ARs), respectively, which are expressed in primary lymphoid organs as well as various immune cells (59). Thus, sex steroids, particularly androgen and estrogens, can modulate immune cell development and immune response and also regulate reproductive functions in males.

Androgen

Men produce 20 times more testosterone than women, and the incidences of autoimmune disease remain relatively lower among men (65–67). Thus, androgens are believed to affect both the development and function of the innate immune response and the adaptive immune system (51, 68). In human males, androgen deficiency is characterized by an increase in serum levels of inflammatory cytokines, such as IL-1β, tumor necrosis factor α (TNF-α), and the number of macrophages in the circulation (69). Furthermore, loss of testicular immune privilege was detected in the mice with deficiency of the androgen receptor in Sertoli cells, revealing the role of androgen in testicular immune privilege (70). Testosterone, as the dominant androgen in testes, its level is decreased in experimental autoimmune orchitis (EAO, a model of male immune infertility) rat. Protective effect is shown in the development of disease and the inflammatory response in EAO rat treated with testosterone supplementation, which prevented the increase of macrophage and reduced the number of $CD4^+$ T cells accompanied with increasing number of regulatory T cells

(Tregs) in testes comparing with the EOA rat without testosterone replacement (71). The mechanism of testosterone actives Tregs is that testosterone induces expression of Foxp3 in human T cells through binding of the AR to gene regulatory sequences, which leads to the generation of $CD4^+CD25^+Foxp3^+$ regulatory T cells, which are viewed as important players in testicular immune tolerance (72). Furthermore, testosterone inhibits the lipopolysaccharide-induced inflammatory response on TNF-α mRNA expression both in Sertoli cells and peritubular cells which support spermatogenesis and transport of spermatozoa as well as testicular immune regulation, while no effect was found in testicular macrophages (73). Taken together, these studies suggested that androgens modulate not only the numbers but also the function and responses of innate immune cells in mammals, as well as the immunosuppressive effect in male reproduction through influencing the numbers and secretion of testicular immune cells. However, the role and mechanism of androgens in regulating the testicular immune status remains to be clarified and elucidated.

Estrogen

Estrogens, as relevant physiological regulators in men, exhibit an immunoenhancing effect (66). Two intracellular ER subtypes (ERα and ERβ) are expressed in the mammalian immune system to regulate the innate and adaptive immune system as well as immune cell development (64, 68, 74). Of note, both ERα and ERβ are expressed by a diverse array of immune cell types, including T cells, B cells, macrophages, dendritic cells (DCs), and NK cells (75, 76). Estrogen regulates immunity and maintains immunometabolic function in males (77, 78). In transgenic male mice that overexpress human aromatase genes (AROM+ mice), increased estradiol promoted testicular macrophage activation; however, testicular macrophages were enhanced in a rat model of EAO, indicating the stimulating effect of estrogens on immunoregulation of male reproductive function (79, 80).

Collectively, sex steroids function as regulators of the immune system, and androgens and estrogens affect different subsets of immune cells. In general, androgens appear to predominantly have immunosuppressive activity, while estrogen exhibit an immunoenhancing effect on immune cells and immune activity (**Figure 1**). Thus, androgens exert suppressive effects in the immune-privileged environment of testes, while estrogens exert immunoenhancing activities in testes, which warrants further investigation.

POSSIBLE CONTRIBUTION OF METABOLISM OF IMMUNE CELLS TO MALE REPRODUCTION

The testicular interstitial space possesses potent immunoregulatory activities through the production of cytokines and other immunoregulatory molecules such as androgens by interacting cell types, including macrophages, DCs, T cells, NK cells, mast cells, and Leydig cells (6, 9). For instance, the anti-inflammatory factor TGF-β and IL-10, can suppress the immune response to maintain the immune homeostasis of testes (6, 9). These immune cells primarily express a high tolerance to germ cell autoantigens,

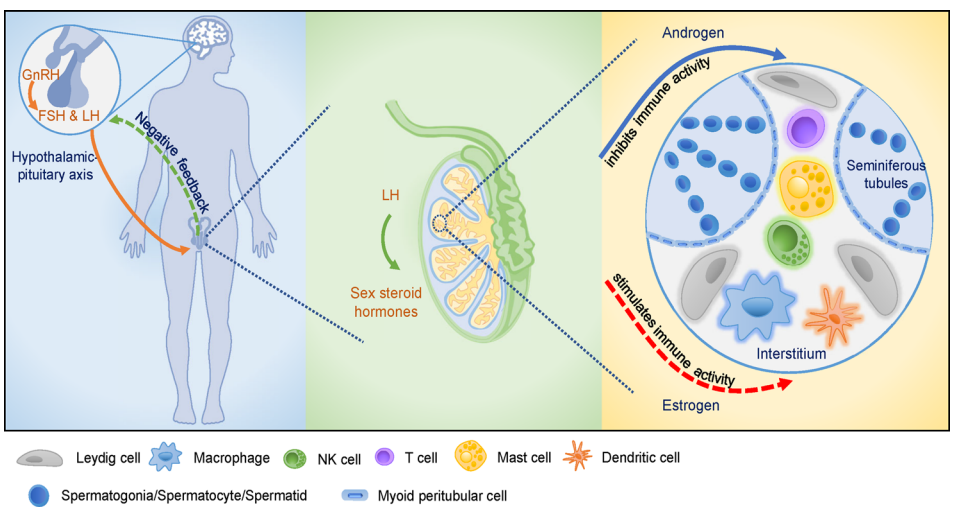

FIGURE 1 | The hypothalamic-pituitary-testicular (HPT) axis and the testicular immune-privileged microenvironment. GnRH stimulates the release of pituitary gonadotropins, induces male reproductive function as well as affects cellular and humoral immune function. GnRH promotes the proliferation of immune cells and modifies cytokines production. Pituitary gonadotropins are involved in cellular and humoral immune development. Sex steroid hormones are secreted by the stimulation of LH that acts on Leydig cells in testis. Androgens and estrogens affect male reproductive function *via* modulation of the immune system and immune response. Various cell types present in the testicular interstitial space, including macrophages, DCs, T cells, NK cells, mast cells, and Leydig cells, providing a unique microenvironment for testicular functions. Androgens play crucial roles in maintaining the integrity of testicular immune-privileged microenvironment (solid arrow), while estrogens seem to play a stimulatory role in testicular immunoregulation which needs further investigations (dotted arrow).

meanwhile maintain protection against microbial infections. At present, the microenvironmental signals like androgens, prostaglandins, and corticosterone have been indicated to influence the phenotype and function of testicular immune cells (81). Since metabolic flux can dictate cell fate like immune cell effector and regulatory function, the field of immunometabolism has seen tremendous development over the past decade (33). Yet metabolic reprogramming in immune cells of testes has not been illustrated. This may be due to a paucity of nonpathological tissue samples in human (82). Conceivably, immunometabolism pattern has been partly established in tumor and gravid uterus which are also immune-privileged sites, which could be used as reference for the new areas of research in immunometabolism in male reproduction. In this article, therefore, we attempt to establish the possible immunometabolic pathways involved testicular function.

Macrophages

In testes, macrophages represented the most abundant immune cells in the interstitial space (83). For example, rat testicular macrophages were accounting for approximately 80% of the testicular leukocytes (84). A recently study in human testes revealed that testicular resident macrophages are approximately 62% of testicular myeloid cells and express 6-fold higher levels of the M2 macrophages marker (CD163) than blood monocytes (85). According to the morphology and localization, human testicular macrophages could be classified into interstitial and peritubular macrophages; but no marker has been found to distinguish both types (86). Unlike in humans, mouse testicular interstitial and peritubular macrophages were characterized by $CD64^{hi}MHCII^{lo}$ and $CD64^{lo}MHCII^{hi}$, respectively (87, 88). Once established in the niche, except the empty niche, these macrophages self-maintain for long periods of time without replenishment from blood monocytes in the steady condition (88). Interstitial macrophages closely contact with Leydig cells, which might contribute to facilitate testosterone. For example, when Leydig cells cultured in testicular macrophages-conditioned medium, the production of testosterone significantly increased, whereas had less effect on conditioned medium from peritoneal macrophages (89). Subsequently, macrophage-derived factor 25-hydroxycholesterol, might works as an exogenous substrate engaging in testosterone production, had been found to increase (90). Moreover, in both the colony stimulating factor1 (CSF1) mutation mouse lacked most macrophage populations and the transient macrophage depletion mouse model, intratesticular testosterone were reduced (91, 92). Testosterone regulated downstream gene expression like *Rhox5* through interacting with androgen receptor in Sertoli cells, and then regulated spermatogenesis processes, including maintenance of spermatogonial numbers and BTB, completion of meiosis by spermatocytes, adherence of elongated spermatids to Sertoli cells, and the release of mature spermatozoa (93, 94). On the other hand, dihydrotestosterone, a derivative of testosterone, modulates levels of glycolysis-related transporters (glucose and monocarboxylate transporter) and enzymes (phosphofructokinase1and lactate dehydrogenase), and consequently acts on glucose metabolism in rat Sertoli cells (95, 96). Glucose metabolism within Sertoli cells is crucial for spermatogenesis since developing germ cells consume lactate produced by Sertoli cells as their main energy source (97). Testicular macrophages might express CSF1 and retinoic acid biosynthesis enzymes ALDH1A2 and RDH10 to promote spermatogonial proliferation and differentiation. In macrophages-depleted testes, followed by ALDH1A2 and RDH10 decrease, spermatogonia differentiation would be disrupted (98). However, it can't identify whether these evidences resulted from peritubular macrophages depletion or interstitial macrophages depletion leading to reduce these factors production by Leydig cells, since the depletion models targeted all macrophages. Winnall and Hedger summarized four subsets of rat testicular macrophages, including $CD68^{+}CD163^{-}$ (21.7%) newly-arrived macrophages and $CD68^{+}CD163^{-}$ infiltrating macrophages accounting for 21.7%, $CD68^{+}CD163^{+}$ intermediate macrophages (36.7%), and $CD68^{-}CD163^{+}$ resident macrophages (42%) (83). Recently, this idea has been renewed by the data, utilizing flow cytometric analyses, that all, not only 57%, testicular macrophages are positive for CD68 and comprised by $CD68^{+}CD163^{+}$ (80%) and $CD68^{+}CD163^{-}$ cells (20%) (81).

In fact, rat testicular macrophages characterized by high level of CD163 that were related to maintain testicular immune privilege through secreting large amounts of the anti-inflammatory cytokine like IL-10, and inducing expansion of immunosuppressive Tregs (81, 85, 99). Similarly, macrophages in mouse testes also display an immunosuppressive phenotype by expressing significantly higher levels of immunosuppressive genes, namely *Mrc1*, *Dab2*, *Igf1*, and *Lgals3* (88). In accordance with these evidences, previous data suggested that the number of $CD25^{+}Foxp3^{+}$ Tregs would increase after coculture of testicular macrophages and splenic T cells (81). In general, classically activated macrophage phenotype or M1 macrophages activated by the stimulation of TLRs through bacterial lipopolysaccharides (LPS) or the cytokine IFN-γ are pro-inflammatory, like peritoneal macrophage. However, rat testicular macrophages are specifically polarized to regulatory phenotype with similar properties as M2 phenotype under LPS/IFN-γ stimulation (99, 100). Even during inflammation resulting from uropathogenic *Escherichia coli* (UPEC), mouse resident macrophages ($F4/80^{hi}CD11b^{lo}$) were only number proliferation, but not transformed to inflammatory macrophages ($F4/80^{lo}CD11b^{hi}$) that impaired testis tissues and spermatogenesis (88). It can be confirmed by the evidence that focal impairment of spermatogenesis induced by UPEC infection in wild type mice was ameliorated in chemokine receptor 2-deficient mice, which lack peripheral blood monocytes due to defective egress of $Ly6C^{hi}$ monocytes from the bone marrow (88). This is partly because testicular macrophages exhibit an attenuated response to inflammatory cues by inhibiting TLR cascade gene expression and blocking the nuclear factor-κB (NF-κB, a proinflammatory transcription factor) signaling pathway (101). As a consequence, the process leads to the low production of prα facilitating the protection of the delicate germ cells from a 'cytokine storm' (82). Meanwhile, testicular macrophages also produce much lower concentration proinflammatory cytokines than peritoneal macrophages to retain bactericidal activities through the

activation protein transcription factor 1 (AP-1) and cAMP response element binding protein (CREB) signaling pathways (100). Secondly, high amounts of testosterone (around100-fold higher than in serum), prostaglandins (PGs, like PGE_2 and PGI_2, around 3000-fold higher than in serum), and corticosterone (around 7-fold higher than in serum) in testicular interstitial fluid are associated with the establishment and maintenance of the immunosuppressive phenotype of M2 macrophage (81). In support, these molecules polarized GM-CSF-induced monocyte-derived M1 macrophages to the M2 macrophage phenotype characterized by significantly expression of IL-10 and CD163 (81). Among these molecules, testosterone and PGE_2 suppressed the activation of the NF-κB signaling pathway by deferring IκBα degradation, and PGE_2 concomitantly activated the CREB and signal transducer and activator of transcription 3 (STAT3) anti-inflammatory signaling pathways in LPS stimulated macrophages. However, corticosterone did not attenuate the activation of the NF-κB signaling pathway and increase the activation of STAT3, but activated the CREB signaling. Endogenous corticosterone produced by testicular macrophages was the principal molecule in maintaining testicular macrophages phenotype and function. This idea could be supported when peritoneal macrophages cultured in testicular macrophages supernatant, the secretion of TNF-α was significantly reduced upon stimulation with LPS, an effect abolished using a corticosterone inhibitor (81). Furthermore, the metabolic reprogramming of immune cells is required for the polarization and activation of macrophages, which is increasingly apparent in macrophage populations derived from the mouse peritoneum (102) and bone-marrow (103, 104). Immunosuppressive M2 macrophages induced by IL-4/IL-13 maintain high levels of oxygen consumption rate to reduce glucose flow through the pentose phosphate pathway (PPP) to oxidative phosphorylation (OXPHOS) and tricarboxylic acid (TCA) cycle (102–104). M2 macrophages also exhibited a significant increase of uptake and oxidation of fatty acids (FAs) which are suppressed in M1 macrophages (105). Testicular somatic cells, such as Sertoli cells, Leydig cells and macrophages, synthesize high levels of FAs metabolites to sustain the M2 phenotype. Coinciding with this, rat testicular prostaglandins that were mainly produced by these cells from arachidonic acid by the action cyclooxygenase (COX) are much higher than in serum under physiological condition (81, 106). However, COX/prostaglandins system was related with infertile patients with impaired spermatogenesis (106). This discrepancy may imply that PGs play distinctly different roles in testes of different species. Thus, the potential mechanism of COX/prostaglandins system on male infertility need to be further investigated. Different from inflammatory macrophages, M2 macrophages metabolize arginine to polyamines that are highly immunosuppressive acting by high levels of arginase 1 (ARG1) (107). Elevated lactate produced by tumor cells has been shown to promote the M2-like polarization and increase ARG1 expression (108). Concomitantly with efficient glycolysis process, Sertoli cells produced abundant lactate and secreted them into seminiferous epithelium for germ cells (97). But whether Sertoli cells-produced lactate polarized testicular macrophages toward the M2 phenotype is less clear.

Conversely, inflammatory M1 macrophages, induced by IFN-γ/LPS, exhibited glucose metabolism shift towards the anaerobic glycolytic pathway and the PPP to meet the rapid energy requirements, and increased demands for biosynthetic precursors used for the synthesis of pro-inflammatory factors (e.g., NO, TNF-α, IL-6) (109). Consequently, this metabolic reprogramming leads to increased lactate, succinate, NADPH necessary for reactive oxygen species (ROS) production (107). Arginine is also a critical nutrient for M1 macrophages to generate cytotoxic nitric oxide (an important pro-inflammatory mediator) by inducible nitric oxide synthase (iNOS) (107). However, in nutrient deficits tumor tissue, an immunologically privileged site, when glycolysis, PPP and TCA cycle were suppressed, the generation of succinate, NADPH and ROS were concomitantly limited, M1 macrophages function were severely limited (107). In this context, testicular interstitial space maintained immunosuppressive state whether partially due to the nutrient constitution, where remains to be investigated.

Overall, the above evidences indicate that testicular macrophages might enhance oxidative metabolism and decrease anaerobic metabolism to maintainM2 macrophages phenotype. In fact, further studies are needed for the metabolism pattern of macrophages in testes, which may help to understand the role of macrophages in spermatogenesis.

Dendritic Cells

Testicular DCs, a small immune cell population within testes, are phenotypically immature and functionally tolerogenic DCs under physiological conditions. They are involved in effector T cell inactivation and Tregs development and are associated with the adaptive immune system of testes under physiological conditions (110). Moreover, immature DCs might be involved in recognition of normal sperm antigens and induction of immune tolerance to protect sperm cells under physiological conditions (110). Fatty acid oxidation (FAO) and OXPHOS are essential catabolic process for the development of immature DCs (111, 112). Notably, drugs (e.g., vitamin-D3) that promote the OXPHOS pathway may facilitate tolerogenic DC (adopted tolerant status) phenotype and function such as the production of IL-10 (113). Moreover, inhibition of FAO prohibited the function of immature DCs and partially restored T cell stimulatory capacity (111). Indoleamine 2,3-dioxygenase (IDO), an enzyme for catalyzing the metabolism of tryptophan and then generating kynurenine, usually maintains a basal level in DCs (114). Functioning as an endogenous ligand for aryl hydrocarbon receptors on T cells, kynurenine has been found to induce the generation of $Foxp3^+$ Tregs and the upregulation of programmed cell death receptor 1 (PD-1) on activated $CD8^+$ T cells, both of which were associated with immunosuppression (115, 116). IDO is reported to induce DCs to initiate immune tolerance and to stimulate the development of Tregs in tumors and pregnant uterus both are immunologically privileged site like testes (117–119). Recently, the IDO-based mechanism has also been identified to be involved in testicular immune privilege (120). The expression of IDO is rapidly increased when DCs

suffer from LPS/IFN-γ-stimulation, leading to limited microbial growth and reduced injurious hyperinflammatory responses (121, 122). However, testicular DCs mildly expressed IDO, meanwhile IDO activity is reduced in EAO rat (120, 123). These differences might be attributed to the fact that the Sertoli cells indirectly inhibit LPS-induced DCs maturation through paracrine effect. Supporting this idea, when bone marrow-derived DCs cocultured with Sertoli cells from mouse testes that secreted galectin-1, the expression of iNOS, COX2, and IDO are decreased, whereas the levels of IL-10 and TGF-β1 are significantly increased in LPS-stimulated DCs (124).

However, DCs maturation under the pathological conditions overcome the immune tolerance by the local activation of autoreactive T cells by upregulating co-stimulatory proteins such as CD40, CD80, CD86, inflammatory cytokines, major histocompatibility complex (MHC) class-II, which trigger autoimmunity and causes male infertility (6). This has been demonstrated in azoospermic testes of human with chronic inflammation and atrophy testes of rats with EAO (12, 125). The predominant metabolic mode of mature DCs following LPS/IFN-γ-stimulation induces a switch from OXPHOS to glycolysis, with a decrease in TCA cycle activity, and an increase in lactate production and flux through the PPP (126–128). Besides, mature DCs induced by LPS also increase the expression of iNOS, which generates NO, a reactive nitrogen species that can inhibit mitochondrial respiration, thereby dampening OXPHOS (129). However, it has not been reported how metabolic reprogramming regulates the development of mature DCs in testes.

Lymphocytes

In normal human and rat testes, lymphocytes were according for 10%-20% of the total leukocyte population and sparsely distributed throughout the interstitial space, whereas B lymphocytes were not found (84, 86). During inflammation induced by infection or autoimmunity, however, the number of lymphocytes, such as effector T helper cells (Th1 and Th17), as well as Tregs, increases significantly within the testicular interstitial space (28, 130). Comparing with peripheral blood where $CD4^+$ T cells were the major lymphocyte subset, T cells in rat testes are predominantly of the $CD8^+$ subset, and a large population of NK cells were also visible (131). This might be consistent with consolidated immunosurveillance and a reduced capacity for initiating antigen-specific immune responses. There was reverse correlation between the largely number of NK cells and the metastatic incidence of gastric, renal, and prostate carcinomas (132).

$Foxp3^+$ Tregs, the powerful immunosuppressive cells, are found in rat, mouse and human testes under physiological conditions, which may be associated with the immunosuppressive characteristics of testes (125, 133, 134). The data about Tregs in human blood reveal that testosterone supplement induces a strong increase in the $CD4^+CD25^+Foxp3^+$ Tregs population *via* Foxp3 through androgen-mediated binding of AR to the *Foxp3* locus (72). However, whether or how testosterone modulates the activation and function of T lymphocytes remains less clear. On the other hand, testosterone might inhibit the activation of $CD8^+$ and $CD4^+$ T-cell subset. When Leydig cells were destroyed by ethane dimethane sulfonate, the number of $CD8^+$ and $CD4^+$ T cells rapidly increased. The addition of testosterone cooperating with recovery Leydig cells would reduce the number of $CD8^+$ and $CD4^+$ T cells to lower than the control levels (135). Similar to Leydig cells, Sertoli cells have been reported to induce the differentiation of $Foxp3^+$ Tregs *via* Notch pathway signaling through secreting JAGGED1 (136). In fact, Tregs generation and suppressive functions are also highly dependent on mitochondrial FAO and OXPHOS to oxidize exogenous FAs, which is stalled by enhanced glycolysis. Numerous regulators of Tregs suppressive function, including adenosine monophosphate-activated protein kinase (AMPK), and transcription factor Foxp3, by inhibiting glycolysis and promoting FAs oxidation through suppression of mTOR activity (137). Foxp3 reduces glucose uptake in Tregs by inhibiting the expression of glucose transporter 1 (GLUT1). Besides, AMPK, another regulator of Tregs suppressive function, inhibits glycolysis, and promotes FAO through the suppression of mTOR activity (137). Interestingly, in response to TLR signals, Tregs upregulate GLUT1 expression and anaerobic glycolysis to promote proliferation and inhibit their suppressive function. In inflammatory testes, although $CD4^+$ and $CD8^+$ Tregs are increased, and TGF-β is expressed, more effector T cell subsets can overwhelm the inhibitory effect of Tregs by producing pro-inflammatory cytokines like TNF-α and IL-6 (138). Thus, Tregs alone may not be sufficient to limit excessive T cells activation in autoimmune settings.

T cells activation leads to dynamic transformation in cell metabolism to protect against pathogens and to coordinate the function of other immune cells. T cells accomplish bioenergetic demands for activation by undergoing anaerobic glycolysis, a process frequently observed in highly proliferative cells in which glucose is fermented into lactate rather than oxidized in mitochondria. Recent studies have reported the dynamic profile of $CD4^+$ and $CD8^+$ T cells after activation and revealed that glucose acts as a crucial contributor to fuel effector responses and proliferation of immune cells (139, 140). PGE_2 secreted by Leydig cells may transform T cells from proinflammatory phenotype (Th1) to anti-inflammatory phenotype (Th2) (141). NK cells, comparable to lymphoid lineage members, also upregulate anaerobic glycolysis and OXPHOS during their activation and effector function, which parallels with the immunometabolism of effector T cells (137). Inconsistent with glucose transport, hypoxia-inducible factor 1α (HIF-1α), and mTOR highlight metabolic control points in both T cells and NK cells. Despite these similar nodes of immunometabolism, NK cells exhibit a differential reliance on OXPHOS for IFN-γ production, while T cells rely profoundly on glycolysis to produce IFN-γ (142, 143). Furthermore, numerous inhibitory molecules, such as IDO and PD-1, alter T cells metabolism by reducing T cells GLUT1 expression and then inhibiting glucose uptake (144, 145). The inhibition of both IDO and PD-1 is also observed in NK cell; however, whether they impair NK cells effector function by altering metabolism remains elusive (146). Given that Sertoli cells express IDO and programmed death-1

ligand-1 (PD-L1) and also inhibit the activation of T cells, and NK cells, it is warranted to elucidate whether Sertoli cells regulate these effector cells by paracrine action to control their metabolism. It is also implicated that Sertoli cells may partly contribute to immunosuppression for the testicular immune privilege in the similar way.

Mast Cells

Mast cells are scarce in rat and mouse, but are more frequent in human, all of which are quiescent under physiological status. Mast cells in testicular interstitial space have long been recognized to regulate steroidogenesis by Leydig cells. A growing body of evidence indicate that increasing number of mast cells is associated with idiopathic male infertilities and spermatogenic disorders (147). Moreover, mast cells are intermingled with testicular peritubular cells in the tubular wall of infertile men and may provide a possible source of highly increased amounts of extracellular ATP. Besides, upon the activation of immune cells, the extracellular ATP may function as a hazardous molecule to peritubular cells by activating their purinoceptors (P2RX4 and P2RX7). Subsequently, ATP-mediated events in peritubular cells lead to enhanced expression of pro-inflammatory molecules like IL-6 and CCL7 (147). Evidence shows that inhibiting glycolytic ATP production may suppress IL-33-induced bone marrow-derived mast cell activation and proinflammatory factor IL-6 and tumor necrosis factor (TNF) production (148). Thus, mast cells may be involved in testicular inflammation *via* their metabolic products.

In conclusion, both the microenvironment and metabolism reprogramming of immune cells participate in the establishment of their phenotype and immunoregulatory function. Mainly, glucose and FA metabolism promote the cell differentiation towards immunologically tolerant cell phenotypes; in contrast, inflammatory phenotype cells use glycolysis as a leading source of energy more than mitochondrial OXPHOS for rapid removal of pathogens (**Figure 2**). The disruption of metabolic reprogramming may result in inflammation, autoimmune-diabetes, metabolic syndrome, and even male infertility. Therefore, exploration of the functions of immune cell metabolism in testes is imperative in further understanding the molecular and cellular processes underlying male infertility. And, this may facilitate the development of novel anti-inflammatory therapeutics targeting immunometabolism.

IMMUNE DYSFUNCTION AND METABOLIC DISORDER IN THE MALE REPRODUCTION

Impact of Metabolic Disorders in Immune Cells and Functions on the Male Reproduction

Although various immune cells have been identified in testes, metabolism of these immune cells remain to be elucidated. Molecular and cellular alterations in the metabolic state under the physiological or pathological conditions in testes remain mostly unexplored. Metabolic reprogramming of immune cells plays a predominant role in regulating their phenotype as well as their plasticity. Considering the abundant immune cells in testes, activation and polarization of macrophages by pro-inflammatory stimuli elicits metabolic reprogramming, further leading to a shift in the balanced mitochondrial metabolism towards ROS generation (149). ROS can stabilize HIF-1α, thus promoting glycolysis and supporting the transcription of the pro-inflammatory cytokine IL-1β (32, 129). IL-1 system may involve in the autocrine regulation of Sertoli cell function *in vitro*, and IL-1β is reported to reduce testicular steroidogenesis of the immature rat that is 21-day-old (150, 151). Besides, it is universally acknowledged that supraphysiological ROS levels lead to defective sperm function by lipid peroxidation of cytomembrane and DNA damage as well as protein oxidation that leads to inactivation of enzymes, which ultimately results in male infertility (152, 153). Types of cytokines secreted from various metabolic processes of different immune cells due to stimulations are not only limited to macrophages, but these cytokines may also conversely influence the functions and metabolism of immune cells (154). Hence, upon activation, immune cells may cause alteration in the cellular metabolism, leading to the secretion of cytokines that may affect testes' normal immune cell functions.

Cytokines Changes in Inflammation in the Male Reproduction

Inflammation of the male reproductive system is inevitably related to changes in the levels of cytokines. Cytokines are released from different immune cells present in the male reproductive system and also in response to foreign antigens and pathogens and chronic inflammation (155). The secretion of cytokines represents the first indication from the innate host defense to combat inflammation of the reproductive tract. Orchitis is one of the common etiological factors related to human subfertility/infertility. Studies on autoimmune orchitis indicated that the initial phase of inflammation comprised of the recruitment of the immune cells, followed by their activation and increased production of pro-inflammatory cytokines such as IL-1 and TNF-α (12, 156). Theses complex array of proinflammatory cytokines affects BTB permeability, which enters the seminiferous epithelium, leading to the induction of apoptosis of germ cells (12). Increasing evidence indicates that elevated levels of cytokines exist in the semen, including IL-1β, IL-6, and IL-8, which are frequently associated with inflammation and infection of the male reproductive system (157–159).

Moreover, inflammation in the male reproductive system has been identified to increase ROS levels, resulting in cell damage concomitantly, apoptosis or necrosis (28, 160). ROS is not only to be involved in the damage of spermatogenic cells and sperm but also impairs Sertoli cells and Leydig cells in testes, which contributes to spermatogenesis dysfunction (161–163). Released pro-inflammatory cytokines in semen during inflammation might modulate the balance of prooxidative and antioxidative systems to the advantage of the oxidative stress, resulting in

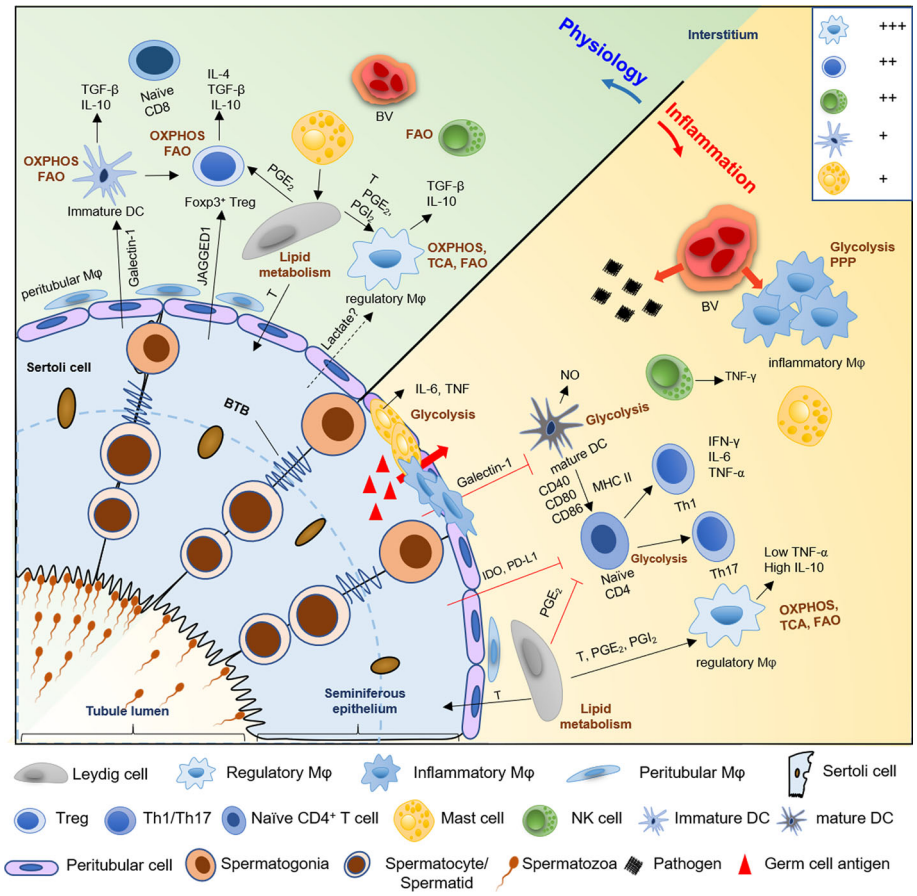

FIGURE 2 | A schematic diagram of the hypothetical metabolic homeostasis of immune cells in testes under physiological or inflammatory condition. In normal testes, immunologically tolerant cell phenotypes, comprising with macrophages (Mφ), immature DCs, Tregs, and regulatory NK cells, principally rely on OXPHOS and fatty acid oxidation pathway to fuel immunosuppressive functions and synthesis of anti-inflammatory cytokines (e.g., IL-10 and TGF-β). However, when testes suffer from pathogens or germ cell antigens attack, the number of macrophages and mast cells are markedly increased, and the location of these cells partially shift from the interstitium to the tubular compartment of infertile men testes. Furthermore, inflammatory phenotype cells such as infiltrating macrophages, mature DCs, effector T helper cells, and mast cells markedly show a metabolic shift towards the anaerobic glycolytic pathway to meet the rapid energy requirements and increased demands for synthesis of proinflammatory cytokine, like IL-6, NO and TNF-α. Then this cause 'cytokine storm' to disrupt the delicate equilibrium between immune privilege and tolerance, which trigger testes inflammation and impair normal spermatogenesis, followed by male infertility. Meanwhile, Sertoli cells also contribute to the immune-privileged status of mammalian testes, especially, maintain immature DCs, and inhibit effector T cells and NK cells *via* paracrine cytokines IDO and PDL-1. Similarly, Leydig cells play an immunoregulatory effect on maintenance of regulatory macrophage phenotype and inhibition of T cells immune responses through secreting lipid metabolites, such as testosterone, PGE_2 and PGI_2. Treg, regulatory T cells; DC, dendritic cell; Th, T helper cell; FAO, fatty acids oxidation; OXPHOS, oxidative phosphorylation; TCA, tricarboxylic acid; PPP, pentose phosphate pathway; T, testosterone; PGE2 and PGI2, prostaglandins E2 and I2; IDO, indoleamine 2,3-dioxygenase; PDL-1, programmed death ligand-1; NO, nitric oxide; BV; blood vessel. +++, most abundant; ++, relatively abundant; +, present (28).

permanent peroxidative damage to spermatozoa, consequent effects in the passage of defective paternal DNA on to the conceptus and fertilizing potential (152, 153, 164, 165).

Systematic Metabolic and Immune Disorders in the Male Reproduction

Metabolic disorders related to systematic diseases may also disrupt the balance of cellar metabolic processes, immune environment, and redox activities. Obesity and metabolic syndrome are characterized by hyperinsulinemia, hyperlipidemia, hyperleptinemia, and chronic inflammations, which may also directly impair testicular functions by dysregulating the HPT axis and immune functions in male reproduction (166, 167). Men with a BMI range from 35 kg m^{-2} to 40 kg m^{-2} have more than 50% reduction in total and free testosterone levels than lean men (168). The decreased level of testosterone is associated with diminished LH and deteriorated semen quality (including reduced sperm count and motility as well as morphologically normal sperm) in men with obesity (169). An obesogenic environment initiates a Th1-lymphocyte and M1-macrophage chronic inflammatory responses that induce pro-inflammatory cytokines and ultimately results in systematic inflammation in the male reproductive system associated with a decrease in immune regulating cells and cytokines (170). Moreover, obesity is identified to be related to increased ROS in semen, which exhibits adverse impacts on the

quality and function of semen (171, 172). Similar impacts of obesity on male reproduction, metabolic syndrome like diabetes mellitus (DM) also disrupt the metabolism of testes that eventually affect spermatogenesis (173).

TARGETING IMMUNOMETABOLISM AS AN ANTI-INFLAMMATORY STRATEGY ON MALE INFERTILITY

Male reproductive system inflammation like epididymitis and orchitis induced by the immune disorder may be linked to male infertility, or benign hyperplasia, or even cancer. Antibiotic therapies are most commonly used to eradicate infection caused by micro-organisms in the male reproductive system; however, according to the European Association of Urology guidelines, the treatment elicited no positive effect on inflammatory alterations and could not reverse functional deficits and anatomical dysfunction (174). Hence, an appropriate selection of specific anti-inflammatory therapy is urgently needed. Indeed, the relationship between immune and metabolism is bidirectional and includes the integrated role of inflammation in the pathogenesis of metabolic disorders, such as obesity and metabolic syndrome caused by unhealthy lifestyle or systematic diseases, and metabolic factors in the regulation of immune cell functions (175). Collectively, these pieces of evidence suggest that therapies targeting immunometabolism might serve as a novel putative strategy for controlling autoimmunity and inflammation (also can be seen in **Table 1**).

Antioxidant Therapy

Excessive ROS production leads to an imbalance of redox and the production of inflammatory cytokines in large amounts (161, 183). Oxidative stress-induced by overproduction of ROS and systematic inflammatory statuses presenting in the body, such as obesity and metabolic syndrome, are associated with male infertility (161). Blocking ROS production is considered as a prior treatment for men with subfertility. Primarily, optimal management strategies, including controlling the elevated inflammatory state and lifestyle modifications with appropriate intervention, are required (170). Adopting a healthy lifestyle, including proper nutritional quality, an appropriate form of physical activity, and effective weight management, represents the most critical strategy to manage metabolic disorders and ensure good health status for male fertility (14). Simultaneous administration of nutraceuticals, such as vitamin C, vitamin E, β-carotenes, magnesium, selenium, zinc, stimulates immune regulating properties (170). In addition, therapeutic drugs, like α-lipoic acid, melatonin, coenzyme Q10, pentoxifylline, and lycopene, are also suggested to reduce metabolic disorder-related inflammatory status in humans (170). These nutraceuticals and drugs that can relieve the inflammatory status present antioxidant properties. Commonly used antioxidants have a positive effect on male fertility, including improvement in basic semen parameters as well as reduction of the levels of ROS and sperm DNA fragment (176). And antioxidants could also improve sperm motility and DNA integrity for infertile men with elevated oxidative stress (177). On the other side, recent randomized controlled trials demonstrated that antioxidants did not improve semen parameters or DNA integrity in infertile men (184, 185). The recent Cochrane Review shows that different types as well as treatment time of antioxidants had different effects on sperm parameters (186). The contradictory conclusions of different research about using antioxidant to improve semen quality might partly result from the heterogeneous nature of the study designs, such as the type of antioxidant, dosages, treatment period, sample size, included criteria of participants with either poor semen quality or high level of oxidative stress. However, there is a considerable variability in the reported antioxidant effect on semen parameters and the Cochrane Review was hard to conclude about the effect of antioxidant on improving sperm quality (186). Thus, the outcomes of antioxidant treatment on male subfertility remains controversial. Further studies, especially with larger sample size and well-designed randomized controlled trials, are needed to confirm the effectiveness of antioxidant supplementation on male fertility.

TABLE 1 | Summary of specific anti-inflammatory therapy on male infertility.

	Management	Consequence	Successful clinical, pre-clinical models	Reference
Antioxidant therapy	lifestyle modifications; antioxidant-rich foods intake; oral antioxidant drug.	reduce the levels of ROS; control the elevated inflammatory state; reduces the sperm DNA damage; improve sperm quality and fertility.	oxidative stress; obesity; metabolic syndrome.	(14, 170, 176, 177)
Targeting immunometabolism therapy	metformin; rapamycin.	inhibit T cells; promotes memory T cells and tissue-resident macrophages; reduces chronic inflammation and ROS; improves insulin sensitivity; increase cholesterol and triglyceride and fatty acid oxidation; improve sperm quality and fertility.	T2DM; hyperglycemia; dyslipidemia.	(178–181)
Hormone therapy	testosterone; aromatase inhibitors.	decreased production of proinflammatory cytokines; maintained the M2 macrophage phenotype; maintain of testicular immunosuppressive status.	experimental autoimmune orchitis.	(82, 182)

ROS, reactive oxygen species; T2DM, type 2 diabetes mellitus.

Targeting Metabolism for Immune Cell Therapy

Metformin, a hypoglycaemic medication primarily used as the first-choice treatment for the management of T2DM, reportedly reduces chronic inflammation and ROS directly, and improves insulin sensitivity, hyperglycemia, and dyslipidemia (178). The anti-inflammatory activity of metformin is predominantly mediated by activation of AMPK and inhibition of NF-κB. Upregulation of AMPK stimulated the levels of cholesterol and triglyceride, and fatty acid oxidation, and inactivates acetyl-CoA (the rate-limiting enzyme in the fatty acid synthesis), thus, led to a switch off the anabolic process (187, 188). Furthermore, metformin has also been proven to inhibit antigen-induced T cell proliferation in an AMPK independent manner, and improve impaired B cell function associated with T2DM *in vivo*, and reduce B cell-intrinsic inflammation *in vitro* (179, 180). Although the effects of metformin on male productive function and fertility is mainly unclear, human and animal studies have shown that this drug also modulates fertility status and sperm quality, particularly in T2DM, through 1) restoring the structure and weight of testes, epididymis, and seminal vesicles, 2) inhibiting of germ cells apoptosis by enhancing the nutritional function of Sertoli cells to produce, 3) increasing sperm count, motility and normal morphology, 4) reducing sperm DNA fragmentation (188, 189). However, either in non-diabetic or in non-T2DM conditions, metformin might cause an adverse effect on the male reproductive system (188). Thus, further studies will be needed to clarify what mechanism is involved in this drug's bidirectional action at different statuses.

Moreover, rapamycin-inhibited mTOR restores cellular homeostasis and promotes tolerance and generation of memory T cells and tissue-resident macrophages (181). Recently, studies have also revealed that in chronic nonbacterial prostatitis models of rats, the activation of the mTOR signaling pathways stimulates inflammatory immune responses by blocking NF-κB and IL-1β while administration of rapamycin reversed these effects (190, 191).

Hormone Therapy

As mentioned earlier, high testosterone concentration helps maintain a testicular immunosuppressive microenvironment. This is mainly attributed to the suppressed NF-κB signaling pathway and decreased production of proinflammatory cytokines, leading to sustained M2-like macrophage phenotype, thereby reducing systemic inflammation (82). Due to testosterone's immunosuppressive properties, some researchers have tried to control testosterone in an EAO animal. Furthermore, they found that testosterone treatment significantly attenuates inflammation progression, mediated by blocking the infiltration of inflammatory immune cells and promoting the expansion of competent $CD4^+CD25^+Foxp3^+$ Tregs in testes (71, 192, 193). Furthermore, aromatase inhibitors increase testosterone in obese males and improve spermatogenesis and sperm quality; however, significant evidence-based studies on the management of male fertility remain lacking (182). Although the adequate concentration of testosterone is critical for spermatogenesis, excessive testosterone through testosterone therapy generally deteriorates fertility parameters in males *via* the negative feedback mechanism and should not be used as part of fertility management (182, 194).

Based on the immunosuppressive properties of Tregs, drugs that stabilize Tregs (including glucocorticoids and NSAIDs) or drugs used to stimulate Tregs differentiation (such as TGF-β and all-trans retinoids) are expected to maximize the benefit of Tregs-based therapies in suppressing autoimmune diseases (138).

COOPERATION OF IMMUNE, ENDOCRINE, AND METABOLISM IN TESTICULAR FUNCTION

Spermatogenesis is a sophisticatedly complex process and involves a coordinated regulation between endocrine, immune, and metabolism in testes. The complex but methodical co-regulation is benefited from the multiplied cell interactions, although BTB separates these cells. As mentioned above, testosterone produced by Leydig cells and are controlled through LH produced in the hypothalamus plays a critical role in the maintenance of immunosuppressive microenvironment for normal spermatogenesis within testes through maintaining regulatory macrophage phenotype and function, inducing $CD4^+CD25^+Foxp3^+$ Tregs expansion, and meanwhile inhibiting $CD8^+$ and $CD4^+$ T cells activation. In turn, T lymphocyte infiltration would decrease Leydig cell population during inflammation resulting from LPS stimulation and virus infection (such as coronavirus disease 2019), whereas the number of Leydig cell would be recovered in αβ, γδ, and CD8 lymphocytes deficient mice (195–197). Macrophage numbers was also significantly decline after Leydig cells were destroyed or the function of Leydig cells were inhibited (84, 198). This might imply that there was relationship between the number of Leydig cells with Macrophage, and T lymphocytes. On the other hand, testosterone is also bound to AR in Sertoli cells to regulate the expression of the spermatogenesis-related gene and regulate glucose metabolism. Furthermore, FSH, acting as the master endocrine regulator of Sertoli cells, stimulated lactate production by Sertoli cells in a HIF-dependent manner (199). Since developing germ cells cannot synthesize lactate, Sertoli cells would converse 75% of their pyruvate production into lactate or pyruvate to fulfill germ cells (200). Tumor cells induced the M2 macrophage phenotype by producing a high lactate level (108). However, there is a doubt whether Sertoli cells-produced lactate would induce immunosuppressive macrophage in testes. Testicular FAO metabolism, particularly PGs production *via* COX2, was controlled by LH, FSH, androgens, and prolactin (106). In turn, PGs acted as an autocrine regulator of Leydig cell steroidogenesis and Sertoli cell function and indirectly regulated sperm maturation (106).

Although the effect of metabolism on testicular immune homeostasis is less clear, the data from either immunologically privileged sites like tumor tissue and pregnant uterus or some normal tissue except testes have been shown that metabolic

reprogramming is necessary for the polarization and activation of immune cells, as mentioned above. For example, oxidative metabolism, such as OXPHOS and FAO pathway, generally markedly increased to promote the immunologically tolerant phenotypes of macrophages, DCs, Tregs, and regulatory NK cells. Conversely, the activation of these immune cells needs higher anaerobic metabolism to meet the rapid energy requirements and produce proinflammatory cytokines, like IL-6, NO, and TNF-α. In this context, it is unquestionable that metabolic reprogramming also plays a vital role in the immunologically privileged characterization of the testis, which remains to be further investigated in subsequent studies. In supporting this, the concentration of testosterone and PGs in testes was higher than in peripheral blood, both of which were synthesized through lipid metabolism by testicular somatic cells. These molecules displayed an immunosuppressive effect on macrophages and T lymphocytes. For example, Sertoli cells act as immunological sentinels of spermatogenesis in partial by forming metabolites, such as PGs, IDO to polarize M2 macrophage and inhibit T and NK cells, respectively (81, 106). On the other hand, when the body suffers from systematic metabolic, the immune homeostasis required for the normal spermatogenesis process will be disturbed. The metabolic disbalance leads to male hypogonadism as well as dysfunction of testicular environment for spermatogenesis. Metabolic disorder with adipose tissue increases the conversion of testosterone to 17β-estradiol and promotes feedback at HTP axis, inhibiting the secretion of both FSH and LH, and finally impairs spermatogenesis (201). This suppression of HPT induced by adipose tissue might be mediated *via* dysregulated leptin signaling and pro-inflammatory cytokines (202). Moreover, obesity and metabolic syndrome, accompanied by excessive fat deposition on the scrotal area, would trigger pro-inflammatory status once adipocytes rupture and ultimately disrupt the spermatogenesis (203). Additionally, a recent experiment revealed that high-fat diet not only induced significant more body weight than their age-matched littermates fed but also impair spermatogenesis by altering glucose and lipid metabolism in Sertoli cells, which lead to Sertoli cells dysfunction and ultimately decreased sperm quality (204). Collectively, the interactions between endocrine, immune and metabolism are essential to maintain the immune environment of the testis and the proper nutrient concentration for the spermatogenic process.

CONCLUSIONS

In summary, the regulation of male reproduction by the HPT axis is, at least in part, through the immune system. The immune cells effectively provide the immunocompetent microenvironment for normal spermatogenesis and subsequent processes, such as sperm maturation. The immune cells develop, activate, and differentiate into unique phenotypes and function in response to the synergistic effects of HPT axis-regulated hormones and the immune microenvironment of the reproductive system. In turn, the metabolic reprogramming of immune cells plays a pivotal role in supporting and modeling the immune microenvironment. There is accumulating appreciation for the part of metabolic alterations in the functions of immune cells. However, the role of immunometabolism on male fertility and whether the HPT axis engages in switching the metabolic flux of immune cells remain to be elucidated. With a well-established understanding of metabolism and immunity, it would be interesting to explore immunometabolism further to clarify the conceptual framework for male reproductive health.

AUTHOR CONTRIBUTIONS

LY and WH have contributed equally to this work. All authors contributed to the article and approved the submitted version.

FUNDING

This review is made possible through the support of the National Key R&D Program of China (2018YFC1003900/2018YFC1003904), Shenzhen Natural Science Foundation (JCYJ20190813161801676) to LD, the German Research Foundation to KT (TH 2126/1-1), and Sanming Project of Medicine in Shenzhen (SZSM201502035).

REFERENCES

1. Ashrafzadeh A, Karsani SA, Nathan S. Mammalian Sperm Fertility Related Proteins. *Int J Med Sci* (2013) 10(12):1649–57. doi: 10.7150/ijms.6395
2. Haschek WM, Rousseaux CG, Wallig MA. "Chapter 18 - Male Reproductive System". In: WM Haschek, CG Rousseaux and MA Wallig, editors. *Fundamentals of Toxicologic Pathology (Second Edition)*, vol. 553–597. San Diego: Academic Press (2010).
3. Diemer T, Hales DB, Weidner W. Immune-Endocrine Interactions and Leydig Cell Function: The Role of Cytokines. *Andrologia* (2003) 35(1):55–63. doi: 10.1046/j.1439-0272.2003.00537.x
4. Dhole B, Kumar A. "Hypothalamic-Pituitary-Testicular Axis". In: *Basics of Human Andrology*. Singapore: Springer (2017). p. 117–34.
5. Hermann BP, Cheng K, Singh A, Roa-De La Cruz L, Mutoji KN, Chen IC, et al. The Mammalian Spermatogenesis Single-Cell Transcriptome, From Spermatogonial Stem Cells to Spermatids. *Cell Rep* (2018) 25(6):1650–1667 e1658. doi: 10.1016/j.celrep.2018.10.026
6. Fijak M, Meinhardt A. The Testis in Immune Privilege. *Immunol Rev* (2006) 213:66–81. doi: 10.1111/j.1600-065X.2006.00438.x
7. Arck P, Solano ME, Walecki M, Meinhardt A. The Immune Privilege of Testis and Gravid Uterus: Same Difference? *Mol Cell Endocrinol* (2014) 382 (1):509–20. doi: 10.1016/j.mce.2013.09.022
8. Stanton PG. Regulation of the Blood-Testis Barrier. *Semin Cell Dev Biol* (2016) 59:166–73. doi: 10.1016/j.semcdb.2016.06.018
9. Zhao S, Zhu W, Xue S, Han D. Testicular Defense Systems: Immune Privilege and Innate Immunity. *Cell Mol Immunol* (2014) 11(5):428–37. doi: 10.1038/cmi.2014.38
10. Meinhardt A, Hedger MP. Immunological, Paracrine and Endocrine Aspects of Testicular Immune Privilege. *Mol Cell Endocrinol* (2011) 335(1):60–8. doi: 10.1016/j.mce.2010.03.022

11. Schuppe H, Meinhardt A. Immune Privilege and Inflammation of the Testis. *Chem Immunol Allergy* (2005) 88:1–14. doi: 10.1159/000087816
12. Jacobo P, Guazzone VA, Theas MS, Lustig L. Testicular Autoimmunity. *Autoimmun Rev* (2011) 10(4):201–4. doi: 10.1016/j.autrev.2010.09.026
13. Chen Q, Deng T, Han D. Testicular Immunoregulation and Spermatogenesis. *Semin Cell Dev Biol* (2016) 59:157–65. doi: 10.1016/j.semcdb.2016.01.019
14. Martins AD, Majzoub A, Agawal A. Metabolic Syndrome and Male Fertility. *World J Mens Health* (2019) 37(2):113–27. doi: 10.5534/wjmh.180055
15. Cheng CY, Wong EW, Yan HH, Mruk DD. Regulation of Spermatogenesis in the Microenvironment of the Seminiferous Epithelium: New Insights and Advances. *Mol Cell Endocrinol* (2010) 315(1-2):49–56. doi: 10.1016/j.mce.2009.08.004
16. Oliveira PF, Alves MG. "Testicular Metabolic Cooperation". In: *Sertoli Cell Metabolism and Spermatogenesis*. Cham: Springer International Publishing (2015).
17. Dias T R, Martins A D, Reis V P, Socorro S M, Silva B, Alves M G, et al. Glucose Transport and Metabolism in Sertoli Cell: Relevance for Male Fertility. *Curr Chem Biol* (2014) 7(3):282–93. doi: 10.2174/2212796807999131128125510
18. Rato L, Alves MG, Socorro S, Duarte AI, Cavaco JE, Oliveira PF. Metabolic Regulation is Important for Spermatogenesis. *Nat Rev Urol* (2012) 9(6):330–8. doi: 10.1038/nrurol.2012.77
19. Li N, Wang T, Han D. Structural, Cellular and Molecular Aspects of Immune Privilege in the Testis. *Front Immunol* (2012) 3:152. doi: 10.3389/fimmu.2012.00152
20. Kaur G, Thompson LA, Dufour JM. Sertoli Cells–Immunological Sentinels of Spermatogenesis. *Semin Cell Dev Biol* (2014) 30:36–44. doi: 10.1016/j.semcdb.2014.02.011
21. Boussouar F, Benahmed M. Lactate and Energy Metabolism in Male Germ Cells. *Trends Endocrinol Metab* (2004) 15(7):345–50. doi: 10.1016/j.tem.2004.07.003
22. Franca LR, Hess RA, Dufour JM, Hofmann MC, Griswold MD. The Sertoli Cell: One Hundred Fifty Years of Beauty and Plasticity. *Andrology* (2016) 4 (2):189–212. doi: 10.1111/andr.12165
23. Jankovic Velickovic L, Stefanovic V. Hypoxia and Spermatogenesis. *Int Urol Nephrol* (2014) 46(5):887–94. doi: 10.1007/s11255-013-0601-1
24. Doyle TJ, Kaur G, Putrevu SM, Dyson EL, Dyson M, McCunniff WT, et al. Immunoprotective Properties of Primary Sertoli Cells in Mice: Potential Functional Pathways That Confer Immune Privilege1. *Biol Reprod* (2012) 86 (1):1–14. doi: 10.1095/biolreprod.110.089425
25. Holdcraft RW, Braun RE. Hormonal Regulation of Spermatogenesis. *Int J Androl* (2004) 27(6):335–42. doi: 10.1111/j.1365-2605.2004.00502.x
26. Zirkin BR, Papadopoulos V. Leydig Cells: Formation, Function, and Regulation. *Biol Reprod* (2018) 99(1):101–11. doi: 10.1093/biolre/ioy059
27. Smith LB, Walker WH. The Regulation of Spermatogenesis by Androgens. *Semin Cell Dev Biol* (2014) 30:2–13. doi: 10.1016/j.semcdb.2014.02.012
28. Hedger MP. "The Immunophysiology of Male Reproduction". In: *Knobil and Neill's Physiology of Reproduction*. San Diego: Academic Press (2015).
29. Qu N, Ogawa Y, Kuramasu M, Nagahori K, Sakabe K, Itoh M. Immunological Microenvironment in the Testis. *Reprod Med Biol* (2020) 19(1):24–31. doi: 10.1002/rmb2.12293
30. Newton R, Priyadharshini B, Turka LA. Immunometabolism of Regulatory T Cells. *Nat Immunol* (2016) 17(6):618–25. doi: 10.1038/ni.3466
31. Van den Bossche J, O'Neill LA, Menon D. Macrophage Immunometabolism: Where Are We (Going)? *Trends Immunol* (2017) 38(6):395–406. doi: 10.1016/j.it.2017.03.001
32. Pearce EJ, O'Neill LAJ. Immunometabolism Governs Dendritic Cell and Macrophage Function. *J Exp Med* (2016) 213(1):15–23. doi: 10.1084/jem.20151570
33. Poznanski SM, Barra NG, Ashkar AA, Schertzer JD. Immunometabolism of T Cells and NK Cells: Metabolic Control of Effector and Regulatory Function. *Inflammation Res* (2018) 67(10):813–28. doi: 10.1007/s00011-018-1174-3
34. Mathis D, Shoelson SE. Immunometabolism: An Emerging Frontier. *Nat Rev Immunol* (2011) 11(2):81. doi: 10.1038/nri2922
35. Eaton SA, Sethi JK. Immunometabolic Links Between Estrogen, Adipose Tissue and Female Reproductive Metabolism. *Biol (Basel)* (2019) 8(1):8. doi: 10.3390/biology8010008
36. Thiele K, Diao L, Arck PC. Immunometabolism, Pregnancy, and Nutrition. *Semin Immunopathol* (2018) 40(2):157–74. doi: 10.1007/s00281-017-0660-y
37. Pearce EJ, Pearce EL. Immunometabolism in 2017: Driving Immunity: All Roads Lead to Metabolism. *Nat Rev Immunol* (2018) 18(2):81–2. doi: 10.1038/nri.2017.139
38. O'Neill LA, Kishton RJ, Rathmell J. A Guide to Immunometabolism for Immunologists. *Nat Rev Immunol* (2016) 16(9):553–65. doi: 10.1038/nri.2016.70
39. Stathopoulou C, Nikoleri D, Bertsias G. Immunometabolism: An Overview and Therapeutic Prospects in Autoimmune Diseases. *Immunotherapy* (2019) 11(9):813–29. doi: 10.2217/imt-2019-0002
40. Plant TM. 60 YEARS OF NEUROENDOCRINOLOGY: The Hypothalamo-Pituitary-Gonadal Axis. *J Endocrinol* (2015) 226(2):T41–54. doi: 10.1530/JOE-15-0113
41. Ramaswamy S, Weinbauer GF. Endocrine Control of Spermatogenesis: Role of FSH and LH/testosterone. *Spermatogenesis* (2014) 4(2):e996025. doi: 10.1080/21565562.2014.996025
42. Huhtaniemi I, Teerds K. "Leydig Cells". In: *Encyclopedia of Reproduction*. Oxford: Academic Press (2018).
43. Meinhardt A, Bacher M, McFarlane JR, Metz CN, Seitz J, Hedger MP, et al. Macrophage Migration Inhibitory Factor Production by Leydig Cells: Evidence for a Role in the Regulation of Testicular Function. *Endocrinology* (1996) 137(11):5090–5. doi: 10.1210/endo.137.11.8895383
44. Meccariello R, Chianese R, Chioccarelli T, Ciaramella V, Fasano S, Pierantoni R, et al. Intra-Testicular Signals Regulate Germ Cell Progression and Production of Qualitatively Mature Spermatozoa in Vertebrates. *Front Endocrinol (Lausanne)* (2014) 5:69. doi: 10.3389/fendo.2014.00069
45. Oliveira PF, Alves MG. "Modulation of Sertoli Cell Metabolism". In: *Sertoli Cell Metabolism and Spermatogenesis*. Cham: Springer International Publishing (2015).
46. Rato L, Meneses MJ, Silva BM, Sousa M, Alves MG, Oliveira PF. New Insights on Hormones and Factors That Modulate Sertoli Cell Metabolism. *Histol Histopathol* (2016) 31(5):499–513. doi: 10.14670/HH-11-717
47. Guma FC, Wagner M, Martini LH, Bernard EA. Effect of FSH and Insulin on Lipogenesis in Cultures of Sertoli Cells From Immature Rats. *Braz J Med Biol Res* (1997) 30(5):591–7. doi: 10.1590/s0100-879x1997000500004
48. Oliveira PF, Alves MG, Rato L, Silva J, Sa R, Barros A, et al. Influence of 5alpha-Dihydrotestosterone and 17beta-Estradiol on Human Sertoli Cells Metabolism. *Int J Androl* (2011) 34(6 Pt 2):e612–20. doi: 10.1111/j.1365-2605.2011.01205.x
49. Raut S, Kumar AV, Deshpande S, Khambata K, Balasinor NH. Sex Hormones Regulate Lipid Metabolism in Adult Sertoli Cells: A Genome-Wide Study of Estrogen and Androgen Receptor Binding Sites. *J Steroid Biochem Mol Biol* (2021) 211:105898. doi: 10.1016/j.jsbmb.2021.105898
50. Alves MG, Rato L, Carvalho RA, Moreira PI, Socorro S, Oliveira PF. Hormonal Control of Sertoli Cell Metabolism Regulates Spermatogenesis. *Cell Mol Life Sci* (2013) 70(5):777–93. doi: 10.1007/s00018-012-1079-1
51. Bhatia A, Sekhon HK, Kaur G. Sex Hormones and Immune Dimorphism. *ScientificWorldJournal* (2014) 2014:159150. doi: 10.1155/2014/159150
52. Tsigos C, Chrousos GP. Hypothalamic-Pituitary-Adrenal Axis, Neuroendocrine Factors and Stress. *J Psychosom Res* (2002) 53(4):865–71. doi: 10.1016/s0022-3999(02)00429-4
53. Segner H, Verburg-van Kemenade BML, Chadzinska M. The Immunomodulatory Role of the Hypothalamus-Pituitary-Gonad Axis: Proximate Mechanism for Reproduction-Immune Trade Offs? *Dev Comp Immunol* (2017) 66:43–60. doi: 10.1016/j.dci.2016.07.004
54. Standaert FE, Chew BP, De Avila D, Reeves JJ. Presence of Luteinizing Hormone-Releasing Hormone Binding Sites in Cultured Porcine Lymphocytes. *Biol Reprod* (1992) 46(6):997–1000. doi: 10.1095/biolreprod46.6.997
55. Tanriverdi F, Gonzalez-Martinez D, Silveira LF, Hu Y, Maccoll GS, Travers P, et al. Expression of Gonadotropin-Releasing Hormone Type-I (GnRH-I) and Type-II (GnRH-II) in Human Peripheral Blood Mononuclear Cells (PMBCs) and Regulation of B-Lymphoblastoid Cell Proliferation by GnRH-I and GnRH-II. *Exp Clin Endocrinol Diabetes* (2004) 112(10):587–94. doi: 10.1055/s-2004-830404

56. Chen H-F, Jeung E-B, Stephenson M, Leung PCK. Human Peripheral Blood Mononuclear Cells Express Gonadotropin-Releasing Hormone (GnRH), GnRH Receptor, and Interleukin-2 Receptor γ-Chain Messenger Ribonucleic Acids That Are Regulated by GnRH *In Vitro*1. *J Clin Endocrinol Metab* (1999) 84(2):743–50. doi: 10.1210/jcem.84.2.5440
57. Morale MC, Batticane N, Bartoloni G, Guarcello V, Farinella Z, Galasso MG, et al. Blockade of Central and Peripheral Luteinizing Hormone-Releasing Hormone (LHRH) Receptors in Neonatal Rats With a Potent LHRH-Antagonist Inhibits the Morphofunctional Development of the Thymus and Maturation of the Cell-Mediated and Humoral Immune Responses. *Endocrinology* (1991) 128(2):1073–85. doi: 10.1210/endo-128-2-1073
58. Mann DR, Howie S, Paulsen DF, Akinbami MA, Lunn SF, Fraser HM. Changes in Lymphoid Tissue After Treatment With a Gonadotropin Releasing Hormone Antagonist in the Neonatal Marmoset (Callithrix Jacchus). *Am J Reprod Immunol* (1998) 39(4):256–65. doi: 10.1111/j.1600-0897.1998.tb00362.x
59. Tanriverdi F, Silveira LF, MacColl GS, Bouloux PM. The Hypothalamic-Pituitary-Gonadal Axis: Immune Function and Autoimmunity. *J Endocrinol* (2003) 176(3):293–304. doi: 10.1677/joe.0.1760293
60. Weigent DA, Blalock JE. Associations Between the Neuroendocrine and Immune Systems. *J Leukocyte Biol* (1995) 58(2):137–50. doi: 10.1002/jlb.58.2.137
61. Carbone F, Procaccini C, De Rosa V, Alviggi C, De Placido G, Kramer D, et al. Divergent Immunomodulatory Effects of Recombinant and Urinary-Derived FSH, LH, and hCG on Human CD4+ T Cells. *J Reprod Immunol* (2010) 85(2):172–9. doi: 10.1016/j.jri.2010.02.009
62. Yesilova Z, Ozata M, Kocar IH, Turan M, Pekel A, Sengul A, et al. The Effects of Gonadotropin Treatment on the Immunological Features of Male Patients With Idiopathic Hypogonadotropic Hypogonadism. *J Clin Endocrinol Metab* (2000) 85(1):66–70. doi: 10.1210/jcem.85.1.6226
63. Bouman A, Heineman MJ, Faas MM. Sex Hormones and the Immune Response in Humans. *Hum Reprod Update* (2005) 11(4):411–23. doi: 10.1093/humupd/dmi008
64. Kovats S. Estrogen Receptors Regulate Innate Immune Cells and Signaling Pathways. *Cell Immunol* (2015) 294(2):63–9. doi: 10.1016/j.cellimm.2015.01.018
65. Klein SL, Flanagan KL. Sex Differences in Immune Responses. *Nat Rev Immunol* (2016) 16(10):626–38. doi: 10.1038/nri.2016.90
66. Roved J, Westerdahl H, Hasselquist D. Sex Differences in Immune Responses: Hormonal Effects, Antagonistic Selection, and Evolutionary Consequences. *Horm Behav* (2017) 88:95–105. doi: 10.1016/j.yhbeh.2016.11.017
67. Trigunaite A, Dimo J, Jorgensen TN. Suppressive Effects of Androgens on the Immune System. *Cell Immunol* (2015) 294(2):87–94. doi: 10.1016/j.cellimm.2015.02.004
68. Ysrraelit MC, Correale J. Impact of Sex Hormones on Immune Function and Multiple Sclerosis Development. *Immunology* (2019) 156(1):9–22. doi: 10.1111/imm.13004
69. Traish A, Bolanos J, Nair S, Saad F, Morgentaler A. Do Androgens Modulate the Pathophysiological Pathways of Inflammation? Appraising the Contemporary Evidence. *J Clin Med* (2018) 7(12):549. doi: 10.3390/jcm7120549
70. Meng J, Greenlee AR, Taub CJ, Braun RE. Sertoli Cell-Specific Deletion of the Androgen Receptor Compromises Testicular Immune Privilege in Mice. *Biol Reprod* (2011) 85(2):254–60. doi: 10.1095/biolreprod.110.090621
71. Fijak M, Schneider E, Klug J, Bhushan S, Hackstein H, Schuler G, et al. Testosterone Replacement Effectively Inhibits the Development of Experimental Autoimmune Orchitis in Rats: Evidence for a Direct Role of Testosterone on Regulatory T Cell Expansion. *J Immunol* (2011) 186(9):5162–72. doi: 10.4049/jimmunol.1001958
72. Walecki M, Eisel F, Klug J, Baal N, Paradowska-Dogan A, Wahle E, et al. Androgen Receptor Modulates Foxp3 Expression in CD4+CD25+Foxp3+ Regulatory T-Cells. *Mol Biol Cell* (2015) 26(15):2845–57. doi: 10.1091/mbc.E14-08-1323
73. Fijak M, Damm LJ, Wenzel JP, Aslani F, Walecki M, Wahle E, et al. Influence of Testosterone on Inflammatory Response in Testicular Cells and Expression of Transcription Factor Foxp3 in T Cells. *Am J Reprod Immunol* (2015) 74(1):12–25. doi: 10.1111/aji.12363
74. Cunningham M, Gilkeson G. Estrogen Receptors in Immunity and Autoimmunity. *Clin Rev Allergy Immunol* (2011) 40(1):66–73. doi: 10.1007/s12016-010-8203-5
75. Giefing-Kröll C, Berger P, Lepperdinger G, Grubeck-Loebenstein B. How Sex and Age Affect Immune Responses, Susceptibility to Infections, and Response to Vaccination. *Aging Cell* (2015) 14(3):309–21. doi: 10.1111/acel.12326
76. Fish EN. The X-Files in Immunity: Sex-Based Differences Predispose Immune Responses. *Nat Rev Immunol* (2008) 8(9):737–44. doi: 10.1038/nri2394
77. Cooke PS, Nanjappa MK, Ko C, Prins GS, Hess RA. Estrogens in Male Physiology. *Physiol Rev* (2017) 97(3):995–1043. doi: 10.1152/physrev.00018.2016
78. Winn NC, Jurrissen TJ, Grunewald ZI, Cunningham RP, Woodford ML, Kanaley JA, et al. Estrogen Receptor-Alpha Signaling Maintains Immunometabolic Function in Males and is Obligatory for Exercise-Induced Amelioration of Nonalcoholic Fatty Liver. *Am J Physiol Endocrinol Metab* (2019) 316(2):E156–67. doi: 10.1152/ajpendo.00259.2018
79. Yu W, Zheng H, Lin W, Tajima A, Zhang Y, Zhang X, et al. Estrogen Promotes Leydig Cell Engulfment by Macrophages in Male Infertility. *J Clin Invest* (2014) 124(6):2709–21. doi: 10.1172/JCI59901
80. Lustig L, Lourtau L, Perez R, Doncel GF. Phenotypic Characterization of Lymphocytic Cell Infiltrates Into the Testes of Rats Undergoing Autoimmune Orchitis. *Int J Androl* (1993) 16(4):279–84. doi: 10.1111/j.1365-2605.1993.tb01192.x
81. Wang M, Fijak M, Hossain H, Markmann M, Nusing RM, Lochnit G, et al. Characterization of the Micro-Environment of the Testis That Shapes the Phenotype and Function of Testicular Macrophages. *J Immunol* (2017) 198(11):4327–40. doi: 10.4049/jimmunol.1700162
82. Meinhardt A, Wang M, Schulz C, Bhushan S. Microenvironmental Signals Govern the Cellular Identity of Testicular Macrophages. *J Leukoc Biol* (2018) 104(4):757–66. doi: 10.1002/JLB.3MR0318-086RR
83. Winnall WR, Hedger MP. Phenotypic and Functional Heterogeneity of the Testicular Macrophage Population: A New Regulatory Model. *J Reprod Immunol* (2013) 97(2):147–58. doi: 10.1016/j.jri.2013.01.001
84. Wang J, Wreford NG, Lan HY, Atkins R, Hedger MP. Leukocyte Populations of the Adult Rat Testis Following Removal of the Leydig Cells by Treatment With Ethane Dimethane Sulfonate and Subcutaneous Testosterone Implants. *Biol Reprod* (1994) 51(3):551–61. doi: 10.1095/biolreprod51.3.551
85. Ponte R, Dupuy FP, Brimo F, Mehraj V, Brassard P, Belanger M, et al. Characterization of Myeloid Cell Populations in Human Testes Collected After Sex Reassignment Surgery. *J Reprod Immunol* (2018) 125:16–24. doi: 10.1016/j.jri.2017.10.043
86. Pollanen P, Niemi M. Immunohistochemical Identification of Macrophages, Lymphoid Cells and HLA Antigens in the Human Testis. *Int J Androl* (1987) 10(1):37–42. doi: 10.1111/j.1365-2605.1987.tb00163.x
87. Mossadegh-Keller N, Gentek R, Gimenez G, Bigot S, Mailfert S, Sieweke MH. Developmental Origin and Maintenance of Distinct Testicular Macrophage Populations. *J Exp Med* (2017) 214(10):2829–41. doi: 10.1084/jem.20170829
88. Wang M, Yang Y, Cansever D, Wang Y, Kantores C, Messiaen S, et al. Two Populations of Self-Maintaining Monocyte-Independent Macrophages Exist in Adult Epididymis and Testis. *Proc Natl Acad Sci USA* (2021) 118(1):e2013686117. doi: 10.1073/pnas.2013686117
89. Yee JB, Hutson JC. Effects of Testicular Macrophage-Conditioned Medium on Leydig Cells in Culture. *Endocrinology* (1985) 116(6):2682–4. doi: 10.1210/endo-116-6-2682
90. Nes WD, Lukyanenko YO, Jia ZH, Quideau S, Howald WN, Pratum TK, et al. Identification of the Lipophilic Factor Produced by Macrophages That Stimulates Steroidogenesis. *Endocrinology* (2000) 141(3):953–8. doi: 10.1210/endo.141.3.7350
91. Cohen PE, Chisholm O, Arceci RJ, Stanley ER, Pollard JW. Absence of Colony-Stimulating Factor-1 in Osteopetrotic (Csfmop/Csfmop) Mice Results in Male Fertility Defects. *Biol Reprod* (1996) 55(2):310–7. doi: 10.1095/biolreprod55.2.310
92. Gaytan F, Bellido C, Morales C, Reymundo C, Aguilar E, Van Rooijen N. Effects of Macrophage Depletion at Different Times After Treatment With

Ethylene Dimethane Sulfonate (EDS) on the Regeneration of Leydig Cells in the Adult Rat. *J Androl* (1994) 15(6):558–64. doi: 10.1002/j.1939-4640.1994.tb00499.x
93. O'Hara L, Smith LB. Androgen Receptor Roles in Spermatogenesis and Infertility. *Best Pract Res Clin Endocrinol Metab* (2015) 29(4):595–605. doi: 10.1016/j.beem.2015.04.006
94. Toocheck C, Clister T, Shupe J, Crum C, Ravindranathan P, Lee TK, et al. Mouse Spermatogenesis Requires Classical and Nonclassical Testosterone Signaling. *Biol Reprod* (2016) 94(1):11. doi: 10.1095/biolreprod.115.132068
95. Rato L, Alves MG, Socorro S, Carvalho RA, Cavaco JE, Oliveira PF. Metabolic Modulation Induced by Oestradiol and DHT in Immature Rat Sertoli Cells Cultured *In Vitro*. *Biosci Rep* (2012) 32(1):61–9. doi: 10.1042/BSR20110030
96. Martins AD, Alves MG, Simoes VL, Dias TR, Rato L, Moreira PI, et al. Control of Sertoli Cell Metabolism by Sex Steroid Hormones is Mediated Through Modulation in Glycolysis-Related Transporters and Enzymes. *Cell Tissue Res* (2013) 354(3):861–8. doi: 10.1007/s00441-013-1722-7
97. Grootegoed JA, Oonk RB, Jansen R, van der Molen HJ. Metabolism of Radiolabelled Energy-Yielding Substrates by Rat Sertoli Cells. *J Reprod Fertil* (1986) 77(1):109–18. doi: 10.1530/jrf.0.0770109
98. DeFalco T, Potter SJ, Williams AV, Waller B, Kan MJ, Capel B. Macrophages Contribute to the Spermatogonial Niche in the Adult Testis. *Cell Rep* (2015) 12(7):1107–19. doi: 10.1016/j.celrep.2015.07.015
99. Winnall WR, Muir JA, Hedger MP. Rat Resident Testicular Macrophages Have an Alternatively Activated Phenotype and Constitutively Produce Interleukin-10 *In Vitro*. *J Leukoc Biol* (2011) 90(1):133–43. doi: 10.1189/jlb.1010557
100. Bhushan S, Tchatalbachev S, Lu Y, Frohlich S, Fijak M, Vijayan V, et al. Differential Activation of Inflammatory Pathways in Testicular Macrophages Provides a Rationale for Their Subdued Inflammatory Capacity. *J Immunol* (2015) 194(11):5455–64. doi: 10.4049/jimmunol.1401132
101. Bhushan S, Meinhardt A. The Macrophages in Testis Function. *J Reprod Immunol* (2017) 119:107–12. doi: 10.1016/j.jri.2016.06.008
102. Newsholme P, Gordon S, Newsholme EA. Rates of Utilization and Fates of Glucose, Glutamine, Pyruvate, Fatty Acids and Ketone Bodies by Mouse Macrophages. *Biochem J* (1987) 242(3):631–6. doi: 10.1042/bj2420631
103. Jha AK, Huang SC, Sergushichev A, Lampropoulou V, Ivanova Y, Loginicheva E, et al. Network Integration of Parallel Metabolic and Transcriptional Data Reveals Metabolic Modules That Regulate Macrophage Polarization. *Immunity* (2015) 42(3):419–30. doi: 10.1016/j.immuni.2015.02.005
104. Vats D, Mukundan L, Odegaard JI, Zhang L, Smith KL, Morel CR, et al. Oxidative Metabolism and PGC-1beta Attenuate Macrophage-Mediated Inflammation. *Cell Metab* (2006) 4(1):13–24. doi: 10.1016/j.cmet.2006.05.011
105. Odegaard JI, Chawla A. Alternative Macrophage Activation and Metabolism. *Annu Rev Pathol* (2011) 6:275–97. doi: 10.1146/annurev-pathol-011110-130138
106. Frungieri MB, Calandra RS, Mayerhofer A, Matzkin ME. Cyclooxygenase and Prostaglandins in Somatic Cell Populations of the Testis. *Reproduction* (2015) 149(4):R169–180. doi: 10.1530/REP-14-0392
107. Leone RD, Powell JD. Metabolism of Immune Cells in Cancer. *Nat Rev Cancer* (2020) 20(9):516–31. doi: 10.1038/s41568-020-0273-y
108. Colegio OR, Chu NQ, Szabo AL, Chu T, Rhebergen AM, Jairam V, et al. Functional Polarization of Tumour-Associated Macrophages by Tumour-Derived Lactic Acid. *Nature* (2014) 513(7519):559–63. doi: 10.1038/nature13490
109. Zhu L, Zhao Q, Yang T, Ding W, Zhao Y. Cellular Metabolism and Macrophage Functional Polarization. *Int Rev Immunol* (2015) 34(1):82–100. doi: 10.3109/08830185.2014.969421
110. Wang P, Duan YG. The Role of Dendritic Cells in Male Reproductive Tract. *Am J Reprod Immunol* (2016) 76(3):186–92. doi: 10.1111/aji.12536
111. Malinarich F, Duan K, Hamid RA, Bijin A, Lin WX, Poidinger M, et al. High Mitochondrial Respiration and Glycolytic Capacity Represent a Metabolic Phenotype of Human Tolerogenic Dendritic Cells. *J Immunol* (2015) 194(11):5174–86. doi: 10.4049/jimmunol.1303316
112. O'Neill LA, Pearce EJ. Immunometabolism Governs Dendritic Cell and Macrophage Function. *J Exp Med* (2016) 213(1):15–23. doi: 10.1084/jem.20151570
113. Ferreira GB, Vanherwegen AS, Eelen G, Gutierrez ACF, Van Lommel L, Marchal K, et al. Vitamin D3 Induces Tolerance in Human Dendritic Cells by Activation of Intracellular Metabolic Pathways. *Cell Rep* (2015) 10(5):711–25. doi: 10.1016/j.celrep.2015.01.013
114. Mellor AL, Munn DH. IDO Expression by Dendritic Cells: Tolerance and Tryptophan Catabolism. *Nat Rev Immunol* (2004) 4(10):762–74. doi: 10.1038/nri1457
115. Liu Y, Liang X, Dong W, Fang Y, Lv J, Zhang T, et al. Tumor-Repopulating Cells Induce PD-1 Expression in CD8(+) T Cells by Transferring Kynurenine and AhR Activation. *Cancer Cell* (2018) 33480-94(3):e487. doi: 10.1016/j.ccell.2018.02.005
116. Mezrich JD, Fechner JH, Zhang X, Johnson BP, Burlingham WJ, Bradfield CA. An Interaction Between Kynurenine and the Aryl Hydrocarbon Receptor can Generate Regulatory T Cells. *J Immunol* (2010) 185(6):3190–8. doi: 10.4049/jimmunol.0903670
117. Pallotta MT, Orabona C, Volpi C, Vacca C, Belladonna ML, Bianchi R, et al. Indoleamine 2,3-Dioxygenase is a Signaling Protein in Long-Term Tolerance by Dendritic Cells. *Nat Immunol* (2011) 12(9):870–8. doi: 10.1038/ni.2077
118. Munn DH, Mellor AL. Indoleamine 2,3-Dioxygenase and Tumor-Induced Tolerance. *J Clin Invest* (2007) 117(5):1147–54. doi: 10.1172/JCI31178
119. Munn DH, Zhou M, Attwood JT, Bondarev I, Conway SJ, Marshall B, et al. Prevention of Allogeneic Fetal Rejection by Tryptophan Catabolism. *Science* (1998) 281(5380):1191–3. doi: 10.1126/science.281.5380.1191
120. Gualdoni GS, Jacobo PV, Sobarzo CM, Perez CV, Matzkin ME, Hocht C, et al. Role of Indoleamine 2,3-Dioxygenase in Testicular Immune-Privilege. *Sci Rep* (2019) 9(1):15919. doi: 10.1038/s41598-019-52192-8
121. Chen Z, Gordon JR, Zhang X, Xiang J. Analysis of the Gene Expression Profiles of Immature Versus Mature Bone Marrow-Derived Dendritic Cells Using DNA Arrays. *Biochem Biophys Res Commun* (2002) 290(1):66–72. doi: 10.1006/bbrc.2001.6147
122. Romani L, Fallarino F, De Luca A, Montagnoli C, D'Angelo C, Zelante T, et al. Defective Tryptophan Catabolism Underlies Inflammation in Mouse Chronic Granulomatous Disease. *Nature* (2008) 451(7175):211–5. doi: 10.1038/nature06471
123. Gandaglia G, Briganti A, Gontero P, Mondaini N, Novara G, Salonia A, et al. The Role of Chronic Prostatic Inflammation in the Pathogenesis and Progression of Benign Prostatic Hyperplasia (BPH). *BJU Int* (2013) 112(4):432–41. doi: 10.1111/bju.12118
124. Gao J, Wang X, Wang Y, Han F, Cai W, Zhao B, et al. Murine Sertoli Cells Promote the Development of Tolerogenic Dendritic Cells: A Pivotal Role of Galectin-1. *Immunology* (2016) 148(3):253–65. doi: 10.1111/imm.12598
125. Duan YG, Yu CF, Novak N, Bieber T, Zhu CH, Schuppe HC, et al. Immunodeviation Towards a Th17 Immune Response Associated With Testicular Damage in Azoospermic Men. *Int J Androl* (2011) 34(6 Pt 2):e536–45. doi: 10.1111/j.1365-2605.2010.01137.x
126. Freemerman AJ, Johnson AR, Sacks GN, Milner JJ, Kirk EL, Troester MA, et al. Metabolic Reprogramming of Macrophages: Glucose Transporter 1 (GLUT1)-Mediated Glucose Metabolism Drives a Proinflammatory Phenotype. *J Biol Chem* (2014) 289(11):7884–96. doi: 10.1074/jbc.M113.522037
127. Krawczyk CM, Holowka T, Sun J, Blagih J, Amiel E, DeBerardinis RJ, et al. Toll-Like Receptor-Induced Changes in Glycolytic Metabolism Regulate Dendritic Cell Activation. *Blood* (2010) 115(23):4742–9. doi: 10.1182/blood-2009-10-249540
128. Tannahill GM, Curtis AM, Adamik J, Palsson-McDermott EM, McGettrick AF, Goel G, et al. Succinate is an Inflammatory Signal That Induces IL-1beta Through HIF-1alpha. *Nature* (2013) 496(7444):238–42. doi: 10.1038/nature11986
129. Kelly B, O'Neill LA. Metabolic Reprogramming in Macrophages and Dendritic Cells in Innate Immunity. *Cell Res* (2015) 25(7):771–84. doi: 10.1038/cr.2015.68
130. Gong J, Zeng Q, Yu D, Duan YG. T Lymphocytes and Testicular Immunity: A New Insight Into Immune Regulation in Testes. *Int J Mol Sci* (2020) 22(1):57. doi: 10.3390/ijms22010057
131. Tompkins AB, Hutchinson P, de Kretser DM, Hedger MP. Characterization of Lymphocytes in the Adult Rat Testis by Flow Cytometry: Effects of Activin and Transforming Growth Factor Beta on Lymphocyte Subsets *In Vitro*. *Biol Reprod* (1998) 58(4):943–51. doi: 10.1095/biolreprod58.4.943

132. Lopez-Soto A, Gonzalez S, Smyth MJ, Galluzzi L. Control of Metastasis by NK Cells. *Cancer Cell* (2017) 32(2):135–54. doi: 10.1016/j.ccell.2017.06.009
133. Jacobo P, Guazzone VA, Jarazo-Dietrich S, Theas MS, Lustig L. Differential Changes in CD4+ and CD8+ Effector and Regulatory T Lymphocyte Subsets in the Testis of Rats Undergoing Autoimmune Orchitis. *J Reprod Immunol* (2009) 81(1):44–54. doi: 10.1016/j.jri.2009.04.005
134. Wheeler K, Tardif S, Rival C, Luu B, Bui E, Del Rio R, et al. Regulatory T Cells Control Tolerogenic Versus Autoimmune Response to Sperm in Vasectomy. *Proc Natl Acad Sci USA* (2011) 108(18):7511–6. doi: 10.1073/pnas.1017615108
135. Hedger MP, Wang J, Lan HY, Atkins RC, Wreford NG. Immunoregulatory Activity in Adult Rat Testicular Interstitial Fluid: Relationship With Intratesticular CD8+ Lymphocytes Following Treatment With Ethane Dimethane Sulfonate and Testosterone Implants. *Biol Reprod* (1998) 58 (4):935–42. doi: 10.1095/biolreprod58.4.935
136. Campese AF, Grazioli P, de Cesaris P, Riccioli A, Bellavia D, Pelullo M, et al. Mouse Sertoli Cells Sustain *De Novo* Generation of Regulatory T Cells by Triggering the Notch Pathway Through Soluble JAGGED1. *Biol Reprod* (2014) 90(3):53. doi: 10.1095/biolreprod.113.113803
137. Poznanski SM, Barra NG, Ashkar AA, Schertzer JD. Immunometabolism of T Cells and NK Cells: Metabolic Control of Effector and Regulatory Function. *Inflammation Res* (2018) 67(10):813–28. doi: 10.1007/s00011-018-1174-3
138. Jacobo P. The Role of Regulatory T Cells in Autoimmune Orchitis. *Andrologia* (2018) 50(11):e13092. doi: 10.1111/and.13092
139. Doedens AL, Phan AT, Stradner MH, Fujimoto JK, Nguyen JV, Yang E, et al. Hypoxia-Inducible Factors Enhance the Effector Responses of CD8(+) T Cells to Persistent Antigen. *Nat Immunol* (2013) 14(11):1173–82. doi: 10.1038/ni.2714
140. Peng M, Yin N, Chhangawala S, Xu K, Leslie CS, Li MO. Aerobic Glycolysis Promotes T Helper 1 Cell Differentiation Through an Epigenetic Mechanism. *Science* (2016) 354(6311):481–4. doi: 10.1126/science.aaf6284
141. Kalinski P. Regulation of Immune Responses by Prostaglandin E2. *J Immunol* (2012) 188(1):21–8. doi: 10.4049/jimmunol.1101029
142. Keating SE, Zaiatz-Bittencourt V, Loftus RM, Keane C, Brennan K, Finlay DK, et al. Metabolic Reprogramming Supports IFN-Gamma Production by CD56bright NK Cells. *J Immunol* (2016) 196(6):2552–60. doi: 10.4049/jimmunol.1501783
143. Keppel MP, Saucier N, Mah AY, Vogel TP, Cooper MA. Activation-Specific Metabolic Requirements for NK Cell IFN-Gamma Production. *J Immunol* (2015) 194(4):1954–62. doi: 10.4049/jimmunol.1402099
144. Eleftheriadis T, Pissas G, Yiannaki E, Markala D, Arampatzis S, Antoniadi G, et al. Inhibition of Indoleamine 2,3-Dioxygenase in Mixed Lymphocyte Reaction Affects Glucose Influx and Enzymes Involved in Aerobic Glycolysis and Glutaminolysis in Alloreactive T-Cells. *Hum Immunol* (2013) 74 (12):1501–9. doi: 10.1016/j.humimm.2013.08.268
145. Gianchecchi E, Delfino DV, Fierabracci A. Recent Insights Into the Role of the PD-1/PD-L1 Pathway in Immunological Tolerance and Autoimmunity. *Autoimmun Rev* (2013) 12(11):1091–100. doi: 10.1016/j.autrev.2013.05.003
146. Beldi-Ferchiou A, Lambert M, Dogniaux S, Vely F, Vivier E, Olive D, et al. PD-1 Mediates Functional Exhaustion of Activated NK Cells in Patients With Kaposi Sarcoma. *Oncotarget* (2016) 7(45):72961–77. doi: 10.18632/oncotarget.12150
147. Mayerhofer A, Walenta L, Mayer C, Eubler K, Welter H. Human Testicular Peritubular Cells, Mast Cells and Testicular Inflammation. *Andrologia* (2018) 50(11):e13055. doi: 10.1111/and.13055
148. Caslin HL, Taruselli MT, Haque T, Pondicherry N, Baldwin EA, Barnstein BO, et al. Inhibiting Glycolysis and ATP Production Attenuates IL-33-Mediated Mast Cell Function and Peritonitis. *Front Immunol* (2018) 9:3026. doi: 10.3389/fimmu.2018.03026
149. Van den Bossche J, Baardman J, Otto Natasja A, van der Velden S, Neele Annette E, van den Berg Susan M, et al. Mitochondrial Dysfunction Prevents Repolarization of Inflammatory Macrophages. *Cell Rep* (2016) 17(3):684–96. doi: 10.1016/j.celrep.2016.09.008
150. Gerendai I, Banczerowski P, Csernus V. Interleukin 1-β Injected Into the Testis Acutely Stimulates and Later Attenuates Testicular Steroidogenesis of the Immature Rat. *Endocrine* (2005) 28(2):165–70. doi: 10.1385/ENDO:28:2:165
151. Huleihel M, Lunenfeld E. Involvement of Intratesticular IL-1 System in the Regulation of Sertoli Cell Functions. *Mol Cell Endocrinol* (2002) 187(1-2):125–32. doi: 10.1016/s0303-7207(01)00690-6
152. Bisht S, Faiq M, Tolahunase M, Dada R. Oxidative Stress and Male Infertility. *Nat Rev Urol* (2017) 14(8):470–85. doi: 10.1038/nrurol.2017.69
153. Tremellen K. Oxidative Stress and Male Infertility–a Clinical Perspective. *Hum Reprod Update* (2008) 14(3):243–58. doi: 10.1093/humupd/dmn004
154. Hotamisligil GS. Foundations of Immunometabolism and Implications for Metabolic Health and Disease. *Immunity* (2017) 47(3):406–20. doi: 10.1016/j.immuni.2017.08.009
155. Ochsendorf FR. Infections in the Male Genital Tract and Reactive Oxygen Species. *Hum Reprod Update* (1999) 5(5):399–420. doi: 10.1093/humupd/5.5.399
156. Lysiak JJ. The Role of Tumor Necrosis Factor-Alpha and Interleukin-1 in the Mammalian Testis and Their Involvement in Testicular Torsion and Autoimmune Orchitis. *Reprod Biol Endocrinol* (2004) 2(1):9. doi: 10.1186/1477-7827-2-9
157. Fraczek M, Kurpisz M. Cytokines in the Male Reproductive Tract and Their Role in Infertility Disorders. *J Reprod Immunol* (2015) 108:98–104. doi: 10.1016/j.jri.2015.02.001
158. Syriou V, Papanikolaou D, Kozyraki A, Goulis DG. Cytokines and Male Infertility. *Eur Cytokine Netw* (2018) 29(3):73–82. doi: 10.1684/ecn.2018.0412
159. La Vignera S, Condorelli RA, Vicari E, Tumino D, Morgia G, Favilla V, et al. Markers of Semen Inflammation: Supplementary Semen Analysis? *J Reprod Immunol* (2013) 100(1):2–10. doi: 10.1016/j.jri.2013.05.001
160. Agarwal A, Rana M, Qiu E, AlBunni H, Bui AD, Henkel R. Role of Oxidative Stress, Infection and Inflammation in Male Infertility. *Andrologia* (2018) 50 (11):e13126. doi: 10.1111/and.13126
161. Barati E, Nikzad H, Karimian M. Oxidative Stress and Male Infertility: Current Knowledge of Pathophysiology and Role of Antioxidant Therapy in Disease Management. *Cell Mol Life Sci* (2020) 77(1):93–113. doi: 10.1007/s00018-019-03253-8
162. Turner TT, Bang HJ, Lysiak JJ. Experimental Testicular Torsion: Reperfusion Blood Flow and Subsequent Testicular Venous Plasma Testosterone Concentrations. *Urology* (2005) 65(2):390–4. doi: 10.1016/j.urology.2004.09.033
163. Darbandi M, Darbandi S, Agarwal A, Sengupta P, Durairajanayagam D, Henkel R, et al. Reactive Oxygen Species and Male Reproductive Hormones. *Reprod Biol Endocrinol* (2018) 16(1):87. doi: 10.1186/s12958-018-0406-2
164. Sikka SC. Oxidative Stress and Role of Antioxidants in Normal and Abnormal Sperm Function. *Front Biosci* (1996) 1:e78–86. doi: 10.2741/a146
165. Martinez P, Proverbio F, Camejo MI. Sperm Lipid Peroxidation and Pro-Inflammatory Cytokines. *Asian J Androl* (2007) 9(1):102–7. doi: 10.1111/j.1745-7262.2007.00238.x
166. Lainez NM, Coss D. Obesity, Neuroinflammation, and Reproductive Function. *Endocrinology* (2019) 160(11):2719–36. doi: 10.1210/en.2019-00487
167. Ray I, Mahata SK, De RK. Obesity: An Immunometabolic Perspective. *Front Endocrinol (Lausanne)* (2016) 7:157. doi: 10.3389/fendo.2016.00157
168. Fui MN, Dupuis P, Grossmann M. Lowered Testosterone in Male Obesity: Mechanisms, Morbidity and Management. *Asian J Androl* (2014) 16(2):223–31. doi: 10.4103/1008-682X.122365
169. Craig JR, Jenkins TG, Carrell DT, Hotaling JM. Obesity, Male Infertility, and the Sperm Epigenome. *Fertil Steril* (2017) 107(4):848–59. doi: 10.1016/j.fertnstert.2017.02.115
170. Leisegang K, Henkel R, Agarwal A. Obesity and Metabolic Syndrome Associated With Systemic Inflammation and the Impact on the Male Reproductive System. *Am J Reprod Immunol* (2019) 82(5):e13178. doi: 10.1111/aji.13178
171. Arafa M, Agarwal A, Al Said S, Majzoub A, Sharma R, Bjugstad KB, et al. Semen Quality and Infertility Status can be Identified Through Measures of Oxidation-Reduction Potential. *Andrologia* (2018) 50(2):e12881. doi: 10.1111/and.12881
172. Dutta S, Majzoub A, Agarwal A. Oxidative Stress and Sperm Function: A Systematic Review on Evaluation and Management. *Arab J Urol* (2019) 17 (2):87–97. doi: 10.1080/2090598X.2019.1599624

173. Alves MG, Martins AD, Cavaco JE, Socorro S, Oliveira PF. Diabetes, Insulin-Mediated Glucose Metabolism and Sertoli/blood-Testis Barrier Function. *Tissue Barriers* (2013) 1(2):e23992. doi: 10.4161/tisb.23992
174. Street EJ, Justice ED, Kopa Z, Portman MD, Ross JD, Skerlev M, et al. The 2016 European Guideline on the Management of Epididymo-Orchitis. *Int J STD AIDS* (2017) 28(8):744–9. doi: 10.1177/0956462417699356
175. Guzik TJ, Cosentino F. Epigenetics and Immunometabolism in Diabetes and Aging. *Antioxid Redox Signal* (2018) 29(3):257–74. doi: 10.1089/ars.2017.7299
176. Majzoub A, Agarwal A. Systematic Review of Antioxidant Types and Doses in Male Infertility: Benefits on Semen Parameters, Advanced Sperm Function, Assisted Reproduction and Live-Birth Rate. *Arab J Urol* (2018) 16(1):113–24. doi: 10.1016/j.aju.2017.11.013
177. Agarwal A, Parekh N, Panner Selvam MK, Henkel R, Shah R, Homa ST, et al. Male Oxidative Stress Infertility (MOSI): Proposed Terminology and Clinical Practice Guidelines for Management of Idiopathic Male Infertility. *World J Mens Health* (2019) 37(3):296–312. doi: 10.5534/wjmh.190055
178. Francomano D, Ilacqua A, Bruzziches R, Lenzi A, Aversa A. Effects of 5-Year Treatment With Testosterone Undecanoate on Lower Urinary Tract Symptoms in Obese Men With Hypogonadism and Metabolic Syndrome. *Urology* (2014) 83(1):167–73. doi: 10.1016/j.urology.2013.08.019
179. Diaz A, Romero M, Vazquez T, Lechner S, Blomberg BB, Frasca D. Metformin Improves *In Vivo* and *In Vitro* B Cell Function in Individuals With Obesity and Type-2 Diabetes. *Vaccine* (2017) 35(20):2694–700. doi: 10.1016/j.vaccine.2017.03.078
180. Zarrouk M, Finlay DK, Foretz M, Viollet B, Cantrell DA. Adenosine-Mono-Phosphate-Activated Protein Kinase-Independent Effects of Metformin in T Cells. *PloS One* (2014) 9(9):e106710. doi: 10.1371/journal.pone.0106710
181. Palsson-McDermott EM, O'Neill LAJ. Targeting Immunometabolism as an Anti-Inflammatory Strategy. *Cell Res* (2020) 30(4):300–14. doi: 10.1038/s41422-020-0291-z
182. Mir J, Ashraf M. Does Weight Loss Improve Fertility With Respect to Semen Parameters— Results From a Large Cohort Study. *Int J Infertil Fetal Med* (2017) 8:12–7. doi: 10.5005/jp-journals-10016-1141
183. Salehi B, Martorell M, Arbiser JL, Sureda A, Martins N, Maurya PK, et al. Antioxidants: Positive or Negative Actors? *Biomolecules* (2018) 8(4):124. doi: 10.3390/biom8040124
184. Schisterman EF, Sjaarda LA, Clemons T, Carrell DT, Perkins NJ, Johnstone E, et al. Effect of Folic Acid and Zinc Supplementation in Men on Semen Quality and Live Birth Among Couples Undergoing Infertility Treatment: A Randomized Clinical Trial. *JAMA* (2020) 323(1):35–48. doi: 10.1001/jama.2019.18714
185. Steiner AZ, Hansen KR, Barnhart KT, Cedars MI, Legro RS, Diamond MP, et al. The Effect of Antioxidants on Male Factor Infertility: The Males, Antioxidants, and Infertility (MOXI) Randomized Clinical Trial. *Fertil Steril* (2020) 113552-560(3):e553. doi: 10.1016/j.fertnstert.2019.11.008
186. Smits RM, Mackenzie-Proctor R, Yazdani A, Stankiewicz MT, Jordan V, Showell MG. Antioxidants for Male Subfertility. *Cochrane Database Syst Rev* (2019) 3:CD007411. doi: 10.1002/14651858.CD007411.pub4
187. Alves MG, Martins AD, Vaz CV, Correia S, Moreira PI, Oliveira PF, et al. Metformin and Male Reproduction: Effects on Sertoli Cell Metabolism. *Br J Pharmacol* (2014) 171(4):1033–42. doi: 10.1111/bph.12522
188. Tavares RS, Escada-Rebelo S, Silva AF, Sousa MI, Ramalho-Santos J, Amaral S. Antidiabetic Therapies and Male Reproductive Function: Where do We Stand? *Reproduction* (2018) 155(1):R13–37. doi: 10.1530/REP-17-0390
189. Maresch CC, Stute DC, Alves MG, Oliveira PF, de Kretser DM, Linn T. Diabetes-Induced Hyperglycemia Impairs Male Reproductive Function: A Systematic Review. *Hum Reprod Update* (2018) 24(1):86–105. doi: 10.1093/humupd/dmx033
190. Su Y, Lu J, Chen X, Liang C, Luo P, Qin C, et al. Rapamycin Alleviates Hormone Imbalance-Induced Chronic Nonbacterial Inflammation in Rat Prostate Through Activating Autophagy *via* the mTOR/ULK1/ATG13 Signaling Pathway. *Inflammation* (2018) 41(4):1384–95. doi: 10.1007/s10753-018-0786-7
191. Zhang L, Liu Y, Chen XG, Zhang Y, Chen J, Hao ZY, et al. MicroRNA Expression Profile in Chronic Nonbacterial Prostatitis Revealed by Next-Generation Small RNA Sequencing. *Asian J Androl* (2019) 21(4):351–9. doi: 10.4103/aja.aja_97_18
192. Aslani F, Schuppe HC, Guazzone VA, Bhushan S, Wahle E, Lochnit G, et al. Targeting High Mobility Group Box Protein 1 Ameliorates Testicular Inflammation in Experimental Autoimmune Orchitis. *Hum Reprod* (2015) 30(2):417–31. doi: 10.1093/humrep/deu320
193. Nicolas N, Muir JA, Hayward S, Chen JL, Stanton PG, Gregorevic P, et al. Induction of Experimental Autoimmune Orchitis in Mice: Responses to Elevated Circulating Levels of the Activin-Binding Protein, Follistatin. *Reproduction* (2017) 154(3):293–305. doi: 10.1530/REP-17-0010
194. Winter AG, Zhao F, Lee RK. Androgen Deficiency and Metabolic Syndrome in Men. *Transl Androl Urol* (2014) 3(1):50–8. doi: 10.3978/j.issn.2223-4683.2014.01.04
195. Vabret N, Britton GJ, Gruber C, Hegde S, Kim J, Kuksin M, et al. Immunology of COVID-19: Current State of the Science. *Immunity* (2020) 52(6):910–41. doi: 10.1016/j.immuni.2020.05.002
196. Yang M, Chen S, Huang B, Zhong JM, Su H, Chen YJ, et al. Pathological Findings in the Testes of COVID-19 Patients: Clinical Implications. *Eur Urol Focus* (2020) 6(5):1124–9. doi: 10.1016/j.euf.2020.05.009
197. Sliwa L, Macura B, Majewska-Szczepanik M, Szczepanik M. Lack of TCRalphabeta+ CD8+ and TCRgammadelta+ Lymphocytes Ameliorates LPS Induced Orchitis in Mice–Preliminary Histological Observations. *Folia Biol (Krakow)* (2014) 62(1):67–71. doi: 10.3409/fb62_1.67
198. Hedger MP, Meinhardt A. Local Regulation of T Cell Numbers and Lymphocyte-Inhibiting Activity in the Interstitial Tissue of the Adult Rat Testis. *J Reprod Immunol* (2000) 48(2):69–80. doi: 10.1016/s0165-0378(00)00071-1
199. Firth JD, Ebert BL, Ratcliffe PJ. Hypoxic Regulation of Lactate Dehydrogenase A. Interaction Between Hypoxia-Inducible Factor 1 and cAMP Response Elements. *J Biol Chem* (1995) 270(36):21021–7. doi: 10.1074/jbc.270.36.21021
200. Crisostomo L, Alves MG, Gorga A, Sousa M, Riera MF, Galardo MN, et al. Molecular Mechanisms and Signaling Pathways Involved in the Nutritional Support of Spermatogenesis by Sertoli Cells. *Methods Mol Biol* (2018) 1748:129–55. doi: 10.1007/978-1-4939-7698-0_11
201. Cardoso AM, Alves MG, Mathur PP, Oliveira PF, Cavaco JE, Rato L. Obesogens and Male Fertility. *Obes Rev* (2017) 18(1):109–25. doi: 10.1111/obr.12469
202. Grossmann M. Hypogonadism and Male Obesity: Focus on Unresolved Questions. *Clin Endocrinol (Oxf)* (2018) 89(1):11–21. doi: 10.1111/cen.13723
203. Pereira SC, Crisostomo L, Sousa M, Oliveira PF, Alves MG. Metabolic Diseases Affect Male Reproduction and Induce Signatures in Gametes That may Compromise the Offspring Health. *Environ Epigenet* (2020) 6(1):dvaa019. doi: 10.1093/eep/dvaa019
204. Luo D, Zhang M, Su X, Liu L, Zhou X, Zhang X, et al. High Fat Diet Impairs Spermatogenesis by Regulating Glucose and Lipid Metabolism in Sertoli Cells. *Life Sci* (2020) 257:118028. doi: 10.1016/j.lfs.2020.118028

Conflict of Interest: The authors declare that the research was conducted in the absence of any commercial or financial relationships that could be construed as a potential conflict of interest.

frontiers in Immunology

ORIGINAL RESEARCH
published: 12 October 2021
doi: 10.3389/fimmu.2021.723409

Seminal Plasma and Seminal Plasma Exosomes of Aged Male Mice Affect Early Embryo Implantation *via* Immunomodulation

Dandan Wang[1†], Kadiliya Jueraitetibaike[1†], Ting Tang[2†], Yanbo Wang[3], Jun Jing[1], Tongmin Xue[2], Jinzhao Ma[1], Siyuan Cao[1], Ying Lin[1], Xiaoyan Li[1], Rujun Ma[1], Xi Chen[3] and Bing Yao[1*]*

[1] Department of Reproductive Medicine, Affiliated Jinling Hospital, Medicine School of Nanjing University, Nanjing, China, [2] Department of Reproductive Medicine, Affiliated Jinling Hospital, Nanjing Medical University, Nanjing, China, [3] School of Life Sciences, Nanjing University, Nanjing, China

Seminal plasma (SP), particularly SP exosomes (sExos), alters with age and can affect female mouse uterine immune microenvironment. However, the relationship between fertility decline in reproductively older males, and SP and sExos age-related changes, which may compromise the uterine immune microenvironment, remains unclear. The present study demonstrated that the implantation rate of female mice treated with SP from reproductively older male mice (aged-SP group) was lower than that of those treated with SP from younger male mice (young-SP group). RNA-sequencing analysis revealed altered levels of dendritic cell (DC)-related cytokines and chemokines in the uteri of the former group compared with those of the latter group. *In vivo* and *in vitro* experiments demonstrated a weaker inhibitory effect of aged SP on DC maturation than of young SP upon stimulation. After isolating and characterizing sExos from young and advanced-age male mice, we discovered that insemination of a subset of the aged-SP group with sExos from young male mice partially recovered the implantation rate decline. Additional *in vivo* and *in vitro* experiments revealed that sExos extracted from age male mice exerted a similar effect on DC maturation as SP of aged mice, indicating an age-related sExos inhibitory effect. In conclusion, our study demonstrated that age-related alterations of sExos may be partially responsible for lower implantation rates in the aged-SP group compared with those in the young-SP group, which were mediated by uterine immunomodulation. These findings provide new insights for clinical seminal adjuvant therapy.

Keywords: seminal plasma, seminal plasma exosomes, dendritic cells, advanced-age male fertility, uterine immune microenvironment, embryo implantation

OPEN ACCESS

Edited by:
Yong-Gang Duan, University of Hong Kong, China

Reviewed by:
Philip Chi Ngong Chiu, The University of Hong Kong, Hong Kong, SAR China
Shiro Kurusu, Kitasato University, Japan

***Correspondence:**
Xi Chen
xichen@nju.edu.cn
Bing Yao
yaobing@nju.edu.cn

†These authors have contributed equally to this work and share first authorship

Specialty section:
This article was submitted to Mucosal Immunity, a section of the journal Frontiers in Immunology

Received: *10 June 2021*
Accepted: *22 September 2021*
Published: *12 October 2021*

Citation:
Wang D, Jueraitetibaike K, Tang T, Wang Y, Jing J, Xue T, Ma J, Cao S, Lin Y, Li X, Ma R, Chen X and Yao B (2021) Seminal Plasma and Seminal Plasma Exosomes of Aged Male Mice Affect Early Embryo Implantation via Immunomodulation. Front. Immunol. 12:723409. doi: 10.3389/fimmu.2021.723409

INTRODUCTION

Due to social pressure, extension of life expectancy, popularization of effective contraception, and the development of assisted reproductive technology, delayed childbirth has become extremely common, highlighting the issue of advanced-age-related fertility decline. Advanced paternal age, which refers to paternal age over 40, are known to significantly impact fertility and offspring health (1), with male age negatively correlated with semen volume, sperm motility, sperm morphology, reproductive hormone levels, testicular function, chromosome structure, and sperm DNA integrity (2–4). Irreversible cell damage and senescence from age-related inflammation and macromolecular dysfunction (5) produce a senescence-associated secretory phenotype (SASP) characterized by the increased release of pro-inflammatory cytokines, chemokines, and tissue-destructive proteases (6). Increased extracellular vesicle (EV) release has been reported in senescent cells, compared with normal cells, indicating an important EV role in SASP development (7). EVs can be largely divided into three groups, among which the smallest EV exosomes (Exos) varying between 0.03 and 0.15 μm are the focus of the attention of most studies in biomedicine, since they regulate multiple intercellular signaling in physiological and pathological situations (8, 9).

Seminal plasma (SP), an important component of male body fluid, is not only a vehicle for carrying spermatozoa to fertilize oocytes but also an essential actor in female immune response regulation and embryo implantation (10–12). Studies have demonstrated that semen can cause an inflammatory response in human female reproductive mucosa, including the production of inflammatory cytokines and chemokines (13–15), upregulation of cyclooxygenase-2 (16), and recruitment of dendritic cells (DCs) and cervical infiltrating neutrophils (14, 17, 18). Interestingly, recent studies have reported that SP may be beneficial to implantation by promoting DC tolerance (19). Tolerant DCs are more resistant to maturation upon various stimulations. Yasuda et al. discovered that immature phenotype made up the main component of uterine DCs (uDCs) 3.5 days post coitum (dpc), indicating that immature DCs may play an important role in successful implantation (20) and demonstrating the influence of male SP on the female reproductive immune microenvironment.

A typical mammalian ejaculation contains trillions of EVs, a primary component of SP. SP exosomes (sExos) and SP provide immunomodulatory functions in the uterus and may be involved in embryo implantation (21).

Based on these previous findings, we hypothesized that during the aging process of advanced-age males, production of senescence-related SP and sExos alters the uterine immune microenvironment, thus affecting embryo implantation. Our research elucidates the influence of SP and sExos from advanced-age male mice on embryo implantation, demonstrating age-related male fertility decline.

MATERIALS AND METHODS

Mice

Specific pathogen-free (SPF) grade 6- to 8-week-, 12- to 14-week-, and 12- to 18-month-old male and 5- to 6-week-old female C57BL/6 mice and 6- to 8-week-old female Institute of Cancer Research (ICR) mice were purchased from Nanjing Medical University Laboratory Animal Co., Ltd. (Certificate number SCXK (Su) 2016-0002). The mice were housed in 12/12-h light/dark cycle, with unrestricted access to food and water. All animal experiments were approved by the Animal Protection and Use Committee of Jinling Hospital and carried out in accordance with institutional guidelines.

Animal Experiment Design

As previously described (22), vasectomies were performed on 12- to 14-week-old (young) and 12- to 18-month-old (aged) male C57BL/6 mice, which were ready for mating, to confirm sterility 2 weeks post-surgery. Estrous cycle smears were used to identify estrus 6- to 8-week-old female ICR mice based on vaginal cytology (23), which were divided into two groups: one (young-SP group) caged with young sterilized male mice and the other (aged-SP group) with aged sterilized male mice. Mating was determined by the presence of a copulatory plug, which was checked at 8:00 a.m. daily, and the day of plug detection was defined 0.5 dpc.

Zygote Collection and Culture

Zygote collection and culture experiments were performed as previously described (24). Briefly, after 46–48 h of 10 IU pregnant mare serum gonadotropin (PMSG) injection, 6- to 8-week-old female ICR mice were injected with human chorionic gonadotropin (HCG) and immediately mated with male mice. Eighteen hours later, the zygotes were harvested and cultured in Quinn's 1026 cleavage medium (CooperSurgical, Trumbull, CT, USA), supplemented with 10% Quinn's 3001 serum protein substitute (CooperSurgical) and paraffin oil, at 37°C under 5% CO_2. The embryos were transferred at the four-cell phase and cultured in Quinn's 1029 blastocyst medium (CooperSurgical), supplemented with 10% Quinn's 3001 serum protein substitute (CooperSurgical), to blastocyst stage for subsequent transfers.

Seminal Plasma Exosomes Administration and Blastocyst Transfer

Copulatory plugs were removed immediately after being detected. For sExos administration, transvaginal injection of 20 μl sExos/mouse was performed at 0.5 dpc or on the morning of estrus day. Briefly, a pipette tip was gently inserted about 5 mm deep into the vaginal lumen of mouse, and 20 μl of sExos was then deposited. For embryo implantation analysis, 16 blastocysts were transferred to each pseudo-pregnant mouse at 3.0 dpc following protocols provided by Pablo Bermejo-Alvarez (22) with little modifications, and mice were euthanized *via* cervical dislocation at 6.5 dpc to analyze implantation rates.

Mouse Uterus RNA Sequencing and Functional Analysis

TRIzol was used to extract total RNA from the uteri of young-SP and aged-SP group female mice at 3.0 dpc, during the pre-implantation window and prior to embryo transfer. RNA integrity and concentration were assessed using the RNA Nano 6000 Assay Kit of the Bioanalyzer 2100 system (Agilent Technologies, Santa Clara, CA, USA). RNA integrity number (RIN) ≥8 was used as a cutoff for RNA integrity. Sequencing libraries were generated using NEBNext® Ultra™ RNA Library Prep Kit for Illumina® (#E7530L, New England BioLabs, Ipswich, MA, USA) following the manufacturer's recommendations. High-throughput sequencing was performed on the Illumina HiSeq 2500 system (Illumina, San Diego, CA, USA) at Annoroad Gene Technology (Beijing, China; http://www.annoroad.com). The original data were filtered and aligned to the reference genome using HISAT2 v2.1.0. Fragments per kilobase of transcript, per million mapped reads were calculated to estimate gene expression levels in each sample. DESeq2 was used to determine differential expression between samples. Genes with $q < 0.05$ and $\log2\ FC > 1$ were identified as differentially expressed genes (DEGs). The Kyoto Encyclopedia of Genes and Genomes (KEGG) enrichments of the DEGs were used to determine their molecular interactions and reaction networks. The p-value ≤0.05 and false discovery rate (FDR) q-value ≤0.05 was considered as statistically significant.

RNA Extraction and Quantitative RT-PCR

Total RNA was extracted from the uteri of young-SP and aged-SP group female mice at 3.0 dpc using a Total RNA Isolation Kit (BEI-BEI Biotech, Zhengzhou, China). The RNA extracted from the uteri of unmated mice between 1:00 p.m. and 4:00 p.m. on the day of estrus was regarded as control. To estimate RNA quality, the ratio of the absorbance contributed by the nucleic acid to the absorbance of the contaminants was calculated and requirements for A_{260}/A_{280} ratios are 1.8–2.2. HisScript III RT SuperMix for qPCR (Vazyme Biotech, Nanjing, China) was used for RT-PCR. AceQ qPCR SYBR Green Master Mix (Vazyme Biotech) was used for qPCR, according to the manufacturer's instructions. The samples were amplified and monitored using a Roche LightCycler 96 Real-time PCR system (Roche Diagnostics, Basel, Switzerland). The fold change in gene expression was calculated using the $2^{-\Delta\Delta Cq}$ method with the housekeeping gene GAPDH as the internal control, which was consistently expressed across samples. Primer-Blast was used to design primers. The primer sequences are listed in **Table 1**. Briefly, primers should have the following properties to ensure the efficiency and specificity: length of 18–24 bases; 40%–60% G/C content; start and end with 1–2 G/C pairs; and melting temperature (Tm) of 50°C–60°C. Primer pairs should have a Tm within 5°C of each other; primer pairs should not have complementary regions.

Uterine Immunohistology and Luminal Fluid Collection

DCs were detected in paraffin-embedded uterine tissues of estrus control, young-SP group, aged-SP group, young-sExos group (perfused with sExos extracted from young male mice), and aged-sExos group (perfused with sExos extracted from aged male mice) females. Intrauterine injection of 10 μg of lipopolysaccharide (LPS; Solarbio, Beijing, China) in a total volume of 25 μl were administered at 0.5 dpc, and uterine luminal fluid was flushed with 50 μl of phosphate-buffered saline (PBS) prior to harvesting uterine tissues at 3.0 dpc. Insoluble material was pelleted at 14,000 × *g* for 10 min, and the supernatant was stored at −80°C until analysis. Uterine tissues were fixed with 4% paraformaldehyde (PFA) in PBS overnight at 4°C and dehydrated in ethanol before paraffin embedding. Tissue sections (3 μM) were cut on a LEiCA RM2016 Rotary Microtome (LEiCA, Shanghai), dewaxed in xylene, and rehydrated. After antigen retrieval process, tissues were surrounded with a hydrophobic barrier using a barrier pen. Non-specific staining between the primary antibodies and the tissue was blocked by incubation in blocking buffer (15% normal rabbit serum (vol/vol) in PBS) at room temperature. Sections were washed in PBS before incubation with anti-CD11c Rabbit pAb (1:100, Servicebio, Wuhan, China) for 1 h. Following washing in PBS, sections were incubated with TRITC-conjugated goat anti-rabbit IgG (1:100, Abcam, Cambridge, UK) overnight at 4°C in a humidified chamber. Sections were washed in PBS before incubation overnight with one of the followings: anti-mouse CD80 fluorescein isothiocyanate (FITC) (1:100, BioLegend, San Diego, CA, USA), anti-mouse CD83 APC (1:100, BioLegend), anti-mouse CD86 FITC (1:100, BioLegend), and anti-mouse MHCII Alexa Fluor® 647 (1:100, BioLegend). Following washing in PBS, DAPI was added, and tissues were incubated for 10 min at room temperature. After rinsing with PBS, tissues were mounted with an anti-fade mounting media. Images were captured using an Eclipse Ci-E microscope (Nikon Instrument, Netherlands). To clearly visualize double-positive cells, the green and red channels were merged using the "AND" gate function in the Image Calculator of ImageJ.

TABLE 1 | Sequence of primers used for real-time quantitative PCR.

Gene name	5′-Sequence-3′
m-Cxcl1-F	CTGGGATTCACCTCAAGAACATC
m-Cxcl1-R	CAGGGTCAAGGCAAGCCTC
m-IL20rb-F	ACCCCTTTAACCGAAATGCAA
m-IL20rb-R	CCTCCAGTAGACCACAAGGAA
m-Fas-F	TATCAAGGAGGCCCATTTTGC
m-Fas-R	TGTTTCCACTTCTAAACCATGCT
m-Cxcl16-F	CCTTGTCTCTTGCGTTCTTCC
m-Cxcl16-R	TCCAAAGTACCCTGCGGTATC
m-Tnfsf10-F	ATGGTGATTTGCATAGTGCTCC
m-Tnfsf10-R	GCAAGCAGGGTCTGTTCAAGA
m-Cx3cl1-F	ACGAAATGCGAAATCATGTGC
m-Cx3cl1-R	CTGTGTCGTCTCCAGGACAA
m-Eda-R	TCAGGGGACTCTGCCACTC
m-Eda-F	CAGGCTGGGCTTTCCAACT
m-Ackr4-F	AGCCAGTACGAAGTGATCTGC
m-Ackr4-R	CTGCGAGCCCAGTGACAAA
m-Il17rb-F	GGCTGCCTAAACCACGTAATG
m-Il17rb-R	CCCGTTGAATGAGAATCGTGT
m-GAPDH-F	TCTTGCTCAGTGTCCTTGC
m-GAPDH-R	CTTTGTCAAGCTCATTTCCTGG

Preparation of Mouse Seminal Plasma

For collecting young SP and aged SP, three 12- to 14-week-old male C57BL/6 mice and three 12- to 18-month-old male

C57BL/6 mice were used, respectively. After being euthanasia, mouse epididymal head, caudal epididymis, prostates, and seminal vesicles were removed from the opened abdominal cavity with microscopic ophthalmic instruments under an anatomical microscope and placed into 600 μl of precooled 0.5% PBS solution. These tissues were cut into small pieces with ophthalmic scissors, and the seminal vesicle fluid was extruded with a sterile syringe tip. The tissue suspension was transferred to a 1.5-ml centrifuge tube and centrifuged at 9,000 × *g* at 4°C for 30 min. The supernatants were collected as young SP and aged SP, respectively, both of which were stored at −80°C before use.

Enzyme-Linked Immunosorbent Assay

The production of interleukin (IL)-12p70, tumor necrosis factor-α (TNF-α), IL-1β, IL-6, IL-10, and transforming growth factor-beta (TGF-β) was measured by ELISA kits (Enzyme-linked Biotechnology, Shanghai, China). Briefly, uterine luminal fluid or cell culture supernatant was added to the reaction buffer containing 50 μl of horseradish peroxidase (HRP)-conjugated reagent, and the wells were sealed and placed in a 37°C water bath for 60 min. Then, the wells were washed, and solutions A and B were added and incubated for another 15 min. The reaction was stopped by adding the termination buffer. The optical density was detected with a Multimode Microplate Reader (BioTek, Winooski, VT, USA). The concentration of each sample was calculated from the standard curve. The limit of these ELISA kits are as follows: mouse IL-12P70: 31.25–1,000 pg/ml; mouse TGF-β: 25–800 pg/ml; mouse IL-10: 12.5–400 pg/ml; mouse IL-8: 3.75–120 pg/ml; mouse IL-6: 3.75–120 pg/ml; mouse IL-1β: 31.25–1,000 pg/ml; and mouse TNF-α: 20–640 pg/ml.

Preparation of Dendritic Cells

As previously described (25), bone marrow from the tibia and femur of euthanized C57BL/6 mice were extracted into a culture dish containing Roswell Park Memorial Institute (RPMI) 1640. The bone marrow cell suspension was centrifuged at 1,000 × *g* for 10 min and subsequently, after the addition of 3 ml of red blood cell lysate, at 1,000 × *g* for 5 min. The cells were cultured in the absence or presence of aged SP (dilution of 1:100), young SP (dilution of 1:100), aged sExos, or young sExos in 6-well plates at 1×10^6 cells per well; and 200 ng/ml of granulocyte-macrophage colony-stimulating factor (GM-CSF) and 200 ng/ml of IL-4 were added. Half of the cell culture medium was refreshed every 3 days. On day 6, non-adherent cells in the culture supernatant and loosely adherent cells harvested by gentle washing with PBS were pooled and used as the starting source of material for most experiments [bone marrow-derived DCs (BMDCs)].

Flow Cytometry and Dendritic Cell Maturation Analysis

BMDCs were stimulated with 1 μg/ml of LPS. After a 24-h culture, the cells were then collected by centrifugation and resuspended in single-cell PBS suspensions. Single-cell suspensions with final cell concentration 1×10^6 cells/ml were blocked with 0.5% bovine serum albumin (BSA) at 4°C for 15 min and incubated with fluorescently labeled antibodies for 30 min. The following antibodies were used for flow cytometry analysis: anti-mouse CD11c PE (0.5 μg/test, BioLegend), anti-mouse CD80 FITC (0.125 μg/test, BioLegend), anti-mouse CD83 APC (0.5 μg/test, BioLegend), anti-mouse CD86 FITC (0.125 μg/test, BioLegend), and anti-mouse MHCII Alexa Fluor® 647 (0.25 μg/test, BioLegend). The cells were subsequently washed, suspended in PBS solution, and analyzed using a BD FACSCalibur flow cytometer (BD Biosciences, Franklin Lakes, NJ, USA). The data were analyzed using FlowJo 7.6.1 software (Tree Star, Inc., Ashland, OR, USA).

Isolation and Characterization of Seminal Plasma Exosomes

The previously collected SP were each diluted with PBS to a total volume of 10 ml and centrifuged at 300 × *g* for 5 min. The supernatant was transferred to a new centrifuge tube and centrifuged at 3,000 × *g* for 10 min to remove cells or other debris and at 10,000 × *g* for 25 min to remove other larger vesicles. The resulting supernatant was then transferred to a matching overspeed centrifuge tube and centrifuged at 110,000 × *g* for 70 min. After the supernatant was transferred into a new tube, 60 μl of PBS was added to resuspend the pellet, which was then filtered with 0.45- and 0.22-μm filters and collected as young sExos and aged sExos, respectively. All centrifugations were carried out under 4°C, and the sExos were stored under −80°C for at most 1 week before use. Epididymosomes were collected following the same procedure as sExos isolation with only epididymal head, and caudal epididymis was used. The presence and purity of sExos were confirmed using H7700 transmission electron microscopy (Hitachi High-Tech, Tokyo, Japan). The sExos size was directly tracked using the Nanosight NS300 system (NanoSight Technology, Malvern, UK). Samples were manually injected into the sample chamber at ambient temperature. Each sample was measured thrice, and the average value was calculated. Finally, data were analyzed using the nanoparticle tracking analysis (NTA) analytical software, version 2.3.

Western Blotting of Seminal Plasma Exosomes

Western blotting was used to identify sExos. Total protein was extracted using a radioimmunoprecipitation assay (RIPA) buffer, and protein samples were fractionated by sodium dodecyl sulfate–polyacrylamide gel electrophoresis (SDS-PAGE), analyzed by Western blotting, and visualized. Membranes were blocked with Albumin Bovine (BSA; Biofroxx, Einhausen, Germany) in TBST (10 mM of Tris, pH 7.5, 150 mM of NaCl, and 0.1% Tween-20) and then probed with primary antibodies overnight at 4°C. The following primary antibodies were used: monoclonal rabbit anti-mouse CD63 antibody (1:2,000, Abcam), monoclonal rabbit anti-mouse TSG101 antibody (1:2,000, Santa Cruz Biotechnology, Dallas, TX, USA), polyclonal CD9 antibody (1:1,000, MultiSciences Biotech, Zhejiang, China), monoclonal rabbit anti-mouse Albumin antibody (1:2,000, Abcam), and monoclonal GAPDH antibody (1:5,000, KangChen Biotech, Shanghai, China). After multiple washes in TBST and incubation with HRP-conjugated secondary antibodies (1:20,000, Beyotime, Shanghai, China), the protein bands were

visualized using an automatic chemiluminescence image analysis system (Tanon Science & Technology, Shanghai, China). The intensities of protein bands were quantitated using ImageJ Gel Analysis program.

Tracing of PKH67-Labeled Seminal Plasma Exosomes in the Uterus

PKH67 Green Fluorescent Cell Linker Kits (Sigma-Aldrich) were used to label sExos lipid bilayers. According to the reagent manufacturer's instructions, 100 μg of freshly isolated sExos was diluted with 500 μl of diluent C and mixed with 500 μl of diluent C, which contained 4 μl of PKH67. After being incubated at room temperature for 5 min, 500 μl of Exosome-depleted FBS Media Supplement (System Biosciences, Palo Alto, USA) was added to halt the staining. The PKH67-labeled pure sExos were then separated from the unbound dye using the ExoQuick exosome precipitation solution (Bomais, Beijing) and were resuspended with 60 μl of PBS. Unstained sExos were used as a negative control. Each mouse was transvaginally injected with 20 μl of PKH67-labeled sExos or control sExos and euthanized 6 h later. The uteri were removed, frozen, and sectioned. After blocking with 2% BSA, slides were incubated overnight with anti-Vimentin antibody (1:200, Abcam) and anti-Cytokeratin 19 antibody (1:400, Abcam) at 4°C and then with secondary antibodies at room temperature for 1 h. The nuclei were then stained with DAB for 15 min, and images were digitized with an IX73 fluorescence microscope (Olympus Corporation, Shinjuku, Tokyo, Japan).

Internalization of Seminal Plasma Exosomes by Bone Marrow-Derived Dendritic Cells

sExos were labeled with PKH67 green fluorescent dye and added to BMDCs cultured in glass-bottom chamber slides. After 24 h of incubation, the cells were placed on poly-L-lysine-coated glass coverslips (12 mm) during 20 min at room temperature. Then cells were washed with PBS and fixed in 4% PFA (10 min on ice) and washed twice with 0.1 mM of glycine in PBS. Subsequently, cells were incubated with a mouse anti-CD11c Rabbit pAb (1:100, Servicebio) for 1 h and revealed with TRITC-conjugated goat anti-rabbit IgG (1:100, Abcam) for 45 min. Then BMDCs were stained with Hoechst for 10 min. Coverslips were mounted on glass slides using Fluoromount and visualized with a LSM 710 laser scanning confocal microscope (Carl Zeiss, Oberkochen, Germany).

Statistical Analysis

GraphPad Prism 8 and SPSS v.20 software packages were used for statistical analysis. Data are expressed as mean ± standard error of the mean. Each experiment was performed in triplicate technical and biological replicates. The differences among different groups and between two groups were assessed by one-way ANOVA with the Holm–Sidak post-hoc test and paired-samples t-test, respectively. For all tests, a bilateral test probability of $p < 0.05$ was considered to represent a statistically significant difference.

RESULTS

Embryo Implantation Rate Reduced in Aged-Seminal Plasma Group

In order to determine whether the effects of SP on embryo implantation were related to male age, we constructed two groups of sterilized male models of different age ranges equal to 20–30 and 40–50 years in humans, using embryo transfer to eliminate maternal and gamete factors, as illustrated by the experimental model diagram in **Figure 1A**. Results showed that the implantation rate of the aged-SP group was significantly lower than that of the young-SP group (**Figures 1B, C**), which indicated age-related effects of SP on embryo implantation.

Uterine Transcriptomics Differed Between Young-Seminal Plasma and Aged-Seminal Plasma Groups

To investigate the possible causes of the disparity in implantation rates between the aged-SP and young-SP groups, we analyzed the RNA sequence of 3.0-dpc uteri from both groups. In hierarchical clustering (data not shown), a sample in the young-SP group was identified as an outlier, which laid in its own branch and extended from the very root of the tree. Outliers increase the variability in data, which decreases statistical power. Consequently, we excluded this outlier, and the principal component analysis of five samples finally included is presented in **Supplementary Figure 1**. As gene cluster maps demonstrate, 632 differentially expressed transcripts were identified, among which 296 genes were upregulated and 336 genes were downregulated (**Figures 2A, B**). The results of KEGG pathway analysis based on these genes primarily identified protein digestion and absorption, basal cell carcinoma, ECM–receptor interaction and cytokine–cytokine receptor interaction (**Figure 2C**). Cytokines have been primarily defined as modulators of the immune system, and the balance in their relative abundance has been shown to impact embryo implantation (26). Among 17 genes included in cytokine–cytokine receptor interaction, nine have been previously identified to be involved in DC migration and maturation. Tolerogenic DCs that are resistant to maturation seemed to be involved in the generation of tolerance to the embryos (27). We therefore validated a subset of mRNAs related to DCs in cytokine–cytokine receptor interaction pathway by qRT-PCR (**Figure 2D**). Results from the qPCR analysis of total RNA extracted from 3.0-dpc uteri during the pre-implantation window and prior to embryo transfer identified an increase of *Cxcl1*, *Il20rb*, *Fas*, *Cxcl16*, *Tnfsf10*, and *Cx3cl1* and a decrease of *Eda*, *Ackr4*, and *Il17rb* expression levels in the uteri of the aged-SP group compared with those of the young-SP group, which were inconsistent with the RNA-seq results. When compared with the virgin control, young-SP group and aged-SP group presented different variation trends, which proposed a complex regulation network of SP on uterine immune status. These results indicated that SP from advanced-age males impacts the embryo implantation-related signaling pathways, especially those

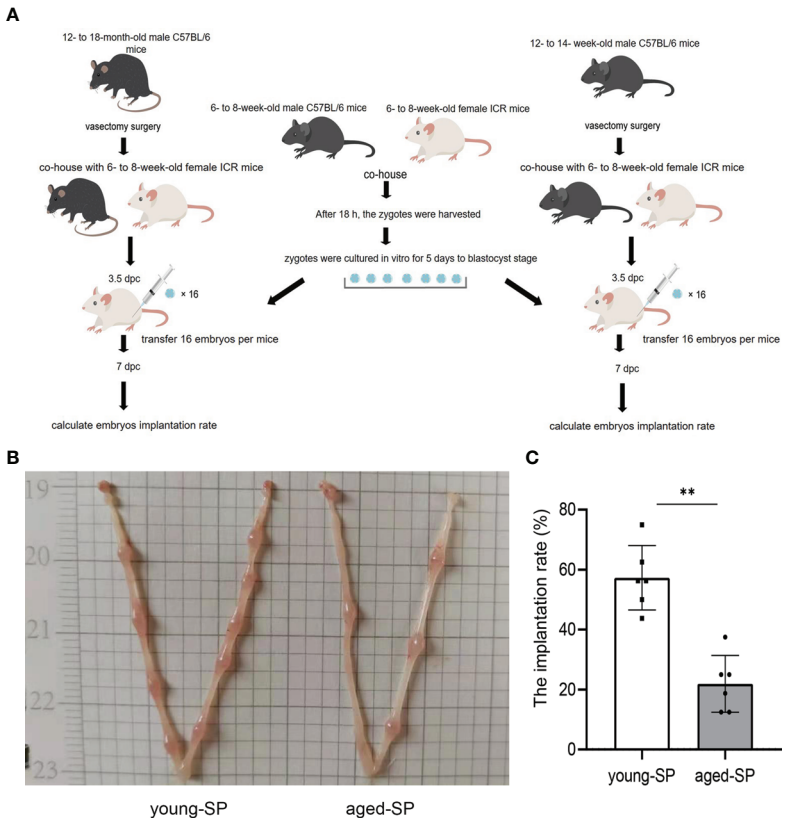

FIGURE 1 | The embryo implantation in the aged-SP group and young-SP group. **(A)** Schematic diagram of experimental design. **(B)** Embryo implantation sites of two groups of recipient female mice on 6.5 dpc. **(C)** Quantitative histogram of embryo implantation rates in two groups of recipient female mice (n = 6). The differences between two groups were assessed by paired-samples t-test. **p < 0.01. The implantation rate (%): the number of implants/number of embryos transferred. SP, seminal plasma; dpc, days post coitum.

involving DC migration and maturation, differently than SP from younger males.

Seminal Plasma Exerted an Inhibitory Effect on Dendritic Cell Maturation, Which Was Attenuated in Advanced Age

To investigate whether DC maturation was involved in the age-related impact of SP on embryo implantation, uterine tissues of young-SP and aged-SP groups were stained with DC maturation markers CD80, CD83, CD86, and MHCII and were visualized. Immunohistology results revealed that both young SP and aged SP could induce DC accumulation in the uteri, while the percentage of mature DCs was higher in aged-SP group than young-SP group (**Figures 3A, B**). Compared with immature phenotype, mature phenotype of DCs produce higher levels of IL-12p70, IL-1b, TNF-a, IL-6, and lower levels of IL-10, TGF-b in response to LPS (19). To further verify whether DC maturation status was altered, uterine luminal fluid in aged-SP and young-SP groups were collected, and ELISA was performed to detect inflammatory cytokines related to DC phenotype (**Figure 3C**). Results showed that the expression profiles of inflammatory cytokines in young-SP group were better aligned with immature DC phenotype than aged-SP group in response to LPS, indicating an inhibitory effect of SP on uterine DC maturation, which was attenuated in the aged-SP group. With emerging evidence showing that SP could impact DC maturation *in vitro*, BMDCs were used as *in vitro* model of DCs to investigate whether a direct impact of SP on DCs existed. CD11c was used to identify BMDCs according to the gating strategy depicted in **Supplementary Figure 2**. Flow cytometry analysis revealed that the expression levels of DC maturation markers CD80, CD83, CD86, and MHCII were higher in the aged-SP group than in the young-SP group (**Figures 4A, B**). In the cell culture supernatant, DC-related inflammatory cytokines presented identical expression profiles as an *in vivo* model (**Figure 4C**). These results indicated that SP exerted an inhibitory effect on DC maturation, which was attenuated in advanced age.

Characterization of Seminal Plasma Exosomes Extracted From Young and Aged Male Mice

sExos have been proposed as the main component of SP to provide immunomodulatory functions in the uterus (21). To investigate whether sExos contribute to the phenotype caused by SP, sExos of the young and aged male groups were extracted, and

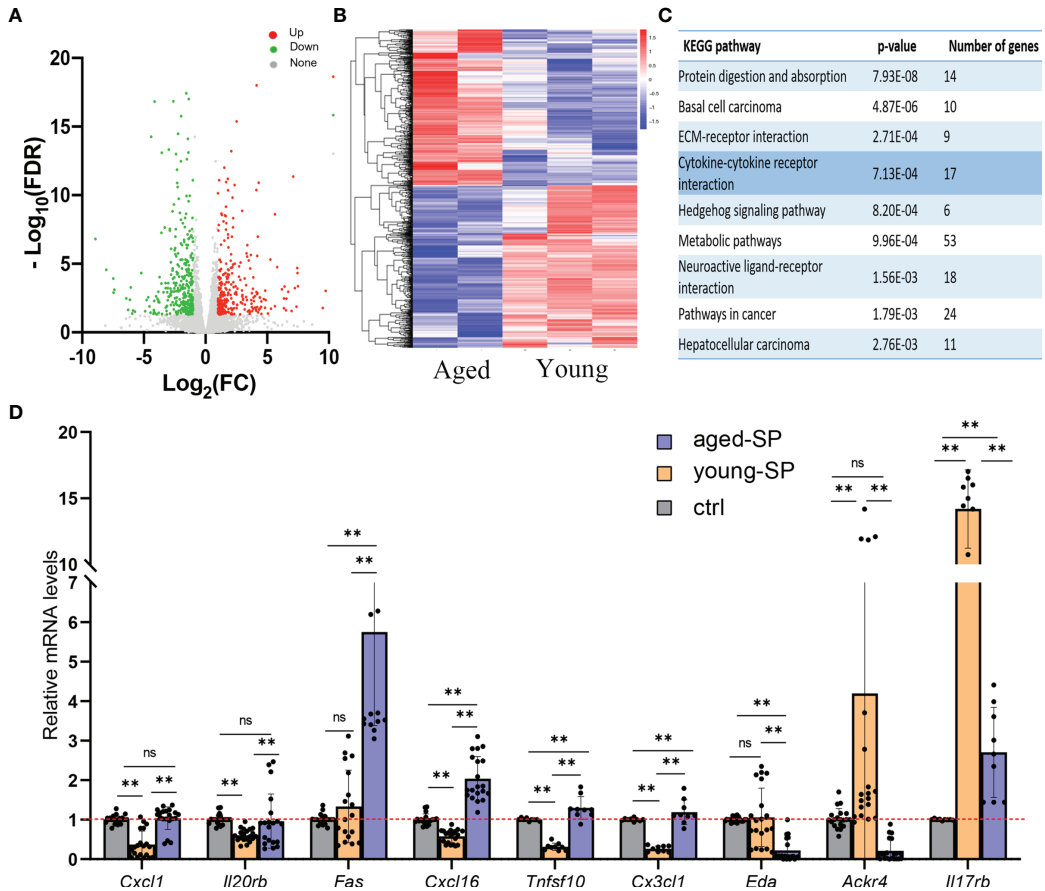

FIGURE 2 | The transcriptomics of the uteri in the young-SP group and aged-SP group. **(A, B)** Volcano map and heatmap depicting clustering and global changes in gene expression for the uterus from aged-SP group and young-SP group as determined by RNA-seq. **(C)** KEGG pathway analysis of transcripts significantly changed. Top nine most highly enriched categories are shown. **(D)** qPCR validation for a subset of genes involved in cytokine–cytokine receptor interaction. *Gapdh* served as an internal control. The differences among different groups were assessed by one-way ANOVA with Holm–Sidak post-hoc test. **p < 0.01. The p-value ≤ 0.05 and FDR q-value ≤ 0.05 were considered as statistically significant. SP, seminal plasma; KEGG, Kyoto Encyclopedia of Genes and Genomes; FDR, false discovery rate; ns, not significant.

further experiments were performed. Western blotting analysis of sExos extracted from young and aged mice verified the presence of universal exosome markers TSG101 and CD63 (**Supplementary Figure 3A**). Further Western blotting analysis of sExos extracted from a single mouse confirmed minor increase without significance in the abundance of sExos with a similar expression level of sExos-positive markers TSG101, CD81, and CD9 in aged group compared with young group (**Figures 5A, B**). Purity was assessed based on the presence of negative marker Albumin, and the results revealed a small amount of Albumin contamination, which were aligned with other literature (28) (**Figures 5A, B**). NTA revealed that the average sExos size of the young and aged groups is, respectively, 102.8 nm and 206.6 nm (**Figures 5C, D**). Transmission electron microscopy analysis verified the presence of separated or clustered membrane-bound particles in the extracted sExos (**Figure 5E**). These results confirmed successful sExos extraction and an increase in the size of sExos from aged male mice.

Intrauterine Perfusion With Young Mouse Seminal Plasma Exosomes Partially Rescued the Decline in Aged-Seminal Plasma Group Embryo Implantation Rate

To further explore whether young mouse sExos have beneficial effects on the decline of aged-SP group embryo implantation rate, remedial experiments were performed. PKH67 immunofluorescence labeling verified sExos entry into the uteri (**Figure 6A**). Further results demonstrated an implantation rate increase in the aged-SP group after perfusion with young sExos (**Figures 6B, C**). Epididymosomes are an important component of the sExos, but in our vasectomized model, epididymosomes would not be present. As such, intrauterine perfusion with epididymosomes extracted from young mice (young epididymosomes) were performed to illustrate whether epididymosomes contributed to the remedial effect of young sExos. Western blotting results confirmed successful extraction of epididymosomes with positive markers CD63, TSG101, and

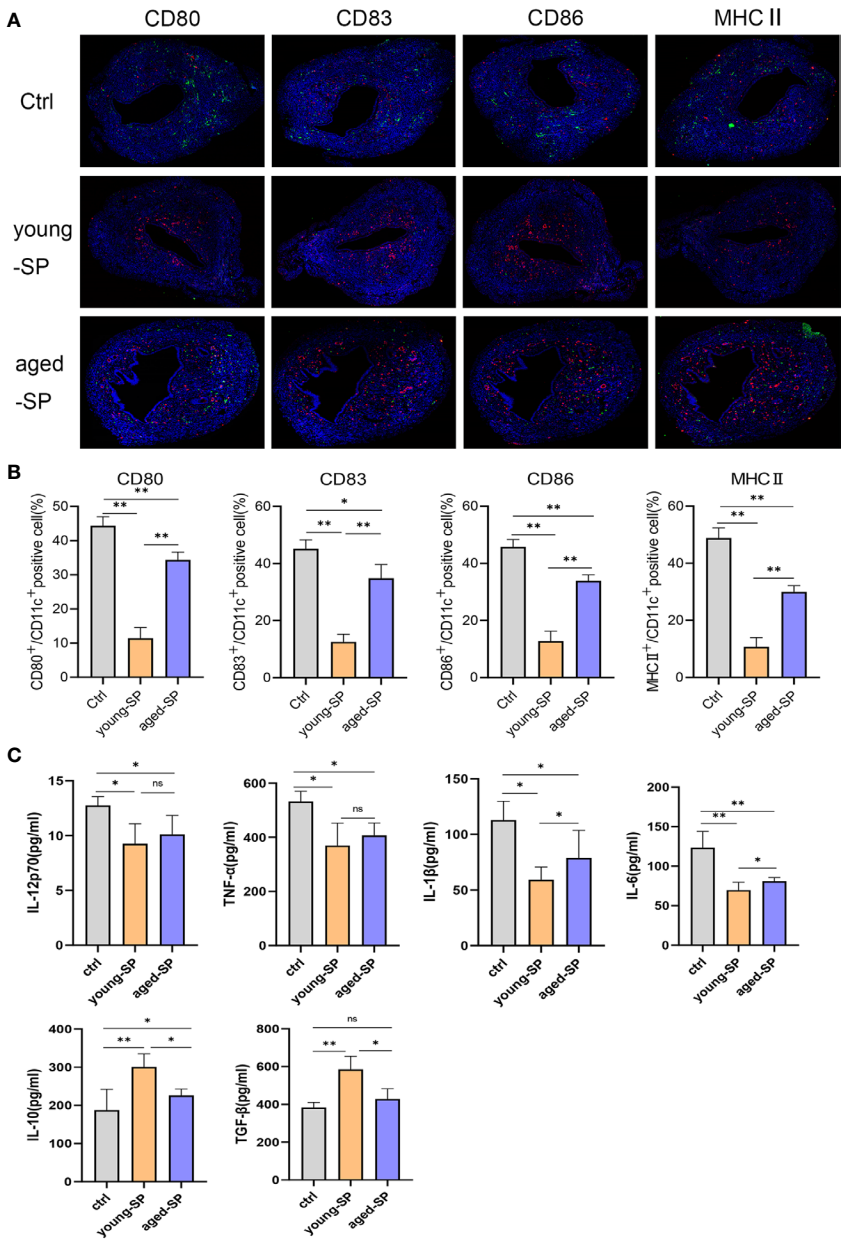

FIGURE 3 | Alterations of uterine DC maturation status between young-SP group and aged-SP group *in vivo*. **(A)** Representative sections of the uteri from control group, young-SP group, and aged-SP group mice, immunostained with anti-CD11c (red) and anti-CD80/CD83/CD86/MHCII (green) antibodies. **(B)** Histomorphometric quantification of DC densities in the myometrium and endometrium of control group, young-SP group, and aged-SP group mice. **(C)** ELISA analysis demonstrating the concentration of IL-12p70, TNF-α, IL-1β, IL-10, TGF-β, and IL-6 in uterine luminal fluid (mean ± SD, n = 6).The differences among different groups were assessed by one-way ANOVA with Holm–Sidak post-hoc test. *p < 0.05 and **p < 0.01. DC, dendritic cell; SP, seminal plasma; ns, not significant.

CD9 and negative marker Albumin (**Supplementary Figure 3B**), while no beneficial impact on declined implantation rate in aged-SP group was observed after exerting young epididymosomes (**Figures 6B, C**). These results revealed the beneficial effect of sExos excluding epididymosomes of young subjects on declined embryo implantation rate in aged-SP group.

Seminal Plasma Exosomes Exerted an Inhibitory Effect on Dendritic Cell Maturation, Which Was Attenuated in Advanced Age

For the purpose of investigating whether sExos participate in SP-related alterations of DC maturation, sExos extracted from young and aged male mice were perfused into the uteri of the virgin

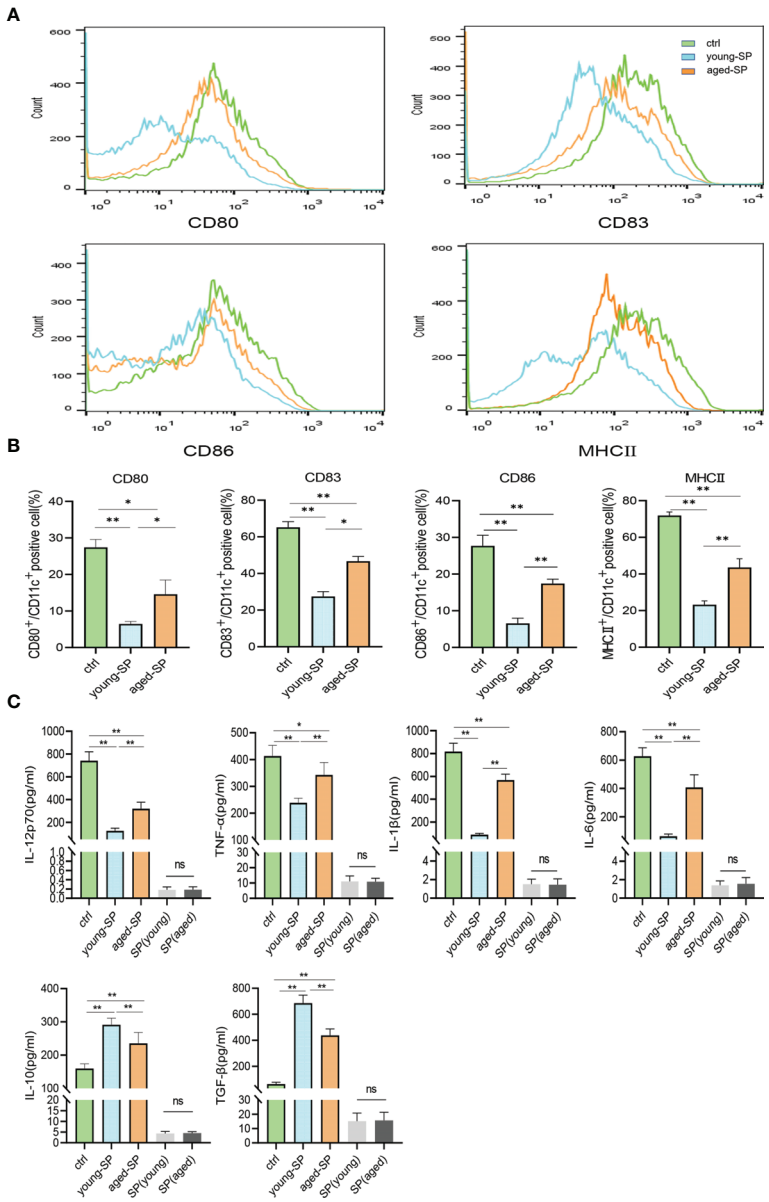

FIGURE 4 | Alterations of BMDC maturation status between young-SP group and aged-SP group *in vitro*. **(A)** Fluorescence-activated cell sorting (FACS) analysis of CD80, CD83, CD86, and MHCII in culture supernatant. The x-axis represents the fluorescence intensity, and the y-axis represents the percentage of positive cells. **(B)** Quantification of CD11c+ CD80+ DC, CD11c+ CD83+ DC, CD11c+ CD86+ DC, CD11c+ MHCII+ DC positive cells as seen in panel A (mean ± SD, n = 6). **(C)** ELISA analysis demonstrating the concentration of IL-12p70, TNF-α, IL-1β, IL-10, TGF-β, and IL-6 in the culture supernatant (mean ± SD, n = 6). The differences among different groups were assessed by one-way ANOVA with Holm–Sidak post-hoc test. *p < 0.05 and **p < 0.01. BMDC, marrow-derived dendritic cell; SP, seminal plasma; DC, dendritic cell; ns, not significant.

female mice. Uterine immunohistology with DC maturation markers demonstrated higher percentage of mature DCs after perfusing aged sExos than young sExos (**Figures 7A, B**). Uterine luminal fluid was also collected to detect inflammatory cytokines related to DC phenotype. An increase of IL-6 and a decrease of IL-10 and TGF-β were observed in aged-sExos group compared with young-sExos group (**Figure 7C**). Although no statistic difference was observed regarding IL-12p70, TNF-α, and IL-1β levels, they all increased in aged-sExos group compared with young-sExos group. Further *in vitro* experiments performed to determine whether aged sExos exerted a similar effect on DC maturation as aged SP revealed higher levels of maturation markers CD80, CD86, and MHCII on the surfaces of aged-sExos-treated group DC (**Figures 8A, B**). ELISA analysis of the cell culture supernatant obtained similar results as uterine luminal fluid, which further verified that aged sExos had a weaker inhibitory effect on LPS-induced DC maturation than young sExos (**Figure 8C**). Increased sExos size may be associated with alterations in sExos composition

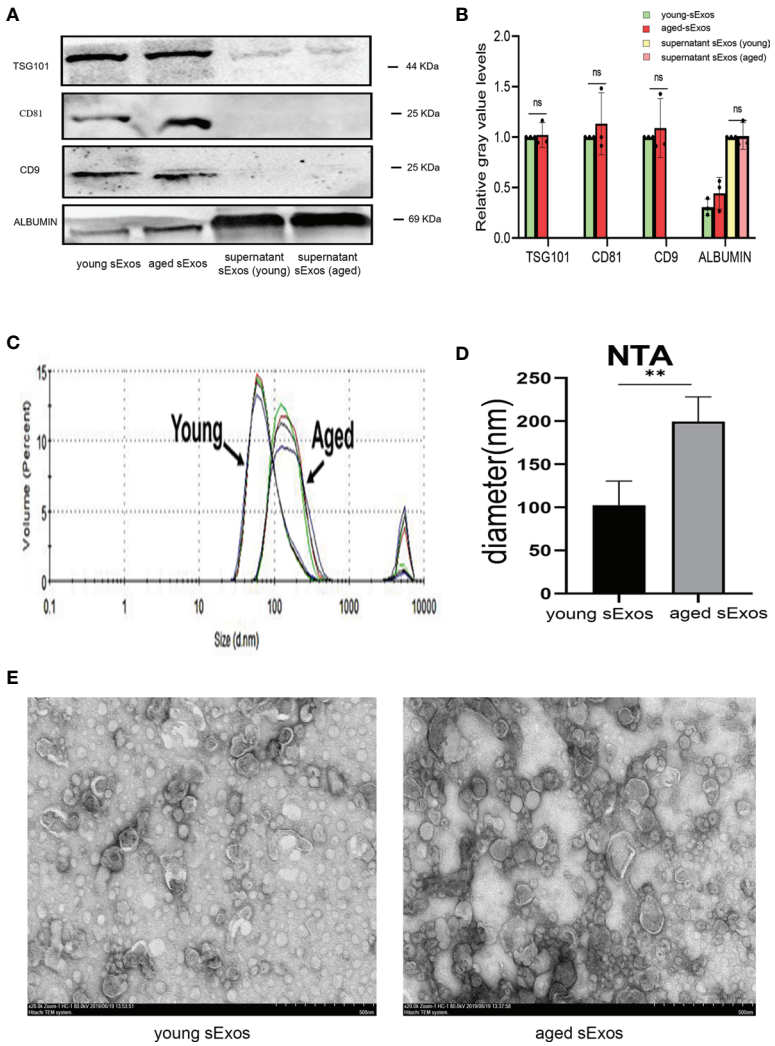

FIGURE 5 | Characterization of sExos extracted from young and aged male mice. **(A)** Western blotting analysis on sExos using antibodies against the positive markers (TSG101, CD81, and CD9) and negative marker Albumin after BCA (Bradford) protein quantification assay. **(B)** Quantification of band intensity as seen in panel **(A, C)** Representative particle size distribution diagrams of sExos from two groups of mice as determined by nanoparticle tracking analysis. **(D)** Quantification of panel C (mean ± SD, n = 6). **(E)** TEM images of sExos isolated from young and aged male mice. Bar = 500 μm. The differences between two groups were assessed by paired-samples t-test. **p < 0.01. sExos, seminal plasma exosomes; BCA, bicinchoninic acid; TEM, transmission electron microscopy; BMDC, marrow-derived dendritic cell; SP, seminal plasma; DC, dendritic cell; ns, not significant.

or internalization ability. Regarding the internalization rate by DCs, no significant difference was found between young-sExos and aged-sExos groups (**Supplementary Figure 4**), which indicated an age-related effect of sExos may be associated with alterations in sExos composition. These results showed that aged sExos acted as main components of aged SP in affecting DC maturation.

DISCUSSION

Function decline in aging semen has been recently identified as another factor besides spermatozoa causing age-related decline in male fertility (29). Emerging evidence has revealed the role of SP in regulating the uterine and fallopian tube environment, thereby enhancing embryo implantation and development (30, 31). Such regulation includes induction of uterine cytokine expression, leading to immune regulation on the uterus of mice (32) and humans (21). The immune cell migration was once believed to be intended for removal of microorganisms and excess sperm (14, 18). However, the SP-induced influx of uterine cytokines and chemokines is now believed to promote maternal tolerance of paternal antigens. T cell-activating macrophages and DCs are recruited into uterine tissue in response to semen-induced cytokine and chemokine signals (33). An article published recently verified migration of uDCs from the periphery just before implantation (20). Their data also showed an increase of immature uDCs on day 3.5 pc, which support the concept that immature DCs may participate in embryo implantation *via*

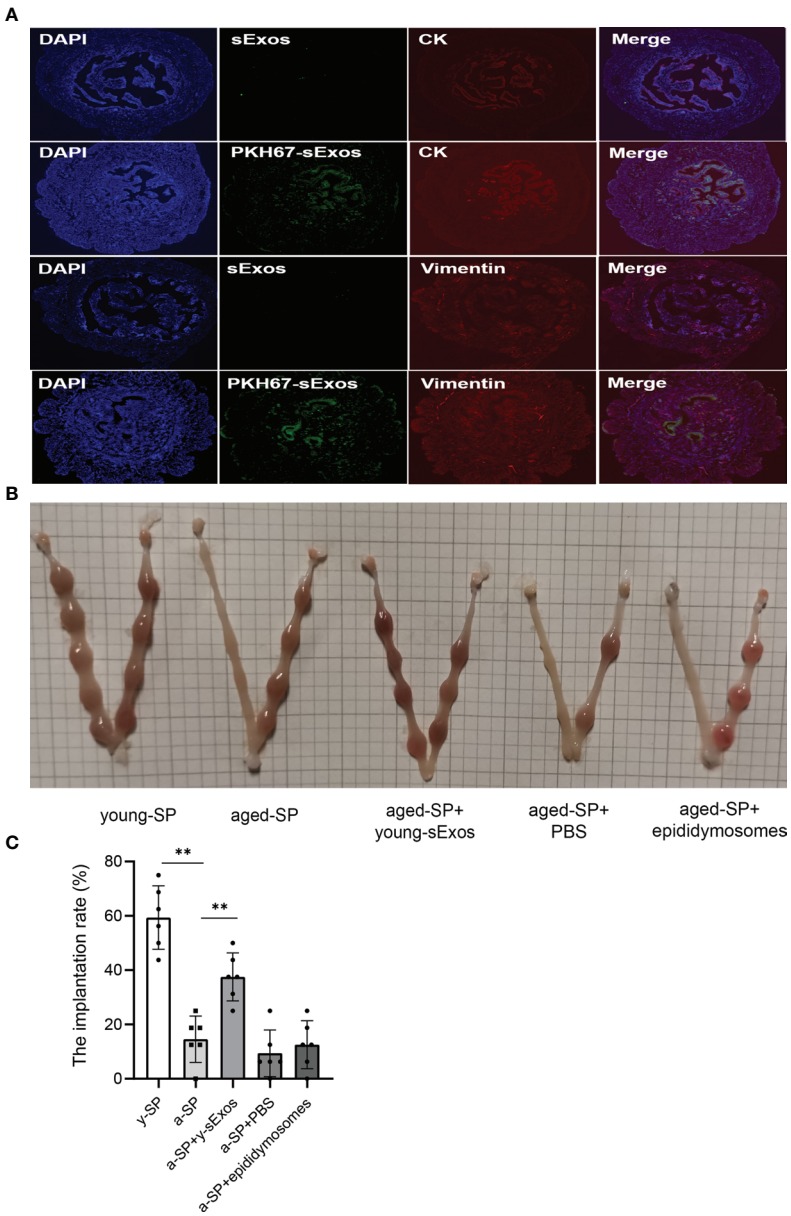

FIGURE 6 | The increase of embryo implantation rate after perfusion with young sExos in the aged-SP group. **(A)** Immunofluorescence staining of the uteri after perfusion with sExos from young male mice. Red fluorescence shows antibody reactivity against Vimentin and Cytokeratin 19, green fluorescence shows PKH67-labeled sExos, and blue fluorescence shows nuclear DAPI reactivity (magnification, ×200). **(B)** Embryo implantation sites of young-SP, aged-SP, aged-SP+young-sExos, aged-SP+PBS, and aged-SP+epididymosomes group female mice on 6.5 dpc. **(C)** Quantitative histogram of the embryo implantation rates in five groups of recipient female mice as seen in panel B (mean ± SD, n = 6).The differences among different groups were assessed by one-way ANOVA with Holm–Sidak post-hoc test. **p < 0.01. sExos, seminal plasma exosomes; SP, seminal plasma; PBS, phosphate-buffered saline; dpc, days post coitum.

regulating fetal–maternal tolerance (34). Numerous studies have revealed an age-related decline in embryo implantation rate, largely mediated by uterine cytokines and chemokine inducement (15, 29, 35). In our results, we found an age-related effect of SP on embryo implantation, accompanied by alterations in uterine cytokines, which may be responsible for the migration or maturation of DCs (36, 37). GM-CSF-derived BMDCs have been used as a model to study DC biology in countless studies. It has generally been thought that non-DCs can be eliminated by early washing steps, discarding highly adherent cells and enriching or sorting for CD11c+ cells. However, recent studies reckon that CD11c+ fraction of GM-CSF cultures comprises macrophages and DCs (38, 39). In our study, we found alterations in DC maturation markers and changes in cytokines involved in successful implantation, which were not specifically secreted by DCs, with emerging evidences verifying their

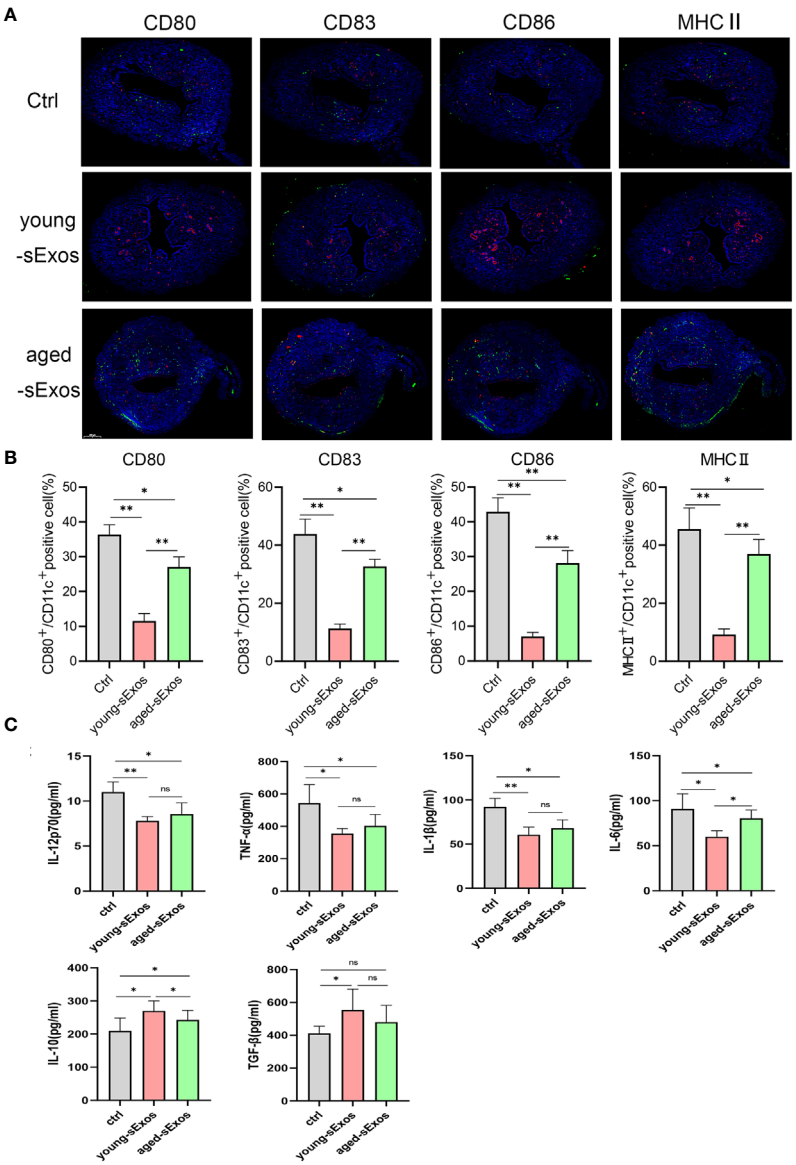

FIGURE 7 | Alterations of uterine DC maturation status between young-sExos group and aged-sExos group *in vivo*. **(A)** Representative sections of the uteri from control group, young-sExos group, and aged-sExos group mice, immunostained with anti-CD11c (red) and anti-CD80/CD83/CD86/MHCII (green) antibodies. **(B)** Histomorphometric quantification of DC densities in the myometrium and endometrium of control group, young-sExos group, and aged-sExos group mice. **(C)** ELISA analysis demonstrating the concentration of IL-12p70, TNF-α, IL-1β, IL-10, TGF-β, and IL-6 in uterine luminal fluid (mean ± SD, n = 6). The differences among different groups were assessed by one-way ANOVA with Holm–Sidak post-hoc test. *p < 0.05 and **p < 0.01. DC, dendritic cell; sExos, seminal plasma exosomes; ns, not significant.

expressions in both DCs and macrophages (39). Therefore, we assumed that the effects observed after various treatments in BMDCs could be mainly attributed to macrophages and DCs, or even CD11c− cells were included. Although we cannot conclude that alterations were mediated by DCs alone, our data do strongly suggest that DCs are at least largely involved. Tolerogenic DCs seemed to be involved in the generation of tolerance to the embryos (27). A previous study showed that DCs tend to differentiate into tolerogenic DCs, which failed to develop a mature phenotype in response to LPS in the presence of SP (19). Our *in vivo* and *in vitro* results confirmed alterations of DC maturation status between young-SP and aged-SP groups, which indicated that the lower implantation rate observed in the aged-SP group may be associated with the diminished inhibitory effect of aged SP on DC maturation.

Semen contains sperm, testosterone (40), soluble proteins—such as TGF-β and interferon-γ (41)—that can interact with cells in the female reproductive tract, and abundant levels of sExos (42), which are mainly secreted from the prostate, and seminal vesicles (43). We successfully isolated and characterized mouse sExos with the presence of positive markers. It has been demonstrated that senescent cells release more Exos with

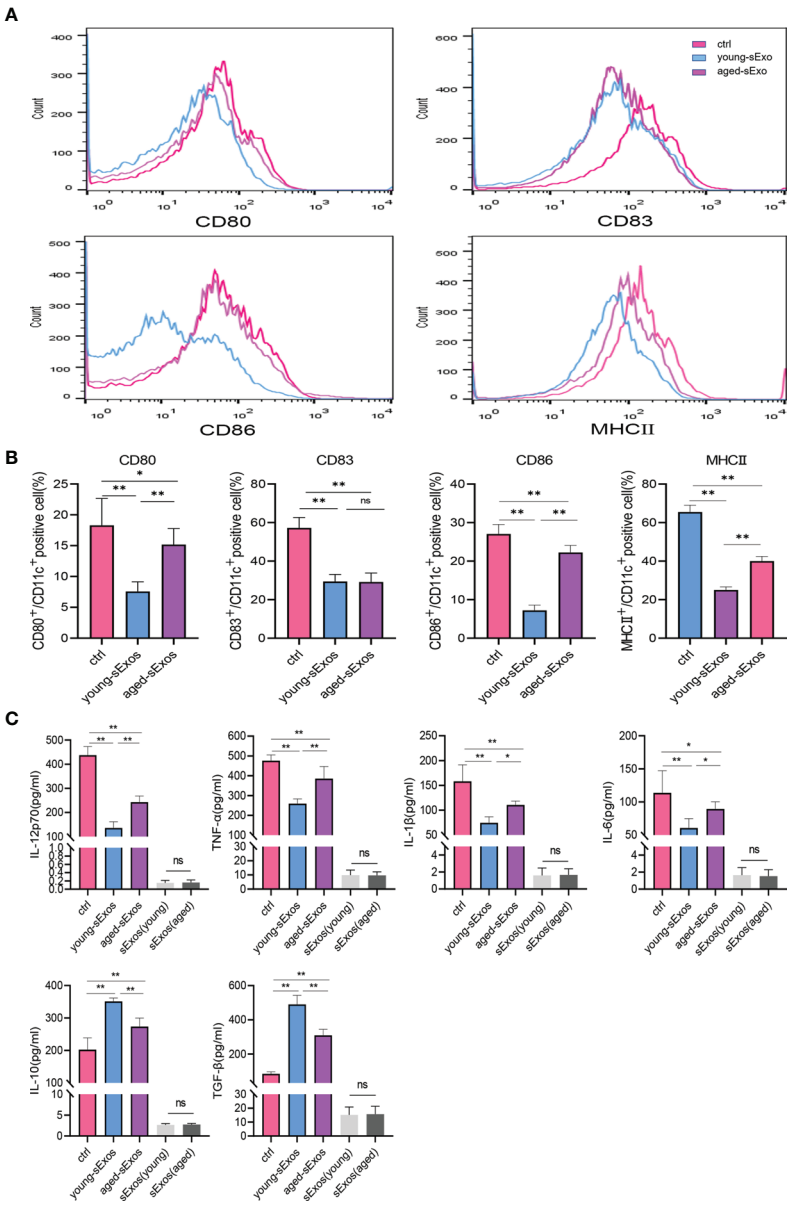

FIGURE 8 | Alterations of BMDC maturation status between young-sExos group and aged-sExos group *in vitro*. **(A)** Fluorescence-activated cell sorting (FACS) analysis of CD80, CD83, CD86, and MHCII in culture supernatant. The x-axis represents the fluorescence intensity, and the y-axis represents the percentage of positive cells. **(B)** Quantification of CD11c+ CD80+ DC, CD11c+ CD83+ DC, CD11c+ CD86+ DC, CD11c+ MHCII+ DC positive cells as seen in panel A (mean ± SD, n = 6). **(C)** ELISA analysis demonstrating the concentration of IL-12p70, TNF-α, IL-1β, IL-10, TGF-β, and IL-6 in the culture supernatant (mean ± SD, n = 6). The differences among different groups were assessed by one-way ANOVA with Holm–Sidak post-hoc test. *p < 0.05 and **p < 0.01. BMDC, marrow-derived dendritic cell; sExos, seminal plasma exosomes; ns, not significant.

different compositions, likely contributing to the SASP (44). No significant difference between young and aged groups was observed regarding the quantity of sExos, which indicated that different phenotypes caused by sExos may be more associated with their composition than quantity. NTA analysis revealed that sExos from the advanced-age group exhibited increased size, consistent with senescent mesenchymal stem cells Exos (45). Increased sExos size may be associated with alterations in sExos composition or internalization ability. With no difference observed in the internalization rate, we hypothesized that there might be age-related changes in the sExos composition. Related research has confirmed that sExos can regulate the immune response and gene expression in the female reproductive tract (11, 46, 47), eventually contributing to embryo implantation and gestation. In our results, young sExos partially recovered the declined implantation rate in the aged-SP group, indicating that

sExos may contribute to the age-related changes of SP. Zhao et al. demonstrated that sExos secreted by 5-aminolevulinic acid photodynamic therapy-treated squamous carcinoma cells can promote DC maturation to exert an anti-tumor immunity function (48). We found that aged sExos exerted a similar effect on DC maturation to aged SP. The current debate over the clinical benefits of sexual intercourse or intrauterine SP perfusion prior to embryo transfer (49–51) has not considered physiological and pathological conditions such as male age. Uterine response intensity and quality are affected by semen composition, including antigen and immunomodulatory adjuvant content. The alteration of SP components under various physiological and pathological conditions may be an immune-mediated quality control process signal to the female reproductive tract (52), leading to different pregnancy and birth outcomes. SP from advanced-age subjects presented no obvious benefits in our study, suggesting that male age should factor into seminal adjuvant therapy.

In conclusion, our study demonstrates that age-related alterations of sExos may be partially responsible for lower implantation rates in the aged-SP group compared with those in the young-SP group, which were mediated by uterine immune status changes. These findings provide new insight and scientific basis for future clinical seminal adjuvant therapy.

DATA AVAILABILITY STATEMENT

The RNA sequencing data associated with this study are publicly available in NCBI (GEO) under the accession number GSE180444.

ETHICS STATEMENT

The animal study was reviewed and approved by The Animal Protection and Use Committee of Jinling Hospital.

AUTHOR CONTRIBUTIONS

BY and XC: study design and final version of manuscript approval. YW, RM ,YL and XL: data acquisition. JM, TX, SC and JJ: data analysis and interpretation. DW KJ and TT: drafting manuscript, performing experiments and responsible for the integrity of the data analysis. All authors contributed to the article and approved the submitted version.

FUNDING

This work was supported by the National Key Research and Development Program of China (2018YFC1004700) and National Natural Science Foundation of China (81971373).

ACKNOWLEDGMENTS

The authors would like to thank Dr. Li Chen for excellent technical support and critically reviewing the manuscript.

SUPPLEMENTARY MATERIAL

The Supplementary Material for this article can be found online at: https://www.frontiersin.org/articles/10.3389/fimmu.2021.723409/full#supplementary-material

Supplementary Figure 1 | Principal component analysis of 5 samples finally included in RNAsequence analysis. Red dots represent female mice in aged-SP group, and green dots represent female mice in young-SP group.

Supplementary Figure 2 | Gating strategy of BMDCs.

Supplementary Figure 3 | Western blotting analysis of sExos and epididymosomes. **(A)** Western blotting analysis on sExos using antibodies against positive exosomal markers (CD63 and TSG101). From left to right: sExos extracted from young male mice; sExos extracted from aged male mice; **(B)** Western blotting analysis on epididymosomes using antibodies against the positive markers (TSG101,CD63 and CD9) and negative marker Albumin after BCA (Bradford) protein quantification assay. From left to right: epididymosomes extracted from young male mice, epididymosomes extracted from aged male mice, remaining supernatant after isolating epididymosomes from young male mice, and remaining supernatant after isolating epididymosomes from aged male mice.

Supplementary Figure 4 | Internalization of sExos by BMDCs Immunofluorescence staining of BMDCs after cultured with sExos from young male mice **(A)** and aged male mice **(B)**. Red fluorescence shows antibody against CD11c, green fluorescence shows PKH67 labeled sExos and blue fluorescence shows nuclear (magnification, ×40). **(C)** Quantification of PKH67 positive CD11c+ cells. The differences between two groups were assessed by paired samples t-test, *P < 0.05 and **P < 0.01. (n=150).

REFERENCES

1. Green RF, Devine O, Crider KS, Olney RS, Archer N, Olshan AF, et al. Association of Paternal Age and Risk for Major Congenital Anomalies From the National Birth Defects Prevention Study, 1997 to 2004. *Ann Epidemiol* (2010) 20(3):241–9. doi: 10.1016/j.annepidem.2009.10.009
2. Kühnert B, Nieschlag E. Reproductive Functions of the Ageing Male. *Hum Reprod Update* (2004) 10(4):327–39. doi: 10.1093/humupd/dmh030
3. Sartorius GA, Nieschlag E. Paternal Age and Reproduction. *Hum Reprod Update* (2010) 16(1):65–79. doi: 10.1093/humupd/dmp027
4. Sharma R, Agarwal A, Rohra VK, Assidi M, Abu-Elmagd M, Turki RF. Effects of Increased Paternal Age on Sperm Quality, Reproductive Outcome and Associated Epigenetic Risks to Offspring. *Reprod Biol Endocrinol* (2015) 13:35. doi: 10.1186/s12958-015-0028-x
5. Chung HY, Sung B, Jung KJ, Zou Y, Yu BP. The Molecular Inflammatory Process in Aging. *Antioxid Redox Signal* (2006) 8(3-4):572–81. doi: 10.1089/ars.2006.8.572
6. Coppé JP, Desprez PY, Krtolica A, Campisi J. The Senescence-Associated Secretory Phenotype: The Dark Side of Tumor Suppression. *Annu Rev Pathol* (2010) 5:99–118. doi: 10.1146/annurev-pathol-121808-102144
7. Carracedo J, Alique M, Ramírez-Carracedo R, Bodega G, Ramírez R. Endothelial Extracellular Vesicles Produced by Senescent Cells: Pathophysiological Role in the Cardiovascular Disease Associated With All Types of Diabetes Mellitus. *Curr Vasc Pharmacol* (2019) 17(5):447–54. doi: 10.2174/1570161116666180820115726

8. Sidhom K, Obi PO, Saleem A. A Review of Exosomal Isolation Methods: Is Size Exclusion Chromatography the Best Option? *Int J Mol Sci* (2020) 21 (18):6466. doi: 10.3390/ijms21186466
9. Kreger BT, Dougherty AL, Greene KS, Cerione RA, Antonyak MA. Microvesicle Cargo and Function Changes Upon Induction of Cellular Transformation. *J Biol Chem* (2016) 291(38):19774–85. doi: 10.1074/jbc.M116.725705
10. Saito S, Shima T, Nakashima A, Inada K, Yoshino O. Role of Paternal Antigen-Specific Treg Cells in Successful Implantation. *Am J Reprod Immunol* (2016) 75(3):310–6. doi: 10.1111/aji.12469
11. Robertson SA, Sharkey DJ. Seminal Fluid and Fertility in Women. *Fertil Steril* (2016) 106(3):511–9. doi: 10.1016/j.fertnstert.2016.07.1101
12. Song ZH, Li ZY, Li DD, Fang WN, Liu HY, Yang DD, et al. Seminal Plasma Induces Inflammation in the Uterus Through the γδ T/IL-17 Pathway. *Sci Rep* (2016) 6:25118. doi: 10.1038/srep25118
13. Sharkey DJ, Tremellen KP, Jasper MJ, Gemzell-Danielsson K, Robertson SA. Seminal Fluid Induces Leukocyte Recruitment and Cytokine and Chemokine mRNA Expression in the Human Cervix After Coitus. *J Immunol* (2012) 188 (5):2445–54. doi: 10.4049/jimmunol.1102736
14. Thompson LA, Barratt CL, Bolton AE, Cooke ID. The Leukocytic Reaction of the Human Uterine Cervix. *Am J Reprod Immunol* (1992) 28(2):85–9. doi: 10.1111/j.1600-0897.1992.tb00765.x
15. Sharkey DJ, Macpherson AM, Tremellen KP, Robertson SA. Seminal Plasma Differentially Regulates Inflammatory Cytokine Gene Expression in Human Cervical and Vaginal Epithelial Cells. *Mol Hum Reprod* (2007) 13(7):491–501. doi: 10.1093/molehr/gam028
16. Joseph T, Zalenskaya IA, Sawyer LC, Chandra N, Doncel GF. Seminal Plasma Induces Prostaglandin-Endoperoxide Synthase (PTGS) 2 Expression in Immortalized Human Vaginal Cells: Involvement of Semen Prostaglandin E2 in PTGS2 Upregulation. *Biol Reprod* (2013) 88(1):13. doi: 10.1095/biolreprod.112.101956
17. Berlier W, Cremel M, Hamzeh H, Lévy R, Lucht F, Bourlet T, et al. Seminal Plasma Promotes the Attraction of Langerhans Cells *via* the Secretion of CCL20 by Vaginal Epithelial Cells: Involvement in the Sexual Transmission of HIV. *Hum Reprod* (2006) 21(5):1135–42. doi: 10.1093/humrep/dei496
18. Pandya IJ, Cohen J. The Leukocytic Reaction of the Human Uterine Cervix to Spermatozoa. *Fertil Steril* (1985) 43(3):417–21. doi: 10.1016/s0015-0282(16)48442-6
19. Remes Lenicov F, Rodriguez Rodrigues C, Sabatté J, Cabrini M, Jancic C, Ostrowski M, et al. Semen Promotes the Differentiation of Tolerogenic Dendritic Cells. *J Immunol* (2012) 189(10):4777–86. doi: 10.4049/jimmunol.1202089
20. Yasuda I, Shima T, Moriya T, Ikebuchi R, Kusumoto Y, Ushijima A, et al. Dynamic Changes in the Phenotype of Dendritic Cells in the Uterus and Uterine Draining Lymph Nodes After Coitus. *Front Immunol* (2020) 11:557720. doi: 10.3389/fimmu.2020.557720
21. Paktinat S, Hashemi SM, Ghaffari Novin M, Mohammadi-Yeganeh S, Salehpour S, Karamian A, et al. Seminal Exosomes Induce Interleukin-6 and Interleukin-8 Secretion by Human Endometrial Stromal Cells. *Eur J Obstet Gynecol Reprod Biol* (2019) 235:71–6. doi: 10.1016/j.ejogrb.2019.02.010
22. Bermejo-Alvarez P, Park KE, Telugu BP. Utero-Tubal Embryo Transfer and Vasectomy in the Mouse Model. *J Vis Exp* (2014) 84):e51214. doi: 10.3791/51214
23. Caligioni CS. Assessing Reproductive Status/Stages in Mice. *Curr Protoc Neurosci* (2009) Appendix 4:Appendix 4I. doi: 10.1002/0471142301.nsa04is48
24. Lin Y, Sui LC, Wu RH, Ma RJ, Fu HY, Xu JJ, et al. Nrf2 Inhibition Affects Cell Cycle Progression During Early Mouse Embryo Development. *J Reprod Dev* (2018) 64(1):49–55. doi: 10.1262/jrd.2017-042
25. Gu AQ, Li DD, Wei DP, Liu YQ, Ji WH, Yang Y, et al. Cytochrome P450 26A1 Modulates Uterine Dendritic Cells in Mice Early Pregnancy. *J Cell Mol Med* (2019) 23(8):5403–14. doi: 10.1111/jcmm.14423
26. Robertson NJ, Brook FA, Gardner RL, Cobbold SP, Waldmann H, Fairchild PJ. Embryonic Stem Cell-Derived Tissues are Immunogenic But Their Inherent Immune Privilege Promotes the Induction of Tolerance. *Proc Natl Acad Sci USA* (2007) 104(52):20920–5. doi: 10.1073/pnas.0710265105
27. Samstein RM, Josefowicz SZ, Arvey A, Treuting PM, Rudensky AY. Extrathymic Generation of Regulatory T Cells in Placental Mammals Mitigates Maternal-Fetal Conflict. *Cell* (2012) 150(1):29–38. doi: 10.1016/j.cell.2012.05.031
28. Baranyai T, Herczeg K, Onódi Z, Voszka I, Módos K, Marton N, et al. Isolation of Exosomes From Blood Plasma: Qualitative and Quantitative Comparison of Ultracentrifugation and Size Exclusion Chromatography Methods. *PloS One* (2015) 10(12):e0145686. doi: 10.1371/journal.pone.0145686
29. Johnson SL, Dunleavy J, Gemmell NJ, Nakagawa S. Consistent Age-Dependent Declines in Human Semen Quality: A Systematic Review and Meta-Analysis. *Ageing Res Rev* (2015) 19:22–33. doi: 10.1016/j.arr.2014.10.007
30. Bromfield JJ. A Role for Seminal Plasma in Modulating Pregnancy Outcomes in Domestic Species. *Reproduction* (2016) 152(6):R223–r232. doi: 10.1530/rep-16-0313
31. Morgan HL, Watkins AJ. The Influence of Seminal Plasma on Offspring Development and Health. *Semin Cell Dev Biol* (2020) 97:131–7. doi: 10.1016/j.semcdb.2019.06.008
32. Schjenken JE, Glynn DJ, Sharkey DJ, Robertson SA. TLR4 Signaling Is a Major Mediator of the Female Tract Response to Seminal Fluid in Mice. *Biol Reprod* (2015) 93(3):68. doi: 10.1095/biolreprod.114.125740
33. Moldenhauer LM, Diener KR, Thring DM, Brown MP, Hayball JD, Robertson SA. Cross-Presentation of Male Seminal Fluid Antigens Elicits T Cell Activation to Initiate the Female Immune Response to Pregnancy. *J Immunol* (2009) 182(12):8080–93. doi: 10.4049/jimmunol.0804018
34. Blois SM, Ilarregui JM, Tometten M, Garcia M, Orsal AS, Cordo-Russo R, et al. A Pivotal Role for Galectin-1 in Fetomaternal Tolerance. *Nat Med* (2007) 13(12):1450–7. doi: 10.1038/nm1680
35. Ibrahim LA, Rizo JA, Fontes PLP, Lamb GC, Bromfield JJ. Seminal Plasma Modulates Expression of Endometrial Inflammatory Meditators in the Bovine†. *Biol Reprod* (2019) 100(3):660–71. doi: 10.1093/biolre/ioy226
36. Blanco P, Palucka AK, Pascual V, Banchereau J. Dendritic Cells and Cytokines in Human Inflammatory and Autoimmune Diseases. *Cytokine Growth Factor Rev* (2008) 19(1):41–52. doi: 10.1016/j.cytogfr.2007.10.004
37. Majumdar A, Capetillo-Zarate E, Cruz D, Gouras GK, Maxfield FR. Degradation of Alzheimer's Amyloid Fibrils by Microglia Requires Delivery of ClC-7 to Lysosomes. *Mol Biol Cell* (2011) 22(10):1664–76. doi: 10.1091/mbc.E10-09-0745
38. Helft J, Böttcher J, Chakravarty P, Zelenay S, Huotari J, Schraml BU, et al. GM-CSF Mouse Bone Marrow Cultures Comprise a Heterogeneous Population of CD11c(+)MHCII(+) Macrophages and Dendritic Cells. *Immunity* (2015) 42(6):1197–211. doi: 10.1016/j.immuni.2015.05.018
39. Erlich Z, Shlomovitz I, Edry-Botzer L, Cohen H, Frank D, Wang H, et al. Macrophages, Rather Than DCs, are Responsible for Inflammasome Activity in the GM-CSF BMDC Model. *Nat Immunol* (2019) 20: (4):397–406. doi: 10.1038/s41590-019-0313-5
40. Narukawa S, Kanzaki H, Inoue T, Imai K, Higuchi T, Hatayama H, et al. Androgens Induce Prolactin Production by Human Endometrial Stromal Cells *In Vitro*. *J Clin Endocrinol Metab* (1994) 78(1):165–8. doi: 10.1210/jcem.78.1.8288699
41. Bromfield JJ. Seminal Fluid and Reproduction: Much More Than Previously Thought. *J Assist Reprod Genet* (2014) 31(6):627–36. doi: 10.1007/s10815-014-0243-y
42. Vojtech L, Woo S, Hughes S, Levy C, Ballweber L, Sauteraud RP, et al. Exosomes in Human Semen Carry a Distinctive Repertoire of Small non-Coding RNAs With Potential Regulatory Functions. *Nucleic Acids Res* (2014) 42(11):7290–304. doi: 10.1093/nar/gku347
43. Rolland AD, Lavigne R, Dauly C, Calvel P, Kervarrec C, Freour T, et al. Identification of Genital Tract Markers in the Human Seminal Plasma Using an Integrative Genomics Approach. *Hum Reprod* (2013) 28(1):199–209. doi: 10.1093/humrep/des360
44. Olivieri F, Albertini MC, Orciani M, Ceka A, Cricca M, Procopio AD, et al. DNA Damage Response (DDR) and Senescence: Shuttled inflamma-miRNAs on the Stage of Inflamm-Aging. *Oncotarget* (2015) 6(34):35509–21. doi: 10.18632/oncotarget.5899
45. Sun L, Zhu W, Zhao P, Zhang J, Lu Y, Zhu Y, et al. Down-Regulated Exosomal MicroRNA-221 - 3p Derived From Senescent Mesenchymal Stem Cells Impairs Heart Repair. *Front Cell Dev Biol* (2020) 8:263. doi: 10.3389/fcell.2020.00263

46. Bai R, Latifi Z, Kusama K, Nakamura K, Shimada M, Imakawa K. Induction of Immune-Related Gene Expression by Seminal Exosomes in the Porcine Endometrium. *Biochem Biophys Res Commun* (2018) 495(1):1094–101. doi: 10.1016/j.bbrc.2017.11.100
47. George AF, Jang KS, Nyegaard M, Neidleman J, Spitzer TL, Xie G, et al. Seminal Plasma Promotes Decidualization of Endometrial Stromal Fibroblasts *In Vitro* From Women With and Without Inflammatory Disorders in a Manner Dependent on Interleukin-11 Signaling. *Hum Reprod* (2020) 35 (3):617–40. doi: 10.1093/humrep/deaa015
48. Zhao Z, Zhang H, Zeng Q, Wang P, Zhang G, Ji J, et al. Exosomes From 5-Aminolevulinic Acid Photodynamic Therapy-Treated Squamous Carcinoma Cells Promote Dendritic Cell Maturation. *Photodiagn Photodyn Ther* (2020) 30:101746. doi: 10.1016/j.pdpdt.2020.101746
49. Chicea R, Ispasoiu F, Focsa M. Seminal Plasma Insemination During Ovum-Pickup–a Method to Increase Pregnancy Rate in IVF/ICSI Procedure. A Pilot Randomized Trial. *J Assist Reprod Genet* (2013) 30(4):569–74. doi: 10.1007/s10815-013-9955-7
50. Qasim SM, Trias A, Karacan M, Shelden R, Kemmann E. Does the Absence or Presence of Seminal Fluid Matter in Patients Undergoing Ovulation Induction With Intrauterine Insemination? *Hum Reprod* (1996) 11(5):1008–10. doi: 10.1093/oxfordjournals.humrep.a019285
51. Crawford G, Ray A, Gudi A, Shah A, Homburg R. The Role of Seminal Plasma for Improved Outcomes During *In Vitro* Fertilization Treatment: Review of the Literature and Meta-Analysis. *Hum Reprod Update* (2015) 21(2):275–84. doi: 10.1093/humupd/dmu052
52. Robertson SA. Immune Regulation of Conception and Embryo Implantation-All About Quality Control? *J Reprod Immunol* (2010) 85(1):51–7. doi: 10.1016/j.jri.2010.01.008

Conflict of Interest: The authors declare that the research was conducted in the absence of any commercial or financial relationships that could be construed as a potential conflict of interest.

Publisher's Note: All claims expressed in this article are solely those of the authors and do not necessarily represent those of their affiliated organizations, or those of the publisher, the editors and the reviewers. Any product that may be evaluated in this article, or claim that may be made by its manufacturer, is not guaranteed or endorsed by the publisher.

frontiers in Immunology

ORIGINAL RESEARCH
published: 26 October 2021
doi: 10.3389/fimmu.2021.743354

S100A9 Activates the Immunosuppressive Switch Through the PI3K/Akt Pathway to Maintain the Immune Suppression Function of Testicular Macrophages

Zun Pan Fan[1], *Mei Lin Peng*[1], *Yuan Yao Chen*[1], *Yu Ze Xia*[2], *Chun Yan Liu*[1], *Kai Zhao*[1] *and Hui Ping Zhang*[1]*

[1] Institute of Reproductive Health, Tongji Medical College, Hua Zhong University of Science and Technology, Wuhan, China, [2] Tongji Medical College, Hua Zhong University of Science and Technology, Wuhan, China

OPEN ACCESS

Edited by:
Kenneth Tung,
University of Virginia, United States

Reviewed by:
Livia Lustig,
University of Buenos Aires, Argentina
Jannette Marie Dufour,
Texas Tech University Health Sciences Center, United States

***Correspondence:**
Hui Ping Zhang
zhpmed@126.com

Specialty section:
This article was submitted to Mucosal Immunity, a section of the journal Frontiers in Immunology

Received: *18 July 2021*
Accepted: *12 October 2021*
Published: *26 October 2021*

Citation:
Fan ZP, Peng ML, Chen YY, Xia YZ, Liu CY, Zhao K and Zhang HP (2021) S100A9 Activates the Immunosuppressive Switch Through the PI3K/Akt Pathway to Maintain the Immune Suppression Function of Testicular Macrophages. Front. Immunol. 12:743354. doi: 10.3389/fimmu.2021.743354

Macrophages are functionally plastic and can thus play different roles in various microenvironments. Testis is an immune privileged organ, and testicular macrophages (TMs) show special immunosuppressive phenotype and low response to various inflammatory stimuli. However, the underlying mechanism to maintain the immunosuppressive function of TMs remains unclear. S100A9, a small molecular Ca^{2+} binding protein, is associated with the immunosuppressive function of macrophages. However, no related research is available about S100A9 in mouse testis. In the present study, we explored the role of S100A9 in TMs. We found that S100A9 was expressed in TMs from postnatal to adulthood and contributed to maintaining the immunosuppressive phenotype of TMs, which is associated with the activation of PI3K/Akt pathway. S100A9 treatment promotes the polarization of bone marrow-derived macrophages from M0 to M2 *in vitro*. S100A9 was significantly increased in TMs following UPEC-infection and elevated S100A9 contributed to maintain the M2 polarization of TMs. Treatment with S100A9 and PI3K inhibitor decreased the proportion of M2-type TMs in control and UPEC-infected mouse. Our findings reveal a crucial role of S100A9 in maintaining the immunosuppressive function of TMs through the activation of PI3K/Akt pathway, and provide a reference for further understanding the mechanism of immunosuppressive function of TMs.

Keywords: S100A9, macrophage polarization, testicular macrophage, immune suppression, orchitis

INTRODUCTION

Macrophage has been classically divided into two polarization programs *in vitro* (1), (1) classically activated macrophages or M1, which are usually stimulated by TH1 type cytokines, resulting in anti-bacterial and pro-inflammatory properties and (2) alternatively activated macrophages or M2, which are induced by TH2 type cytokines, resulting in anti-inflammatory, pro-repair phenotype. Generally, M1 play a major role in the early stage of infection to resist pathogens, while M2 play a

major role in the recovery stage to promote tissue repair (2). Polarized macrophages display different patterns of glucose metabolism, M1-type macrophages are characterized by rapid glycolysis ability, while M2-type macrophages are mainly characterized by oxidative phosphorylation (3). Macrophage polarization is modulated by local microenvironment, and different polarization status affects the outcome of inflammation (4).

As first-line immune defense cells against inflammation in the testis, testicular macrophages (TMs) show unique tolerance to pathogens and play a key role in maintaining the immune privileged state of the testis and spermatogenesis (5). Tissue-resident TMs are usually M2 under physiological conditions, exhibited immuno-suppressive feature by secreting high levels of IL10 or TGFβ, and showed an inactivation of NF-κB signaling during inflammatory stimulation (6). The immunosuppression phenotype of rat TMs is associated with high levels of immunomodulatory molecules in testicular interstitial fluid, such as testosterone, prostaglandin, and corticosterone (7). Other molecules such as activin A, 25-HC may also affect the phenotype of testicular macrophages (8). However, the mechanism of regulating the immunosuppressive function of TMs remains unclear.

Notably, S100A9, a Ca^{2+} binding protein (9), which is mainly derived from macrophages, regulates immune function by affecting the phenotype of macrophages in neonatal mouse intestinal tissue under physiological conditions. Intestinal tissues from $S100a9^{-/-}$ neonatal mouse showed altered phenotype of colonic lamina propria macrophages in colon with reduced IL-10 and TGF-β (secreted by M2-type macrophage) mRNA level, downregulated expression of CX3CR1 protein (macrophage marker), and fewer regulatory T cells (10). In the blood of human newborn, S100A9, which is higher than adult under physiological conditions, inhibits the ability of fast-glycolysis (M1-type feature) in neonatal cord blood-derived macrophages, causing impaired ability of reaction to pathogens (11). Therefore, S100A9 is closely associated with the activation of M2 macrophages under physiological condition. However, the role of S100A9 in TMs has not been studied.

PI3K/Akt signaling is a critical pathway that converges metabolic and inflammatory signals to regulate macrophage response and modulate activation phenotype (12). The activation of PI3K signaling is a critical molecular switch that controls macrophage immune suppression function in cancer and other disorders (13); PI3K signaling through Akt and m-TOR inhibits NF-κB activation, leading to an immunosuppressive function during inflammation (13). Significant upregulation of S100A9, accompanied by activation of PI3K/Akt pathway, has been found in various diseases related to immune escape, such as colitis (14), breast cancer (15), and psoriasis (16). However, whether S100A9 affects the polarization of TMs by activating PI3K/Akt pathway remains unknown.

In the present study, we tested the proportion of M2-type TMs in mouse from postnatal to adulthood and S100A9 expression in TMs. The effect of S100A9 on the polarization of mouse TMs was verified *via* the intervention of tasquinimod (S100A9 inhibitor). The function of S100A9 *in vitro* on the polarization of bone marrow-derived macrophages was determined by exogenous supplementation of S100A9. The effect of S100A9 on the PI3K/Akt pathway was evaluated by the knockdown or overexpression of S100A9 in Raw264.7 mouse macrophage cell line. Finally, we verified that elevated S100A9 following UPEC-infection contributed to maintain the M2 polarization of TMs through the activation of PI3K/Akt pathway.

MATERIALS AND METHODS

Animals

C57BL/6 mice (2-, 4-, 6-, 8- and 10-week-old) (2week, n=15; 4week, n=12; 6week, n=32; 8week, n=35; 10week, n=8) were obtained from the Animal Centre of Tongji Medical College. All animals were housed and handled in strict accordance with the guidelines approved by the Animal Care and Use Committee of Tongji Medical College, Huazhong University of Science and Technology (No. 2019_S326).

Bacterial Culture and Animal Treatment

Urinary pathogenic *E. coli* (UPEC) strain CFT073 was propagated, and UPEC-induced experimental orchitis model was prepared as previously described (17). The testis, epididymis, and vas deferens of male C57BL/6 mice were fully exposed after anaesthesia. Approximately 8×10^4 per 10 μl of UPEC saline suspension was injected into the vas deferens proximal to the caudal epididymis. The sham group was injected with the same amount of PBS. Ligation was performed at the injection site to prevent the spread of infection. The S100A9 protein (RD, 2065-S9-050) was dissolved in PBS. Tasquinimod (S100A9 inhibitor, ABR-215050, MCE, 254964-60-8) was dissolved in dimethyl sulfoxide (DMSO) and diluted with PBS to adjust the concentration of DMSO to 3%. On day 2 post-infection, ABR-215050 (S100A9 inhibitor, 20 mg/kg) and LY294002 (50 mg/kg) were injected into the upper, middle and lower pole of UPEC-infected mouse testis (at a two-day interval, twice totally). The concentration of S100A9 was adjusted and injected about 10-15ul into each testicle. DMSO (3%) was injected into the testis as control.

Identification of Testis Infection and Sample Collection

The animals were sacrificed on the 7th day after infection. Testicular tissues were collected for subsequent experiments. A small piece of testicular tissue was taken from control and UPEC-infected groups, homogenized and diluted in 1ml of sterile PBS. 100ul testicular homogenate was evenly coated on LB solid medium and incubated at 37°C overnight. The CFU of UPEC and control group was compared the next day.

Western Blot Analysis

Total protein was extracted from macrophages by radio-immunoprecipitation assay (RIPA) buffer containing cocktail

protease inhibitor and phosphor–protease inhibitor (Servicebio, G2006/G2007). Protein concentration was determined using BCA kit (Thermo Fisher, 23225). Equal amounts of protein (5–25 μg) were loaded in appropriate concentration of sodium dodecyl sulphate (SDS)–polyacrylamide gel electrophoresis and transferred into polyvinylidene fluoride (PVDF) membrane. The membranes were blocked with 5% bovine serum albumin and incubated at 4°C overnight with the following primary antibodies: rabbit anti-S100A9 (1:1,000, abcam,242945), rabbit anti-PI3K (1:1,000, CST, 4257), rabbit anti-AKT (1:1,000, CST, 4691), rabbit anti-p-AKT (1:1,000, CST, 4060), rabbit and rabbit anti-β-actin (1:1,000, CST, 4970). The membranes were then incubated with goat anti-rabbit secondary antibody (1:4,000, Biosharp) for 2 h at room temperature. Protein bands were detected using Femto-light chemiluminescence kit (Omni-ECL, SQ201) and chemiluminescence-gel imaging system ECL (Board, USA). The results were analysed with help of the Image J software. Densitometry values were normalized to total β-actin.

Single-Cell Suspension of Testicular Interstitial Cells

The animals were sacrificed after anesthesia, and their testicles were removed. Interstitial cells were isolated as previously described (17). After careful dissection of tunica albuginea, the de-capsulated testes were digested with 1 mg/ml collagenase I (Sigma, USA) and 10 μg/ml DNase I in a shaking water bath at 34°C for 15 min. When the tubules were dispersed, digestion was terminated. The tubules were then filtered with a 200-mesh sieve, and the filtrate was centrifuged at 800 ×*g* for 5 min. RBC was removed with erythrocyte lysate. After resuspension with PBS, the single-cell suspension of testicular interstitial cells was obtained.

Flow Cytometry

Interstitial cells were collected and stained according to the manufacturer's instructions. The following antibodies were used: anti-mouse CD16/32 (Biolegend, 156604), Zombie-APC/CY7 (Biolegend, 423106), FITC anti-mouse CD45 (Biolegend, 103108), PE anti-mouse F4-80 (Biolegend, Clone: BM8, 123110), PE/cyanine5 anti-mouse CD86 (Biolegend, 105016), and Brilliant Violet 605™ anti-mouse CD206 (Biolegend, 141721). The labelled cells were detected using a flow cytometer (Cytek Aurora or BD LSRII). Data were analysed using FlowJo software (Version 10.4.0, USA).

Immunofluorescence Staining

The testicular tissue was fixed in 4% paraformaldehyde, subjected to gradient dehydration, embedded with Tissue-tek OCT (AKURA, 4583), snap frozen in liquid nitrogen, and cut into 5 μm-thick sections. After antigen retrieval, the slides were permeabilized with 0.5% Tritox-100, blocked with 5% BSA, and then incubated with rabbit anti-S100A9 (1:1,000, Abcam, 242945) and Alexa Fluor® 594 anti-mouse F4/80 (1:100, Biolegend, 123140) as primary antibodies. The secondary antibody was goat anti-rabbit Alexa Fluor 488(1:100). The nuclei were stained with DAPI, and images were acquired using fluorescence microscope (Mshot, MF43).

Immunohistochemistry

The testis was fixed in 4% paraformaldehyde, embedded with paraffin wax, and cut into 5 μm-thick sections. The slides were dewaxed in xylene and rehydrated in gradient alcohol solution. After antigen retrieval, the slides were added with 3% hydrogen peroxide to prevent endogenous peroxidase formation and then blocked with 3% BSA. The expression of S100A9 was detected by incubation with primary rabbit anti-S100A9 (1:1,000, Abcam, 242945) and appropriate secondary antibodies.

Magnetic-Activated Cell Sorting for TMs

The interstitial cells were counted, resuspended in 0.5–1 ml auto MACS running buffer (Miltenyi,130-091-221-1), and incubated for 15 min at 4°C in the dark with Anti-F4/80-MicroBeads (Miltenyi, 130-110-443) according to the manufacturer's instructions. The cells were washed and centrifuged at 300 ×*g* for 10 min. Cellular suspension was loaded into the LS separation column previously rinsed with 3 ml of MACS running buffer and attached to MACS separator (Miltenyi, 130-042-301). The positive fraction (F4/80 positive macrophage) was attached to the column, while the negative fraction was eluted through the column (discarded). The magnetically labelled cells were flushed immediately by firmly pushing the plunger into the column. The cells were identified through FCM by using PE anti-mouse F4-80 (Biolegend, Clone: BM8, 123110). The purity of TMs was about 85%.

RNA Isolation and qPCR

The total RNA of BMDMs and TMs was extracted using TRIzol reagent (Invitrogen, 15596018, China) according to the manufacturer's recommendation, and then transcribed into cDNA by using HiScript II Q RT SuperMix for qPCR (11123 ES, China). qRT-PCR amplification was performed using Hieff qPCR SYBR Green Master Mix (112101ES03, China) on LightCycler®96 (Roche, Basel, Switzerland). The prime sequences are shown in **Table 1**. Relative mRNA levels were normalized to β-actin expression and determined using the $2^{-\Delta\Delta CT}$ method.

Plasmid Construction and Transfection

S100A9 over-expressing vector, shRNA-expressing vector and their negative control plasmid were purchased from Genomeditech (Shanghai, China). The entire S100A9 sequence was included in the S100A9-overexpression vector. BamHI and XhoI sites were inserted in the overexpression vector PGMLV-CMV-MCS-EF1-ZsGreen1-T2A-Puro through a double-restriction enzyme digest. Three shRNAs targeting S100A9 were constructed by pGMLV-SC5 RNAi lentivirus vector. Plasmid titers were detected using Nanodrop2000 (Thermo Scientific, USA) and transfected into RAW 264.7 cell lines by

TABLE 1 | Primers used for qPCR in this study.

Mouse	Sense 5′-3′	Anti-sense 5′-3′
IL10	TTCTTTCAAACAAAGGACCAGC	GCAACCCAAGTAACCCTTAAAG
TGFβ1	CCAGATCCTGTCCAAACTAAGG	CTCTTTAGCATAGTAGTCCGCT
S100A9	CACAGTTGGCAACCTTTATGAA	TCATACACTCCTCAAAGCTCAG

using High-gene Transfection reagent (Abclone, RM09014) according to the manufacturer's instruction. The sequences and primers are shown in Supplementary material (**Supplementary Table S1**).

Statistical Analysis

All data were presented as mean and standard deviation (mean ± SD). GraphPad Prism 7 (GraphPad Software, USA) was used for data analysis through analysis of variance and Dunnett's multiple comparisons test. P-value < 0.05 indicated significant difference.

RESULTS

S100A9 Is Associated With Immunosuppressive Phenotype of TMs

We first tested the expression of S100A9 in the testis. We found that S100A9 was expressed in the TMs of mouse from postnatal to adulthood based on F4/80 and S100A9 dual immunofluorescence localization (**Figure 1** and **Supplementary Figure S1**).

CD68 was expressed in most TMs of rats (5) and distinguished by $CD68^+CD163^-$(M1) and $CD68^+CD163^+$(M2). In mouse, no definite markers are available to identify TM1 and TM2; core macrophage markers such as CXC3R1, F4/80, CD11b, and AIF, are expressed in most TMs in mouse (18). CD80, CD86 and cytokines such as IL1, TNF-a are usually secreted by M1 (1, 19–22), while CD163 and CD206 were used to mark M2 in mouse (21–24).

Thus, in the present study, we observed the change of TMs in mouse by flow cytometry by using $CD45^+$ (leukocyte marker), $F4/80^+$ (macrophage marker), $CD206^+$ (M2 marker), and $CD86^+$ (M1 marker). Testicular interstitial cells were collected, and the percentage of $CD45^+$ leukocyte, $CD45^+F4/80^+$macrophage, $CD45^+F4/80^+CD206^+CD86^-$ M2, and $CD45^+F4/80^+CD206^-CD86^+$ M1 groups were analysed using flow cytometry (**Figure 2A** and **Supplementary Figure S2**). We found that the total number of leukocytes and macrophages in testis was increased with the development of testis (**Supplementary Figure S3**); the proportion of M2-TMs increased gradually from postnatal (2 weeks) to adulthood (≥ 6 weeks) and became stabilized at approximately 90% after the sixth week (**Figure 2B**). Almost all adult testicular macrophages expressed CD206, and most of them were M2 after 6 weeks. TMs were collected using magnetic-activated sorting by using F4/80 magnetic beads and the purity was identified by FCM (**Figure 2C** and **Supplementary Figure S4**). Then, we compared the mRNA expression of S100A9 (**Figure 2D**) in TMs from week 2 to week 10. Notably, the change trend of S100A9 in TMs was consistent with the increasing trend of M2 macrophages in testis. Therefore, S100A9 may be related to maintaining the immunosuppressive phenotype of testicular macrophages.

S100A9 Maintains the M2 Polarization State of Testicular Macrophages

To further clarify whether S100A9 plays a role in regulating TMs polarization, we injected tasquinimod (S100A9 inhibitor) and S100A9 into testis. DMSO was used as the control group. The percentage of M1 (marked as $CD45^+F4/80^+CD206^-CD86^+$) and M2 (marked as $CD45^+F4/80^+CD206^+CD86^-$) in each group was detected by FCM analysis (**Figure 2E** and **Supplementary Figure S5**). No obvious change was observed in DMSO and S100A9 group compared with the control group. Treatment with tasquinimod (S100A9 inhibitor) substantially decreased the M2:TM ratio from 90.0% to 58.7%, and the M1:TM ratio increased from 1.10% to 24.5% between the control and tasquinimod group. This result was similar with the treatment by LY294002 (PI3K inhibitor). M2:TM ratio decreased from 90.0% to 69.4%, and the M1:TM ratio increased from 1.10% to 18.04% between the control and LY294002 group. Therefore, S100A9 contributes to maintain the immunosuppressive phenotype of TMs through the activation of PI3K/Akt pathway.

S100A9 Treatment Promotes the Polarization of Bone Marrow-derived Macrophages to M2 *In Vitro*

We isolated and cultured mouse bone marrow-derived macrophages (BMDMs, designated as M0) *in vitro* (**Figure 3A**) and stimulated them with S100A9 (1 μg/ml), IL-4 (10 ng/ml, designated as M2) and IFN-γ (50 ng/ml, designated as M1) for 48 h, respectively. DMSO (0.3%) was used as the control. Tasquinimod (10 μmol/ml, inhibitor of S100A9) was compared with the S100A9 group. M1/M2 subpopulation in each group was distinguished by the expression of M1 ($CD45^+F4/80^+CD86^+$) and M2 ($CD45^+F4/80^+CD206^+$), as shown in **Figures 3B, C** and **Supplementary Figure S6**. We obtained an extremely similar trend (the ratio of M2/M1) between IL4 and S100A9 group, and the ratio of M2/M1 was reversed with the treatment of tasquinimod (**Figure 3D**). We also found that S100A9 significantly increased the mRNA expression of IL10 and TGFβ (**Figures 3E, F**) in the S100A9 group, and treatment with tasquinimod significantly decreased the expression of IL10 and TGFβ, which were usually secreted by M2-type macrophages. Thus, S100A9 stimulation promoted the polarization of BMDMs from M0 to M2 *in vitro*.

S100A9 Activates the PI3K/Akt Pathway in Raw 264.7 Macrophages

To verify whether S100A9 can activate the immunosuppression switch of macrophages to maintain the immunosuppressive phenotype by activating PI3K/Akt pathway, we overexpressed and knocked down S100A9 in mouse RAW264.7 macrophage cell line. PI3K inhibitor (LY294002) was used to inhibit the activation of the PI3K/Akt pathway. Then, the expression levels of S100A9, PI3K, Akt, and p-Akt in the five groups, namely, the control, S100A9 knockdown (S100A9-KD), S100A9 overexpression (S100A9-OE), S100A9-KD+S100A9, and S100A9-OE+LY294002 group, were tested (**Figure 4A** and **Supplementary Figure S7**). In comparison with the control group, the expression of S100A9 significantly increased after overexpression, decreased in S100A9-KD group, and then reversed after exogenous supplementation (**Figure 4B**). The

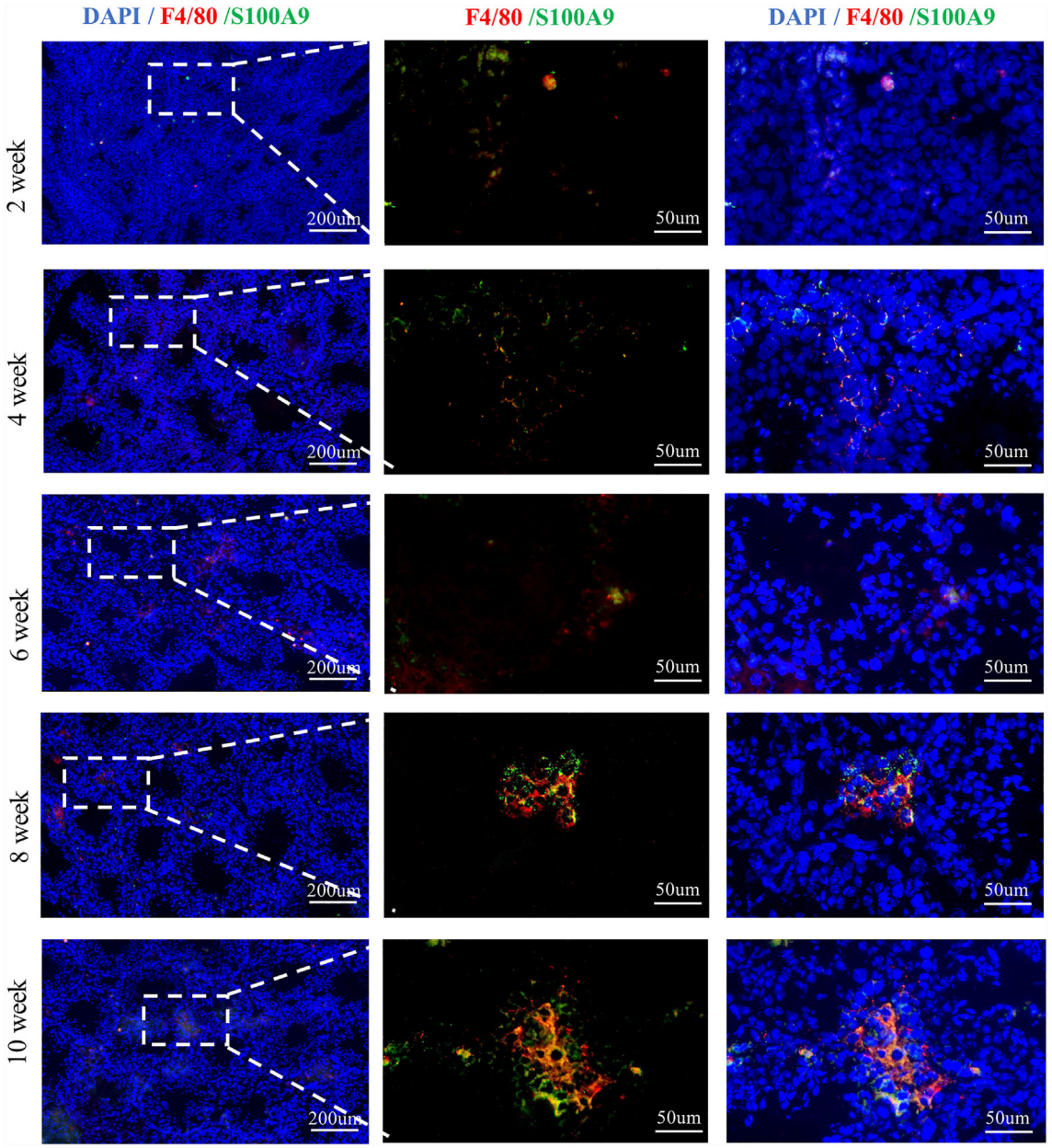

FIGURE 1 | S100A9 expressed in testicular macrophages of mouse from weeks 2 to 10. Double immunofluorescence staining of S100A9 and mouse macrophage marker (F4/80) in testis from weeks 2 to 10 (scale bar: 200 and 50μm).

expression of PI3K showed no obvious change in each group (**Figure 4C**). In comparison with the control group, the ratio of p-Akt/Akt was significantly upregulated in the S100A9-OE group. Treatment with LY294002 significantly attenuated the upregulation ratio of p-AKT/Akt (**Figure 4D**). The ratio of p-Akt/Akt was significantly downregulated in S100-KD group, but the ratio then significantly increased with the supplementation of S100A9 (**Figure 4D**). Hence, S100A9 overexpression activates the PI3K/Akt pathway.

Expression of TM-Derived S100A9 Increase in UPEC-Induced Orchitis

We successfully established the mouse UPEC model according to previous methods (17). The testes of the two groups (**Figure 5A**) were mashed and smeared on a bacterial plate. Compared with the control group, the generation of strains was visible to the naked eye in UPEC group (**Figure 5B**). The TMs of mouse were collected using F4/80 magnetic beads at the seventh day after UPEC infection to detect the expression of S100A9 (**Figure 5C**). The

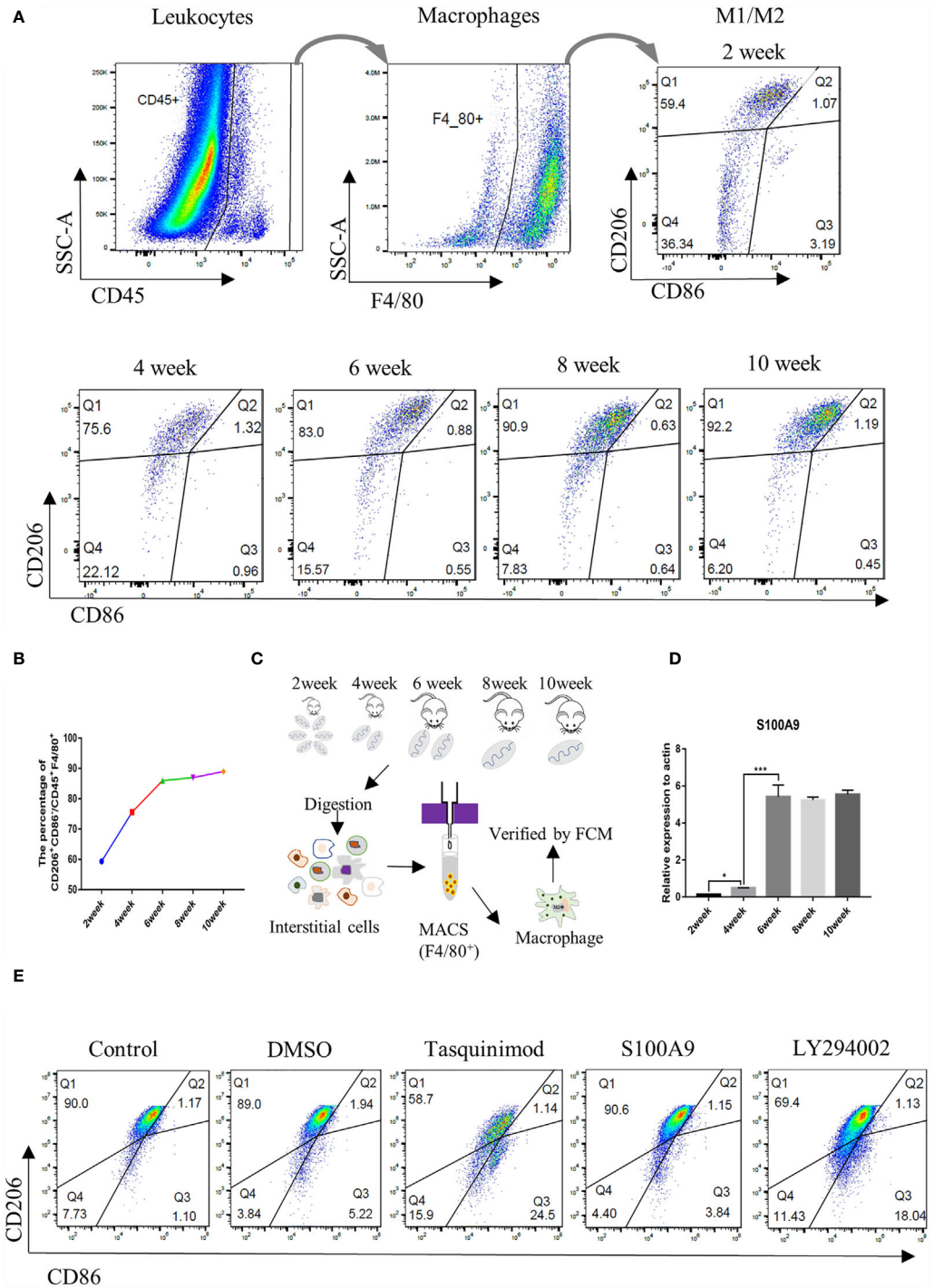

FIGURE 2 | Ratio of M2 TMs and S100A9 mRNA expression increases with the development of mouse testis. **(A)** Gating strategy that describes $CD45^+F4/80^+$ mouse testis fraction and the distinction of M2 ($CD206^+CD86^-$) and M1 ($CD206^-CD86^+$) population, represented by Q1 and Q3 respectively (2week, *n*=4/group; 4-6week, *n*=3/group; 8-10week, *n*=2/group). **(B)** Percentage of M2Φ in different age of TMs by FCM. **(C)** Flow chart of preparation for TMs, testes from weeks 2 to 10 were digested and interstitial cells were incubated with F4/80 magnetic beads (2week, *n*=8/group; 4-6week, *n*=6/group; 8-10week, *n*=4/group). TMs were obtained by magnetic cell sorting (MACS), and the purity was verified by flow cytometry for subsequent experiment. **(D)** Relative mRNA expression of S100A9 at different ages of TM (2week, *n*=6/group; 4-6week, *n*=5/group; 8-10week, *n*=4/group). **(E)** Percentage of M2Φ in adult mouse testis (8week, *n*=2/group) under physiological conditions decreased with the treatment of S100A9 inhibitor (tasquinimod) or PI3K inhibitor (LY294002), compared with the control group. DMSO and S100A9 groups were used as control. Data represent the mean ± standard error (n=2-3). Significant differences between the two groups are indicated as $^*P < 0.05$, $^{***}P < 0.001$; comparisons between groups using one-way ANOVA followed by Dunnett's multiple comparisons test.

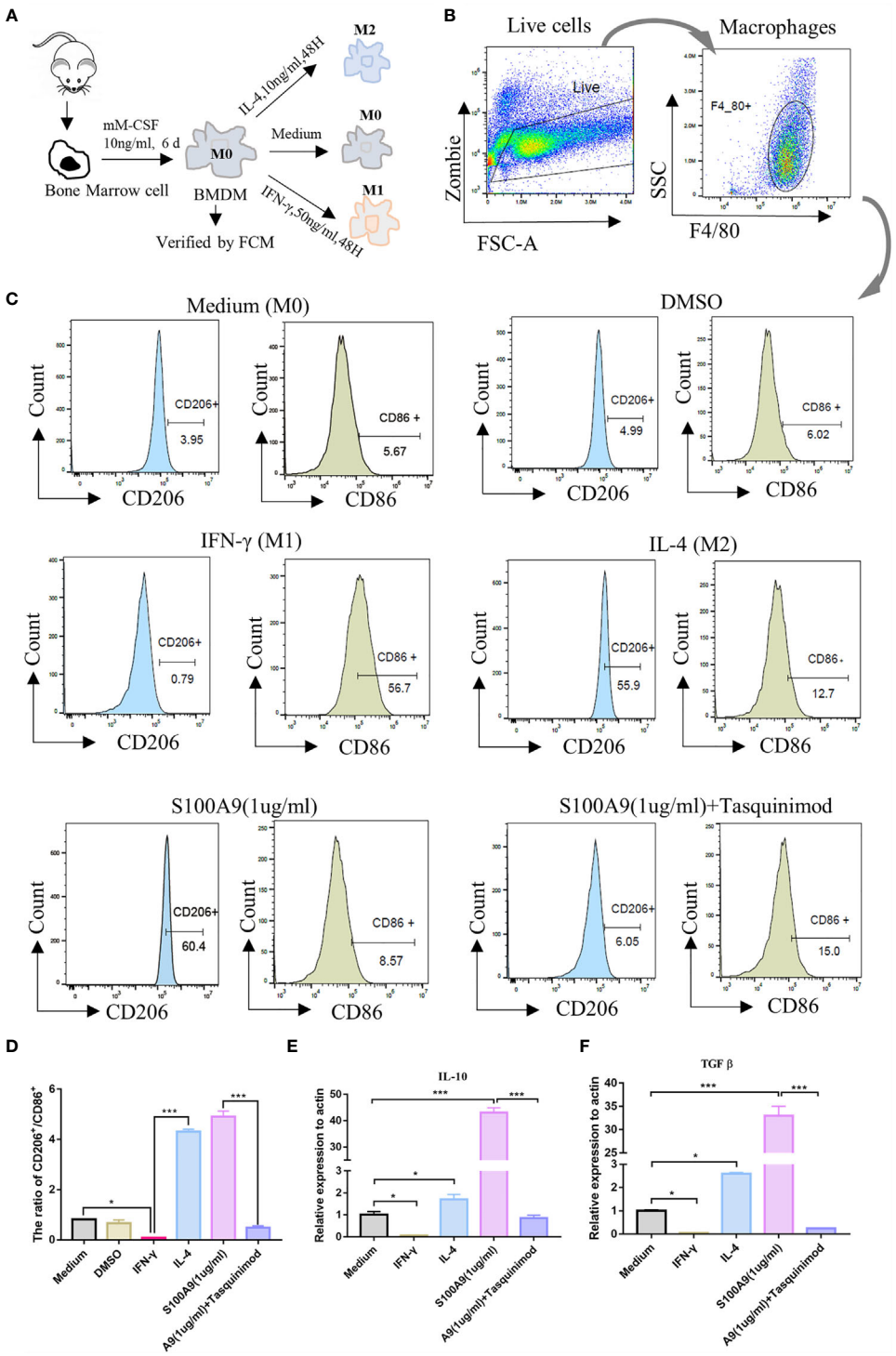

FIGURE 3 | S100A9 treatment promotes the polarization of bone marrow-derived macrophages to M2 *in vitro*. **(A)** Mouse (6week, *n*=4/group) bone marrow single cell suspension was collected through a 70μm filter, and removed red blood cells by red cell lysis solution. BMDMs (M0) were induced with mM-CSF (10 ng/ml, 6 days) in RPMI1640 medium. Further polarization was achieved by adding 50 ng/ml IFN-γ (M1), 10 ng/ml IL-4 (M2), DMSO (0.3%), S100A9 (1 μg/ml) and S100A9 (1 μg/ml)+tasquinimod (10 μmol/ml) for 48 more hours. **(B, C)** Immunotyping was performed by flow cytometric analysis to detect live cells, macrophage surface markers (F4/80$^+$), M1-MΦ marker (CD86$^+$), and M2-MΦ marker (CD206$^+$). **(D)** The ratio of CD206$^+$ and CD86$^+$ in different groups. **(E, F)** Relative mRNA expression of IL10 and TGFβ in different groups. Data represent the mean ± standard error(*n*=3–5). *P < 0.05, ***P < 0.001. comparisons between groups using one-way ANOVA followed by Dunnett's multiple comparisons test.

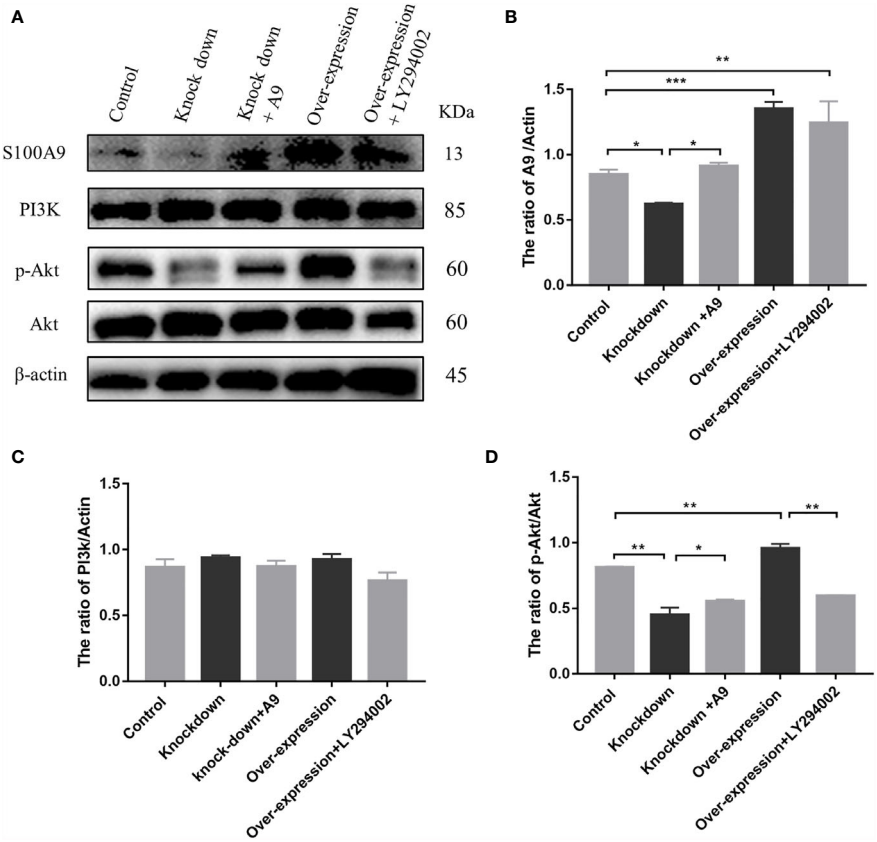

FIGURE 4 | S100A9 treatment activates PI3K/Akt pathway in Raw 264.7 macrophage cells. **(A)** Western blot results and quantification data of S100A9, PI3K, p-Akt, and Akt expression in different groups. Quantification data of Western blot analysis results for the ratio of **(B)** S100A9/Actin, **(C)** PI3K/Actin, and **(D)** p-Akt/Akt. Data are presented as mean ± standard error (n=2–3); *P < 0.05, **P < 0.01, ***P < 0.001; comparisons between groups using one-way ANOVA followed by Dunnett's multiple comparisons test.

purity of TMs was verified by FCM (**Supplementary Figure S4**). Western blot (**Figures 5D, E** and **Supplementary Figure S8**) analysis and immunohistochemistry (**Figure 5F**) showed that the expression of S100A9 in TMs was significantly increased after UPEC infection. Double-immunofluorescence staining (**Figure 5G** and **Supplementary Figure S8**) of F4/80 and S100A9 showed increased expression of S100A9 in testis following UPEC infection.

Inhibition of S100A9 or Blocking of the PI3K/Akt pathway Reduce the Proportion of M2-TMs Following UPEC-Induced Orchitis

Although the expression of S100A9 increased following UPEC infection, the percentage of M1-TM (marked as $CD45^+F4/80^+CD86^+CD206^-$) increased from 1.10% to 5.69%, and M2-TM (marked as $CD45^+F4/80^+CD206^+CD86^-$) decreased from 90% to 80.7% (**Figures 2E**, **5H**). To further identify S100A9 contributes to M2 polarization of TMs through the activation of PI3K/Akt pathway, we injected tasquinimod (S100A9 inhibitor) or LY294002 (PI3K inhibitor) individually into the mouse testis two days after UPEC infection. On the seventh day after infection, the percentage of M1 and M2 in each group was detected by FCM analysis (**Figure 5H** and **Supplementary Figure S5**). Treatment with tasquinimod further decreased the ratio of M2-TM from 80.7% to 65.9% but increased the ratio of M1-TM from 5.69% to 26.5% between the UPEC and UPEC + tasquinimod group. Treatment with LY294002 (inhibitor of PI3K) also attenuated M2-TM from 80.7% to 72.1% but increased the ratio of M1-TM from 5.69% to 21.4% between UPEC and UPEC+LY294002 group (**Figure 5H**). S100A9 inhibitor and PI3K inhibitor both decreased the ratio of M2-TMs. Therefore, the elevated S100A9 following UPEC infection contributed to maintain the M2 polarization of TMs through the activation of PI3K/Akt pathway. This finding is consistent with the phenomenon we observed in physiological conditions.

DISCUSSION

Overall, this study found a new role of S100A9 in maintaining the immunosuppression phenotype of TMs. We elucidated the mechanism by which S100A9 can maintain the

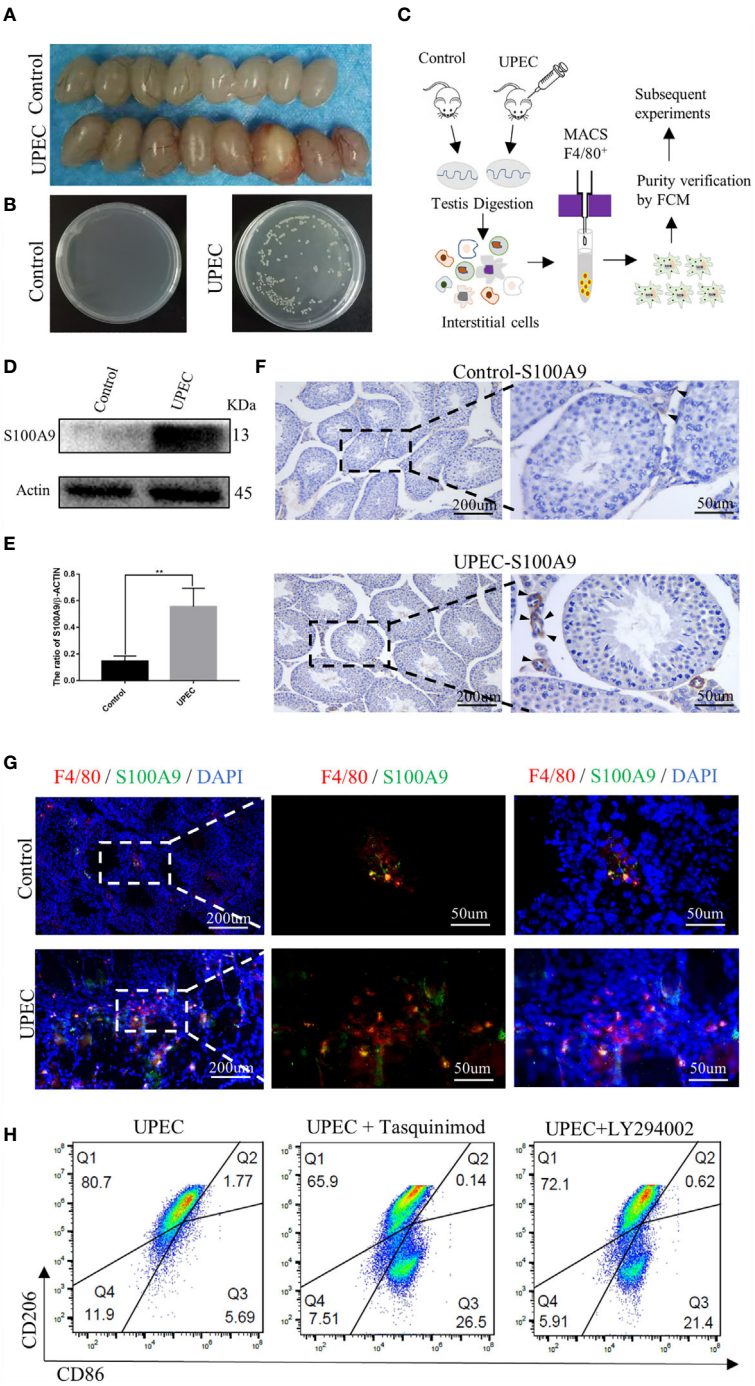

FIGURE 5 | S100A9 expression increased in TMs and treatment with tasquinimod or LY294002 attenuated the ratio of M2-TMs following UPEC-induced orchitis. **(A)** Comparison of testis between the control and UPEC infection groups (8week, n=4/group). **(B)** The growth of the colonies after homogenization and plating of testis tissues in the control and UPEC groups (n=4/group). **(C)** Flow chart of preparation for TMs, testes from control and UPEC group were digested and interstitial cells were incubated with F4/80 magnetic beads (8week, n=4/group). TMs were obtained by magnetic cell sorting (MACS), and the purity was verified by flow cytometry for subsequent experiment. **(D, E)** Western blot analysis results and quantification data of S100A9 expression in TMs of control and UPEC group (8week, *n*=4/group). Data represent the mean ± standard error. $^{**}P < 0.01$. **(F)** Immunohistochemistry staining result of S100A9 in the control and UPEC group testis (8week) at the 7th day after infection. Black arrows showed the expression of S100A9 (scale bar: 200, 50 μm). **(G)** Double immunofluorescence staining of S100A9 and mouse macrophage marker (F4/80) in the testis (8week) of control and UPEC group (scale bar: 200, 50 μm). **(H)** Flowcytometric analysis of total TMs (8week, *n*=2/group) was marked as $CD45^{+}F4/80^{+}$. Percentage of M2Φ in testis decreased with the treatment of S100A9 inhibitor (tasquinimod) or PI3K inhibitor (LY294002), compared with the UPEC group.

immunosuppressive phenotype *via* the activation of PI3K/Akt pathway, an immunosuppressive switch in macrophages. In addition, elevated S100A9 following UPEC-infection contributes to maintaining the M2-type polarization of TMs. Our findings enriched the understanding of the immunosuppressive phenotype of TMs and pave the way to explore the fate of testicular inflammation.

Based on our results, S100A9 expressed in TMs of mouse. The mRNA expression of S100A9 and the proportion of M2-TMs gradually increased with testicular development and remained relatively stable after sperm maturation (at 6 weeks later). Almost all adult testicular macrophages showed M2 types under physiological conditions, and this property may help in maintaining the immune-privileged state of testis to ensure that the antigens on the mature sperm surface are not attacked by themselves. S100A9 inhibitor significantly downregulated the proportion of M2-TMs from 90.0% to 58.7%, this confirming the crucial role of S100A9 in maintaining the M2 polarization state of testicular macrophages.

Bone marrow-derived macrophages induced by macrophage colony-stimulating factor were usually used for *in vitro* studies of macrophage polarization because of its unchanged original "activation" status of macrophages (25). We found that S100A9 promoted the polarization of bone-marrow-derived macrophages from M0 to M2 *in vitro* and increased the mRNA expression of IL-10 and TGFβ. This result is consistent with the findings in myelodysplastic syndromes (MDS) (26), in which S100A9 lead abnormal increase of myeloid-derived suppressor cells and suppressive cytokines IL-10 and TGF-β and finally contributed to immunosuppression, inflammation, and cancer. This result also explains why testicular macrophages secreted a large amount of IL-10 during inflammation stimuli and showed an immunosuppression phenotype (7).

Considering the inability of primary testicular macrophages proliferation *in vitro*, we overexpressed and knockdown S100A9 in Raw 264.7 macrophage cell line and confirmed that S100A9-OE activates the immunosuppressive switch of macrophages through the activation of PI3K/Akt pathway. Finally, we validated this phenomenon by inhibiting S100A9 and PI3K pathways in UPEC-induced orchitis. The elevated S100A9 in orchitis helps in maintaining the M2 polarization of TMs and attenuated the ratio of M1, which usually represent the ability of macrophages to resist bacteria. Similarly, the inhibition of S100A9 or PI3K pathways reduced the M2 ratio of TMs in control and UPEC group. Our results are consistent with the results of a study about fetal cord blood-derived macrophages. The high level of S100A9 in fetal cord blood altered the phenotype of fetal cord blood macrophages by preventing m-TOR expression and inhibiting glycolysis (11). Therefore, an attenuated response to inflammatory stimuli was observed. Rapid glycolysis is a characteristic of M1 macrophages. m-TOR, as a key sensor of nutrient status, is the downstream signal of the PI3K/Akt pathway, and is inhibited by activating the PI3K/Akt axis (12). Moreover, the phenotype of colonic lamina propria macrophages in S100A9$^{-/-}$ mice was altered, and the level of IL10 and TGF-β secreted by M2 macrophages decreased; the number of CX3CR1 protein (macrophage marker) was also decreased (10), which is consistent with our results. Overall,

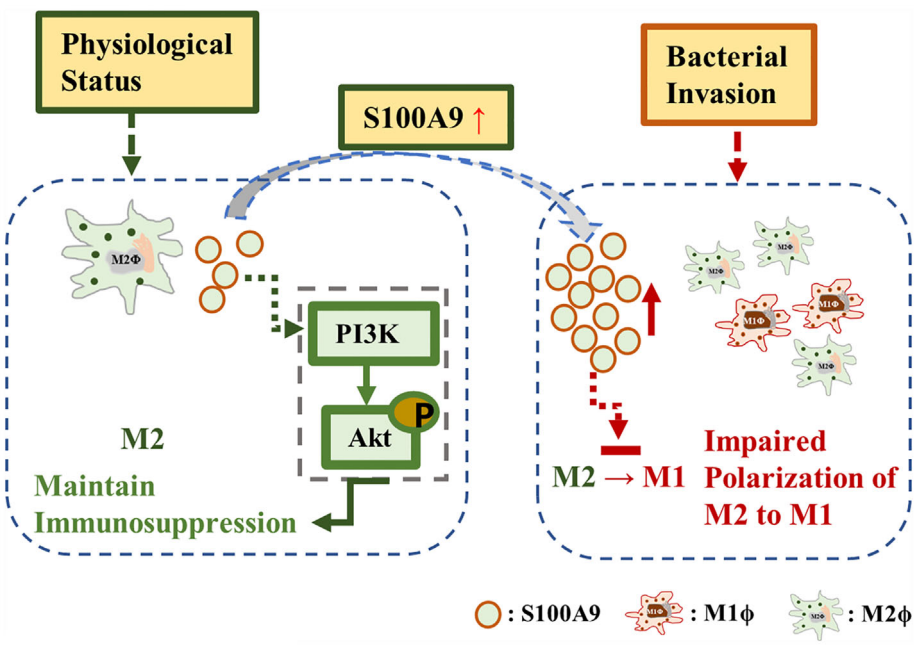

FIGURE 6 | S100A9 mechanism. S100A9 contributed to maintain the M2 polarization of testicular macrophages through the activation of PI3K/Akt pathway under physiological condition. During inflammation, the elevated S100A9 weakened the polarization of testicular macrophages from M2 to M1.

our results revealed a new role of S100A9 in maintaining the immune suppression phenotype of TMs.

Besides, S100A9 contributes to maintain the polarization of M2 TMs, which may impair their ability to resist bacterial in the early stage of infection, but it may also promote the transformation of acute inflammation to chronic (2) and accelerate the repair of tissues in the late stage of infection. In human orchitis, persistent chronic inflammatory response following acute orchitis is often accompanied by a large number of immune cell infiltration in testis and severe fibrosis around seminiferous tubules (27). Among infertile men with genital tract infection, up to 25% of infertile men experience local inflammatory reaction and immune cell infiltration by testicular biopsies (28). The positive effect of targeting S100A9 has been observed in many chronic inflammatory diseases with abnormal tissue repair, such as pulmonary fibrosis (29), renal fibrosis (30), atherogenesis (31), and systemic sclerosis phenotype (32). Whether S100A9 mediates testicular inflammation during the long recovery process following acute infection needs further study.

In conclusion, our study reveals a previously unrecognized function of S100A9 in TMs, in which it maintains the immune suppression phenotype of TMs *via* the activation of the PI3K/Akt pathway for a better understanding of the special immunosuppressive function of TMs (**Figure 6**). In orchitis, elevated S100A9 contributes in maintaining the M2 polarization of TMs, which partly explain the immunosuppressive phenotype of TMs to bacterial stimulation. Whether S100A9 can affect the inflammatory outcome in testis and promote tissue repair by affecting the polarization of macrophages to M2 worth further study.

DATA AVAILABILITY STATEMENT

The original contributions presented in the study are included in the article/**Supplementary Material**. Further inquiries can be directed to the corresponding author.

ETHICS STATEMENT

The animal study was reviewed and approved by Committee of Tongji Medical College, Huazhong University of Science and Technology.

AUTHOR CONTRIBUTIONS

ZF and YC designed the study. ZF and MP performed the experiment. YX assembled the data. ZF and CL wrote the paper. KZ and HZ revised manuscript. All authors read and approved the submitted manuscript version.

FUNDING

This work was supported by the National Natural Science Foundation of China (Grant No. 8187061007).

SUPPLEMENTARY MATERIAL

The Supplementary Material for this article can be found online at: https://www.frontiersin.org/articles/10.3389/fimmu.2021.743354/full#supplementary-material

REFERENCES

1. Sica A, Mantovani A. Macrophage Plasticity and Polarization: *In Vivo* Veritas. *J Clin Invest* (2012) 122(3):787–95. doi: 10.1172/JCI59643
2. Shapouri-Moghaddam A, Mohammadian S, Vazini H, Taghadosi M, Esmaeili SA, Mardani F, et al. Macrophage Plasticity, Polarization, and Function in Health and Disease. *J Cell Physiol* (2018) 233(9):6425–40. doi: 10.1002/jcp.26429
3. Viola A, Munari F, Sánchez-Rodríguez R, Scolaro T, Castegna A. The Metabolic Signature of Macrophage Responses. *Front Immunol* (2019) 10:1462. doi: 10.3389/fimmu.2019.01462
4. Locati M, Curtale G, Mantovani A. Diversity, Mechanisms, and Significance of Macrophage Plasticity. *Annu Rev Pathol* (2020) 15:123–47. doi: 10.1146/annurev-pathmechdis-012418-012718
5. Mossadegh-Keller N, Sieweke MH. Testicular Macrophages: Guardians of Fertility. *Cell Immunol* (2018) 330:120–5. doi: 10.1016/j.cellimm.2018.03.009
6. Bhushan S, Meinhardt A. The Macrophages in Testis Function. *J Reprod Immunol* (2017) 119:107–12. doi: 10.1016/j.jri.2016.06.008
7. Wang M, Fijak M, Hossain H, Markmann M, Nüsing RM, Lochnit G, et al. Characterization of the Micro-Environment of the Testis That Shapes the Phenotype and Function of Testicular Macrophages. *J Immunol (Baltimore Md: 1950)* (2017) 198(11):4327–40. doi: 10.4049/jimmunol.1700162
8. Barakat B, O'Connor AE, Gold E, de Kretser DM, Loveland KL. Inhibin, Activin, Follistatin and FSH Serum Levels and Testicular Production Are Highly Modulated During the First Spermatogenic Wave in Mice. *Reprod (Cambridge England)* (2008) 136(3):345–59. doi: 10.1530/REP-08-0140
9. Wang S, Song R, Wang Z, Jing Z, Wang S, Ma J. S100A8/A9 in Inflammation. *Front Immunol* (2018) 9:1298. doi: 10.3389/fimmu.2018.01298
10. Willers M, Ulas T, Völlger L, Vogl T, Heinemann AS, Pirr S, et al. S100A8 and S100A9 Are Important for Postnatal Development of Gut Microbiota and Immune System in Mice and Infants. *Gastroenterology* (2020) 159(6):2130–45.e2135. doi: 10.1053/j.gastro.2020.08.019
11. Dreschers S, Ohl K, Lehrke M, Möllmann J, Denecke B, Costa I, et al. Impaired Cellular Energy Metabolism in Cord Blood Macrophages Contributes to Abortive Response Toward Inflammatory Threats. *Nat Commun* (2019) 10(1):1685. doi: 10.1038/s41467-019-09359-8
12. Vergadi E, Ieronymaki E, Lyroni K, Vaporidi K, Tsatsanis C. Akt Signaling Pathway in Macrophage Activation and M1/M2 Polarization. *J Immunol (Baltimore Md: 1950)* (2017) 198(3):1006–14. doi: 10.4049/jimmunol.1601515
13. Kaneda MM, Messer KS, Ralainirina N, Li H, Leem CJ, Gorjestani S, et al. Pi3kγ Is a Molecular Switch That Controls Immune Suppression. *Nature* (2016) 539(7629):437–42. doi: 10.1038/nature19834
14. Zhang X, Wei L, Wang J, Qin Z, Wang J, Lu Y, et al. Suppression Colitis and Colitis-Associated Colon Cancer by Anti-S100a9 Antibody in Mice. *Front Immunol* (2017) 8:1774. doi: 10.3389/fimmu.2017.01774
15. Moradpoor R, Gharebaghian A, Shahi F, Mousavi A, Salari S, Akbari ME, et al. Identification and Validation of Stage-Associated PBMC Biomarkers in Breast Cancer Using MS-Based Proteomics. *Front Oncol* (2020) 10:1101. doi: 10.3389/fonc.2020.01101
16. Ge H, Li B, Chen W, Xu Q, Chen S, Zhang H, et al. Differential Occurrence of Lysine 2-Hydroxyisobutyrylation in Psoriasis Skin Lesions. *J Proteomics* (2019) 205:103420. doi: 10.1016/j.jprot.2019.103420
17. Li Y, Su Y, Zhou T, Hu Z, Wei J, Wang W, et al. Activation of the NLRP3 Inflammasome Pathway by Prokineticin 2 in Testicular Macrophages of Uropathogenic Escherichia Coli- Induced Orchitis. *Front Immunol* (2019) 10:1872. doi: 10.3389/fimmu.2019.01872

18. Mossadegh-Keller N, Gentek R, Gimenez G, Bigot S, Mailfert S, Sieweke MH. Developmental Origin and Maintenance of Distinct Testicular Macrophage Populations. *J Exp Med* (2017) 214(10):2829–41. doi: 10.1084/jem.20170829
19. Krausgruber T, Blazek K, Smallie T, Alzabin S, Lockstone H, Sahgal N, et al. IRF5 Promotes Inflammatory Macrophage Polarization and TH1-TH17 Responses. *Nat Immunol* (2011) 12(3):231–8. doi: 10.1038/ni.1990
20. Lescoat A, Ballerie A, Jouneau S, Fardel O, Vernhet L, Jego P, et al. M1/M2 Polarisation State of M-CSF Blood-Derived Macrophages in Systemic Sclerosis. *Ann Rheumatic Dis* (2019) 78(11):e127. doi: 10.1136/annrheumdis-2018-214333
21. Dessing MC, Tammaro A, Pulskens WP, Teske GJ, Butter LM, Claessen N, et al. The Calcium-Binding Protein Complex S100A8/A9 has a Crucial Role in Controlling Macrophage-Mediated Renal Repair Following Ischemia/Reperfusion. *Kidney Int* (2015) 87(1):85–94. doi: 10.1038/ki.2014.216
22. Hasan D, Chalouhi N, Jabbour P, Hashimoto T. Macrophage Imbalance (M1 vs. M2) and Upregulation of Mast Cells in Wall of Ruptured Human Cerebral Aneurysms: Preliminary Results. *J Neuroinflamm* (2012) 9:222. doi: 10.1186/1742-2094-9-222
23. Zhou X, Li W, Wang S, Zhang P, Wang Q, Xiao J, et al. YAP Aggravates Inflammatory Bowel Disease by Regulating M1/M2 Macrophage Polarization and Gut Microbial Homeostasis. *Cell Rep* (2019) 27(4):1176–89.e1175. doi: 10.1016/j.celrep.2019.03.028
24. Olsson A, Nakhlé J, Sundstedt A, Plas P, Bauchet AL, Pierron V, et al. Tasquinimod Triggers an Early Change in the Polarization of Tumor Associated Macrophages in the Tumor Microenvironment. *J Immunotherapy Cancer* (2015) 3:53. doi: 10.1186/s40425-015-0098-5
25. Ushach I, Zlotnik A. Biological Role of Granulocyte Macrophage Colony-Stimulating Factor (GM-CSF) and Macrophage Colony-Stimulating Factor (M-CSF) on Cells of the Myeloid Lineage. *J Leukocyte Biol* (2016) 100(3):481–9. doi: 10.1189/jlb.3RU0316-144R
26. Chen X, Eksioglu EA, Zhou J, Zhang L, Djeu J, Fortenbery N, et al. Induction of Myelodysplasia by Myeloid-Derived Suppressor Cells. *J Clin Invest* (2013) 123(11):4595–611. doi: 10.1172/JCI67580
27. Mikuz G, Damjanov I. Inflammation of the Testis, Epididymis, Peritesticular Membranes, and Scrotum. *Pathol Annu* (1982) 17(Pt 1):101–28.
28. Schuppe HC, Pilatz A, Hossain H, Diemer T, Wagenlehner F, Weidner W. Urogenital Infection as a Risk Factor for Male Infertility. *Deutsches Arzteblatt Int* (2017) 114(19):339–46. doi: 10.3238/arztebl.2017.0339
29. Araki K, Kinoshita R, Tomonobu N, Gohara Y, Tomida S, Takahashi Y, et al. The Heterodimer S100A8/A9 Is a Potent Therapeutic Target for Idiopathic Pulmonary Fibrosis. *J Mol Med (Berlin Germany)* (2021) 99(1):131–45. doi: 10.1007/s00109-020-02001-x
30. Tammaro A, Florquin S, Brok M, Claessen N, Butter LM, Teske GJD, et al. S100A8/A9 Promotes Parenchymal Damage and Renal Fibrosis in Obstructive Nephropathy. *Clin Exp Immunol* (2018) 193(3):361–75. doi: 10.1111/cei.13154
31. Kraakman MJ, Lee MK, Al-Sharea A, Dragoljevic D, Barrett TJ, Montenont E, et al. Neutrophil-Derived S100 Calcium-Binding Proteins A8/A9 Promote Reticulated Thrombocytosis and Atherogenesis in Diabetes. *J Clin Invest* (2017) 127(6):2133–47. doi: 10.1172/JCI92450
32. Wu Y, Li Y, Zhang C, Xi A, Wang Y, Cui, et al. S100a8/A9 Released by CD11b+Gr1+ Neutrophils Activates Cardiac Fibroblasts to Initiate Angiotensin II-Induced Cardiac Inflammation and Injury. *Hypertension (Dallas Tex: 1979)* (2014) 63(6):1241–50. doi: 10.1161/HYPERTENSIONAHA.113.02843

Conflict of Interest: The authors declare that the research was conducted in the absence of any commercial or financial relationships that could be construed as a potential conflict of interest.

Publisher's Note: All claims expressed in this article are solely those of the authors and do not necessarily represent those of their affiliated organizations, or those of the publisher, the editors and the reviewers. Any product that may be evaluated in this article, or claim that may be made by its manufacturer, is not guaranteed or endorsed by the publisher.

frontiers | Frontiers in Immunology

REVIEW
published: 26 May 2022
doi: 10.3389/fimmu.2022.809247

Exposed and Sequestered Antigens in Testes and Their Protection by Regulatory T Cell-Dependent Systemic Tolerance

*Jessica Harakal[1,2,3], Hui Qiao[1,3], Karen Wheeler[2,3], Claudia Rival[1,3], Alberta G. A. Paul[1,3], Daniel M. Hardy[4], C. Yan Cheng[5], Erwin Goldberg[6] and Kenneth S. K. Tung[1,2,3]**

[1] Department of Pathology, University of Virginia, Charlottesville, VA, United States, [2] Department of Microbiology, University of Virginia, Charlottesville, VA, United States, [3] Bierne B. Carter Center for Immunology Research, University of Virginia, Charlottesville, VA, United States, [4] Cell Biology and Biochemistry Department, Texas Tech University Health Science Center (HSC), Lubbock, TX, United States, [5] Center for Biomedical Research, Population Council, New York, NY, United States, [6] Molecular Biochemistry Department, Northwestern University, Evanston, IL, United States

OPEN ACCESS

Edited by:
Tanima Bose, Ludwig Maximilian University of Munich, Germany

Reviewed by:
Markus Xie, Immunology Discovery, Genentech, United States
Livia Lustig, University of Buenos Aires, Argentina

***Correspondence:**
Kenneth S. K. Tung
kst7k@virginia.edu

Specialty section:
This article was submitted to Mucosal Immunity, a section of the journal Frontiers in Immunology

Received: *04 November 2021*
Accepted: *07 February 2022*
Published: *26 May 2022*

Citation:
Harakal J, Qiao H, Wheeler K, Rival C, Paul AGA, Hardy DM, Cheng CY, Goldberg E and Tung KSK (2022) Exposed and Sequestered Antigens in Testes and Their Protection by Regulatory T Cell-Dependent Systemic Tolerance. Front. Immunol. 13:809247. doi: 10.3389/fimmu.2022.809247

Continuous exposure of tissue antigen (Ag) to the autoantigen-specific regulatory T cells (Treg) is required to maintain Treg-dependent systemic tolerance. Thus, testis autoantigens, previously considered as sequestered, may not be protected by systemic tolerance. We now document that the complete testis antigen sequestration is not valid. The haploid sperm Ag lactate dehydrogenase 3 (LDH3) is continuously exposed and not sequestered. It enters the residual body (RB) to egress from the seminiferous tubules and interact with circulating antibody (Ab). Some LDH3 also remains inside the sperm cytoplasmic droplets (CD). Treg-depletion in the DEREG mice that express diphtheria toxin receptor on the Foxp3 promoter results in spontaneous experimental autoimmune orchitis (EAO) and Ab to LDH3. Unlike the wild-type male mice, mice deficient in LDH3 (wild-type female or LDH3 *NULL* males) respond vigorously to LDH3 immunization. However, partial Treg depletion elevated the wild-type male LDH3 responses to the level of normal females. In contrast to LDH3, zonadhesin (ZAN) in the sperm acrosome displays properties of a sequestered Ag. However, when ZAN and other sperm Ag are exposed by vasectomy, they rapidly induce testis Ag-specific tolerance, which is terminated by partial Treg-depletion, leading to bilateral EAO and ZAN Ab response. We conclude that some testis/sperm Ag are normally exposed because of the unique testicular anatomy and physiology. The exposed Ag: 1) maintain normal Treg-dependent systemic tolerance, and 2) are pathogenic and serve as target Ag to initiate EAO. Unexpectedly, the sequestered Ags, normally non-tolerogenic, can orchestrate *de novo* Treg-dependent, systemic tolerance when exposed in vasectomy.

Keywords: testis autoantigens and autoantibodies, exposed and sequestered testis autoantigens, the residual bodies and cytoplasmic droplets, experimental and human autoimmune orchitis, post-vasectomy tolerance versus orchitis, Foxp3+ regulatory T cells and systemic tolerance

1 INTRODUCTION

Inbred mice thymectomized between day 1 and day 5 (d3tx) after birth spontaneously develop autoimmune disease in the ovary, prostate, stomach, testis and/or lacrimal gland (1). All the diseases are preventable by the early implantation of lymphoid organs from normal syngeneic donors (1–3). This seminal observation led to discovery of the CD4+ Foxp3+ CD25+ regulatory T cells (Treg) crucial for organ-specific autoimmune disease prevention (4–6). Peripheral Tregs may develop "naturally" in the thymus (nTregs), or may have converted from Foxp3-negative "conventional" CD4+ T cells in the periphery (pTregs) (7). The CD4+ nTregs develop in response to tissue auto-peptides expressed in the thymic medulla – a process controlled by unique Ag presenting dendritic cells (8), the transcription regulator *AIRE* (9), the transcription factor *Fezf2* (10), and the chromatin remodeler Chd4 (11). Relevant to this review are 1) the idiopathic male infertility that occurs in autoimmune polyendocrinopathy syndrome 1 with or without *AIRE* mutation (12, 13), 2) the orchitis detectable in the *Fezf2* NULL mice (10), 3) the Tregs that develop in the periphery in response to self or foreign peptides presented by tolerogenic Ag presenting cells in appropriate cytokine environment (14–16), and 4) autoimmune sequel of human vasectomy.

Tregs control T effector cell responses in the regional lymph node (LN) of the target organ and prevent autoimmune disease (17). There is enrichment of Treg function in the normal regional LN for prevention of disease in the target organ. Whereas 0.5 million Tregs pooled from all LNs of normal mice are required to adoptively suppress autoimmune ovarian disease in d3tx mice, only 30,000 Tregs from the ovary-draining LN are sufficient (17). This finding applies equally to the Tregs in LN draining the prostate and lacrimal glands (18). The enrichment of disease-specific Treg in regional LN requires continuous exposure to relevant Ag from the target organ. For instance, ablation of prostate Ag by neonatal orchiectomy deprives prostate-specific Treg enrichment in the prostate-draining LN without affecting Treg enrichment in LN draining the lacrimal gland. Indeed, Treg enrichment in the prostate-draining LN can be quickly restored in the orchiectomized mice when prostate Ag are re-expressed upon testosterone treatment (18–21). These findings, initially conducted using polyclonal Tregs, have been confirmed and extended by studies using Ag-specific Tregs (21, 22). Therefore, Ag accessibility, controlled at the level of the target organs can influence systemic tolerance initiated in the thymus (23–25). In this context, the sperm Ag in the normal testis has long been considered unique in that they are all sequestered from the immune system and are beyond regulation by systemic tolerance.

The Ag relevant to experimental autoimmune orchitis (EAO) are expressed in post-meiotic germ cells inside the seminiferous tubules (SFT). They are separated from the interstitial space by the blood-testis barrier (BTB) provided by the Sertoli cells with their basal and apical tight junctions (26). Rodent sperm Ag appear at about 2 weeks after birth (27). Thereafter, a large quantity of numerous novel testis-specific antigens are synthesized and expressed in the meiotic germ cells (28). Murine spermatogenesis occurs in 12 stages along the length of an adult seminiferous tubule, each defined by unique composition and arrangement of the germ cells (29). However, the first wave of spermatogenesis initiated at puberty is synchronous for all tubules (30). After they differentiated from the haploid spermatids, sperm released into the seminiferous tubular lumen would traverse the straight tubules, the rete testis, the ductus efferentes, and enter the caput epididymis. Further transit through the epididymis body and tail complete sperm maturity (28). This paradigm of testis biology has led to the concept that sperm Ag of late ontogeny are sequestered in a completely closed epithelial environment; they do not communicate with the immune system including with Tregs, and are unable to maintain "neonatal" tolerance (28, 31–33). Accordingly, local Ag independent mechanisms (or local immune privilege), operating in the testis and epididymal interstitial spaces, are essential for immune protection of testicular Ag. The idea of Ag sequestration was also a rationale behind the application of highly immunogenic cancer/testis Ag (CTA) as cancer vaccine candidates (34). However, sperm Ag sequestration, the lack of systemic tolerance, and the natural hyper-immunogenicity of CTA are not evidence-based.

Several studies have argued against the complete sequestration of sperm Ag. First, mice immunized with testis homogenate in incomplete Freund's adjuvant do not develop EAO but they produce Ab that react with the diploid preleptotene spermatocytes located outside the BTB, indicating that germ cells outside the BTB are immunogenic (23, 35). Second, d3tx mice develop autoimmune orchitis and epididymitis, and the disease is prevented by infusion of T cells from normal syngeneic donors. This suggests the existence of testis-specific Treg (36). Third, the preferential accumulation of inflammatory cells at the straight tubule in adoptive EAO transfer (37), is likely due to reduced mechanical barrier in this location (38). Nonetheless, a long-standing question remained. How do testis-specific T cells receive their tolerogenic Ag signal, and how do effector T cells and Ab engage their target sperm Ag in the testis to initiate EAO if the Ag are completely sequestered?

The first definitive evidence against complete sperm Ag sequestration was obtained in a study that documented continuous sperm Ag egress from normal SFT and the protection of the exposed Ag by Treg-dependent systemic tolerance (25). Herein, we review the published experiments, including the mechanism of Ag egress and systemic tolerance controlled by the Tregs. We also document that some other sperm Ag, which lack the properties of the exposed sperm Ag, are indeed sequestered. We first encountered the sequestered sperm Ag in 2011 when we investigated mice with unilateral vasectomy (Uni-Vx) (39). We were puzzled by the absence of the anticipated post-vasectomy robust Ab response to sperm. Instead, we found rapid induction Ag-specific Tregs against ZAN, an acrosomal sperm Ag subsequently confirmed to be sequestered (25, 39, 40).

2 FINDINGS

We present our results in two parts. Part 1 will summarize our published studies on the responses to three individual sperm Ag in normal mice (25). Part 2 will describe the findings from our

earlier research on the Uni-Vx mice, which, in retrospect, is highly pertinent to our findings in Part 1 (39, 40).

2.1 Part 1: Accessibility and Immunological Studies on Meiotic Germ Cell Antigens Located in Seminiferous Tubules of Normal Mice

2.1.1 Detection of LDH3 and Transgenic Ovalbumin Egress From the SFT to Interstitial Space

Lactate dehydrogenase 3 (LDH3) is a cytoplasmic Ag of meiotic germ cells located inside normal ST. LDH3 first appears at postnatal week 2. To detect LDH3 egress from the SFT, we injected rabbit Ab against mouse LDH3 intravenously into normal 8 week-old male mice (27). Twelve hours later, we detected immune complexes as granular deposits of rabbit IgG in mice injected with LDH3 Ab. The immune complexes were localized outside the BTB and surrounded 20% of the SFT (25). To support the LDH3 specificity of the immune complexes, we did not detect them in the *Ldh3* null mice injected with LDH3 Ab or in wildtype (WT) mice injected with Ab against ovalbumin (OVA). In addition, immune complexes were not detected beyond the testis, including the caput, corpus, and cauda epididymis.

We also investigated the sperm Ag zonadhesin (ZAN), located in the inner acrosomal membrane (41). In contrast to LDH3, we did not detect evidence of egress of ZAN, a sperm acrosomal Ag. Therefore, both LDH3 and ZAN exist in the SFT behind the BTB, but only LDH3 egresses from the SFT. While the Sertoli cells and the BTB may prevent the entrance of macromolecules into the SFT lumen (42), they do not inhibit the egress of all sperm Ag into the interstitial space.

2.1.2 LDH3 and Transgenic Ovalbumin Egress From the Seminiferous Tubule as Contents of the Residual Body

Following LDH3 Ab injection, immune complex formation is dependent on the age of the mice; they are detected in 5 week-old mice but not in mice at the ages of 3, 4, or 4.5 weeks. The onset at 5 weeks coincides with the onset of spermiation, a process wherein elongated haploid spermatids transform into sperm in the first wave of synchronous spermatogenesis (30). At spermiation, the redundant cytoplasm and plasma membrane from the late spermatid are packaged into: 1) a large residual body (RB) retained in the SFT, and 2) a smaller cytoplasmic droplet (CD) that remains attached to the sperm until they leave the caput epididymis (25, 43, 44). To investigate the hypothesis that LDH3 is exported as the content of the RB, we utilized mice expressing transgenic OVA on the protamine 1 promoter (the OVA-Hi), at 10 μg of extractable OVA per gram of testis, as a surrogate sperm-specific cytoplasmic Ag in elongated spermatid and sperm (25). We also utilized the Scleraxis-GFP mice with Sertoli cell-specific fluorescence (25) as well as Ab to the testis isoform of angiotensin-converting enzyme as a RB marker (45).

We detected LDH3 in the RB of normal WT mouse testis by indirect immunofluorescence. Intense staining of OVA was also noted in the RB of the OVA-Hi mice that co-localizes with LDH3. Detection was maximal at stage IX of the spermatogenic cycle (25). Some RB, engulfed by Sertoli cells, appears as dual-fluorescence labeled star-shaped objects. However, some RB retains their normally round shape and are distributed from the apex to the base of the SFT epithelium. Importantly, these RB stain positively for OVA and LDH3 and have no Scleraxis-GFP co-stain (not shown). Thus, they are located outside the Sertoli cell cytoplasm. In addition, strong OVA staining appears inside the basal cytoplasm of the Sertoli cells, as droplets in the adjacent interstitial space in OVA-Hi mice, and inside interstitial macrophages. To show OVA egress from the SFT, we intravenously injected OVA-Hi mice with OVA Ab. This led to immune complex formation on the surface of SFT outside the BTB, some inside the interstitial F4/80+ macrophages.

Therefore, not all RB are engulfed and destroyed by the Sertoli cells. Some RB located outside the Sertoli cells remain intact until they reach the base of the Sertoli cells. At that location, spermatid Ag appears to be transported into the interstitial space *via* the basal Sertoli cell cytoplasm. These findings are consistent with an electronic microscopic study of labeled rat RB by Xiao et al. (46). After sperm are released at stage IX, the RB were described to move rapidly to the edge of the SFT, change into lipid inclusions and lipid particles, and were discharged into interstitial space. However, the definitive movement of sperm Ag from Sertoli cell to the interstitial space requires more detailed investigation.

The differential sequestration status between LDH3 and ZAN is confirmed recently based on proteomic and mass spectroscopic analyses of the testis interstitial fluids and serum proteins (47). The authors proposed two hypothetical mechanisms for meiotic Ag egress from the ST. One is *via* the RB at stage IX of the spermatogenic cycle (25) and the second to occur earlier, at spermatogenic cycle stages VI and VII prior to RB formation.

2.1.3 Immunological Evidence for: A) Exposed Status of LDH3 and Transgenic OVA, B) Tregs as Their Tolerance Mechanism, and C) Sequestered Status of ZAN

First, we detected differences in the immunogenicity of LDH3 and ZAN between Ag-positive mice and Ag-negative mice (23, 25). WT male C57BL/6 mice immunized with testis homogenate in adjuvant do not produce Ab to LDH3. In contrast, robust LDH3 Ab responses are elicited in both LDH3-deficient *Ldh3* null male C57BL/6 mice and female WT C57BL/6 mice. Importantly, the treatment of the LDH3-immunized WT male mice with CD25 Ab (PC61), which depletes ~60% of Tregs for 5 weeks (39), enhanced their LDH3 Ab levels to the level of the immunized-WT female mice. By comparison, male and female WT mice immunized with testis homogenate produce comparable and strong ZAN Ab responses and the male response to ZAN was unaffected by Treg depletion by CD25 Ab. These results indicated that WT male mice are tolerant to the exposed LDH3 and their Tregs maintain the unresponsive state to LDH3. In contrast, male C56BL/6 mice are not tolerant to the sequestered ZAN Ag.

Second, Treg depletion alone (without Ag immunization) resulted in spontaneous EAO and Ab against LDH3 but not against ZAN. Injection of diphtheria toxin depletes 95% of Tregs

from the LN and spleen of male B6AF1-DEREG mice that express transgenic diphtheria toxin receptor on Foxp3-positive Tregs (48). After 3 diphtheria toxin injections, 40% of the mice spontaneously develop EAO. The severe testis pathology includes: 1) increase in interstitial accumulation of macrophages with the M1 phenotype, a concomitant reduction in the M2 macrophages and macrophage invasion into the ST; 2) focal peri-tubular immune complexes composed of IgG2 and complement component C3 in 70% of mice; 3) molecular, functional, and ultrastructural evidence of a defective BTB, 4) reduction in spermatogenesis, epididymal sperm content, and testis weight. Because the immunopathology and the LDH3 Ab response in the Treg-depleted DEREG mice are preventable by reconstitution of Tregs from normal WT mice, Treg depletion must be responsible for the LDH3 Ab response and the autoimmune orchitis pathology. Most likely, when Tregs are depleted, the altered innate functional properties of the Ag presenting cells (49) allows the exposed testis Ag, including LDH3, to stimulate pathogenic autoimmune T cell response.

Third, we compared the immune response to OVA between the OVA-Hi mice and OVA-Lo mice that express 40-fold lower level of transgenic OVA in the elongated spermatid (25). The OVA-Hi mice immunized with OVA in adjuvant do not respond to OVA. In contrast, similarly immunized OVA-Lo mice mount a strong Ab and T cell responses to OVA and its T cell epitope and develop severe EAO. Moreover, T cells from their regional LN of the injection site adoptively transfer EAO to OVA-Hi or OVA-Lo recipients but not to the WT BALB/c recipients. Compared with the OVA-Hi mice, only a trace amount of rabbit IgG is detected in <5% of the SFT of OVA-Lo mice injected with rabbit Ab to OVA. The results indicate that although OVA-Lo mice do not expose sufficient OVA to maintain tolerance to OVA, the amount of OVA that egresses from the SFT is sufficient to be presented as target Ag for the effector T cells and Ab to initiate EAO. This finding indicates that the quantity of available target Ag expression also influences Treg-dependent tolerance versus autoimmunity (50). It also indicates that different mechanisms of EAO pathogenesis are responsible for disease induced by high versus low tissue expression or accessibility.

2.2 Part II: Unilateral Vasectomy Exposes Epididymal Sperm Ag and Causes Rapid Emergence of ZAN-Specific Tregs and Testis-Specific Tolerance

Because ZAN has the properties of a foreign Ag, we expected it to stimulate a robust Ab response when it becomes exposed. In 2011 and 2013, we tested this hypothesis in WT mice subjected to Uni-Vx, in which the intact contralateral gonad monitors the systemic responses to sperm release in the ipsilateral epididymis. The result from this unintentional study was unexpected.

Epithelial cell apoptosis and desquamation occur in the epididymis within 24 hours after Uni-Vx and sperm are extruded into the interstitial space. To our surprise, the Uni-Vx mice did not have detectable testis Ag-specific or ZAN-specific immune responses for the next 3-4 months (39, 40). This is not because the mice are unresponsive to ZAN. Instead, a response to ZAN emerges only when their Tregs were partially depleted. We confirmed this by two approaches. First, Treg depletion by CD25 monoclonal Ab at the time of Uni-Vx led to a spontaneous Ab to ZAN, CD4 T cell responses to ZAN peptide, and severe bilateral autoimmune orchitis transferable by regional LN CD4 T cells. Second, mice with Uni-Vx alone developed testis Ag-specific tolerance; specifically, the Uni-Vx mice no longer develop EAO when immunized with testis Ag and adjuvants although they developed experimental autoimmune encephalomyelitis when immunized with brain Ag. Importantly, the tolerance state to the testis Ag also depends on Tregs and is preventable by CD25 monoclonal Ab treatment. These findings on ZAN indicate that even sequestered testis Ag, when exposed, can lead to *de novo* testis Ag-specific Treg responses that tempers an excessive immune response against the sequestered self-Ag, as seen in tissue injury and testis infections.

The ZAN-specific Tregs emerge rapidly following uni-Vx. When Treg depletion is delayed for 7 days from the time of Uni-Vx (day 0), the Treg-dependent tolerance against ZAN is no longer reversible (40). The ZAN-specific Tregs most likely represents iTregs since normal mice have no detectable Treg-dependent tolerance to ZAN. In addition, we showed that the Treg induction in uni-Vx is affected in mice with genetic deficiency in PD1 ligand and not in PD1, a finding consistent with the involvement of iTregs in post-transplantation tolerance (51). Interestingly, the Treg-depleted uni-Vx mice produced Ab responses against ZAN but not LDH3, suggesting that sufficient nTregs maintain tolerance to LDH3 despite CD25 monoclonal Ab treatment.

The ZAN-specific tolerance after Uni-Vx is long lasting. Compared to age-matched control mice, the Uni-Vx mice showed resistance to testis Ag induction of sperm Ab and EAO up to 12–16 months (40). However, at 4-5 months after Uni-Vx, low levels of serum ZAN Ab emerge, and the Ab titers amongst individual mice fluctuate over time. We interpret the findings to indicate a gradual decline in Treg control, followed by an imbalance between the Treg and effector T cell responses. The imbalance may be triggered by tissue pathology occurring in the ipsilateral testis and epididymis due to mechanical obstruction of vasectomy. They include severe fibrosis in the epididymis and reduction in spermatogenesis confined to the vasectomized testis (40). In view of these new findings, it is important to further investigate the immune sequelae of clinical vasectomy, a health issue of national and international importance. Moreover, infertility often occurs after vasectomy reversal despite the return of adequate sperm counts (52).

3 SUMMARY AND CONCLUSIONS

We have reviewed the supporting evidence that Ag in the normal testis, relevant to testicular autoimmunity, are not completely sequestered. In **Figure 1**, we illustrate the anatomy of normal mouse testis and the pathways by which Ags in haploid germ cells located behind the BTB can egress from the SFT as contents of the RB. The process appears to involve an undefined exocytosis pathway of the basal Sertoli cells. The exposed testis Ag is presented to Ag-specific Tregs in sufficient quantity to maintain

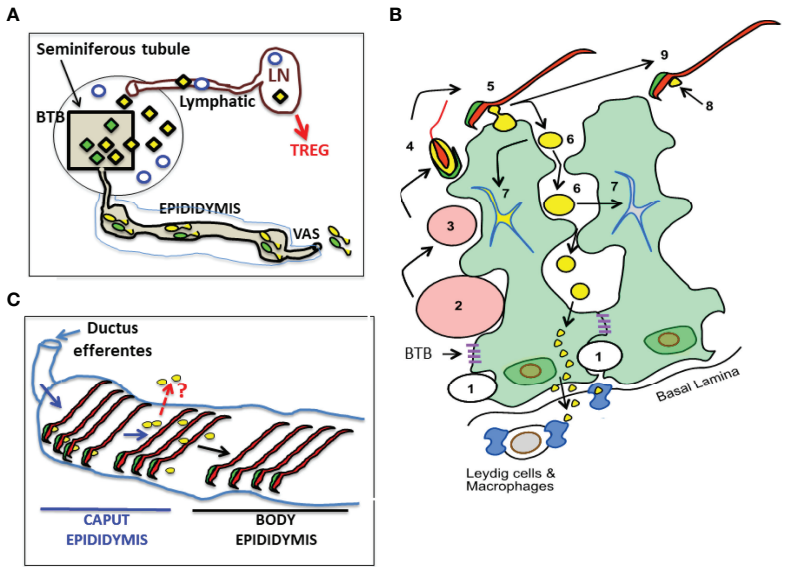

FIGURE 1 | A Landscape of Cellular Antigens in Testicular, Epididymal and Regiona Lymph Node (LN) Compartments. **(A)** The blood-testis barrier (BTB) divides normal testis into the seminiferous tubule and the interstitial compartment. The Ag of the interstitial space, located outside the BTB, including the Leydig cells (empty blue circles), spermatogonia, and preleptotene spermatocytes (not shown) are likely to be exposed. Seminiferous tubule contains all the unique Ag in meiotic germ cells (diamonds). Unexpectedly, some meiotic germ cell antigens (yellow diamonds) continuously egress into interstitial space and reach the regional LN *via* the afferent lymphatic, while other antigens are sequestered (green diamonds). **(B)** A cartoon showing the location and fate of male germ cell development adjacent to two Sertoli cells (with green cytoplasm). Spermatogonia (*1*) traverse the BTB to become spermatocytes (*2 and 3*), and early spermatids (*4*) that develops acrosome (in green), cytoplasm (in yellow), nucleus and tail (in red). Spermiation occurs when late spermatid (*5*) becomes sperm (*9*). Some meiotic germ cell cytoplasm becomes the residual body (RB) (*6*) while others become the cytoplasmic droplet (CD) that attaches to the sperm (*8*). Most RB are engulfed and destroyed by Sertoli cell (*7*). However, some RB stay outside the Sertoli cells until reaching their base, and enter the interstitial space. Systemic Treg-dependent tolerance mechanism protects the meiotic cell antigens in RB and CD (example: LDH3). The sequestered meiotic germ cell antigens (example: ZAN in sperm acrosome) are not protected by systemic tolerance in normal mice. **(C)** The CDs (yellow spheres), initially attached to the sperm in the caput epididymis, soon disappear and are undetectable in the body epididymis. A question (in red): Do the exit of CD Ag in epididymis represent an additional pathway of sperm Ag egress?

physiological tolerance in normal mice. However, in individuals destined to develop testicular autoimmune disease, the exposed testis Ag can become the immunogen, trigger a pathogenic autoimmune response, and maintain the pathogenic process of EAO (24). EAO can result from a multitude of genetic and environmental factors (53–55), including loss of Treg function, conversion of Treg to effector T cells, response to foreign Ags *via* molecular mimicry (56), and disruption of local regulation (57).

The process of meiotic Ag egress in the SFT also highlights the process of molecular recycling in spermatogenesis that involves the Sertoli cells. In addition to the re-utilization of RB contents in spermatogenesis and spermiogenesis, the apical-to-basal directional movement of macromolecules in the normal SFT epithelium is also documented for the re-utilization of iron in spermatogenesis, and for the recycling of tight junctional molecules in BTB biosynthesis (58–61)

In contrast to the exposed testis Ag, some testicular Ag are normally sequestered behind the BTB. They are normally non-tolerogenic and are not protected by the nTreg. However, when they become exposed, as demonstrated by vasectomy, the normally sequestered Ag can rapidly elicit iTreg that prevent or temper concomitant autoimmune responses against them. Remarkably, the Ag-specific iTreg response is strong enough to maintain tolerance for many months after vasectomy. It is possible that when the sequestered sperm Ag are exposed by bacterial or viral infections, or other types of injuries, they too can induce an iTreg-dependent mechanism for protection (16). Study on the Uni-Vx mice also reveals that major complications of vasectomy result from simple vas obstruction rather than systemic immune mechanism (40).

Our work emphasizes the importance of the Treg-dependent systemic immune protection of male germ cell Ags. It compliments the extensive research on local regulation in the testis, but by no means minimize the importance of local regulation. However, the findings of Treg-depleted DEREG mice indicate that loss of Treg alone can be sufficient to cause EAO. Future research will focus on how the systemic mechanism and local mechanisms are complimentary and function in concert.

AUTHOR CONTRIBUTIONS

KT and JH designed the experiments that constitute this review. KT, JH, HQ, KW, CR, AP, DH, YC, and EG conducted the experiments and analyzed the data. JH, DH, EG, YC provided experimental tools or generate the mouse models. KT and JH wrote the manuscript. All authors contributed to the article and approved the submitted version.

FUNDING

The study was supported by NIH grants RO1 AI 41236 and RO1 AI 51420.

ACKNOWLEDGMENTS

The authors are grateful to the very helpful advice from Rex Hess and Esther Meyron-Holtz.

REFERENCES

1. Nishizuka Y, Sakakura T. Thymus and Reproduction: Sex-Linked Dysgenesia of the Gonad After Neonatal Thymectomy in Mice. *Science* (1969) 166:753–5. doi: 10.1126/science.166.3906.753
2. Kojima A, Prehn RT. Genetic Susceptibility to Post-Thymectomy Autoimmune Diseases in Mice. *Immunogenetics* (1981) 14:15–27. doi: 10.1007/BF00344296
3. Sakaguchi S, Takahashi T, Nishizuka Y. Study on Cellular Events in Post-Thymectomy Autoimmune Oophoritis in Mice: II. Requirement of Lyt-1 Cells in Normal Female Mice for the Prevention of Oophoritis. *J Exp Med* (1982) 156:1577–86. doi: 10.1084/jem.156.6.1577
4. Sakaguchi S, Sakaguchi N, Asano M, Itoh M, Toda M. Immunologic Self-Tolerance Maintained by Activated T Cells Expressing IL-2 Receptor Alpha-Chains (CD25). Breakdown of a Single Mechanism of Self-Tolerance Causes Various Autoimmune Diseases. *J Immunol* (1995) 155:1151–64.
5. Fontenot JD, Gavin MA, Rudensky AY. Foxp3 Programs the Development and Function of CD4+CD25+ Regulatory T Cells. *Nat Immunol* (2003) 4:330–6. doi: 10.1038/ni904
6. Hori S, Nomura T, Sakaguchi S. Control of Regulatory T Cell Development by the Transcription Factor Foxp3. *Science* (2003) 299:1057–61. doi: 10.1126/science.1079490
7. Chen W, Jin W, Hardegen N, Lei K-J, Li L, Marinos N, et al. Conversion of Peripheral CD4+CD25- Naive T Cells to CD4+CD25+ Regulatory T Cells by TGF-Beta Induction of Transcription Factor Foxp3. *J Exp Med* (2003) 198:1875–86. doi: 10.1084/jem.20030152
8. Savage PA, Klawon DEJ, Miller CH. Regulatory T Cell Development. *Annu Rev Immunol* (2020) 38:421–53. doi: 10.1146/annurev-immunol-100219-020937
9. Anderson MS, Venanzi ES, Klein L, Chen Z, Berzins SP, Turley SJ, et al. Projection of an Immunological Self Shadow Within the Thymus by the Aire Protein. *Science* (2002) 298:1395–401. doi: 10.1126/science.1075958
10. Takaba H, Morishita Y, Tomofuji Y, Danks L, Nitta T, Komatsu N, et al. Fezf2 Orchestrates a Thymic Program of Self-Antigen Expression for Immune Tolerance. *Cell* (2015) 163:975–87. doi: 10.1016/j.cell.2015.10.013
11. Tomofuji Y, Takaba H, Suzuki HI, Benlaribi R, Martinez CDP, Abe Y, et al. Chd4 Choreographs Self-Antigen Expression for Central Immune Tolerance. *Nat Immunol* (2020) 21:892–901. doi: 10.1038/s41590-020-0717-2
12. Abramson J, Husebye ES. Autoimmune Regulator and Self-Tolerance - Molecular and Clinical Aspects. *Immunol Rev* (2016) 271:127–40. doi: 10.1111/imr.12419
13. Schuppe H-C, Meinhardt A, Allam JP, Bergmann M, Weidner W, Haidl G. Chronic Orchitis: A Neglected Cause of Male Infertility? *Andrologia* (2008) 40:84–91. doi: 10.1111/j.1439-0272.2008.00837.x
14. Schmidt SV, Nino-Castro AC, Schultze JL, Lutz MB, Granucci F. Regulatory Dendritic Cells: There is More Than Just Immune Activation. *Front Immunol* (2012) 3:274. doi: 10.3389/fimmu.2012.00274
15. Guo Zheng S, Chen L, Guo Z, Zhang B, S-q L, Zhu K, et al. Lineage Tracking the Generation of T Regulatory Cells From Microbial Activated T Effector Cells in Naïve Mice. *Front Immunol* (2020) 1:3109. doi: 10.3389/fimmu.2019.03109
16. Zhu K, He C, Liu S-Q, Qu M, Xie T, Yang X, et al. Lineage Tracking the Generation of T Regulatory Cells From Microbial Activated T Effector Cells in Naïve Mice. *Front Immunol* (2020) 10:3109. doi: 10.3389/fimmu.2019.03109
17. Samy ET, Setiady YY, Ohno K, Pramoonjago P, Sharp C, Tung KSK. The Role of Physiological Self-Antigen in the Acquisition and Maintenance of Regulatory T-Cell Function. *Immunol Rev* (2006) 212:170–84. doi: 10.1111/j.0105-2896.2006.00404.x
18. Setiady YY, Ohno K, Samy ET, Bagavant H, Qiao H, Sharp C, et al. Physiologic Self Antigens Rapidly Capacitate Autoimmune Disease-Specific Polyclonal CD4+ CD25+ Regulatory T Cells. *Blood* (2006) 107:1056–62. doi: 10.1182/blood-2005-08-3088
19. Taguchi O, Nishizuka Y. Self Tolerance and Localized Autoimmunity: Mouse Models of Autoimmune Disease That Suggest Tissue-Specific Suppressor T Cells Are Involved in Self Tolerance. *J Exp Med* (1987) 165:146–56. doi: 10.1084/jem.165.1.146
20. Taguchi O, Kontani K, Ikeda H, Kezuka T, Takeuchi M, Takahashi T, et al. Tissue-Specific Suppressor T Cells Involved in Self-Tolerance Are Activated Extrathymically by Self-Antigens. *Immunol* (1994) 82:365–9.
21. Leonard JD, Gilmore DC, Dileepan T, Nawrocka WI, Chao JL, Schoenbach MH, et al. Identification of Natural Regulatory T Cell Epitopes Reveals Convergence on a Dominant Autoantigen. *Immunity* (2017) 47:107–17.e8. doi: 10.1016/j.immuni.2017.06.015
22. Klawon DEJ, Gilmore DC, Leonard JD, Miller CH, Chao JL, Walker MT, et al. Altered Selection on a Single Self-Ligand Promotes Susceptibility to Organ-Specific T Cell Infiltration. *J Exp Med* (2021) 218:20200701. doi: 10.1084/jem.20200701
23. Garza KM, Agersborg SS, Baker E, Tung KS. Persistence of Physiological Self Antigen Is Required for the Regulation of Self Tolerance. *J Immunol* (2000) 164:3982–9. doi: 10.4049/jimmunol.164.8.3982
24. Alard P, Thompson C, Agersborg SS, Thatte J, Setiady Y, Samy E, et al. Endogenous Oocyte Antigens Are Required for Rapid Induction and Progression of Autoimmune Ovarian Disease Following Day-3 Thymectomy. *J Immunol* (2001) 166:4363–9. doi: 10.4049/jimmunol.166.7.4363
25. Tung KSK, Harakal J, Qiao H, Rival C, Li JCH, Paul AGA, et al. Egress of Sperm Autoantigen From Seminiferous Tubules Maintains Systemic Tolerance. *J Clin Invest* (2017) 127:1046–60. doi: 10.1172/JCI89927
26. Dym M, Fawcett DW. The Blood-Testis Barrier in the Rat and the Physiological Compartmentation of the Seminiferous Epithelium. *Biol Reprod* (1970) 3:308–26. doi: 10.1093/biolreprod/3.3.308
27. Hintz M, Goldberg E. Immunohistochemical Localization of LDH-X During Spermatogenesis in Mouse Testes. *Dev Biol* (1977) 57:375–84. doi: 10.1016/0012-1606(77)90222-6
28. Mital P, Hinton BT, Dufour JM. The Blood-Testis and Blood-Epididymis Barriers Are More Than Just Their Tight Junctions. *Biol Reprod* (2011) 84:851–8. doi: 10.1095/biolreprod.110.087452
29. Russell LD, Ettlin RA, Sinha Hikim AP, Clegg ED. *Histological and Histopathological Evaluation of the Testis. 1st ed*. Clearwater, FL: Cache River Press (1990).
30. Oakberg EF. Duration of Spermatogenesis in the Mouse and Timing of Stages of the Cycle of the Seminiferous Epithelium. *Am J Anat* (1956) 99:507–16. doi: 10.1002/aja.1000990307
31. Hedger MP. Macrophages and the Immune Responsiveness of the Testis. *J Reprod Immunol* (2002) 57:19–34. doi: 10.1016/S0165-0378(02)00016-5
32. Fijak M, Meinhardt A. The Testis in Immune Privilege. *Immunol Rev* (2006) 213:66–81. doi: 10.1111/j.1600-065X.2006.00438.x
33. Li N, Wang T, Han D. Structural, Cellular and Molecular Aspects of Immune Privilege in the Testis. *Front Immunol* (2012) 3:152. doi: 10.3389/fimmu.2012.00152
34. Simpson AJG, Caballero OL, Jungbluth A, Chen Y-T, Old LJ. Cancer/Testis Antigens, Gametogenesis and Cancer. *Nat Rev Cancer* (2005) 5:615–25. doi: 10.1038/nrc1669
35. Yule TD, Montoya GD, Russell LD, Williams TM, Tung KS. Autoantigenic Germ Cells Exist Outside the Blood Testis Barrier. *J Immunol* (1988) 141:1161–7.
36. Taguchi O, Nishizuka Y. Experimental Autoimmune Orchitis After Neonatal Thymectomy in the Mouse. *Clin Exp Immunol* (1981) 46:425–34.
37. Tung KS, Yule TD, Mahi-Brown CA, Listrom MB. Distribution of Histopathology and Ia Positive Cells in Actively Induced and Passively Transferred Experimental Autoimmune Orchitis. *J Immunol* (1987) 138:752–9. doi: 10.1111/j.1749-6632.1987.tb25096.x
38. Figueiredo AFA, Hess RA, Batlouni SR, Wnuk NT, Tavares AO, Abarikwu SO, et al. Insights Into Differentiation and Function of the Transition Region

Between the Seminiferous Tubule and Rete Testis. *Differentiation* (2021) 120:36–47. doi: 10.1016/j.diff.2021.06.002
39. Wheeler K, Tardif S, Rival C, Luu B, Bui E, Del Rio R, et al. Regulatory T Cells Control Tolerogenic Versus Autoimmune Response to Sperm in Vasectomy. *Proc Natl Acad Sci USA* (2011) 108:7511–6. doi: 10.1073/pnas.1017615108
40. Rival C, Wheeler K, Jeffrey S, Qiao H, Luu B, Tewalt EF, et al. Regulatory T Cells and Vasectomy. *J Reprod Immunol* (2013) 100:66–75. doi: 10.1016/j.jri.2013.08.004
41. Hickox JR, Bi M, Hardy DM. Heterogeneous Processing and Zona Pellucida Binding Activity of Pig Zonadhesin. *J Biol Chem* (2001) 276:41502–9. doi: 10.1074/jbc.M106795200
42. Meng J, Holdcraft RW, Shima JE, Griswold MD, Braun RE. Androgens Regulate the Permeability of the Blood-Testis Barrier. *Proc Natl Acad Sci USA* (2005) 102:16696–700. doi: 10.1073/pnas.0506084102
43. Yuan S, Zheng H, Zheng Yan ZW. Proteomic Analyses Reveal a Role of Cytoplasmic Droplets as an Energy Source During Epididymal Sperm Maturation. *PLoS One* (2013) 8:e77466. doi: 10.1371/journal.pone.0077466
44. Au CE, Hermo L, Byrne E, Smirle J, Fazel A, Kearney RE, et al. Compartmentalization of Membrane Trafficking, Glucose Transport, Glycolysis, Actin, Tubulin and the Proteasome in the Cytoplasmic Droplet/HERMES Body of Epididymal Sperm. *Open Biol* (2015) 5:150080. doi: 10.1098/rsob.150080
45. Atanassova N, Lakova E, Bratchkova Y, Krasteva G, Donchev M. Expression of Testicular Angiotensin-Converting Enzyme in Adult Spontaneously Hypertensive Rats. *Folia Histochem Cytobiol* (2009) 47:117–22. doi: 10.2478/v10042-009-0002-6
46. Xiao CY, Wang YQ, Li JH, Tang GC, Xiao SS. Transformation, Migration and Outcome of Residual Bodies in the Seminiferous Tubules of the Rat Testis. *Andrologia* (2017) 49:e12786. doi: 10.1111/and.12786
47. O'Donnell L, Rebourcet D, Dagley LF, Sgaier R, Infusini G, O'Shaughnessy PJ, et al. Sperm Proteins and Cancer-Testis Antigens Are Released by the Seminiferous Tubules in Mice and Men. *FASEB J* (2021) 35:e21397. doi: 10.1096/fj.202002484R
48. Lahl K, Loddenkemper C, Drouin C, Freyer J, Arnason J, Eberl G, et al. Selective Depletion of Foxp3+ Regulatory T Cells Induces a Scurfy-Like Disease. *J Exp Med* (2007) 204:57–63. doi: 10.1084/jem.20061852
49. Steinman RM. Dendritic Cells: Understanding Immunogenicity. *Eur J Immunol* (2007) 37.Suppl 1:S53–60. doi: 10.1002/eji.200737400
50. Plotz PH. The Autoantibody Repertoire: Searching for Order. *Nat Rev Immunol* (2003) 3:73–8. doi: 10.1038/nri976
51. Riella LV, Paterson AM, Sharpe AH, Chandraker A. Role of the PD-1 Pathway in the Immune Response. *Am J Transplant* (2012) 12:2575–87. doi: 10.1111/j.1600-6143.2012.04224.x
52. Lee R, Goldstein M, Ullery BW, Ehrlich J, Soares M, Razzano RA, et al. Value of Serum Antisperm Antibodies in Diagnosing Obstructive Azoospermia. *J Urol* (2009) 181:264–9. doi: 10.1016/j.juro.2008.09.004
53. del Rio R, McAllister RD, Meeker ND, Wall EH, Bond JP, Kyttaris VC, et al. Identification of Orch3, A Locus Controlling Dominant Resistance to Autoimmune Orchitis, as Kinesin Family Member 1c. *PLoS Genet* (2012) 8:e1003140. doi: 10.1371/journal.pgen.1003140
54. Ma RZ, Gao J, Fillmore PD, Meeker ND, Tung KSK, Watanabe T, et al. Identification of Bphs, an Autoimmune Disease Locus, as Histamine Receptor H1. *Science* (2002) 297:620–3. doi: 10.1126/science.1072810
55. Zhao Z, Qiao H, Ge Y, Kannapel CC, Sung SSJ, Gaskin F, et al. Autoimmune Experimental Orchitis and Chronic Glomerulonephritis With End Stage Renal Disease Are Controlled by Cgnz1 for Susceptibility to End Organ Damage. *Clin Immunol* (2021) 224:108675. doi: 10.1016/jclim.2021.108675
56. Luo AM, Garza KM, Hunt D, Tung KSK. Antigen Mimicry in Autoimmune Disease: Sharing of Amino Acid Residues Critical for Pathogenic T Cell Activation. *J Clin Invest* (1993) 92:2117–23. doi: 10.1172/JCI116812
57. Lustig L, Guazzone VA, Tung KSK. Autoimmune Orchitis and Autoimmune Ovarian Disease. In: NR Rose, IR Mackay, editors. *The Autoimmune Diseases*, *6th*. London: Elsevier (2019).
58. Yan HHN, Mruk DD, Lee WM, Cheng CY. Blood-Testis Barrier Dynamics are Regulated by Testosterone and Cytokines *via* Their Differential Effects on the Kinetics of Protein Endocytosis and Recycling in Sertoli Cells. *FASEB J* (2008) 22:1945–59. doi: 10.1096/fj.06-070342
59. Leichtmann-Bardoogo Y, Cohen LA, Weiss A, Marohn B, Schubert S, Meinhardt A, et al. Compartmentalization and Regulation of Iron Metabolism Proteins Protect Male Germ Cells From Iron Overload. *AJP Endocrinol Metab* (2012) 302:E1519–30. doi: 10.1152/ajpendo.00007.2012
60. Smith BE, Braun RE. Germ Cell Migration Across Sertoli Cell Tight Junctions. *Science* (2012) 338:798–802. doi: 10.1126/science.1219969
61. Vogl AW, Young JS, Du M. New Insights Into Roles of Tubulobulbar Complexes in Sperm Release and Turnover of Blood-Testis Barrier. *Int Rev Cell Mol Biol* (2013) 303:319–55. doi: 10.1016/B978-0-12-407697-6.00008-8

Conflict of Interest: The authors declare that the research was conducted in the absence of any commercial or financial relationships that could be construed as a potential conflict of interest.

Advantages of publishing in Frontiers

OPEN ACCESS
Articles are free to read for greatest visibility and readership

FAST PUBLICATION
Around 90 days from submission to decision

HIGH QUALITY PEER-REVIEW
Rigorous, collaborative, and constructive peer-review

TRANSPARENT PEER-REVIEW
Editors and reviewers acknowledged by name on published articles

Frontiers
Avenue du Tribunal-Fédéral 34
1005 Lausanne | Switzerland

Visit us: www.frontiersin.org
Contact us: frontiersin.org/about/contact

REPRODUCIBILITY OF RESEARCH
Support open data and methods to enhance research reproducibility

DIGITAL PUBLISHING
Articles designed for optimal readership across devices

FOLLOW US
@frontiersin

IMPACT METRICS
Advanced article metrics track visibility across digital media

EXTENSIVE PROMOTION
Marketing and promotion of impactful research

LOOP RESEARCH NETWORK
Our network increases your article's readership